Report Series

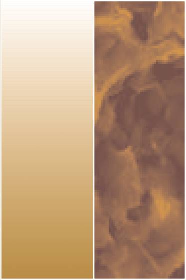

Dossier 2005 Argile

Tome

Phenomenological evolution of a geological repository

December 2005

ANDRA
Agence nationale
pour la gestion des déchets radioactifs

The present English version is a translation of the original “*Dossier 2005 Argile*“ documentation written in French, which remains ultimately the reference documentation.

In order to be consistent through the various documents, while the word ''storage'' (''*entreposage*'' in French) refers only to temporary management (in terms of concept and facility), ''disposal'' (in term of concept) and ''repository'' (in terms of facility or installation) refers to long term management of high level long lived radioactive waste (''*stockage*'' in French for these words).

This document is the result of a collective effort involving numerous partners and contractors working alongside Andra personnel.

As was suggested following the review of file 2001, Andra decided to call on external experts for the rereading of file 2005.
Andra would therefore like to thank the following:

- **Michel Bues** (teacher at the Ecole Nationale Supérieure de Géologie)
- **Hubert Doubre** (teacher at the Université Paris Sud)
- **Marc Panet** (mining civil engineer, Member of the Académie des Technologies)
- **Bernard Poty** (Research Director Emeritus of the CNRS)

who provided recommendations assisting with the drafting of this document.

Contents

Contents 5

Table of illustrations 15

1 Introduction 27

1.1 Purpose of the Volume as part of the Dossier 2005 Argile 29

1.2 Inputs 30

1.3 Structure of the "Evolution Phenomenologique du stockage géologique" Volume 31

1.4 Representation of process space and time scales 32

1.5 Predicting the phenomenological evolution over time, especially over the long term 32

2 The Meuse/Haute Marne site, HLLL waste and disposal concepts 35

2.1 Introduction 37

2.2 The Meuse / Haute-Marne site and the Callovo-Oxfordian layer (Elion, 2005) 38

2.3 HLLW and spent fuels (Andra, 2005e) 42

2.3.1 Main categories of HLLW 43
2.3.2 Spent fuels after passing through EDF PWR reactors or CEA experimental reactors 45
2.3.3 Radioactive waste production analysis scenarios 48
2.3.4 Primary reference waste packages 48

2.4 Repository concepts (Andra, 2005i) 64

2.4.1 Long-term safety and reversibility 64
2.4.2 Design issues addressing the safety and reversibility requirements 66

2.5 Implications of the architecture of the repository on the phenomenological evolution of the repository and its geological environment 84

2.5.1 Simplification and control of the phenomenological evolution 84
2.5.2 Engineered structures presenting a marked typology with regard to phenomenological behaviour 84
2.5.3 Major components of the geological medium and the repository 86

3 The initial state of the geological medium before the repository was built 93

3.1 Introduction 95

3.2 The general setting 95

3.2.1 The geological features of the site 97
3.2.2 The seismo-tectonic setting 102
3.2.3 Hydrogeology and water chemistry 105
3.2.4 The natural geothermal field 107
3.2.5 The natural mechanical stress field 108

3.3 The different geological formations 109

3.3.1 The Callovo-Oxfordian layer 109
3.3.2 The formations surrounding the Callovo-Oxfordian 148

3.4 Tectonics and fracturing 158

3.4.1 Tectonic history of the sector 158
3.4.2 The scale of fracturing in the Meuse/Haute-Marne sector 159
3.4.3 Marne / Poissons diffuse fracture zone 162
3.4.4 The impact of fracturing on the hydraulic properties of the formations 164

3.5 The surface environment 165

3.5.1 Climate 165
3.5.2 Geological basement to geomorphological model 166
3.5.3 Resources (surface hydrology and hydrogeology) 167
3.5.4 Soils 169
3.5.5 Flora and fauna 170
3.5.6 Human activities 170

3.6 Summary of the initial state of the geological medium 171

3.6.1 Geological aspects: a simple structure and one homogeneous Callovo-Oxfordian layer in the sector 171
3.6.2 Thermal aspects: a geothermal system free of anomaly 172
3.6.3 Hydraulic aspects: a weakly permeable Callovo-Oxfordian with slow flow in the surroundings 172
3.6.4 Chemical aspects: an homogeneous formation with pore water at equilibrium, weakly alkaline, carbonate, sodiocalcic and reducing 173
3.6.5 Mechanical aspects: a simple natural stress field, coherent with knowledge of the Paris Basin 174
3.6.6 Surface environment: characteristics inherited from the climatic history and geomorphological evolution 174

4 Phenomenological processes 175

4.1 The main phenomenological processes relating to the repository 177

4.1.1 Thermal load due to exothermic waste 177
4.1.2 Hydraulic processes: hydraulic head discharge, desaturation, resaturation combined with hydrogen production, and return to a new hydraulic equilibrium 177
4.1.3 Chemical processes: interface reactions with the near-field argillites and clayey components, corrosion of metal components and chemical degradation of concrete 178

4.1.4 Mechanical pressure discharge and damage processes in the Callovo-Oxfordian layer in the near field of the repository, followed by a return to mechanical equilibrium 178

4.2 Main THMCR processes relating to geodynamic evolution 179

4.2.1 Internal geodynamics 179
4.2.2 Climatic changes 179

4.3 Timescales of the major THMC processes and radionuclide release and transfer 179

4.4 Spatial organisation of the phenomenological evolution of the repository and its geological environment: independence and similarities 181

5 Thermal load 185

5.1 Introduction 187

5.2 The modes of heat transfer given off by waste packages in the repository and the surrounding geological formations 187

5.2.1 Within the geological medium 187
5.2.2 In the repository 189

5.3 Spatial organisation of the thermal load 191

5.3.1 On the scale of the repository and surrounding geological medium 191
5.3.2 On a repository zone scale 191

5.4 Thermal loads of C waste and spent fuel repository zones 194

5.4.1 On a disposal cell scale 194
5.4.2 On a repository module scale 195
5.4.3 On a repository zone scale 196
5.4.4 On a site scale 196

5.5 Thermal load of the B waste repository zone 199

5.6 Summary of the thermal load of the repository 203

5.6.1 Thermal independence of the repository zones 203
5.6.2 Maximum temperatures reached in the short term in the disposal cells 203
5.6.3 Homogenisation of temperatures in the disposal modules and zones 203
5.6.4 Generally moderate thermal gradients 203
5.6.5 Limited duration of the thermal load 204
5.6.6 Low thermal loads on the Callovo-Oxfordien layer on a macroscopic scale and on the surrounding formations 204
5.6.7 Sensitivity of the analysis with regard to the reversible management process 205

6 Flow and transfer in solution and as gas 209

6.1 Introduction 211

6.1.1 The implications of water flows on other phenomena 211
6.1.2 The driving forces behind water flow evolution 211

6.1.3 Spatial organisation of the processes as determined by the repository design: independence and similarity 211
6.1.4 Chapter outline 212

6.2 The hydraulic behaviour of the surrounding formations under the effect of the repository 217

6.2.1 The initial hydraulic head drop 217
6.2.2 The Tithonian limestone: rapid return to hydraulic equilibrium 218
6.2.3 The Kimmeridgian and the carbonated Oxfordian: hydraulic head drop and desaturation 218
6.2.4 Repository closure and return to a new hydraulic equilibrium 222
6.2.5 The hydraulic evolution of the surrounding rocks following repository-induced hydraulic disturbance 223

6.3 The hydraulic behaviour of the Callovo-Oxfordian under the effect of the repository 223

6.3.1 Hydraulic head drop and desaturation during the operating phase 223
6.3.2 Repository resaturation during post-closure and the effect of the hydrogen produced by metal corrosion 235
6.3.3 Solute transport in the repository and Callovo-Oxfordian until the return to a new hydraulic equilibrium 258
6.3.4 Conclusion 260

6.4 Summary on flows and the transfer in dissolved and gaseous form 263

6.4.1 A framework for chemical and mechanical evolutions in the repository followed by radionuclide release and transfer 263
6.4.2 Two specific driving factors behind the flows 263
6.4.3 Hydraulic evolution of the repository: the involvement of various processes until the return to a new state of hydraulic equilibrium 264
6.4.4 Solute transport that is dominated by diffusion in the Callovo-Oxfordian 268
6.4.5 The production and migration of very small quantities of radionuclides in gaseous form 268
6.4.6 Geodynamic evolution causes significant modification to the water flow and transport in the surrounding rocks over the million years 268
6.4.7 Phenomenological elements that are important for reversibility 269

7 Chemical phenomena 271

7.1 Introduction 273

7.1.1 The result of desequilibria 273
7.1.2 Evolution principally concerning the repository and the near-field Callovo-Oxfordian layer 274
7.1.3 Independence and similarities of chemical evolution 274
7.1.4 Two categories of structure in terms of chemical evolution 274
7.1.5 Organisation of the chapter 274

7.2 Chemical evolution of structures ventilated during the repository operational period: Type B waste disposal cells, drifts and shafts 275

7.2.1 Oxidising disturbance in argillites in structure walls due to desaturation 276
7.2.2 Atmospheric carbonation of structural concretes 278
7.2.3 Corrosion of metal structural components 281
7.2.4 Alkaline disturbance of argillites by the concrete in infrastructure components 284

7.2.5 Alteration processes of type B waste disposal packages 284
7.2.6 Summary of information concerning the chemical evolution of ventilated structures during the operational phase 286

7.3 Chemical evolution of disposal cells of type C waste and spent fuel 287

7.3.1 Corrosion of the coating, lining and containers inside disposal cells....................288
7.3.2 Chemical evolution of the engineered barrier of spent fuel disposal cells 292
7.3.3 Chemical evolution of near-field argillites of type C waste and spent fuel disposal cells...295
7.3.4 Dissolution of the glass matrix 296
7.3.5 Spent fuel assemblies...301
7.3.6 Alkaline Disturbance at the Disposal cell Hydraulic head 307
7.3.7 Other Chemical Processes at the Hydraulic head of C waste & Spent Fuel Disposal cells 312

7.4 Chemical Evolution of B waste disposal cells in Post-Closure Status 312

7.4.1 Transition to anoxic redox conditions, then to reducing conditions......................314
7.4.2 Chemical degradation of cementitious materials in B waste disposal cells...........314
7.4.3 B waste packages...319
7.4.4 Argillite alkaline disturbance in near-field B waste disposal cells.......................326

7.5 Chemical evolution of drift and shaft seals in the post-closure phase 328

7.5.1 Alkaline perturbation of seal cores and hydraulic keys due to concrete components 328
7.5.2 Alkaline perturbation of argillites in the near field close to drift and shaft seals 330
7.5.3 Corrosion of metal components of drift and shaft seals 330

7.6 Chemical evolution of drifts and shafts in the post-closure phase 331

7.6.1 Chemical deterioration of cement based shaft components...................................331
7.6.2 Alkaline perturbation in the near field geological environment close to the shafts..331
7.6.3 Alkaline perturbation of drift and shaft backfill in the post-closure phase 332

7.7 Chemical evolution of Callovo-Oxfordian argillites in the far field...............332

7.8 Chemical evolution of the surrounding formations (Dogger and carbonated Oxfordian)..332

7.9 Summary of the chemical evolution of the repository and its geological environment 333

7.9.1 An important component of the phenomenological evolution of the repository..333
7.9.2 Slow chemical evolution mainly affecting the repository and the Callovo-Oxfordian in the very near field 333
7.9.3 A limited number of major processes...334
7.9.4 Important phenomenological elements for reversibility.......................................336

8 Mechanical evolution of the repository and the surrounding geological medium 339

8.1 Introduction 341

8.1.1 A component in the phenomenological evolution of the repository......................341

8.1.2 Effect of intrinsic mechanical behaviour of the argillites and thermal, hydraulic and chemical evolutions of the repository 341
8.1.3 An evolution mainly concerning the repository and the Callovo-Oxfordian layer in the near-field 342
8.1.4 Independence and similarity of the mechanical evolution 342
8.1.5 Three categories of engineered structure in terms of mechanical evolution 342
8.1.6 Organisation of the chapter on mechanical behaviour 343

8.2 Creation of an initial excavation damaged zone (EDZ): excavating the engineered structures and instantaneous mechanical relaxation 343

8.2.1 Various mechanical behaviours according to the geological formations crossed 345
8.2.2 An initial, variable EDZ according to the depth under consideration and the orientation of the engineered structure 347
8.2.3 Extent of the initial EDZ around the various repository engineered structures 348
8.2.4 Convergence relating to the initial mechnical relaxation 353
8.2.5 Permeability of the initial EDZ 355

8.3 Mechanical evolution of ventilated engineered structures during repository operating phase: drifts, B waste disposal cells and shafts 357

8.3.1 Thermal, hydraulic and chemical contexts 357
8.3.2 Shafts, B waste disposal cells and drifts not subjected to a rise in temperature 360
8.3.3 Drifts subjected to a rise in temperature 363

8.4 Mechanical evolution of B waste disposal cells and drifts in post-closure phase 363

8.4.1 Closure of B waste disposal cells and drifts 363
8.4.2 Loading of ground support/liner and commencement of EDZ healing 365
8.4.3 Mechanical evolution with the gradual chemico-mechanical degradation of the engineered structure components 367

8.5 Mechanical evolution of C waste disposal cells and spent fuel disposal cells 369

8.5.1 Mechanical behaviour of the useful part and the disposal cell hydraulic head 369
8.5.2 Thermal, hydraulic and chemical contexts 369
8.5.3 Organisation over time of the mechanical evolution of the disposal cells 370
8.5.4 Thermo-mechanical loading from emplacing the packages and installing the disposal cell plug 373
8.5.5 Saturation of the swelling clay in the plug and the engineered barrier (around 100 years) 375
8.5.6 Mechanical evolution up to rupture of the lining and/or liner 378
8.5.7 Mechanical evolution after rupture of the lining and liner and before rupture of the over-packs 381
8.5.8 Mechanical evolution with corrosion of over-packs 384

8.6 Mechanical evolution of seals 386

8.6.1 Creation of seals 386
8.6.2 The thermal, hydraulic and chemical contexts of the mechanical evolution of the seals after closure. 391
8.6.3 Seal saturation phase and development of swelling pressure 394

8.6.4 After resaturation, as the mechanical properties of the support bases and ground supports/liners evolve 396
8.6.5 In the overlying formations of the Callovo-Oxfordian layer 398

8.7 Large-scale mechanical evolution 399

8.7.1 The effects of the repository 399
8.7.2 Effects of erosion and tectonics or seismicity 399

8.8 Summary of mechanical evolution 401

8.8.1 Mechanical impact of the repository limited to the near-field in the Callovo-Oxfordian 401
8.8.2 No significant consequence on the hydraulic and chemical evolutions of the geological medium 402
8.8.3 Mechanical evolution of the repository and the Callovo-Oxfordian in the near-field marked by three major periods 402
8.8.4 Elements with respect to reversibility 403
8.8.5 Limited evolution of the initial EDZ from its creation to its healing 404
8.8.6 Maintenance of the hydraulic properties of the disposal cell plugs and the seals over time 405

9 Geodynamic evolution of the Callovo-Oxfordian, the surrounding geological formations and the surface environment 407

9.1 Introduction 409

9.2 Internal geodynamics 409

9.3 Climate change 410

9.4 Consequences of climate change 416

9.4.1 Periodic formation and disappearance of permafrost 416
9.4.2 Biosphere evolution 418

9.5 Topographic changes 420

9.6 Effects of the evolutions on geological formations and surface environments 423

9.6.1 Callovo-Oxfordian 423
9.6.2 Surrounding formations 423
9.6.3 Surface environment 426

9.7 Summary of the geodynamic evolutions of geological formations and surface environments 427

9.7.1 For the Callovo-Oxfordian layer 427
9.7.2 For the surrounding formations 428
9.7.3 For the surface environments 428

10 Radionuclide release and transfer 431

10.1 Introduction 433

10.1.1 The Release and Transfer of Radionuclides: Phenomena Governed by the Evolution of the Repository 433

10.1.2 The Organisation of the Chapter on the Release and Transfer of Radionuclides 433

10.2 The Release of Radionuclides by Waste Packages 435

10.2.1 C Waste Packages 435
10.2.2 Spent Fuel Packages 437
10.2.3 B Waste Packages 440

10.3 The Transfer of Radionuclides in the Repository Structure 446

10.3.1 The Physical and Chemical Conditions in the Repository Cells 449
10.3.2 Retention in the Repository Cells 451
10.3.3 The Transfer of Radionuclides in the Repository: Transfer Paths and Typical Time Frame 458

10.4 Transfer of Radionuclides in Solution in the Callovo-Oxfordian Layer from the Repository and into the Surroundings 460

10.4.1 Phenomenology of the Callovo-Oxfordian Layer From the Perspective of Radionuclide Release Time for Waste Packages 460
10.4.2 Transfer in the Callovo-Oxfordian Layer 461

10.5 The Transfer of Radionuclides in the Surroundings 468

10.5.1 The General Characteristics of Transfer in the Surrounding Formations and the Effects of Geodynamic Evolution 468
10.5.2 The Transfer of Mobile Radionuclides Leaving the Callovo-Oxfordian Layer 472

10.6 The Transfer of Radionuclides to the Biosphere and Humans 474

10.6.1 The Overall Model of Radionuclide Transfer into the Biosphere: Direct and Indirect Transfer 475
10.6.2 The Transfer of Radionuclides in the Current Biosphere for the Plateaux Zones of the Meuse/Haute-Marne Site 479
10.6.3 The Transfer of Radionuclides in the Current Biosphere in the Case of the Valley Zones 481
10.6.4 The Effect of Geodynamic Evolution on the Transfer of Radionuclides 481

10.7 Summary 483

10.7.1 The Effects of Thermal, Hydraulic, Chemical, Mechanical and Geomorphicological Evolutions on the Release and Transfer of Radionuclides 483
10.7.2 Radionuclides with Specific Behaviour in Terms of Solubility and Retention 484
10.7.3 Slow and Limited Release of Radionuclides Beyond the Repository 484
10.7.4 Migration of Very Soluble Long-Lived Radionuclides Not Sorbed in the Callovo-Oxfordian Layer 485
10.7.5 Transfer of Radionuclides to the Surroundings Influenced by Geodynamic Evolution 485
10.7.6 The Transfer of Radionuclides to the Biosphere and Humans 486
10.7.7 Important Phenomenological Elements for Reversibility 486

11 Uncertainties relating to the phenomenological description 489

11.1 Uncertainty Concerning the Method of Operation and Closure of the Repository 491

11.2 Examination of Uncertainties Concerning the Available Data and Phenomenological Interpretations 492
11.2.1 The Characteristics of the Callovo-Oxfordian Layer 492
11.2.2 Bulk Permeability 492
11.2.3 Diffusion and retention properties 493
11.2.4 The Repository and the Callovo-Oxfordian Layer in the Near Field 493
11.2.5 Surrounding Formations 496
11.2.6 Representation of Couplings 497

11.3 Conclusion 498

12 Synthesis 499

12.1 Main characteristics of the approach 501

12.2 General description of repository phenomena and repository life history 502
12.2.1 Evolution shaped by the characteristics of the Callovo-Oxfordian stratum and repository design 502
12.2.2 A combination of processes that vary in importance over time 503
12.2.3 Very limited evolution of the Callovo-Oxfordian layer as a whole over the next million years 504
12.2.4 Evolution of flow in surrounding formations over the next million years 504
12.2.5 Slow release of radionuclides from waste packages governed by repository installations and geological medium 504

12.3 Lessons 505

Bibliographic References 507

Table of illustrations

Figures

Figure 1.1.1 General structure of the Dossier 2005 Argile 29
Figure 2.2.1 Geographic location of the Meuse / Haute-Marne site 38
Figure 2.2.2 Geological location of the Meuse / Haute-Marne site within the Paris Basin 38
Figure 2.2.3 Geological cross-section at the Meuse / Haute-Marne site 39
Figure 2.2.4 3D geological block diagram of the Meuse / Haute-Marne site 40
Figure 2.2.5 Perimeter of the transposition zone around the Meuse / Haute-Marne site and position of boreholes drilled by Andra in the sector 41
Figure 2.3.1 See-through diagram of primary vitrified waste package and photograph of R7T7 nuclear glass 43
Figure 2.3.2 Diagram of B waste package containing hulls, end caps and compacted technological radioactive waste (B5 waste package, see Table 2.3.2) 45
Figure 2.3.3 Diagram of a PWR fuel assembly 46
Figure 2.3.4 See-through diagram of a spent fuel assembly and various cross-sections of a spent fuel rod after passing through the reactor 47
Figure 2.3.5 Basic diagram of the location of the radionuclides within a spent fuel rod and a UOX pellet after passing through the reactor 47
Figure 2.3.6 Diagrams and dimensions of vitrified waste reference packages 50
Figure 2.3.7 Diagrams and dimensions of B waste reference packages 52
Figure 2.3.8 Activation product and fission product activity of each reference package in Bq par package (Short-lived activity: half-life = 6 years; Medium-lived activity: 6 years < half-life = 30 years; Long-lived activity: half-life > 30 years 56
Figure 2.3.9 Actinide activity of each reference package in Bq par package (Short-lived activity: half-life = 6 years; Medium-lived activity: 6 years< half-life = 30 years; Long-lived activity: half-life > 30 years) 56
Figure 2.3.10 Relative distributions (%) of ^{14}C, ^{36}Cl, ^{59}Ni, ^{94}Nb, ^{99}Tc, ^{129}I and ^{135}Cs, inventories in B waste, C waste and spent fuels (not including CU3) for the four waste management scenarios 57
Figure 2.3.11 Relative distributions (%) of ^{14}C, ^{36}Cl, ^{59}Ni, ^{94}Nb, ^{99}Tc, ^{129}I, ^{135}Cs, total uranium and total plutonium inventories in B waste reference packages for waste management scenario S1b 58
Figure 2.3.12 Heat release curves for C waste reference packages and spent fuels (Andra, 2005e) 60
Figure 2.3.13 Heat release curves for B waste reference packages (Andra, 2005e) 61
Figure 2.4.1 Diagram of the repository's location in the middle of the Callovo-Oxfordian layer (reference location of the underground research laboratory) 66
Figure 2.4.2 Example of the general organisation of the repository (case of waste production scenario S1a) 70
Figure 2.4.3 Example of a basic diagram of a B waste disposal package 72
Figure 2.4.4 Diagram of a C waste disposal package 73
Figure 2.4.5 Diagram of a CU1 spent fuel disposal package 74

Figure 2.4.6 Basic diagram of a B waste package disposal cell in operating configuration 75
Figure 2.4.7 Basic diagram of a C waste package disposal cell in operating configuration 76
Figure 2.4.8 Basic diagram of a C waste disposal cell filled with disposal packages in operating configuration 77
Figure 2.4.9 Basic diagram of a spent fuel disposal cell filled with disposal packages in operating configuration 77
Figure 2.4.10 Basic diagram of a sealed C waste disposal cell 79
Figure 2.4.11 Basic diagram of a sealed spent fuel disposal cell 80
Figure 2.4.12 Basic diagram of a drift seal (longitudinal cross-section) 81
Figure 2.4.13 Basic diagram of a sealed B waste disposal cell 81
Figure 2.4.14 Basic diagram of a B waste disposal cell seal (longitudinal cross-section) 82
Figure 2.4.15 Basic diagram of an access shaft seal (longitudinal cross-section) 83
Figure 3.2.1 Available data and location of the work done by Andra in the Meuse/Haute-Marne sector 96
Figure 3.2.2 Schematic diagram of the formation of the Paris basin from the Palaeozoic to the present day 98
Figure 3.2.3 3D block diagram of the geological structure of the Paris basin at the present day 99
Figure 3.2.4 Lithological succession directly above the Meuse/Haute-Marne site 100
Figure 3.2.5 3D block diagram of the geological structure of the Meuse/Haute-Marne sector 101
Figure 3.2.6 3D block diagram of the lithology and relief of the Meuse/Haute-Marne sector 103
Figure 3.2.7 Geodynamic setting of Eastern France: the relationship between seismicity and crustal thickness (Andra, 2005h, chapitre 35) 104
Figure 3.2.8 3D block diagram of hydrogeological systems in the Meuse/Haute-Marne sector 106
Figure 3.2.9 Profile of geothermal temperatures in the sedimentary series at the Meuse/Haute-Marne site (Bauer, 2005) 107
Figure 3.2.10 Orientation of the current state of stress in the Meuse/Haute-Marne sector (Andra, 2005h ; Grellet et al., 1993) 108
Figure 3.3.1 Geometry of the sedimentary series in the Meuse/Haute-Marne sector 109
Figure 3.3.2 Isohypses at the top of the Callovo-Oxfordian in the Meuse/Haute-Marne sector (in m NGF) 110
Figure 3.3.3 Thickness of the Callovo-Oxfordian in the Meuse/Haute-Marne sector (on the right) determined from isohypses at the top and bottom of the formation (on the left) 110
Figure 3.3.4 Vertical organisation of the Callovo-Oxfordian directly above the Meuse/Haute-Marne site 112
Figure 3.3.5 Lateral homogeneity of the Callovo-Oxfordian in the Meuse/Haute-Marne sector 113
Figure 3.3.6 Schematic representation of the deposition of 3 Callovo-Oxfordian sequences 113
Figure 3.3.7 Calcite concentrations, isotopic composition of Sr and δ^{13}C in calcite in borehole HTM 102 (according to (Lavastre, 2002 ; Maes, 2002)—Domain

of marine calcites for $\delta^{13}C$ (Podlaha et al., 1998), domain of isotopic composition of Sr in Callovo-Oxfordian seawater (Koepnick et al., 1990)) 115
Figure 3.3.8 Schematic representation of the Callovo-Oxfordian texture and porosity..........121
Figure 3.3.9 Conceptual model of formation porosity (based on mercury porosimetric measurements and nitrogen adsorption curves) (Andra, 2005h, chapitre 12).....122
Figure 3.3.10 Profile of apparent hydraulics heads measured in the Callovo-Oxfordian directly above the Meuse / Haute-Marne underground research laboratory (compilation of measurements available at the end of March 2005) 128
Figure 3.3.11 Schematic representation of the Callovo-Oxfordian and its surroundings in the context of an osmotic system 131
Figure 3.3.12 Evaluation of the vertical hydraulic head gradient through the Callovo-Oxfordian, deduced from charges in the surroundings 135
Figure 3.3.13 Vertical profile of the whole Callovo-Oxfordian for measured values of the diffusion coefficient for tritiated water (HTO) 142
Figure 3.3.14 Vertical profiles of chlorides in the Callovo-Oxfordian and its surroundings on a sectoral scale 145
Figure 3.3.15 Schematic diagram of lithologies and porous horizones in the Dogger limestone at the Meuse/Haute-Marne site...150
Figure 3.3.16 Organisation of water flow in the Dogger limestone at the present time...........150
Figure 3.3.17 Hydraulic head field and chloride concentration of Dogger limestone pore water in the Meuse/Haute-Marne sector 151
Figure 3.3.18 Deposition environment of an carbonated Oxfordian platform – Example of the terminal mid-Oxfordian platform according to (Carpentier, 2004 ; Université de Lyon I, 2002)..152
Figure 3.3.19 Morphology of porous horizons (Hp1 to Hp4) of Oxfordian carbonate based on 3D seismic data 153
Figure 3.3.20 Extension of the Middle Oxfordian porous facies in the Meuse/Haute-Marne sector...155
Figure 3.3.21 Representation of the porous horizons in the carbonated Oxfordian at the present time 155
Figure 3.3.22 Organisation of water flow in carbonated Oxfordian at the present time 156
Figure 3.3.23 Schematic diagram of the Marly Kimmeridgian...157
Figure 3.3.24 Schematic representation of Barrois Limestones 158
Figure 3.4.1 The different tectonic structures in the Meuse/Haute-Marne sector 160
Figure 3.4.2 Diagram of microfracturing in the Callovo-Oxfordian......................................161
Figure 3.4.3 Boundaries of the Marne / Poissons diffuse fracture zone.................................164
Figure 3.5.1 Variation of mean temperatures and rainfall at Saint-Dizier 166
Figure 3.5.2 The different morphological models around the Meuse/Haute-Marne site at the present time 167
Figure 3.5.3 Schematic representation of surface water flow at the Meuse/Haute-Marne site at the present time and its relationship with the lithological units 168
Figure 3.5.4 Schematic distribution of different soils on the Meuse/Haute-Marne site at the present time 169
Figure 3.5.5 Schematic distribution of large natural units on the Meuse/Haute-Marne site at the present time...170
Figure 3.6.1 Schematic representation of water flow and solute transport in the geological medium in its initial state 173

Figure 4.3.1 Chronogram of the major phenomena affecting the repository and its geological environment (based on the conventional hundred-year repository construction/operation/closure time diagram) 180
Figure 5.3.1 Thermal load of the various repository zones on a site scale.............................193
Figure 5.4.1 Temperature evolution in and around a C1 waste disposal cell emplaced in a repository after a 60-year storage period..195
Figure 5.4.2 Temperature evolution in and around a CU2 spent fuel disposal cell emplaced in a repository after a 90-year storage period 195
Figure 5.4.3 Temperature evolution in the centre of the access drifts to CU2 spent fuel disposal cells (90-year storage period) and to C1 waste disposal cells (60-year storage period) assuming rapid backfilling of the access drifts (30 years after package emplacement)...196
Figure 5.4.4 Representation of the thermal load of C waste repository zones at various times (scenario S1a – total reprocessing of spent UOX and MOX fuels)...........197
Figure 5.4.5 Representation of the thermal load of spent fuel repository zones at various times (scenario S2 with direct disposal of spent UOX and MOX fuels) 198
Figure 5.5.1 Temperature evolution in and around a disposal cell of cladding waste (reference packages B5.2 emplaced in the repository after a ten-year storage period) and a disposal cell of bituminised waste (reference packages B2.1 emplaced in the repository after a one-year storage period) with no ventilation period following package emplacement 200
Figure 5.5.2 Temperature evolution in and around a cladding waste disposal cell (reference packages B5.2 emplaced in a repository after a ten-year storage period) with no ventilation period following package emplacement and with ventilation maintained for ten years..201
Figure 5.5.3 Representation of the thermal load of the B waste repository zone at various times under the assumption that the disposal cells are closed immediately after emplacing the packages 202
Figure 5.6.1 Time chart of the thermal load in the various repository zones and the Callovo-Oxfordian layer on a macroscopic scale (on the basis of the conventional 100-year repository creation/operation/closure time chart) 208
Figure 6.2.1 Diagram showing flow diections and a profile of the initial hydraulic head in the Callovo-Oxfordian and its surrounding rocks..217
Figure 6.2.2 Diagram of hydraulic disturbances caused by the repository in the Callovo-Oxfordian and surrounding rocks during the operating phase. 218
Figure 6.2.3 Schematic representation of the hydraulic head drop by the shafts created in the Hp1-4 horizon of the carbonated Oxfordian 220
Figure 6.3.1 Representation of the evolution of temperature and relative hygrometry of air along a schematical ventilation path 225
Figure 6.3.2 General diagram of the ventilation-induced desaturation process during the operating phase and the generation of hydrogen in the post-closure phase. (Not to scale are the structure dimensions and the significance of phenomena)..229
Figure 6.3.3 Schematic representation of the quasi-stationary saturation profile obtained in a drift that remained open for at least a decade...232
Figure 6.3.4 Evolution with time of the hydraulic pressure profile in the argilites radially surrounding the centre line of a drift open for several decades and subject to thermal loading 234
Figure 6.3.5 Evolution with time the hydraulic pressure profile in the argilites radially surrounding to the centre line of a spent fuel cell 234

Figure 6.3.6 Diagram of the main hydrogen migration paths to the access drift before and after resaturation of the ways from a spent fuel disposal cell plug 239
Figure 6.3.7 General resaturation pattern at the scale of the repository. The upper part of the shaft seal is resaturated by water from the carbonated Oxfordian. The rest of the repository is resaturated with water from the Callovo-Oxfordian. 240
Figure 6.3.8 Diagram of the hydrogen transfer path ways in the repository and the surrounding Callovo-Oxfordian...241
Figure 6.3.9 Isopressure curves at peack pressure (about year 2,000) of water in the Callovo-Oxfordian around the drift of a spent fuel repository module. The water flows are divergent from the drift to the argillites. The ordinates scale in this figure is expanded by a factor of 15...246
Figure 6.3.10 Isopressure curves of water in the Callovo-Oxfordian around a drift of a spent fuel repository module (at about year 9,000). The water flows are convergent towards the drift. The ordinates scale in this figure is expanded by a factor of 15 247
Figure 6.3.11 Diagram of the water flow at the scale of the repository following its total resaturation...248
Figure 6.3.12 Example of water flow lines crossing the repository after return to hydraulic equilibrium: Most of the flow lines travelling through the repository join the Callovo-Oxfordian argillites and do not end up in the shaft...249
Figure 6.3.13 Diagram of the hydraulic heads in the geological layers after return to hydraulic equilibrium following the impact of the repository 250
Figure 6.3.14 Diagram of the resaturation of a B waste cell. Evolution of the type of water flow before and after seepage into the emplacement gaps. Zoom is on the individual stacks of waste packages...252
Figure 6.3.15 Time chart giving the degree of saturation in the various components of a B waste repository module and the associated effects and couplings (on the basis of the conventional century-long construction/operating/repository closure time chart)...253
Figure 6.3.16 Time chart giving the hydrogen gas pressure in the various components of a B waste repository module and the associated effects and couplings (on the basis of the conventional century-long construction/operating/repository closure time chart) 254
Figure 6.3.17 Time chart giving the water saturation in the various components of a C waste or spent fuel repository module (on the basis of the conventional century-long construction/operating/repository closure time chart)..................256
Figure 6.3.18 Time chart giving the gas pressure in the various components of a C waste or spent fuel repository module (on the basis of the conventional century-long construction/operating/repository closure time chart) 257
Figure 6.3.19 Diagram of the solute transport modes from the repository, at the scale of the Callovo-Oxfordian and its surrounding rocks on the Meuse/Haute-Marne site, and after return to hydraulic equilibrium 260
Figure 6.3.20 Schematic representation of water flow rates across the repository and solute migration modes within the repository, after return to hydraulic equilibrium...262
Figure 7.3.1 Schematical representation of the progression of corrosion of the lining and over-pack in a type C waste cell, from several hundred, several thousands and tens of thousands of years 290

Figure 7.3.2 Schematical representation of the progression of corrosion of the lining, container and insert in a spent fuel disposal cell after several hundred, several thousand and tens of thousands of years....291
Figure 7.3.3 Schematical representation of the perturbation of the iron/swelling clay engineered barrier of a spent fuel disposal cell, after a few tens of thousands of years....294
Figure 7.3.4 Simplified curve for the dissolution of the glass matrix over time for a generic type R7T7 glass (type C2 packages) (Andra, 2005m)....298
Figure 7.3.5 Simplified representation of the evolution of the dissolution of oxide pellets with time for the long type CU, UOx3 spent fuel (Andra, 2005d ; Andra, 2005m)....304
Figure 7.3.6 Schematic representation of the alkaline disturbance of swelling clay plugs in C waste disposal cells over 100,000 years....309
Figure 7.4.1 Schematic representation of the progressive degradation of type CEM V concrete coating / support of a B waste disposal cell (Bourbon, 2005)....317
Figure 7.4.2 Evolution of dose rates ($Gy.h^{-1}$) in contact with primary B reference packages (evaluation on the side of the package) (Andra, 2005a)....320
Figure 7.4.3 Simplified representation of the degradation of bituminized sludges over time (Andra, 2005d)....323
Figure 7.4.4 Schematic representation of the degradation stages of bituminized sludges....324
Figure 7.4.5 Schematic representation of alkaline disturbance in clays of B waste disposal cells and degradation of support / coating concrete over 100,000 years (Jacquot & Dimier, 2005)....327
Figure 7.5.1 Diagram of the alkaline perturbation of a drift seal around the hydraulic cut-off: pH field a) at 20,000 years and b) at 500,000 years (Jacquot & Michau, 2005)....329
Figure 7.9.1 Chronogram for the main chemical processes in the B waste, C waste and spent fuel disposal cells (based on the chronogram for the 100 year period set by convention for building / operation / closure of the repository)....338
Figure 8.2.1 Geometry of the initial EDZ based on the orientation of the engineered structures with respect to the state of natural stress....348
Figure 8.2.2 Sample network of connected microfissures obtained by simulating the excavation of an engineered structure oriented s_H using the PFC code....356
Figure 8.3.1 Time chart of the mechanical evolution of a B waste cell: thermal, hydraulic and chemical contexts during construction, operating and post-closure phases (based on a conventional, hundred-year time chart of the construction/operation/closure of a repository)....358
Figure 8.3.2 Loading on the ground support/liner from argillite creep and the evolution of the EDZ around a B waste disposal cell during the operating phase....362
Figure 8.4.1 Loading on ground support/liner and evolution of EDZ around an exothermic B waste disposal cell during hte first thousands of years after closure....366
Figure 8.4.2 Evolution of the EDZ around a B waste disposal cell with the chemical degradation of the concretes (beyond 10,000 years)....368
Figure 8.5.1 Time chart of the mechanical evolution of a C waste cell: thermal, hydraulic and chemical contexts during construction, operating and post-closure phases (based on a conventional hundred-year time chart of the construction/operation/closure of a repository)....371
Figure 8.5.2 Time chart of the mechanical evolution of a spent fuel cell: thermal, hydraulic and chemical contexts during construction, operating and post-

closure phases (based on a conventional hundred-year time chart of the construction/operation/closure of a repository) 372
Figure 8.5.3 Evolution of the EDZ under the effect of the rise in temperature and the deferred convergence aorund a C waste disposal cell (hypothesis of maximum clearances) 374
Figure 8.5.4 Resaturation process of the swelling clay - example of C waste disposal cell plug....................376
Figure 8.5.5 Diagrams showing evolution of EDZ around a C waste disposal cell and a spent fuel disposal cell under thermo-mechanical coupling (timescale of 100 to 150 years)....................377
Figure 8.5.6 Diagrams showing evolution of EDZ around a C waste disposal cell and a spent fuel disposal cell before rupture of the lining and liner (timescale of several hundred to thousands of years)....................380
Figure 8.5.7 Diagrams showing evolution of EDZ around a C waste disposal cell and a spent fuel disposal cell after rupture of the lining and before rupture of the over-pack (timescale of several thousands to several tens of thousands of years)....................383
Figure 8.5.8 Diagrams showing evolution of EDZ around a C waste disposal cell and a spent fuel disposal cell after discharge of strength of over-packs and in the long term (timescale of tens of thousands of years)....................385
Figure 8.6.1 Creation of a radial hydraulic cut-off around a drift and filling with blocks of compacted swelling clay: feasibility test at Mont Terri....................387
Figure 8.6.2 Numerical modelling of the creation of a hydraulic cut-off around a drift: interruption of the fractured zone the length of the hydraulic cut-off....................388
Figure 8.6.3 Simplified diagrams illustrating the interruption of the fractured zone around the hydraulic cut-off in a drift seal....................389
Figure 8.6.4 Time chart of the mechanical evolution of a drift seal: thermal, hydraulic and chemical contexts during construction and post-closure phases (based on a conventional hundred-year time chart of the construction/operation/closure of a repository) 393
Figure 8.6.5 Numerical modelling of the effects of the load applied by swelling pressure of the swelling clay in the hydraulic cut-off in the argillites: recompression of EDZ fissures 394
Figure 8.6.6 Simplified diagrams illustrating the recompression of the EDZ fissures under the load applied by the swelling pressure of the swelling clay and by argillite creep and swelling around a drift seal (timescale of a thousand years)....................395
Figure 8.6.7 Simplified diagrams illustrating the generalised loading of a drift seal as cement-based degradation takes place (beyond 100,000 years) 398
Figure 9.3.1 Variations in temperature in the Antarctic (Vostok) over the last 400,000 years (from Petit et al., 1999)....................411
Figure 9.3.2 Schematic representation of the main climatic phases during a glacial/interglacial cycle, for a situation comparable to that of the Meuse/Haute-Marne site 412
Figure 9.3.3 Ice cap areas and principal environments during the last glacial maximum (Berger, 1992)....................413
Figure 9.3.4 Simulations of the volume of ice in the Northern hemisphere over the next 100,000 years (according to Loutre & Berger, 2000)....................414
Figure 9.3.5 Natural climate change scenarios for the Meuse/Haute-Marne region (according to BIOCLIM, 2003a) 414

Figure 9.3.6 Climate change according to a scenario with major anthropic disturbance for the next million years at the Meuse/Haute-Marne site (according to BIOCLIM, 2003a)....................415
Figure 9.4.1 Conceptual model of future permafrost at the Meuse/Haute-Marne site 417
Figure 9.4.2 Schematic representation of the "boreal" stage of the climate cycle - Vegetation and biosphere evolution around the underground research laboratory site 418
Figure 9.4.3 Schematic representation of the "tundra" stage of the climate cycle - Vegetation and biosphere evolution around the site 419
Figure 9.5.1 Spatial variability in long-term average erosion rates on the scale of the sector....................421
Figure 9.5.2 Evolution in the morphology of the sector from the present day to one million years' time 422
Figure 9.6.1 Schematic representation of the change in flows in the calcareous Oxfordian between the present day and one million years' time....................425
Figure 9.6.2 Schematic representation of the vertical hydraulic head gradient in the Callovo-Oxfordian between the present day and one million years' time..........426
Figure 9.7.1 Time chart of the effects of geodynamic evolutions on the geological medium and surface environment (on the basis of the conventional 100-year repository creation/operation/closure time chart) 427
Figure 10.2.1 Chronogram of the Degradation Processes of Reference Packages (Based on the Conventional Secular Chronogram for Manufacture / Operation / Closure of the Repository) 445
Figure 10.4.1 Diagram Showing the Distribution of the Mass of Iodine 129 between the Repository Components and the Callovo-Oxfordian Formation at Different Times for Repository Zones C1-C2. The percentages include the mass that has disappeared via radioactive decay (calculated on the basis of Andra, 2005m) 462
Figure 10.4.2 Diagram Showing the Distribution of the Mass of Iodine 129 between the Repository Components and the Callovo-Oxfordian Layer at Different Times for Repository Zone SF1. The percentages include the mass that has disappeared via radioactive decay (calculated on the basis of Andra, 2005m) 463
Figure 10.4.3 Diagram Showing the Distribution of the Mass of Chlorine 36 between the Repository Components and the Callovo-Oxfordian Layer at Different Times for Repository Zones C1-C2. The percentages include the mass that has disappeared via radioactive decay (calculated on the basis of Andra, 2005m) 463
Figure 10.4.4 Diagram Showing the Distribution of the Mass of Chlorine 36 among the Repository Components and the Callovo-Oxfordian Formation at Different Times for SF1 Spent Fuel Repository Zones. The percentages include the mass that has disappeared via radioactive decay (calculated on the basis of Andra, 2005m) 464
Figure 10.4.5 Diagram Showing the Distribution of the Mass of Selenium 79 among the Repository Components and the Callovo-Oxfordian Formation at Different Times for the C1-C2 Repository Zone. The percentages include the mass that has disappeared via radioactive decay (calculated on the basis of Andra, 2005m) 464
Figure 10.4.6 Diagram Showing the Distribution of the Mass of Selenium 79 among the Repository Components and the Callovo-Oxfordian Formation at Different

Times for SF1 Spent Fuel Repository Zones. The percentages include the mass that has disappeared via radioactive decay (calculated on the basis of Andra, 2005m) 465

Figure 10.5.1 Organisation of the (Horizontal and Vertical) Advective and (Essentially Vertical) Diffusive Transport Components in the Callovo-Oxfordian and Surrounding Formations. The size of the arrows are representative of the relative intensity of the transport in the various formations 469

Figure 10.5.2 Diagram Showing the Fluctuation of the Water Table on the Regional Scale Over the Course of a Glacial Cycle 470

Figure 10.5.3 Diagram Showing the Development of the Paths and a Plume of Solutes in the Calcareous Oxfordian Formation Downstream from the Meuse/Haute-Marne Site over the Next Million Years 473

Figure 10.6.1 Model of Transfer in the form of a Matrix in Several Segments of the Biosphere (IAEA, 2003) 475

Figure 10.6.2 The Main Transfer Paths in the Biosphere 476

Figure 10.6.3 Model of Transfer from the Geosphere to the Biosphere on the Meuse/Haute-Marne Site 480

Tables

Table 2.3.1 List of vitrified waste reference packages in the inventory model 50
Table 2.3.2 List of B waste reference packages in the design inventory model 53
Table 2.3.3 List of standard spent fuel assemblies...54
Table 2.3.4 Global quantitative data for the number and volume of B and C waste packages and the number of spent fuel assemblies in the design inventory model as per the waste production scenarios 55
Table 2.3.5 Maximum dose rate in contact with various primary packages upon conditioning in disposal packages for subsequent disposal 61
Table 2.4.1 Distribution of B waste reference packages per cell 71
Table 2.4.2 Estimation of the maximum dose rates in contact with the various disposal packages upon placement in the repository 74
Table 3.3.1 The main characteristics of the Callovo-Oxfordian in its initial condition.........147
Table 5.6.1 Thermal load of the various repository zones (repository located at a depth of 500 m)..207
Table 8.2.1 Numerical modelling assessments of geometries and extensions of the initial EDZ in the Callovo-Oxfordian argillites for the various repository engineered structures (Barnichon & Su, 2005a) (Barnichon & Su, 2005c) (Su & Barnichon, 2005)...351

Insets

Inset 2.1 Radioactive elements formed in reactor fuel assemblies 42
Inset 2.2 List of 144 radionuclides selected for the radioactive inventory of HLLW packages 59
Inset 2.3 Radiation emitted by radionuclides 62
Inset 2.4 Origin of heat release from HLLW packages and spent fuels 63
Inset 2.5 Thermal criteria adopted for the repository design 68
Inset 2.6 Swelling clays (Andra, 2005f, Tome 1) (1/2) 87
Inset 2.7 MX80 methodological swelling clay selected for geological repository studies 89
Inset 2.8 Composition of cement-based repository materials and chemistry of their interstitial waters (Andra, 2005f, Tome 2) 90
Inset 2.9 General characteristics of metallic repository materials 91
Inset 3.1 Geochemical and isotopic tracers: Principles and applications (1/2) 116
Inset 3.2 Definition of the transposition zone 119
Inset 3.3 Water structure in saturated and unsaturated argillites 124
Inset 3.4 Callovo-Oxfordian (very low) permeability measurements (Andra, 2005h, chapitre 16) (1/2) 125
Inset 3.5 Water flow in natural porous media: Darcy's law 127
Inset 3.6 Phenomena responsible for over pressure in deep clay formations (1/2) 129
Inset 3.7 Chemical osmosis in a porous medium 132
Inset 3.8 Solute transfer phenomena (Carnahan, 1985) 137
Inset 3.9 Equation for solute transport in porous media (1/2) 138
Inset 3.10 Anionic exclusion 140
Inset 3.11 Determination of pore water chemistry in undisturbed argillites (Altmann & Jacquot, 2005) (1/2) 144
Inset 4.1 Phenomenological interactions in the Callovo-Oxfordian layer: Estimated times and distances relating to thermal, hydraulic and chemical interactions 182
Inset 5.1 Evaluations of the thermal load of the repository 188
Inset 5.2 The modes of heat transfer 189
Inset 6.1 Hydrogen production in the repository (1/2) 213
Inset 6.2 Modelling of hydraulic phenomena (1/2) 215
Inset 6.3 Notion on the degree 221
Inset 6.4 The relative hygrometry of the air and the suction in a porous medium 227
Inset 6.5 The sorption - desorption curves of porous environments 230
Inset 6.6 The sorption - desorption curves of porous 231
Inset 6.7 The conceptual model of gas transport in dense clay environments (1/2) 242
Inset 7.1 Oxidation of pyrites (FeS2) 277

Inset 7.2	Atmospheric carbonation of cement-based materials (1/2)	279
Inset 7.3	Corrosion of non or lightly alloyed steels (1/3)	282
Inset 7.4	Radiolysis of the bitumen matrix	286
Inset 7.5	Iron (metal) /clay (argillites and swelling clay) disturbance	295
Inset 7.6	The structure of (boro)silicated glass	297
Inset 7.7	Dissolution phases of silicated glasses	299
Inset 7.8	The dissolution products of silicated glasses	300
Inset 7.9	Structure of oxide pellets and assembly sheaths	302
Inset 7.10	Radiolysis of water	305
Inset 7.11	Radiolytic dissolution of a UO2 / PuO2 pellet (1/2)	306
Inset 7.12	Alkaline disturbance in clays (argillites and swelling clay)	311
Inset 7.13	Water reactivity of cement-based materials	315
Inset 7.14	Aqueous degradation of bituminized sludges (B2 reference packages)	325
Inset 8.1	EDZ or damaged zone around the engineered structures	344
Inset 8.2	The law of short-term mechanical behaviour of the argillites (1/2)	346
Inset 8.3	Deferred mechanical behaviour of the argillites	354
Inset 8.4	Hydromechanical coupling in the argillites	359
Inset 8.5	Coupled thermo-hydro-mechanical behaviour of the argillites	360
Inset 10.1	Toxic Chemical	434
Inset 10.2	Radionuclide Behaviour in Glass Alteration Products	436
Inset 10.3	The Location and the Distribution of Radionuclides in Spent Fuel Assemblies	439
Inset 10.4	The Location and the Distribution of Radionuclides in B4 and B5 Types of Waste	443
Inset 10.5	Sorption Properties of the Clay	446
Inset 10.6	The Retention and Transport of Solutes	447
Inset 10.7	The Retention Properties (Solubility and Sorption) of Radionuclides in Swelling Clay (1/2)	452
Inset 10.8	Organic Complexing Agents Contained in B waste or Originating from the Degradation of Organic B waste	455
Inset 10.9	The Solubility and Sorption of Radionuclides in Cement-Based Materials (1/2)	456
Inset 10.10	Gaseous Radionuclides in Repository Conditions	460
Inset 10.11	The Retention Properties (Solubility and Sorption) of Radionuclides in Callovo-Oxfordian(1/2)	466
Inset 10.12	Model of the Transfer of Radionuclides in Soils	477
Inset 10.13	The Model of Radionuclide Transfer to Plants	479

1

Introduction

1.1 Purpose of the Volume as part of the Dossier 2005 Argile 29

1.2 Inputs 30

1.3 Structure of the "Evolution Phenomenologique du stockage géologique" Volume 31

1.4 Representation of process space and time scales 32

1.5 Predicting the phenomenological evolution over time, especially over the long term 32

1.1 Purpose of the Volume as part of the Dossier 2005 Argile

The Law of 30 December 1991 (Loi n°91-1381) entrusted Andra with the task of assessing the feasibility of high-level and long-lived radioactive waste (HLLL waste) repositories in deep geological formations. This volume of the Dossier 2005 Argile records the results of the aforementioned study, focussing on the phenomenological evolution of the repository and its geological environment over time. It is based on the characteristics of the clay formation studied at the underground research laboratory at the Meuse / Haute-Marne site, in the east of France.

The feasibility study is based on evaluation of the conditions under which a repository could be built, operated and managed in a reversible manner, closed, and then monitored while it evolves without further human intervention. The study covers the full spectrum of French high-level and long-lived radioactive waste, including existing radioactive waste and radioactive waste liable to be produced in the short- and medium-term. It sets out to ensure that the safety of employees and the general public is not compromised at any time, and that the environment remains protected.

The French language version of this volume entitled «Evolution Phénomenologique du stockage géologique» belongs to level 2 of the dossier 2005 architecture, alongside the "Safety assessment of a geological repository" (Andra, 2005j) and "Architecture and management of a geological repository" (Andra, 2005i) volumes, with which it shares certain elements relating to the repository's design and geological context. It is positioned upstream of the former, and downstream of the latter (Figure 1.1.1).

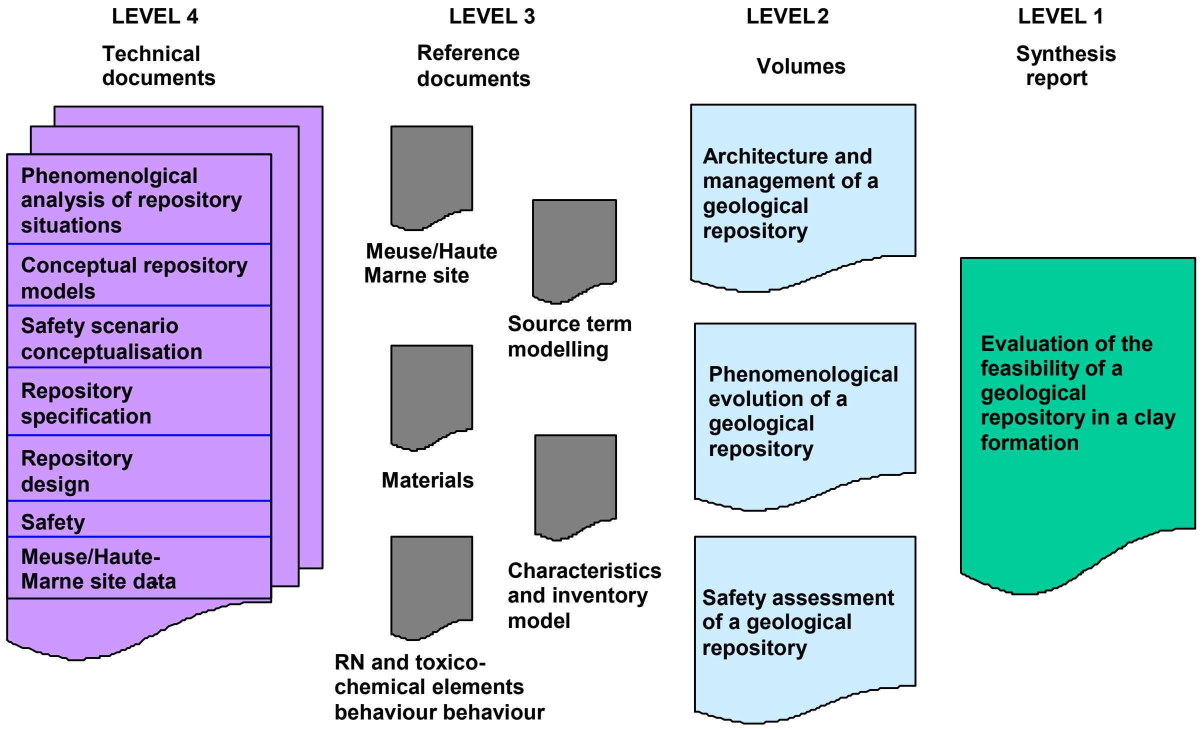

Figure 1.1.1 General structure of the Dossier 2005 Argile

The purpose of this document is to outline the existing knowledge that provides a basis for describing the set of phenomena and processes that govern the evolution of the repository and its environment over a period of one million years. This description benefits from the research conducted by Andra over the last fifteen years. This research has involved many French and overseas laboratories and research centers. The document also draws on research in fields that are only indirectly connected with the subject of radioactive waste disposal in geological formations, but which provide additional information to that obtained directly by Andra and its partners, whether through analogies with natural and engineered repository components, or through transposable analytical, experimental and modelling strategies. This report also includes the latest results obtained at the underground research laboratory and from the sample probes in the first experimental drift located at –445 m.

1.2 Inputs

The "Architecture et gestion du stockage géologique" volume (Andra, 2005i) which is on the same level in the dossier as this document, specifies the nature and geometry of the various repository components, together with its general architecture and operating process.

The "Evolution Phénomenologique du stockage géologique" Volume has been developed from a set of upstream documents on levels 3 and 4 in the Dossier 2005's document architecture (Figure 1.1.1):

- The reference knowledge documents on level 3 of the 2005 file's architecture, which concern the site (Andra, 2005h), radionuclides (Andra, 2005g), radioactive waste package release models (Andra, 2005d), radioactive waste inventory model (Andra, 2005e) and repository materials[1] (Andra, 2005f).
- The Phenomenological Analysis of Repository Situations (PARS) (Andra, 2005a ; Andra, 2005b), which provides a space-time description of the various phenomena affecting the repository's components and its environment. This analysis is based on a detailed description of the aforementioned components. It identifies the major processes and determines the uncertainties associated with them.
- The conceptual models described in the level 4 notes, based on the geological and engineered components and the major processes identified in the PARS. The notes accompanying each conceptual model reflect the best available knowledge, providing a picture of the phenomenology that can be applied in safety calculations. Uncertainties are represented either by ranges in parameter values or by alternative models.

Although this document draws on all these components of the dossier 2005, it has a different structure and focus. Specifically, it is not a reference knowledge document inasmuch as it draws from these level 3 documents only the information that serves to justify the description of the repository's evolution. It does, however, aim to provide an all-round synthesis of the scientific results reported in the reference knowledge documents.

It does not concentrate on the repository's safety, although the description of the repository's evolution can be applied directly when developing safety scenarios. The document also contains information in support of the proposed choices or options relating to the repository's architecture and reversible management. This information is provided via an analysis that covers not only the repository's long-term behaviour but also the processes involved in its operation on a hundred-year scale; this scale has been adopted by convention but can be extended to cover a multi-century period. It also contributes to the safety assessment, and in particular, the conclusion contains a ranked vision of the uncertainties that are an input for the safety calculations and related sensitivity analyses.

---

[1] The expression "repository materials" covers all materials used in the engineered repository components, other than waste and primary waste packages. Swelling clays, concrete and steel are the main repository materials.

1.3 Structure of the "Evolution Phenomenologique du stockage géologique" Volume

As already stated, this document fits between the volume introducing the repository's architecture and reversible management and the volume covering the safety assessment. To link these three documents and make them easier to read, section 2 of the «Evolution Phénomenologique du stockage géologique» volume reiterates the key aspects of the repository's design and management that are necessary in order to describe the phenomenological evolution.

Describing the phenomenological evolution of a set of engineered components (disposal cells, disposal modules, drifts, access shafts, etc.) and natural components (host rock and surrounding geological formations strata) implies adopting a structure that gives the reader an overall view of the sequence of processes that govern the repository's phenomenological evolution. Consequently, this volume has been designed to transpose the current state of knowledge into a scientific narrative spanning the million-year period adopted for the analysis (Andra, 2005j). In view of the chronology, sequencing and linkages between the described processes, this narrative cannot be totally linear. It is organised using an overall chronogram representing the repository's phenomenological evolution, in which the main phenomena are classified not by their order of appearance but by their influence on the development of other phenomena. Thus, the descriptions of the thermal (T), hydraulic (H), chemical (C) and mechanical (M) processes precede (in the above order) the repository's geodynamic evolution and the release and transfer of the radionuclides.

The complete description of the repository's phenomenological evolution is based on a presentation of the initial state (prior to construction and any disturbances) that aims to inform the reader about the T-H-M-C-[2] equilibria that characterise the local and regional geological environment of the Meuse / Haute-Marne site (cf. § 3 on the initial state of the geological environment).

In opting to consider the major phenomena that affect the phenomenological evolution of the repository and its geological environment one after the other, it is important not to overlook the linkages between them. Accordingly, each of the chapters relating to the THCM processes[2] (cf. § 5, 6, 7 and 8), contains an introduction and a summary linking to the upstream and downstream chapters, respectively. The summaries are designed to give readers the basic information that will enable them to understand the subsequent chapter(s). More specifically, each summary contains a paragraph devoted to the repository's reversibility, which (i) identifies the major phenomenological states over the course of the hundred-year period adopted by convention for the construction, operation and closure of the repository, and (ii) specifies any phenomenological evolutions relating to the non-closure of part or all of the repository over a multi-century timescale.

In each chapter, the phenomenology is described wherever necessary for each type of structure or group of structures, according to their geometry, the materials used or the related mode of operation. Although this organisation creates a degree of redundancy in the document, it is considered necessary in order to give a clear picture of the behaviour of each of the repository's main componants, and mark their independence in terms of phenomenological evolution.

The major phenomena and any uncertainties liable to affect them are listed at the end of the document (cf. § 11 and 12) This list provides a link with the "Safety Assessment" volume, thereby allowing the reader to obtain information to justify the safety choices and the conceptualisation of the safety models and the manner in which they are treated.

---

[2] THCM is the acronym that stands for the set of Thermal, Hydraulic, Chemical and Mechanical phenomena and processes. Biological processes (bacterial activity) are treated as Chemical processes, although in international literature they are sometimes identified separately and represented by the letter B. Similarly, the letter R is sometimes used to refer to radiological processes such as radiolysis of water under the effect of radioactive radiation. Given the similarity of their main effects, they have been assimilated to Chemical processes.

1.4 Representation of process space and time scales

A clear perception of space and time extensions of THCM processes and related disturbances is essential in order to properly understand the sequencing of, and where applicable, the linkages between the various processes in terms of time and space. To this end, time diagrams based on those described in the dedicated document (Chabiron & Plas, 2005) have been inserted into the text, with the overall aim of situating the release and migration of radionuclides and toxic chemical in relation to each process.

The time diagrams have been intentionally limited to the period of one million years, the cut-off point for safety calculations based on representative radioactive half-lives and the main phenomena affecting the repository's evolution. This cut-off point does not itself limit the continuation of processes such as those relating to geodynamic activity or the degradation of certain repository components. Rather, it defines a time envelope capable of representing the phenomena that are relevant to the understanding of the phenomenological evolution of the repository and its geological environment.

Some time-related aspects are not expressly included, such as biosphere sequencing or the continuous analysis of geodynamic evolution on the hydrogeological system. These aspects are nevertheless taken into consideration in the form of a series of snapshots taken at key periods, allowing the related transients to be described.

1.5 Predicting the phenomenological evolution over time, especially over the long term

Predicting the phenomenological evolution of the repository and its geological environment over a one million-year timescale may initially appear a risky enterprise. In this respect, the hundred-year to multi-century timescale of the repository's operational, observation and reversibility period seems easier to grasp by the layman, in particular via the feedback on the behaviour of underground engineered structures that has been generated by civil engineering and mining sources for decades.

However, the 'one million years' unit of time is commonly used in the earth sciences and astronomy. Scientists in these fields are accustomed to characterising and predicting sometimes complex phenomenological processes, or at least their trends, over time scales much longer than a million years.

In this broad context, predicting the phenomenological evolution of the repository and its geological environment is a relevant exercise. The approach is based on the very principle of a repository in a deep geological formation and the design options proposed for the repository.

- In regional terms, the fact that a geological environment has stabilised over a period of several millions or tens of millions of years implies that significant internal geodynamic changes may not need to be considered for the analysis period. Locally, in the particular area under consideration, the Callovo-Oxfordian layer has simple geometric characteristics and a geological history that is straightforward and largely free from disturbances. It is also characterised by its very limited exchanges of matter with its environment and by interactions between fluids and rocks (i.e. solids) that are the result of early processes that occurred tens of millions of years ago, at least. This stability, combined with the layer's uniformity and intrinsic properties mean that the studied geological system's characteristics can be established using existing scientific and technical means. The geological environment's past behaviour and properties provide a solid foundation for predicting its evolution over the next million years. In particular, the choice of a deep geological formation as the site of the repository means that the formation (and therefore the repository) are insaturated from the effect of surface changes, allowing these properties to remain intact over time.

The favourable geological characteristics of the Meuse/Haute-Marne site are described in chapter 3, on the initial environment, and in chapter 9 on the geological environment's geodynamic evolution.

- The options selected by the repository designer, notably relating to its architecture and materials, help to control the phenomenological processes that take place over time in the repository and the surrounding geological environment. The choice of a compartimentazed architecture is intended to limit phenomenological interactions within the repository. Similarly, the choice of natural or pseudo-natural materials such as concrete, clay, unalloyed or weakly-alloyed steel and glass, for example, is also designed to simplify the phenomenological processes and enhance our ability to evaluate their behaviour over time, notably by comparing them with similar naturally-occurring materials (Andra, 2005f).

The repository's design measures are described in chapter 2, and mentioned in chapters 5, 6, 7 and 8 which describe the thermal, hydrological, chemical and mechanical components of the repository's phenomenological evolution.

2

The Meuse/Haute Marne site, HLLL waste and disposal concepts

2.1 Introduction 37

2.2 The Meuse / Haute-Marne site and the Callovo-Oxfordian layer (Elion, 2005) 38

2.3 HLLW and spent fuels (Andra, 2005e)..42

2.4 Repository concepts..64

2.5 Implications of the architecture of the repository on the phenomenological evolution of the repository and its geological environment 84

2.1 Introduction

The description of the phenomenological evolution of the repository and its geological environment is based on three points covered successively in this chapter: The Meuse / Haute-Marne site, the waste and the repository concepts.

- **(i)** The characteristics of the Meuse / Haute-Marne site, and particularly those of the Callovo-Oxfordian layer considered for the repository feasibility study, are described in detail in the reference knowledge documents (Andra, 2005h). They are covered in chapter 3 of the present document, which describes the initial state of the geological medium prior to construction of the repository.
- **(ii)** At this stage, for the purpose of introducing the repository concepts, we shall limit ourselves to (i) defining the site's geographic location and its geological context within the Paris Basin, and (ii) providing a brief description of the Callovo-Oxfordian layer and its surrounding formations.
- **(iii)** HLLW, spent fuels and repository concepts are specifically covered in the “Architecture et gestion du stockage géologique” volume (Andra, 2005i). The present chapter only covers the general characteristics of waste and repository concepts so as to facilitate the understanding of the phenomenological evolution of the repository. Nevertheless, later in this document, within the scope of the description of the phenomenological evolution of the repository and its geological environment, detailed characteristics of HLLW, spent fuels and repository concepts are specified whenever necessary.

First, the typology of the HLLW and spent fuels is specified (origin of the radioactive waste, primary packages, quantitative and radiological inventories, physical and chemical characteristics of the radioactive waste or primary packages, heat release, etc.). For this purpose, the various radioactive waste production scenarios considered are described, along with their basic hypotheses, particularly those regarding existing non-conditioned radioactive waste and future radioactive waste.

Secondly, a description of long-term safety functions and repository reversibility is provided (Andra, 2005j).

Finally, the general architecture of the repository, primary packages, storage cell and the repository management and closure procedures adopted to satisfy the safety functions and reversibility requirements are covered, with special emphasis on the fractioned and modular repository design concept, the choice of repository materials, and the thermal criteria selected for the repository design.

- **(iv)** A final summary serving as an introduction to the rest of the document covers the main concepts associated with the phenomenological evolution of the repository and its geological environment, namely stressing the specific characteristics of the constitutive materials and design-related measures adopted to simplify and control this evolution.

2.2 The Meuse / Haute-Marne site and the Callovo-Oxfordian layer (Elion, 2005)

The Meuse / Haute-Marne site is defined as the authorised perimeter for the construction of the underground research laboratory. It is located in Eastern France, on the boundary between the Meuse and Haute-Marne departments (Figure 2.2.1).

Figure 2.2.1 Geographic location of the Meuse / Haute-Marne site

Geologically, the Meuse / Haute-Marne site is part of the eastern region of the Paris Basin (Figure 2.2.2). In this region, the Paris Basin is composed of alternating sedimentary layers (predominantly argillaceous) and limestone layers, deposited in a stable marine environment during the Jurassic, between 165 and 135 million years ago (see section 3). These layers have a simple and regular geometric structure, slightly sloping towards the northwest (1.5 to 2 degrees) in accordance with the general structure of the Paris Basin (bowl-shaped structured centred in the Paris area).

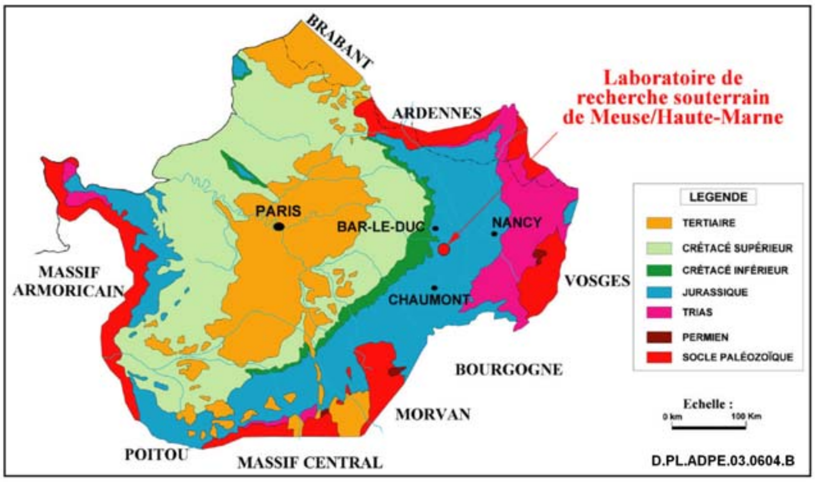

Figure 2.2.2 Geological location of the Meuse / Haute-Marne site within the Paris Basin

Within the sedimentary sequence, the Callovo-Oxfordian layer has been selected for the repository feasibility study (Figure 2.2.3). It is surrounded by two geological formations (underlying Dogger and overlying carbonated Oxfordian) containing aquiferous sedimentary horizons with low permeabilities and slow runoffs (approximately one kilometre per hundred thousand years for the Darcy water velocity)

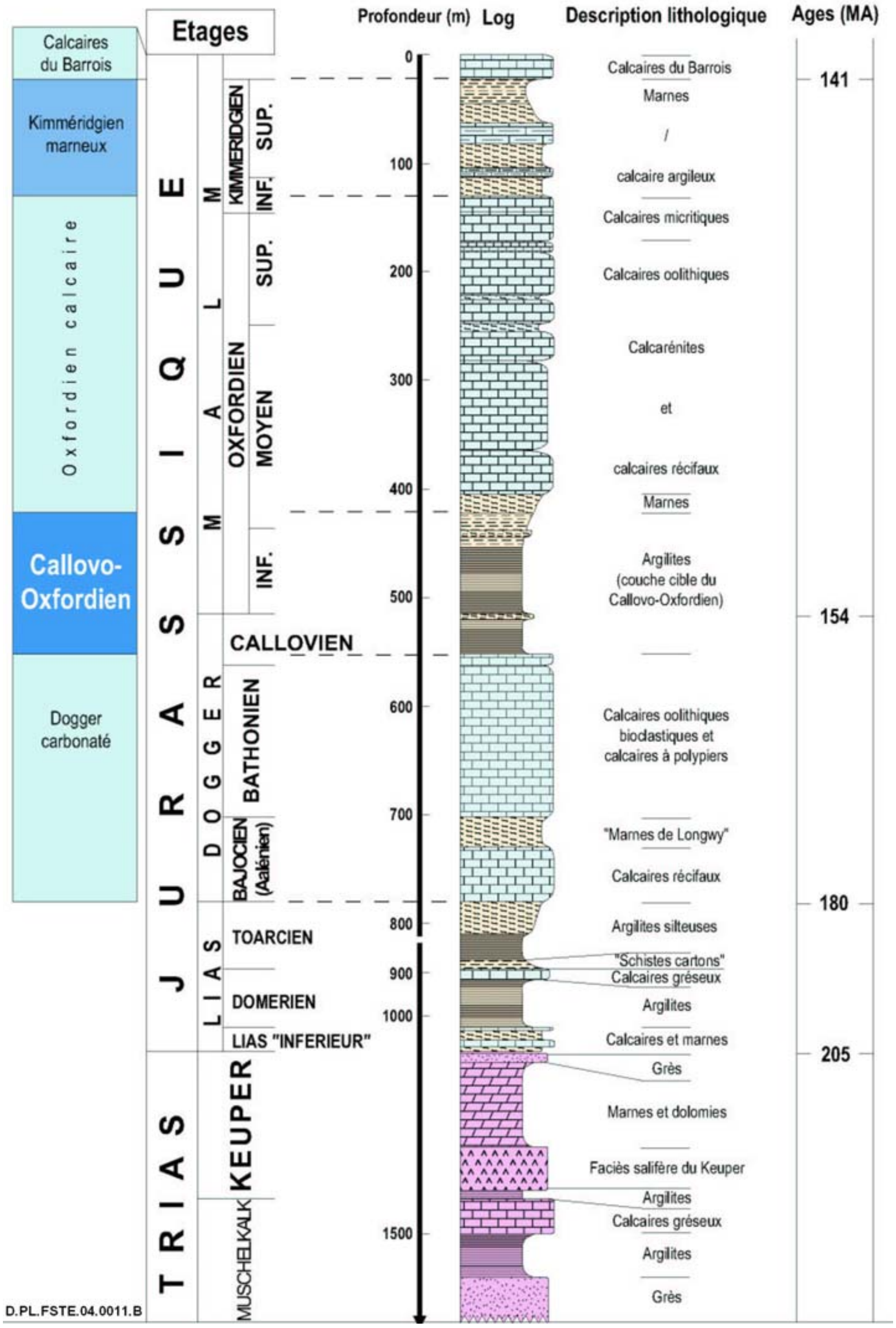

Figure 2.2.3 *Geological cross-section at the Meuse / Haute-Marne site*

The structural framework is stable, with natural mechanical stresses oriented in a stable manner for the past 20 million years. The site is located apart from large regional faults such as the Marne fault towards the southwest (Figure 2.2.4).

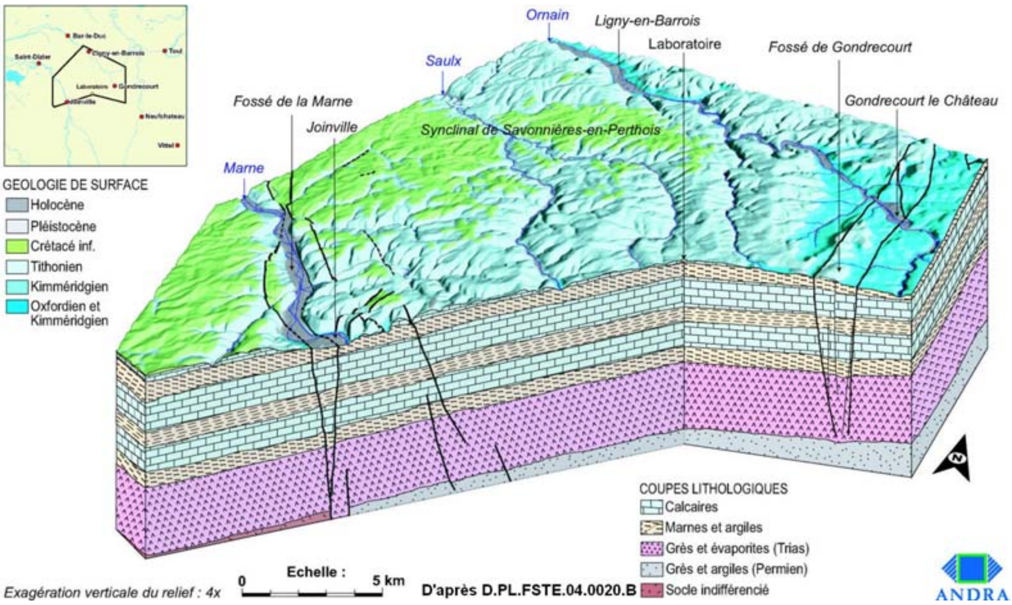

Figure 2.2.4 3D geological block diagram of the Meuse / Haute-Marne site

From a seismotectonic perspective, the Paris Basin is a stable zone with very low seismicity, remote from active zones such as the “Fossé Rhénan” towards the east, the Alps (southeast), the Massif Central (south) and the Massif Armoricain (west). There is no detectable neotectonic activity or significant local seismic activity in the Meuse / Haute-Marne sector, as indicated by the national seismic monitoring network and that implemented by Andra. The maximum seismic hazard physically possible is estimated at 6.1 ± 0.4 (with epicentre located 6 km from the site).

The Callovo-Oxfordian layer is an argillaceous layer at least 130 meters thick, laterally homogeneous, with low porosity (15 %) and low permeability (Darcy water velocity of approximately 3 centimeters after 100,000 years), consisting of argillaceous mineral phases (smectites, illites and illite/smectite interlayers) representing up to 60 % of its mass, as well as silts (fine quartzes) and carbonates. The 3D seismic data produced by Andra shows no faults with a vertical throw exceeding 2 meters within the layer. Directional boreholes confirm the absence of secondary (subseismic) faults. Moreover, only a few microfissures, stable and not affecting water flow, have been observed in over 4 km of core samples, and some of them are sealed with sulphates (celestine), which is indicative of a precocious formation during the compaction of deposits.

The characteristics of the Callovo-Oxfordian layer have been acquired shortly after its deposition. The layer has subsequently remained undisturbed, as indicated by Sr and $\delta^{13}C$ isotopic markers, geological thermometers (maximum paleo-temperature of approximately 40 °C) and the near absence of minerals formed at a later date (beyond 10 million years).

The argillaceous mineralogical composition of the argillites gives the Callovo-Oxfordian layer high retention capabilities. This is combined with low diffusion coefficient values, particularly for anions, due to the very small porosity of the argillites. Half the porosity of 15 to 18 % is occupied by bound water. The pores have an average size of 50 nm corresponding to a weak accumulation of a few water molecules. An electrostatic repulsion of the anions occurs within the smaller pores due to the existence of negative charges on the surface of the argillaceous minerals. The retention of cations is high. The natural tracer profiles (^{37}Cl, ^{11}B, ^{4}He) and the marked differences in chloride concentration between the base of the carbonated Oxfordian and the roof of the Callovo-Oxfordian confirm the presence of slow solute transport processes.

Finally, the argillites have mechanical properties favouring the feasibility of underground engineered structures at the depth of the Callovo-Oxfordian layer in the transposition zone (simple compression resistance > 21 MPa) and also significant thermal properties (thermal conductivity of between 1.4 and 2,7 W.m^{-1}.K^{-1}, depending on the stratigraphy).

Based on the position of the underground research laboratory, one define a transposition zone within which the Callovo-Oxfordian layer has physical and chemical properties similar to those observed at the laboratory (Figure 2.2.5). Its surface area is approximately 250 km². The depth of the Callovo-Oxfordian roof varies from 420 m at the underground research laboratory to over 600 m along the dip direction, and the thickness of the layer varies from 130 m at the laboratory to 160 m towards the north.

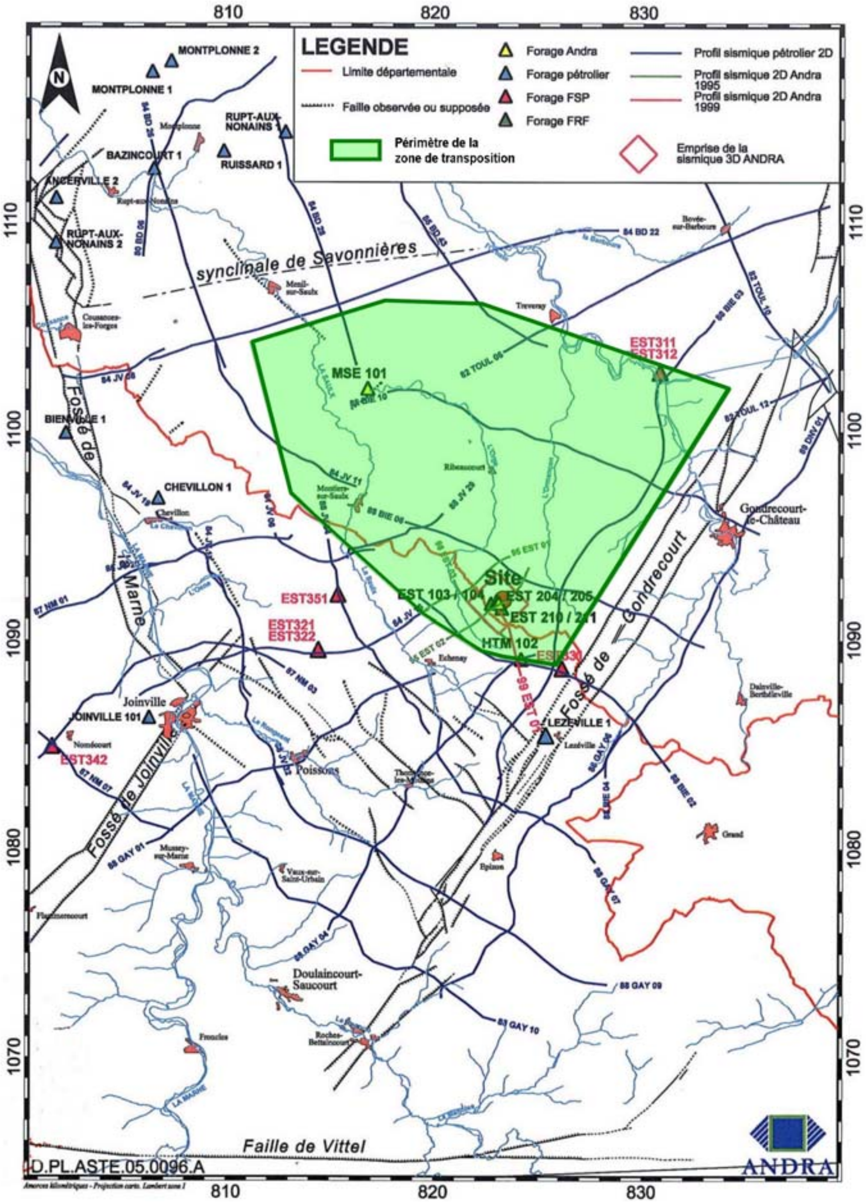

Figure 2.2.5 *Perimeter of the transposition zone around the Meuse / Haute-Marne site and position of boreholes drilled by Andra in the sector*

2.3 HLLW and spent fuels (Andra, 2005e)

HLLW is produced by the electronuclear industry (EDF and COGEMA) and by research and national defence activities (CEA). At present, this radioactive waste mainly comes from spent fuels discharged from EDF electrical production reactors and subsequently reprocessed in COGEMA plants at La Hague to separate the uranium and plutonium. It contains short-lived radioelements, generally in large quantities (high-level), and long-lived radioelements in medium to very large quantities, i.e., actinides, fission products and activation products (Inset 2.1).

Spent fuels are considered as recoverable nuclear materials, and therefore not as radioactive waste. They are nevertheless taken into account for the repository feasibility study, so as to cover all possible scenarios without prejudging the future organisation of the electronuclear industry.

The radioactive waste and radioactive waste package inventory (type and quantity) takes into account all the radioactive waste already produced, as well as that possibly generated by existing nuclear facilities. As far as future radioactive waste production is concerned, this implies the formulation of radioactive waste production and conditioning hypotheses, particularly regarding the management of electronuclear facilities.

Inset 2.1 ***Radioactive elements formed in reactor fuel assemblies***

Three types of radioactive elements are formed through in-reactor fission reactions:

- ✓ **Actinides**: These nuclei have a higher atomic number (2) than uranium and are created through neutron captures not followed by fission. Actinides draw their name from actinium (Z=89), a heavy metal preceding uranium in Mendeleiev's table but having similar chemical properties. Uranium, which exists in natural state, is also an actinide.

  The actinide produced most abundantly in reactors is plutonium, led by its main isotope, plutonium-239 (^{239}Pu), which is fissile. Reactors produce other actinides in lesser quantities, referred to as 'minor' actinides for that reason. The principal minor actinides are neptunium-237 (^{237}Np), americium-241 and 243 (^{241}Am and ^{243}Am) and curium-244 and 245 (^{244}Cm and ^{245}Cm). However, the production of minor actinides is low in comparison with that of fission products and plutonium.

- ✓ **Fission products**: They result from the fission of heavy nuclei (such as ^{235}U) or from the disintegration of fission fragments (this is the case with ^{129}I, for example).

  Fission products belong to a large number of chemical species. Most of them attach themselves to the fuel as solid oxides. Some are metals that remain in place, while others are rare gases such as ^{85}K.

- ✓ **Activation products**: They are mainly formed in the various structural alloys of the fuel assemblies via bombardment by neutrons or other particles.

Certain fission products and activation products are gaseous or extremely volatile, such as ^{3}H and ^{85}Kr (completely) or ^{36}Cl, ^{14}C and ^{129}I (partly). They are located **(i)** in the free spaces of the rods (gaps between pellets and sheaths, or upper part of rods after diffusion outside grains and pellets reactor), **(ii)** in grain joints, **(iii)** in pellet fissures/cracks, **(iv)** in grains (as inclusions), and **(v)** in the pores of restructured pellet zones (RIM).

It must be noted that certain radioactive elements may be both a fission product and an activation product, such as ^{14}C for example.

The spent fuel assemblies are transported to the reprocessing plants and dismantled. The spent fuel rods are sheared and then dissolved in nitric acid. The plutonium and uranium are extracted from this solution using chemical methods. The recovered uranium is re-enriched to form fuel. The plutonium is used to produce new fuels composed of a mixture of uranium oxide and plutonium oxide (mixed oxides, or 'MOX') already used in one third of French PWRs. The residue solutions resulting from the chemical treatment with nitric acid mainly contain fission products and activation products. They are calcinated and vitrified to constitute vitrified primary radioactive waste packages. The structural elements of the spent fuel assemblies mainly contain activation products. They are conditioned in concrete or compacted and then placed in stainless steel drums to constitute some primary B waste packages.

2.3.1 Main categories of HLLW

There are two main categories of high-level and/or long-lived radioactive waste.

2.3.1.1 C waste (also referred to as vitrified or high-level waste)

This type of radioactive waste corresponds to unrecoverable materials in high-level solutions resulting from the reprocessing of spent fuels in the COGEMA plants at La Hague and Marcoule. These solutions are a mixture of fission products, actinides and activation products. They are evaporated, and the solid materials obtained (containing radioactivity) are calcinated and dissolved at high temperature in a borosilicate glass matrix. The result is then poured into 316L stainless steel drums to constitute the primary vitrified radioactive waste packages (Figure 2.3.1).

Once the glass has been poured, the radioactive elements are distributed homogenously within the glass matrix in various chemical forms, either incorporated into the vitreous network or as metallic inclusions.

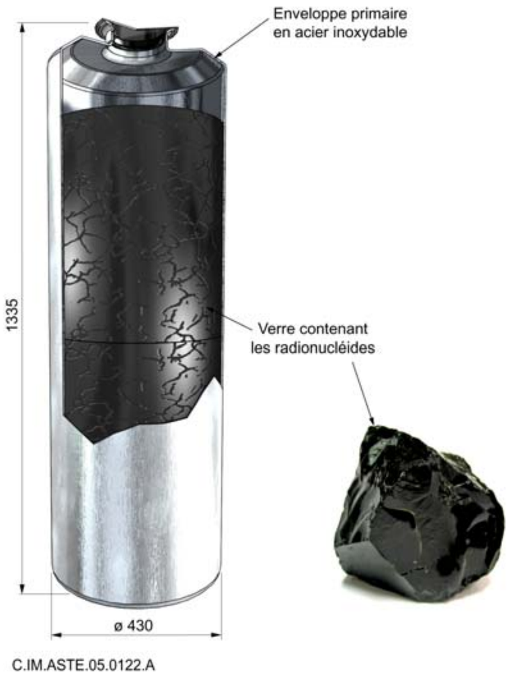

Figure 2.3.1 *See-through diagram of primary vitrified waste package and photograph of R7T7 nuclear glass*

2.3.1.2 B waste (also referred to as ILLW[3])

This type of radioactive waste mainly consists of intermediate-level long-lived radioactive waste resulting from the reprocessing of spent fuels and from the operation and maintenance of reprocessing plants or electronuclear facilities. It also includes radioactive waste produced by CEA nuclear research centres.

There are many different types of B waste, i.e., 'cladding radioactive waste' (metallic structural elements of fuel assemblies, such as zircalloy fuel rod cladding, fuel assembly support grids, etc.), intermediate-level effluent treatment sludges (co-precipitation salts), and 'technological radioactive waste' (filters or pumps). Metals constitute a significant part of B waste, but it also includes organic and inorganic compounds such as bitumen, plastics, cellulose, etc.

B waste contains actinides, but due to its origin it usually also includes activation products and fission products. The radionuclides are for the most part homogenously distributed within the radioactive waste. Only a fraction is located on the surface of the radioactive waste (this is the case with fission products such as ^{129}I, located in the first microns of the inner face of the zircalloy cladding).

B waste is conditioned using three methods, depending on the type:

- bituminisation, in the case of effluent treatment sludges, for example
- concreting
- compaction, in the case of hulls, end caps and technological waste, for example.

---

[3] ILLW: Intermediate-level long-lived waste

The conditioned waste is placed in concrete or steel drums. The packages obtained constitute the primary B waste packages (Figure 2.3.2).

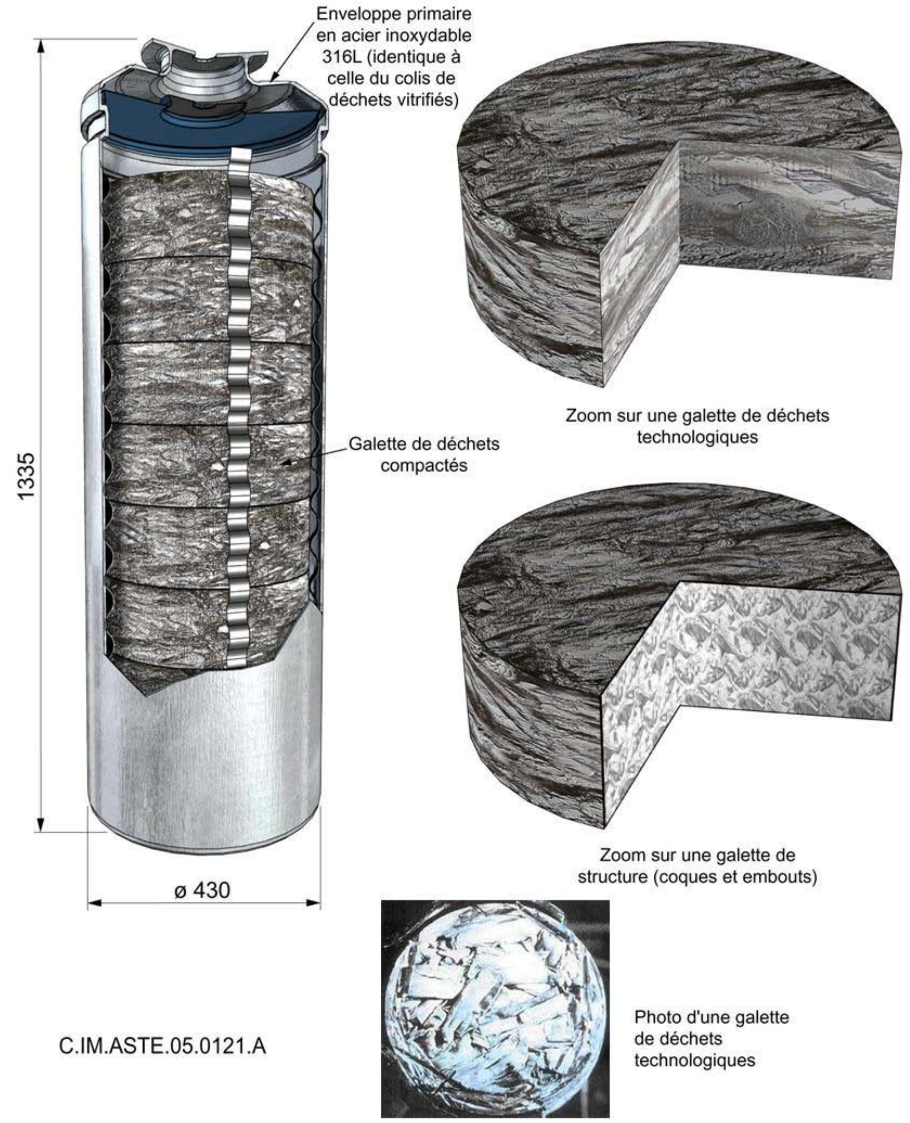

Figure 2.3.2 *Diagram of B waste package containing hulls, end caps and compacted technological radioactive waste (B5 waste package, see Table 2.3.2)*

2.3.2 Spent fuels after passing through EDF PWR reactors or CEA experimental reactors

A nuclear fuel assembly comprises a rod bundle consisting of a zircalloy cladding containing UO_2 or $(U\text{-}Pu)O_2$ fuel pellets referred to as 'UOX' and 'MOX', respectively. These pellets are formed through sintering of oxide grains. The rods are approximately 4 meters long and their upper and lower parts are sealed with 2 welded plugs. The stack of rod pellets, representing approximately 95 % of the rod length, is mechanically stabilised by a helicoidal inconel spring in the upper part of the rod.

A series of metallic grids mechanically supports the fuel assembly rod bundle. In the upper part of the fuel assembly, a device consisting of a metallic head plate and a 'spider' ensures the handling of the fuel assembly and the passage of reactor control rods. Figure 2.3.3 shows an EDF PWR fuel assembly.

The various metallic components of an assembly are referred to as structural elements.

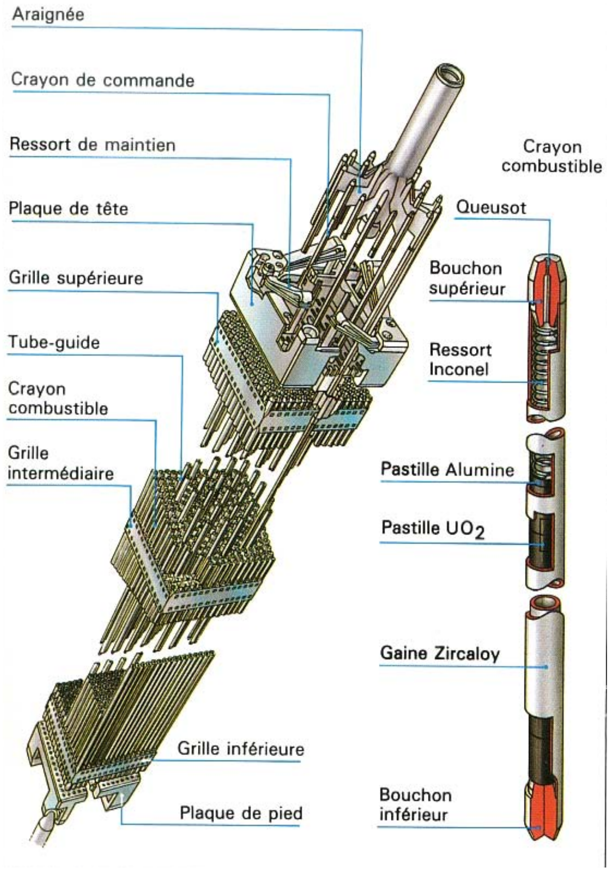

Figure 2.3.3 *Diagram of a PWR fuel assembly*

In the reactor, the assemblies undergo significant physical and chemical modifications with respect to their initial state. In particular, the pellets show fissures and differences in grain size associated with recrystallisation processes. A layer of oxidised zirconium (zirconia) a few microns thick is formed on the inner and outer faces of the zircalloy cladding.

The fission reactions of the uranium and plutonium in the reactor lead to the formation of actinides, fission products and activation products. These radionuclides are located within the oxide pellets and structural elements. The actinides are mainly distributed in the oxide pellets, and more specifically in the oxide grains Certain fission and activation products formed in the pellets, such as ^{14}C, are volatile (or gaseous) under in-reactor temperature and pressure conditions. They may then partially migrate outside the oxide grains and accumulate in gaps, particularly in the upper part of the rods (Figure 2.3.3), in grain joints and in fissures, as shown in figure 2.3.4 and figure 2.3.5. The structural elements mainly contain activation products such as ^{59}Ni, ^{93}Zr and ^{94}Nb located by nature in the mass of structural elements. More specifically, the cladding contains ^{129}I incorporated into the zirconia layer during fission reactions.

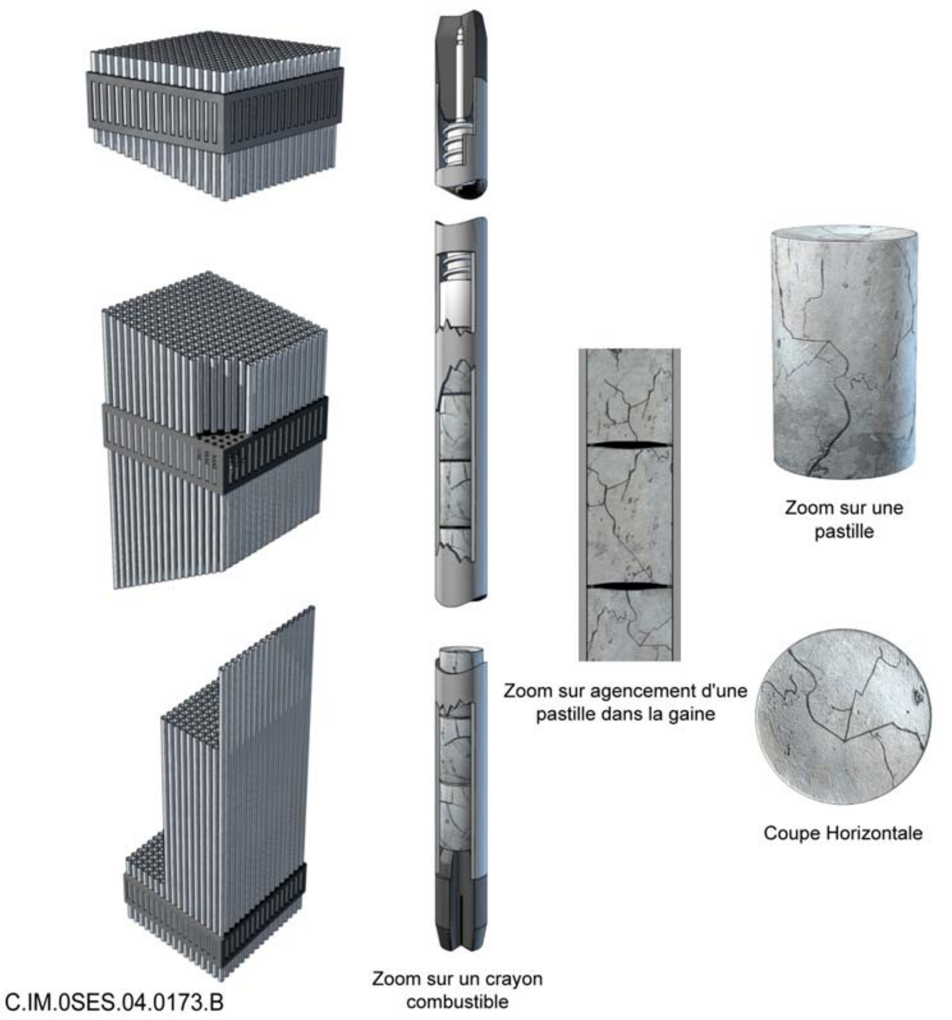

Figure 2.3.4 *See-through diagram of a spent fuel assembly and various cross-sections of a spent fuel rod after passing through the reactor*

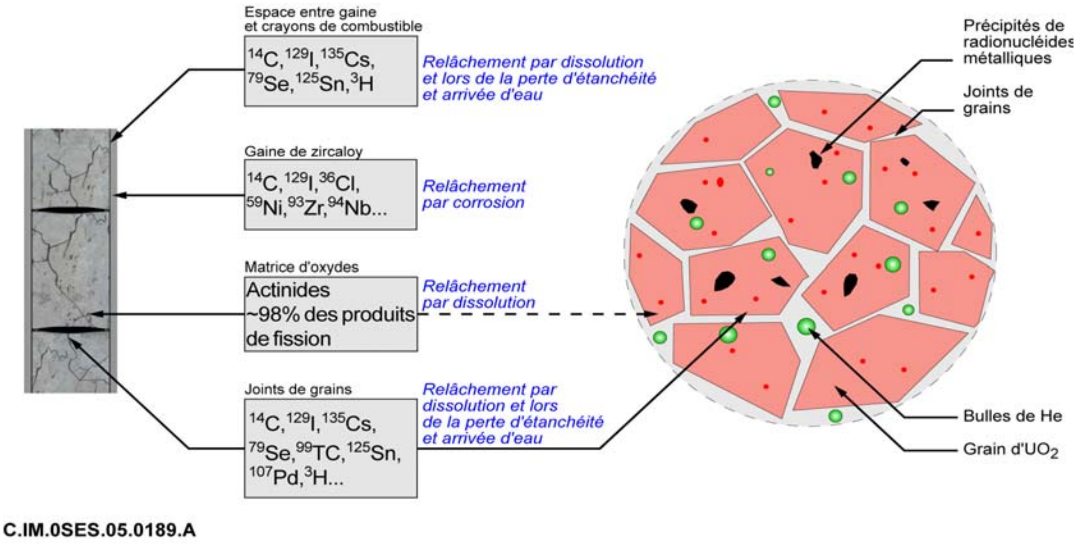

Figure 2.3.5 *Basic diagram of the location of the radionuclides within a spent fuel rod and a UOX pellet after passing through the reactor*

2.3.3 Radioactive waste production analysis scenarios

Fifty-eight PWRs commissioned between 1977 and 1999 are currently in operation. The mass of nuclear fuel discharged from these reactors during their entire period of operation is estimated at 45,000 tonnes of heavy metal. This estimate is based on a combination of hypotheses regarding **(i)** the average lifetime of reactor units (forty years), **(ii)** the energy produced (16,000 terawatt-hours of cumulated production), and **(iii)** the progressive increase in fuel burnup rates in reactors.

Based on these hypotheses, four nuclear fuel management scenarios (i.e. waste production scenarios) are adopted to conduct the repository studies. The principle of these scenarios is to encompass various possible industrial strategies without seeking to privilege any of them in particular. This approach covers a very broad range of radioactive waste types, allowing for a technical analysis of questions associated with the various packages (Andra, 2005e).

- The first three management scenarios correspond to the reprocessing of spent fuels discharged from reactors:
    - complete reprocessing of UOX and MOX spent fuels discharged from EDF reactors, with production of all types of vitrified radioactive waste reference packages (management scenario **S1a**)
    - reprocessing of UOX fuels associated with the production of C1 and C2 vitrified radioactive waste (management scenario **S1b**)
    - reprocessing of UOX fuels only associated with the production of C1 vitrified radioactive waste (management scenario **S1c**)

Scenarios S1b and S1c are used to study the possibility of increasing the concentration of waste in the glass (with respect to packages currently produced). This higher concentration would result in a slightly greater heat release from the packages (see section 5).

- The fourth management scenario (**S2**) assumes the continuation of UOX reprocessing until 2010 and its subsequent end. It supports an exploratory study of the direct disposal of UOX and enriched uranium fuels, as wells as MOX fuels (as in scenarios S1b and S1c).

In order to apply these scenarios in terms of conditioned waste, the hypotheses adopted for existing non-conditioned waste and future waste consist of maintaining the industrial processes currently implemented by waste producers (vitrification, compaction, cementation and bituminisation).

2.3.4 Primary reference waste packages

The two main categories of HLLW and spent fuels include various types of families differentiated by their origin, chemical composition, radionuclide inventory, number, conditioning or physical and chemical behaviour (see section 2.4.2.6).

In order to simplify the repository design, these families are grouped into reference packages according to a three-level classification that constitutes the design inventory model (Andra, 2005e). Level 1 mainly corresponds to the composition and the conditioning method. Levels 2 and 3 address the diversity of families within the same level 1 reference package, particularly with respect to their phenomenological behaviour within the repository.

2.3.4.1 C waste reference packages

C waste is grouped into five level 1 reference packages based on origin and heat release with respect to radiolement content (Table 2.3.1).

C0 vitrified waste packages correspond to old waste productions. There are three subsets (level 2) corresponding to the following:

- **(i)** reprocessing of spent fuels from natural uranium-graphite-gas reactors (Sicral type NUGG fuels) and Phenix fast neutron reactors in the PIVER plant at Marcoule between 1969 and 1981 (PIVER vitrified waste)
- **(ii)** reprocessing of NUGG fuels previously processed in the COGEMA plant at La Hague, currently stored while awaiting conditioning (UMo vitrified waste)
- **(iii)** reprocessing of NUGG fuels since 1978 in the COGEMA vitrification facility at Marcoule (AVM vitrified waste). C0 reference packages differ from other vitrified waste reference packages, particularly in their dimensions.

Reference packages C1 to C4 correspond to two groups:

- ***Vitrified waste resulting from current production (or considered in the short term)*** due to the reprocessing of PWR UOX and enriched uranium fuels in the COGEMA plants at La Hague.

  This includes C1 reference packages corresponding to the current processing of UOX1 fuels (reactor burnup rate: 33 GWd.t^{-1}), UOX2/enriched uranium fuels (reactor burnup rate: 45 GWd.t^{-1}) and UOX3 fuels (reactor burnup rate: 55 GWd.t^{-1}) and C2 reference packages corresponding to the processing of UOX2/enriched uranium fuels (reactor burnup rate: 45 GWd.t^{-1}) and UOX3 fuels (reactor burnup rate: 55 GWd.t^{-1}).

- ***Hypothetical future vitrified waste*** corresponding to glass production that can be possibly considered in the COGEMA plant at La Hague.

  A first subset (C3 packages) corresponds to glasses resulting from the conditioning of fission product solutions from UOX and MOX fuels. These glasses are defined as consisting of a mixture of 15 % MOX and 85 % UOX2.

  A second subset (C4 packages) corresponds to vitrified waste resulting from the processing of UOX fuels and containing a small additional load of plutonium. The incorporation of plutonium in the glass is fixed as a mass percentage (approximately 4 kg per package). The plutonium incorporated comes from UOX2 fuels.

The various reference packages are shown in figure 2.3.6

Table 2.3.1 List of vitrified waste reference packages in the inventory model

Reference packages		Level 1	Level 2	Description	Remarks
Vitrified waste	C	**C0**	C0.1	PIVER vitrified waste	Reference packages from old production
			C0.2	UMo vitrified waste	
			C0.3	AVM vitrified waste	
		C1		Current uranium oxide/enriched uranium vitrified waste	Reference packages from current production or considered in the short term, i.e., conditioning in CSD-V vitrified waste reference packages (316L stainless steel drum)
		C2		Future uranium oxide/enriched uranium vitrified waste	
		C3		UOX/MOX vitrified waste	Hypothetical future reference packages (conditioning similar to C1 and C2 packages)
		C4		UOX + Pu vitrified waste	

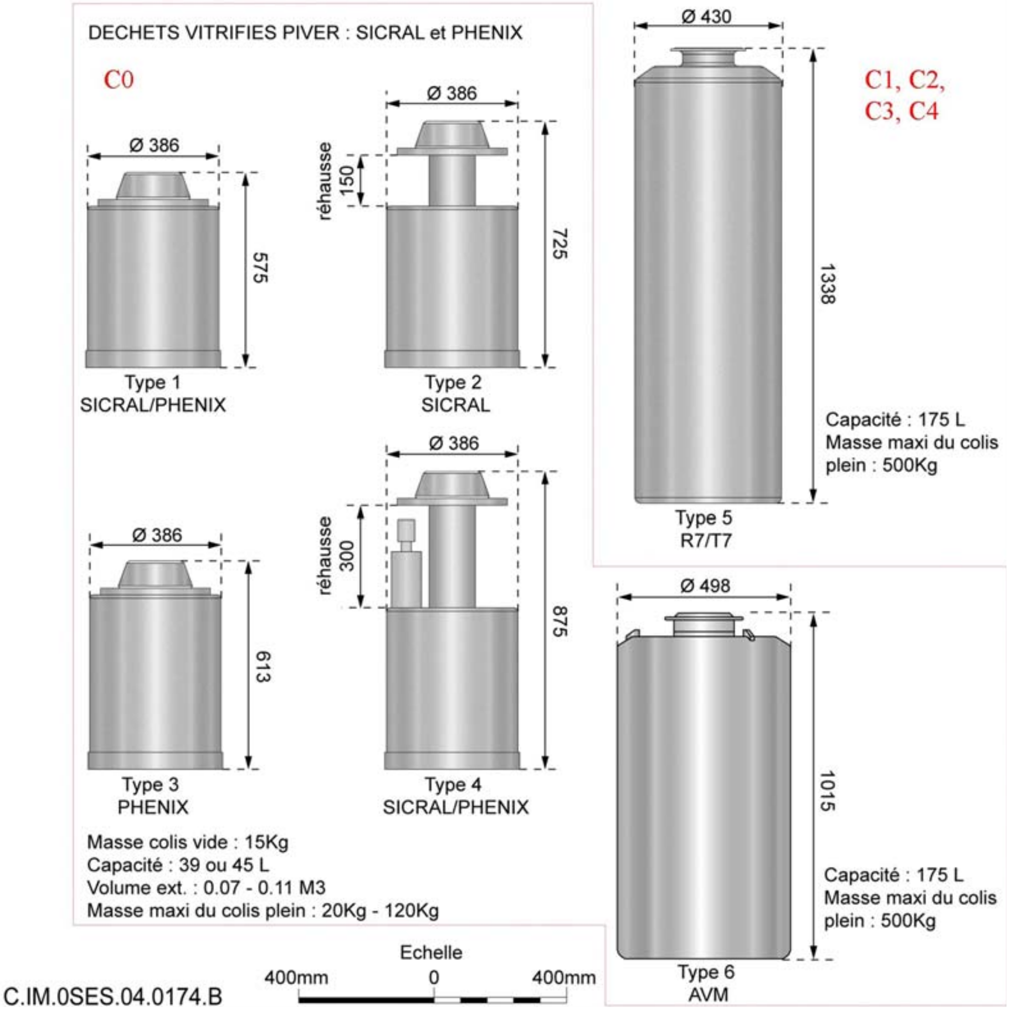

Figure 2.3.6 Diagrams and dimensions of vitrified waste reference packages

2.3.4.2 B waste reference packages

The various types of B waste are grouped into eight level 1 reference packages according to type and conditioning method (bituminisation, compaction or cementation) (Table 2.3.3). I.e., activated metallic waste from nuclear reactors (B1), bituminised liquid effluent treatment sludges (B2), cemented or compacted technological waste (B3), cemented cladding waste (B4), compacted cladding waste (B5), cladding and technological waste placed in drums (B6), sources (B7), and waste containing radium and americium (B8).

The large diversity of B waste leads to distinguishing between level 2 and level 3 B waste reference packages whenever necessary.

- B2.1 and B2.2 reference packages correspond to different package geometries.
- B3 reference packages are grouped based on the materials used for the containers and the homogenous or heterogeneous character of the radioactive conditioned waste, i.e.:
    - B3.1: heterogeneous waste contained in concrete envelopes
    - B3.2: homogenous waste contained in concrete envelopes
    - B3.3: heterogeneous waste contained in metallic envelopes

Level 3 corresponds to the chemical nature of the waste, the risk of hydrogen production and the package dimensions. Level 3 reference packages associated with level 2 reference packages (B3.1, B3.2 and B3.3) are classified in order of increasing size, i.e.:

- B3.1.1, B3.1.3, B3.2.1, B3.2.2, B3.3.2: packages potentially generating hydrogen
- B3.1.2, B3.3.1, B3.3.3, B3.3.4: packages containing organic matter and generating hydrogen

- B5 reference packages are differentiated according to waste type and associated characteristics (chemical, radiological, thermal):
    - B5.1 / B5.2: These reference packages differ from other cladding waste conditioned in CSD-C containers on account of their greater thermicity and the presence of technological waste. They are used to distinguish two potentially different CSD-C populations based on technological waste content, i.e., B5.1 corresponds to technological waste containing organic matter, whereas B5.2 does not contain any.
    - B5.3: cladding waste only, no organic matter, very low thermicity (due to age of waste)
    - B5.4: magnesian waste, no organic matter, no thermicity
- B6 reference packages are differentiated according to waste type, materials and envelope geometry:
    - B6.1: envelope geometry different from that of reference packages B6.2 to B6.5 (identical)
    - B6.2: cladding waste consisting of steel, zircalloy and inconel
    - B6.3: magnesian cladding waste
    - B6.4: packages containing organic technological waste and generating hydrogen
    - B6.5: packages only containing metallic technological waste
- B7 and B8 reference packages are also differentiated according to waste type, materials and envelope geometry.

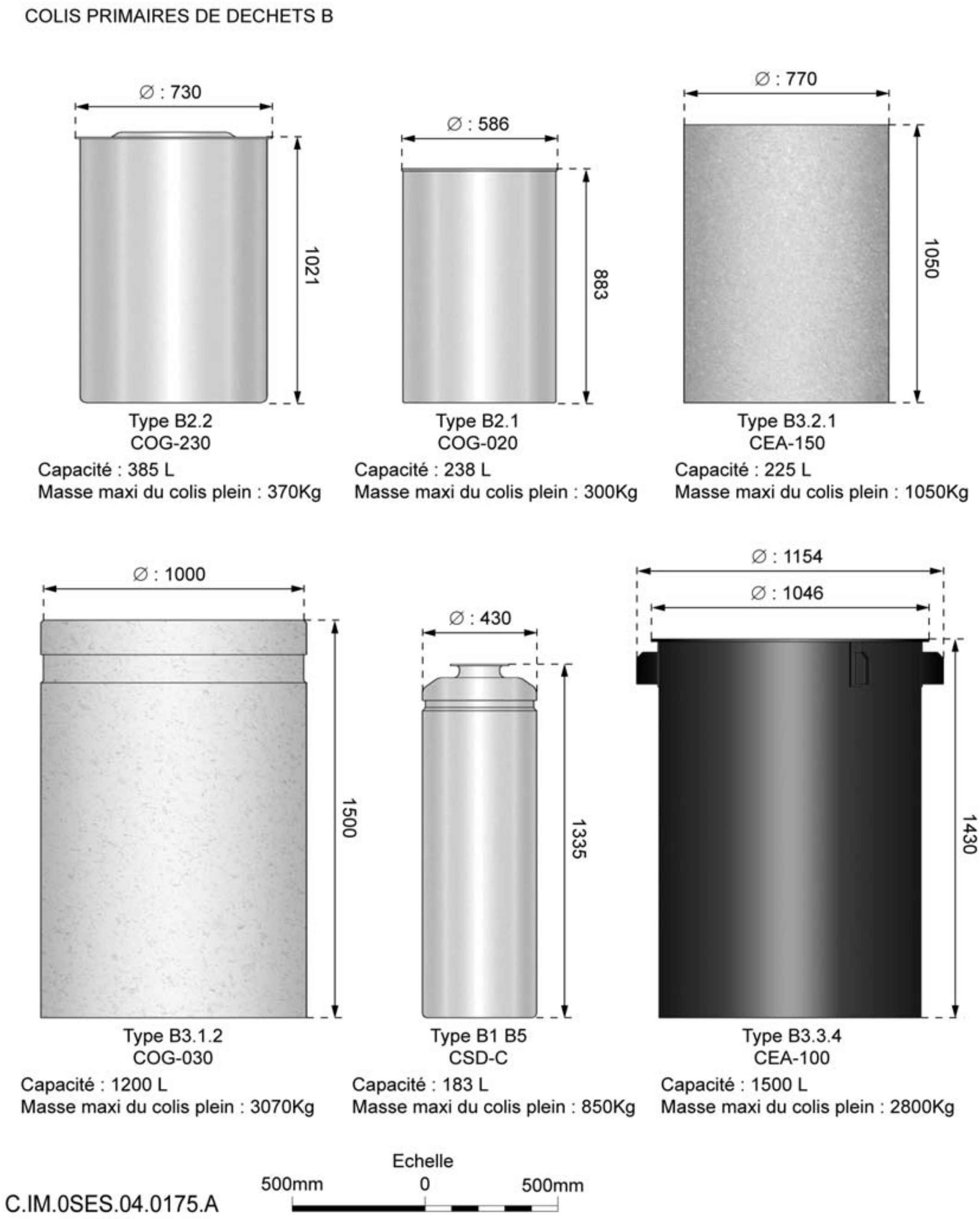

Figure 2.3.7 Diagrams and dimensions of B waste reference packages

Table 2.3.2 *List of B waste reference packages in the design inventory model*

Reference packages		Level 1	Level 2	Level 3	Description
Activation product waste	**B**	**B1**			CSD-C containing activation product waste from PWRs and fast reactors
Bituminised waste		**B2**	B2.1		238 and 245-litre bitumen drums
			B2.2		428-litre bitumen drums
Technological and miscellaneous waste, cemented or compacted		**B3**	B3.1	B3.1.1	1,000-litre concrete containers possibly reconditioned in metallic containers
				B3.1.2	Concrete containers (CAC and CBF-C'2) containing various technological waste
				B3.1.3	1800-litre concrete containers containing miscellaneous waste
			B3.2	B3.2.1	500-litre concrete containers (sludges and concentrates)
				B3.2.2	1200-litre concrete containers (CBF-C'2) containing CEDRA and AGATE waste
			B3.3	B3.3.1	Standard compacted waste containers (CSD-C) containing alpha waste
				B3.3.2	Multipurpose storage drums containing cemented pulverulent waste
				B3.3.3	500-litre steel containers containing miscellaneous waste
				B3.3.4	870-litre steel containers containing miscellaneous waste
Cemented cladding waste		**B4**			Drums containing cemented hulls and end caps
Compacted cladding waste with or without technological waste		**B5**	B5.1		CSD-C containers containing a mixture of hulls, end caps and technological waste (including organic waste)
			B5.2		CSD-C containers containing a mixture of hulls, end caps and metallic technological waste
			B5.3		CSD-C containers containing PWR cladding waste (HAO) without technological waste
			B5.4		CSD-C containers containing magnesian cladding waste
Cladding and technological waste placed in drums		**B6**	B6.1		180-litre steel containers containing AVM operating waste
			B6.2		Multipurpose storage drums containing metallic cladding waste
			B6.3		Multipurpose storage drums containing magnesian cladding waste
			B6.4		Multipurpose storage drums containing metallic and organic technological waste
			B6.5		Multipurpose storage drums containing metallic technological waste
Sources		**B7**[*]	B7.1		Source blocks
			B7.2		CSD-C containers containing PWR primary and secondary source rods
			B7.3		Multipurpose storage drums containing sealed sources
Waste containing radium and americium		**B8**[*]	B8.1		Multipurpose storage drums containing radiferous lead sulphate
			B8.2		870-litre steel containers containing lightning rods with radium or americium
			B8.3		Multipurpose storage drums containing ORUM

([*] B7 and B8 reference packages are not covered in the rest of this document)

2.3.4.3 Spent fuels

The spent fuel taken into account comes from decommissioned reactor sectors, research reactors (NUGG, EL4), national defence activities and PWR reactors.

There are three types of level 1 reference packages. The first two correspond to EDF PWR uranium oxide/enriched uranium fuels (CU1) and MOX fuels (CU2). The third type corresponds to CEA fuels (CU3).

For CU1 and CU2 reference packages, the reference fuel assembly corresponds to an advanced 2nd generation FRAGEMA design with thickened guide tubes and zirconium alloy cladding. The following are distinguished:

- UOX fuel assemblies for 900 MWe PWRs (AFA-2GE 'short' fuel assemblies[4])
- UOX/enriched uranium and MOX fuel assemblies for 1300 MWe and 1450 MWe PWRs (AFA-2LE 'long' fuel assemblies[4])

CU3 fuels include research reactor and nuclear propulsion fuels (national defence). These are not included in the design inventory model scenarios and are not covered in the present document.

Table 2.3.3 List of standard spent fuel assemblies

Standard spent fuel assemblies		**Level 1**	**Level 2**		**Description**	**Remark**
Spent fuels	**EDF PWR fuels**	**CU1**			PWR uranium oxide and enriched uranium spent fuels	The reference fuel assembly corresponds to an advanced 2nd generation FRAGEMA design with thickened guide tubes and zirconium alloy cladding.
		CU2			PWR MOX spent fuels	
	CEA fuels	**CU3***			Research reactors and national defence	

(* CU3 spent fuels are not covered in the rest of this document)

2.3.4.4 Inventories of the number of reference packages

Table 2.3.4 shows the inventories of the number of HLLW packages and spent fuel assemblies for the four waste production scenarios. These inventories are based on the hypothesis of maintaining the industrial processes currently implemented by waste producers (vitrification, compaction, cementation, bituminisation) for existing non-conditioned waste and future waste. They are based on cautious hypotheses, using figures corresponding to a conservative level of expected waste production, particularly so as to taken into account the uncertainties regarding the future of certain types of ILLW.

---

[4] Assemblies AFA-2GE and AFA-2LE have the same configuration (17x17 rods, 12.6 mm pitch, 214x214 mm cross-sectin) but different total lengths: 4120 mm for AFA-2GE and 4870 mm for AFA-2LE, hence the terms short and long.

Table 2.3.4 *Global quantitative data for the number and volume of B and C waste packages and the number of spent fuel assemblies in the design inventory model as per the waste production scenarios*

	S1a		**S1b**		**S1c**		**S2**	
Reference package	**Number**	**Volume (m^3)**	**Number**	**Volume (m^3)**	**Number**	**Volume (m^3)**	**Number**	**Volume (m^3)**
B1	2,560	470	2,560	470	2,560	470	2,560	470
B2	104,990	36,060	104,990	36,060	104,990	36,060	104,990	36,060
B3	32,940	27,260	32,940	27,260	32,940	27,260	30,390	24,540
B4	1,520	2,730	1,520	2,730	1,520	2,730	1,520	2,730
B5	42,600	7,790	39,900	7,300	39,900	7,300	13,600	2,490
B6	10,810	4,580	10,810	4,580	10,810	4,580	10,810	4,580
B7	3,045	1,440	3,045	1,440	3,045	1,440	3,045	1,440
B8	1,350	775	1,350	775	1,350	775	1,350	775
Total for B waste reference packages	**199,815**	**81,105**	**197,115**	**80,615**	**197,115**	**80,615**	**168,265**	**73,085**
C0	4,120	700	4,120	700	4,120	700	4,120	700
C1	4,640	810	4,640	810	38,350	6,710	4,640	810
C2	990	170	27,460	4,810	0	0	5,920	1,040
C3	13,320	2,330	0	0	0	0	0	0
C4	13,250	2,320	0	0	0	0	0	0
Total for C waste reference packages	**36,320**	**6,330**	**36,220**	**6,320**	**42,470**	**7,410**	**14,680**	**2,550**
Total for B/C	**236,135**		**238,735**		**244,985**		**240,945**	

CU1	0		0		0		54,000*	
CU2	0		5,400		5,400		4,000	
Total for spent fuel assemblies	**0**		**5,400**		**5,400**		**58,000**	

*: number of 4 UOX disposal packages: 13 500

Table 2.3.4 leads to the following conclusions:

- The number of B waste reference packages varies little from one scenario to another.
- In the B waste category, four reference packages constitute the majority in terms of number of packages: **(i)** bituminised sludge packages (B2), **(ii)** technological and miscellaneous waste packages, cemented or compacted (B3), **(iii)** cladding waste with or without technological waste, compacted (B5), and **(iv)** cladding and technological waste placed in drums (B6).
- B waste packages represent over 80 % of the number of reference packages (sum of B and C packages and spent fuel assemblies), regardless of the waste management scenario considered. They are followed by the C waste packages (between 6 and 17 % of the total number of reference packages), with spent fuel assemblies last in the list.

This vast quantity of B waste packages is unrelated to their inventory of radioelements, which amounts to less than 1 % of the total activity of HLLW (see 2.3.4.5)

2.3.4.5 Radioactive inventories of the reference packages

The radioactive inventories of reference packages have been determined by considering only radionuclides with half-lives exceeding six months, and based on feedback from safety analyses previously conducted by Andra and foreign counterparts (Andra, 2005j). This leads to a list of 144 radionuclides including fission products, activation products and actinides, as shown in inset 2.2. Like the number of reference packages, the radioactive inventory varies depending on the waste production scenario considered (Andra, 2005e).

So the reference packages differ in terms of radioactive inventory. Figure 2.3.8 and figure 2.3.9 respectively show the activation/fission product activity and the actinide activity per reference package.

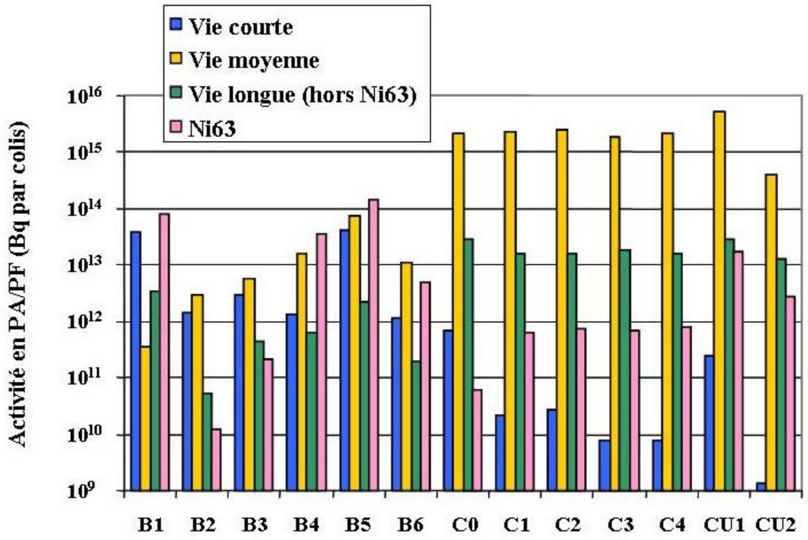

Figure 2.3.8 *Activation product and fission product activity of each reference package in Bq par package (Short-lived activity: half-life = 6 years; Medium-lived activity: 6 years < half-life = 30 years; Long-lived activity: half-life > 30 years*

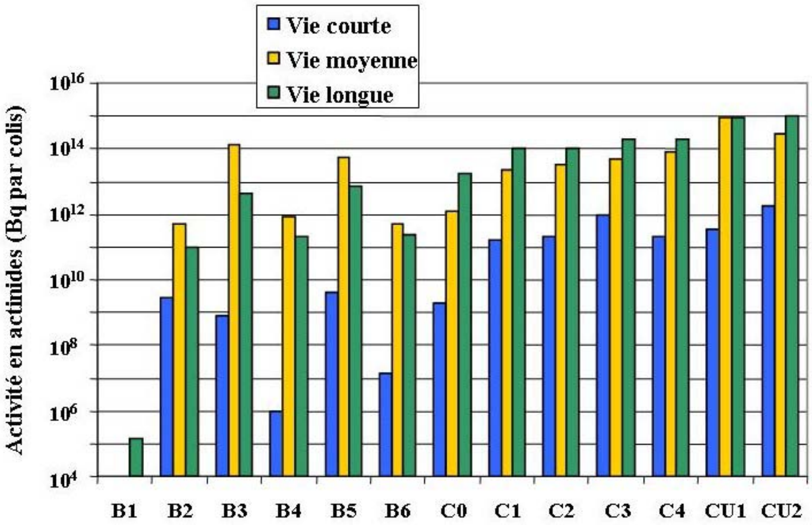

Figure 2.3.9 *Actinide activity of each reference package in Bq par package (Short-lived activity: half-life = 6 years; Medium-lived activity: 6 years< half-life = 30 years; Long-lived activity: half-life > 30 years)*

Figure 2.3.10 shows a few radionuclide inventories (long-lived in particular) for the four waste production scenarios. C waste and spent fuels clearly represent the vast majority of the radioactive inventory for most radionuclides (in comparison with B waste packages). It can also be seen that the total inventory varies from one scenario to another. B waste is predominant for activation products formed preferentially in fuel assembly structural elements, such as ^{14}C, ^{94}Nb and ^{59}Ni and, to a lesser extent, ^{36}Cl.

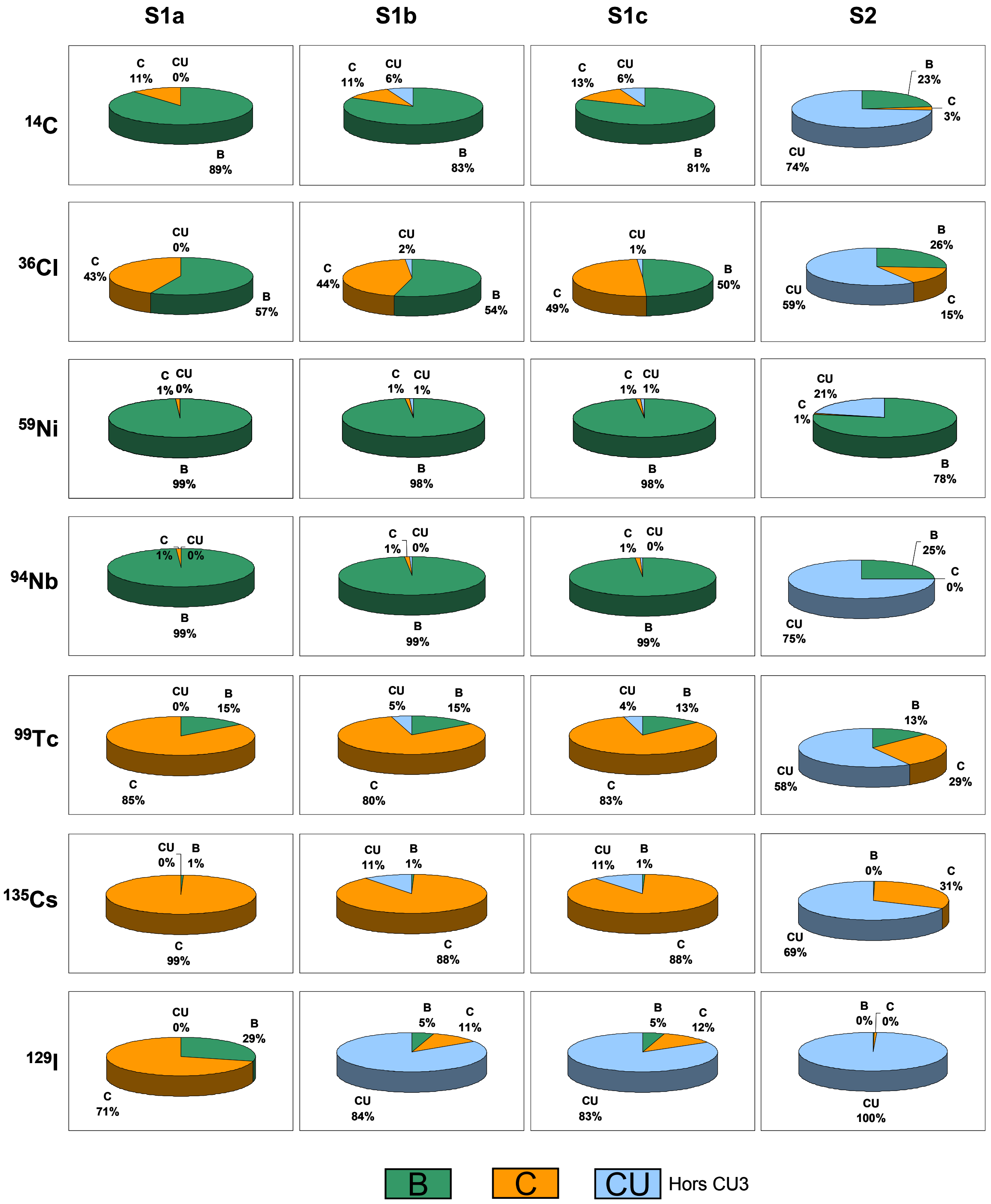

Figure 2.3.10 Relative distributions (%) of ^{14}C, ^{36}Cl, ^{59}Ni, ^{94}Nb, ^{99}Tc, ^{129}I and ^{135}Cs, inventories in B waste, C waste and spent fuels (not including CU3) for the four waste management scenarios

Figure 2.3.11 shows the relative inventories of B waste reference packages for scenario S1b and for a few radionuclides. It can be seen that B5 packages represent the majority in terms of fission and activation products. For the other reference packages, inventories vary depending on the radionuclide considered.

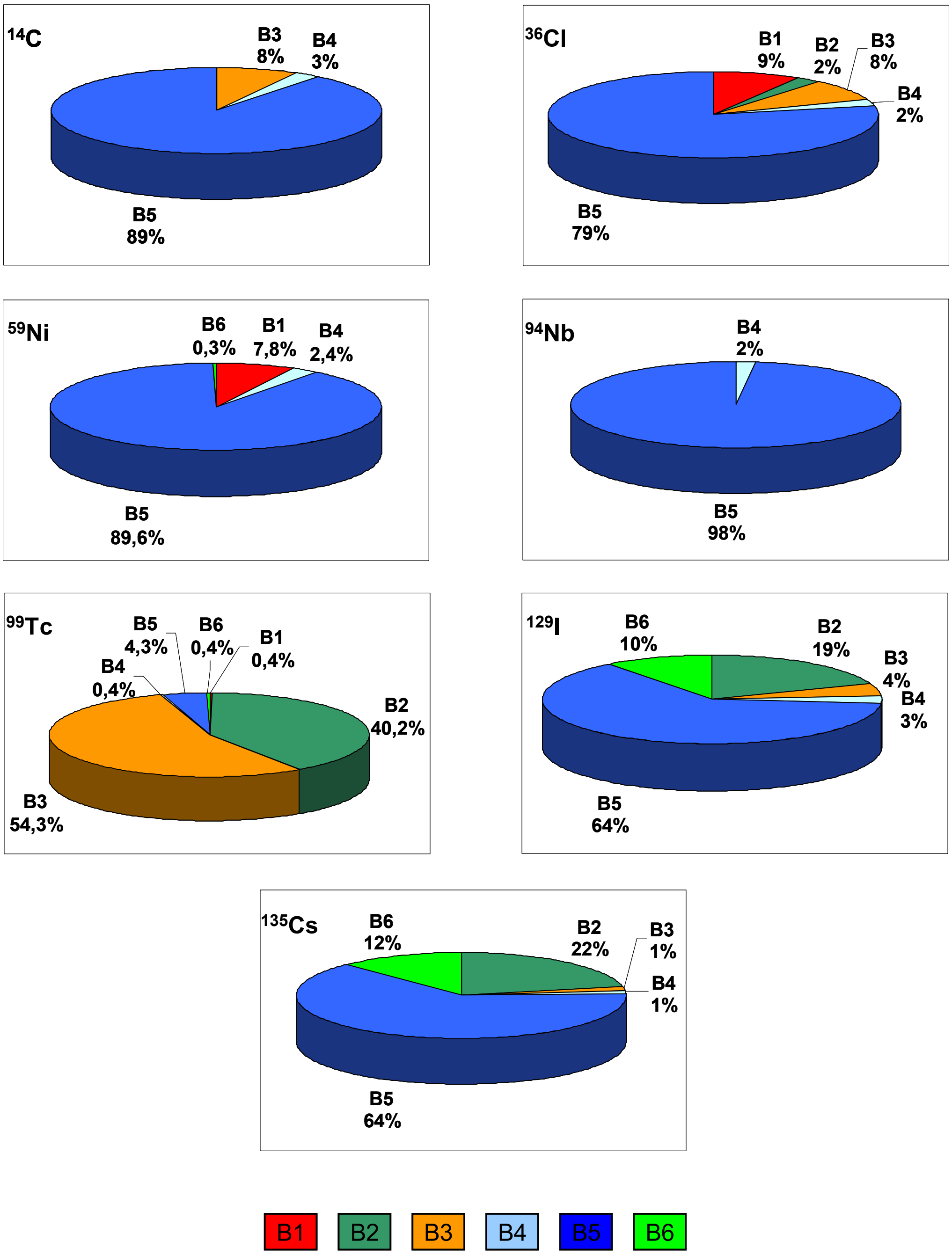

Figure 2.3.11 *Relative distributions (%) of ^{14}C, ^{36}Cl, ^{59}Ni, ^{94}Nb, ^{99}Tc, ^{129}I, ^{135}Cs, total uranium and total plutonium inventories in B waste reference packages for waste management scenario S1b*

Inset 2.2 ***List of 144 radionuclides selected for the radioactive inventory of HLLW packages***

Isotope	Half-life (years)	Isotope	Half-life (years)	Isotope	Half-life (years)	Isotope	Half-life (years)
Actinides							
^{226f}**Ra**	$1.60\cdot10^{3}$	^{236f}U	$2.34\cdot10^{7}$	^{244f}**Pu**	$8.00\cdot10^{7}$	^{247f}**Bk**	$1.38\cdot10^{3}$
^{228f}**Ra**	5.75	^{238f}U	$4.47\cdot10^{9}$	^{241f}**Am**	$4.33\cdot10^{2}$	^{249f}**Bk**	$8.76\cdot10^{-1}$
^{227f}**Ac**	$2.18\cdot10^{1}$	^{235f}**Np**	1.08	^{242m}**Am**	$1.41\cdot10^{2}$	^{248f}**Cf**	$9.13\cdot10^{-1}$
^{228f}**Th**	1.91	^{236f}**Np**	$1.52\cdot10^{5}$	^{243f}**Am**	$7.37\cdot10^{3}$	^{249f}**Cf**	$3.51\cdot10^{2}$
^{229f}**Th**	$7.34\cdot10^{3}$	^{237f}**Np**	$2.14\cdot10^{6}$	^{242f}**Cm**	$4.46\cdot10^{-1}$	^{250f}**Cf**	$1.31\cdot10^{1}$
^{230f}**Th**	$7.54\cdot10^{4}$	^{210f}**Pb**	$2.20\cdot10^{1}$	^{243f}**Cm**	$3.00\cdot10^{1}$	^{251f}**Cf**	$8.89\cdot10^{2}$
^{232f}**Th**	$1.41\cdot10^{10}$	^{236f}**Pu**	2.90	^{244f}**Cm**	$1.81\cdot10^{1}$	^{252f}**Cf**	2.65
^{231f}**Pa**	$3.28\cdot10^{4}$	^{238f}**Pu**	$8.77\cdot10^{1}$	^{245f}**Cm**	$8.50\cdot10^{3}$	^{252f}**Es**	1.29
^{232f}U	$6.98\cdot10^{1}$	^{239f}**Pu**	$2.41\cdot10^{4}$	^{246f}**Cm**	$4.73\cdot10^{3}$	^{254f}**Es**	$7.54\cdot10^{-1}$
^{233f}U	$1.59\cdot10^{5}$	^{240f}**Pu**	$6.56\cdot10^{3}$	^{247f}**Cm**	$1.60\cdot10^{7}$		
^{234f}U	$2.46\cdot10^{5}$	^{241f}**Pu**	$1.44\cdot10^{1}$	^{248f}**Cm**	$3.40\cdot10^{5}$		
^{235f}U	$7.04\cdot10^{8}$	^{242f}**Pu**	$3.74\cdot10^{5}$	^{250f}**Cm**	$8.00\cdot10^{3}$		

Isotope	Half-life (years)	Isotope	Half-life (years)	Isotope	Half-life (years)	Isotope	Half-life (years)
Fission products and activation products							
^{3f}**H**	$1.23\cdot10^{1}$	^{85f}**Kr**	$1.07\cdot10^{1}$	^{129f}**I**	$1.57\cdot10^{7}$	^{209f}**Po**	$1.00\cdot10^{2}$
^{10f}**Be**	$1.60\cdot10^{6}$	^{87f}**Rb**	$4.80\cdot10^{10}$	^{134f}**Cs**	2.06	^{157f}**Tb**	$9.82\cdot10^{1}$
^{14f}**C**	$5.73\cdot10^{3}$	^{90f}**Sr**	$2.91\cdot10^{1}$	^{135f}**Cs**	$2.30\cdot10^{6}$	^{158f}**Tb**	$1.81\cdot10^{2}$
^{22f}**Na**	2.60	^{93f}**Zr**	$1.53\cdot10^{6}$	^{137f}**Cs**	$3.00\cdot10^{1}$	^{154f}**Dy**	$2.85\cdot10^{6}$
^{26f}**Al**	$7.20\cdot10^{5}$	^{91f}**Nb**	$6.80\cdot10^{2}$	^{133f}**Ba**	$1.05\cdot10^{1}$	^{163f}**Ho**	$4.57\cdot10^{3}$
^{32f}**Si**	$1.72\cdot10^{2}$	^{92f}**Nb**	$3.50\cdot10^{7}$	^{137f}**La**	$6.00\cdot10^{4}$	^{166m}**Ho**	$1.20\cdot10^{3}$
^{36f}**Cl**	$3.02\cdot10^{5}$	^{93m}**Nb**	$1.64\cdot10^{1}$	^{144f}**Ce**	$7.80\cdot10^{-1}$	^{171f}**Tm**	1.92
^{39f}**Ar**	$2.69\cdot10^{2}$	^{94f}**Nb**	$2.03\cdot10^{4}$	^{143f}**Pm**	$7.26\cdot10^{-1}$	^{173f}**Lu**	1.37
^{42f}**Ar**	$3.30\cdot10^{1}$	^{93f}**Mo**	$3.50\cdot10^{3}$	^{144f}**Pm**	$9.95\cdot10^{-1}$	^{174f}**Lu**	3.31
^{40f}**K**	$1.28\cdot10^{9}$	^{97f}**Tc**	$2.60\cdot10^{6}$	^{145f}**Pm**	$1.77\cdot10^{1}$	^{176f}**Lu**	$3.61\cdot10^{10}$
^{41f}**Ca**	$1.03\cdot10^{5}$	^{98f}**Tc**	$4.20\cdot10^{6}$	^{146f}**Pm**	5.53	^{172f}**Hf**	1.87
^{44f}**Ti**	$4.72\cdot10^{1}$	^{99f}**Tc**	$2.13\cdot10^{5}$	^{147f}**Pm**	2.62	^{178n}**Hf**	$3.10\cdot10^{1}$
^{49f}**V**	$9.04\cdot10^{-1}$	^{106f}**Ru**	1.01	^{145f}**Sm**	$9.31\cdot10^{-1}$	^{182f}**Hf**	$8.99\cdot10^{6}$
^{53f}**Mn**	$3.70\cdot10^{6}$	^{101f}**Rh**	3.30	^{146f}**Sm**	$1.03\cdot10^{8}$	^{179f}**Ta**	1.77
^{54f}**Mn**	$8.56\cdot10-^{1}$	^{102f}**Rh**	2.90	^{151f}**Sm**	$8.87\cdot10^{1}$	^{186m}**Re**	$2.00\cdot10^{5}$
^{55f}**Fe**	2.70	^{102m}**Rh**	$5.67\cdot10^{-1}$	^{150f}**Eu**	$3.42\cdot10^{1}$	^{194f}**Os**	5.99
^{60f}**Fe**	$7.51\cdot10^{6}$	^{107f}**Pd**	$6.50\cdot10^{6}$	^{152f}**Eu**	$1.33\cdot10^{1}$	^{192n}**Ir**	$2.41\cdot10^{2}$
^{57f}**Co**	$7.43\cdot10^{-1}$	^{108m}**Ag**	$4.18\cdot10^{2}$	^{154f}**Eu**	8.60	^{193f}**Pt**	$5.07\cdot10^{1}$
^{60f}**Co**	5.27	^{110m}**Ag**	$6.84\cdot10^{-1}$	^{155f}**Eu**	4.96	^{195f}**Au**	$5.10\cdot10^{-1}$
^{59f}**Ni**	$7.50\cdot10^{4}$	^{109f}**Cd**	1.27	^{148f}**Gd**	$7.45\cdot10^{1}$	^{194f}**Hg**	$5.20\cdot10^{2}$
^{63f}**Ni**	$1.00\cdot10^{2}$	^{113m}**Cd**	$1.41\cdot10^{1}$	^{150f}**Gd**	$1.79\cdot10^{6}$	^{204f}**Tl**	3.78
^{65f}**Zn**	$6.69\cdot10^{-1}$	^{119m}**Sn**	$8.02\cdot10^{-1}$	^{153f}**Gd**	$6.63\cdot10^{-1}$	^{202f}**Pb**	$5.26\cdot10^{4}$
^{68f}**Ge**	$7.41\cdot10^{-1}$	^{121m}**Sn**	$5.00\cdot10^{1}$	^{208f}**Bi**	$3.68\cdot10^{5}$	^{205f}**Pb**	$1.52\cdot10^{7}$
^{79f}**Se**	$6.50\cdot10^{4*}$	^{126f}**Sn**	$1.00\cdot10^{5}$	^{210m}**Bi**	$3.00\cdot10^{6}$	^{207f}**Bi**	$3.80\cdot10^{1}$
^{81f}**Kr**	$2.10\cdot10^{5}$	^{125f}**Sb**	2.73	^{208f}**Po**	2.90		

* The May 2005 update of the NEA's national data base (JEFF-3.1 : Joint Evaluated Fission and Fusion File), used by Andra, shows an increase in the half-life of selenium 79 - by a factor of approximately 17 - to a period of 1.1 million years (Andra, 2005j)

2.3.4.6 Heat release of the reference waste packages

The radioactivity present in HLLW and spent fuel assemblies (Inset 2.3) is accompanied by a release of heat (Inset 2.4).

C waste packages and spent fuel assemblies release significant quantities of heat due to their high radioactivity, i.e., several thousand watts per C waste package upon production, and several thousand watts per spent fuel assembly 3 years after discharging from the reactor. Correlatively to radioactive decay, the heat release then decreases during a period ranging from several hundreds of years (C waste) to several thousands of years (spent fuels) (Figure 2.3.12).

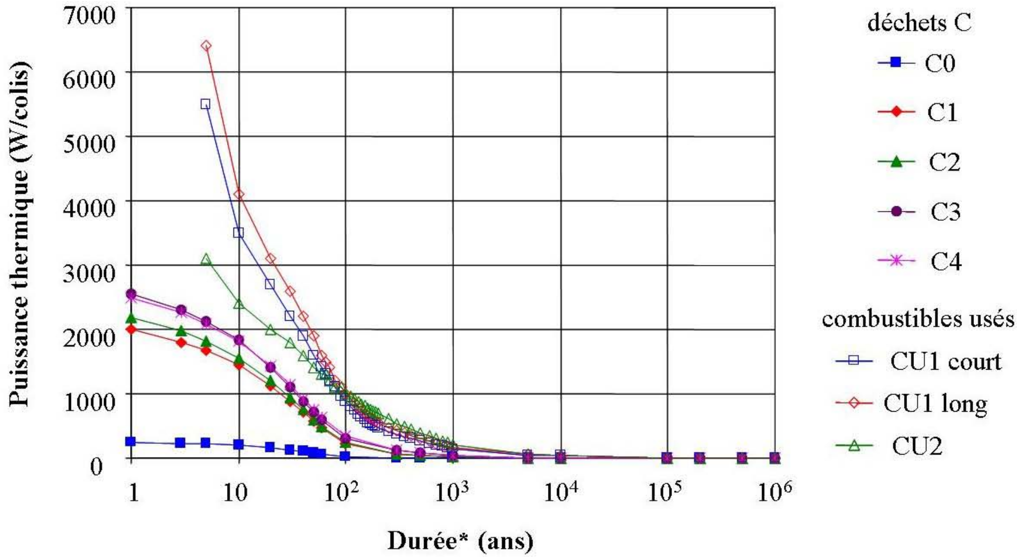

a) à l'échelle du million d'années

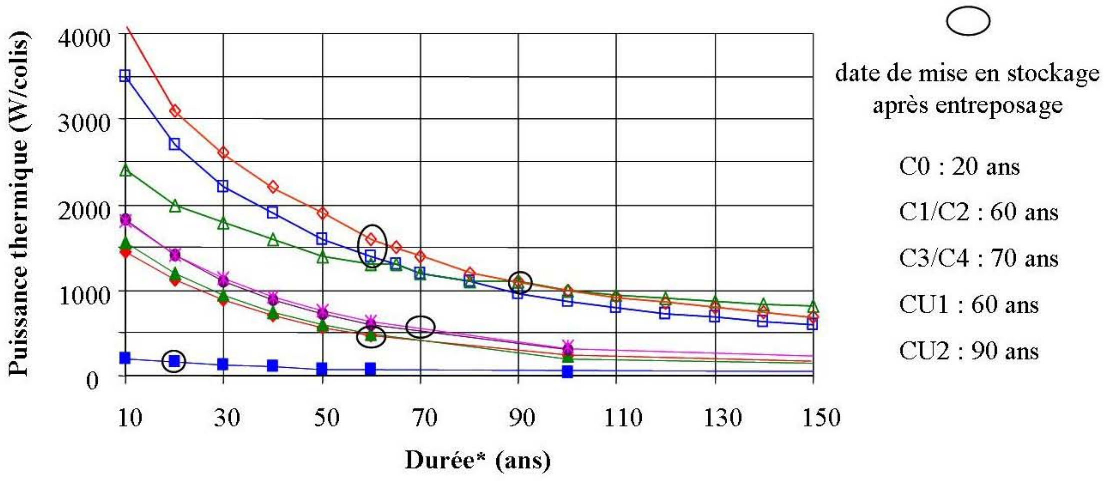

b) à l'échelle 10 – 150 ans

* durée comptée à partir de : la date de production pour les déchets C
la date de sortie du réacteur pour les combustibles usés

Figure 2.3.12 Heat release curves for C waste reference packages and spent fuels (Andra, 2005e)

Given the lower radioactivity of B waste packages with respect to C waste packages and spent fuel assemblies, they release little or no heat. Among B waste packages, B1 and B5 are considered as slightly exothermic. Their heat release ranges from a few watts to a few tens of watts upon package production and decreases very strongly over a few tens of years (Figure 2.3.13).

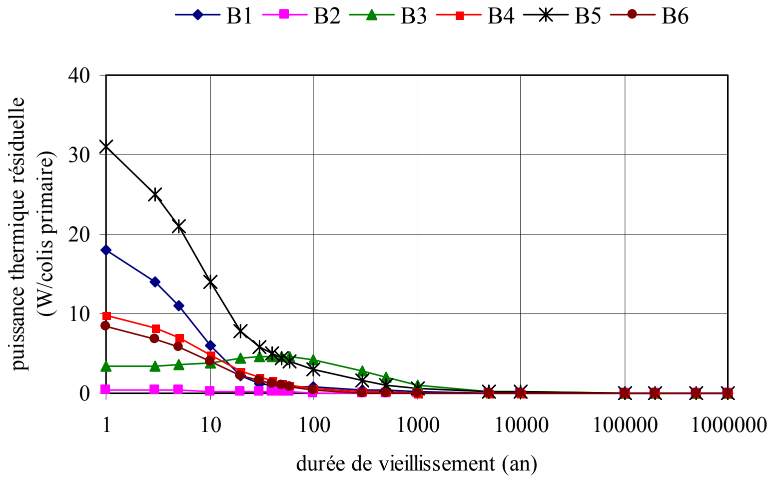

Figure 2.3.13 Heat release curves for B waste reference packages (Andra, 2005e)

2.3.4.7 External dose rates of primary packages

The βγ activity of primary waste packages causes external radiation (Inset 2.3). Among primary packages, C waste packages (to a lesser degree), spent fuels and B1 and B5 packages are associated with the highest external irradiation levels (Andra, 2005i), as indicated in table 2.3.5.

Table 2.3.5 Maximum dose rate in contact with various primary packages upon conditioning in disposal packages for subsequent disposal

Types of waste	Primary package type	Content type	Maximum dose rate in contact with primary packages or spent fuel assemblies ($Sv.h^{-1}$)
B	**B1**	Compacted activation waste	25
	B2	Bituminised waste	2
	B3	Compacted or cemented technological waste	0.5
	B4	Cemented cladding waste	0.5
	B5	Compacted cladding waste with or without technological waste	15
	B6	Cladding and technological waste placed in drums	2
C	**C**	Vitrified waste	250
Spent fuels	**CU1**	UOX/enriched uranium spent fuel assemblies	25
	CU2	MOX spent fuel assemblies	15

Inset 2.3 ***Radiation emitted by radionuclides***

Radionuclides emit three types of radiation:

Alpha (α) radiation

Alpha (α) radioactivity results from the emission of a helium nucleus composed of 2 protons and 2 neutrons (electric charge +2). It mainly concerns heavy nuclei, i.e., actinides. These nuclei are unstable and emit a light helium nucleus to decrease their electric charge and thereby become more stable. The Coulombian repulsion energy released during an alpha disintegration takes the form of kinetic energy shared by the α particle and the recoiling nucleus. The α particles carry away approximately 98 % of the energy, i.e., a few million electronvolts (MeV). α radiation is stopped very quickly by matter (it travels a few centimeters through air and a sheet of paper stops it).

The periodes alpha disintegration half life are often long, as in the case of thorium-232 (^{232}Th) and uranium-238 (^{238}U), which take billions of years to disintegrate. But radium-226 (^{226}Rd), for example, has a disintegration half life of 1,600 years.

Gamma (γ) radiation

Gamma radiation is of the same type as X rays or the light emitted by atoms (electromagnetic radiation), but the energy transported is much higher, i.e., 100,000 to a few million electronvolts. Gamma radiation generally follows an alpha (α) or beta (β) disintegration or the capture of a neutron by a nucleus. These events generally leave the nucleus in an excited state, i.e., with additional energy as compared to its natural or 'fundamental' state. The nucleus then loses this over energy in one or more steps, emitting an electromagnetic energy grain (gamma photon) each step. Gamma radiation is very penetrating (it can pass through several centimeters of lead).

Beta (β) radiation

β^- radioactivity results from the emission of an electron and an antineutrino accompanying the transformation of a neutron into a proton. β^+ radioactivity corresponds to the transformation of a proton into a neutron with the emission of a positron and a neutrino. The disintegration energy is shared among the three participants, i.e., the recoiling nucleus, the electron (or positron) and the antineutrino (or neutrino). The nucleus, whose mass is very large compared to that of the other participants, carries away practically no energy. Since over neutrons are frequent among natural radioactive nuclei, β^- radioactivity is by far the most frequently observed. β radiation is more penetrating than α radiation but less so than γ radiation. It travels a few meters through air and a sheet of aluminium will stop it.

An example of β^- radioactivity is potassium-40 (^{40}K), a very long-lived natural isotope of Potassium that is contained naturally in the human body and disintegrates into calcium-40 (^{40}Ca).

Inset 2.4 ***Origin of heat release from HLLW packages and spent fuels***

Radiation-matter interactions

The radioactive elements contained in the waste emit β/γ and α radiation that is partially or completely slowed down within the waste and/or the waste conditioning matrix (in glass, for example). All or part of this radiation's kinetic energy is then transformed into heat.

The quantity of heat released over time by the waste therefore mainly depends on the type and quantity of radioactive elements contained and decreases proportionally to their radioactive decay.

γ radiation contributes more significantly to the total heat release than α radiation. It mainly corresponds to short to medium-lived radionuclides, particularly ^{137}Cs (radioactive half-life of approximately 30 years) or ^{60}Co (approximately 5.2 years).

Vitrified waste and spent fuels

Vitrified waste and spent fuel assemblies have high inventories of ^{137}Cs. This is the reason for their particularly high heat release, i.e., several thousand watts during the first ten years after vitrified waste package production, or after exiting the reactor in the case of spent fuel assemblies. The total β/γ activity then decreases by a factor of approximately 2 every 30 years (half-life of ^{137}Cs), attaining a few hundred watts after 100 years. Beyond a few hundred years, the β/γ emitters are less numerous than the medium and long-lived α emitters. The heat release is then mainly due to the α emitters, and less heat is released (in the order of a few tens of watts). Spent fuels have a higher α emitter inventory and a slower thermal decay rate than vitrified waste.

B waste

^{60}Co (higher inventory than ^{137}Cs) plays the leading role in B waste heat release, particularly for B5 and B1 reference packages. Due to its half-life of 5 years, a significant decrease in B waste heat release occurs during the first tens of years, attaining values ranging from a few watts to less than 1 watt per primary package after 100 years.

2.4 Repository concepts (Andra, 2005i)

The technical options proposed for the design of underground installations and disposal packages satisfy three requirements (Andra, 2005i):

- long-term safety functions;
- reversibility and flexible operation;
- security and operating safety.

Compactness is also sought.

They are defined based on **(i)** HLLW and spent fuel inventories and characteristics and **(ii)** the various characteristics (geometric, geological, geochemical, hydrogeological, geomechanical, etc.) of the Callovo-Oxfordian layer.

2.4.1 Long-term safety and reversibility

2.4.1.1 Long-term repository safety functions

The main objective of the long-term management of high-level long-lived waste (HLLW) is to protect humans and the environment from the risks associated with the existence of said waste, both during the industrial operating phase and in the long term. The solution provided by the repository is based on the confinement of the waste in the Callovo-Oxfordian layer. This is ensured in a passive manner over large periods of time (designed for up to a million years).

In addition, the repository architectures and concepts proposed include the implementation of reversibility and appropriate measures to facilitate it. Andra associates it with repository management flexibility.

This objective is recalled in basic safety rule no. III.2.f: "The short and long-term protection of humans and the environment is the fundamental objective assigned to a deep geological waste disposal facility". This protection of humans and the environment is ensured by preventing the dissemination of the radionuclides contained in the waste, without relying on maintenance or surveillance in the long term. The basic safety rule specifies the following: ""It (the protection of humans and the environment) must be ensured for all risks associated with the dissemination of radioactive substances in all the situations taken into account, without depending on institutional controls for which there is no certainty beyond a limited period of time" (RFS n° III.2.f, 10 juin 1991).

In order to prevent radioactive dissemination over the different time scales considered, various safety functions are conferred to a deep geological repository. These safety functions mutually complement one another, thereby optimising the global performance of the system. They offer a certain degree of redundancy to ensure better resistance to failures or external aggressions.

It must first be noted that the deep repository protects the waste from erosion phenomena and principal human activities which affect only a superficial thickness of the terrain over a period of hundreds of thousands of years (see section 9 on long-term geological and climatic changes).

Within this context, the safety functions can be summarised as follows:

(i) ***Preventing the circulation of water inside the repository***

Deep geological formations are initially saturated with water. Water flow near the waste constitute the main factor capable of altering the packages and allowing the release of radioactive elements inside the repository (see section 7 on the chemical evolution of the repository). A circulation of this water therefore constitutes a potential radionuclide transfer mode (see section 10 on radionuclide transport).

(ii) ***Limiting the release of radionuclides and immobilising them in the repository*** (i.e., protecting the waste)

Since water flow into the waste cannot be excluded in the long term (see section 6 on the hydraulic evolution of the repository and its geological environment), it is important to limit the release of radionuclides into the water and to immobilise them in the waste as much as possible.

In order to achieve this, the first step is to implement waste packages preventing the dispersion of radionuclides (for example, by means of the matrix in which the radionuclides are incorporated or the containers in which the waste is placed). The aqueous alteration of the waste and their conditioning is limited by placing the waste in favourable, physical and chemical environnements.

(iii) ***Delaying and attenuating radionuclide migration towards the environment***

In order to protect humans and the environment from radionuclides possibly released by the waste, the released flux must be delayed and attenuated over space and time.

The Callovo-Oxfordian formation has been chosen for its low permeability and solute diffusion coefficient values and its high retention capabilities. Radionuclide migration can also be delayed within certain repository components.

For this purpose, it is necessary:

- **to make the most of the favourable properties of the Callovo-Oxfordian argillites** (low permeability, retention capabilities, geochemical properties, hydrogeological environment). The age of the formation, its tectonic stability and its depth ensure a great stability of the Callovo-Oxfordian layer's properties over a period of a million years.

And, correlatively:

- **to preserve the favourable properties of the geological medium and limit the perturbations induced by the repository**, by controlling perturbations possibly due to i) the excavation of the underground engineered structures (particularly the mechanically damaged zone of the Callovo-Oxfordian layer around the repository structures), ii) added materials (particularly the effect of concrete pore water on argillites) and iii) the presence of waste (and associated thermal loading in particular).

2.4.1.2 Taking reversibility into account

Reversibility can be defined as the possibility of progressive and flexible control of disposal processes, granting future generations a freedom of choice regarding the repository.

Within this perspective, the disposal process can be broken down into a series of steps to be completed. The goal is to provide maximum flexibility for managing each step, particularly by allowing the possibility of a standby and observation period before deciding to proceed to the next step (or return to a previous step).

Reversibility therefore covers a larger scope of action than package 'recoverability' and can be evaluated in terms of the following:

(v) capacity to remove stored packages;
(vi) capacity to intervene in the disposal process;
(vii) possibility to modify the design of the engineered structures during the disposal process.

Reversibility contributes to providing a means to control the repository based on the expectations of the various generations concerned.

2.4.2 Design issues addressing the safety and reversibility requirements

2.4.2.1 Repository location in the middle of the Callovo-Oxfordian layer

In order to take into account the nearly horizontal geological structure of the Callovo-Oxfordian layer and preserve a sufficient minimum distance between the repository and the surrounding formations, the repository is constructed on a single plane within the layer.

At the location of the Meuse / Haute-Marne underground research laboratory, the Callovo-Oxfordian layer has a thickness of approximately 135 meters. The repository is therefore positioned in the middle of the Callovo-Oxfordian layer. This corresponds to a distance of 65 meters between the roof and wall of the layer and the midplane of the repository, thus ensuring a clearance of 60 meters of argillites between the repository (average thickness: 10 meters) and the surrounding carbonated Oxfordian and Dogger formations (Figure 2.4.1).

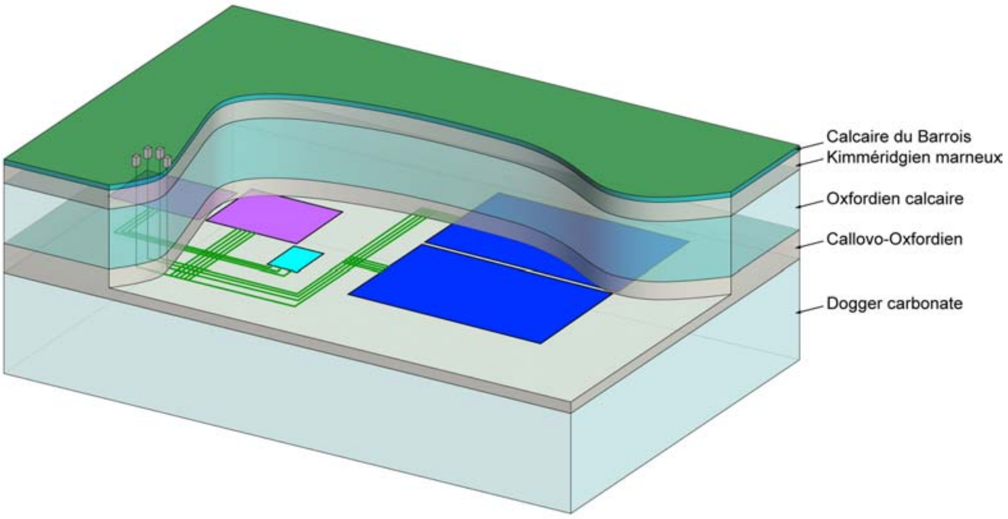

Figure 2.4.1 Diagram of the repository's location in the middle of the Callovo-Oxfordian layer (reference location of the underground research laboratory)

The thickness of the Callovo-Oxfordian layer increases from the underground research laboratory over the rest of the transposition zone (refer to the definition provided in section 2.2 and Inset 3.2) ; For any other position of the repository within the transposition zone, the distance of 65 meters between the roof of the layer and the midplane of the repository is adopted by convention.

2.4.2.2 Orientation of the engineered structures to limit mechanical perturbations

In order to limit the mechanical stresses exerted by the repository structures on the argillites in the near-field (particularly to prevent the formation of a excavated disturbed zone in the near field with permeability zone larger than this of undisturbed argillites, which could increase water fluxes within the repository or significantly decrease the migration times of the radionuclides released by the packages), the disposal cells and the drifts accommodating the repository's hydraulic closure seals are oriented in the direction of the major mechanical stress (see section 8)

2.4.2.3 Compactness of the repository to limit mechanical perturbations

Empty spaces and residual gaps within the repository after its closure are generally minimised to ensure a compactness limiting mechanical deformations of the repository and its geological environment. This is the purpose of the drift backfill (as dense as possible).

2.4.2.4 Limiting the increase in temperature associated with the heat release from waste packages

- **Maximum temperature of 90 °C for C waste and spent fuels**

C waste and spent fuels are characterised by significant heat release. At this stage of the studies, in order to remain within a temperature domain that is currently well understood in terms of **(i)** evolution of the materials, **(ii)** knowledge and modelling of the phenomena involved and **(iii)** limited or negligible impact on the properties of the repository components and Callovo-Oxfordian layer, a maximum temperature of 90 °C is defined for C waste in contact with argillites and for spent fuels in contact with the buffer (Inset 2.5).

- **Maximum temperature of 70 °C for B waste (exothermic)**

For B waste, the maximum temperature adopted is 70 °C. More specifically, the B2 reference package (bituminised sludges) disposal modules are designed to keep the temperature inside the disposal cells below 30 °C, thus preserving the integrity of the bitumen and its confinement capabilities (Inset 2.5).

- **Temporary storage period prior to disposal for C waste and spent fuels**

The maximum temperature requirements imply an adapted distribution of the packages (disposal cells) within the repository (see section 2.4.2.5 below) and a interim storage period for the various options proposed, i.e.:

- 60 years for C1 and C2 packages;
- 70 years for C3 and C4 packages;
- 60 years for CU1 packages;
- 90 years for CU2 packages.

Inset 2.5 ***Thermal criteria adopted for the repository design***

The 'thermal' dimensioning of the repository mainly consists of defining the number of waste packages per cell, the distances between adjacent disposal cells and the interim storage periods for waste packages (i.e., heat energy upon placement in the repository). It is based on the definition of 'thermal criteria' corresponding to maximum temperature thresholds or admissible temperature ranges for the various repository components. Given the current knowledge base, these thresholds are defined with respect to **(i)** the available data concerning the phenomenological behaviours of repository components and radionuclides, and **(ii)** the effects of temperature on said behaviours.

Status and control of knowledge regarding phenomenological behaviours

- ✓ In general, temperatures above 100 °C associated with high temperature gradients (exceeding a few degrees per metre) increase the chemical reactivity of argillites, concretes and metals and are the cause of complex hydraulic and mechanical phenomena. Moreover, under such conditions, there are numerous experimental difficulties in acquiring phenomenological knowledge. At this stage of the repository feasibility studies, it has therefore been decided to define a maximum temperature of 100 °C within the repository, particularly for clays (argillites and swelling clays). A margin of 10 °C, i.e., a **maximum admissible temperature of 90 °C**, has been adopted so as to take into account the uncertainties regarding the thermal properties and models associated with the thermal dimensioning of the repository, particularly for C waste and spent fuels. This maximum temperature excludes the boiling of liquid water and limits the mineralogical transformations of the argillites and swelling clay-based components.

- ✓ However, since the chemical behaviour of the cement-based materials is not well understood at temperatures beyond 70-80 °C, a maximum temperature of 80 °C has been defined for the cement-based materials of B waste disposal cells. A margin of 10 °C corresponding to a **maximum admissible temperature of 70 °C** has therefore been adopted for the thermal dimensioning of B waste disposal cells. More specifically, in the case of **bituminised sludge packages**, a **maximum temperature of 30 °C** has been defined so as to limit the creep rate and chemical reactivity of the bitumen.

Effects of temperature on the release and migration of radionuclides within the repository and the Callovo-Oxfordian layer (leak tightness of C waste and spent fuel containers)

The aqueous dissolution rate of glass increases exponentially with temperature, namely beyond 50 °C. The absence of water in contact with the glass matrix during the period when package core temperatures exceed 50 °C therefore prevents an overly important initial dissolution regime of the glass. After the transient phase of initial dissolution, the dissolution kinetics of the glass is controlled by the solute transport conditions, the chemistry of the waters and retention properties of the external environment. This data is poorly understood for temperatures exceeding 50 °C and high thermal gradients. The same applies to the behaviour of radionuclides in a solution, for both vitrified waste and spent fuels.

It is therefore necessary to ensure the **leak tightness of C waste and spent fuel containers when the temperature in the environment near the packages exceeds 50 °C**. For vitrified waste primary packages, this leak tightness is ensured by the over-pack design.

2.4.2.5 Modular and compartmented repository design

The modular and compartmented repository design makes it possible to:

- to ensure a large flexibility in terms of waste management, repository operation and reversibility
- to limit the phenomenological interactions between the various waste categories (and families within the same category), particularly thermal interactions, and thereby preserve radionuclide confinement properties
- to limit the consequences of altered events due to failure or intrusion in the repository.

- **Repository zones dedicated to different types of waste**

The repository consists of distinct zones separated by several hundreds of meters from one another, i.e., the access shaft zone (connecting to the surface) and dedicated waste disposal zones (B, C0, C, CU1, CU2). A network of connecting drifts connects the repository zones and the access shafts (Figure 2.4.2).

As far as the repository design is concerned, the following can be distinguished:

- B and C0 waste repository zones characterised by *non-exothermic or slightly exothermic packages* that can be placed in the repository without a prior interim storage period. These zones require relatively small horizontal footprints and small quantities of construction work. The dimensioning of these zones and the connecting drifts to service them does not appear to be significantly affected by the date of placement in the repository or by construction and operating rhythms.
- C waste (other than C0) and CU1 and CU2 spent fuel repository zones characterised by *highly exothermic packages* requiring a significant interim storage period. These zones require large horizontal footprints and large quantities of construction work. The dimensioning of these repository zones and their connecting drifts is affected by the date of placement in the repository and by construction and operating rhythms.

- **Modularity and compartmentation of each disposal zone**

In order to satisfy the compartmentation and modularity requirements ensuring long-term safety and favouring flexibility and progressiveness in repository construction and operation, the repository zones are subdivided into sub-zones, modules and disposal cells (Figure 2.4.2).

In order to separate waste with different behaviours (B waste packages) and ensure flexible construction and operation (C waste and spent fuel packages), each repository zone is divided into 2 to 4 *sub-zones* each comprising several *modules*.

The *disposal modules* constitute the base elements of the repository's compartmentation in accordance with long-term safety requirements. Each zone is thus divided into at least a dozen disposal modules[5].

Regarding organisation, the disposal modules may be subdivided into operating units each devoted to a single activity (construction, operation or closure) during a period of several months or years.

In zone B, each module consists of a *cell* and its *access drift* and constitutes an *operating unit*. In the C waste and spent fuel zones, each module consists of several tens of *disposal cells* and three associated *access drifts*, and is subdivided into two *operating units*.

Figure 2.4.2 shows the general architecture of the repository for waste production scenario S1a.

---

[5] For zones with low inventories, the number of modules may be less than 10.

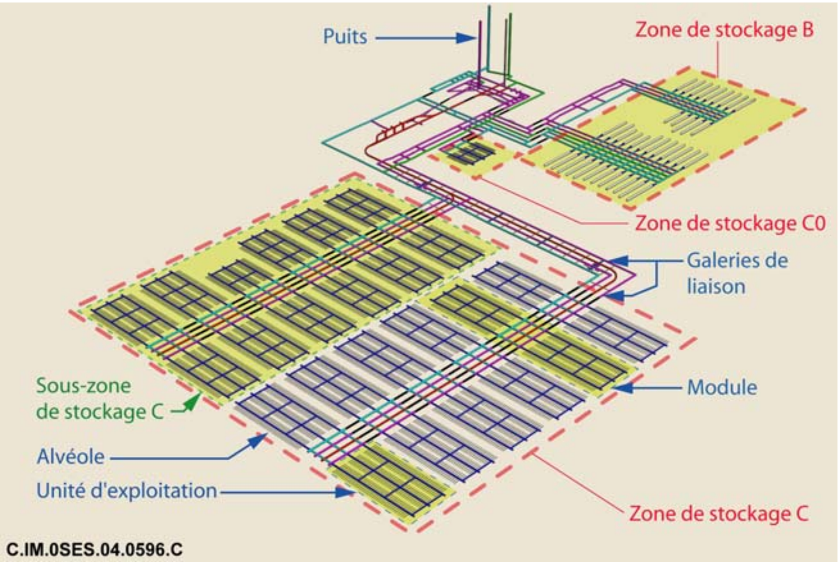

Figure 2.4.2 *Example of the general organisation of the repository (case of waste production scenario S1a)*

- **B waste disposal cells dedicated according to the presence of organic compounds and/or hydrogen production**

B packages have various different physical and chemical characteristics. In order to prevent and limit phenomenological interactions between packages, repository zone B is subdivided into two sub-zones:

- sub-zone 1 receives packages not containing organic matter
- sub-zone 2 receives packages containing organic matter

In each sub-zone, an inter-cell distance of 72 m (5 times the diameter of the disposal cells) has been adopted so as to minimise the mechanical interactions between disposal cells.

It must be noted that sub-zone 1 also corresponds to the most radioactively active and hottest B waste packages. This separation therefore keeps hot waste packages at a distance, particularly with respect to the bitumen packages of sub-zone 2, which are sensitive to heat.

This subdivision corresponds to three types of disposal cells (Table 2.3.4):

Sub-zone 1

- ***Disposal cells*** that contain waste comprising no organic compounds but producing hydrogen through radiolysis of the concrete in the primary packages
- ***Disposal cells*** that contain waste comprising no organic compounds and producing no hydrogen through radiolysis

Sub-zone 2

- ***Disposal cells*** corresponding to B waste (mainly bituminised waste) containing organic compounds or matter and producing hydrogen through radiolysis of the organic matter.

Table 2.4.1 Distribution of B waste reference packages per cell

B waste reference packages grouped in distinct disposal cells
B3.1.1 – B3.1.3 – B3.2 – B3.3.2 – B4
B1 – B5.2 – B5.3
B2 – B3.1.2 – B3.3.1 – B3.3.3 – B3.3.4 – B5.1

- **Modularity of C waste and spent fuel repository zones limiting the thermal loading and allowing flexibility**

The organisation of the repository zones is similar to the general architecture of the repository. Their design and dimensioning are very strongly determined by thermal considerations. To facilitate the organisation of their construction, operation and closure, these zones are divided into sub-zones approximately 2 km long and 1.5 km wide. Each sub-zone is divided into 8 to 12 operating units. Each operating unit comprises 80 to 220 disposal cells. The disposal cells are spaced approximately 15 to 20 meters apart so as to contribute to the observance of the maximum temperature criterion (90 °C).

- **Grouped access shafts**

The surface facilities and underground facilities are connected by a group of shafts shared by all repository zones and compatible with all fluxes generated by the various waste production scenarios (S1a, S1b, S1c and S2). There are 4 shafts respectively ensuring package transfers, air return, personnel transfers and material transfers associated with the construction, operation and closure of the repository.

The shafts are grouped together in a zone with a radius of approximately 200 m, off-centred with respect to the repository zones. The access shaft zone may be located upstream of the hydraulic load gradient in the carbonated Oxfordian with respect to the repository zones.

The useful diameter of the shafts varies from 6.5 m for the personnel shaft to approximately 10 to 11.5 m for the other shafts. The shafts are made impermeable to the Barrois limestones by a moulded wall. In the Callovo-Oxfordian layer, the shafts have a concrete support / coating approximately 1.7 m thick.

- **Connecting drift network**

The disposal modules are connected to the shafts via *connecting infrastructures* consisting of parallel *connecting drift* network. This network is hierarchised into *main connecting drifts* linking the shaft zone to the various repository sub-zones and *secondary connecting drifts* within each sub-zone. This hierarchisation allows for flexible construction and operation of the repository by making the various sub-zones independent from one another.

The diameter of the drifts has been voluntarily limited to the smallest possible cross-section on account of the fluxes passing through these drifts. The useful diameter of the connecting drifts is about 5 meters, with horseshoe cross-section.

The drifts are supported by projected concrete 20-cm thick and coated with B60 concrete 35 or 65 cm thick, depending on the orientation of the drifts with respect to the natural mechanical stresses.

2.4.2.6 Dedicated containers and disposal packages for different types of waste

B and C waste primary packages and spent fuel assemblies are conditioned in disposal packages prior to placement in the repository. The disposal packages are placed in the disposal cells (Andra, 2005i).

- **B waste concrete disposal packages**

B waste primary packages are grouped in concrete containers according to package type so as to minimise handling and facilitate standardisation of operations (Figure 2.4.3). They consist of an canister and a cover.

Various types of containers may be used so as to take into account the specific characteristics of the reference packages. For example, for reference packages producing hydrogen (such as bituminised sludge packages), the covers are designed to allow the evacuation of the hydrogen produced.

B waste disposal packages consist of a concrete container, B waste primary packages and filling material. The disposal packages are stacked inside the disposal cells.

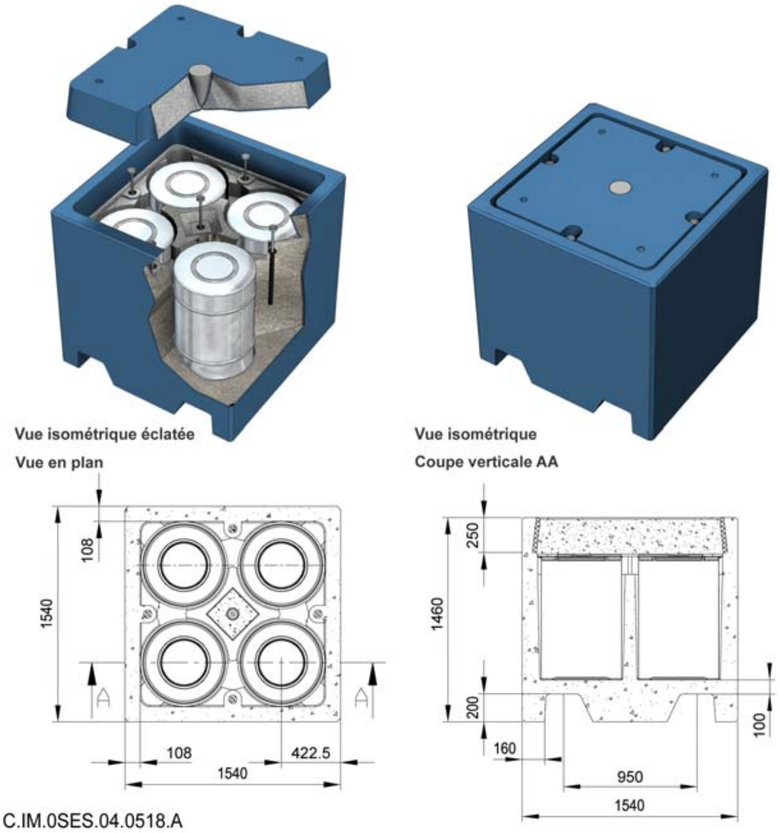

Figure 2.4.3 Example of a basic diagram of a B waste disposal package

- **Thick carbon steel over-pack for C waste primary packages and thick carbon steel container for spent fuels**

Each C waste primary package is placed in a carbon steel over-pack 55 mm thick. This consists of two parts welded together, i.e. a body consisting of a cylindrical canister with integrated bottom and a cover (Figure 2.4.4)

The spent fuel assemblies are conditioned in a carbon steel container consisting of a cylindrical shell approximately 110 mm thick and a welded cover. CU1 spent fuel assemblies are placed in the container in groups of four, separated inside the container by an iron and possibly preconditioned in a stainless steel cladding. CU2 disposal packages only comprise a single assembly (Figure 2.4.5).

The thick carbon steel overpack and container enable handling and possible removal of packages for reversibility purposes. Their mechanical resistance and slow corrosion guarantee leak tightness over a period defined as approximately 4,000 years for vitrified waste and 10,000 years for spent fuels.

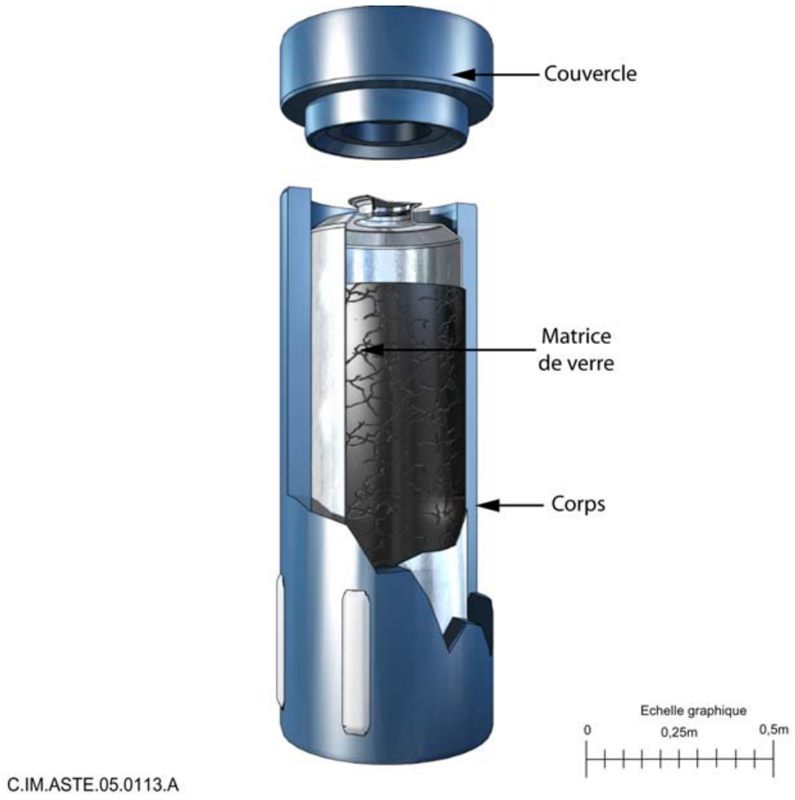

Figure 2.4.4 Diagram of a C waste disposal package

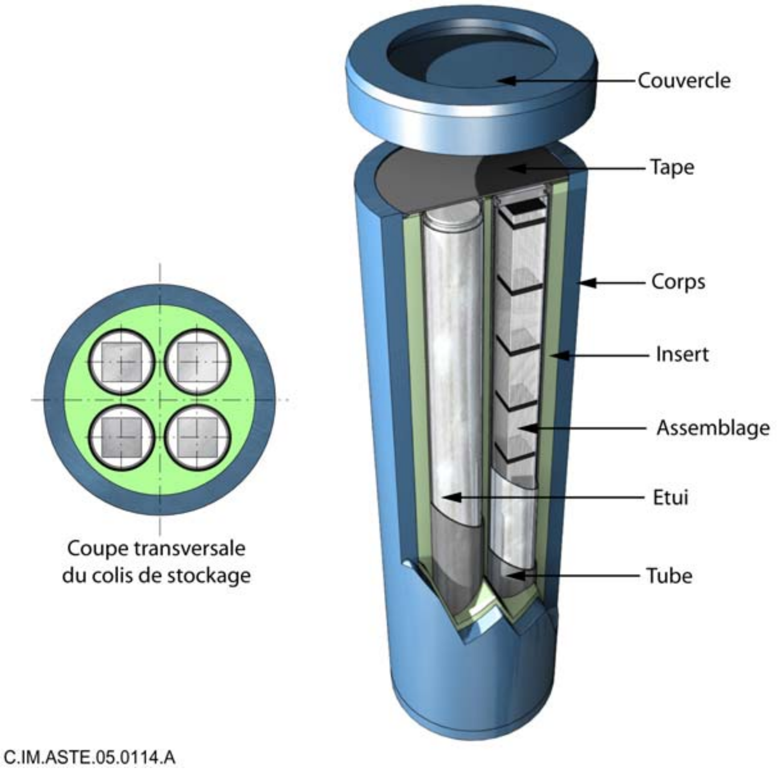

Figure 2.4.5 Diagram of a CU1 spent fuel disposal package

In the disposal cells, the C waste and spent fuel disposal packages are arranged horizontally inside a metallic lining (see section 2.4.2.7). Buffers similar to the disposal packages and filled with an inert material are placed between the disposal packages to contribute to maintaining the temperature inside the disposal cells below 90 °C (Figure 2.4.8, Figure 2.4.9). The number of disposal packages varies from 6 to 18 for C waste disposal cells and 3 to 4 for spent fuel disposal cells.

- **Decreased external dose rates with disposal packages**

The canister of the disposal packages contribute to decreasing the external dose rates due to βγ radiation with respect to the primary packages (see section 2.3.4.7). This is particularly the case with C waste and spent fuels due to the thickness of their metallic container, as indicated in table 2.4.2.

Table 2.4.2 Estimation of the maximum dose rates in contact with the various disposal packages upon placement in the repository

Type of waste	Type of disposal package	Type of disposal package envelope	Maximum dose rate in contact with disposal package ($Sv.h^{-1}$)
B	B1, B5	Concrete	≤ 10
	B2	Concrete	≤ 1
	B3, B4	Concrete	
C	C	Steel	≤ 10
CU	CU1	Steel	≤ 0.1
	CU2	Steel	≤ 0.01

2.4.2.7 Disposal cells specifically designed for each type of waste (Andra, 2005i)

- **Concrete tunnels for B waste**

The disposal cell selected is a subhorizontal dead-end tunnel with an excavated diameter of approximately 10 to 12 meters and a useful length of 250 meters. It is coated with concrete and comprises a concrete roller slab. The cell constitutes an irradiating chamber in which the packages are stacked. For this purpose, a supplementary volume of concrete is added to the coating so as to constitute a disposal chamber with a rectangular section dimensions suited for the shape of the stack of packages. The decimetric gaps left between the disposal packages (i.e., total empty space between disposal packages amounting to less than 5 % of the excavated cross-section) allows for easy removal of disposal packages for reversibility purposes.

The disposal cell is ventilated throughout its operating period to evacuate gases produced by packages, thereby also contributing to decreasing the temperature during the first years of package disposal. It is connected to the access infrastructure by an entrance drift with an excavated diameter of between 7 and 8 m. This drift is sealed upon closure of the disposal cell.

The B waste disposal cell concept is illustrated in figure 2.4.6.

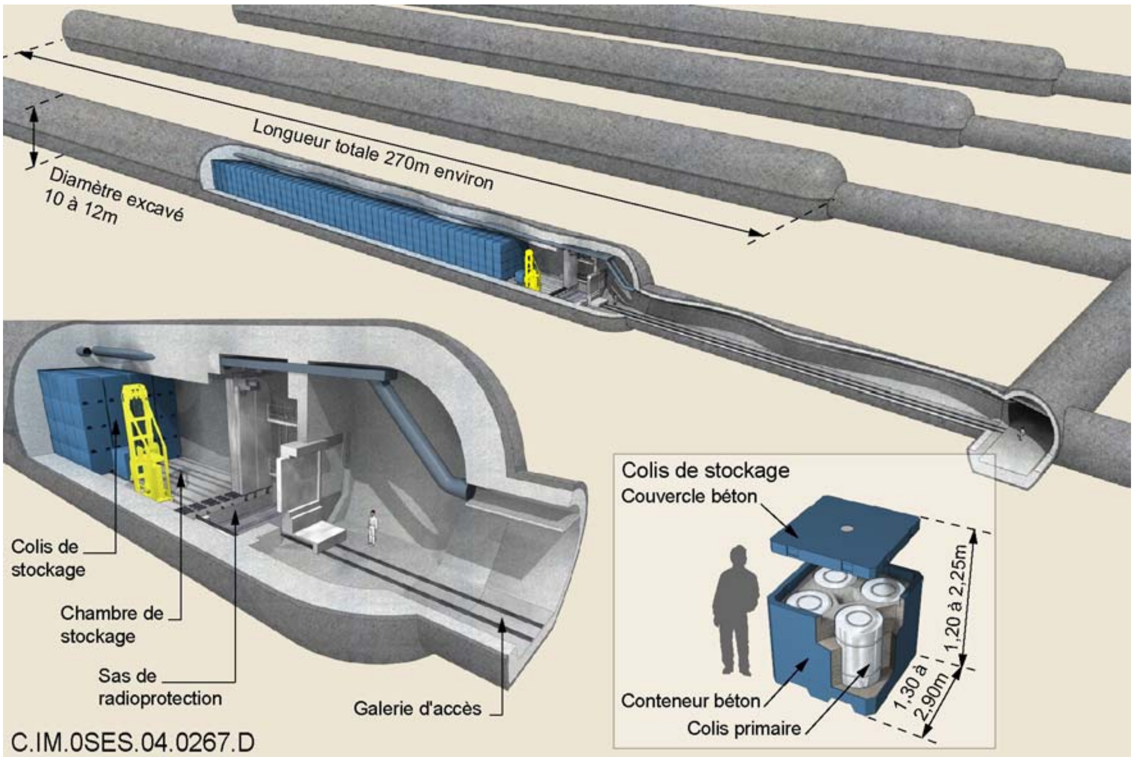

Figure 2.4.6 Basic diagram of a B waste package disposal cell in operating configuration

- **Small-diameter tunnels for C waste and spent fuels**

The C waste and spent fuel package disposal cells are subhorizontal dead-end tunnels approximately 40 m long comprising a 'useful part' to accommodate the disposal packages and a cell head to seal the cell. They are constructed and operated from the access shafts. Each tunnel has an inner lining consisting of a thick, low or non-alloy steel tube in which the disposal packages are inserted. This lining has a thickness ranging of between 25 mm (C waste and CU2 spent fuels) and 40 mm (CU1 spent fuels) allowing for the possible removal of packages for reversibility purposes.

The C waste disposal cell concept adopted is a tunnel whose diameter corresponds to that of the disposal package (approximately 0.7 m), with the steel inner lining then serving as a support base (see Figure 2.4.7 and Figure 2.4.8). The tunnel for the spent fuel packages has a larger diameter (approximately 3 m and 2.5 m for CU1 and CU2 packages, respectively). A coating consisting of a thick, perforated, low or non-alloy steel tube supports it. The space between the argillites and the inner lining is filled with a swelling clay-based material implemented in the form of rings and constituting buffer (Figure 2.4.9).

The heat produced by the C waste and spent fuels is only evacuated through passive conduction in the geological environment. No ventilation is required for this process. The disposal cells are closed with an operating plug (leak tight cover) that prevents the exchange of air between the disposal cells and the access drifts.

The C waste and spent fuel disposal cell concepts are illustrated in figure 2.4.7, figure 2.4.8 and figure 2.4.9.

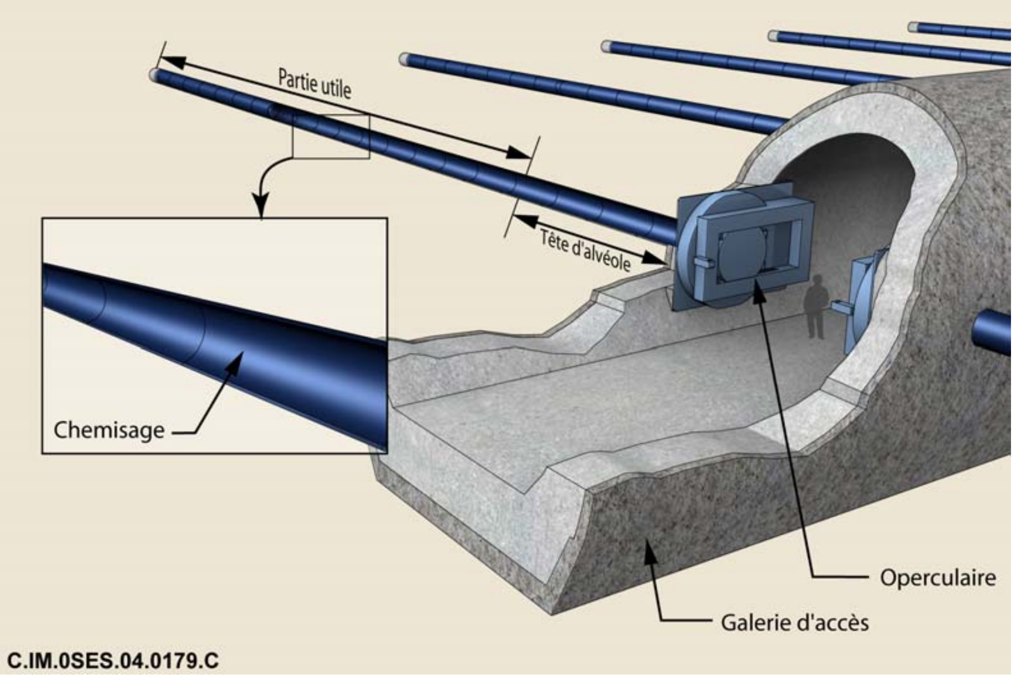

Figure 2.4.7 Basic diagram of a C waste package disposal cell in operating configuration

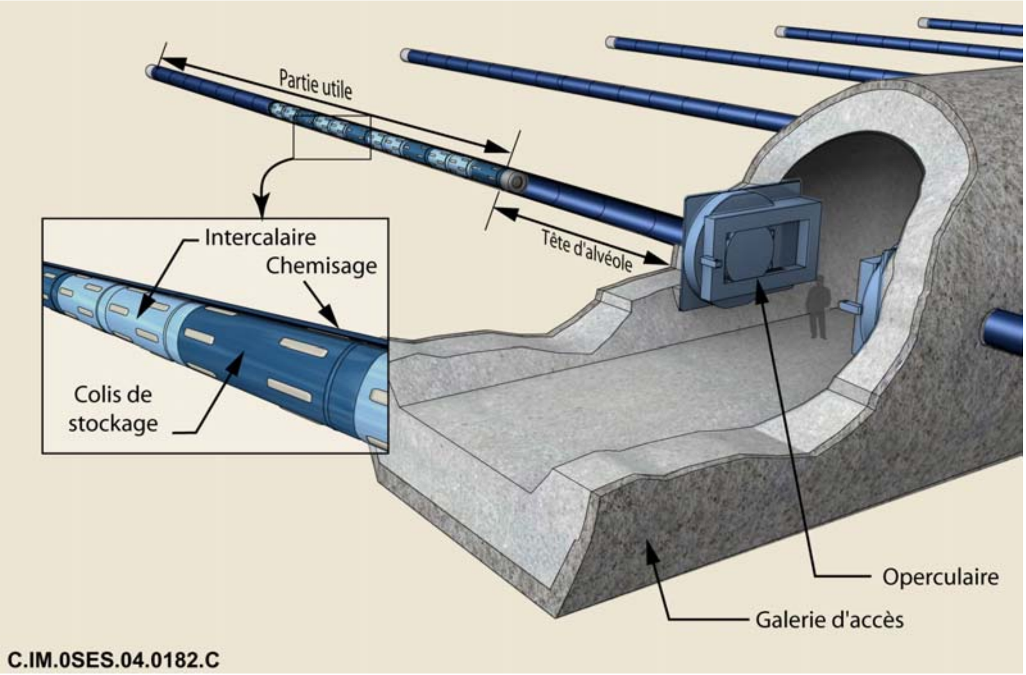

Figure 2.4.8 *Basic diagram of a C waste disposal cell filled with disposal packages in operating configuration*

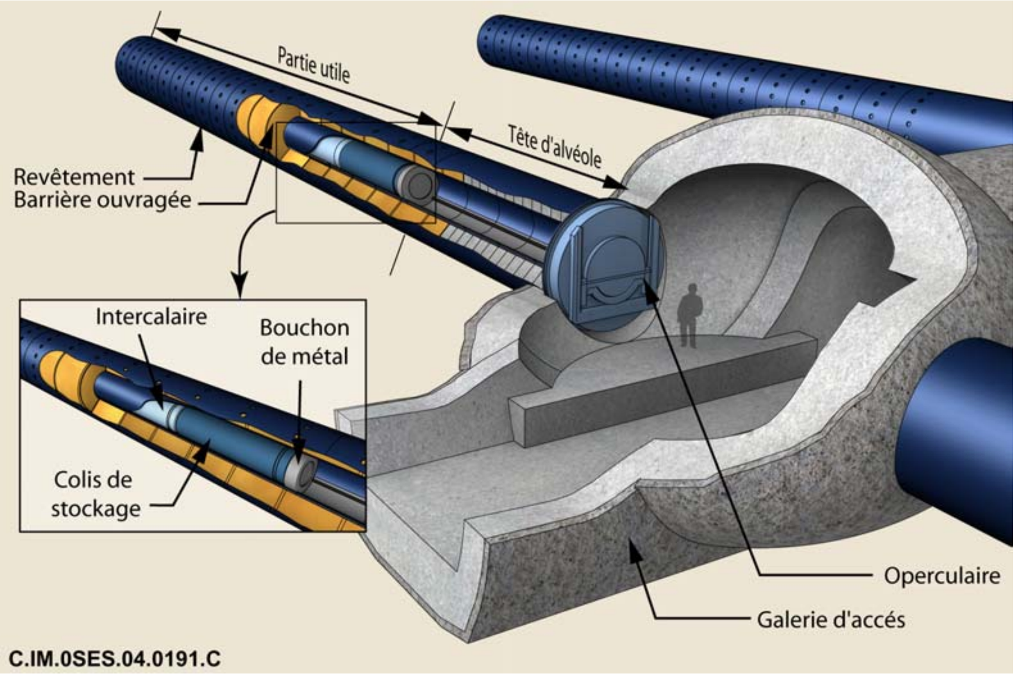

Figure 2.4.9 *Basic diagram of a spent fuel disposal cell filled with disposal packages in operating configuration*

2.4.2.8 Step-by-step repository management until its closure

- **Progressive and flexible general procedure**

In order to ensure the repository's flexibility and reversibility, its construction, operation and closure are based on a series of successive steps. This principle applies from the overall repository system (access shafts and repository zones) to the disposal modules and disposal cells within a repository zone. It can be summed up as follows:

Step 1: The disposal packages are placed in a cell. The disposal cell is sealed by a device that can be opened (to enable the placement of disposal packages) and then resealed temporarily (to isolate the cell from the access drift connected to it and accessible).

Step 2: This step is characterised by the sealing of the disposal cell. The drift connected to the disposal cell (or group of disposal cells) still remains accessible.

Step 3: The disposal module is sealed and in final configuration. The access drifts connected to the disposal module are still accessible. The closure of the disposal module includes backfilling the internal access drifts connected to it.

Step 4: The connecting drifts between one or more disposal modules are also sealed. Only the connecting drifts leading to the repository zone are considered as accessible.

Step 5: The engineered structures connecting the surface facilities and the underground facilities are sealed. All of the disposal modules and repository zones connected to these structures are then in post-closure configuration.

- **Flexible chronogramfor repository construction, operation and closure**

Due to the flexible management principle and the progressiveness of the production of waste packages and placement in the repository, the various steps involved in the construction, operation and closure of the repository are completed over a secular to plurisecular time period. More specifically, this time period may vary depending on the waste production management scenario and the choice of duration to proceed from one step to another. By convention, a secular duration is adopted as the reference.

The repository's design according to distinct zones for each type of waste (B, C0, C1/C2/C3/C4, CU1, CU2 and CU3) effectively allows a large degree of flexibility in the time diagrams for the construction, operation and closure of each of these zones. Nevertheless, as we will see in chapters 5, 6, 7, 8, 9 and 10 describing the phenomenological evolution of the repository and its geological environment, the modularity of the repository also leads to phenomenological evolutions that are nearly independent for each zone and similar for disposal modules of the same repository zone, thereby minimising the impact of the time diagrams on these evolutions.

To perform the analysis of the phenomenological evolution, a conventional reference chronogram of secular duration is used. This chronogramcorresponds to a progressive waste management with regard to thermicity and covers all the waste, i.e.:

- first the non-exothermic or slightly exothermic waste packages not requiring prior interim storage (B waste and C0 vitrified waste reference packages) are placed in the repository for a period of approximately 40 years,
- then the C1, C2, C3 and C4 vitrified waste packages are placed in the repository for a period of 50 years (scenarios S1a and S1b) or less (S2),
- finally, the spent fuel packages are placed in the repository for a period of approximately 30 years (scenario S2) prior to its definitive closure.

Regarding sensitivity, the analysis is conducted over a plurisecular period of the chronogramfor the construction, operation and closure of the repository.

2.4.2.9 Progressive and structured closure of the repository

- **Installation of repository-specific components**

The closure of the repository is achieved by constructing engineered structures whose functions are to limit the mechanical deformations of surrounding argillites in the long term, to minimise water circulation and to fractionate the repository.

These functions are assigned to different types of engineered structures, i.e., the mechanical deformations of the argillites are essentially limited by means of a support or by backfilling all the drifts. Water flows are minimised by means of seals (low-permeability localised structures). Various seals are installed in locations favouring their efficiency and redundancy. They also ensure the compartmentation of the repository.

The closure of the repository falls within the scope of the step-by-step disposal process, with each type of engineered structure ensuring a step of the process, as summarised below:

- installation plugs at the head of the C waste and spent fuel disposal cells
- installation of seals in the access drifts of the B waste disposal cells
- backfilling of the drifts
- installation of seals at specific points in the repository zone drifts
- sealing of the access shafts.

- **C waste and spent fuel disposal cell plugs**

The closure of the C waste disposal cells consists of removing the lining at the head of the disposal cells and installing a swelling clay plug and a non-reinforced concrete plug (Figure 2.4.10).

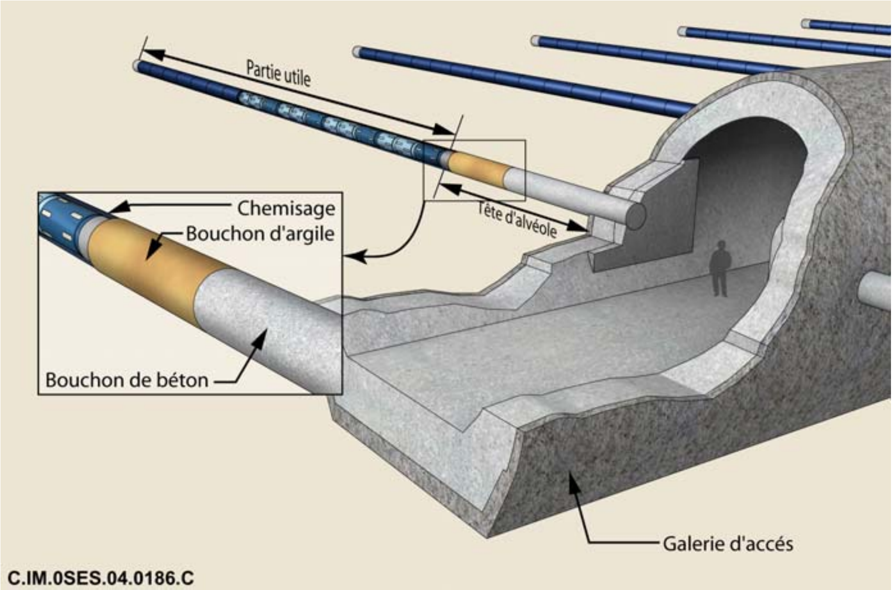

Figure 2.4.10 Basic diagram of a sealed C waste disposal cell

The closure principle for spent fuel disposal cells is the same as for C waste disposal cells, but the metal support is left in place at the head of the cell (Figure 2.4.11).

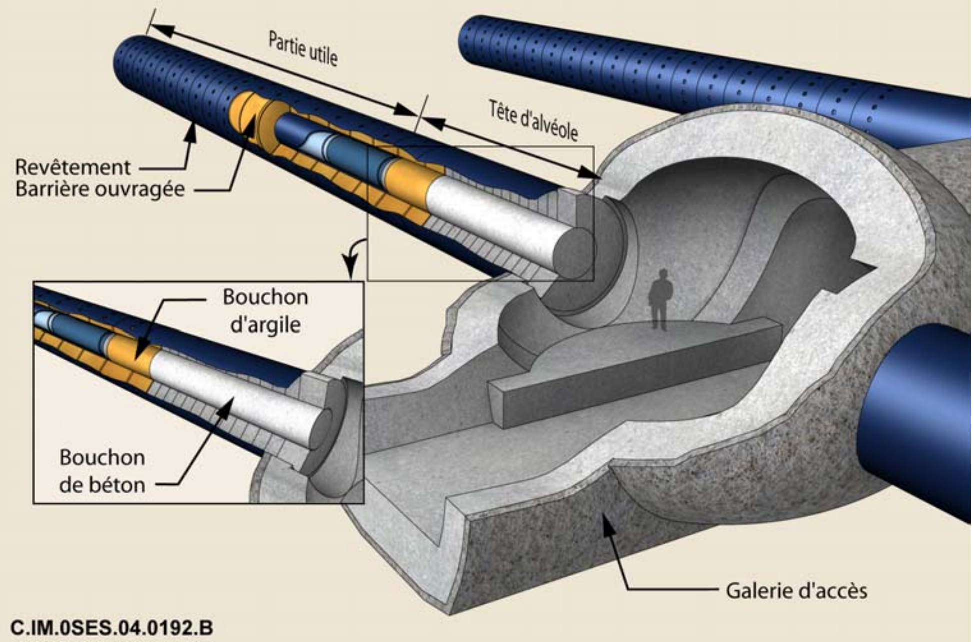

Figure 2.4.11 Basic diagram of a sealed spent fuel disposal cell

- **B waste disposal cell and drift seals**

Each drift seal consists of a swelling clay-based core giving the engineered structure its very low permeability characteristics, and concrete support bases ensuring the mechanical confinement of the core. On both sides, over a distance of approximately 30 meters, the drift backfill has better mechanical properties than the conventional backfill so as to contribute to the mechanical confinement of the engineered structure (Figure 2.4.12).

The swelling clay seal comprise (i) cores approximately 40 meters long, (ii) local hydraulic keys approximately 30 cm thick and 1.5 to 3.0 m deep ensuring hydraulic cutoff of the fractured zone of the argillites, whereas the concrete coating of the drifts is kept in place elsewhere along the core.

Swelling clay is adopted as the base material for the core and hydraulic keys due to its very low permeability and its swelling and deformation capabilities allowing it, in the presence of water, to fill the gaps left during the core's construction and ensure proper contact with the drift wall. As a result, once the clay has swelled, the core will no longer offer the water any preferential flow paths. Finally, its natural character and its chemical compatibility with the argillites will ensure great durability. Two techniques for implementing the swelling clay core are considered, i.e., pellets (or a mixture of pellets and powder) and precompacted blocks.

The non-reinforced High Pergormance concrete support bases are intended to limit the core's volumic expansion by mechanically withstanding the swelling pressure developed by the swelling clay, particularly during the core's transient hydration and swelling phase. In the very long term, the support backfills must assume the role of the concrete support bases, if necessary. For this purpose, they consist of a mixture of excavated argillites and sand with similar proportions.

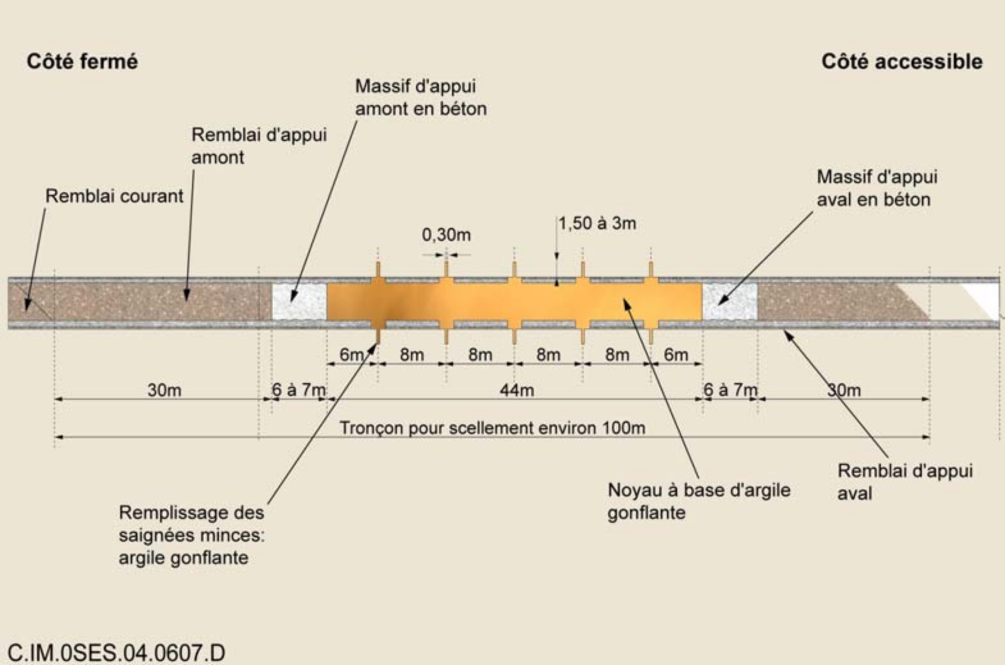

Figure 2.4.12 Basic diagram of a drift seal (longitudinal cross-section)

The access drift of the B waste disposal cells is similar to a conventional drift. The seals of the B waste disposal cells are similar to those of the drifts, with dimensions adapted to the specific configuration of the disposal cells (Figure 2.4.13 and Figure 2.4.14).

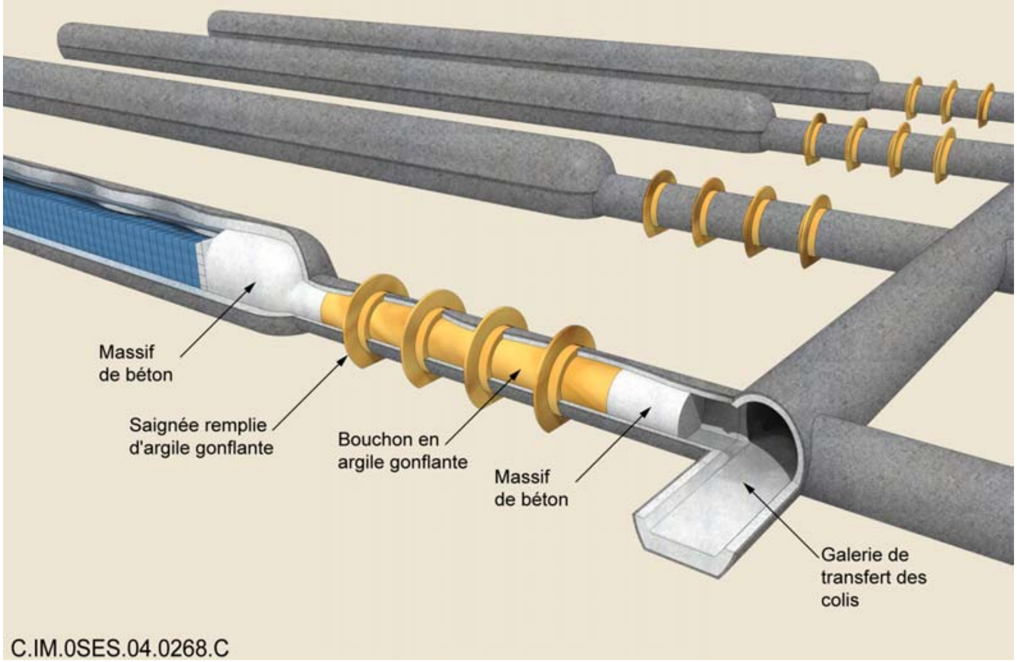

Figure 2.4.13 Basic diagram of a sealed B waste disposal cell

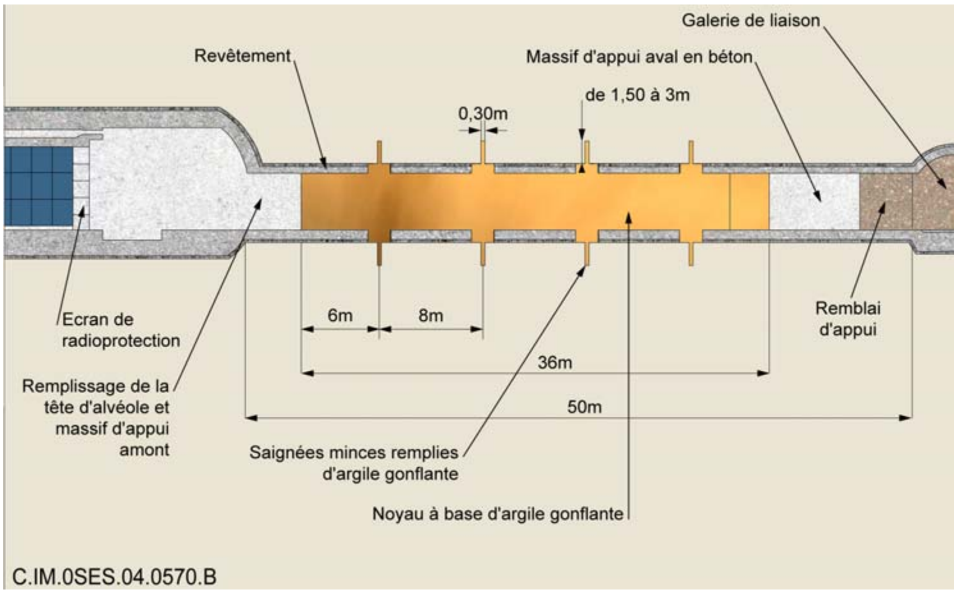

Figure 2.4.14 Basic diagram of a B waste disposal cell seal (longitudinal cross-section)

- **Drift backfill**

The backfill must support the pressure of the argillites after the rupture of the drift lining and minimise rock deformations in the long term, thereby preventing or limiting the expansion of the excavated damaged zone around the engineered structures. For this purpose, **(i)** the empty spaces left behind must be as small as possible and **(ii)** the backfill material must have a sufficient bearing capacity as soon as it is installed. The stiffness of the material then increases with the creep compression exerted by the argillites.

Since a significant volume of backfill is required (several million cubic meters), it has been decided to reuse the excavated argillites as the base material for the backfill, thereby reducing added material requirements.

The backfill consists of excavated argillites reconditioned (20 mm crushing) after being stored in heaps. Its water content is close to the Standard Proctor Optimum value[6], i.e., 10 to 15 %. A dry density of at least 1.6 is sought for the backfill when installed, with a swelling potential of one to a few percents. Installation will be performed through ramming in horizontal layers (lower part of the drift) and inclined layers (top).

Near the seals, the backfill also ensures mechanical confinement (Figure 2.4.12).

- **Shaft seal**

A seal is installed *in the upper part of the Callovo-Oxfordian layer so as* ***to isolate the repository*** from the overlying geological formations. Its permeability must be as low as possible. As in the case of the drifts, the **core** of this seal consists of a swelling clay-based material. It rests on a ***concrete support base*** occupying the base of the shaft and extending through the drifts connected to it over a pluridecametric distance. The mechanical robustness of this base ensures the stability of all the closure structures superimposed in the shaft. The weight of the overlying materials may eventually contribute to the confinement of the swelling core. A concrete support base anchored in the rock is constructed above the core to play a mechanical role during the resaturation phase.

---

[6] Standard Proctor Optimum is a normalised test to determine the most favourable water content for a material's compaction. A water content slightly higher than the Standard Proctor Optimum value favours the mechanical resistance of the backfill during resaturation.

The seal isolating the repository is implemented over the greatest possible height in the upper part of the Callovo-Oxfordian layer, where the argillites have a greater mechanical resistance than in the middle of the formation. The thickness of these more resistant layers is at least 30 meters (38 m directly above the underground research laboratory). The knowledge acquired suggests that the construction of the shafts will not lead to the appearance of a fractured zone. It is therefore planned to lay the coating over the entire height of the core during the construction of the seal, thus ensuring direct contact of the swelling material with the argillites.

The seal isolating the repository is covered with a **backfill** up to the top of the carbonated Oxfordian. The material used is identical to that of the drift backfill. Above the backfill, an ***aquifer separation seal*** is constructed to separate the more permeable levels of the covering formations (carbonated Oxfordian, Kimmeridgian and Tithonian). For example, it can be located in the lower marly level of the Kimmeridgian formation, with a height of 10 to 15 meters and a constitution similar to that of the first seal. In the upper part of the shaft, a backfill completes the filling up to the surface.

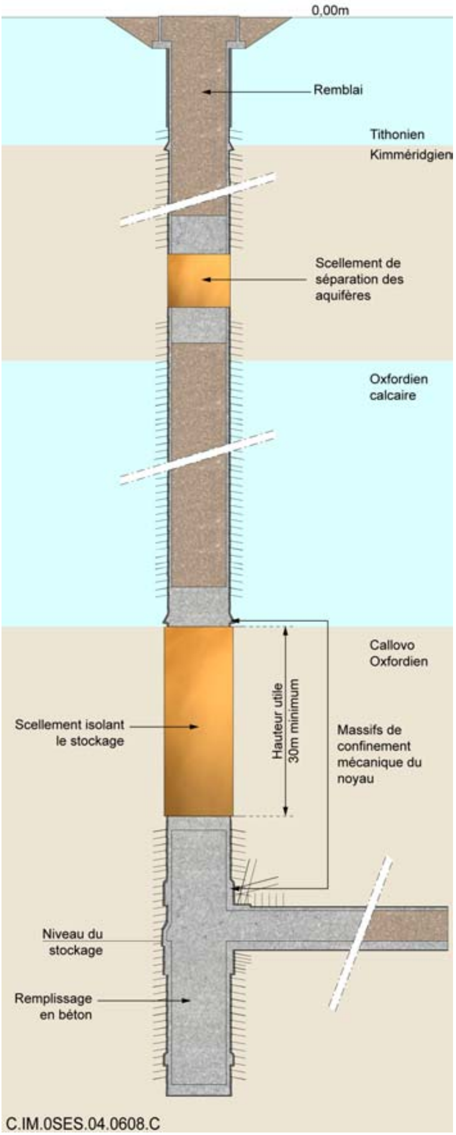

Figure 2.4.15 Basic diagram of an access shaft seal (longitudinal cross-section)

2.5 Implications of the architecture of the repository on the phenomenological evolution of the repository and its geological environment

The repository design proposed is intended to meet the safety and reversibility objectives (Andra, 2005j). For this purpose, it is based on current knowledge of the phenomenological behaviour of the repository and its geological environment. It also contributes to controlling this behaviour, namely the complexity and extension of the processes in space and time.

2.5.1 Simplification and control of the phenomenological evolution

The simplification and control of the repository's phenomenological evolution are principles adopted to ensure repository safety and reversibility. Various design measures contribute to achieving this goal.

- Compartmented and modular repository architecture with distinct and separate reference package repository zones (and distinct and separate disposal modules within each repository zone).

The objective here is to limit or prevent any phenomenological interaction between repository zones and between disposal modules within the same zone, thereby effectively minimising the complexity of their phenomenological evolutions. The repository then behaves as a sum of elementary repositories that are nearly independent with regard to phenomenological evolution.

- Minimisation of maximum temperatures in the repository and its geological environment.

The primary objective is to maintain the repository and its geological environment within a temperature domain preserving the natural properties of the Callovo-Oxfordian layer and repository components.

- Choice of constitutive materials for the engineered structures of the repository.

The objective is to limit the chemical perturbations within the repository and the Callovo-Oxfordian layer and to maintain a favourable physical and chemical environment for the waste packages so as to limit the release of radionuclides.

- Mechanical dimensioning of the underground engineered structures.

The objective is to limit mechanical perturbations, particularly mechanical damage of the argillites in the near field of the engineered structures (installation of coating, distance between two adjacent structures equal to at least five times the diameter, minimisation of empty spaces, disposal cells oriented in the direction of major stress, etc.).

2.5.2 Engineered structures presenting a marked typology with regard to phenomenological behaviour

The nature of the repository components and operating procedures determine the phenomenology observed in the repository and the surrounding geological medium during both the operating / reversibility phase and the post-closure phase. We can therefore identify three major characteristics of the repository engineered structures, which can further be combined.

2.5.2.1 Engineered structures distinct in terms of constitutive materials

The following types of engineered structures can be distinguished:

- Engineered structures in which clay and metals prevail, such as the C waste and spent fuel disposal cells (Inset 2.6, Inset 2.7 and Inset 2.9) ;
- Engineered structures in which concrete and metals prevail, such as the B waste disposal cells (Inset 2.8) and engineered structures comprising a majority of clay associated with concrete, such as the seals and backfills.

Corrosion and hydrogen production (correlatively) are important processes in the phenomenological evolution of the first type of engineered structures. The second type is marked by the chemical degradation of the concrete and by chemical interactions between the cementitious waters and the clays (argillites and swelling clays).

2.5.2.2 Engineered structures distinct in terms of ventilation during operation

The following can be distinguished:

- Engineered structures which are closed (in terms of air exchange with the drift) due to the implementation of temporary measures (leak tight cover), such as C waste and spent fuel disposal cells
- Engineered structures kept open and ventilated during all or part of the repository operating phase until its closure, such as the B waste disposal cells and especially the drifts and access shafts

Ventilation and the presence of oxygen in particular determine the redox and saturation conditions of the engineered structures. These two parameters have significant effects on the chemical and mechanical processes within the engineered structures (corrosion of metallic components or chemical degradation of concretes, for example).

2.5.2.3 Engineered structures distinct in terms of heat release

The following can be distinguished:

- Engineered structures with high thermicity, such as the C waste and spent fuel disposal cells
- Engineered structures with little or no thermicity, such as the drifts, access shafts and B waste disposal cells

Temperature constitutes a parameter of the chemical, hydraulic and mechanical processes. Although the proposed design is intended to minimise increases in temperature within the repository, the amplitude, kinetics and duration of said increases in temperature constitute phenomenological evolution data.

2.5.3 Major components of the geological medium and the repository

In the repository system design and safety assessment, certain elements are assigned specific functions. Others, such as the drifts and surrounding formations, do not play an explicit role (Andra, 2005j).

As a result, during the post-closure phase the safety of the repository is ensured by a number of natural components and privileged engineered components intended to limit the return of radionuclides towards humans and the environment, i.e.:

- The **Callovo-Oxfordian layer**, namely on account of its past (and future) stability over several millions of years, as well as its low permeability and high retention properties.
- The **seals**, which ensure the general hydraulic closure of the repository.
- The swelling clay engineered barrier of the spent fuel disposal cells and the swelling clay plugs of the C waste and spent fuel disposal cells. Like the seals, they contribute to the hydraulic closure of the repository (at the disposal cell level).
- The **spent fuel and C waste containers**. Their function is to ensure the complete confinement of radionuclides during periods where (i) short and medium-lived radionuclides still have significant activity and (ii) the increase in temperature in and around the repository is still significant (for example, beyond 50 °C for vitrified waste).
- The **B waste package containers**, which delay and limit the release of radionuclides over a *minimum* period ranging from few thousand to ten thousand years.
- The waste conditioning matrixes, such as the glass matrix, the spent fuel oxide pellets or the retreatment sludge bitumen matrix. After the discharge of container confinement capabilities, the conditioning matrixes limit the release of radionuclides over long periods of time (i.e., a minimum of tens of thousands of years).

Inset 2.6 ***Swelling clays (Andra, 2005f, Tome 1) (1/2)***

Swelling argillaceous minerals

Swelling clays mainly consist of swelling argillaceous minerals (**smectites**) and 'secondary' minerals (carbonates, quartz, feldspars, pyrite, oxyhydroxides). The smectites (and other argillaceous minerals) belong to the phyllosilicates group. They are present in the form of very small crystals (a few microns at the most) appearing in all surface domains (alterites, soils, sediments) or subsurface domains (diagenesis, hydrothermal alterations). The crystals (or crystallites) result from the stacking of layers that adhere to one another to form polycrystalline particles. At the upper scale, the crystals or polycrystalline particles (possibly but not necessarily associated with secondary minerals) form aggregates. The assembled aggregates and possible secondary minerals form the swelling clays.

Each flake consists of a stack of two base layers: a) the tetrahedric layer formed by tetrahedrons SiO_4^{4-} or AlO_4^{5-} constituting a two-dimensional array, and b) the octahedric layer formed by two octahedrons in a hexagonal symmetrical array (see figure below).

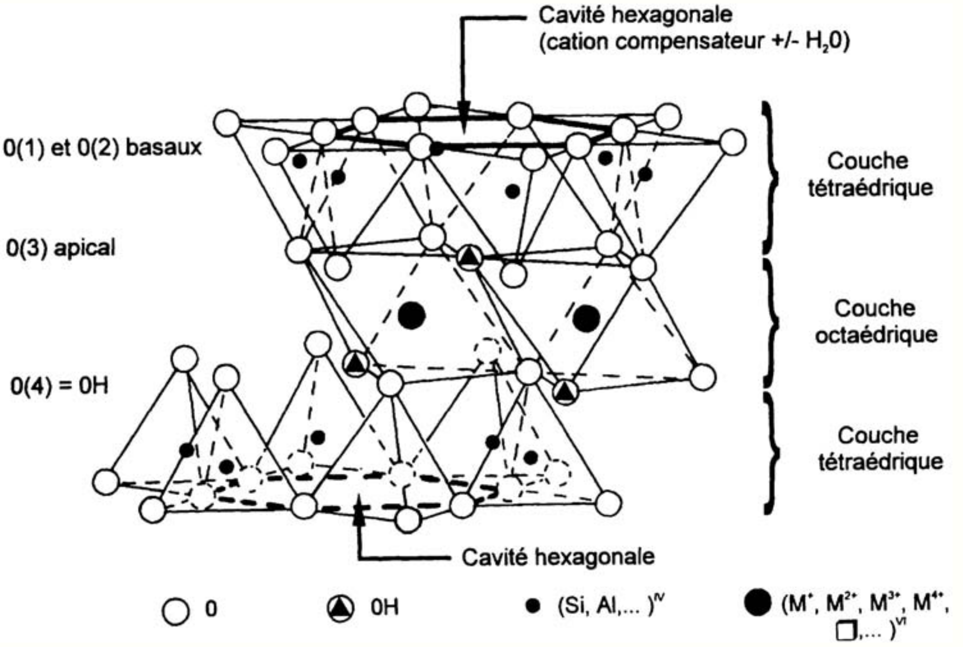

3D representation of the structure of a 2:1 clay of smectite type (flake consisting of 2 tetrahedric layers surrounding 1 octahedric layer) (Petit *et al.*, 1999, d'après Grim, 1968)

Specific characteristic of smectites: Charge deficit and interfoliar swelling

The crystalline structure of swelling minerals corresponds to 2:1 layers (TOT) (see figure below). Cationic substitutions may occur in the tetrahedric layer ($Si^{4+} \rightarrow Al^{3+}$) and in the octahedric layer ($R^{3+} \rightarrow R^{2+}$), creating a deficit of positive charges in the 2:1 flake. This deficit is compensated by the addition of a cationic interfoliar layer in the crystalline structure. The number of interfoliar cations depends on their valency and the value of the interfoliar charge. For the smectites, this charge may vary between 0.30 and 0.65 for a composition of $O_{10}(OH)_2$ type, thereby modifying the chemical and physical properties of the layers. The cations are weakly fixed in the interfoliar space. They are completely exchangeable, and polar molecules such as water may penetrate this space, conferring the expansion capacity of the layers (swelling) through adsorption of the polar molecules. This expansion is proportional to the number of water layers (0 to 3). This number mainly depends on the type of interfoliar cation and the partial pressure (P/P_0) of the water. The maximum hydration of the smectites becomes infinite pour Na^+ and Li^+ and corresponds to 3 layers of water for Ca^{2+}, Mg^{2+} and Ba^{2+}. Potassium allows 2 layers of water in montmorillonites (octahedric charge) and only 1 layer in other smectites.

Swelling clays (2/2)

Swelling pressure and low permeabilities to water

During the adsorption of water, a diffuse distribution of cations is formed around the layers, particularly a forced concentration of ions creating an 'ionic atmosphere'. Since the positive charges of the cations and the negative charges of the layers are physically separated, the system can be considered as a dual electric layer similar to an osmometre with a semi-permeable membrane consisting of an argillaceous flake. There is therefore an osmotic pressure gradient in the inter-flake space, which produces a repulsion force. At the scale of the swelling clay, the various repulsion forces observed in the layers are transmitted to the particles and then to the aggregates, thereby determining the swelling pressure. If deformation is prohibited, for a given interfoliar cation the swelling pressure will increase proportionately to the clay density.

This close relationship between the water and the layers (and with the aggregates in general) is also the cause of the low permeability of the swelling clays ($\leq 10^{-11}$ m.s^{-1}).

Inset 2.7 ***MX80 methodological swelling clay selected for geological repository studies (Andra, 2005f, Tome 1)***

Mineralogical composition

MX80 is the methodological swelling clay selected by Andra to conduct the repository feasibility studies. It is a natural clay found in Wyoming (USA). It consists of approximately 80 % smectite, 20 % secondary minerals (quartz et cristobalite, sodiocalcic feldspars (plagioclases), potassic feldspars (microcline or sanidine), biotite – phlogopite, carbonates such as calcite and ankerite, sodiocalcic phosphate of buchwaldite type, pyrite and hematite) and minerals in trace quantities (titanium (0.1 %) and zirconium, sulphates such as anhydrite, and barytine-celestine).

The X-ray diffraction analysis shows that the smectite contains no interlayers. It consists of a low charge montmorillonite with a structural formula per half-mesh:

$(Si_{3.98}Al_{0.02})(Al_{1.55}Fe^{3+}_{0.09}Fe^{2+}_{0.08}Mg_{0.28})O_{10}(OH)_2Na_{0.18}Ca_{0.10}$, with mixed Na(2/3)-Ca(1/3) interfoliar lining

The argillaceous fraction (< 2 µm) represents 84.6 % of the total mass, which is close to the smectite content. This fraction contains traces of quartz and biotite, whereas the sand and silt fractions are enriched with secondary minerals. The cationic exchange capacity, determined for a purified fraction, is 87.5 meq/100g. The specific surface is estimated at approximately 30 $m^2.g^{-1}$, which is relatively high, especially considering that bentonite only consists of approximately 80 % montmorillonite.

Preparation for use in the repository

Once extracted and treated (grinding, crushing, drying), the MX80 clay appears in the form of a grey powder with larger particles. In order to be used as a repository material, this powder is then compacted using various techniques to obtain objects of various shapes and sizes, i.e., bricks, tori and granulates (pellets). This compaction eliminates the macroporosity (diameter > 50 nm) without modifying the distribution of the mesopores. At millimetric scale, the pore network remains completely connected. The dry densities amount to 1.6 $g.cm^{-3}$ for a water saturation degree generally comprised between 70 and 90 %. This compaction then gives the MX80 clay the strong swelling and low permeability properties (see figure below) required for the hydraulic closure structures of the repository (plugs of disposal cell, seals of drift and access shaft).

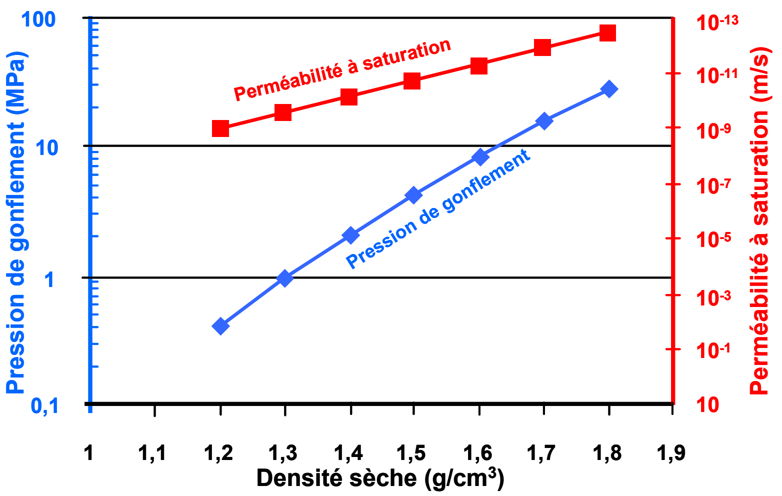

Swelling pressure and water permeability curves for MX80 swelling clay

Inset 2.8 ***Composition of cement-based repository materials and chemistry of their interstitial waters (Andra, 2005f, Tome 2)***

Formulations studied

The concrete formulations studied by Andra consist of **calcareous granulates**, to avoid alkali reactor problems and the release of alkaline cations (Na, K), and two types of cements:

- **CEM I**, with a **Portland clinker** content of over 95 %
- **CEM V** (slag and ash cements), composed of 25 to 60 % Portland clinker, 20 to 45 % **high furnace slags**, and 20 to 45 % **flying ashes** from fossil fuel thermal plants.

The cement load is approximately 400 kg.m^{-3} for CEM I and 450 kg.m^{-3} for CEM V. From a mechanical perspective, the concretes studied therefore belong to the **High Performance Concrete** class, with a simple compression resistance exceeding 60 MPa.

Chemistry of the cement-based waters and chemical degradation state of the concretes

During cement hydration, the presence of highly soluble alkaline oxides (Na_2O and K_2O) and alkaline-terrous oxides (MgO, CaO) in the clinker leads to the formation of hydrates that are stable in an alkaline medium, giving the interstitial waters of the concretes an alkaline character with a pH level of between 10.4 and 12.5. The main hydrates concerned are portlandite $Ca(OH)_2$, whose pH balance is close to 12.5 (acid-alkaline buffer), and hydrated calcium silicates, with a stability domain ranging from approximately 12.5 to 10.5, depending on the calcium to silica ratio (C/S). At the low end, the brucite $Mg(OH)_2$ has a pH balance of 10.4. The pH level of the interstitial waters may be controlled in the concrete formulation so as to not exceed the target value of 12.5.

The chemical evolution of a concrete upon contact with pure water or the Callovo-Oxfordian waters can be described in a simplified manner according to the various chemical states encountered during the dissolution of the reactive cement-based poles described above (see figure below).

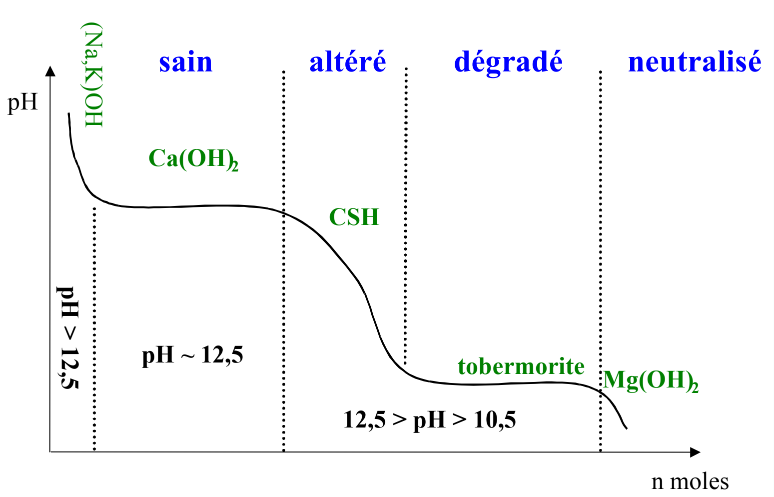

Diagram of the successive chemical degradation states of concretes as a function of the pH level of the pore water

Inset 2.9 ***General characteristics of metallic repository materials (Andra, 2005f, Tome 3)***

Two types of metallic materials are formed in the repository (not including the zircalloy cladding of the spent fuel assembly rods):

- **Stainless steels** or passivatable alloys (Fe-Cr-Ni- Mo)

They mainly constitute a) the *primary canister of various B waste primary packages such as bituminised sludge packages* (B2) and compacted hull / end cap and compacted technological waste packages (B5), and b) the *primary canister of vitrified waste packages*. In the latter case, a refractory stainless steel (Z156CN2313) with a carbon content decreased to 0.08 % is used to avoid intergranular corrosion, whereas the more standard SI 309L grade is employed for the primary *canister* of B waste primary packages.

The dominant mechanism in stainless steel corrosion is the propagation of pits or crevices, but the corrosion rates may be very low, less than a few tens of µm per year, particularly under reducing conditions (expected after repository closure) or in the presence of chlorides. Welding operations are delicate, and welds potentially constitute privileged corrosion areas.

- **Low-alloy and non-alloy steels**

These steels mainly constitute a) the *containers of C waste and spent fuel disposal packages* and b) the *infrastructure components of the disposal cells of said packages (lining, support)*.

The choice of low or non-alloy steels for the containers is based on the technological capabilities demonstrated (metallurgy, weldability, etc.), their good mechanical and chemical properties (predictability of corrosion) and limited cost (base material and manufactured object). P235 non-alloy steel has been selected for the container studies due to the following:

  - good weldability (low carbon content)
  - structure less sensitive to cold fissuring in the welding zone (low elastic limit)
  - sufficient elastic limit to withstand an isotropic external stress of at least 12 MPa
  - no need for thermal treatment after welding

Generalised corrosion is the dominant mechanism in the corrosion of low or non-alloy steels. Corrosion kinetics in an argillaceous medium are well understood due to significant experience feedback, i.e., long exposure tests and laboratory studies to identify corrosion mechanisms. Under reducing conditions, the corrosion rate is approximately *a few µm per year at the most*. Corrosion resistance for several thousands to tens of thousands of years can be expected for pluridecimetric thicknesses, since very low values (less than a few tenths of µm per year) have been experimentally observed. Under anoxic or reducing conditions, the corrosion rate of these steels varies little with changes in the chemical composition of the waters in the surrounding environment. Chemical composition and metallurgical structure (possibly subject to local modifications by welding) do not have a significant effect on corrosion. Finally, localised corrosion may be observed, particularly during the first stages of corrosion in an oxidising medium, but its relative importance compared to generalised corrosion decreases with time.

For the infrastructure components of vitrified waste and spent fuel disposal cells, other steel grades are considered, such as P355 or S355 steels for example, which have a higher mechanical resistance than P235 steels but present more significant risks of stress corrosion and fragilisation by hydrogen.

3

The initial state of the geological medium before the repository was built

---

3.1 Introduction 95

3.2 The general setting 95

3.3 The different geological formations 109

3.4 Tectonics and fracturing 158

3.5 The surface environment 165

3.6 Summary of the initial state of the geological medium 171

3.1 Introduction

The current state of the geological sedimentary formations and the units they form (basin for example) results from the accumulation and superposition of a series of geological phenomena which marked their history from the time the sediments were deposited to the present day. Reconstituting this history requires a multiscale approach, from tectonic plate to basin to region, and then finally to the site being considered.

This is why this chapter first discusses the geological setting on the scale of the Paris basin, then of the Meuse/Haute-Marne sector, which covers an area of 40 km from East to West and 60 km from North to South, centred on the position of the underground research laboratory (Figure 3.2.1). It describes the phenomenological status (hydrogeological, chemical, thermal and mechanical) of the entire series which is on a level with the current site (see § 3.2). Sections 3.3.1 and 3.3.2 give a more accurate description of the characteristics of the Callovo-Oxfordian and surrounding units. The different scales of fracturing and their effect on the characteristics of the formations are covered in section 3.4. Finally, section 3.5 presents the surface environment.

3.2 The general setting

The Paris Basin, with its sedimentary series of varied facies and aureolar layout, has been the subject of many geological studies, notably within a context of resource detection campaigns (water, oil, gas, coal, etc.), both on the surface and at depth. These studies have accumulated an impressive knowledge base. The general geological setting of the Paris basis is therefore very well documented.

Within this general context, the Meuse/Haute-Marne site on the Eastern edge of the Paris basin belongs to an area with no potential for these resources, especially coal and oil. The areas of interest for coal resources are located in the extension of the Sarre-Lorraine Basin, mainly within the formations from the Westphalian era (Donsimoni, 1981). Reconstitutions of the Palaeozoic substrate throughout the region carried out based on seismic data and results from deep boreholes show that the Westphalian is only present to the North of the sector. At site level, this Palaeozoic substrate takes the form of a thick clastic series (several thousands of metres), from the Permian and Stephanian era, less rich in organic matter without any major seams of bitumous coal (Andra, 2005h, chapitre 8). The depth of this series, greater than 3,500 m, rules out mining and coal gas exploitation. This Permian and Stephanian series, like the overlying clastic Triassic layer, has poor reserve characteristics and water with high salinity removing any geothermal interest from these formations (Andra, 2005h, chapitre 8). Concerning oil, the approaches made on a basin-wide scale, particularly by the IFP (Espitalié *et al.*, 1987), during the 1970s and 80s, showed that the areas of interest lie more to the West, towards the centre of the basin. In the area around the site, as throughout the entire Eastern aureole, the main potential parent rocks (Lias clays) are immature and therefore incapable of expressing the kerogen they contain in the form of hydrocarbons (Hanzo & Espitalié, 1994 ; Kruge *et al.*, 1997 ; Landais *et al.*, 1989). Therefore, since the mid 1980s, this region has been excluded from intense oil prospecting campaigns, unlike the central zone of the basin, which explains the lower density of boreholes and seismic profiles in the area around the site.

- From the mid 1990s, Andra's work in site characterisation and the installation of the underground research laboratory completed the old existing drilling and geophysical data as well as information on the surface geology. This work was organised in several phases (Figure 3.2.1) (Andra, 2005h, chapitre 6) ;
- From 1991 to 1998, preliminary work was carried out on a sectoral scale, reprocessing existing geophysics data and reinterpreting old borehole data, producing detailed land surveys, five deep boreholes and a 2D seismic reflection campaign;
- In 1999 and 2000, before construction of the underground research laboratory, the work done consisted of a 3D seismic reflection campaign covering 4 km², four hydrogeological and

geochemical boreholes on the laboratory platform, and two geological boreholes drilled along the axis of the future access shafts;

- In 2003, eight boreholes on five platforms (FSP campaign) were made throughout the sector, to improve definition of the limits of hydrogeological knowledge on this scale;
- In 2004, eight boreholes, four of which were directional (FRF campaign), explored the geological medium with the aim of measuring the properties of the Callovo-Oxfordien layer and its surroundings in the immediate neighbourhood of the site;
- Finally, since August 2000, sinking the laboratory access shaft has led to the collection of in situ information through scientific monitoring of this operation (geological monitoring, sampling, geomechanical characterisation,…). This monitoring was completed in 2004 with the data produced from excavation of the experimental drift at -445 m, as well as the first results of the experiments performed there**.**

These investigations provided the information permitting the building of a site and sectoral scale model, contributing to the knowledge acquired more broadly in the basin and leading to a report on the initial state of the site.

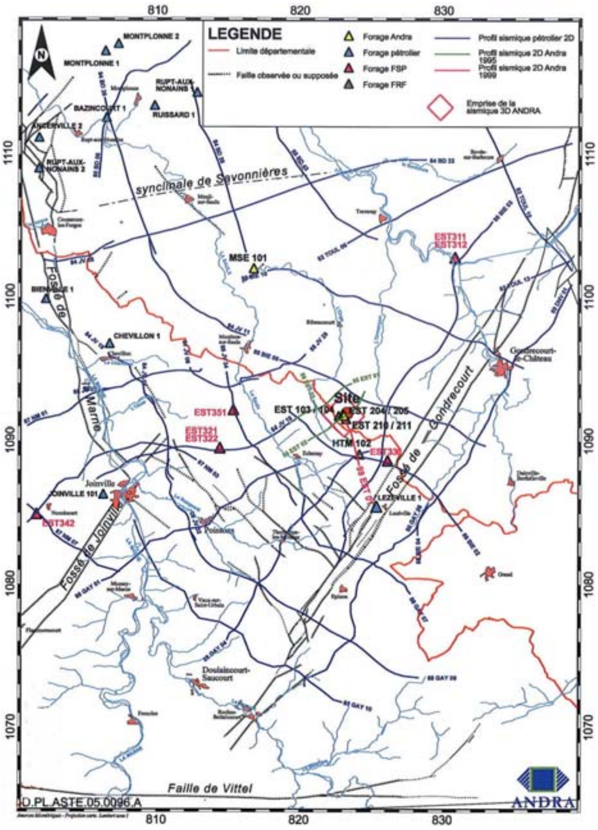

Figure 3.2.1 *Available data and location of the work done by Andra in the Meuse/Haute-Marne sector*

3.2.1 The geological features of the site

3.2.1.1 At the scale of the Paris Basin

The history of the Paris basin begins on a flat substrate inherited from palaeozoic history. During the secondary era, from 250 to 135 million years ago, over an area largely exceeding the current geographical limits of the Paris basin, sedimentary series, initially predominantly continental (Lower Triassic), then oceanic (Upper Triassic, Jurassic), were deposited in thick layers, in a relatively stable tectonic context, providing the lithological units with large lateral extensions. During this epoch, the basin largely opened towards the East (Figure 3.2.2, a and b) (Dercourt *et al.*, 1993 ; Mégnien, 1980). The layers outcropping in the Meuse/Haute-Marne sector date from the end of the secondary era. Due to the calm context of this epoch, the immersed zones, especially during the period of high sea level (corresponding to deposits of clay formations), were far-reaching. Thus the Callovo- Oxfordian sedimentation field covers the whole Paris Basin, between the emerged zones formed by the Ardennes and London-Brabant massifs to the North, the massif armoricain to the West and the Massif de Bohème to the East. Within this zone, the Callovo-Oxfordian mainly displays sedimentation with marl and clay dominance on the shoal corresponding to the Burgundy platform, where this sedimentation is more carbonated (Andra, 2005h, chapitre 10). When the sea retreated 120 My ago, due to the opening of the Atlantic, sedimentation began once again during the Cretaceous, notably with chalk deposits (Figure 3.2.2, c) (Cavelier *et al.*, 1980a). It was during the tertiary era (65 My ago) that the basin gradually assumed its current structure, following various tectonic phases, (Bergerat, 1985 ; Villemin, 1986): the Pyrenean phase (which corresponds to the collision between the African plate and the West European plate), the Oligocene extension phase (about 34 My ago, responsible for the formation of the Rhine rift valley) and finally the compressive phase initiated by the Alpine thrust (from 23 My ago to the present day). Under the action of these successive phases, the edges of the Paris basin were raised, emerged and subjected to erosion. Marine and then lagoonal deposits were restricted to the centre of the basin (Figure 3.2.2, d) (Mégnien, 1980). From the Neogene (23 My ago), the sea retreated fully and the topographical models evolved towards the present setting: erosion leaving the more resistant formations in relief, particularly limestones, while rapidly removing the softer clay formations (Figure 3.2.2, e). Over the past three million years, strong climatic cycles have been alternating extremely cold periods with temperate periods about every 100,000 years. During the cold periods, subsoil may remain frozen to a depth of more than 100 meters all the year round (which is then referred to as permafrost) (Berger, 1992). These climatic cycles also helped influence the topographical models and the rhythm with which river beds were incised (Mégnien, 1980).

The general structure of the basin is currently in the shape of a bowl filled with a succession of sedimentary layers, the oldest of which outcrop on the edges, with the most recent in the centre of the basin in the Ile de France. The aureole of Jurassic land outcropping is thus very visible on the whole eastern part of the basin, proof of the continuity of deposits during this period: from south of the Ardennes, Lorraine, the limits of Burgundy, the buttresses of the Massif Central and right up to the limits of Poitou. In the western part of the basin, these formations are partially covered by later Cretaceous deposits. This continuity is also ensured at depths (Figure 3.2.3). On a level with the Brie area, the secondary and tertiary filling is more than 3,000 m thick.. It is only about 1,800 m at the site location, because of the erosion of more recent terrain. This structure is locally affected by faults, the largest of which date back to the primary history of the basin basement (Bray, Vittel faults, etc.). These faults may have been active throughout the entire history of the basin (Bergerat, 1985 ; Coulon, 1992). Generally speaking, the ratio between basin filling (subsidence) and its diameter is 5/1,000, which characterises stable platform basins (Cavelier *et al.*, 1980b).

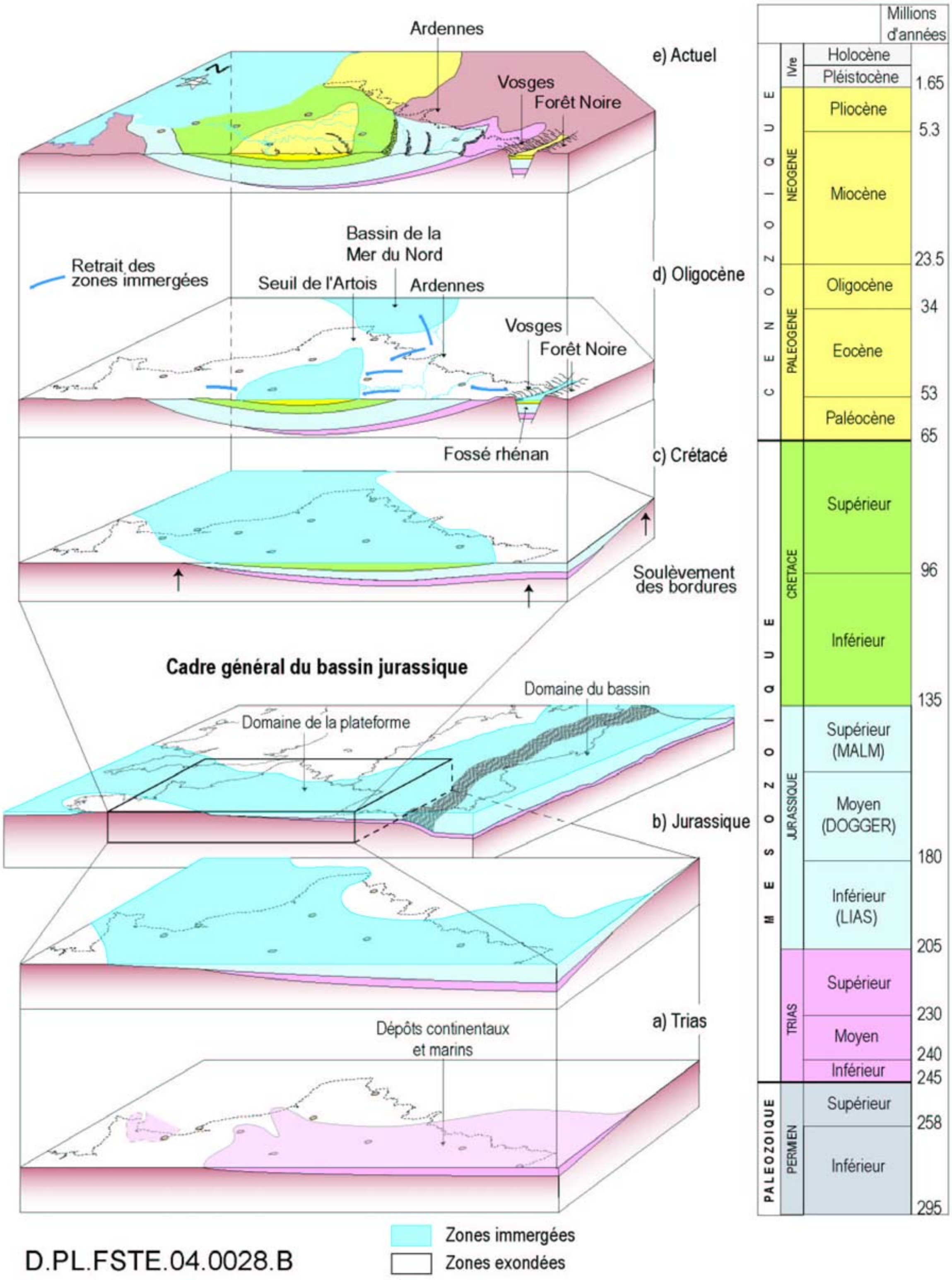

Figure 3.2.2 *Schematic diagram of the formation of the Paris basin from the Palaeozoic to the present day*

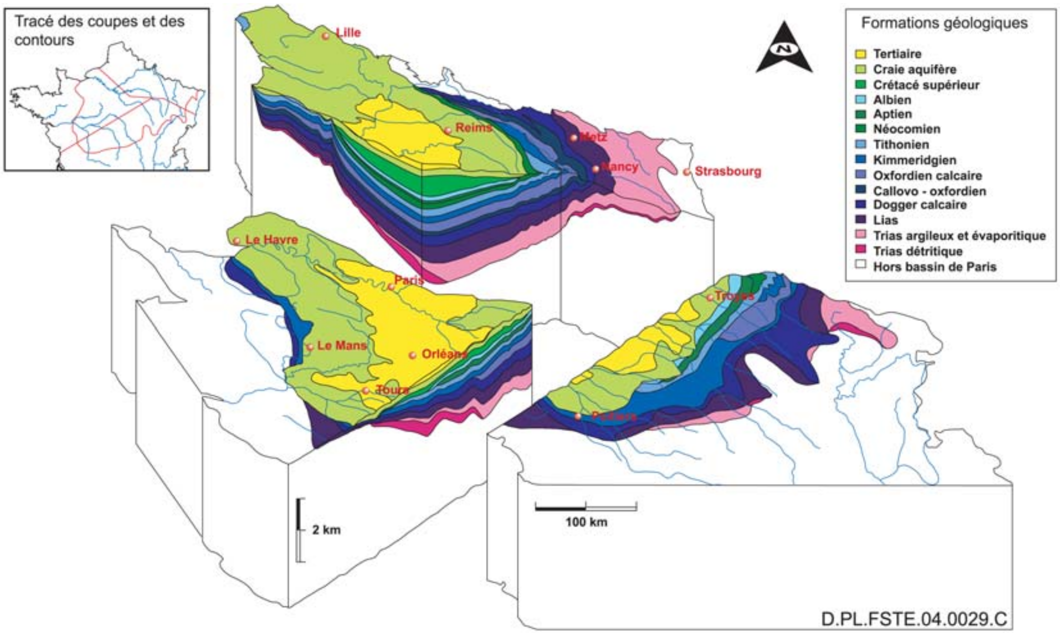

Figure 3.2.3 3D block diagram of the geological structure of the Paris basin at the present day

3.2.1.2 At the sectoral scale

In the several hundred square kilometers sector containing the site, the first 1,000 meters of formations, including the Callovo-Oxfordian and its surroundings, consist of a set of layers deposited in a marine environment during the Dogger and the Malm (180 to 135 My ago). This sedimentary series consists of alternating limestone formations and predominantly clayey formations, corresponding to variations in the conditions of deposition during each epoch. These variations result from a combination of basin subsidence and variations in sea-level (Guillocheau *et al.*, 2002): The limestone formations are deposited in shallow environments whereas the clay-rich formations were laid down in deeper water (about one hundred meters) and therefore further from the coast. Given the stable tectonic context of the basin during the Jurassic (cf. § 3.2.1.1), these formations show great lateral continuity. At the end of the Jurassic and in the lower Cretaceous, the region was emerged for the first time. Sedimentation resumed in a continual fashion during the Upper Cretaceous with chalk deposits at sector level of around 300 metres, thick depending on the different palaeothermal episodes (cf. § 3.3.1.3). During all the Tertiary and the Quaternary, the region remained emerged when the area definitively retreated due to the effects of the raising of the basin edges (André, 2003). During this period, erosion stripped off the lands from the Upper Cretaceous, leaving the Jurassic series in outcrops. The sedimentary series, such as observed nowadays in the sector is formed from bottom to top (and from East to West at outcrops) by (Figure 3.2.4):

- the Dogger limestone formation, resting on Liassic marls and clays;
- the Callovo-Oxfordian clayey formation;
- the mid- to upper-Oxfordian limestone formation;
- the marly Kimmeridgian, marking a new deeper deposition environment;
- Tithonian limestones (Barrois limestones) outcropping at site level;
- thin clayey-sandy Cretaceous cover (veneer) capping the highest topographical points.

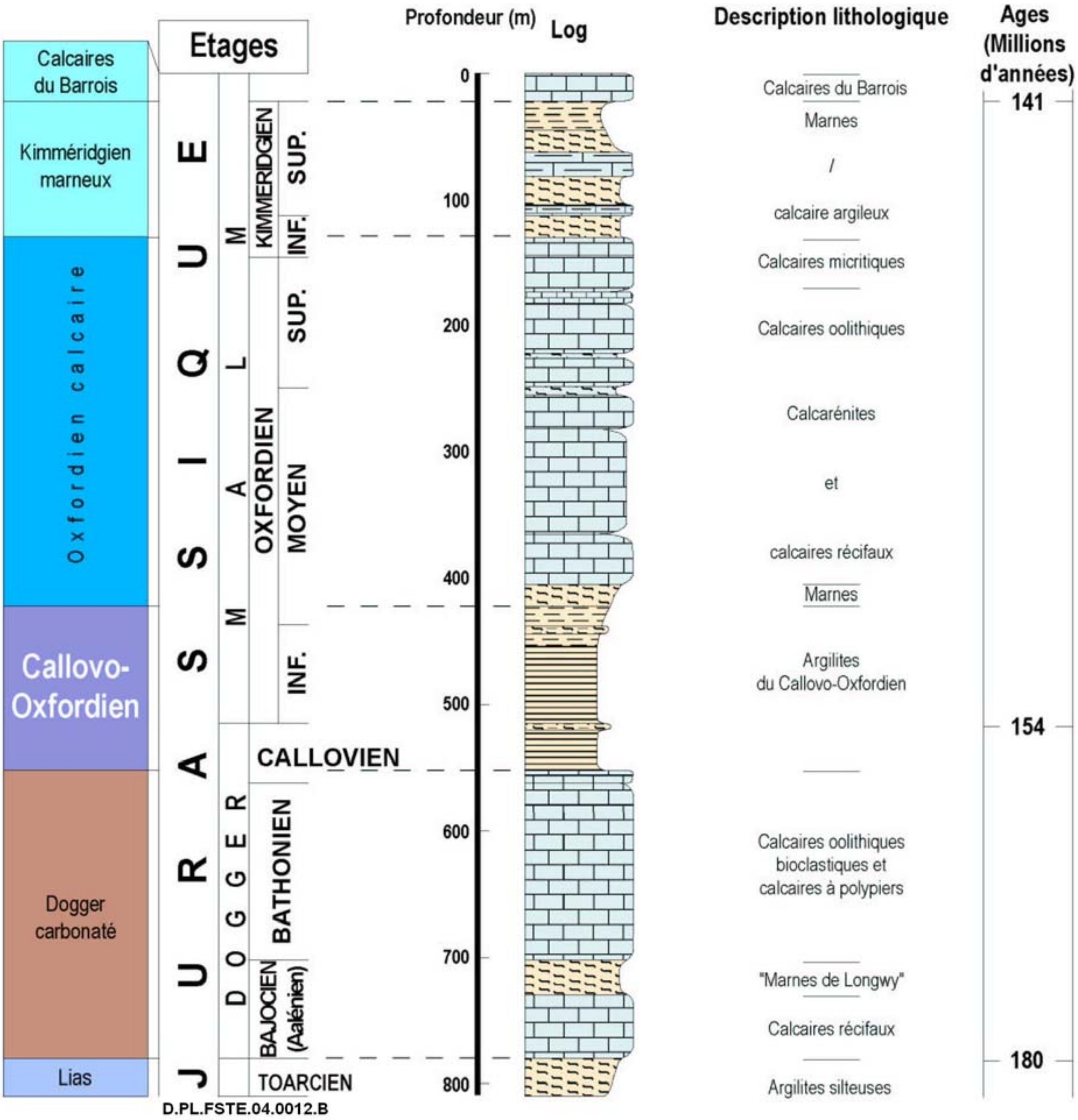

Figure 3.2.4 Lithological succession directly above the Meuse/Haute-Marne site

Coherent with the general structure of the Paris basin, in the Meuse/Haute-Marne sector these sedimentary layers show a simple, monoclinal structure over several hundred km², with a shallow but regular dip from 1° to 1.5° towards the North-West (Figure 3.2.5) (Elion, 2005 ; Trouiller & Benabderrahmane, 2005). This structure is locally affected by slight long wavelength deformations (decakilometric), including the Savonnières syncline in the north of the sector. The regional faults enclosing the sector (Marne and Poissons faults running North-North-West/South-South-East, the Gondrecourt graben running North-North-East/South-South-West and the Vittel East/West fault), which affect the entire secondary series, were subjected to only minor movement during the period of deposition of these formations, having been most active later on during the Tertiary (Trouiller & Benabderrahmane, 2005) (cf.§ 3.4).

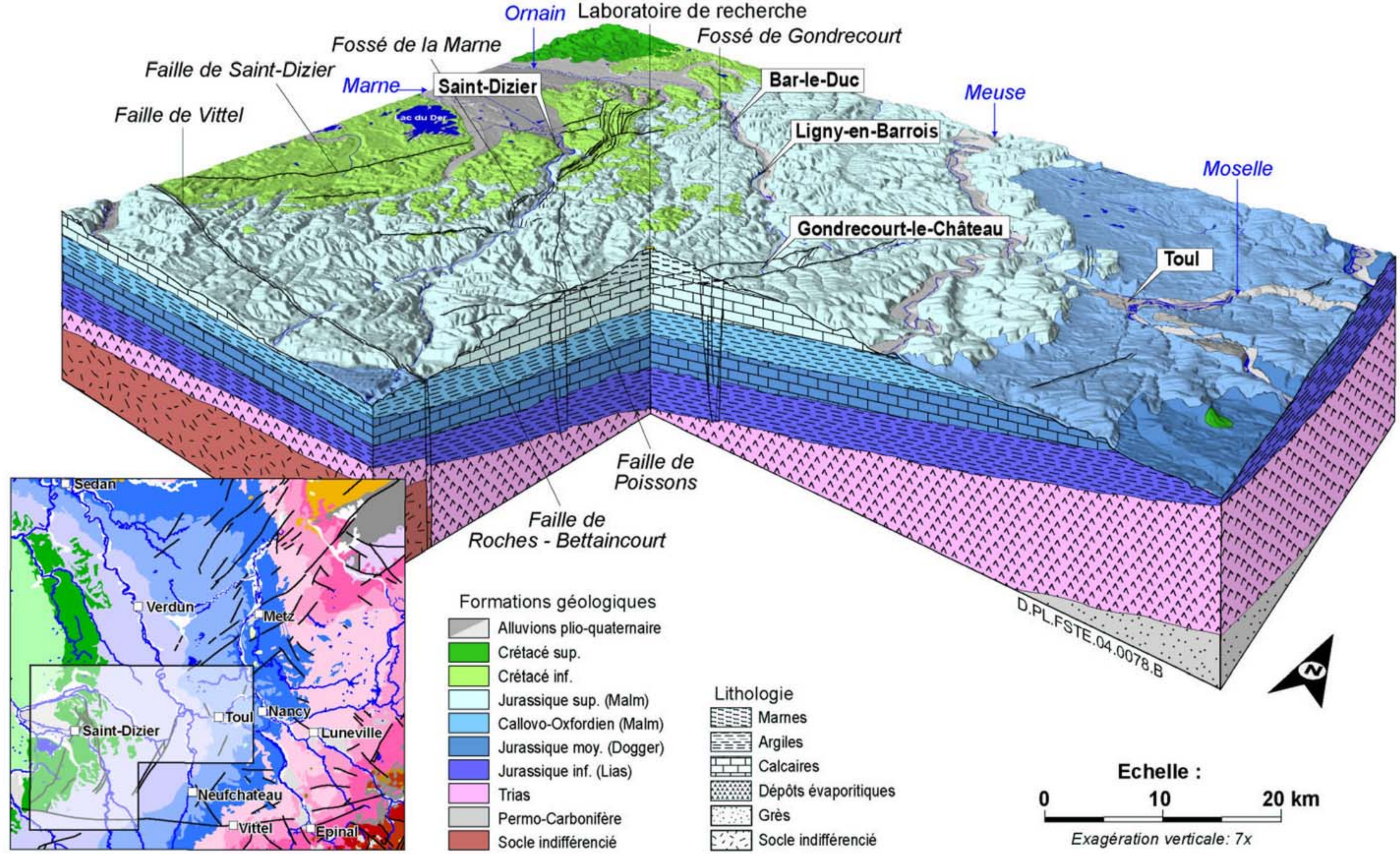

Figure 3.2.5 *3D block diagram of the geological structure of the Meuse/Haute-Marne sector*

The alternating limestones-clays and regional dip of 1° to 1.5°, engenders a typical sloping relief at the outcrops. Thus, overlying the clay zones forming depressions, the more resistant limestone beds appear in the form of slopes about one hundred meters high, with fronts extending Westwards across vast plateaux (Figure 3.2.6). The soils, corresponding to the sedimentary alteration, are thin and stony on slopes, deeper and loamy in clay depressions. The relief also controls surface runoff, surface water tending to flow to the bottom of the slope, thus developing disymmetrical stream systems. Thus, in the Eastern part of the sector, the Moselle and the Meuse rivers flow towards the North, guided by the Dogger and Oxfordian slopes. In the Western part of the sector, the region is drained towards the North and North-West by the Marne and its affluents (Ornain, Saulx, Rongeant). These flow in the direction of dip of the layers, incising deeply into the Barrois Limestones. The tributary basins thus determined result from the complex evolution of flow upstream of these rivers, which is linked to erosion and catchment phenomena (see § 9.5 and (Brulhet, 2005b)).

The current morphology, linked to the lithology of outcropping layers, is therefore the result of successive topographical evolutions initiated since the final retreat of the sea from this part of the Paris basin (at the end of the Cretaceous, around 65 My ago). These superficial processes have had little effect at depth (Brulhet, 2005b).

The sedimentary series can be considered to be generally at steady-state hydraulically, chemically, thermally and mechanically given the relatively long period (several My) of system stability. This state of equilibrium relative to the main events has been maintained for several My and evolves only slowly. Only modifications due to climatic variations at 100,000 year intervals create transient disturbances (essentially hydraulic in the surroundings) which do not affect significantly the mean long term (10^6 years) values chemical or mechanical states.

3.2.2 The seismo-tectonic setting

The current convergence between the African plate and the European plate is slow between a few millimeters and one centimetre per year (Le Pichon, 2004). Most of this movement is absorbed by deformation in mountain zones (North Africa and the Alps at French latitude). The rest of the movement is absorbed by slipping along major faults in the plate: this is notably the case of the West European rift. Here there is significant seismicity as well as deformation recognised as tectonic in origin. Slipping along the most active faults is about 0.01 to 0.1 mm.year^{-1} in the Lower Rhine rift and 0.01 to 0.001 mm.year^{-1} in Alsace (Brulhet, 2005a). At such velocities, and considering the large size of the faults, it is possible to engender earthquakes of a magnitude reaching 7.0 ± 0.4 in the Rhine rift, with a return period of between 10,000 and 250,000 years. Outside these zones, any movements are even weaker and only concern regional faults affecting the basement (Brulhet, 2005a) (Marne and Vittel faults for example – see § 3.4). In these faults, any slipping is very slow, estimated at 0.001 and 0.0001 mm.year^{-1}, depending on the size of the fault.

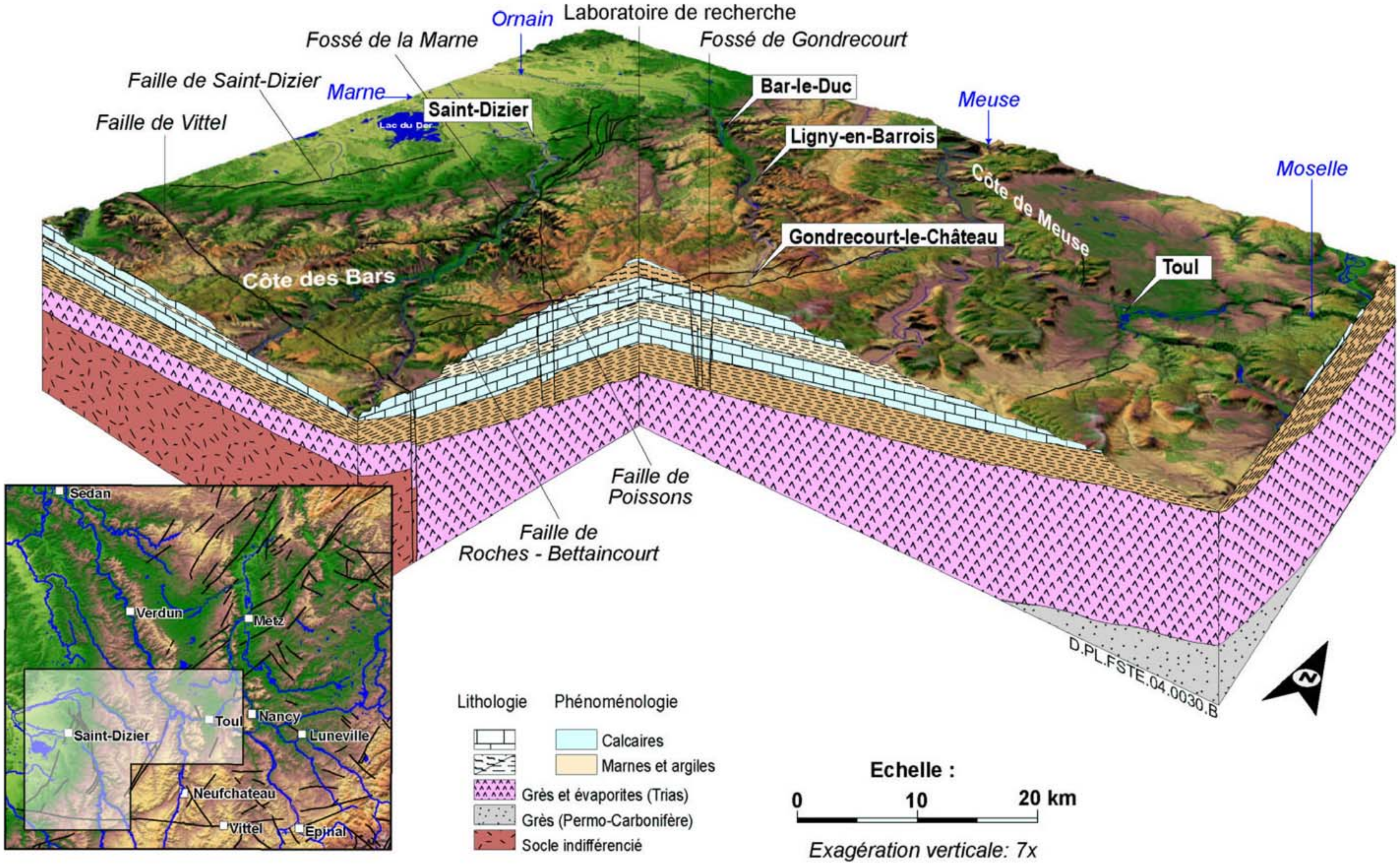

Figure 3.2.6 *3D block diagram of the lithology and relief of the Meuse/Haute-Marne sector*

These considerations explain why, outside the active zones located on its edges (particularly the Rhine graben system), the Paris basin is a region of very low seismicity.

In this intraplate area, the Meuse/Haute-Marne sector also appears to be a remarkable part of the West European plate. The lithosphere here is of uniform thickness, contrasting with the regions further east, particularly the Rhine graben valley (Figure 3.2.7). This uniformity is characteristic of stable, largely undeformed zones. The zone appears to be aseismeic, with respect to both historic seismicity and recent geological periods: indeed, no quaternary evidence of tectonic activity has been found along the major faults surrounding the sector. The sector is therefore a very stable zone from a seismo-tectonic point of view. The maximum possible earthquakes in this context are estimated at around 6.1 ± 0.4 along the regional faults enclosing the sector (Gondrecourt graben, Marne faults), with return periods of between 100,000 and 1,000,000 years (see § 9.2).

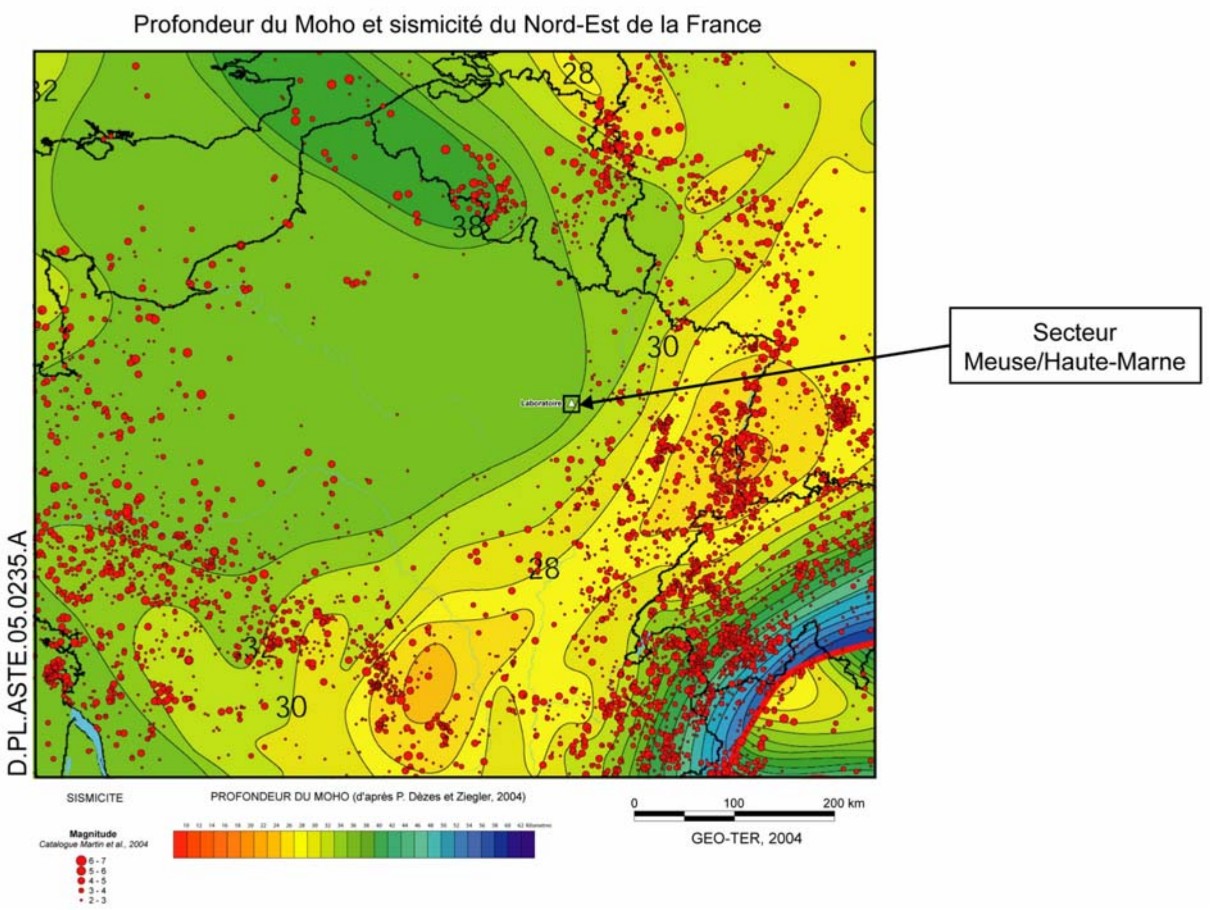

Figure 3.2.7 *Geodynamic setting of Eastern France: the relationship between seismicity and crustal thickness (Andra, 2005h, chapitre 35)*

3.2.3 Hydrogeology and water chemistry

3.2.3.1 Water flows within and between formations

The hydrogeological setting on a sectoral scale depends on the lithological succession of the different layers: limestone layers behave like aquifers whereas clay formations act as impermeable horizons. In aquifers, circulation is organised from outcrops near plateaux, where surface alterations (action of rainwater) strongly increase permeability, frequently giving rise to karstification. On the surface, these aquifers flow towards the rivers. At depth, because of the dip, the lithological continuity of the layers and the presence of impermeable formations on either side of the aquifers, flow through the sector is globally within the aquifers, in a Westerly and North-Westerly direction, towards the centre of the basin, then towards the English Channel (Figure 3.2.8) (Gonçalvès, 2002 ; IFP, 2004 ; Trouiller & Benabderrahmane, 2005 ; Wei *et al.*, 1990). The presence of impermeable horizons prevents any significant vertical flow from one aquifer to another. Only regional accidents such as the Marne faults or the Gondrecourt rift could allow communication between aquifers during certain periods, such as the Oligocene (extensive phase). This vertical drain role may also be played by current faults, particularly the Marne faults, which runs parallel to the major North-North-West/South-South-East horizontal stress field (Trouiller & Benabderrahmane, 2005) (cf. § 3.2.4).

This hydraulic independence of aquifer formations leads to different hydraulic head fields between one aquifer and the next. The Dogger head field therefore has only low gradients of about 10^{-3} m.m^{-1} on a sectoral scale, flowing towards the South-West (see. § 3.3.2.1). The carbonated Oxfordian head field has slightly steeper gradients (around $5 \cdot 10^{-3}$ m.m^{-1}) running in slightly different directions (North-West to West - see § 3.3.2.2). The low permeabilities recorded in these carbonate formations (10^{-8} to 10^{-10} m.s^{-1} depending on the tested interval (Trouiller & Benabderrahmane, 2005) and the low kinematic porosities (less than 10 %) impose slow advective transfer velocity of a few to ten kilometers per million years, on a sectoral scale, as confirmed by the results of isotopic analyses (particularly ^{36}Cl for the carbonated Oxfordian) (Buschaert & Giffaut, 2005).

This organisation of water flows on a regional scale is also reflected in the contrasting chemical and isotopic characteristics of the water in these formations. These waters change from oxidising, near the surface, to reducing at depth. Under the marly Kimmeridgian directly above the site, because of the low water velocity, the Oxfordian and Dogger waters are in equilibrium with the solid phases of the carbonate minerals making up the porous horizons. They all have a neutral pH close to 7-7.5. Dogger water is more saline (by a few g.L^{-1}) than Oxfordian (less than 1 g.L^{-1}). This salinity level of Dogger water seems to be reflected, throughout the basin, by vertical transfers of saline Triassic water to the Dogger, along the lines of regional accidents during their successive occurrence during the Paris basin's history, but given the time scale concerned, also through the diffusion of Triassic chlorides through Lias clays (see § 3.3.2.1).

This difference in salinity between the formations lying above and below the Callovo-Oxfordian, demonstrates the barrier role it plays with respect to the flow and transport of solutes. This role is also illustrated by the chlorine concentration profile, which is compatible with that of a low permeability medium in which diffusion is dominant and has reached steady state (Altmann & Coelho, 2005). These observations are coherent with all the Callovo-Oxfordian permeability measurements made in boreholes or from samples. These are generally low, between 10^{-13} and 10^{-14} m.s^{-1} (see § 3.3.1.6) limiting flow and thereby allowing the solid phases to control the water chemistry (see § 3.3.1.8). In this formation, the hydraulic head fields are determined by the conditions at the boundaries set by the supra- and underlying aquifers (see § 3.3.1.6).

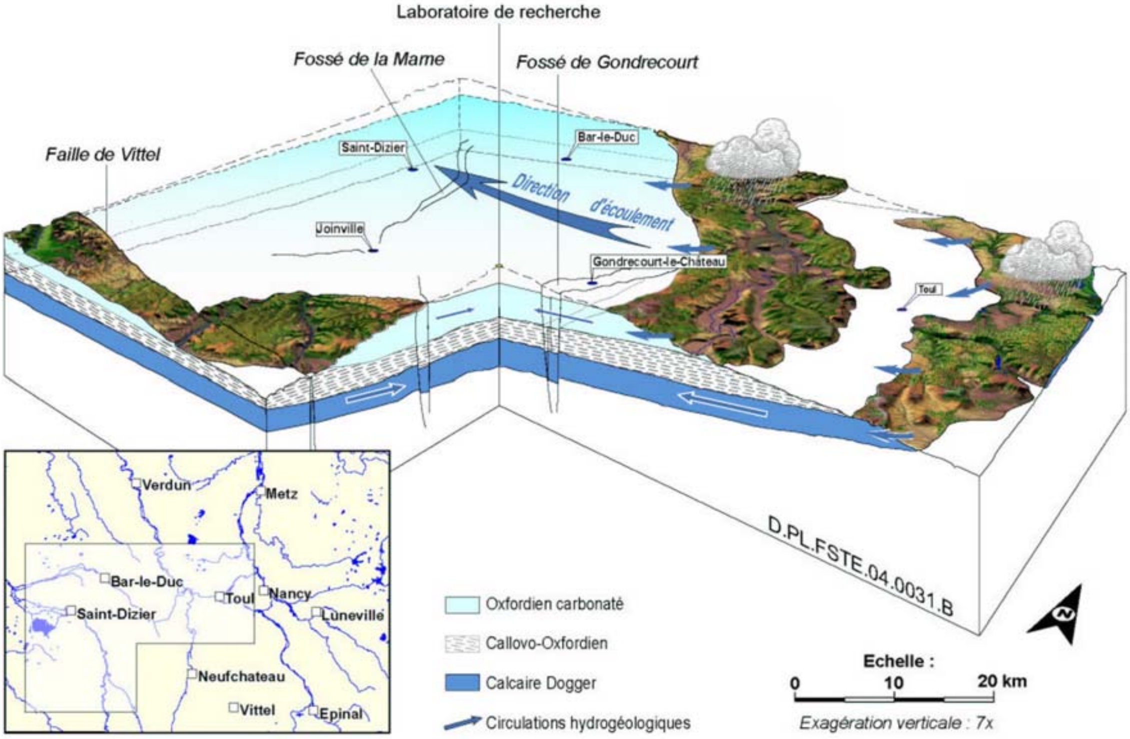

Figure 3.2.8 3D block diagram of hydrogeological systems in the Meuse/Haute-Marne sector

3.2.3.2 The effects of past climatic cycles

For the past three My, glacial-interglacial climatic cycles at roughly 100,000 year intervals, have led to the blockage of infiltration at outcrops and outlets at exits during glacial periods or even blocked circulation within the formations depending on the depth of permafrost (see § 9.4 and (Brulhet, 2005b)). These transient and reversible disturbances had very little impact on average water velocity at depth. They slow already low velocities speeds even further and have little effect on the chemical equilibria of deep formations, which are controlled by the mineral phases.

On the other hand, past climatic cycles have altered surface morphology through erosion, with greater and irreversible effects on zones close to the surface:

- the structural surfaces of the limestone plateaux have slowly eroded (10 to 20 meters per 500,000 years), initiating slope reduction (by several kilometers over the same time) (Brulhet, 2005b),
- the valleys were incised much faster: at about 50 to 80 meters per 500,000 years (Brulhet, 2005b).

Therefore, aquifer supply zones (recharging on the plateaux) and outlets (notably in the valleys) have moved gradually as morphological modifications took place and some parts of the deep groundwater have gradually become surface deposits. These phenomena are slowly changing the hydrogeological circulation. The effects of these continuous changes on water in the Callovo-Oxfordian and surrounding formations, are only perceptible over long periods (several million years), the water remaining in equilibrium with the solid phases (Brulhet, 2005b). At depth, all the formations have therefore been at chemical equilibrium, in a stationary condition for several million years, controlled by water and solute flow through the system and solid phases present.

3.2.4 The natural geothermal field

The thermal state of the various formations is determined by the flow of heat of crustal origin, considered to have been constant over the last few million years, the thermal properties of sedimentary formations and the cycles of variations in mean ground temperature which have succeeded each other over the past few hundred thousand years. These are rapidly damped with depth. Only the climatic cycles with the longest periods (glacial-interglacial cycles of 100,000 years) have had greater impact, with the 0 °C isotherm descending to 300 m (see § 5.6.3). The heritage of past cycles, particularly the last glacial maximum, is recorded today by just a few degree temperature drop at a depth of more than 500 meters (Andra, 2005a, fiche 14). Therefore, the sedimentary series directly above the Meuse/Haute-Marne site currently records a temperature of 10 °C close to the surface (corresponding to annual ground surface temperatures), increasing to 22 °C in the Callovo-Oxfordian (Figure 3.2.9) and 28 °C at the base of the Dogger.

The mean gradient is 2.3°C/100 m (Bauer, 2005) and (Andra, 2005a, fiche 16). Homogeneous throughout the transposition zone, it is distinctly lower than that observed elsewhere in the basin, which is around 3.3 °C/100 m (BRGM & ELF Aquitaine, 1976). Variations in thermal gradient with depth, determined essentially by variations in thermal conductivity of the formations, are very small. In the Callovo-Oxfordian, variations in clay content (see § 3.3.1.4) are also the cause of very slight variations in this gradient. No sudden variation, generally associated with aquifers and major water flow, has been observed, which agrees with the hydrogeological model for the sector, generally characterised by slow water flow.

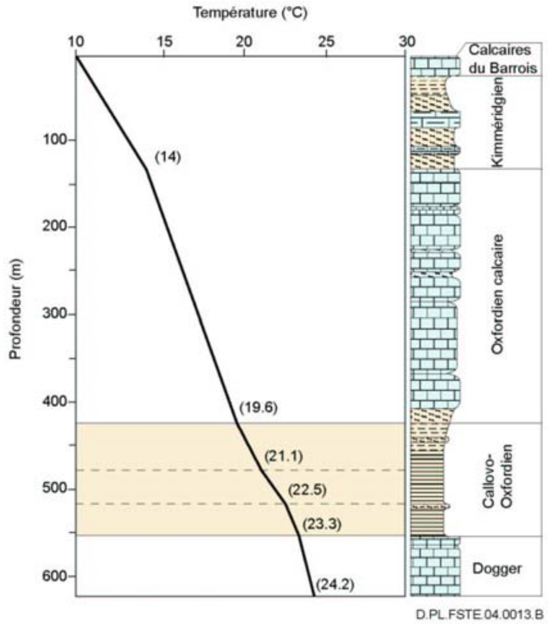

Figure 3.2.9 *Profile of geothermal temperatures in the sedimentary series at the Meuse/Haute-Marne site (Bauer, 2005)*

3.2.5 The natural mechanical stress field

At the start of the Alpine compressive regime in the Miocene (23 My ago), a stress regime oriented West-North-West/East-South-East was set up across the whole West European plate. This regime is still in place today (Bergerat, 1985 ; Brulhet, 2005a) (Figure 3.2.10). The fact that the region is more than 350 kilometers from the Alpine front and its slow plate velocities explains the stability of this stress regime. It controls the horizontal stresses exerted on all the formations in the sector, thus determining anisotropic horizontal stresses with a major stress oriented N155° (Andra, 2005h, chapitre 9) and a minor perpendicular stress. These orientations are coherent with observations made in France (Grellet *et al.*, 1993) and on the scale of the West European plate (Rebaï *et al.*, 1992). The ratio between the amplitudes of these two stresses (major stress/minor stress) is around 1 to 1.2 for the central part of the Callovo-Oxfordian and distinctly higher in the surroundings formations. In the sedimentary series, the vertical component of stress corresponds to the weight of the overlying terrain. It is close to the minor horizontal stress. This value is about 12 MPa for the Callovo-Oxfordian medium, directly above the underground research laboratory (depth 500 m).

This state of stress should remain perennial over the next million years. Indeed, if stress values change gradually as superficial layers are eroded, the general orientation of the stress field will stay the same for a single formation.

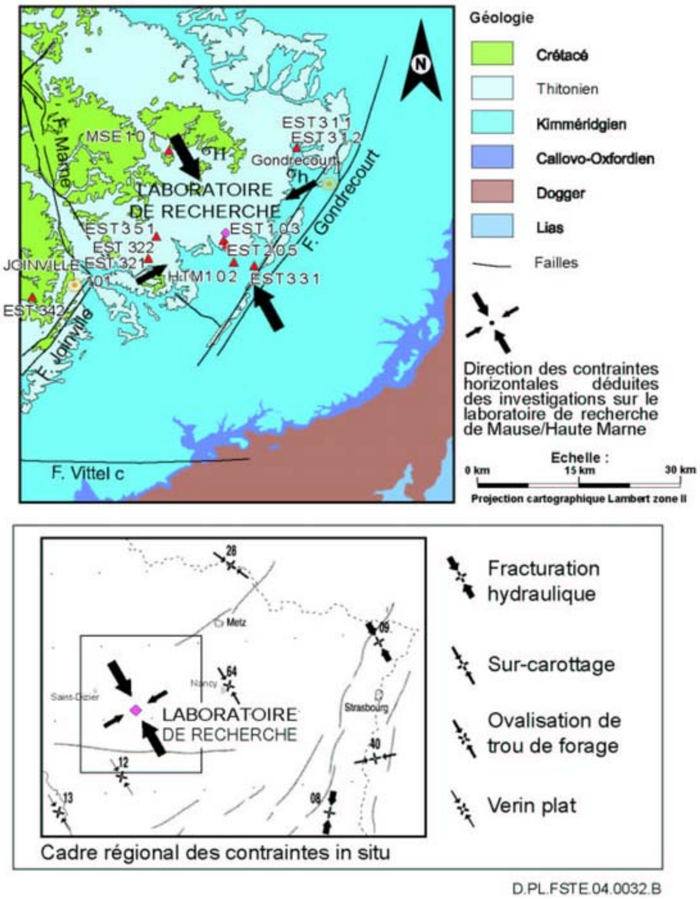

Figure 3.2.10 *Orientation of the current state of stress in the Meuse/Haute-Marne sector (Andra, 2005h ; Grellet et al., 1993)*

3.3 The different geological formations

The previous section described the general geological and phenomenological setting of the sedimentary series, first on a scale of the Paris basin, then of the sector. This section concentrates more on presenting the characteristics of each formation in its current state. One begin with the Callovo-Oxfordian layer (see § 3.3.1) followed by the underlying Dogger (see § 3.3.2.1) and the overlying Oxfordian limestones (see § 3.3.2.2) respectively, and finally the surface formations of Kimmeridgian marls and Barrois limestones are described (see § 3.3.2.3).

3.3.1 The Callovo-Oxfordian layer

3.3.1.1 Geometry of the layer

The Callovo-Oxfordian (argillites) forms a homogeneous clay-rich layer, the top of which is at a depth of 420 meters directly above the underground research laboratory. Because of the dip of these layers towards the North-West, this depth increases gradually to more than 600 meters fifteen kilometers to the North (Figure 3.3.1, Figure 3.3.2). At the same time, the thickness of the layer varies from 130 meters to about 160 meters from South to North-West. Seismic geophysical data and correlations between boreholes show that this variation is gradual at the scale of the whole sector and is coherent with the initial topography, of low contrast, having determined the sedimentation of this formation about 155 million years ago (Figure 3.3.3) (Elion, 2005).

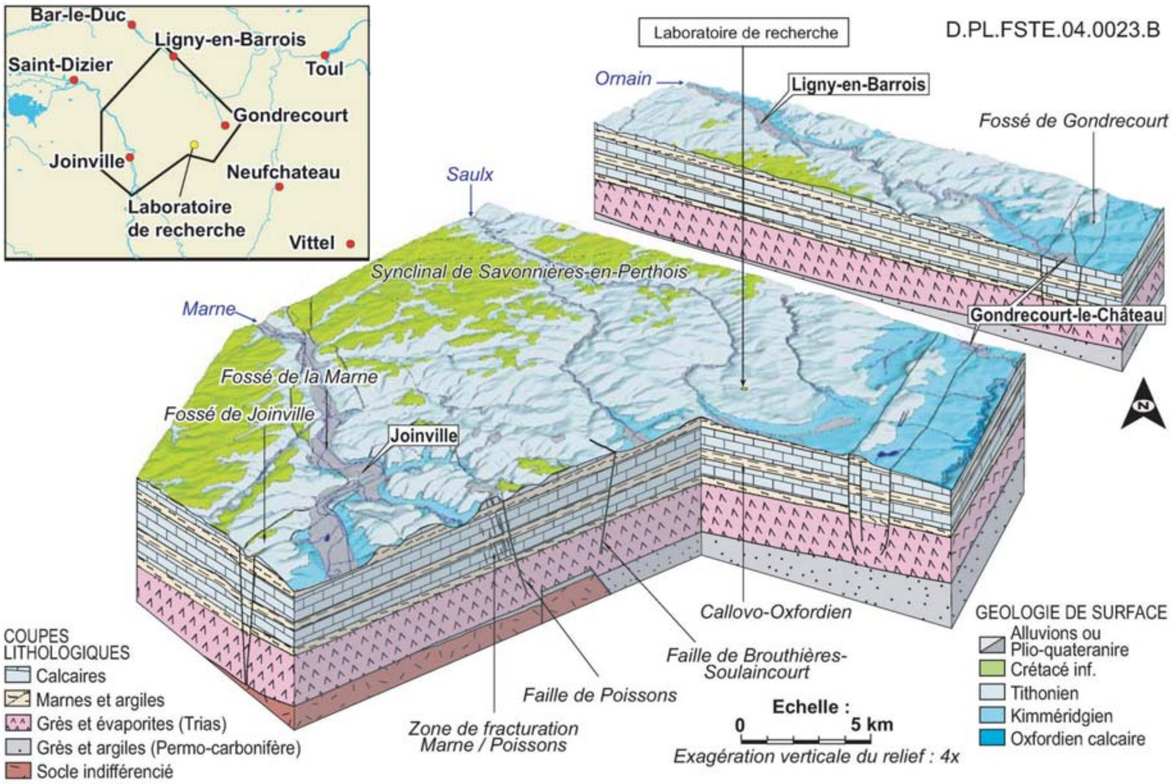

Figure 3.3.1 Geometry of the sedimentary series in the Meuse/Haute-Marne sector

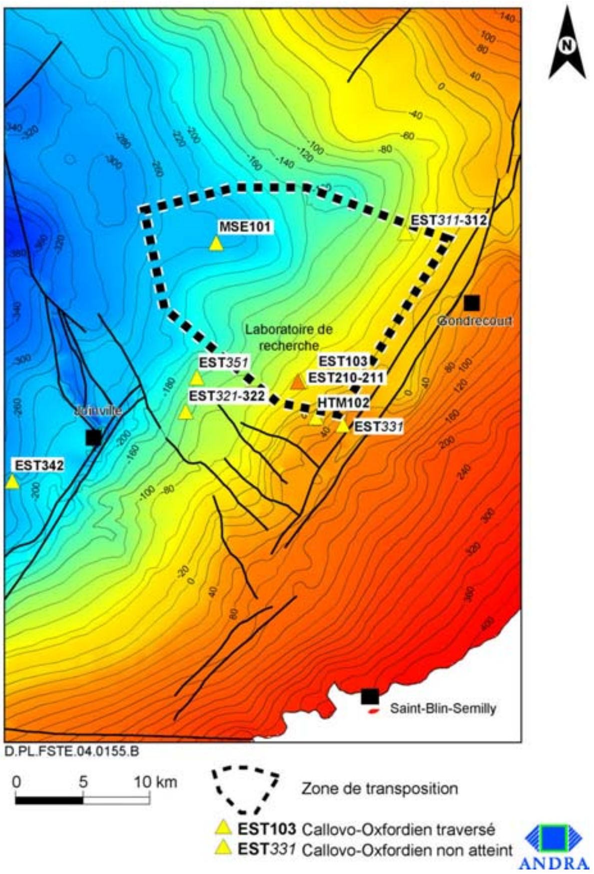

Figure 3.3.2 *Isohypses at the top of the Callovo-Oxfordian in the Meuse/Haute-Marne sector (in m NGF)*

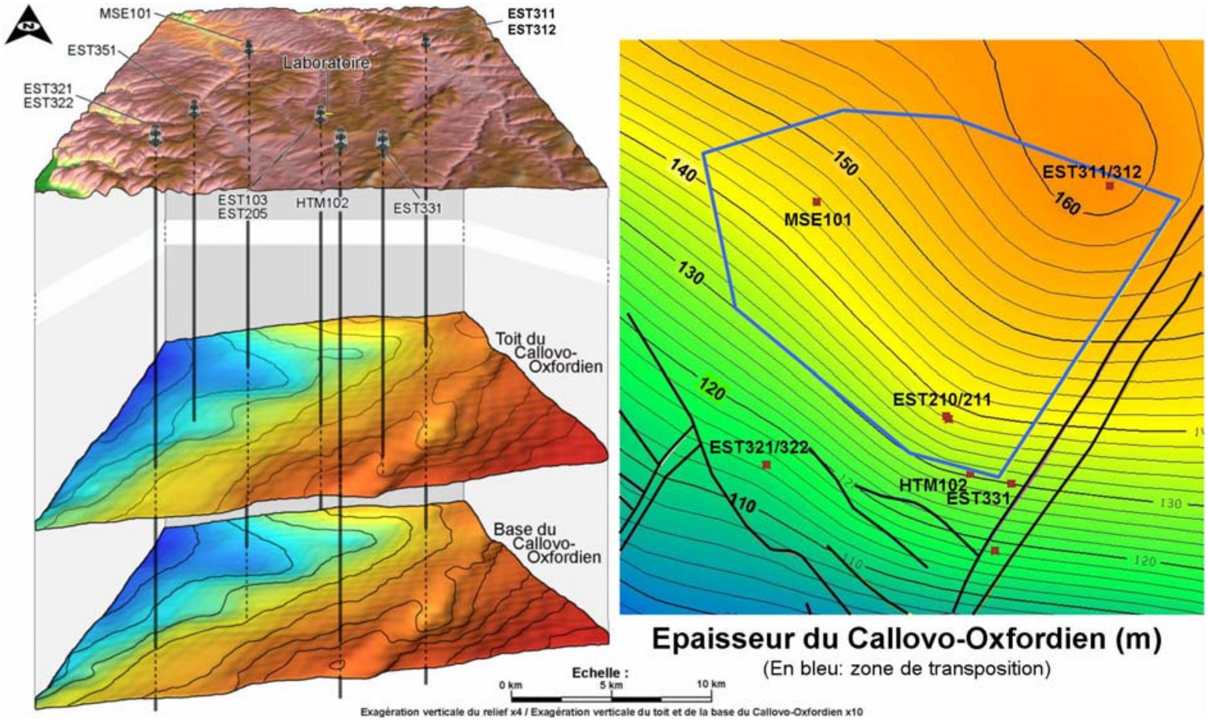

Figure 3.3.3 *Thickness of the Callovo-Oxfordian in the Meuse/Haute-Marne sector (on the right) determined from isohypses at the top and bottom of the formation (on the left)*

3.3.1.2 The main mineral phases and internal structure

The Callovo-Oxfordian layer was deposited under about one hundred meters of water during periods of high sea-level, in an open, calm marine environment (Guillocheau *et al.*, 2002). The nearest emerged zones are in the "London-Brabant" range, currently known as the Ardennes (Pellenard *et al.*, 1999).

This distance from the sources of sediment supply explains the fine granulometry of the rock constituents. The Callovo-Oxfordian displays three main mineralogical phases:

- an argillaceous phase (from 25 to 60 % of the total rock mass), formed by the following components:
    - interstratified illite/smectite (from 10 to 30 % of the total rock mass),
    - micas and illite (up to 20 % of the total rock mass),
    - kaolinite in the lower part of the layer (from 5 to 10 % of the total rock mass) and,
    - a few per cent of chlorites distributed throughout its entire thickness,
- a carbonate phase (from 20 to 40 % of the mass, essentially calcite with a few per cent of dolomite) and,
- a quartz phase of low granulometry (silts), for a proportion of between 20 and 30 % of the mass.

These three main phases are accompanied by so-called accessory phases (notably pyrite), in mass quantities of less than a few percent (Elion, 2005) (Figure 3.3.4).

Vertically, the gradual proportional variations in the main mineralogical phases are organised in three decametric sedimentary sequences which express low cyclic variation in relative sea-level at the time of deposition (transgressive-regressive cycles each lasting about 2 to 3 My). The sequence boundaries are defined unambiguously in the sector (Figure 3.3.4):

- the lower sequence rests directly on Dogger limestones, thus defining zone S0;
- the bases of the second and third sequences (zones S1 and S2) are marked by the presence of small carbonate levels;
- finally, the top of the layer (zone S2b) provides a diagraphic marker which is easy to correlate from one borehole to the next.

Within each sequence, flood maxima, corresponding to the greatest depth of water reached during deposit of the sediments, is marked by an enrichment in clay minerals. The central part of the layer, around the flooding maximum of the second sequence (zone S1b, level studied for installation of a repository), includes up to 60 % of these minerals. This level also corresponds to a mineralogical change in the argillaceous phase, revealing a passage of interlayer illite-smectite type I/S R=1 at the base of an I/S R=0 type towards the top. This change, which takes place over a few meters, is not diagenetic in origin, but is linked to sedimentation conditions: it reflects the movement of sediment supply sources linked to high sea-level conditions at the time of deposition (Pellenard *et al.*, 1999). The upper sequence shows a higher concentration of carbonates. These are revealed in the form of nodules and small decimetric to metric carbonate levels (Figure 3.3.4).

Laterally, on a sectoral scale, these sequences are found over long distances, with only slight variations in mineral composition for each of them (a few %) (Figure 3.3.4). Therefore, the only distinct trend revealed is a very slight enrichment in quartz (5 to 10 %) when moving fifteen kilometers to the North from the site (Elion, 2005). The same applies to variations in thickness (a few meters) in each sequence, these being very gradual. Only the lower sequence, controlled by the topography of the layer substrate, shows greater variation in thickness (about twenty meters in the domain concerned) (Figure 3.3.5 and Figure 3.3.6). This difference can be used to control geological barrier thicknesses on a sectoral scale, on either side of S1b surface, the level studied for possible installation of a repository. It is on the basis of these data that certain thickness criteria have been selected to define the transposition zone (total thickness of layer, upper geological barrier thickness from the repository- Inset 3.2). The constancy of these sequences gives evidence of the calm tectonic and sedimentary context during the period of deposition. Within the sector, this context is used to predict the lack of a gap in sedimentation of any size likely to disturb the continuity of the layer (Elion, 2005) and the absence of sand lenses (turbidites) within the layer, particularly given the distance from the sources of supply (emerged zones), notably during the period of high sea-level (Elion, 2005).

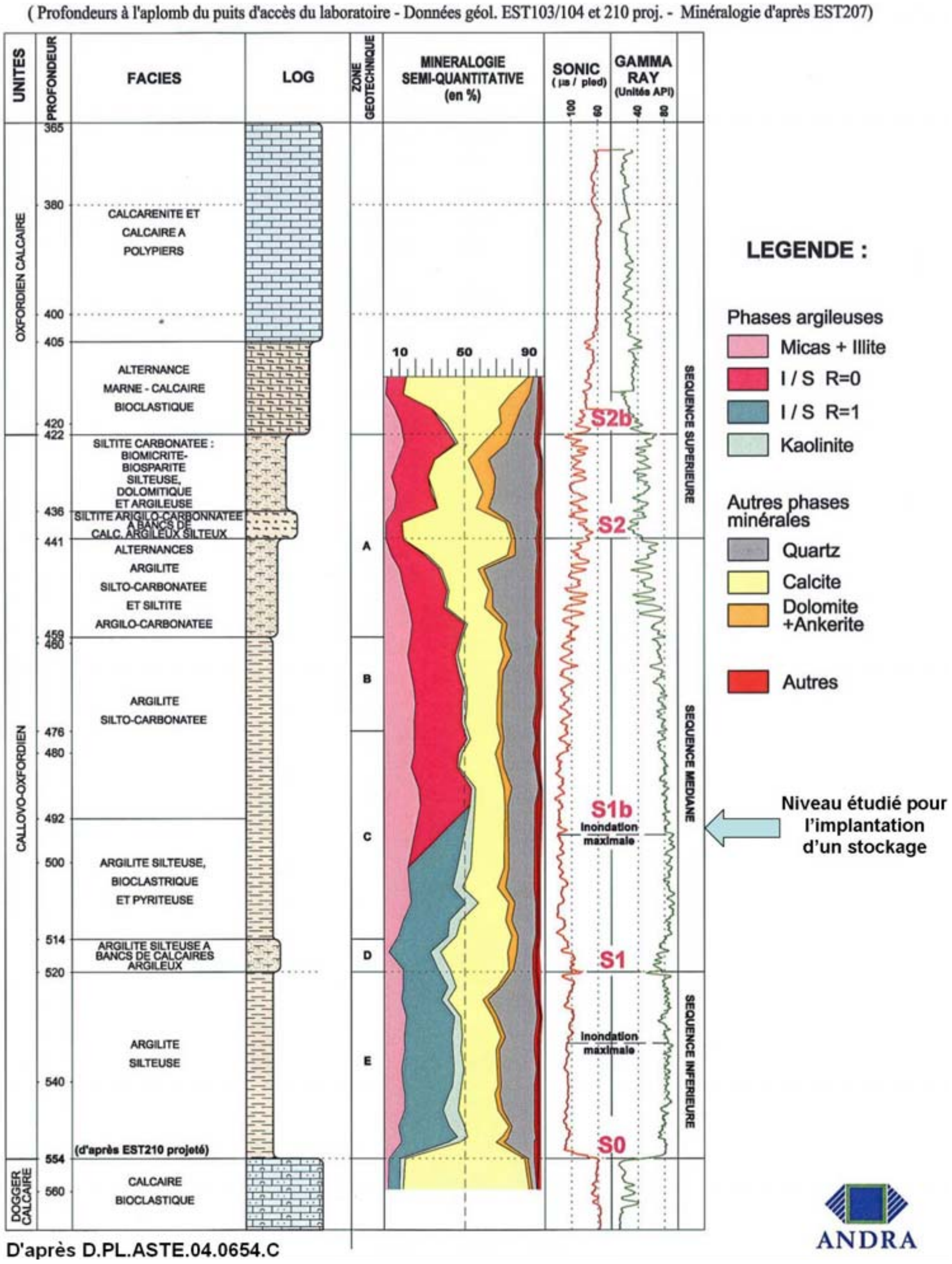

D'après D.PL.ASTE.04.0654.C

Figure 3.3.4 *Vertical organisation of the Callovo-Oxfordian directly above the Meuse/Haute-Marne site*

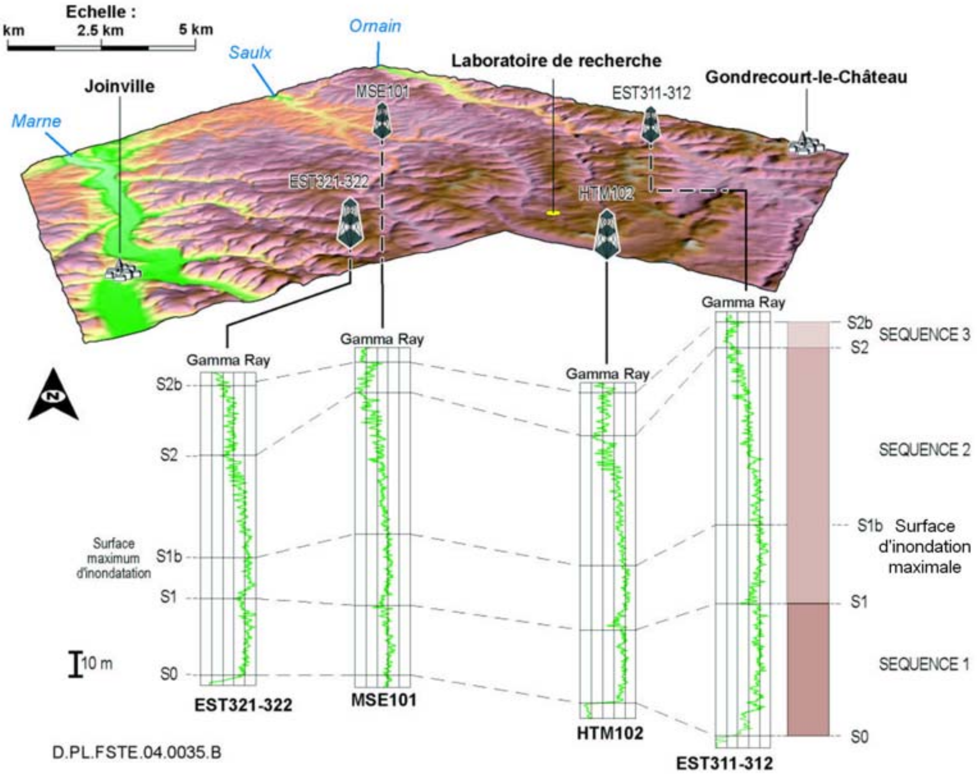

Figure 3.3.5 Lateral homogeneity of the Callovo-Oxfordian in the Meuse/Haute-Marne sector

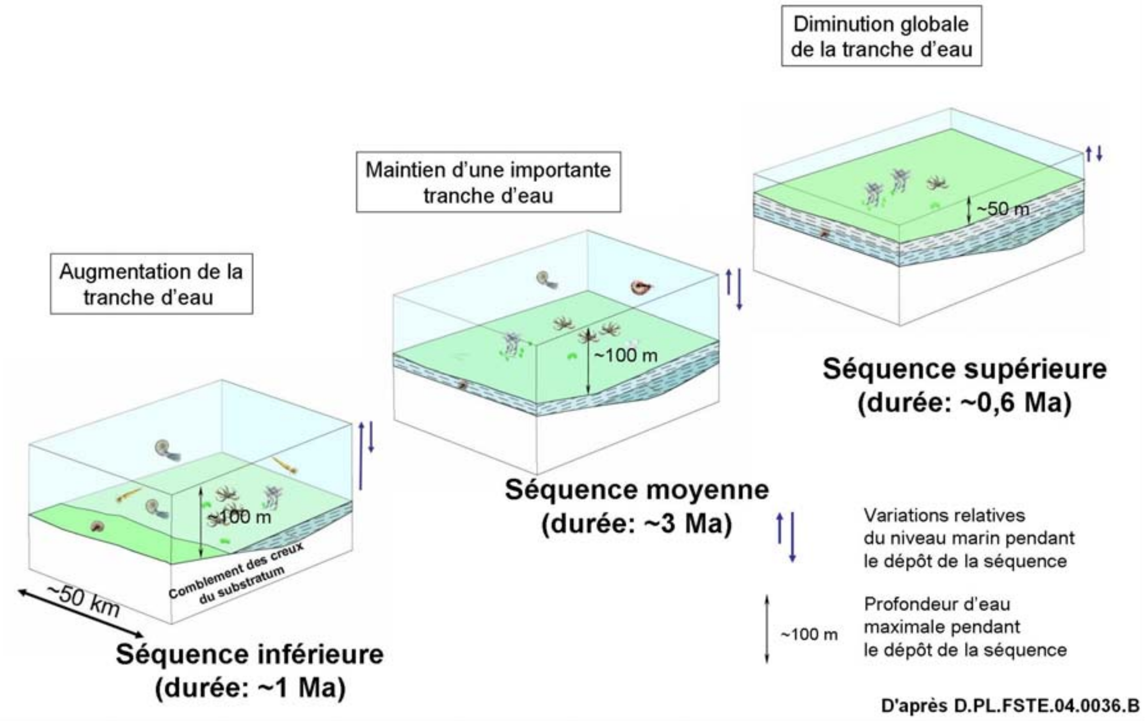

Figure 3.3.6 Schematic representation of the deposition of 3 Callovo-Oxfordian sequences

3.3.1.3 Evolution of the layer since its deposition

Between the end of deposition and the end of the Jurassic (150 – 135 My), the layer was covered by at least 500 meters of sediment (Elion, 2005). It then underwent different successive diagenetic processes. The first of these processes was gradual compaction of the sediment, with expulsion of water under the weight of later deposits. Physicochemical changes then took place (mineral dissolution and precipitation), controlled by increased pressure and temperature linked to burial and fluid circulation. These processes had very little effect on the layer during the period, given the shallow depth of burial of the layer by the end of the Jurassic (500 to 600 meters).

Later on, the major events in geological history marking the end of the Cretaceous (retreat of the sea) and during the Tertiary (Pyrenean phase, Oligocene distension followed by the Alpine phase) had little effect on the formation. Its current characteristics were essentially acquired during the Cretaceous, as shown by dating the last diagenetic episode (more than 100 My ago). This episode, of low intensity, concerned certain exchanges between clays and carbonates in very small volumes of rock (Clauer *et al.*, 2001). The initial phases, notably the clay minerals, were not affected by major modifications of their crystal chemistry and texture (Rousset & Clauer, 2003). The very limited nature of neoformations in these minerals makes it difficult to determine the duration and extension of the diagenetic phase. However, periods of about ten million years have been suggested on the basis of studies of a specific level, enriched in smectite minerals (Rousset & Clauer, 2003). Isotopic analyses performed on the carbonate phase (notably Sr and $\delta^{13}C$ – Inset 3.1) gave results within the ranges of characteristic values for Callovo-Oxfordian seawater throughout the Callovo-Oxfordian thickness (Lavastre, 2002 ; Maes, 2002) (Figure 3.3.7). The vertical evolution of isotopic compositions also shows good correlation with sea-level variation, as deduced from sequential interpretations. The original marine signature of carbonate cements is therefore preserved, demonstrating the limited diagenesis affecting the carbonate fraction. Generally speaking, the diagenetic phenomena recorded by the Callovo-Oxfordian are early, very discrete and of regional extension. They are therefore not likely to be the cause of heterogeneity at the scale of the transposition zone.

Further burial under Cretaceous sediment remains limited (around 300 meters), considering the site's position close to the edge of the basin. The maximum temperature reached by the layer remains low, around 40 °C, as shown by the analyses performed on the various temperature markers available, notably the study of maturity of organic material (Andra, 2005h, chapitre 11). This Cretaceous sediment was eroded during the Tertiary, bringing the layer to its current temperature (22 °C) which is considered to be stationary (see § 3.2.4). These temperature levels and conditions of burial are much lower than those needed for mineralogical transformation of clay phases (e.g. for smectites to be transformed into illites). In sedimentary basins, these transformations only begin at temperatures higher than 80 °C and are only detectable beyond 100 °C, with a mean geothermal gradient of 3 °C/100 m, indicating depths greater than 2,500 m (Chamley, 1989). Transformation kinetics are also slow at these low temperatures: the total transformation of smectites to illites would need about one hundred million years at 80 °C (Pytte & Reynolds, 1989).

The Callovo-Oxfordian is therefore a geological formation formed 155 million years ago in a stable context. Mineralogical transformations after the deposit of the layer are processes of regional extent, involving exchanges in the limited volumes of rock and mainly affecting carbonated cements. On the scale of the layer geological evolution, these phenomena occur at an early stage, before 100 million years.The moderate thermal evolution of the layer throughout its history was not enough to initiate mineralogical transformation of clay phases (notably illitisation).

This diagenetic evolution of regional extent and limited in intensity does not call into question initial layer architecture. This takes the form of a sedimentary unit with well limited geometry showing the three deposit sequences on major surfaces. The lateral homogeneity of the Callovo-Oxfordian, which results from the conditions of deposits on the formation and its diagenetic evolution is therefore thus controlled over a zone of several hundreds of km².This homogeneity, as well as consideration of layer behaviour during digging of the structures (depending on the mechanical properties of the rock presented below), have led to the definition of a zone of around 250 km² corresponding to a domain geologically equivalent to that of the underground research laboratory, known as a transposition zone (Inset 3.2).

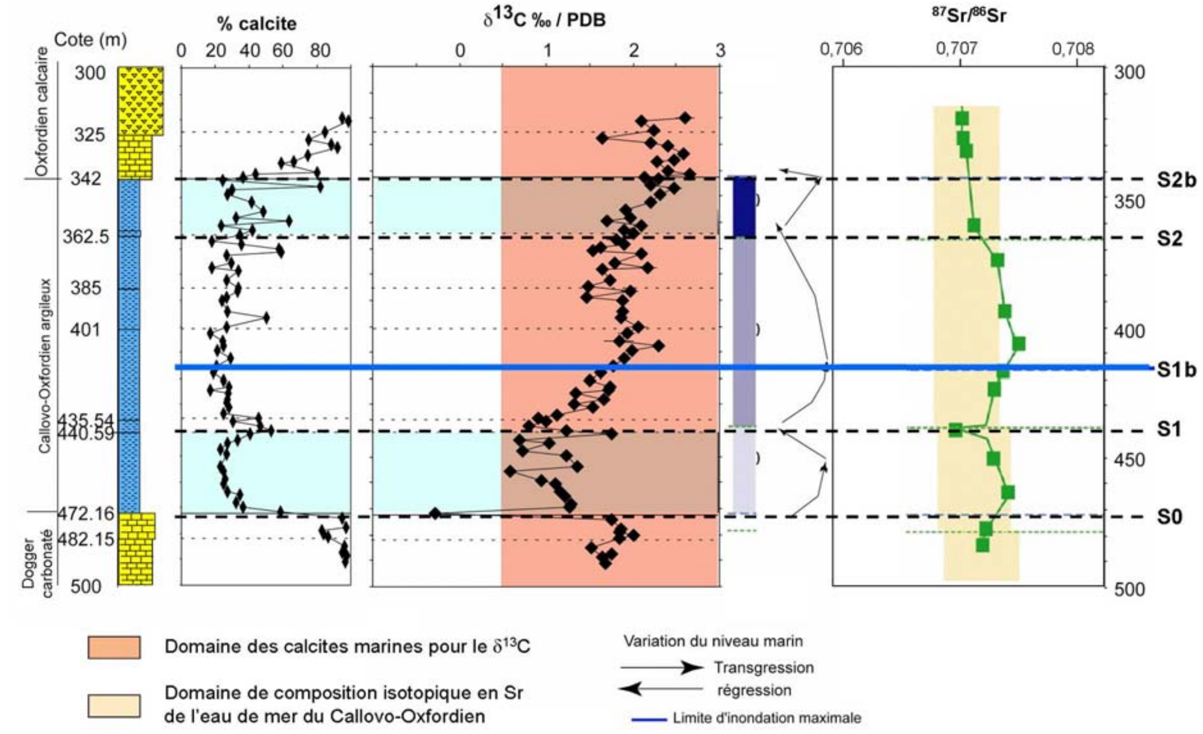

Figure 3.3.7 *Calcite concentrations, isotopic composition of Sr and $\delta^{13}C$ in calcite in borehole HTM 102 (according to (Lavastre, 2002 ; Maes, 2002)—Domain of marine calcites for $\delta^{13}C$ (Podlaha et al., 1998), domain of isotopic composition of Sr in Callovo-Oxfordian seawater (Koepnick et al., 1990))*

Inset 3.1 ***Geochemical and isotopic tracers: Principles and applications (1/2)***

Natural chemical and isotopic tracers measured in the pore water of geological formations and/or mineral phases, provide information on the behaviour of solutes naturally present in these formations, so that transport parameters such as velocities can be generally validated or water-rock interactions identified in time and space.

Natural anionic tracers (chlorine and bromine) in water are studied to follow the movements of solutes in the formations. Indeed, these interact very little with the mineral matrix and display identical behaviour relative to different processes. The Cl/Br ratio is an indicator of the source and evolution of water: it is about 300 for seawater and several thousand for the dissolution of evaporites.

The ratios between different **stable isotopes of a single element** reposition the sample analysed relative to an initial, so-called standard environment (the isotopic fractionation ratio being known for this environment). The isotope ratio between two stable isotopes of a single element is generally rounded to the isotopic ratio of the standard using the following formula (here for two stable chlorine isotopes):

$$\delta^{37}Cl = \left(\frac{{}^{37}Cl / {}^{35}Cl^{\,\acute{e}ch.}}{{}^{37}Cl / {}^{35}Cl^{\,std}} - 1 \right) * 1000$$

Therefore, the concentrations of stable water isotopes (δ^2H, calculated from the ^{2}H/H ratio and δ^{18}O, determined from the ^{18}O/^{16}O ratio) help determine its origin as marine or meteoric. The same applies to analyses of chlorine isotopes which, because of the different mobility rates of the two stable isotopes (^{37}Cl and ^{35}Cl), can also be used to identify transport processes, particularly diffusive processes.

More specifically, in **solid phases**, concentrations of Strontium (^{87}Sr/^{86}Sr) and Carbon (^{13}C/^{12}C) isotopes are used to determine the media in which the minerals were formed and evaluate water-rock interactions (diagenetic phenomena).

The same types of analyses can also be performed on **gases taken in samples**:

- the stable isotopes of water vapour give a measurement which is independent of that of formation water (sometimes difficult to extract for clay-rich media);
- the carbon in dissolved CO_2 is measured as an indicator of the water's equilibrium with carbonate phases compared with the δ^{13}C determined in the carbonate phases detected;
- alkane isotopes are characterised to determine the origin and maturity of gases found in the samples;
- rare gases, helium and, above all, argon, are produced more or less continuously in the rock. The study of rare gas distribution profiles helps characterise the transport mode according to the accumulations or dilutions observed.

Natural radioactive isotope markers are studied to determine residence times.
This applies to the study of radioactive imbalance in the ^{238}U radioactive decay chain (presented below).

$${}^{238}U \xrightarrow[4{,}469.10^{9}\,a]{\alpha} {}^{234}Th \xrightarrow[24{,}1\,j]{\beta} {}^{234}U \xrightarrow[2{,}445.10^{5}\,a]{\alpha} {}^{230}Th \xrightarrow[75200\,a]{\alpha} {}^{226}Ra \xrightarrow[1602\,a]{\alpha} {}^{222}Rn.........{}^{206}Pb$$

The principle is based on calculating the ratio of activities between two elements in the chain, which, at equilibrium (closed medium) must be 1. Imbalance indicates fractionation, revealing a disturbance in the medium. This study reveals the recent evolution of the system (about 800,000 years).

Geochemical and isotope tracers: Principles and applications (2/2)

Studying certain **natural or artificial radionuclides** leads to absolute dating of water, based on radioactive decay. A broad time spectrum is now covered by techniques which are already available or in the process of development.

- **Tritium** is a radioactive isotope of hydrogen, with a half-life of about 12 years. It does not exist naturally, so its presence in the environment results from nuclear testing in the 1950s and 1960s. It is used to date recent water which has infiltrated over less than 50 years.
- **Carbon-14, chlorine-36** and **krypton-81** are three radioactive isotopes which are produced naturally in the atmosphere in quantities which are more or less constant (or known) over time. These isotopes infiltrate underground water tables in rainwater and are then no longer in contact with the atmosphere. Using the half-life of these isotopes, their residence time in the water can then be measured. ^{14}C has a half-life of 5,730 years, so that water can be dated to about 40,000 years. Isotopes with long half-lives such as ^{36}Cl (300,000 years) and ^{81}Kr (229,000 years) are used to determine residence times in water which is several tens of thousands of years or up to one million years old.

3.3.1.4 Mechanical and thermal properties

The internal architecture of the rock matrix layer conditions its mechanical behaviour and consequently the breackdown of the formation into geomechanical zones. This zoning is based on the formation's clay content and is therefore closely linked to the sequential breakdown described above (see § 3.3.1.2). Laterally, the sequential breakdown and its correlations are used to extrapolate this geomechanical zoning, in coherence with lithological variations throughout the transposition zone.

Vertically, three zones with marked differences in mechanical behaviour can be distinguished, in connection with the percentage of clay in the rock (Figure 3.3.4) (Andra, 2005h, chapitre 25).

- The upper zone (zone "A") is about 37 m thick directly above the site. It displays average behaviour which is more rigid than the underlying zones. Alternating more or less carbonate-rich beds leads to wide dispersion of mechanical properties. Strength and the deformation module have average values of 27 MPa and 6,000 MPa respectively.
- The median zone (zone "B/C") is about 55 m thick. This zone corresponds to a gradual increase in deformability (reduced rigidity) and a gradual reduction in the zone's resistance from top and bottom towards the centre of the zone, this being correlated with increased clayiness. The most deformable zone is on a level with the installation of the repository structures. The average properties of the zone are 4,500 MPa for the deformation module and 21 MPa for compression strength. Short-term flow speeds (first weeks to first months) are estimated at 10^{-2} to 10^{-3} year^{-1}. In the longer term, after the first year, these speeds are 10^{-4} year^{-1}. In this zone, these speeds are about 4 times higher than in zone "A".
- The lower zone (zone "D/E"), 40 meters thick, has a mean mechanical strength of about 21 MPa and a deformation modulus of about 6,000 to 7,000 MPa. The homogeneity of sedimentation in this zone is reflected in the low variability of physical properties (density, porosity) and slight variability in mechanical parameters according to variability in carbonate levels (locally more rigid behaviour). This variability is observed towards the top of this zone (carbonate interval separating the lower sequence from the median sequence).

Under the effect of gravity, argillite sedimentation induces preferential orientation of clay particles. Consequently, it stratifies the structure of the matrix, giving rise to the slight anisotropy of these mechanical properties.

Thermal conductivity in the Callovo—Oxfordian is anisotropic because of this stratification (about 1.3 to 1.9 $W.m^{-1}.K^{-1}$ vertically and 1.9 to 2.7 $W.m^{-1}.K^{-1}$ horizontally). It varies only slightly over the height of the layer, also linked to its clay content and hence geomechanical zoning.

Inset 3.2 **Definition of the transposition zone**

The transposition zone is the result of a procedure involving searching, in the sector studied, for a geographical domain considered to be geologically equivalent to the underground research laboratory site, both from the point of view of geometry and in properties of confinement of the Callovo-Oxfordian formation as well as the characteristics of disturbances engendered by a repository. Mapping of this zone is based on the following list of parameters:

- thickness of the layer;
- preservation of the formation's physicochemical properties, which result from the conditions under which the sediments were deposited and their later evolution (diagenesis, tectonics), evaluation of this being based on (i) lithological variability, vertically (mineralogical succession, especially clay mineral content) and horizontally (variations on the relative proportions of the principal rock constituents), and (ii) distance from major faults;.
- factors controlling the extension of disturbances around the underground structures (intrinsic strength of the rock, amplitude of stresses, ...).

These parameters are used to define a limited zone (see figure below) (Andra, 2005h, chapitres 21 et 28):

- to the South, by the minimum thickness of 130 m (zone in which there is still at least 65 m of formation above surface S1b, the level studied for installation of a repository);
- to the East by the Gondrecourt graben, one kilometre from the repository;
- to the North by a line schematically materialising the facies variations expected in the layer (notably quartz enrichment), based on controls made at boreholes MSE101 and EST311;
- to the West by a maximum depth of layer criterion (about 630 m at S1b), controlling the extension of disturbances, particularly mechanical, when excavating the structures, which appears to be more restrictive than the criterion applied to avoid the Marne faults.

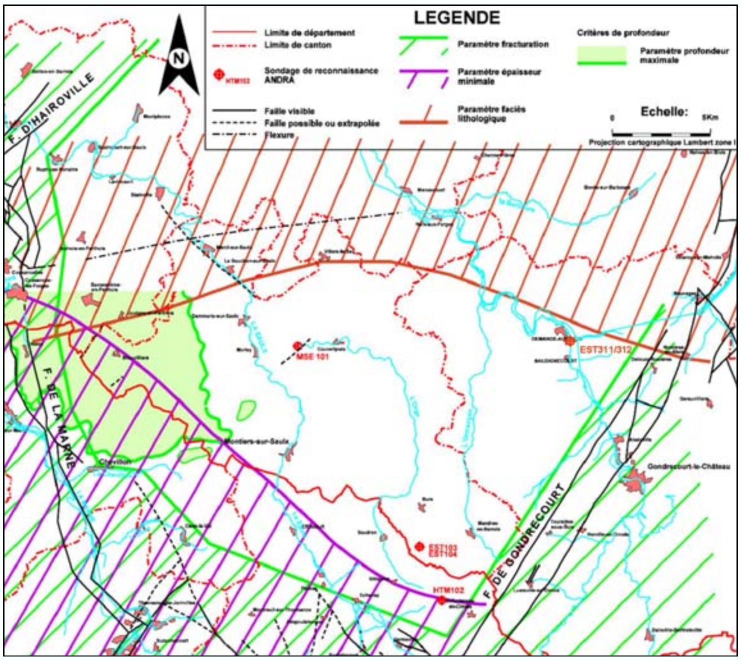

Definition of the transposition zone

The zone thus defined, covering an area of about 250 km², remains schematic with certain limits (to the north in particular) based on criteria which are more qualitative than quantitative. However, given the expected constancy of the properties of the Callovo-Oxfordian within these boundaries, it can be used to delineate the area of interest for studying a repository, based on cautious hypotheses.

3.3.1.5 Textural properties and porosity

The initial mineralogical composition and diagenetic history of the Callovo-Oxfordian argillites are such that the mineralogical and textural characteristics, have been remained relatively constant for more than 100 My.

The porous volume depends on the arrangement of the three main mineral phases (Andra, 2005h, chapitre 12):

- The clay phases (largest – 60 % maximum) are in the form of aggregates of clay minerals (platelets of more or less regular shapes) from several tens to one hundred micrometers long and a few tens of nanometers thick. These aggregates act as a matrix and are roughly organised in flexuous beds, according to stratification;
- small quartz-bearing detritic elements (5 to 10 micrometers), are distributed evenly in this matrix;
- the carbonate phase is displayed is the form of elements of variable sizes, some being fairly large (up to millimetre scale), which are bioclasts and automorphic crystals resulting from secondary neoformations following diagenetic events.

Because of the relative proportions of the clay phases and the other phases, detritic and calcite elements are not in connection and appear to be dispersed throughout the matrix.

This arrangement produces two types of porosity within the rock (Andra, 2005h, chapitre 12) (Figure 3.3.8, Figure 3.3.9):

- porosity within the clay matrix (around the aggregates and particles of clay), depending on the sizes of inframicrometric pores and described as meso- and microporosity (roughly 90 % of porous volume);
- porosity at the interface between the clay matrix and quartz particles and bioclasts, depending on the sizes of micrometric pores and inframicrometric pores for neoformed carbonates, described as macroporosity (around 10 % of porous volume).

The total porous volume thus defined is about 18 % of the total volume of the rock. This porosity induces considerable tortuosity linked to inter-organisation of the clay aggregates.

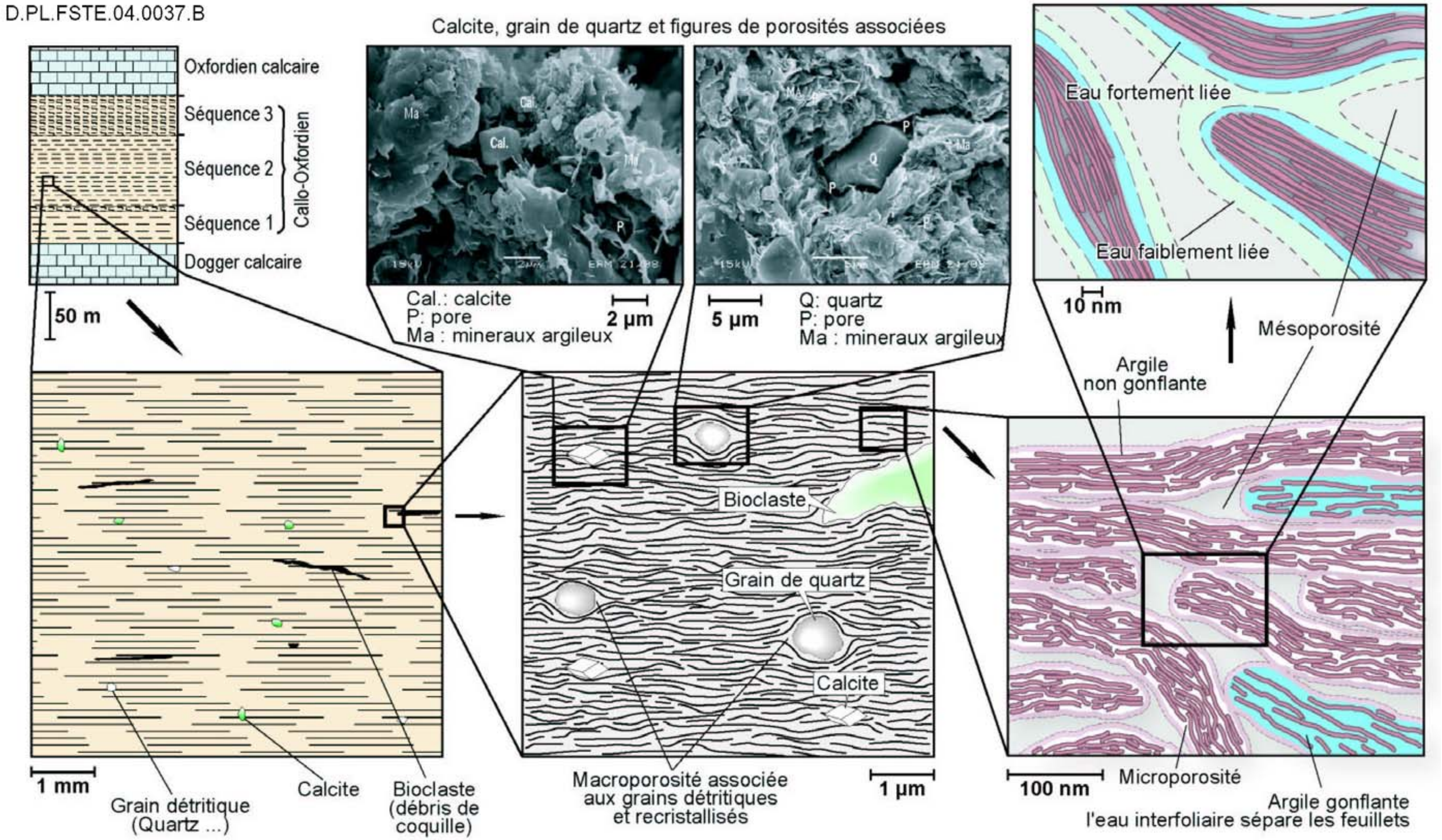

Figure 3.3.8 *Schematic representation of the Callovo-Oxfordian texture and porosity*

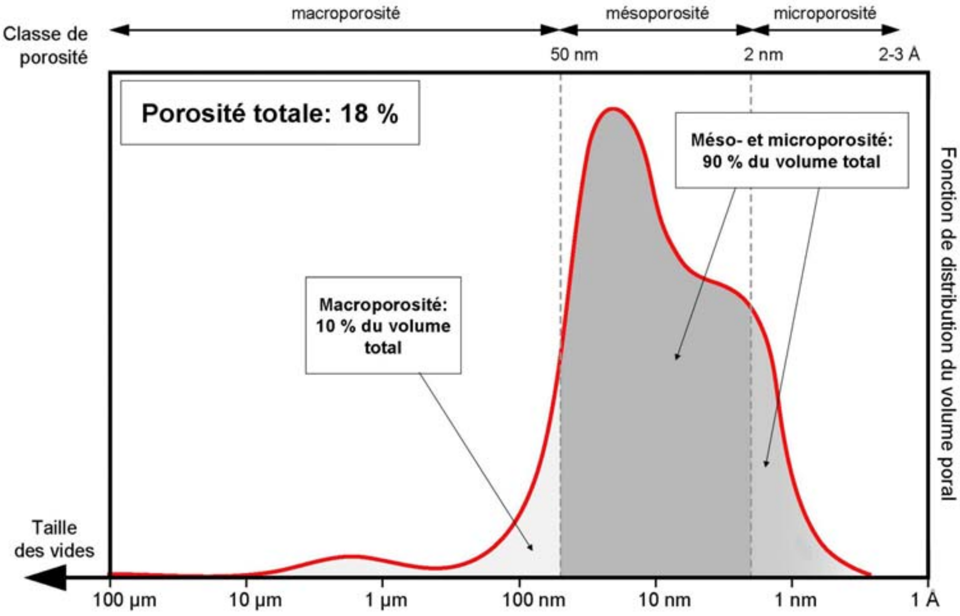

Figure 3.3.9 *Conceptual model of formation porosity (based on mercury porosimetric measurements and nitrogen adsorption curves) (Andra, 2005h, chapitre 12)*

3.3.1.6 Pore water and water flow in the Callovo-Oxfordian

Generally speaking, the water is more structured (*i.e.* organised in a network) close to the surfaces of minerals, particularly close to those with a residual electrical charge. In a porous medium, this defines bound water, and therefore non-mobile water and free water unaffected by this effect. (Inset 3.3)

Clay particles carry a permanent charge and high specific surface area and herefore have a major effect on water structure in the immediate surroundings (Andra, 2005h, chapitre 12), unlike quartz or carbonates which do not have permanent charges and much smaller specific surface areas.

A thin layer of clay-bound water is therefore formed around the clay particles, which may plug some pores "electrochemical gap"). For sediment such as the Callovo-Oxfordian argillites, the pores thus obstructed by this "electrochemical gap" are about 10 to 20 nanometers wide (Andra, 2005h, chapitre 12) (Figure 3.3.8). The rock's porosity being essentially distributed throughout the clay matrix, the proportion of clay-bound water, in contact with the particles, is high. It accounts for about 50 % of the water in the total porosity (Altmann & Coelho, 2005 ; Altmann & Jacquot, 2005). This clay-bound water is not involved in flow within the rock.

These textural properties give the Callovo-Oxfordian formation low permeability throughout its thickness (Altmann & Coelho, 2005 ; Altmann & Jacquot, 2005). The different measurements made, both on samples and in boreholes, give coherent values between 10^{-14} m.s^{-1} and 10^{-13} m.s^{-1} (Altmann & Coelho, 2005 ; Altmann & Jacquot, 2005) (Inset 3.4). It should be noted that the lowest permeability values (about 10^{-14} m.s^{-1}) are deduced from the analyses of pressure recorded by EPG probes, thus providing access to reliable values for a significant volume of rock. The highest value deduced from an EPG measurement is around $4{\cdot}10^{-13}$ m.s^{-1}. This range of values is also coherent with the first results of experiments in progress on the Meuse / Haute-Marne site (PEP experiments: measurement of interstitial pressure and permeability of argillites and REP: monitoring the argillite response to shaft excavation). When all these measurements are reviewed in perspective there is no evidence of real permeability anisotropy. This anisotropy would be the consequence of the organisation of clay minerals, inherited from the conditions during sedimentation and would fall within the range given above. This is also coherent with certain specific measurements made on samples of gas, which show anisotropy to a factor of 10 between horizontal and vertical permeability (Zhang & Rothfuchs, 2004).

This low permeability of the Callovo-Oxfordian, linked to low hydraulic head gradients on either side of the formation, controls slow vertical water flow (Inset 3.5). The velocities of this water flow are fairly different in detail because of the medium's pore structure. Moreover, some pores are not connected and cannot take part in the water flow. A so-called kinematic porosity is therefore defined, which is a fraction of total porosity, used macroscopically to calculate mean water flow velocity in the direction of the hydraulic head gradient. For the Callovo-Oxfordian, this kinematic porosity has been taken as being the same as the fraction of free water in the rock, i.e. about 9 %, corresponding to half the total porosity. The very low permeability determines average flow speeds within the layer (Darcy velocity, inset 3.5) at around 3 cm per 100,000 years, which corresponds to a water transfer velocity of about 30 cm per 100,000 years, considering the kinematic porosity.

Inset 3.3 ***Water structure in saturated and unsaturated argillites***

In a porous medium there are interactions between the various non-miscible fluids in the pore volume, and also between the fluids and various solids constituting the solid matrix.

In a water-saturated porous medium, which is the initial state of the geological layers penetrated by the various repository structures, the following structural conditions of water can typically be distinguished (following figure) (Andra, 2005h, chapitre 12):

- free water, which is not significantly affected by the interaction between water and the solid matrix. This water moves under the effect of gravity. The porosity it occupies is called kinematic porosity. In this porosity, the pores are larger than the characteristic dimensions of about 2.10^{-8} m. In granular media such as gravel or sand, in which all the pores are large, kinematic porosity can be taken as total porosity and forces other than gravity (capillary, Van de Waals...) can be ignored, including the surface effects of the grains constituting these media which are not usually electrically charged;
- the weakly bound water is in small pores in which the capillary forces are higher than the force of gravity. That is why this water is also called capillary water. Typically, the size of the pores is between $2 \cdot 10^{-8}$ m and $3 \cdot 10^{-9}$ m. This water can only be removed from the medium through desaturation. As desaturation takes place, increasingly small pores are desaturated. The suction forces necessary for this extraction increase gradually during the process, because the capillary pressure is inversely proportional to the radius of the pore (Inset 6.5 and Inset 6.6). This type of water is found in cemented, diagenetic or crystalline media (sandstone and fine limestone, granite, ...) and also in clays;
- strongly bound water, in which capillary forces are weaker than electrochemical forces close to the surface of certain minerals such as clays. These forces act only over very short distances, just a few nanometers. They develop mainly in clays and require major suction forces to move the water they hold on the surface of the clay sheets. In the Callovo-Oxfordian argillites, suction forces of several tens of MPa are required to move this water;
- water which is an integral part of clay minerals. This is structural water (independent of the degree of hydration) and interfoliar water. In certain clays this water may be mobile. This is the case for bentonites, which do not have the same chemical composition when they are desaturated as they do when saturated, which partly contributes to their swelling property. For Callovo-Oxfordian argillites, this water cannot be removed from the solid matrix and cannot therefore take part in flow.

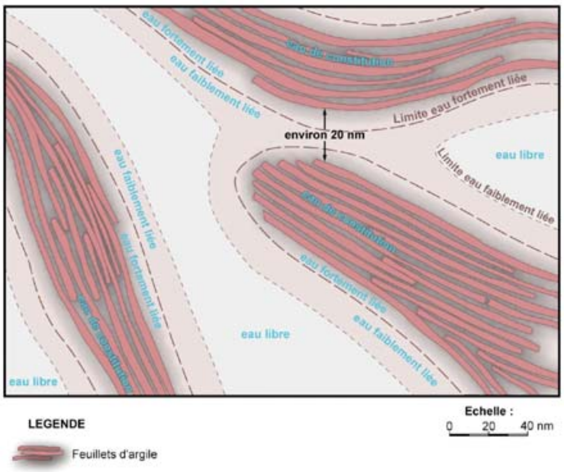

Diagram of the structure of water and the scale of pores in argillites

Inset 3.4 ***Callovo-Oxfordian (very low) permeability measurements (Andra, 2005h, chapitre 16) (1/2)***

Along with the diffusion coefficient, permeability is an important element for the assessment of radionuclide transfer capacities within the Callovo-Oxfordian. These two parameters together make it possible to assess the dominant transfer mode, between advection and diffusion and ultimately the radionuclide transfer time from the repository to surrounding formations (cf. § 3.3.1.7). Expected permeability of Callovo-Oxfordian argillites are several orders of magnitude less than those currently encountered in aquifer formations, so that permeability measuring systems conventionally used in hydrogeology prove to be inappropriate as they are. Low water flow rates brought into play in mediums with permeability of less than 10^{-10} m/s require high precision instruments and consideration of any artefacts. Thus, achieving a stationary water flow system and a measurable water flow rate normally requires injection of a fluid at high pressure gradients. Too high a gradient could lead to modification of the porosity due to the hydraulic and mechanical coupling and turbulent water flows, even movement of adsorbed water. Water flow measurements thus run the risk of being erroneous and their interpretation based on one of Darcy's laws results in an error in permeability measurement. In addition to this, the problem arises of scale of measurement representativity for the thickness of at least 130 m of the Callovo-Oxfordian layer.

In order to gain better access to argillite permeability, Andra deployed a set of methods (and instruments) specially designed and adapted from conventionally used methods, both for samples and *in situ* in boreholes.

The most routinely used method consists of causing temporary and limited disturbance of the fluid pressure in the medium and measuring the resumption of pressure balance. This method known as a pulse-test can be used in boreholes, between packers, but also on small-sized samples (of around ten centimetres), in laboratories where it completes measurement under steady-state operating conditions.

Other experimental systems, specially developed, also facilitate access to permeability of the medium:

- it is possible to use the transient phase of pressure recovery, recorded after the installation of pressure sensors in the formation (electromagnetic pressure gauges). Analysis of this transient phase determines, based on inverse modelling, confidence intervals for each parameter including permeability controlling pressure increase in the chamber;

- on samples, interpretation of water sorption/desorption isotherms and of hydrological profiles determines porosity depending on the degree of saturation. Thus the following items can be measured::
  - either hydrological profiles in the sample during their resaturation, as permeability is calculated based on several profiles, corresponding to different durations and based on the sorption/desorption curve,
  - or evolution kinetics of the sample mass related to disturbance of a capillary pressure imposed on this sample, as permeability to liquid is calculated by solving the equation of mass transfer in a non-saturated medium.

Each of these methods (laboratory measurements and investigations *in situ*) has advantages and disadvantages. *In situ* measurements provide access to larger scales than laboratory measurements. Moreover, they have the advantage of being carried out under mechanical and hydraulic conditions which are those of the natural medium. Laboratory measurements involve smaller-sized samples, less representative of large-scale permeability, but making it possible to strictly control experimental conditions (fluids used, mechanical stress, sample deformation, etc). They are carried out with instruments of metrological precision higher than those for investigations *in situ*. On the other hand, the sample can be damaged when it is taken despite precautions taken (prompt emplacement in confinement cells).

Callovo-Oxfordian (very low) permeability measurements (Andra, 2005h, chapitre 16) (2/2)

Lastly, measurement durations vary greatly according to the method used. ”Pulse-test” type measurements in boreholes are made over short periods of time (about a day) whereas measurements of samples are carried out over long durations (around a week). Assessments based on pressure increases in closed chambers are made over far longer periods of time (several months to several years) providing optimum determination of their formation pressure and permeability.

Measuring campaigns carried out by Andra on the Callovo-Oxfordian used all these experimental systems:

- tests have been conducted on the various boreholes, on the site of the underground research laboratory and also on the transposition zone scale (mainly in boreholes MSE101 and HTM102) and at different intervals in the layer,
- measurements in closed chambers (EPG) have been made on the same underground laboratory site and at different stratigraphic levels of the layer,
- lastly, numerous measurements of permeability have been made on samples, as this review area is especially the subject of a specific research programme and of comparison of results obtained within the framework of the FORPRO research group agreement between Andra and the CNRS (Forpro, 2003)

All the results obtained made it possible to (i) assess Callovo-Oxfordian permeability with a good level of confidence (and consistent with results of measurements in Opalinus clays in the underground laboratory of Mont Terri and in Benken); (ii) show permeability homogeneity throughout the layer, absence of scale effect and low anisotropy, at the most of factor ten between horizontal and vertical permeability.

Inset 3.5 ***Water flow in natural porous media: Darcy's law***

The causes of water displacement in a porous medium are pressure gradients on the one hand and external forces on the other. In naturally porous media the other forces can generally be reduced to gravity. The combination of these two effects, pressure gradient and gravity, are used to define the hydraulic head. Darcy's law links hydraulic head to water flow rate:

$$\vec{U} = -\overline{\overline{K}}\,\overrightarrow{gradH}$$

With:
U: average flow rate of water through the porous medium, or Darcy's velocity
K: coefficient of permeability ($m.s^{-1}$)
$H = \frac{p}{\rho g} + z$: hydraulic head (m of water column)
p: pressure (Pa)
ρ: water density ($kg.m^{-3}$)
g: acceleration due to gravity ($m.s^{-2}$)
z: altitude (m)

The hydraulic head gradient is the main force driving water movement in a porous medium, but not the only one. Experimental observations have recorded water movement under the effect of other gradients, mainly:

- the electric potential gradient, gradE, responsible for the electro-osmotic effect;
- the thermal gradient, gradT, responsible for the thermo-osmotic effect;
- the chemical concentration gradient, gradC, responsible for the chemical osmotic effect.

Darcy's law can be summarised therefore by:

$$\vec{U} = -\overline{\overline{K}}_1\,\overrightarrow{gradH} - \overline{\overline{K}}_2\,\overrightarrow{gradE} - \overline{\overline{K}}_3\,\overrightarrow{gradT} - \overline{\overline{K}}_4\,\overrightarrow{gradC}$$

which can be rearranged and written as:

$$\vec{U} = -\overline{\overline{K}}_1\left(\overrightarrow{gradH} + \overline{\overline{\sigma_E}}\,\overrightarrow{gradE} + \overline{\overline{\sigma_T}}\,\overrightarrow{gradT} + \overline{\overline{\sigma_C}}\,\overrightarrow{gradC}\right)$$

With σ_E, σ_T, σ_C representing the respective coefficients of efficacy for electro-osmosis, thermo-osmosis and chemical osmosis.

Pore water in the Callovo-Oxfordien is at a higher pressure than the pore water in the surrounding Dogger and Oxfordian limestone. Interstitial pressure measurements directly above the site, obtained using EPG and in measuring chambers *in situ* highlight, in a replicable and consistent manner, overpressure of between 20 and 40 metres over total Callovo-Oxfordian thickness (Andra, 2005h)). Near the layer boundaries, a steep pressure gradient with the surrounding layers is observed (Figure 3.3.10). Over pressures are frequently observed in the clay-rich formations of sedimentary basins. The possible origins are presented in inset 3.6 (Altmann & Coelho, 2005 ; Grauls, 1999).

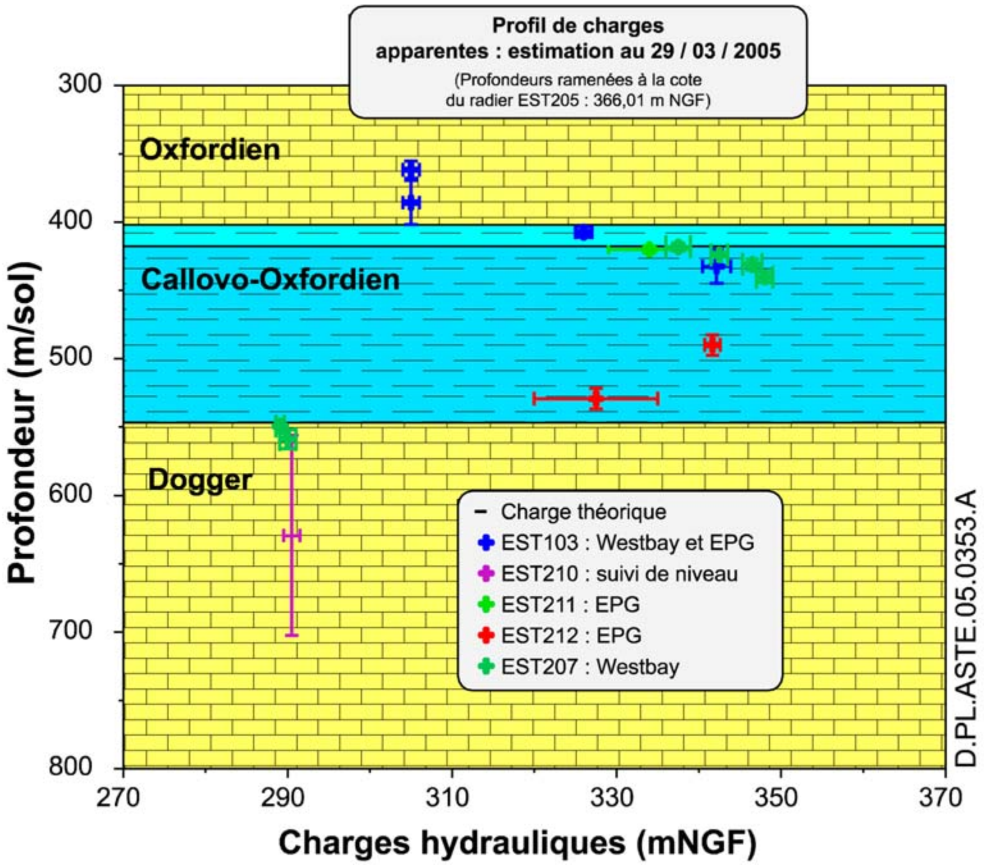

Figure 3.3.10 *Profile of apparent hydraulics heads measured in the Callovo-Oxfordian directly above the Meuse / Haute-Marne underground research laboratory (compilation of measurements available at the end of March 2005)*

Inset 3.6 ***Phenomena responsible for over pressure in deep clay formations (1/2)***

In sedimentary basins, clay formations often display higher interstitial pressures than the lithostatic stress or even higher than those measured in their surroundings. The main forces driving these over pressures are either an increase in the volume of fluid (under thermal stress, for example) or a reduction in pore volume (particularly under mechanical stress), or effects linked to boundary conditions or their modification over time. All the main causes are summarised in the following figure.

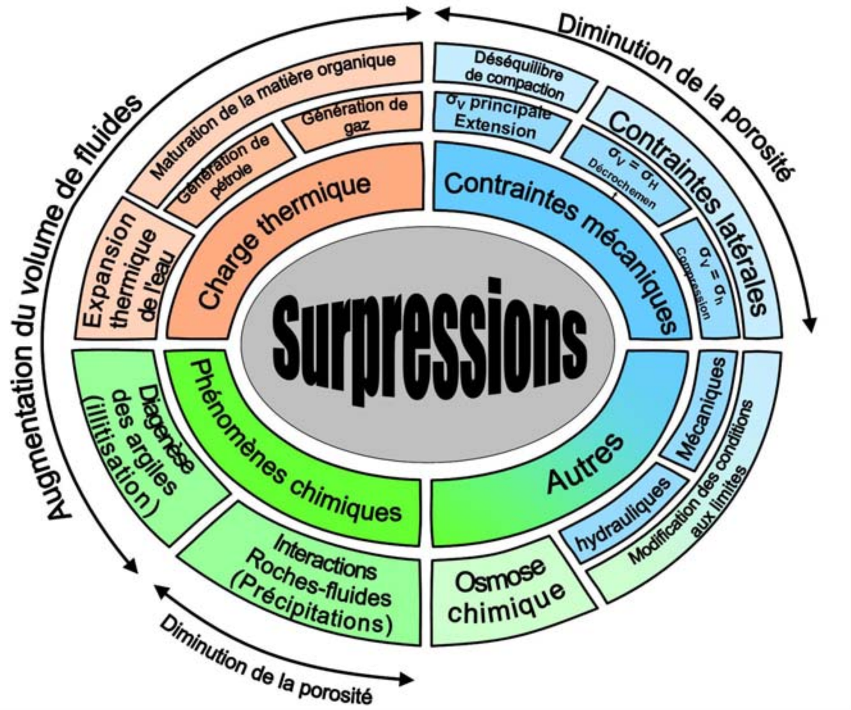

Figure based on Grauls, 1999, modified.
Phenomena responsible for over pressures in geological formations

- The causes linked to **mechanical stress** are:
  - imbalance due to compaction (or sub-compaction) observed when clay sediments, not yet consolidated, are in an early stage of diagenetic evolution with high concentrations of water. In this case, the over pressure results from interstitial water absorbing part of the weight of the underlying sedimentary pile.
  - the gradual deformation of the sedimentary skeleton under the effect of tectonic stresses which do not allow the pressure equilibrium to be restored in the formation by water flowing out of it, when there are less permeable zones at the top and bottom of the formation.

- The causes linked to **thermal charge** are all responsible for an increase in the volume of fluid:
  - either by the production of liquid or gaseous hydrocarbons during kerogen cracking;
  - or by the thermal expansion of water.

Phenomena responsible for over pressure in deep clay formations (2/2)

- The causes linked to **chemical stress** are essentially diagenetic:
    - the transformation of smectites into illites (illitisation) releases water which was bound to the smectite, thereby helping increase the volume of this water;
    - fluid-solid interactions and the neoformation of mineral phases (carbonates for example) reducing the porosity of the argillites.
- **Conditions at layer boundaries** (and their modification over time) may also be responsible for over pressures.
    - This is the effect of modifying hydraulic conditions at the boundaries, in the surroundings at the top and bottom of the layer: the cessation of aquifer charging at outcrops during glaciation cycles, changes in surface hydraulics,…). In this case, rebalancing in the clay layer, which has lower permeability, has not had time to eliminate them.
    - It may also be due to the existence, in the past, of a greater mechanical load on the layer. The reduction in load may be due to partial erosion of the sedimentary column or the disappearance of a thick layer of ice, for example. As in the previous case, the clay layer has not had time to restore equilibrium under the new conditions.
- Finally, **chemical osmosis** is also a cause of these over pressures, the driving force, in this case, being differences in the water's chemical activity between two porous media (Inset 3.7).

Examples in numerous basins show that over pressure does not have a single cause, but many different contributions are involved.

At the current state of knowledge, for the Callovo-Oxfordian, most of the causes potentially responsible for over pressure can be eliminated.

- Mechanically, the Callovo-Oxfordian is a consolidated formation with characteristics acquired several tens of My ago (see § 3.3.1.3), so the subcompaction phenomenon cannot apply. Generally speaking, any explanation which leads to a fall in porosity under the influence of natural stresses can be eliminated. Quantitative analyses of this phenomenon (Altmann & Coelho, 2005) show that the values of rock parameters (permeabilities and flow speeds) are not enough to explain the over pressure measured, and require that permeabilities in the base of the Oxfordian at the top of Dogger be much over than measured.
- The weak thermal charge (both present and past see §3.3.1.3) in the layer eliminates the thermal expansion of water and maturation of organic material.
- Illitisation is also excluded since the temperatures and depths of the layer reached during its history are inadequate (see § 3.3.1.3). Other diagenetic phenomena (concerning carbonate precipitation) are also limited, as has been seen, and are old events (dating from a hundred million years ago, see § 3.3.1.3).
- Quantitative evaluation of hydraulic modifications at the boundaries, under the effect of glaciation cycles, shows that these could indeed lead to transient over pressure in the Callovo-Oxfordian on the site, with an effect of several meters (Gonçalvès *et al.*, 2004). This is much lower than the values measured and cannot be solely responsible for the phenomenon observed in the Callovo-Oxfordian.
- The fact that there was a mechanical load on the layer in the past is not significant either, in that, on the one hand, glaciers were always absent directly above the site and, on the other, the erosion

kinetics are slow (a few tens of meters per My on the plateaux) and progressive over time (Brulhet, 2005b), much less than the time scale required for rebalancing pressure in the layer, at around 10,000 years (see § 6). These phenomena are not, therefore, likely to create over pressure by hydraulic imbalance.

The same applies to measuring artefacts linked to the flow of argillites around the chamber, evaluation of which shows that, even if it was present, it could not explain the whole amplitude of over pressure measured (Andra, 2005h, chapitre 19).

Only osmosis seems likely to explain the amplitude of the over pressure measured (Inset 3.7). A large number of studies have evoked osmosis and the semi-permeable behaviour of clay media to explain over pressure and transient flow observed in geological sequences comprising low permeability clay rich layers (Goguel, 1987 ; Horseman *et al.*, 1996 ; Neuzil, 2000).

The following figure (Figure 3.3.11) shows one way of representing the Callovo-Oxfordian and its surroundings in the context of an osmotic system. In this case, osmosis is responsible for water flow by diffusion from the surrounding Dogger and carbonated Oxfordian into the Callovo-Oxfordian to compensate for the lower chemical activity of water in the clay-rock pore spaces. This flow ceases once equilibrium is reached.

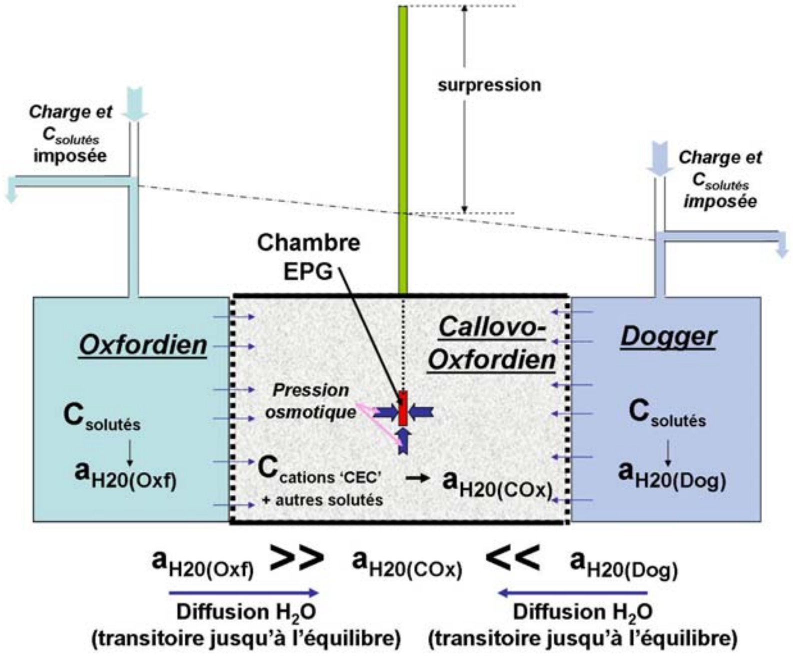

Figure 3.3.11 *Schematic representation of the Callovo-Oxfordian and its surroundings in the context of an osmotic system*

Inset 3.7 ***Chemical osmosis in a porous medium (1/2)***

Chemical osmosis involves the displacement of water linked to a concentration gradient of elements (solutes) dissolved in it. It is usually seen when two solutions of different concentrations are brought into contact and the solutes cannot move homogeneously from one medium to the other by diffusion. This result can be obtained by inserting a semi-permeable membrane between the solutions. In this case, the passage of solutes is prevented and that of the only solvent (water) is allowed. The water then diffuses from the less concentrated solution into the more concentrated solution to restore equilibrium. When this is reached, a difference in hydraulic head is observed between the two solutions (see diagram below).

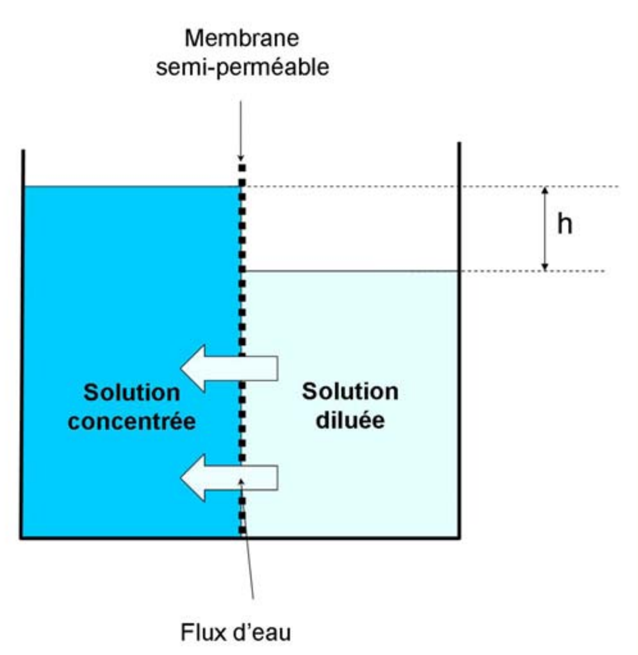

Diagram of chemical osmosis principale

Therefore, osmosis involves the transfer of water molecules by diffusion from a region of higher water chemical activity to a region of lower activity (the activity of water in a solution is its molar fraction, i.e. the ratio between the number of molecules of water and the total number of molecules in solution).

This phenomenon can also be seen where there are two porous media in contact, but the diffusion of solutes from one to the other is prevented. This may be due to two different causes:

- one of the media has pores which are smaller than the molecules (mechanical exclusion) or,
- one of the media has pore surfaces which carry electrical charges, which prevent the transfer of similarly charged ions (exclusion due to electrostatic repulsion).

Chemical osmosis in a porous medium (2/2)

If constant porous volumes are considered, the diffusion of water towards the most concentrated medium increases its hydrostatic pressure relative to the other medium. This difference in pressure causes Darcian counter-flow of water proportional to the hydraulic head field. If there is no exchange of solute molecules, the system evolves towards a stationary state characterised by a difference in stable pressure and zero net flow of water (diffusion + Darcian). If the system is closed to exchanges of material and energy with the environment, the water is in a state of thermodynamic equilibrium: the sum of its chemical potential (proportional to its activity) and mechanical potential (proportional to hydrostatic pressure) is zero. The difference in pressure between the two media is therefore the osmotic pressure.

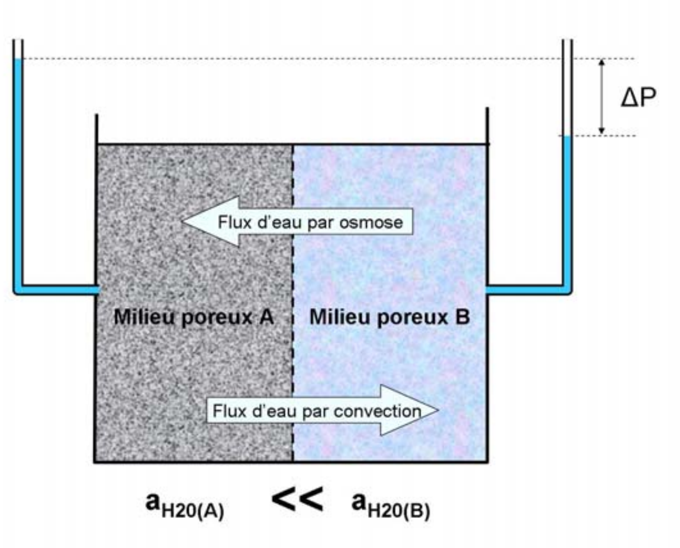

Diagram of chemical osmosis principale in a porous medium

The theory (as decribed by (Horseman *et al.*, 1996) for example, shows that, in so far as the phenomena prevent solutes from passing from one reservoir to the other are efficient, this osmotic pressure is expressed as:

$$\Delta P = -\,Cste\,\ln\frac{a_A}{a_B}$$

a_A and a_B being the activities of water at equilibrium in concentrated and dilute reservoirs.

A certain number of observations on the Meuse/Haute-Marne site seem to be incompatible with using a model for osmosis which only takes into account the concentrations of solutes in pore water (free water) (Altmann & Coelho, 2005) (Andra, 2005h, chapitre 16). In particular, the over pressure measured is considerable between the base of the layer and the Dogger (Figure 3.3.10) whereas the concentrations of solutes in pore solutions are very similar (see § 3.3.1.8). Under these conditions, a model based only on the concentration of solutes in pore water predicts a very slight over osmotic pressure. Moreover, cation and anion diffusion coefficients which differ from zero show that tha Callovo-Oxfordian doesn't prevent the migration of solutes by diffusion for chemical solution of water from the Meuse/Haute-Marne site.

However, there are other processes and other populations of solutes, to keep solute concentrations higher in the Callovo-Oxfordian and its surroundings (Altmann & Coelho, 2005). Indeed, the various studies performed on Callovo-Oxfordian pore water show that the composition of this solution (and thus eventually the activity of pore water in the argillites) is controlled by **(i)** the compensation of over (or inadequate) charges in clay phases by oppositely charged ions, **(ii)** the solubility balance imposed by the local mineral system and **(iii)** the concentrations of species in solution not controlled by fluid-rock interactions, particularly chlorides (Altmann & Jacquot, 2005).

Distribution of the major constituents of the mineral system (carbonates, clays,…) responsible for the first two phenomena described above, varies very little throughout the thickness of the formation. On the other hand, certain characteristics of clay minerals evolve, particularly the Cation Exchange Capacity (C.E.C., Inset 10.5), and the chloride concentration (major uncontrolled species) which falls systematically and linearly between the bottom and the top of the Callovo-Oxfordian. This concentration profile for the Callovo-Oxfordian is constrained by conditions at the Dogger-Oxfordian boundaries (see § 3.3.1.8). Chloride exchanges between the Dogger and the Oxfordian are considered to be part of the permanent regime, which is why the profile is stable over time. Because of the nature of these different processes, the chemical activity of water (its molar fraction) can be considered to be constant in time at every point in the Callovo-Oxfordian. In this case, the relationship described in inset 3.7 may then apply.

The value of chemical activity in the pore water of the Callovo-Oxfordian depends on the concentrations of dissolved species and clay mineral charge compensating ions. Current knowledge indicates that the total concentration of dissolved species varies around 0.1 M in the Callovo-Oxfordian. This concentration includes the species controlled locally by interaction between fluids and minerals and those which are exchanged permanently across the Callovo-Oxfordian (mainly chlorides). This concentration is therefore slightly variable through the thickness of the layer. In the Dogger, the total concentration of dissolved species is of the same order of magnitude as it is at the base of the Callovo-Oxfordian. It is much lower in the carbonated Oxfordian (around 0.01 M). Concerning ions which compensate for the permanent charges in clay minerals, the total concentration can be estimated from the cation exchange capacity. The various evaluations performed (Altmann & Coelho, 2005) (Andra, 2005h, chapitre 16) show that only a fraction of these compensating ions (those not directly attached to the surface of the clays, around 5 to 15 % of all these ions) is necessary to lower the water activity sufficiently to generate the observed pore pressures. This estimate is coherent with the results of studies of the structure and effects of the double layer on the process of transport in a highly compacted clay medium (Revil & Leroy, 2004). The total concentration of solutes in the pore water, including the fraction of compensating ions, then becomes much higher than that of the moving pore water in the argillites: if 15 % of the compensating ions are assumed to affect the activity of moving pore water, the total concentration gives values varying between 0.24 and 0.31 M. This variation can be explained by the variation in percentage of clay minerals, the type of interlayer minerals I/S R=0 and I/S R=1 which give different C.E.C values, and the chloride concentration in the Callovo-Oxfordian pore water. The activity of pore water in the argillites is then weaker than that of the two surrounding formations (factor 2 to 3 relative to the Dogger and 20 to 30 relative to the carbonated Oxfordian). The profiles of over osmotic pressure calculated on this basis are coherent with that measured (which shows over pressure throughout the thickness of the Callovo-Oxfordian, with steep gradients close to the boundaries) (Altmann & Coelho, 2005) (Andra, 2005h, chapitre 16).

Osmotic pressures are thought to depend on both the composition of the moving pore water and the CEC bearing phases, which explains the strong contrasts observed with the surrounding formations. Within the same layer, the disymmetry of the over pressure profile can be explained by both variations in C.E.C and in chloride concentrations (Altmann & Coelho, 2005).

This over pressure developed very early in the history of the layer: as soon as it had acquired the characteristics observed at the present time, about 100 My ago (see § 3.3.1.3). The profile of this over pressure has only evolved slightly since then, in connection with the chemical changes taking place in the water in surrounding beds, until about 30 My ago (corresponding to the end of the diagenetic processes in the carbonates, see § 3.3.2.1 and 3.3.2.2). In the absence of major modifications in the system, it has remained very stable since this date.

If it is considered that the over pressure measured is stable over time, the net flow of water corresponding to osmosis is then zero in the Callovo-Oxfordian and between it and its surroundings. Indeed, flow by diffusion due to the gradient of water chemical activity is counter-balanced by the Darcian flow induced by the hydraulic head gradient thus created (Inset 3.7). This osmosis will therefore not affect flow within the layer, which will be characterised by a permanent regime controlled only by the hydraulic head fields imposed by the surroundings. This flow can therefore be represented by Darcy's law based only on conditions at the hydraulic boundaries in the surroundings.

These determine a hydraulic head gradient field in the transposition zone from (i) 0.2 $m.m^{-1}$ to the south involving vertical downward flow to (ii) 0.3 $m.m^{-1}$ to the north and north-west involving a vertical upward flow (Figure 3.3.12).

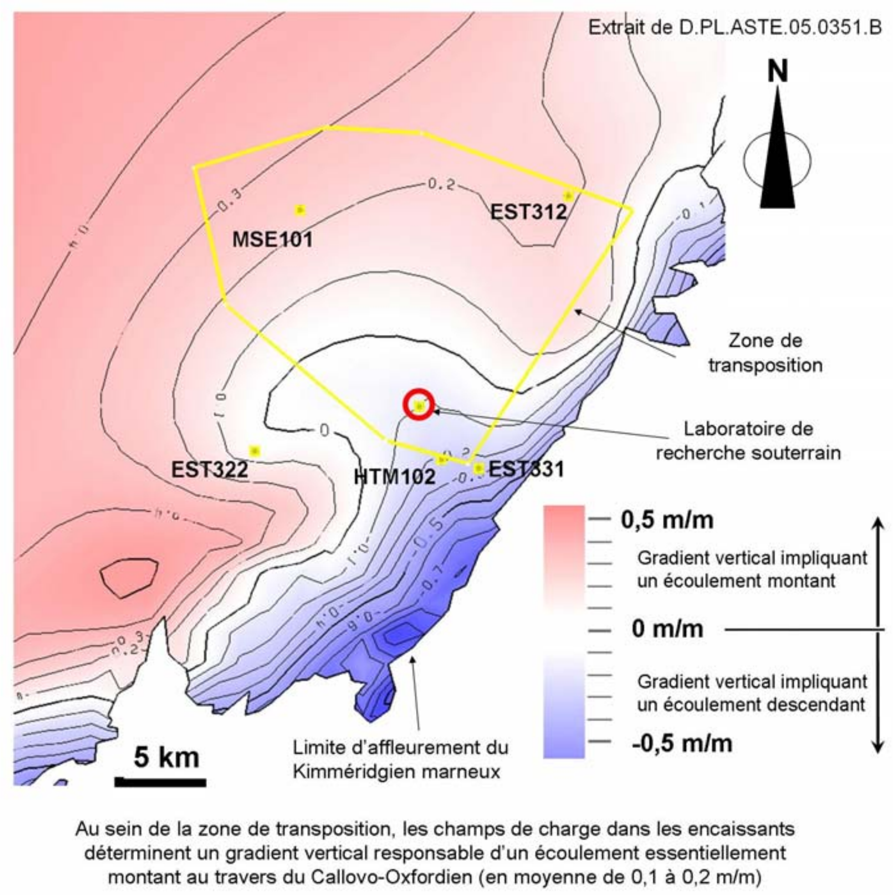

Au sein de la zone de transposition, les champs de charge dans les encaissants déterminent un gradient vertical responsable d'un écoulement essentiellement montant au travers du Callovo-Oxfordien (en moyenne de 0,1 à 0,2 m/m)

Figure 3.3.12 Evaluation of the vertical hydraulic head gradient through the Callovo-Oxfordian, deduced from charges in the surroundings

The suggested explanation for the origin of these over pressures in the Callovo-Oxfordian therefore matches the available data. However, it must be supported and refined relative to the data which will be obtained in the underground research laboratory. The osmotic origin of the over pressures measured implies that they have no impact on flow in the Callovo-Oxfordian. The over pressures measured remain very weak (20 to 40 m, i.e. 0.2 to 0.4 MPa). In the event of the minor participation of phenomena other than osmosis in these over pressures, the order of magnitude of the vertical gradient through the layer is not called into question. In the unlikely event that the over pressure is anything other than osmotic in origin, it would have limited impact on flow in the Callovo-Oxfordian. It would lead to hydraulic head gradients measured in the layer being around one $m.m^{-1}$ very locally, close to the formation boundaries. Under these conditions, diffusion remains dominant.

3.3.1.7 Transport of solutes in the Callovo-Oxfordian

Within a porous medium such as the Callovo-Oxfordian in its initial state, the solute transfer to be considered would be that which takes place under the effect of natural gradients in the formation on a macroscopic scale (Inset 3.8) (Carnahan, 1985).

For the Callovo-Oxfordian in its natural state, certain solute transfers can be neglected.

- Electrical potential gradients are only expressed on a microscopic scale. Their effect, which explains the behaviour of ions of different charges, is implicitly taken into account, on a macroscopic scale, in the values of parameters for the main phenomena (coefficient of diffusion accessible porosity) (Altmann & Coelho, 2005).
- Thermal gradients, under natural conditions (see § 3.2.3.1), are not high enough for water (thermo-osmosis) or solute (thermo-diffusion) transfer to take place in the Callovo-Oxfordian (Coelho, 2005).
- The only two possible "driving forces" for transfer at present are therefore the hydrostatic pressure gradient (responsible for chemical advection and kinematic dispersion) and the gradient of chemical activity (responsible for solute diffusion) (Inset 3.9).

Inset 3.8 ***Solute transfer phenomena (Carnahan, 1985)***

Within the context of the theory of irreversible processes, “Onsager” theory, a series of transfer phenomena is possible depending on the various gradients and the entity transported, as shown in the following table:

		Gradient			
		Electrical potential	**Hydraulic head**	**Concentration**	**Temperature**
Entity transported	**Electrical charge (C..m^{-2}.s^{-1})**	**Electrical conduction** (Ohm's Law)	**Electrical advection** (Rouss Effect)	**Exclusion current** (Membrane potential)	**Thermoelectric** (Seeback effect / Thompson effect)
	Solvent (water) (m^3..m^{-2}.s^{-1})	**Electro-osmosis**	**Hydraulic conduction** (Advection) Darcy's law	**Chemical osmosis**	**Thermo-osmosis**
	Solute s (mols. m^{-2}.s^{-1})	**Electro-diffusion** (Electrophoresis)	**Chemical advection** (Reverse osmosis)	**Chemical diffusion** (Fick's law)	**Thermodiffusion** (Soret Effect)
	Heat (J.m^{-2}.s^{-1})	**Peltier effect**	**Thermofiltration**	**Dufour effect**	**Thermal conduction** (Fourrier's law)

In this table, transport phenomena (so-called "diagonals") link the flow of a given entity to the gradient of the same type, noted in red and named as a law (Darcy's law, Fick's law...). Other phenomen are said to be "non-diagonal" and are some times named as effects (Soret effect, Dufour effect…).

Concerning solutes, the main natural transfer phenomena are therefore:

- chemical advection involving solute transfer by water flow (due to the hydrostatic pressure gradient);
- electrodiffusion, due to the electric potential gradient;
- thermodiffusion, due to the temperature gradient;
- diffusion due to the concentration gradient, governed by Fick's law.

Inset 3.9 ***Equation for solute transport in porous media (1/2)***

The transport phenomena generally used to describe solute transport in permeable porous media are advection, hydraulic dispersion and diffusion.

Advection corresponds to solute transfer by water flow. It depends on Darcy's velocity, solute concentration and kinematic porosity (porosity accessible to the solute for advection).

Hydraulic dispersion is linked to the heterogeneities of the water velocity field in convective flow. This depends on the concentration gradient and the average speed of the fluid (Darcy's velocity). In most of the situations encountered in hydrogeology, it also depends on a variable, called dispersivity, which represents the size of the largest heterogeneities encountered along the route followed by the solutes. This variable is determined empirically.

Molecular diffusion results from the Brownian movement of (solute) molecules which tends to reduce the differences in concentration existing at different points in a medium considered to be continuous. Apart from the concentration gradient, diffusion depends on a variable called effective coefficient of diffusion. Diffusive flow takes place through so-called diffusion accessible porosity. For a given medium, notably the Callovo-Oxfordian, where there is great fluid/solid interactions, the effective coefficient of diffusion and accessible porosity are parameters specific to each solute.

The equation for transfer of a solute in a porous medium is written as:

$$\frac{\partial \omega C}{\partial t} = -div(F_c + F_{dc} + F_d) + m \qquad (1)$$

with:
ω: solute accessible porosity (-)
C: concentration ($kg.m^{-3}$)
F_c: convective flow ($kg.m^{-2}.s^{-1}$)
F_{dc}: kinematic dispersion flow ($kg.m^{-2}.s^{-1}$)
F_d: diffusive flow ($kg.m^{-2}.s^{-1}$)
m: source of solute ($kg.m^{-2}.s^{-1}$)

In general, the following expressions are used in porous media for F_c , F_{dc} and F_d:

$F_c = qC$ with q Darcy's velocity (water flow in $m.s^{-1}$) (2a)

$F_{dc} = \alpha q gradC$ with α dispersivity (m) (2b)

$F_d = D_e gradC$ with D_e effective diffusion coefficient (De) in $m^2. s^{-1}$ (2c)

By integrating expressions (2a) to (2c) in equation (1), this gives:

$$\frac{\partial \omega C}{\partial t} = div((\alpha q + D_e) gradC - qC) + m \qquad (3)$$

Equation for solute transport in porous media (2/2)

To determine which of the three transfer modes, advection or diffusion/dispersion, is dominant on a macroscopic scale over a distance L, an adimensional number, known as Peclet's number, Pe, used for large scales, can be calculated:

$$Pe = \frac{qL}{\alpha q + D_e} \qquad (4)$$ with L, distance of transfer (m)

In a one-dimensional medium, this number represents the ratio between dispersive diffusion and advective flows. When it is much greater than 1, the advective flow is smaller than the dispersive one. On the contrary, when it is much smaller than 1, the dispersive diffusion flow is smaller than the convective route time.

From a dimensional point of view, it also represents the ratio between the two terms (αq+D_e)gradC and qC on the right hand side of equation (3). When Peclet's number on a large scale is much greater than 1, this means that the term (αq+D_e)gradC can be ignored relative to qC, and that advection is therefore dominant over dispersion/diffusion in terms of solute flow. When it is much less than 1, the advective term can be ignored relative to the dispersive/diffusive term in terms of solute flow.

Therefore, when Peclet's number on a large scale is much greater than 1, advection is both the fastest mode of transport and the dominant mode of transport in terms of flow. On the other hand, when Peclet's number on a large scale is much smaller than 1, dispersion/diffusion is predominant, in terms of both transfer speed and solute flow.

- When Peclet's number on a large scale is much smaller than 1, transport is dominated by diffusion and equation (3) can be reduced to:

$$\frac{\partial \omega C}{\partial t} = div(D_e gradC) + m \qquad (5)$$

- When Peclet's number on a large scale is much greater than 1, advection is predominant. equation (3) can then be reduced to:

$$\frac{\partial \omega C}{\partial t} = div(q(\alpha gradC - C)) + m \qquad (6)$$

- When transport is essentially diffusive, equation (5) is expressed in one dimension, in the form of a parabolic equation:

$$\frac{\partial C}{\partial t} = D_p \frac{\partial^2 C}{\partial^2 x} \qquad (7)$$

D_p being the coefficient of diffusion of the pore:

$$D_p = \frac{De}{\omega} \qquad (8)$$

Characteristic diffusion times can be estimated from equation (7) (Inset 4.1).

Transport parameters depend on the textural and poral properties of the Callovo-Oxfordian. Argillite porosity is essentially porosity within the clay matrix, consisting of small pores (see § 3.3.1.5), determining the tortuous pathways used for transfer and hence, the coefficients of diffusion which are strongly diminished for all species, by about 10^{-12} $m^2.s^{-1}$ for anions to by about 10^{-10} $m^2.s^{-1}$ for cations (see values in Table 3.3.1) (Altmann & Coelho, 2005). Transport velocity is therefore largely influenced by the chemical species, notably ionic charge in solution (Inset 3.10).

Inset 3.10 **Anionic exclusion**

The clay sheets in Callovo-Oxfordian argillites have specific electrochemical properties, notably an over of negative electric charge on their surface. Anions therefore tend to be pushed towards the centre of the pores.

The structure Callovo-Oxfordian argillite porosity also includes a large proportion of very small pores (Altmann & Coelho, 2005). However, because of the electric repulsion exerted on anions by the clay sheets, anions cannot access pores smaller than twenty nanometers (Altmann & Coelho, 2005). A great many pores in Callovo-Oxfordian argillites are therefore accessible to water and cations, but not to anions (see Following figure). This is known as anion exclusion.

On the macroscopic scale, the main effect of this phenomenon is a reduction in anion diffusion properties (diffusion coefficient and porosity accessible to diffusion) compared with those of cations and the water itself. These weaker anion diffusion properties are very clearly illustrated by anion diffusion experiments conducted on Callovo- Oxfordian samples (Andra, 2005h, chapitre 19).

It is possible that this phenomenon also affects anion advection, because anions are not found in the total water flow, but these effects have not yet been studied in Callovo-Oxfordian argillites, solute transport being largely dominated by diffusion.

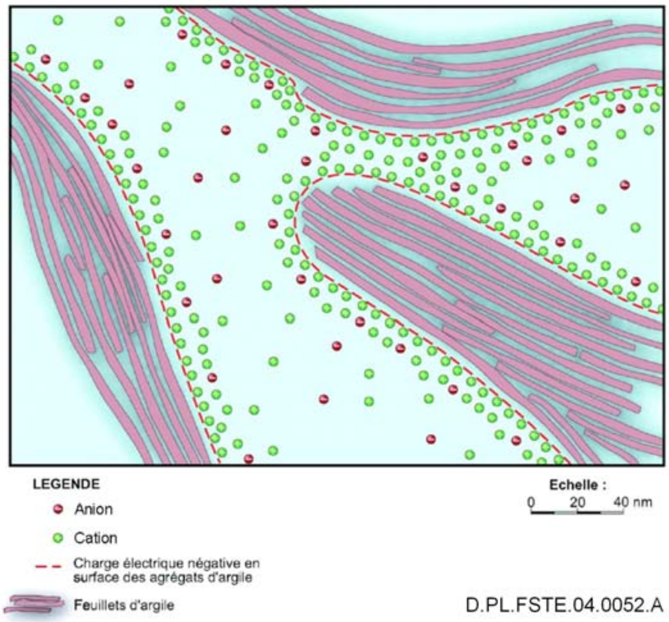

Diagram of Anion Exclusion principle

Generally, cations are attracted by negatively charged clay sheets. They are therefore usually found closer to the surface of these sheets than the anions. The affinity of cations (and certain anion) for rock surfaces varies depending on the chemical nature of the species at the mineral surface (cf. § 10.4). The rate of propagation of a concentration front of a solute will vary as a function of affinities, decreasing as affinity goes up. Most cations are therefore more or less well absorbed onto the surfaces of clay sheets, which slow their movement down relative to anions. Cations which display strong affinity for clay sheets therefore move only a few meters per million years.

However, not all cations have specific affinity for chemical sites on the surface of clay sheets (cf. § 10.4) and are therefore not sorbed. For cations which are not sorbed, the effective diffusion coefficient measured on samples is approximately 2.5 10^{-10} $m^2.s^{-1}$ whereas the porosity accessible to diffusion is 18 % (Altmann & Coelho, 2005)). These values are confirmed *in situ* by the initial results of the DIR experimental programme (Andra, 2005h, chapitre 19). These non-sorbed cations diffuse into Callovo-Oxfordian argillites, covering, on average, about one metre every ten years, ten metres in a thousand years and take more than a hundred thousand years to cross the total thickness of the layer i.e. 130 m (characteristic diffusion time being proportional to the square of the distance covered, Inset 4.1 and Inset 3.10).

Anions are subject to anion exclusion (Inset 3.10). This phenomenon pushes the anions towards the centre of the pores. This explains why anion diffusion coefficients and their porosity accessible to diffusion are lower compared to cations: about 5.10^{-12} $m^2.s^{-1}$ and 5 % respectively. The values obtained from measuring samples (Altmann & Coelho, 2005)) are consistent with the initial results from the DIR experimental programme conducted in the underground research laboratory (Andra, 2005h, chapitre 19). Since anions are repulsed from solid surfaces, they are generally retained less than cations. A theoretical evaluation of characteristic transfer times (see the calculation in Inset 4.1) shows that a non-sorbed anion in Callovo-Oxfordian argillites covers, on average, about one metre every hundred years, ten meters in over a thousand years and takes several million years to cross the total thickness of the layer.

This phenomenon is also sensitive to the chemical composition of pore water, notably its ionic force, which controls extension of the zone of influence of mineral surfaces over ion distribution in solutions (Inset 3.10 and (Altmann & Coelho, 2005)). The effective diffusion coefficients and diffusion accessible porosity values vary very little throughout the layer (Figure 3.3.13, showing diffusion coefficients of tritiated water, a neutral chemical species). This constancy reflects the lithological and textural homogeneity of the Callovo-Oxfordian (Altmann & Coelho, 2005).

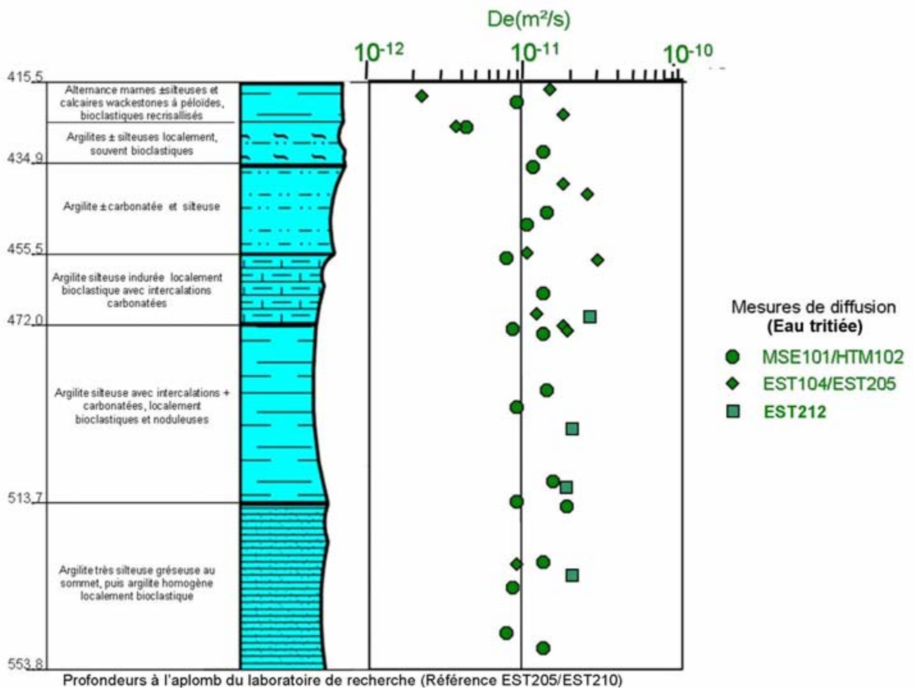

Figure 3.3.13 *Vertical profile of the whole Callovo-Oxfordian for measured values of the diffusion coefficient for tritiated water (HTO)*

Advection corresponds to solute transfer by water flow. This phenomenon therefore depends directly on the hydrodynamic characteristics of the formation: permeability and hydraulic head gradient (see § 3.3.1.6). Kinematic porosity is the porosity accessible to this phenomenon and is used to calculate the average water velocity of transfer through the porous medium. By abstracting hydraulic dispersion, linked to heterogeneities in the water velocity field (Inset 3.9), the characteristic transport time for advection is the flow time, i.e. one million years to cover a few meters and several tens of millions of years to cross the Callovo-Oxfordian layer (see § 3.3.1.6). These characteristic times are one or two orders of magnitude longer than transport times for anion and cation diffusion as presented above.

In the Callovo-Oxfordien layer, the calculation of Peclet's number on a large scale (Inset 3.9) is very small, about 0.02 for anions (Altmann & Coelho, 2005), and confirms the predominance of diffusion. The interpretations of salinity profiles for the Callovo-Oxfordian (see § 3.3.1.8), and the profiles of natural tracers in pore water (particularly chlorine isotopes, Inset 3.1) (Altmann & Coelho, 2005) are coherent with existence of a steady state system dominate by diffusion from Dogger to Oxfordian diffusion in the Callovo-Oxfordian. Theoretical transfer times (see calculation in Inset 4.1) through the layer are therefore long: from several thousand to several million years for non-retarded anion species which are the most mobile. This observation is coherent with the preliminary results of studies of rare gases in pore water (notably He, Inset 3.1) (Andra, 2004a).

Evaluations performed on the basis of the different possible scenarios responsible for over pressure (see § 3.3.1.6) show that, even taking into account the over pressure actually affecting the hydraulic head gradient in the Callovo-Oxfordian (and thus non-osmotic in origin), this predominance of diffusion over advection remains valid (Altmann & Coelho, 2005). Estimates of Peclet's number calculated in these cases, on maximalist bases and outside probable phenomenological domains, show that it is at most between 0.3 and 0.9.

3.3.1.8 The chemical composition of pore water in the Callovo-Oxfordian

The low solute transfer velocities and high surface area to volume ratios lead to strong interactions between pore water, with the minerals controlling the final composition of water in the formation. Thus, the concentrations of dissolved species are considered to be at thermodynamic equilibrium for the Callovo-Oxfordian in its initial state, this equilibrium being controlled by certain mineral phases in the argillites themselves.

The low content of water, 7 to 8 % weighted (Altmann & Jacquot, 2005), and low permeability of the Callovo-Oxfordien are insufficient for direct analysis of pore water composition. This was determined on the basis of analyses of samples from the Callovo-Oxfordian and geochemical models (Inset 3.11). Results from the PAC experimental programme in the underground research laboratory confirm the main characteristics of pore water composition thus determined (especially certain significant parameters such as ionic force, chloride and major anion concentration and total cation concentration) (Andra, 2005h, chapitre 18). This composition is considered to be homogeneous throughout the thickness of the formation, in coherence with its overall lithological homogeneity (Altmann & Coelho, 2005 ; Altmann & Jacquot, 2005). The composition of water thus evaluated has a neutral pH (slightly more than 7). It is reducing, as indicated by the presence of pyrite and organic material. Chemically, the water is calcium-sodium carbonate in nature. The analyses of stable isotopes in the water (Andra, 2004a), confirmed by those performed on dissolved gases (H_2O and CO_2), (Inset 3.1), (Girard *et al.*, 2002) show that this was clearly of meteoric origin. This water has therefore replaced the original seawater by diffusion from the surroundings. This process took place over a period extendings over several hundred million years from the time when meteoric water could circulate in the surroundings, i.e. at least 65 million years, during the Cretaceous (Andra, 2005h, chapitre 18). This circulation, which was locally triggered right from the end of the Jurassic (first retreat of the sea), is related to the generalised emersion of the Paris Basin between the end of the Cretaceous and the Tertiary, 65 million years ago. This emersion, related to the raising of the basin edges caused outcropping of the major argillaceous-carbonated units of the Jurassic, mainly in the entire eastern part of the Paris basin, thus enabling meteoric water to circulate within aquifer formations as from this epoch (see § 3.2.1.1) (André, 2003). Data concerning stable carbon isotopes ($\delta^{13}C$, Inset 3.1) in the dissolved bicarbonates (Girard *et al.*, 2003) demonstrate the chemical and isotopic equilibrium of pore water with the carbonate phases. This chemical equilibrium confirms the slow transfer velocities already revealed in this medium (see § 3.3.1.7). The CO_2 partial pressures measured for the formation are, on average, between 7.2 and 3.1 mbar (0.72 and 0.31 MPa), corresponding to CO_2 partial pressure Logs of -2.15 and -2.51 respectively. The water is also sulphated and chlorinated (chlorinity being determined analytically). Other elements (major cations and silicon) are controlled by the different mineral phases (Altmann & Jacquot, 2005) (Table 3.3.1).

The concentrations of certain mobile species (notably chlorine) vary throughout the thickness of the layer (between 1,000 and 500 mg.L^{-1}, from bottom to top for Cl^- (Lavastre, 2002), directly above the site), reflecting an exchange of these species between the Callovo-Oxfordian and surrounding formations. On a sectoral scale, these profiles show (Figure 3.3.14):

- control of the salinity profile in the Callovo-Oxfordian by Dogger salinity (considerably higher in the North-East – EST311/312 boreholes-than in the South-West - EST321/322 boreholes) ;
- low salinities in the carbonated Oxfordian, contrasting with those of the Callovo-Oxfordian and the Dogger. These low salinities are controlled by convective water flow in this surrounding formation which dilutes rising flow by diffusion through the Callovo-Oxfordian (Andra, 2004c).

These observations support the image of very limited exchanges through the layer, over a long time-scale of about ten million years, with diffusion being predominant. These exchanges are thought to take place in a quasi permanent regime (Altmann & Coelho, 2005).

Inset 3.11 ***Determination of pore water chemistry in undisturbed argillites (Altmann & Jacquot, 2005) (1/2)***

In general terms, at depths, pore water chemistry in a natural porous medium results from chemical interactions of this water with solid phases (minerals) which it is composed of. In macroscopic terms, this chemistry is characterised by a set of parameters such as pH and Eh, the redox potential), alkalinity, ion concentration (for example Na^+, K^+, Ca^{2+}, Mg^{2+}, Cl^- and SO_4^{2-}) and inorganic carbon content. Most of these parameters are controlled by solid/solution chemical reactions with mineral phases (mineral solubility and ion exchange). On the other hand, a small number of parameters, such as chloride ion concentration, are not controlled by such balances but result from formation of the porous medium and/or its background, mainly solute exchanges with other surrounding porous mediums. This is for example the case for Callovo-Oxfordian argillites whose chloride concentration results from their marine origins and then from exchanges with the surrounding formations.

Complete characterisation of interstitial water chemistry in porous mediums is generally accessible from water samples and their chemical analysis. That is not the case for deep clay formations for which only a limited number of parameters is accessible to direct experimental measuring. On the one hand, given their low permeability, only very small quantities of water can be sampled. On the other hand, a significant part of the pore water is not free: it is related to clay minerals on their surface and sometimes makes up their structure. This is especially the case for Callovo-Oxfordian argillites with very small-sized pores (cf. § 3.3.1.5 and Inset 3.3). In addition, there are the electrostatic processes of clay minerals, especially smectites (cf. § 3.3.1.2), which result in the development of an anionic exclusion process (Inset 3.10) and to a non-homogenous spatial distribution of solutes within the pores. The issues therefore arise of the very definition of interstitial water and how to gain access to it.

These issues have been the subject of significant research work for more than ten years, mainly involving Boom clay in Mol in Belgium (European project (Griffault *et al.*, 1996), and then Opalinus clay in the underground research laboratory in Mont Terri (Pearson *et al.*, 2003). The works in Mont Terri resulted in definition and validation of methodology applied to Callovo-Oxfordian argillites. This is based on coupling of some data accessible for the characterisation of intact argillites, thermodynamic modelling of the balance of dissolution - precipitation reactions and ion exchange and the characterisation of water balance with crushed argillites. The choice of the balanced thermodynamic approach rather than the kinetics approach is justified by the slow rate of water flows and of solute transfers in argillites compared to the characteristic times of chemical kinetics.

Parameters which can be measured by experiments are: total water content, total chloride ion concentration, mineralogical composition, cation exchange capacity and sorbed cation population, laws of mass action governing these exchanges and carbonate activity.

Chlorides predominantly contribute to ionic force which in turn profoundly affects other solid/solution balances. However, chloride ion concentration cannot only be defined from the total chlorine content in the rock and from total porosity, due to anionic exclusion which results in preferential localisation of chlorides in free water. Chloride ion concentration is thus specifically deduced from squeezing tests on argillite samples taken from boreholes and permeability measuring tests with kinematic porosity measurement.

Determination of pore water chemistry in undisturbed argillites (Altmann & Jacquot, 2005)(2/2)

The parameters obtained from experiments are then used in geochemical modelling to determine other parameters, especially pH, Eh, ionic force, alkalinity and concentrations of the major elements (Na, K, Ca, Mg, Sr, Si and S). In order to do so, minerals contributing to chemical balances must be defined, mainly for cationic exchanges, consistent with the phase rule. Of the minerals observed in experiments, only those without any dissolution facies are retained and are thus considered as in equilibrium with interstitial water. As an example, sodium concentrations are controlled by ion exchanges, whereas calcium and sulphate contents are controlled by calcite ($CaCO_3$) and celestine ($SrSO_4$) respectively. This modelling was carried out with the geochemical calculation code PHREEQC-2 (Parkhurst & Appelo, 1999). Modelling robustness is assessed with sensitivity studies mainly focussing on parameters such as the partial pressure value of CO_2, minerals retained and the type of minerals controlling solution concentration of a solute.

These works thus proposed a reference model for chemical composition of interstitial water in Callovo-Oxfordian argillites and intervals of extreme values possible for all major parameters of interstitial water (Table 3.3.1). The main characteristics of the reference model thus determined are confirmed by results from the PAC experimental programme carried out in the underground laboratory, the aim of which is to define *in situ* the composition of argillite pore water.

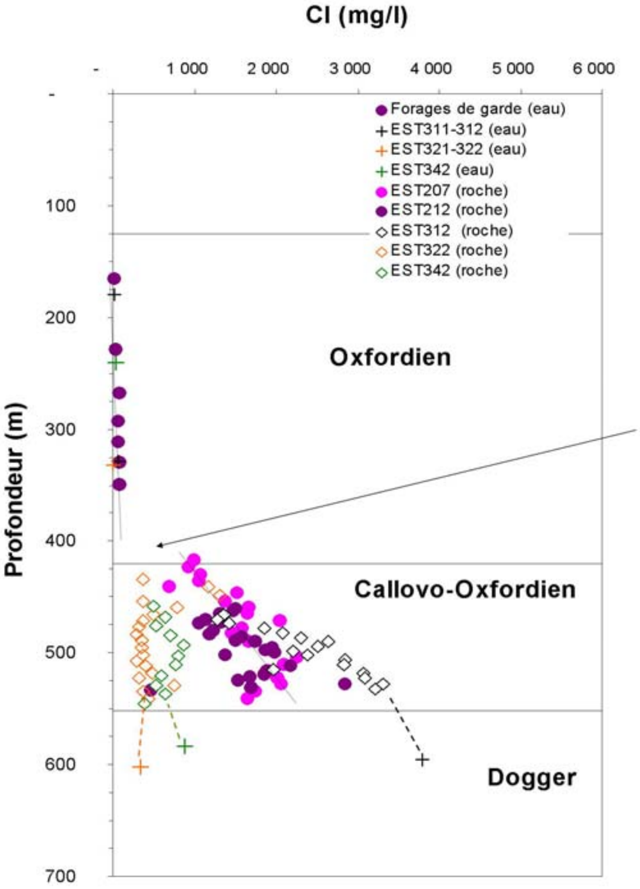

La rupture de teneurs en chlorures, observée sur le site (forages EST207, EST212 et forages de garde), au dessus du Callovo-Oxfordien correspond à une dilution par les flux convectifs horizontaux dans l'Oxfordien carbonaté, des flux montants par diffusion au travers du Callovo-Oxfordien.

Pour chaque forage:

- A la base du Callovo-Oxfordien, la salinité est proche de celle du Dogger, montrant un contrôle des teneurs en chlorures par ce dernier.
- Les profils dans le Callovo-Oxfordien, diminuant progressivement vers le toit de la formation, traduisent des échanges lents, à diffusion dominante.

Figure 3.3.14 Vertical profiles of chlorides in the Callovo-Oxfordian and its surroundings on a sectoral scale

3.3.1.9 Summary of the main characteristics of the Callovo-Oxfordian

The Callovo-Oxfordian formation thus appears to be a layer which was deposited under calm conditions and has evolved in a stable environment for tens of millions of years. This layer displays simple, regular geometry in the area studied and is more than 130 m thick in the transposition zone. Over this area, it shows great homogeneity of thermal, mechanical, hydraulic and chemical properties. All the results obtained indicate a medium with a strongly confining character, with the layer acting as a barrier.

The Callovo-Oxfordian is well isolated from its surface environment. Apart from any possible transient phenomena (impact of the latest climatic changes, see § 3.2.3.2) affecting the conditions at the layer boundaries and having only limited impact on the layer in general, the formation is at equilibrium under current conditions, given the location of the site within a stable part of the basin, the depth of the layer and its mineralogical and textural properties being acquired very early in its geological history.

The following table summarises the main characteristics of the Callovo-Oxfordian in its initial condition.

Table 3.3.1 The main characteristics of the Callovo-Oxfordian in its initial condition.

Caractéristics			Values	
Geometry (transposition zone)	Thickness		130 to 160 m	
	Dip		1 to 1.5° NW	
	Depth (centre of the layer)		500 to 630 m	
Mineralogical composition (in mass)	Clays	Interlayer minerals I/S	15 to 30 %	25 to 60 %
		Micas / Illite	5 to 20 %	
		Kaolinite	a few to 10 %	
		Chlorites	a few %	
	Carbonates		15 to 50 %	
	Quartz		25 to 35 %	
	Organic materials		0.5 to 2 %	
	Pyrite		2 to 3 % (maximum)	
Thermal conductivity			$1.3 – 1.9\ W.m^{-1}.K^{-1}$ $1.9 – 2.7\ W.m^{-1}.K^{-1}$	
Stress status			Orientation: σ_H : N155°E $\sigma_H / \sigma_h = 1$ to 1.3 $\sigma_h = \sigma_v$= weight of terrain	
Mechanical properties (zone B/C)	Deformation module		4,000 MPa	
	compression strength		21 MPa	
	flow speed		To several months : 10^{-2} to 10^{-3} $year^{-1}$ After the first year :10^{-4} $year^{-1}$	
Permeability			About 10^{-14} to 10^{-13} $m.s^{-1}$ The anisotropy of horizontal/vertical permeability is within this range of values (max. factor 10)	
Total porosity			18 %	
Diffusion coefficient	Anions		10^{-12} to 10^{-11} $m^2.s^{-1}$	
	Cations		$2.5 \cdot 10^{-11}$ to $5 \cdot 10^{-10}$ $m^2.s^{-1}$	
Accessible porosity	Anions		5 %	
	Cations		18 %	
Chemistry of interstitial water (maximum and minimum values according to (Altmann & Jacquot, 2005)	pH		6.9 to 7.6	
	Eh		-180 to -150 mV	
	Ionic force		0.09 to 0.12 M	
	Cl^-		$1.2 \cdot 10^{-2}$ to $3 \cdot 10^{-2}$ $mol.L^{-1}$	
	SO_4^{2-}		$3.4 \cdot 10^{-2}$ to $3.4 \cdot 10^{-3}$ $mol.L^{-1}$	
	Ca^{2+}		10^{-2} to $1.5 \cdot 10^{-2}$ $mol.L^{-1}$	
	Na^+		$2.5 \cdot 10^{-2}$ to $4.4 \cdot 10^{-2}$ $mol.L^{-1}$	
	Carbonates (HCO_3^-)		$7.5 \cdot 10^{-4}$ to $3.4 \cdot 10^{-3}$ $mol.L^{-1}$	
	Log P_{C02}		-2.96 to -1.63	

3.3.2 The formations surrounding the Callovo-Oxfordian

The two carbonate formations immediately above and below the Callovo-Oxfordian, the Dogger and the carbonated Oxfordian, are limestone, aquiferous units, which set the boundary conditions, notably hydraulic and chemical, of the Callovo-Oxfordian layer (Figure 3.2.4).

3.3.2.1 The Dogger

The Dogger, resting on Lias clays, is a 300 m thick formation. On the scale of the Paris Basin, it represents the development of major carbonate platforms, under a very shallow sea, in a tropical environment. These conditions are responsible for the wide variety of facies observed (shelly debris, calcareous sand, reefs,....) which are deposited by currents and during sea-level changes. These rapid variations are found both laterally and vertically (Guillocheau *et al.*, 2002 ; Trouiller & Benabderrahmane, 2005). A more clayey interval, which is found everywhere in Eastern France ("Longwy Marls"), separating the two Bajocian and Bathonian limestone units, marks deepening relative to deposit conditions. At the top of the formation, the nacreous Slab, very rich in shelly debris, marks the passage from the Dogger to the Callovo-Oxfordian (Figure 3.2.4).

Just after it was deposited, the Dogger was subjected to a series of diagenetic processes which controlled successive phases of carbonate dissolution and recrystallisation. These processes, classic to carbonate formations, are part of a continuous evolution (Choquette & Pray, 1972):

- the first phases are early and take place during and just after deposition of the sediment ;
- the following phases are linked to burial of the series ;
- finally, the latest phases concern denudation of the sedimentary series and its emergence at outcrop.

These processes are very different from those which affected the Callovo-Oxfordian: for the latter, diagenetic phenomena were early and involved only restricted volumes of rock, given its low permeability. For the carbonates, which were originally strongly porous and permeable, the diagenetic processes involved greater volumes of fluids and were highly dependent on palaeocirculation within the formations.

On a scale of the basin, the hydrogeological modelling methods used for the Dogger, suggest a major diagenetic event at the start of the Tertiary (from -65 to -50 My) (Gonçalvès, 2002). This dating agrees with geochemical evaluations performed on the site, demonstrating that the last cementation, in the form of cement blocking porosity in all the granular facies, was linked to an inflow of meteoric water (notable $\delta^{18}O$ results) (Buschaert *et al.*, 2004 ; Vincent, 2001). Therefore, the later evidence of diagenesis in the carbonates must be linked to the outcropping of the formations after the Cretaceous, allowing infiltration of meteoric water at the outcrops. This infiltration may also have been facilitated locally by fault movement, particularly during the Oligocene which was a period of distension. During these distensive phases, these accidents may also play a part in short-circuiting deep formations and allow fluids from different aquifer formations to mix in the neighbourhood of these events. The influence of these accidents during these processes, revealed in the centre of the Paris Basin (Worden *et al.*, 1999 ; Worden & Matray, 1995), is suggested, in the sector, by the isotopic signature of fracture filling. On the edges of fault zones (Gondrecourt graben and close to the Poissons fault), this fracture filling indicates a possible contribution by Triassic fluid (Buschaert, 2001 ; Maes, 2002). Nevertheless, this fault contribution is limited in time and space. In particular, this scheme can only be envisaged during periods of tectonic extension, which means prior to the Miocene (-23 My) and are not expected in the future (see § 3.2.1 and 3.2.2). This contribution is also very slight when compared with the processes governing the infiltration of meteoric water at outcrops, which has been continuous since the Cretaceous and will contine on into the future.

The petrophysical characteristics, as observed at present, were therefore acquired at least 30 million years ago. The lack of recent evolution of this system is illustrated by the lack of $^{234}U/^{238}U$ imbalance in the carbonate matrices (Inset 3.1) (Deschamps, 2003), even though very discrete imbalance has been noted in the region of stylolitic joints (Deschamps *et al.*, 2004), in the Dogger as well as the carbonated Oxfordian, which seems to indicate that these joints could have made a recent contribution to fluid transfer. However, this contribution remains very local, within the joints themselves, and is limited in terms of flow since the imbalance is very slight.

Generally speaking, these major diagenetic processes, expressed regionally on the scale of the Eastern boundary of the Paris Basin, are linked to fluid circulation in limestones. These dissolution processes, near outcrop zones, and precipitation when the formation is underground, depend heavily on the volumes of fluids involved and their renewal. They have no influence on the carbonate cements in the Callovo-Oxfordian argillites, which are more impermeable, as indicated by the marine signature which has been preserved in these cements (see § 3.3.1.3).

These diagenetic processes are responsible for weak porosities (6 to 10 %) and the global permeability of the Dogger (from 10^{-10} to 10^{-9} $m.s^{-1}$). They are the cause of lower permeability (by 1 to 2 orders of magnitude) than that measured in the centre of the basin (Krakenberger, 1983), further from the influence of meteoric water. Only a few extension zones covering several kilometers, isolated within the compact limestones and independent of facies, seem less affected by these phenomena (Figure 3.3.15). Their porosities and permeabilities are then considerably higher (15 % and 10^{-8} $m\ s^{-1}$ respectively) than the rest of the formation.Water productivity levels in these porous horizons are low: around one litre per minute or less (Andra, 2004b). Deep water circulation takes place mainly within these horizons. Directly above the site, the low permeability of the carbonates results in slow flow rates: Hydrogeological modelling indicates that water velocities (in the sense of Darcy's law) of a few hundred meters per million years (Trouiller & Benabderrahmane, 2005), are much slower (more than two orders of magnitude) than the average regional velocities modelled on the scale of the Paris basin (Wei *et al.*, 1990). These velocities correspond to advective transfer distance for a non-sorbed solute, at just a few kilometers per million years.

These deep circulations are organised from outcrops in the plateaux zones. Flow on a sectoral scale in the Dogger limestone is coherent with that observed on the scale of the basin: it flows West towards the centre of the basin. Figure 3.3.16) (IFP, 2004). In general, the hydraulic head gradient is very low: 0.2 to 0.4 per thousand to the North-East of the sector studied to 2 per thousand in the South-West, in the regions of EST322 bore hole (Figure 3.3.17).

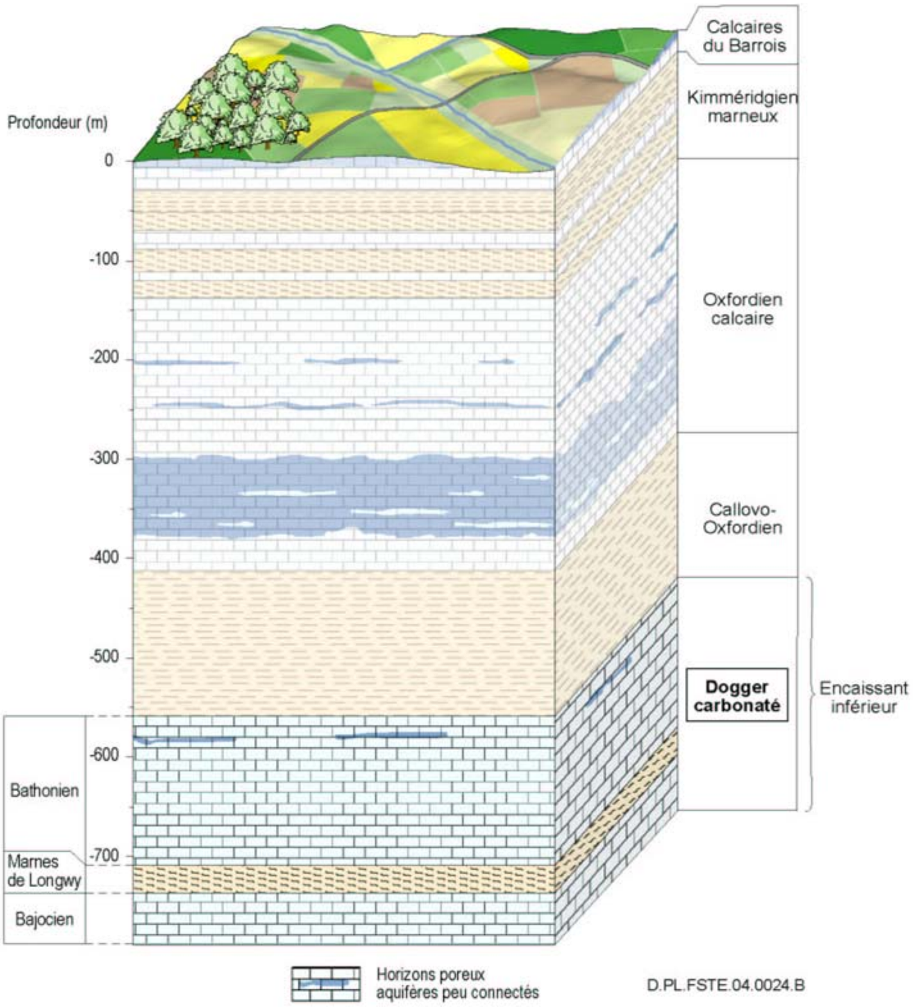

Figure 3.3.15 *Schematic diagram of lithologies and porous horizones in the Dogger limestone at the Meuse/Haute-Marne site*

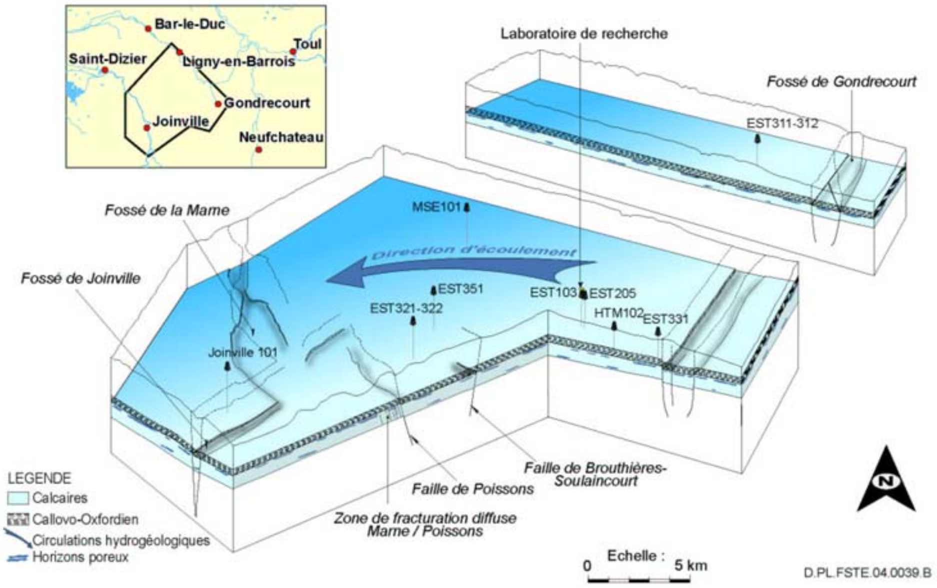

Figure 3.3.16 *Organisation of water flow in the Dogger limestone at the present time*

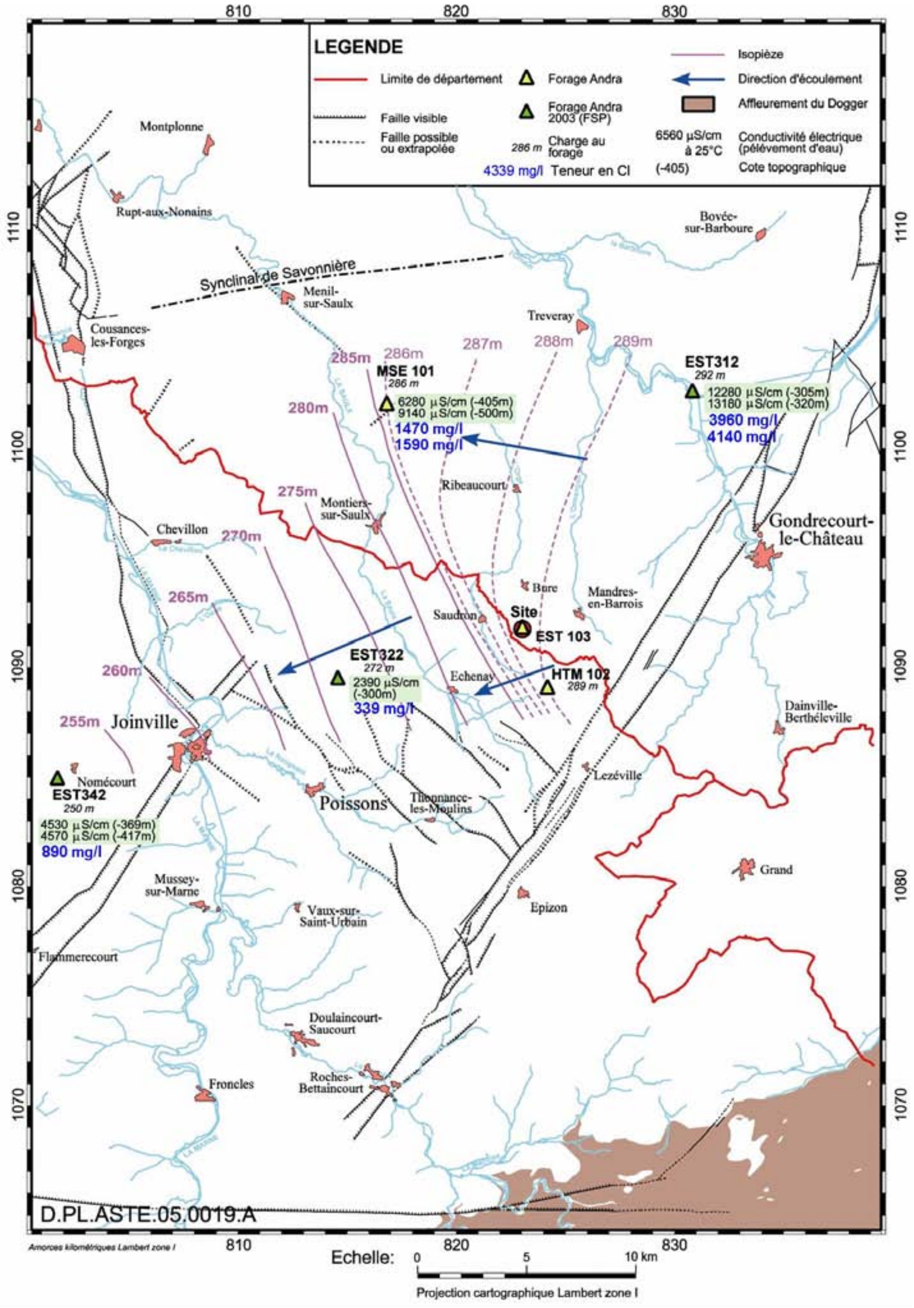

Figure 3.3.17 *Hydraulic head field and chloride concentration of Dogger limestone pore water in the Meuse/Haute-Marne sector*

Given the very long contact times, it is safe to conclude that Dogger water is at chemical equilibrium with the formation. Measurments show that this is heavily-mineralised, chloride-sulphate-sodium type water with a neutral pH (slightly more than 7) and reducing in character; it is chemically close to that observed in the same formation elsewhere in the Paris basin (Andra, 2005h, chapitre 18). This water, of meteoric origin (see above) has a long residence time (about a million years in MSE101 borehole), as indicated by the rare gas measurements (Dewonck, 2000).

On the scale of the basin, as already mentioned above, successive fault movements in major regional faults (notably the Bray fault), and particularly the movement associated with the end-Cretaceous phase (-65 My) and Oligocene (-34 My), seem to have facilitated vertical transfer between aquifers (Gonçalvès, 2002 ; Matray & Chery, 1995). On the scale of the eastern aureole of the Paris Basin, the particular methods used involving helium isotopes (Marty *et al.*, 2003) show that the Lias clays effectively isolate the Triassic and Dogger aquifers. Within this context, the triassic isotope signatures found in the calcite filling fractures close to major fault appear to be a very local phenomenon, reflecting communications which were very limited over time. This is illustrated by the differences in salinity between the aquifers: about a hundred g.L^{-1} for the Triassic (BRGM & ELF Aquitaine, 1976) and a few g.L^{-1} for the Dogger (see § 3.3.1.8). Nevertheless, Dogger salinities remain high for meteoric water: they seem to have been acquired by the diffusion of triassic salt through the Lias clay (Andra, 2005h, chapitre 18). These exchanges therefore take place, on the scale of the basin, over long periods of several million years. The differences in chlorine concentrations in the Dogger, observed on a more local sectoral scale (from about 4 g.L^{-1} in the North-East, to about 0.3 g.L^{-1} around EST322 borehole, are coherent with the electrical conductivities measured, Figure 3.3.17) and can be linked to the faster circulation elsewhere in the sector which leads to dilution of this triassic salt (see § 3.4.3).

3.3.2.2 Carbonated Oxfordian

Above the Callovo-Oxfordian, the carbonated Oxfordian displays deposition conditions fairly similar to those of the Dogger: over a thickness of about 300 m, it consists of different superposed carbonate platforms (Figure 3.2.4). However, the deposition environments are much more contrasted than for the Dogger. Instead of one vast platform which is alternately covered and exposed by waves and tides, well-separated environments can be distinguished for each of the carbonated Oxfordian platforms. The coarse-grained facies, which correspond to shallow water at the time of deposition (clayey sands, lagoon facies, reefs…) are generally in the North-East of the sector (near Commercy) whereas beyond Joinville in the South-West, more clay-rich basin facies are developing (Trouiller & Benabderrahmane, 2005 ; Vincent, 2001) (Figure 3.3.18).

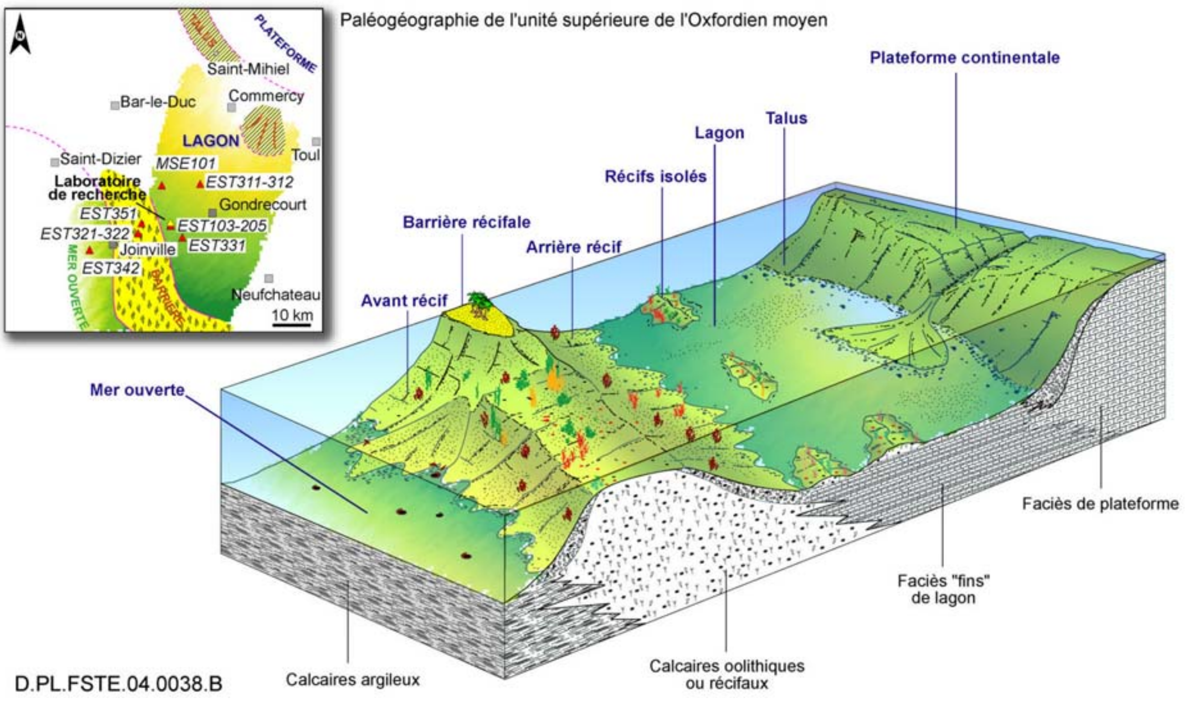

Figure 3.3.18 *Deposition environment of an carbonated Oxfordian platform – Example of the terminal mid-Oxfordian platform according to (Carpentier, 2004 ; Université de Lyon I, 2002)*

Under its cover, the unit is affected by major diagenesis, similar to that affecting the Dogger As was the case in the Dogger, this diagenesis is responsible for more intense recrystallisation in the sector than in other areas of the Paris Basin, notably in granular facies. Therefore, throughout the formation, global permeabilities are low: around 10^{-9} m.s^{-1}, two orders of magnitude less than those measured towards the centre of the Paris basin. However, some levels of the carbonated Oxfordian, mainly fine-grained facies, have higher porosities and permeabilities than the rest of the formation. These so-called "porous" horizons are defined directly above the underground research laboratory and identified by numbers 1 to 7, i.e. Hp1 to Hp7 They are mainly precise facies (carbonate lagoon mud, inter-reefal facies…), which are homogeneous and in which secondary "chalky" diagenesis has transformed the primary facies into a fine, homogeneous micrite, with high porosity relative to the rest of the formation (Trouiller & Benabderrahmane, 2005). The organisation of these porous levels is therefore linked directly to the initial sedimentary deposition conditions, which explains their global geometry and correlation with stratification as shown by the 3D seismic data recorded on the site (Figure 3.3.19). At this scale, these data illustrate well that the distribution of the most porous zones can become irregular, thereby explaining the difficulty in correlating detail, although without causing much change in the global hydrodynamic characteristics of the formation (Vigneron *et al.*, 2004).

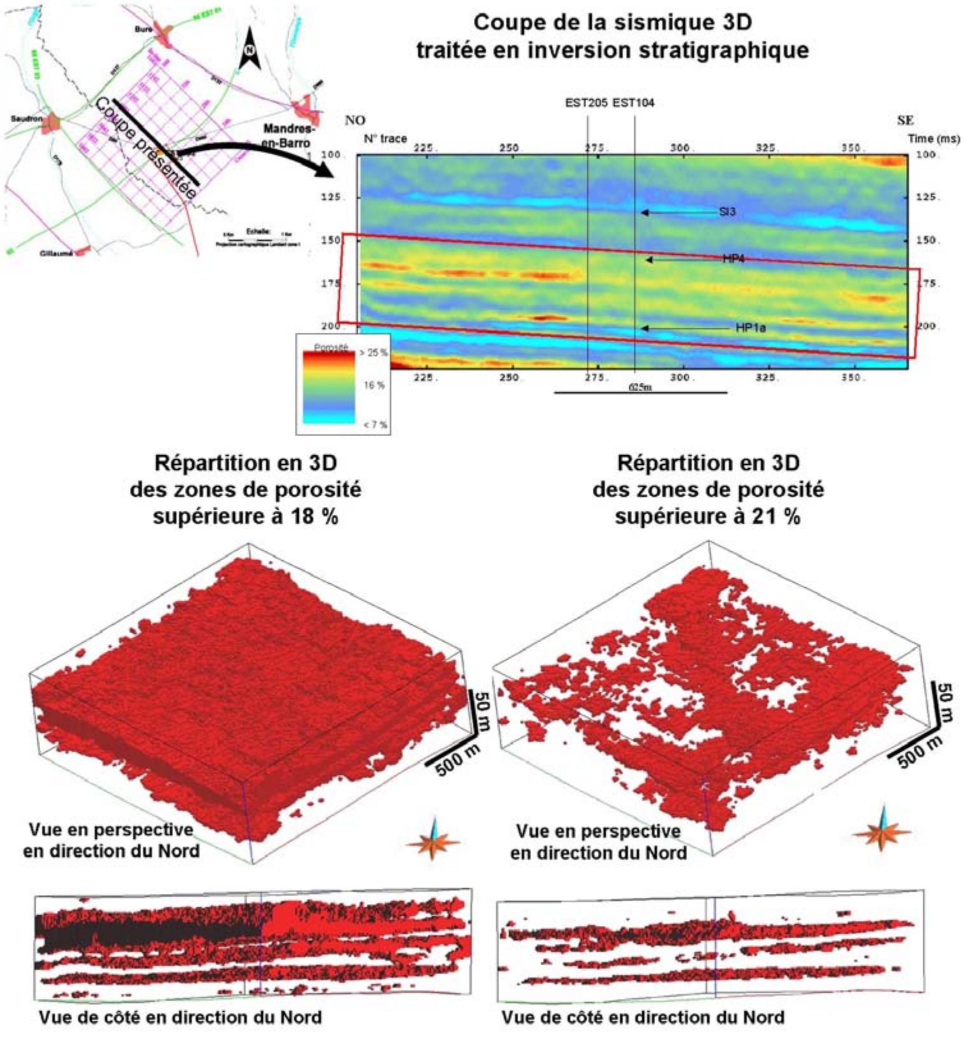

Les données de sismique 3D permettent d'illustrer la morphologie des horizons poreux, qui apparaissent continus et s'organisent globalement selon la stratification (à gauche). Cependant, l'étude des zones les plus poreuses et les plus perméables (à droite) montre que ces dernières peuvent présenter une connectivité moindre, en accord avec les données de puits.

Figure 3.3.19 Morphology of porous horizons (Hp1 to Hp4) of Oxfordian carbonate based on 3D seismic data

At the sectoral scale, their distribution, extension and continuity can therefore be deduced from the distribution of corresponding sedimentary facies (Carpentier, 2004 ; Université de Lyon I, 2002), even though it seems difficult to achieve fine detailed correlation. Therefore, regional knowledge and different data collected from deep boreholes drilled throughout the sector are used to provide a general definition of the extensions of the main porous facies in the formation (Trouiller & Benabderrahmane, 2005) Above the facies representing deposition of the first carbonate platform, slightly permeable can be distinguish throughout the sector facies (facies C3a/C3b: permeability levels of about 10^{-11} $m.s^{-1}$):

- a unit made up of porous horizons (Hp1 to Hp4) recognised in the North-West part of the sector and made up mainly of lagoon facies (Figure 3.3.18). These horizons display porosity levels of about 20 % and maximum permeabilities of around 10^{-8} $m.s^{-1}$. They are separated within more compact limestones (porosities of 15 % and permeabilities of 10^{-9} $m.s^{-1}$). A few kilometers South and West of the site, the results of boreholes EST321 and EST351 show that the transformation of these lagoon facies into recrystallised facies, then, further on into clay basin facies (Joinville region) is reflected in the disappearance of these porous horizons (Figure 3.3.20) ;
- In the Upper Oxfordian, porous horizons (Hp5 to Hp7), thinner than the lower porous horizons (Hp1 to Hp4), are systematically found in boreholes, but are difficult to correlate from one borehole to the next. They are more continuous and better represented in the North-Eastern part of the sector but are not systematically found in the South-Western part (Trouiller & Benabderrahmane, 2005).

It is mainly within these porous horizons that water circulation takes place (Figure 3.3.20 and Figure 3.3.21). Productivity levels in boreholes are low for all the porous horizons: a few litres per minute. These productivity levels may, however, be higher when the formation is close to outcropping (in the valleys for example, see EST311 borehole (Andra, 2004b)) or when there are fractures (EST321 borehole see § 3.4.3). Because of the low permeability of these porous horizons (about 10^{-8} $m.s^{-1}$ at most), flow rates directly above the site are low: In the transposition zone, hydrogeological modelling indicates average Darcy velocities of about one kilometre per million years. These velocities correspond to real water movement velocity (permeability divided by kinematic porosity) and advective transfer times for a non-sorbed solute, at about one kilometre per hundred thousand years. These transfer velocities are confirmed by isotopic analyses (see below). They vary very little in the transposition zone, because of the slight variations in horizontal hydraulic head gradient, the average value of which is about 10^{-2} $m.m^{-1}$.

As for the Dogger, regional water flow is globally directed from the source zones consisting of plateaux in the South and East of the site, in which the formation is karstified, towards the centre of the Paris basin. However, from the site, part of this flow moves towards the Marne valley in the South-West, because the top of the Oxfordian limestone outcrops in this valley (Figure 3.3.22), (IFP, 2004 ; Trouiller & Benabderrahmane, 2005). For trajectories directly above the Meuse/Haute-Marne site, this outcrop zone in the Marne valley represents a natural outlet from the carbonated Oxfordian aquifer in the sector today.

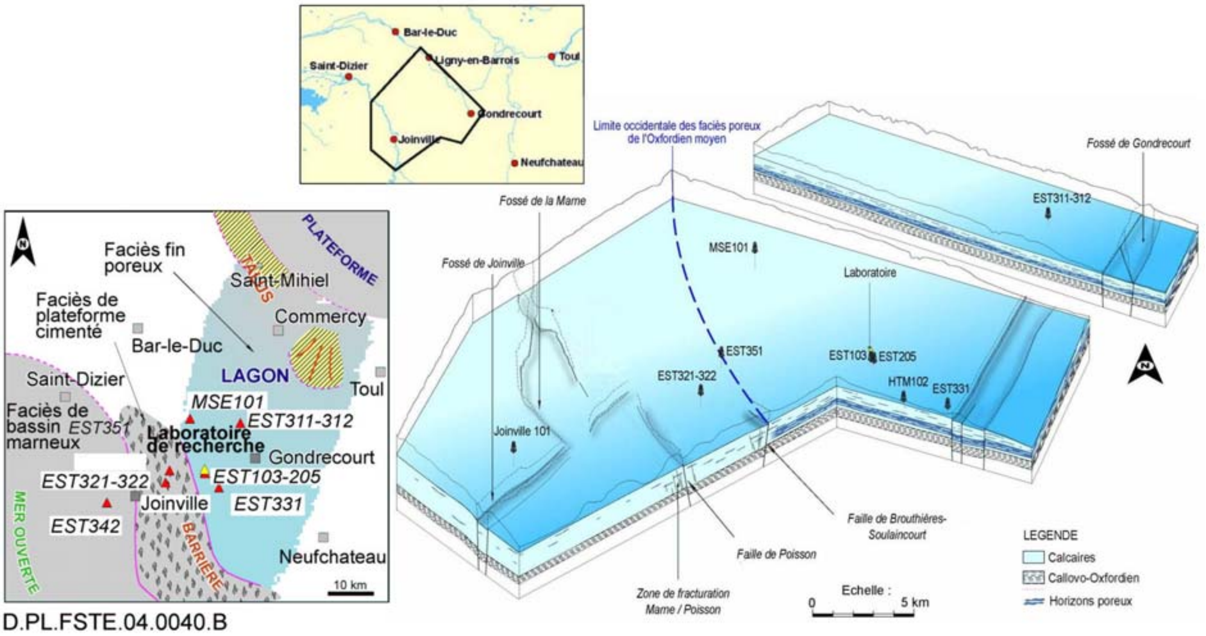

Répartition des faciès poreux de l'Oxfordien moyen

Extension géographique des horizons poreux Hp1 à Hp4 (sur la base de l'extension des faciès fins de lagon)

Figure 3.3.20 Extension of the Middle Oxfordian porous facies in the Meuse/Haute-Marne sector

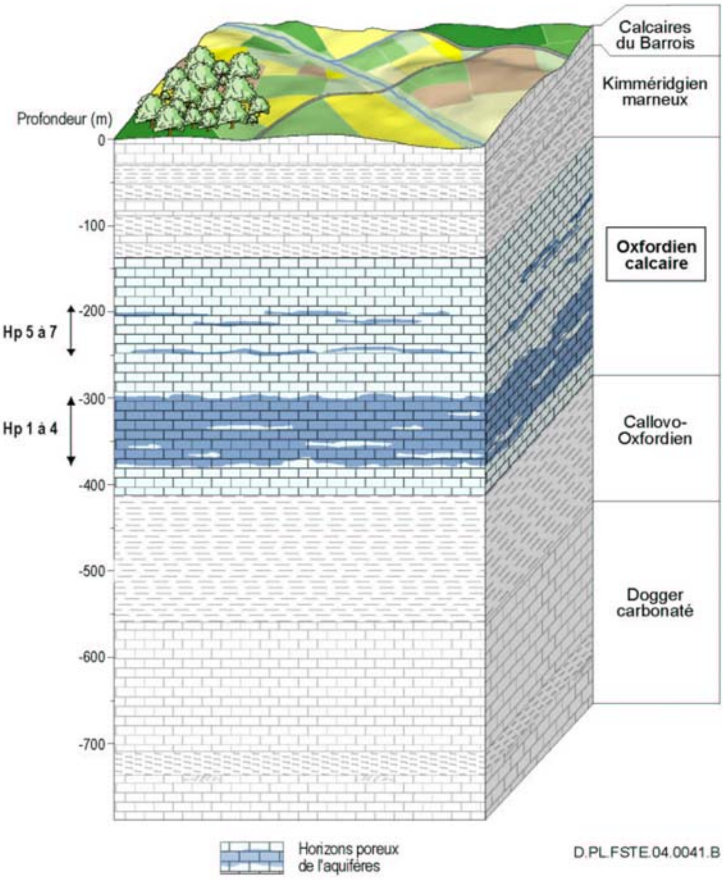

Figure 3.3.21 Representation of the porous horizons in the carbonated Oxfordian at the present time

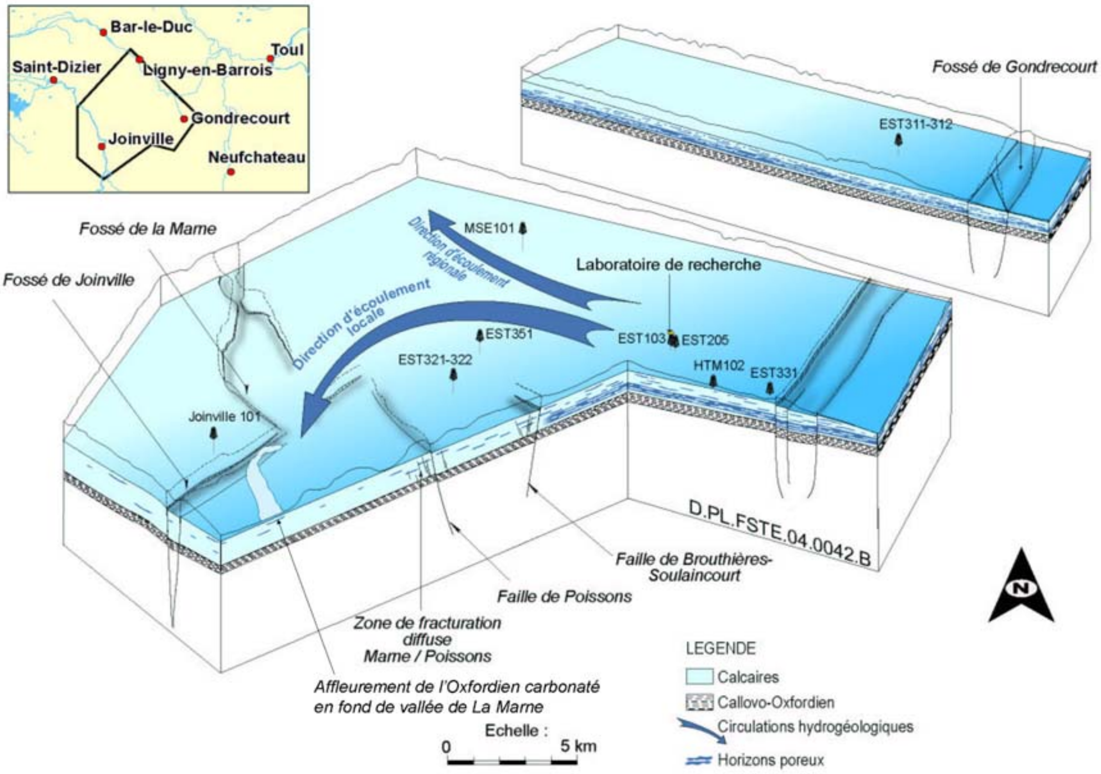

Figure 3.3.22 Organisation of water flow in carbonated Oxfordian at the present time

One consequence of flow through the well-differentiated porous horizons in the carbonated Oxfordian is that there is distinct chemical separation, directly above the site, for water between the lower porous horizons and the upper porous horizons (Trouiller & Benabderrahmane, 2005):

- the chemical facies of water in the lower horizons is sodium carbonate; this is reducing, with a neutral pH (7.5);
- the water facies in the upper horizons is magnesium carbonate, also with a pH of 7.5 but less reducing or even mildly oxidising.

These differences must be linked to the slightly different geological history of these two units, particularly with respect to deposition environments, palaeocirculation and diagenetic processes. But in both cases this is ancient water, of meteoric origin, not very saline (about 1g.L^{-1}) and geochemically evolved, at equilibrium with the formation. The low level of open fracturing revealed on monitoring excavation of the access shafts (only one productive structure observed, decametric in height, with a low flow rate of about 10^{-2} l.mn^{-1} - see § 3.4 and (Andra, 2004c)) does not therefore, generally allow vertical transfer of fluid from one set of porous horizons to the next. The analyses performed using chlorine-36 isotopes indicate, that this water is about 400,000 years old directly above the site (Buschaert & Giffaut, 2005), thus confirming the slow circulation velocities (about one kilometre per 100,000 years on average), reconstituted by hydrogeological modelling (IFP, 2004 ; Trouiller & Benabderrahmane, 2005).

3.3.2.3 Marly Kimmeridgian and Barrois Limestones

Above the carbonated Oxfordian, the Kimmeridgian displays more clay-rich facies. 110 m thick directly above the site, this formation consists of marls alternating with clayey limestones (Figure 3.3.23). These facies indicate further deepening of water during deposition of the formation.

These deposition conditions, like the Callovo-Oxfordian, explain the great constancy of facies and the thickness of this layer on a regional scale. When it outcrops, its initially low permeability underground, around 10^{-11} to 10^{-12} m.s^{-1} (Andra, 2003b), increases to about 10^{-7} m.s^{-1} because of surface alterations more specifically affecting the carbonate intervals (Trouiller & Benabderrahmane, 2005).

Under cover, the Kimmeridgian pore water displays a facies fairly similar to that of the upper carbonated Oxfordian horizons: reducing water, magnesium bicarbonate facies and a pH of 7.5. At the outcrops (or under cover for the part in contact with the Barrois Limestone aquifer), the formation is subjected to an oxidising environment which profoundly changes this facies (particularly with oxidation of pyrite, sulphate production and increasing concentration of iron in solution) and the water naturally becomes oxidising (Andra, 2003b). These marls separate the aquifer layer of carbonated Oxfordian from that of the Barrois Limestone (Trouiller & Benabderrahmane, 2005)

Directly above the site, the hydraulic head gradient through the formation is high at 0.4 m.m^{-1}, thereby confirming the semi-permeability of marly Kimmeridgian, both above ground and under cover (Andra, 2005a, situation 16).

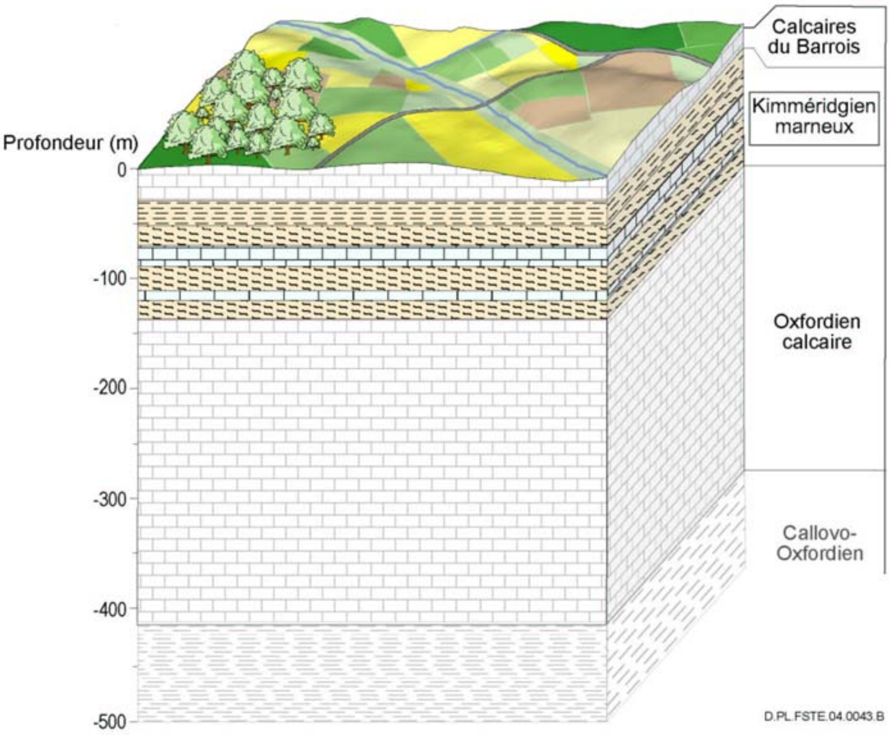

Figure 3.3.23 Schematic diagram of the Marly Kimmeridgian..

The Barrois Limestone, which outcrops in a large part of the sector, corresponds to the reinstallation of large carbonate platforms with calcareous muds on the scale of the Paris Basin. The formation is more than 200 m thick when it is complete. The initial type of limestone (more or less vacuolar clayey limestone) and its evolution at outcrops under the action of meteoric water, separates this formation into two units with quite different behaviour (Figure 3.3.24) (Trouiller & Benabderrahmane, 2005):

- a base unit (representative of the laboratory surroundings) about thirty meters thick, in which karstic developments are limited;
- an upper unit, which may reach several meters thick, in which karsts are frequent. They are all the more developed in that Cretaceous sandy clay is preserved above the formation (Brulhet, 2005b ; Trouiller & Benabderrahmane, 2005).

No matter which unit is considered, water flow in this surface aquifer fluctuates rapidly with pluviometry. Transfer, globally in a North-West direction, is rapid (several hundred to thousands of meters per day). Because the groundwater is rapidly recharged with meteoric water, water in the formation is oxidising and displays a calcium bicarbonate facies which is more or less chlorinated (Andra, 2003c) and (Andra, 2005a, situation 17).

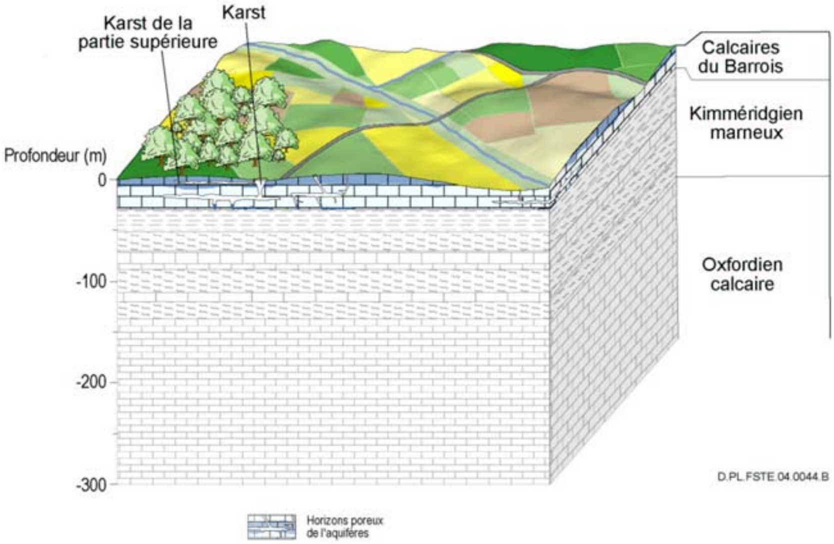

Figure 3.3.24 Schematic representation of Barrois Limestones

3.4 Tectonics and fracturing

3.4.1 Tectonic history of the sector

The Meuse/Haute-Marne site is located in a tectonically calm zone, away from regions marked by major tectonic phases.

On a sectoral scale, only the major faults (Marne faults, Poissons fault, Vittel fault), anchored in the basement rock and inherited from pre-Jurassic history, are likely to have been under extension during deposition of the terminal Dogger and Malm layers (Guillocheau *et al.*, 2002 ; Trouiller & Benabderrahmane, 2005), these movements being poorly documented on a scale of the Paris basin (Guillocheau *et al.*, 2000). During the Cretaceous, this reactivation was more complicated, alternating extension and compression (Guillocheau *et al.*, 2000).

It was really from the end of the Cretaceous and during the Tertiary that the structural organisation, as seen today, was installed (Bergerat, 1985) and (Andra, 2005h, chapitre 9):

- the Pyrenean phase (about -65 My), corresponding to the instigation of a compressive regime North/South to North-East/South-West, reactivated these strike slip accidents (horizontal displacement);
- at the end of the Eocene and in the early Oligocene (-34 My), this compressive regime was followed by a roughly East-West extensive regime. This was notably responsible for the formation of the Rhine rift valley. In the sector, this regime reactivated existing faults, extending them and creating new North-North-East/South-South-West structures (Gondrecourt graben, Joinville graben), anchored in Triassic saliniferous layers;

- finally, since the early Miocene (-23 My), the region has been subject to a compressive regime, linked to the Alpine thrust, running globally North-West/South-East, episodically remobilising the strike-slip faults. This regime, which is still in place today (see § 3.2.5), is responsible for the tectonic uplift affecting the entire Paris basin at present. Evaluations of the rate of this uplift in the sector of the Meuse/Haute-Marne site (based on valley subsidence dynamics) are estimated at one hundred meters per million years (Brulhet, 2005b). These evaluations are coherent with those given for the whole Paris basin (Pomerol, 1978).

3.4.2 The scale of fracturing in the Meuse/Haute-Marne sector

Fracturing in the sector, resulting from this tectonic history, is revealed on different scales (Andra, 2005h, chapitre 9).

- The regional faults (Marne faults, Poissons fault, Gondrecourt graben, Joinville graben and Vittel fault) enclose the sector (Figure 3.4.1). These faults, with vertical displacement of about fifty meters or more, cross the entire Jurassic series. They absorb most of the deformation which has affected the sector as is shown by their history, which corresponds to the major tectonic phases, and by the weakness of deformation outside these fault zones.
- Secondary faults also affect the whole Jurassic series, but with less vertical displacement and extension. They display similar evolution to that of the regional faults to which they are associated. They are thus particularly found to the South of the site, around the Poissons fault, in a zone linking the Marne faults and the Gondrecourt graben (Figure 3.4.1).
- Minor faults (displacement less than 5 m) form a fracture family not observed at present in the boreholes in the sector. It is out of reach of classic 2D seismic investigation methods. 3D seismic methods can be used to detect tectonic objects with as little as two metres of displacement. On the actual laboratory site, no structures of this type have been detected, an observation confirmed by the directional boreholes drilled during the FRF campaign (Andra, 2004a). By analogy with the secondary faults, these minor faults, several kilometres apart and potential extensions of several hundred metres, are likely to affect several formations at a time (Elion, 2005 ; Trouiller & Benabderrahmane, 2005). They should preferably be encountered close to regional accidents. The disposal concepts (notably the modularity of the architecture used) are such that the possible existence of these faults, judged to be highly unlikely in the transposition zone (Elion, 2005) can be ignored.
- On a smaller scale, there are microstructures corresponding to objects displaying small amounts of displacement (much less than a metre) and extension (several metres to decametric). The term "microstructures" is used to group extremely varied objects (such as joints and tension gashes) which represent discontinuities within the layers. They may be tectonic in origin or linked to the diagenetic history of the sediment (expulsion of water for example). Their distribution is therefore linked to both geographic location (fault proximity) and the type of sediment (argillite or limestone) and its own behaviour during the geological history of the zone.

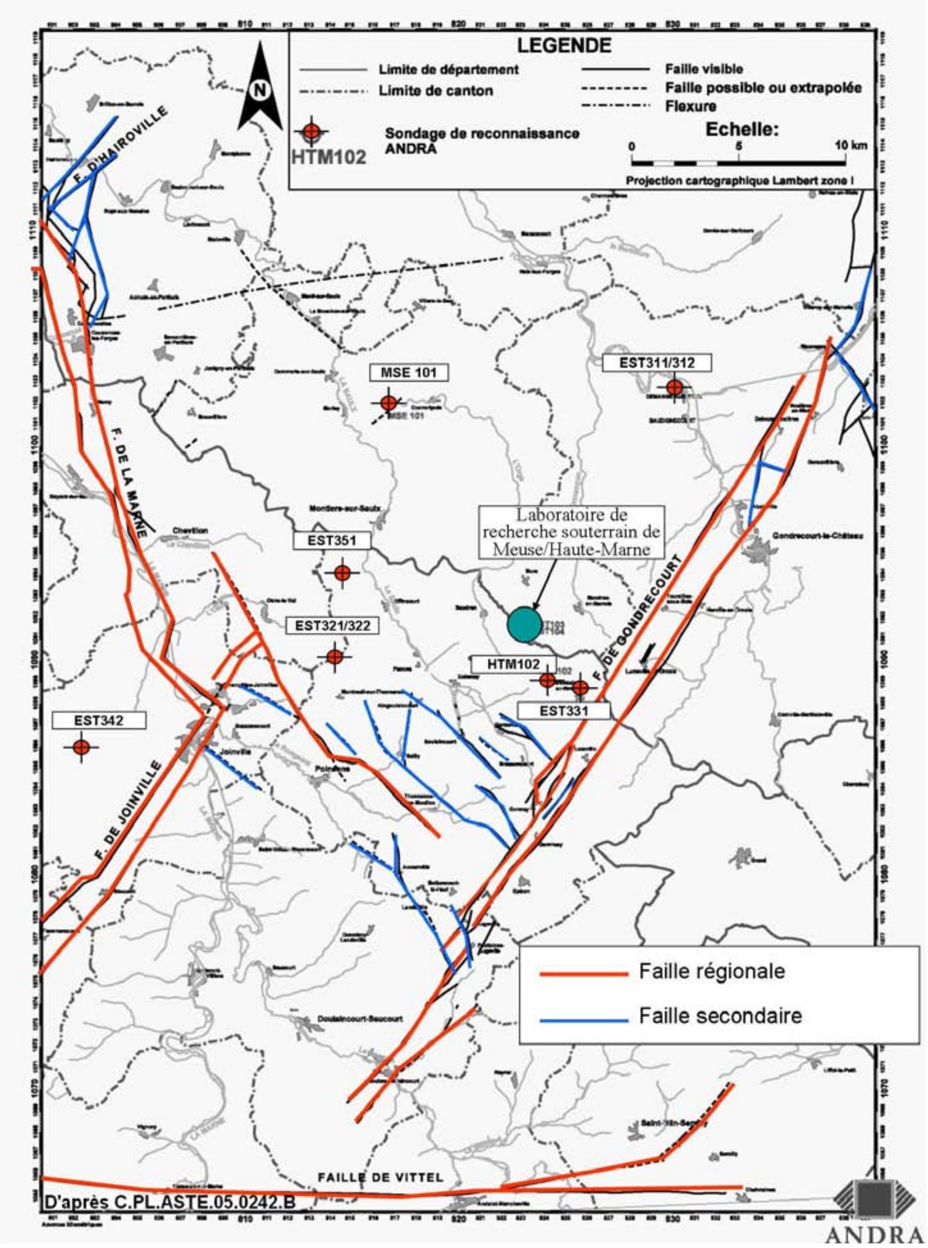

Figure 3.4.1 The different tectonic structures in the Meuse/Haute-Marne sector

Thus, in the Dogger and carbonated Oxfordian (Trouiller & Benabderrahmane, 2005), these microstructures are denser at outcrops close to regional faults (2 to 4 joints per metre). Under cover and with increasing distance from accidents, the microfracturing observed remains strong on a sectoral scale (spacing typically less than one metre to one metre). However, it is often cemented with calcite, as shown by observations made during construction of the access shafts of the underground research laboratory (Andra, 2004c).

Microstructures are rare in the Callovo-Oxfordian: several tens of microstructures, with no movement, were encountered over more than 1,300 m of cored boreholes. These structures are usually cemented with calcite or celestine, indicating early cementation during compaction (Andra, 2004a ; Elion, 2005). Investigations via inclined boreholes, performed on the site, revealed less space between structures in the upper part (estimated at about thirty meters) than in the rest of the layer (hectametric) and emphasise the influence of lithology on the distribution of microstructures (upper facies are richer in carbonate and therefore more fragile) (Andra, 2004a ; Elion, 2005) (Figure 3.4.2).

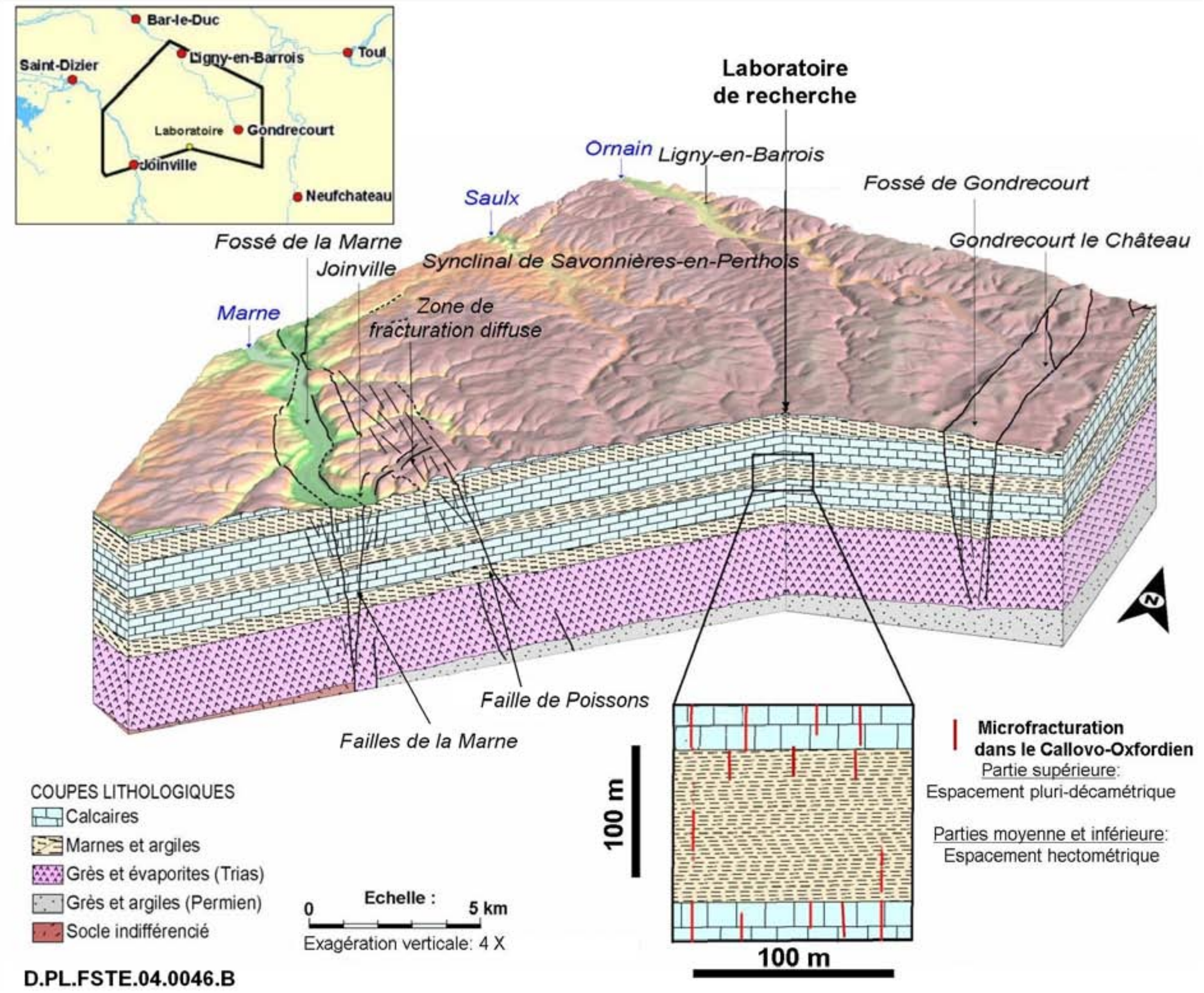

Figure 3.4.2 Diagram of microfracturing in the Callovo-Oxfordian

Furthermore, the 3D seismic data (Andra, 2005h, chapitre 9) revealed structures in the Bajocian and Bathonian which are N120°E oriented and may have been interpreted as fractures. They show an apparent maximum "displacement" (of about 3 to 4 meters) at the roof of the Longwy marls, and are then rapidly attenuated upwards, where they are apparently sealed into the Bathonian and do not not appear to have any influence on the top of the Dogger limestone. On the scale of resolution of 3D seismic data, they do not, therefore, affect the base of the clay Callovo-Oxfordian, with no offset, even minimal, visible at the horizon including the top of the Dogger limestone. One of the objectives of the FRF borehole campaign was to identify these structures and evaluate their potential impact in terms of microfracturing, not detectable by seismic methods, in the Callovo-Oxfordian layer (Andra, 2004a). The borehole results, compared with the 3D seismic data and geophysical investigations made in the boreholes, have led to these structures being interpreted in connection with reefal constructions at the top of the Bajocian, these possibly being controlled by faults in the pre-existing underlying formations at the time these constructions were installed (Andra, 2005h, chapitre 9). The boreholes confirm:

- in the Bathonian, dampening of microfractures developing directly above these structures, interpreted as compaction figures;
- the absence of fracturing and microfracturing in the Callovo-Oxfordian associated with these structures.

3.4.3 Marne / Poissons diffuse fracture zone

Boreholes EST321 and EST322 encountered an influx of water in the carbonated Oxfordian, associated with joints generally oriented N150° with infracentimetric to centrimetric openings, leading to overall transmissivity rates, deduced from pumping tests, three orders of magnitude higher than those in other boreholes in the sector. These structures, of tectonic origin, as indicated by their preferential orientation, have been enlarged in Oxfordian limestones by dissolution phenomena (Andra, 2004b ; Andra, 2004c). Boreholes EST321 and EST322 are located close to the Poissons fault, in the prolongation of a network of secondary faults, all oriented N150°E (Figure 3.4.1). This series of accidents is developed South-West of the site, between the Gondrecourt graben and the Marne faults. The Poissons fault and these secondary faults are well identified on both the existing seismic cross-section, which shows them crossing the whole Jurassic series, and on the surface. The results of these boreholes therefore confirm the observations made at outcrops, indicating that microfracturing is more developed in the surrounding carbonates close to the faults (see § 3.4.2).

Hydraulic measurements at boreholes EST321 and EST322 show:

- a difference in hydraulic head of 6 m between the Dogger and the carbonated Oxfordian, of the same order of magnitude as that observed on the site (see Figure 3.3.12),
- water from the Dogger and carbonated Oxfordian with very different geochemical characteristics (several orders of magnitude for chloride concentrations, for example – 300 mg.L^{-1} for the Dogger and less than 2 mg.L^{-1} for the carbonated Oxfordian).
- These elements indicate that, in spite of the faults identified by seismic data in south-east of these boreholes and throughout the thickness of the series, including in the Callovo-Oxfordian, the latter still acts as a semi-permeable barrier between the Dogger and the carbonated Oxfordian in this zone. The different faults identified and the joints revealed in the boreholes do not therefore create a short-circuit between the Dogger and the Oxfordian.

All the pore water of the carbonated Oxfordian in the sector is more than 40,000 years old according to the results of ^{14}C analyses (Inset 3.1). However, stable isotope analyses show that the water in EST321 borehole is considerably younger than the water in other boreholes in the sector (notably EST311 borehole and MSE101 which, like EST321, are located hydraulically downstream of the site) (Andra, 2004b). The chlorine content of pore water of the carbonated Oxfordian in the sector diminishes with the relative age of this water, with weaker concentrations observed at borehole EST321 (less than 2 mg.L^{-1}). These results indicate a dilution of carbonated Oxfordian pore water with recent meteoric water in the area of borehole EST321. The apparent age of the sampled pore water is still more than 40,000 years however. This dilution can be linked to transmissive structures revealed in the carbonated Oxfordian in this borehole and the possible existence of links from the carbonate aquifer and the surface close to it.

It should be noted that, for the Dogger, the results of geochemical and isotopic analyses display the same trends. All the Dogger water in the sector is ancient, with the values of $_{14}$C concentration being on the limit of detection. However, in the same way as for the carbonated Oxfordian, comparative analyses of stable isotopes in the water show that Dogger water in EST322 is more recent (Andra, 2004b). The variation in Dogger salinity is also organised in the same way as in the carbonated Oxfordian (but with higher chloride concentrations). The highest levels of salinity, about 4 g.L$_{-1}$, are in the North-east, in the borehole EST312. The weakest, around 0.3 g.L$_{-1}$, are observed in borehole EST322, to the West of the site (Figure 3.3.17). These results suggest circulation which is also faster in the Dogger in this zone, leading to greater dilution of chlorides rising by diffusion from Triassic horizons. However, borehole EST322 has not revealed any fracturing in the Dogger, which means that this faster flow cannot be directly linked to transmissive microfracturing.

These different elements form the basis of a diffuse fracture zone revealed, in which, due to the proximity of faults, fracturing and microfracturing are potentially more intense in the carbonates, notably Oxfordian, so that more rapid water flow is observed in this zone than in other parts of the sector. This diffuse fracturing is probably organised in "corridors" oriented N150° which means that it is not present throughout the zone. It has no influence on the hydrodynamic properties of the Callovo-Oxfordian and does not therefore modify global hydrogeological scheme in the sector. Only water residence times in carbonate formations are affected locally. However, these residence times are long (more than 40,000 years at least) according to the results of ^{14}C analyses (Andra, 2004b ; Andra, 2004c).

The size of the objects concerned is not enough for a deterministic representation to be made. The boundaries of this zone are intended, above all, to define a perimeter within which the probability of detecting this type of structure is higher (see the probabilitistic representation made for the needs of hydrogeological modelling (IFP, 2004)). These boundaries (Figure 3.4.3), which form more of an "envelope", remain approximate, given the small number of control points. They are partly based on tectonic structures recognised on the surface and in seismic data and partly on borehole results. Borehole EST351, which records flow rates in the carbonated Oxfordian, of the same order of magnitude as those measured in the sector ($20.1mn^{-1}$), is excluded from it. These elements are used to define the North-East boundary of the zone according to the direction of surface faults, passing approximately through the Saulx valley in the South and extending to the Marne faults. This diffuse fracture zone, mapped according to the proximity of accidents recognised on the surface and seismically, develops outside the transposition zone (Inset 3.2), which is, by definition, far from the fault zones.

Generally speaking, the representation of this zone, based mainly on borehole results from platform of boreholes EST321/322, remains to be confirmed.

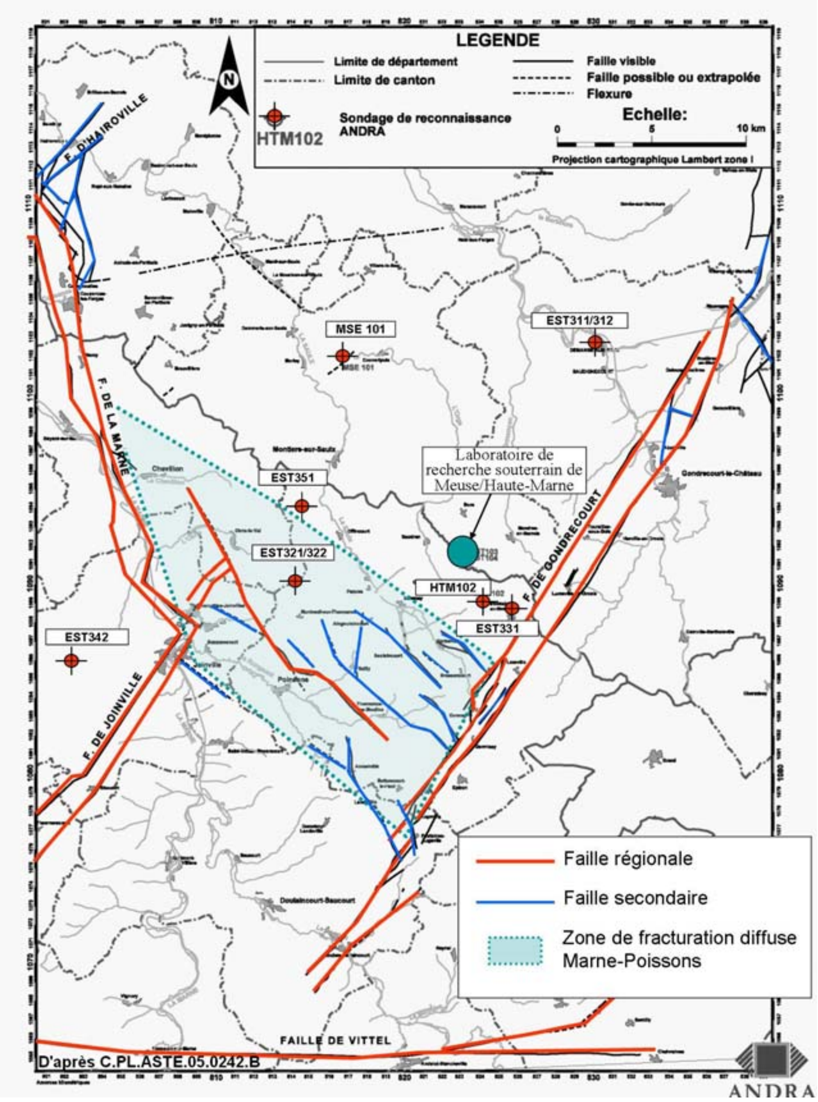

Figure 3.4.3 *Boundaries of the Marne / Poissons diffuse fracture zone*

3.4.4 The impact of fracturing on the hydraulic properties of the formations

Of all these different scales of fracturing, only regional faults can play a hydraulic role affecting all the formations. Although their vertical displacement of around a hundred meters is unlikely to bring different aquifer formations directly above each other (Dogger at the same level as carbonated Oxfordian, for example), on the other hand, it may act as an impermeable barrier (by bringing an aquifer formation in contact with an aquitard.

Outside the diffuse fracture zone and generally with increasing distance from tectonic accidents, microfracturing in the carbonated Oxfordian does not create any path for vertical transfer of fluids (see § 3.3.2.2), as is shown by the differences in water composition between upper and lower porous horizons. Monitoring shaft drilling revealed only one transmissive structure, extending over several meters, in this formation (Andra, 2004c), providing a good demonstration of the slight impact, in general, of microfracturing in the carbonated Oxfordian water flow regime, essentially controlled by porous horizons. Nevertheless, this microfracturing is enough to provide hydraulic continuity in transmitting the charge throughout the porous horizons.

In the Dogger, no transmissive structures were found in the boreholes. Given the high level of calcite recrystallisation observed generally in microfractures in this formation within the sector, the formation does not play a part in water flow. Furthermore, the long residence time for water in this formation, as for the Oxfordian, is not very compatible with flow through a fractured network (see § 3.3.2.1). Any impact by microfracturing in the Dogger can therefore only be interpreted as very local, close to faults.

In the Callovo-Oxfordian, hydraulic tests performed on the various intervals, particularly directly above the rare structures revealed in the upper part of the formation (structures cemented by calcite or celestine, see § 3.4.2), demonstrated the lack of impact of these structure on the layer's permeability (Andra, 2004a ; Elion, 2005).

Therefore, given:

- the distance, by definition (Inset 3.2) of the regional accident from the transposition zone limit and zones linked to these accidents, recognised on the surface (therefore the diffuse fracture zone);
- the lack of impact of the rare microstructures recognised, on Callovo-Oxfordian permeability, as well as a vertical hydraulic head gradient imposed by the surroundings, excluding the transmissive structures crossing the formation;
- the small part played by microstructures with respect to water flow in the surroundings outside the diffuse fracture zone and close to the faults, since this essentially horizontal water flow is controlled by porous horizons being generally organised according to stratification;

within the transposition zone, there is no expected modification of properties in those volumes of the Callovo-Oxfordian and surrounding carbonate formations, due to fracturing.

3.5 The surface environment

The climate at the site, the geological substrate and hydrogeology of the sector all determine the geomorphological model of the site. These elements condition the surface soil and hydrogeology and therefore, fauna, flora and human activities. The term "surface environment" or "biosphere" includes all these constituents (Texier & Leclerc-Cessac, 2005).

3.5.1 Climate

In this part of Eastern France, the climate is temperate-oceanic. With their North-South orientation and altitude (over 300 meters), the hills of the Meuse form an initial barrier to air masses from the West and South-West (dominant winds) crossing the Paris Basin. The forced ascendance is reflected in the high rainfall (up to 1,000 – 1,100 mm.year^{-1}) distributed throughout the year. Locally, the main valleys (Marne, Meuse, Moselle) record lower rainfall at about 700 mm.year^{-1}) (Andra, 2005a, situation 2).

Current mean annual temperatures oscillate around 10 °C with daily minima of -2 °C in winter and maxima of 24 °C in summer (Figure 3.5.1). Air humidity levels are high: around 75 % in summer and 85 to 87 % in winter (Andra, 2005h, chapitre 14).

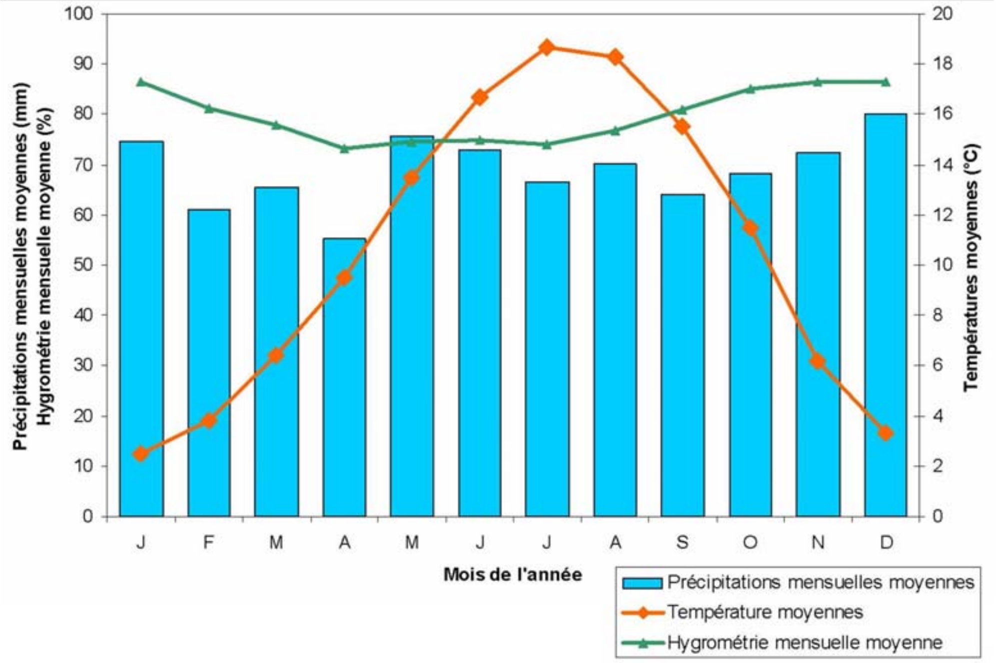

Figure 3.5.1 Variation of mean temperatures and rainfall at Saint-Dizier

3.5.2 Geological basement to geomorphological model

At outcrops in the sector, the alternating soft clay and strong limestone layers and general dip of these layers to the West and North-West are responsible for a typically hilly landscape with views from South and East towards the North-West (Brulhet, 2005b) over:

- the carbonated Oxfordian plateau forming the Meuse hills, overhanging the depression created by the Callovo-Oxfordian clays (Figure 3.2.6),
- plus further West, the marly depression of the Kimmeridgian, within which intervals of clayey limestone form small, highly visible mounds in the landscape Figure 3.2.6 and Figure 3.5.2),
- the Barrois Limestones, in the form of a vast plateau, are capped by a Lower Cretaceous veneer (sand and red clay) and incised by rivers. To the East of the site, several mounds belonging to the Barrois Limestone line the edge of the Gondrecourt graben (Figure 3.5.2).

Relief is the result of continuous evolution since the sector emerged at the end of the Cretaceous and is linked to its tectonic evolution.

For 3 My, alternating glacial-interglacial cycles have led to this tectonic origin being overlain by periodic modifications, linked to the cyclicity of climatic evolution (Brulhet, 2005b). These modifications particularly concern the development and retreat of permafrost. The dynamics of these evolutions are presented in § 9.3.

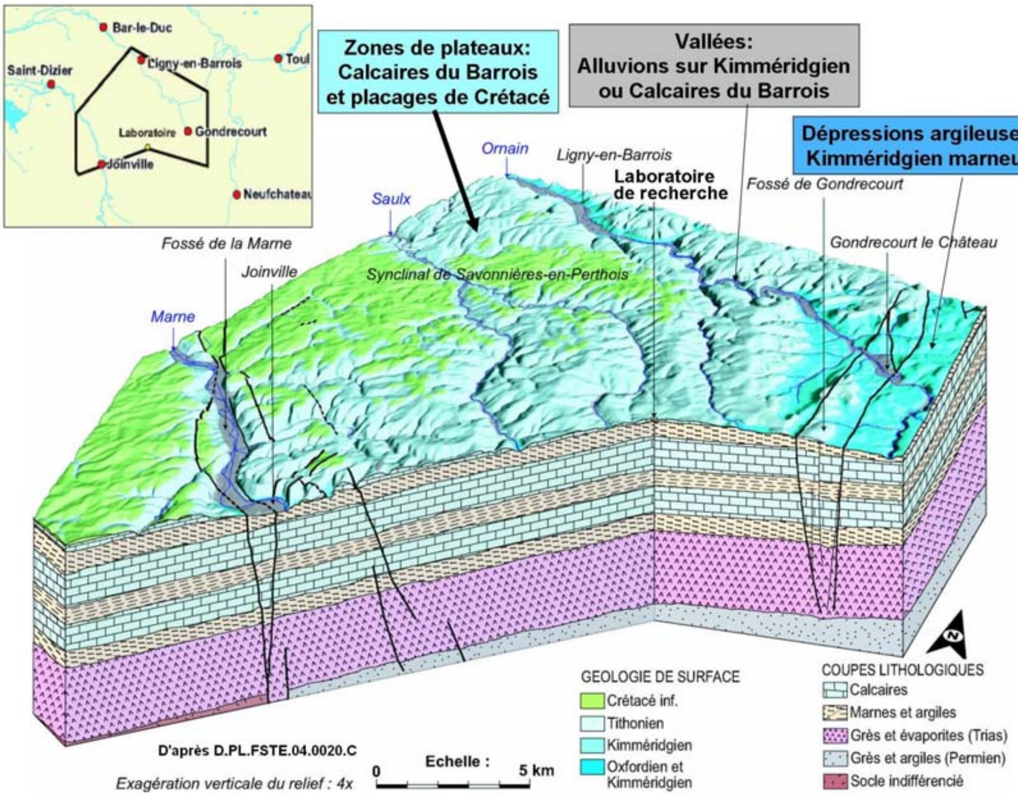

Figure 3.5.2 The different morphological models around the Meuse/Haute-Marne site at the present time

3.5.3 Resources (surface hydrology and hydrogeology)

The topography controls surface water flow, with surface water tending to flow to the foot of the hills. To the West of the sector, the region is drained to the North and North-West by the Marne and its affluents (Ornain, Saulx, Rongeant). These flow in the direction of dip of the layers, deeply incising the Barrois Limestones. The dynamics of this incision are closely linked to recent tectonics in the sector as well as successive glacial and interglacial periods (Brulhet, 2005b). Thus, the most "efficient" periods of erosion are at the start of glacial periods, during cold damp climatic episodes with marked frosts. This heritage explains the current valley morphology, with valleys too large for the meandering streams wandering around their alluvial plains (Brulhet, 2005b ; Texier & Leclerc-Cessac, 2005). The valleys are seasonally flooded during the wettest months.

The valley bottoms are natural outlets from the Barrois limestones (see Figure 3.5.3). These outlets take the form of karstic springs with output strongly influenced by precipitation, but which can reach several $m^3.min^{-1}$ (Andra, 2005a, situation 17). These springs are found essentially when the upper part of the Barrois Limestones has been incised. The karsts of the upper part of the Barrois limestones are also responsible for losses from certain rivers (the Orge downstream of Saudraon and Couvertpuis, the Saulx in the North of the sector) (Brulhet, 2005b). For the lower part, where there are no karsts, water flow rates from the rare springs are very low (a few tens of L/min at most) and intermittent.

This difference in hydraulic behaviour between the two Barrois limestone units depends on their underground water sources. When the lower part (the first thirty meters of the formation) outcrops, as is the case at the underground research laboratory, the water sources are too small and either not exploited or very little: water flow rates at boreholes are around 10 to 15 $L.min^{-1}$, as shown by the measures taken around the site (Andra, 2003c) and (Andra, 2005a, situation 17). According to karstic developments, these borehole productivities can become very high in the upper part (up to 500 $L.min^{-1}$), which is enough for the resource to be used to satisfy the needs of human communities (for example springs at Rupt-aux-Nonains and Cousances-les-Forges, in the north of the sector (Andra, 2005a, situation 17).

The intercalation of marly limestones in the Kimmeridgian also constitutes a source of water close to the outcrops. Borehole productivities are 200 to 300 L.min^{-1} at most. The springs flow at rates which can reach 1 m^3.min^{-1} at most, but with rapid variations which reveal the low level of reserves in these aquifers (Andra, 2005a, situation 16). Under cover, the formation becomes unproductive (Andra, 2003b ; Trouiller & Benabderrahmane, 2005).

The carbonate formations surrounding the Callovo-Oxfordian (carbonated Oxfordian and Dogger) are unproductive at the underground research laboratory site, because of their low permeability (see § 3.3.2.1 and 3.3.2.2). Evaluations based on borehole data provided by Andra, give flow rates of a few l.min^{-1} (Andra, 2004b). When they are fractured, as is the case, for example, at borehole EST321 (see § Figure 3.4.2), water flow rates may be much higher, from several tens to a hundred l.min^{-1} (rates determined over a short test period, the duration of which is not guaranteed) (Andra, 2004b).

At the outcrop, these formations are productive, like the Barrois limestones, because of karstification: they are then likely to flow at high rates (several m^3.min^{-1} or more). This is particularly the case for the carbonated Oxfordian in the Marne valley in the South of the sector (Andra, 2005a, situation 15).

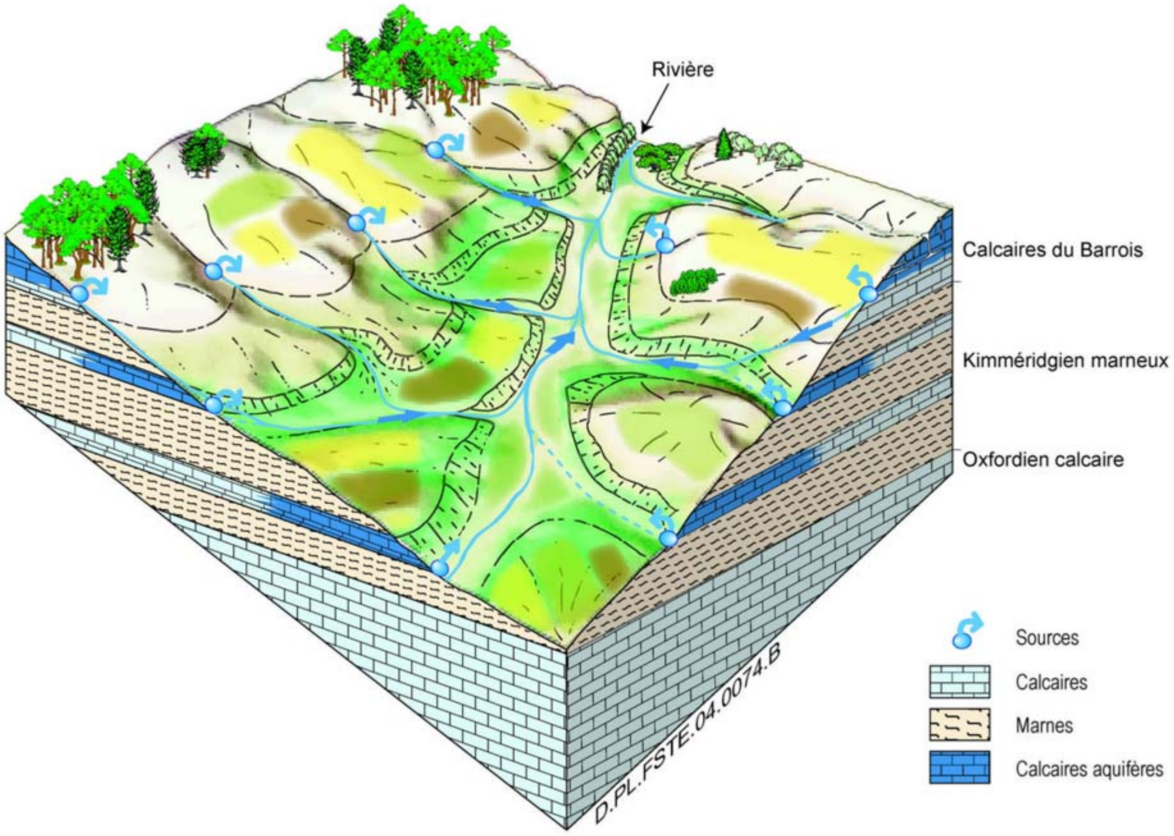

Figure 3.5.3 *Schematic representation of surface water flow at the Meuse/Haute-Marne site at the present time and its relationship with the lithological units*

3.5.4 Soils

The main types of soils are distributed according to the nature of the substrate (limestone or clay) and the geomorphological situation in question (thalweg, valley bottom) (Andra, 2005h, chapitre 22).

On the plateaux, the soils are linked to the limestone substrate (Figure 3.5.4). In most cases these are thin, more or less pebbly and loamy depending on the topographical model (Texier & Leclerc-Cessac, 2005). In the thalwegs, soils are predominantly loamy and may be very thick (up to 3 m) (Andra, 2005h, chapitre 22). In the long term, these soils are maintained from one glacial/interglacial cycle to the next, and only evolve with climatic fluctuations in detail, because of the process of pedogenesis (dissolution of the substrate), deposition and aeolian erosion (loess - loam) and/or periglacial action (cryoturbation, periglacial erosion) (Brulhet, 2005b).

On the slopes, soil development depends on climatic conditions. During glacial periods, the slopes are subject to erosion (active landslips, gravity slides) which limits the establishment of soil, depending on detailed morphology and exposure. During interglacial periods, such as the present time, soils are stabilised with the installation of plant cover (Brulhet, 2005b). The slopes therefore display soils which are not very evolved, are thin, pebbly and carbonate-rich (Texier & Leclerc-Cessac, 2005) (Figure 3.5.4).

In the marly depressions, soils are thin and mainly clay (Texier & Leclerc-Cessac, 2005).

In the valley bottoms, soils are eroded, then "neoformed" with each climatic cycle (see § 9.4.2). Thin, relatively unevolved soils are established on limestone-rich alluvium/colluvium. They are loamy in nature, with flood deposits (from seasonal floods) (Texier & Leclerc-Cessac, 2005) (Figure 3.5.4). They are locally hydromorphic, when the valley is situated on marls (upstream parts of the Saulx, the Orge and the Rongeant in particular).

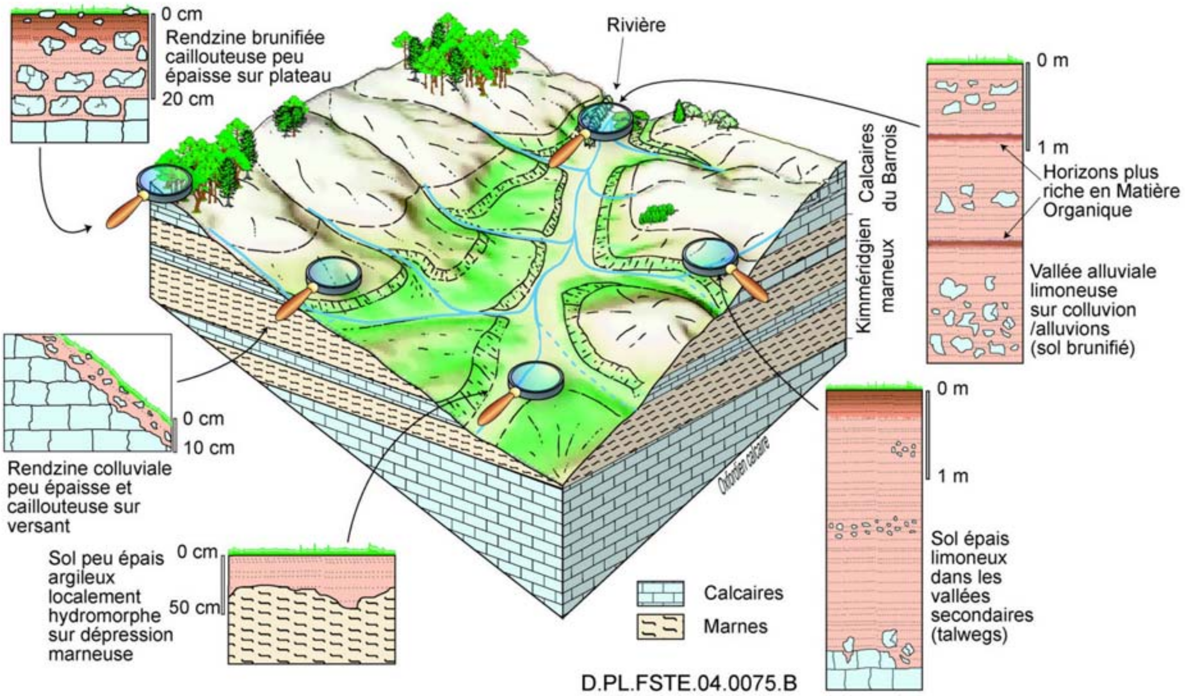

Figure 3.5.4 *Schematic distribution of different soils on the Meuse/Haute-Marne site at the present time*

3.5.5 Flora and fauna

The climate and soils are suitable for high plant potential and good crop productivity (Texier & Leclerc-Cessac, 2005).

On the plateaux and slopes, agricultural areas have been gradually replacing the mixed temperate forest (deciduous and conifers) over the past few thousand years, although there are still large areas of forest (particularly Montiers forest), mostly in the form of small wooded hills (Andra, 2005h, chapitre 22), (Figure 3.5.5).

The valley bottoms are occupied by meadows (water meadows or not depending on the soil) (Figure 3.5.5).

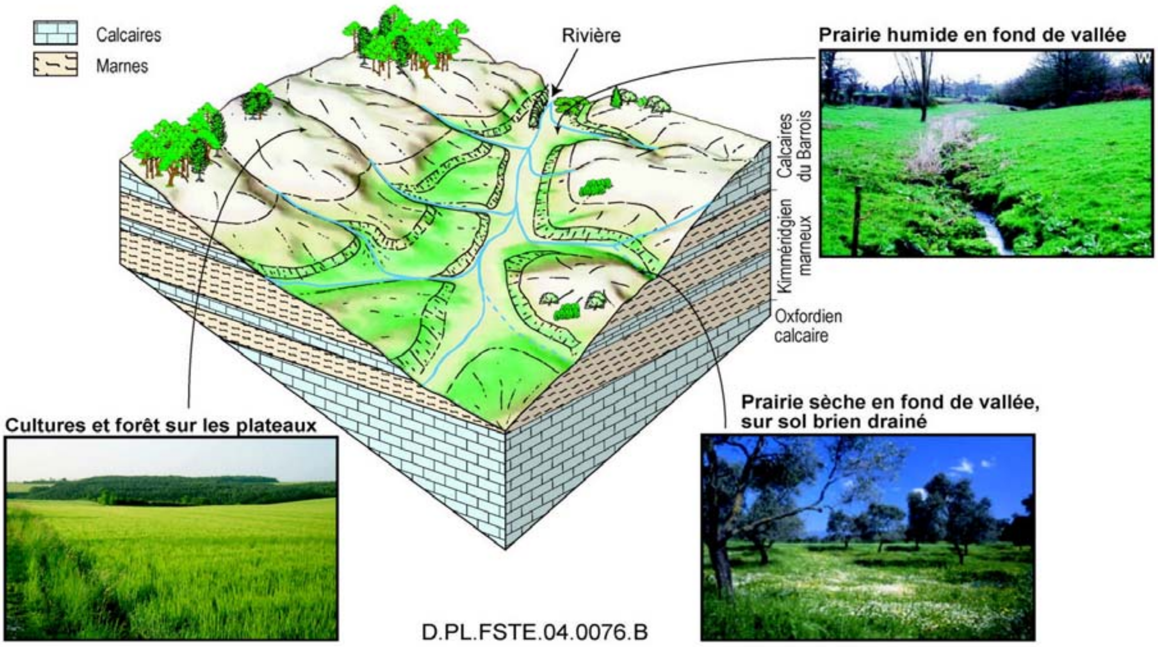

Figure 3.5.5 Schematic distribution of large natural units on the Meuse/Haute-Marne site at the present time.

The alternation and diversity of the environment means that a wide variety of numerous fauna is maintained and developed (birds and mammals, game in particular). This wealth of fauna is also maintained by the good distribution of water sources and wet zones throughout the sector. Thus, all the food chains are particularly well represented (Andra, 2005h, chapitre 22).

3.5.6 Human activities

Habitations are essentially grouped in the valleys close to water sources. Only a few farms are isolated on the plateaux. The main activity in the sector is agriculture, centred on the production of cereals and oilseed crops and beef raising (Texier & Leclerc-Cessac, 2005).

3.6 Summary of the initial state of the geological medium

This summary of the initial state of the geological medium is intended to extract the most important points from the previous elements so that a context is set for the following chapters which will describe the evolution of this medium under the influence of a repository and geodynamic processes.

3.6.1 Geological aspects: a simple structure and one homogeneous Callovo-Oxfordian layer in the sector

The geological medium displays a simple structure. It is in the form of a stack of large dimension contrasting lithological units (alternately carbonates and clays), well identifiable, with flat geometry, showing very little variation in thickness, and continuous on a scale of the transposition zone and the sector. It is perfectly coherent with the general geometry of deposits on the scale of the Paris Basin.

Within these large units, the Callovo-Oxfordian is a predominantly clay-rich layer, varying from a minimum of 130 m up to 160 m thick and between 500 and 630 m deep in the transposition zone. Vertically, the layer is organised in three sedimentary sequences, the boundaries of which are underlined by thin carbonate deposits which can be correlated over large distances. The central part of the Callovo-Oxfordian is the most clayey zone (up to 60 % clay minerals). The top of the layer (last 30 to 40 m) is characterised by carbonate enrichment. In the transposition zone and beyond, it shows very little lateral variation in lithology.

This formation is surrounded by two massive carbonate units (Dogger and Oxfordian limestones), not outcropping in the transposition zone. The layers which outcrop in the transposition zone (marly Kimmeridgian in the valleys and Barrois limestones on the plateaux), by their flat structure, uniform dip and differences in lithology, produce a characteristic sloping relief with plateaux zones deeply incised by river valleys.

The unit is very slightly deformed. The sector is surrounded by faults which have absorbed the main tectonic deformations occurring during its geological history. In the East, the Gondrecourt fault can be identified, the Marne faults in the West, and South-West of the site is a zone linked to the Poissons fault, with possible extension of a series of minor faults recognised on the surface, known as a diffuse fracturing zone. In this latter zone, there is microfracturing in the carbonated Oxfordian, linked to dissolution phenomena, recognised in boreholes, but its boundaries, currently defined as an "envelope", are still to be confirmed. It could locally induce faster flow in this formation without disturbing overall hydrogeological function, particularly the barrier role played by the Callovo-Oxfordian. The generally very flat geometrical setting is only disturbed close to major faults, with maximum displacement being less than one hundred meters. The transposition zone is located away from these major accidents and the diffuse fracture zone. Investigations performed to date have not revealed any detectable discontinuity of tectonic origin in this transposition zone (i.e. with vertical displacement of more than 5 m, which could be reduced to 2 m on the site of the underground research laboratory).

The petrophysical characteristics of the formations were acquired very early in the area's geological history, either at the time of deposition or shortly afterwards, or during diagenetic phases, the most recent of which are contemporary with Tertiary history. The textural properties of the Callovo-Oxfordian were acquired during the early history of the formation. These properties are responsible for its low permeability, which is homogeneous throughout the formation (10^{-13} to 10^{-14} m.s^{-1}). The latest diagenetic phases were responsible for the low permeability observed in the Dogger and carbonated Oxfordian when under cover, on a scale of the Eastern aureole of the Paris basin. These latest phases are linked to the outcropping of carbonate formations in the East of the sector, and the circulation of water of meteoric origin. They do not affect the more impermeable Callovo-Oxfordian. The Callovo-

Oxfordian and its surroundings therefore give evidence of very slow evolution over several tens of millions of years, so that it can be said that these formations are, at depth, at equilibrium over this time scale.

3.6.2 Thermal aspects: a geothermal system free of anomaly

The sector does not display any geothermal anomaly relative to the rest of the Paris basin but the temperature gradient is lower than average, at about 2.3 °C/100 m, i.e. a temperature of about 23 °C in the middle of the layer, directly above the underground research laboratory. It is essentially controlled by natural crustal flow and climatic variations on the surface. These are linked to past climatic cycles and are dampened at depth. They therefore have very little effect on the Callovo-Oxfordian. Phases of glacial maxima led to the development of surface permafrost and temporary penetration of the 0 °C isotherm as far as the carbonated Oxfordian at most. The thermal properties of the Callovo-Oxfordian are relatively homogeneous throughout the thickness of the layer. They are anisotropic because of stratification (from 1.3 to 1.9 $W.m^{-1}.K^{-1}$ vertically and 1.9 to 2.7 $W.m^{-1}.K^{-1}$ horizontally).

3.6.3 Hydraulic aspects: a weakly permeable Callovo-Oxfordian with slow flow in the surroundings

Current hydrogeology in the sector results from slow evolution over several million years, particularly under the effect of the erosion of surface terrain leading to the migration of recharging areas and the creation of new outlets in the valleys. During this evolution, the installation of permafrost during glacial cycles created reversible disturbances in the carbonated Oxfordian, for which the duration of about 20,000 years per 100,000 year cycle is brief on a scale of several million years.

The vertical alternation of weakly permeable carbonate layers and clay layers limits vertical flow. The differences in water salinity between the Dogger and carbonated Oxfordian (see below) are coherent with the low permeabilities measured in the Callovo-Oxfordian: at 10^{-13} to 10^{-14} $m.s^{-1}$. These low values, which are homogeneous throughout the height of the layer, are controlled by the texture of the argillites and on the basis of low lateral variability throughout the layer, can be extrapolated to the whole transposition zone. They determine the slow water velocity within the layer (Figure 3.6.1). Over pressure relative to the surroundings, was measured in the Callovo-Oxfordian at about thirty to forty meters. At the current state of knowledge, the amplitude of this over pressure can only be interpreted by invoking osmosis. It does not affect water flow in the Callovo-Oxfordian. This essentially vertical water flow is controlled by the hydraulic head gradient between the two surrounding carbonates. Within the transposition zone, this gradient is low (0.2 $m.m^{-1}$ responsible for descending flow towards the south to 0.3 $m.m^{-1}$ responsible for ascending flow towards the formation north and north-west). In the surroundings, water flow is essentially horizontal (Figure 3.6.1). In accordance with the general structure of this whole eastern part of the Paris basin, this water flow is directly globally towards the centre of the basin to the West. For a fraction of the water flow from the site, and only for the carbonated Oxfordian, a single local outlet exists to the West of the site, towards the Marne valley which incises the formations to a considerable depth. All the other trajectories, for both the Oxfordian and the Dogger, display regional water flow towards the centre of the Paris basin.

The low permeabilities of the Dogger and Oxfordian limestones impose a slow water flow velocity in the sector, about one kilometre per hundred thousand years, or even less in the Dogger. The major faults in the sector do not play a marked hydraulic role in deep circulation, although on the scale of the Paris basin, exchanges between aquifers have been revealed across regional faults. In these surrounding formations, borehole water flow rates are slow, a few litres per minute. In the fractured zones, borehole water flow rate can be higher.

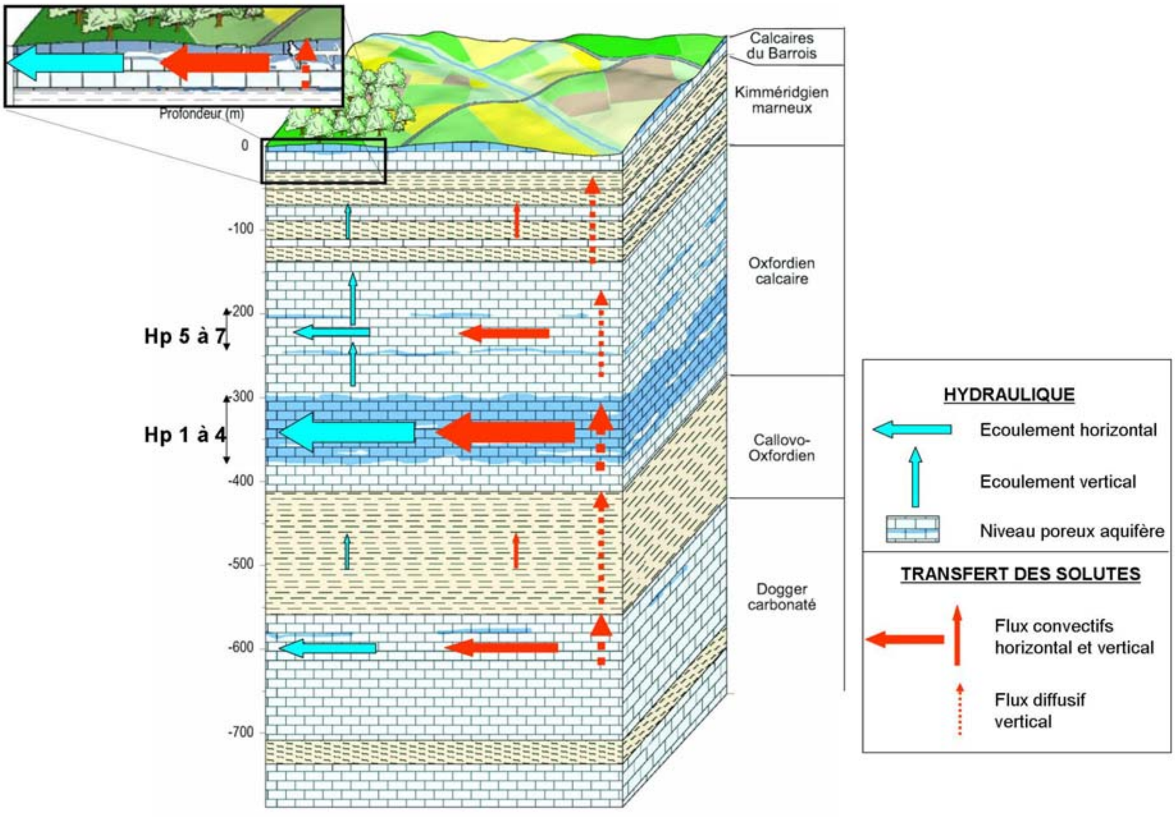

Figure 3.6.1 *Schematic representation of water flow and solute transport in the geological medium in its initial state*

3.6.4 Chemical aspects: an homogeneous formation with pore water at equilibrium, weakly alkaline, carbonate, sodiocalcic and reducing

The long solution residence times in both the Callovo-Oxfordian and its surroundings, imposes a chemical state close to equilibrium at depth, with pore water of globally homogeneous composition for each formation. Generally speaking, pore water in the formations is reducing, carbonate-rich and near natural pH. In particular, the pore water of the Callovo-Oxfordian records charges of chlorides and sulphates. The chemical composition of the pore water is relatively to be homogeneous throughout the thickness of the formation as well as laterally, in coherence with its global lithological homogeneity and low variability on the scale of the transposition zone. The Dogger displays high total salinities (up to about 4 $g.L^{-1}$) which control the salinities of the Callovo-Oxfordian. Within the Callovo-Oxfordian, salinity decreasing towards the top of the formation is characteristic of a medium in which diffusion is the dominant means of transport. In the carbonated Oxfordian, salinities (less than 1 $g.L^{-1}$) are less than those observed at the top of the layer, showing that there is dilution by horizontal water flow in this aquifer (Figure 3.6.1). Generally speaking, the very marked differences in chemical and isotopic compositions of Dogger and carbonated Oxfordian water illustrate the generally impermeable nature of the Callovo-Oxfordian.

Past climatic cycles have not altered pore water chemistry in the Callovo-Oxfordian, notably because of its chemical buffer capacity. There may have been disturbances in the carbonated Oxfordian, but over limited periods and with no irreversible chemical effect.

3.6.5 Mechanical aspects: a simple natural stress field, coherent with knowledge of the Paris Basin

The current state of natural mechanical stresses has been the same for more than twenty million years. The vertical stress corresponds to the weight of the terrain. The horizontal stress is slightly anisotropic (with an σ_H / σ_h anisotropy ratio of 1 to 1.2), the major stress being oriented North-North-West/South-South-East. This direction is found throughout the Paris basin and results from compression of the entire West European plate following the Alpine thrust.

Deformation velocities are slow and the sector is far from currently active deformation zones. Displacement rates along the planes of basement faults in the sector are estimated at less than 10^{-6} m.year^{-1}. This explains the seismically calm nature of this part of the Paris Basin, corroborated by the lack of evidence of quaternary tectonic activity on the faults in the sector.

The intrinsic mechanical behaviour in the Callovo-Oxfordian layer depends on the percentage of clay and can be subdivided into three zones, according to variations in this percentage. The median zone, richer in clay and including the laboratory site, is more deformable than the upper and lower zones, the latter notably displaying more rigid behaviour because of the carbonate intercalations. The velocity of creep during the first weeks, estimated at 10^{-2} to 10^{-3} year^{-1} in the central part of the Callovo-Oxfordian, is about four times lower in the upper part (zone "A"). This central zone displays compression resistance of about 20 MPa and a modulus of deformation of 4,500 MPa.

3.6.6 Surface environment: characteristics inherited from the climatic history and geomorphological evolution

For outcropping formations (Kimmeridgian, Barrois Limestones), the impact of internal and external geodynamic evolution has been greater. Thus, the main characteristics of these formations and the current biosphere: distribution of water resources, durability (on the plateaux) or neoformation (in the valleys) of soils, distribution of different cultivated, wooded zones, etc. are the heritage of past climatic cycles and evolutions of the general geomorphological model in the sector over the last few million years.

4

Phenomenological processes

4.1 The main phenomenological processes relating to the repository 177

4.2 Main THMCR processes relating to geodynamic evolution 179

4.3 Timescales of the major THMC processes and radionuclide release and transfer 179

4.4 Spatial organisation of the phenomenological evolution of the repository and its geological environment: independence and similarities 181

Many different phenomena are involved in the phenomenological evolution of the repository and its geological environment. However, it is possible to identify a set of major processes that act as a guide for the analysis and description of the phenomenological evolution undertaken in the following chapters.

Starting from the existing state of equilibrium, two specific drivers are responsible for the phenomenological evolution of the repository and its geological environment:

- The repository itself,
- The natural geodynamic evolution of the geological environment, characterised by climate-driven evolution on the surface and internal geodynamic changes (tectonic mouvements).

4.1 The main phenomenological processes relating to the repository

In view of a) the characteristics of the geological environment when in equilibrium, as described in chapter 3, and b) the repository's characteristics, as described in chapter 2, the repository is a source of various types of disturbance (THMC) that influence both the repository itself and the surrounding geological environment (i.e. the Callovo-Oxfordian layer and, to a much lesser extent, the surrounding geological formations).

4.1.1 Thermal load due to exothermic waste

Placing type C waste and spent fuel packages (and to a lesser extent, weakly exothermic category B waste) into the repository (cf. § 2.3.3) causes a gradual increase in the temperature of the corresponding repository zones and the surrounding geological environment (mainly the Callovo-Oxfordian clay layer). Because the heat emitted by waste packages gradually decreases, this temperature rise is transient, rising to a peak and then decaying until the repository and its surrounding geological environment return to the natural geothermal temperatures.

4.1.2 Hydraulic processes: hydraulic head discharge, desaturation, resaturation combined with hydrogen production, and return to a new hydraulic equilibrium

The geological formations are initially saturated and in a state of hydraulic equilibrium, as described in chapter 3. The repository is responsible for a series of hydraulic disturbances over time; these disturbances can be categorised as follows:

- Initially, the creation of the repository immediately causes a discharge of hydraulic head (i.e. a fall in water pressure) in each of the formations above the Callovo-Oxfordian layer around the access shafts, and within the Callovo-Oxfordian layer around all of the structures (dgrabens, disposal cells and access shafts). During the operational phase, the hydraulic head discharge propagates around the structures that are kept open. As well as the hydraulic head discharge, ventilation with non water-saturated air in ventilated structures desaturates the argillites in the immediate vicinity of those structures.
- Air is trapped as the successive structures (especially the grabens) are closed. The hydraulic head discharge and desaturation processes cease, and the repository and the argillites in the near field subject to desaturation during the operational phase begin to resaturate. This resaturation is influenced by the hydrogen produced as a result of corrosion of the repository's metal components, in particular in the C waste and spent fuel disposal cells. When the repository has been totally saturated, a new state of hydraulic equilibrium forms in the repository and the Callovo-Oxfordian layer around the repository zones.

4.1.3 Chemical processes: interface reactions with the near-field argillites and clayey components, corrosion of metal components and chemical degradation of concrete

Repository design measures attempt to minimise the chemical disturbances in the repository and the Callovo-Oxfordian layer. The repository nevertheless remains an intrinsic source of chemical disturbances. Furthermore, these disturbances are affected by the thermal disturbances and the aforementioned hydraulic processes. These chemical disturbances result mainly from the introduction of materials and fluids from beyond the Callovo-Oxfordian layer. These materials and fluids are:

- Either out of equilibrium with the chemistry of the pore water and solids in the Callovo-Oxfordian layer, as is the case, for example, with the concrete in B waste disposal cells, or the oxygen of the ventilation air,
- Or near a state of equilibrium with the Callovo-Oxfordian layer, as is the case with the swelling clays used for seals and disposal cell plugs or the excavated disturbed argillites in graben backfill.

In addition to the indirect chemical consequences relating to the thermal disturbances that affects the repository and the Callovo-Oxfordian layer as a whole, most of the chemical disturbances are located at the interfaces, owing in particular to the slow transfer of solutes in and around the repository. The main issues are:

- ***For the repository***: chemical degradation of man-made components, including aqueous degradation of concrete in contact with the pore water of the argillites, corrosion of the metals present in containers and waste, transformation of swelling clays in contact with iron and concrete or the transformation of disturbed backfill argillites, aqueous corrosion of glass and aqueous dissolution of the oxide matrices in spent fuel;
- ***For the Callovo-Oxfordian layer***: the oxidising disturbance linked caused by the presence of ventilation air combined with desaturation in the near field of the ventilated structures, alkaline disturbance in contact with the concrete repository components (B waste disposal cells and grabens) and the disturbance caused by iron in contact with metal components (C waste disposal cell linings and spent fuel disposal cell linings and supports).

4.1.4 Mechanical pressure discharge and damage processes in the Callovo-Oxfordian layer in the near field of the repository, followed by a return to mechanical equilibrium

When structures are created, the pressure on the surrounding argillites is immediately reduced, as characterised by the appearance of a zone of disturbed rock at the interface, called the Excavation Damaged Zone (EDZ). The mechanical behaviour of the repository in general, and of the EDZ in particular, as well as the behaviour of the near-field Callovo-Oxfordian layer, subsequently evolve during the operational period, and change further following closure under the effect of the thermal load, hydraulic processes such as desaturation and resaturation, and chemical processes.

Over the long term, argillite creep and the gradual chemical degradation of repository components, including container corrosion or chemical attack on concrete by the pore water of the argillites, for example, are responsible for the repository's mechanical evolution, and ultimately a new state of mechanical equilibrium, similar to the current state, at the scale of the repository.

4.2 Main THMCR processes relating to geodynamic evolution

4.2.1 Internal geodynamics

The Meuse/Haute-Marne site is extremely stable with respect to internal geodynamic phenomena. Any isostatic movements are very small. Accordingly, climatic changes will be the main driver of geodynamic evolution over the next million years and beyond.

4.2.2 Climatic changes

Extrapolating existing data or combining this data with human disturbances, and in particular the massive release of greenhouse gases, astronomical climate theory leads us to consider the following two scenarios for the Meuse/Haute-Marne facility:

- Either a continuation of the quaternary climate cycles, i.e. alternating glacial and interglacial cycles at intervals of approximately 100,000 years,
- Or a period of warming lasting several tens of thousands of years, followed by a return to natural climate cycles after around 500,000 years.

These climate changes are responsible for erosion that does not reach the Callovo-Oxfordian layer but does locally alter the morphology of the surface terrain. Thus, valleys deepen and coastlines recede, outcrops of the various geological formations slowly move, new karstic systems develop and river capture phenomena evolve. Over the million-year study period, such morphology changes affect the water drainage patterns, and therefore the transport of solutes, in the surrounding geological formations, especially those above the repository. Nevertheless, solute transport in the Callovo-Oxfordian layer within the transposition zone is unaffected, remaining dominantly diffusive as is currently the case (cf. § 3).

4.3 Timescales of the major THMC processes and radionuclide release and transfer

The major THMC processes already described develop over different time periods, as shown in the Figure 4.3.1, although in time (after a few tens of thousands of years to one hundred thousand years) they tend to revert towards a new state of equilibrium or very slow evolution.

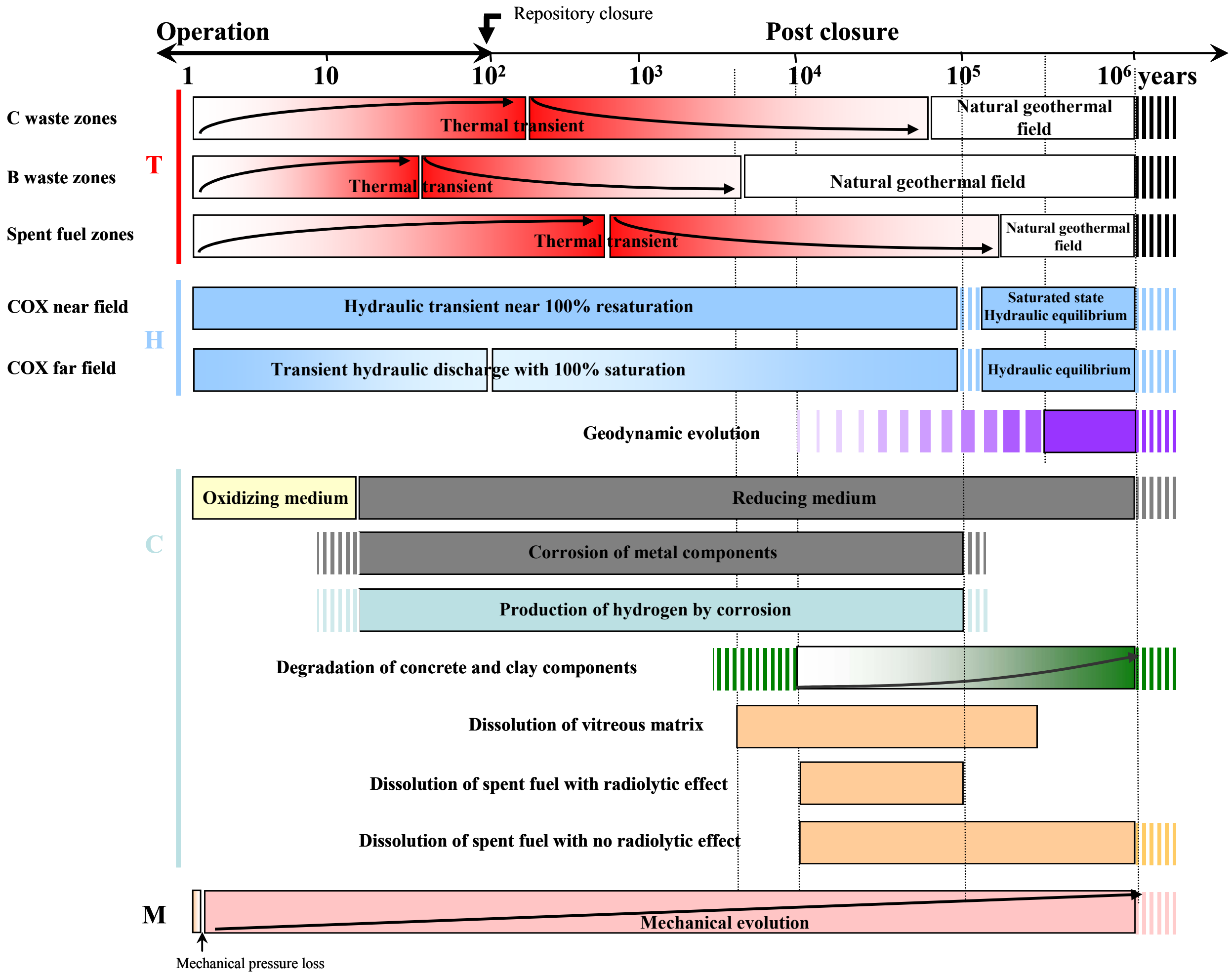

Figure 4.3.1 *Chronogram of the major phenomena affecting the repository and its geological environment (based on the conventional hundred-year repository construction/operation/closure time diagram)*

Broadly:

- Geodynamic processes occur over a timescale of at least one million years;
- Thermal loading occurs over a timescale of several tens of thousands of years, although they peak in the repository within a few decades or centuries;
- Hydraulic processes in the repository and the Callovo-Oxfordian layer take place over a timescale of approximately 100,000 years, prior to total saturation of the repository after around 200,000 years, accompanied by a return to a state of hydraulic equilibrium in the repository and the surrounding Callovo-Oxfordian layer;
- Apart from the redox transient, which appears a short-lived phenomenon when considered on a million-year timescale, the chemical processes develop mainly after ten thousand years and last a few hundred thousand or even a million years. More specifically, the metal components, and in particular the C waste and spent fuel containers corrode over a period lasting from a few thousand years to a few tens of thousands of years;
- Mechanical processes, which are largely dependent on the hydraulic processes and the chemical degradation of the repository components extend primarily over the same timescales as those processes. However, they develop naturally over a million years at least, owing to the very slow natural creep of the argillites;

- Radionuclide release is largely dependent on chemical processes such as corrosion of metal containers, aqueous dissolution of packaging matrices (e.g. the glass in vitrified waste) or dissolution of spent fuel oxide pellets. Accordingly, the timescale for this process extends from a few tens of thousands of years to several hundred thousand years or more. Once released, radionuclides migrate into the Callovo-Oxfordian layer over a period of several hundred thousand years, via the general solute transfer process described in chapter 3.

4.4 Spatial organisation of the phenomenological evolution of the repository and its geological environment: independence and similarities

Any complex spatial organisation of the phenomenological evolution of the repository and its geological environment is prevented or limited by (i) the repository's compartmentalised modular design, (ii) the thickness of the Callovo-Oxfordian layer, which offers a clearance of at least 60 m between the repository and the surrounding formations, (iii) the specific properties of the Callovo-Oxfordian layer, including its low permeability and a relative ability to act as a chemical buffer, and (iv) the presence of seals and disposal cell plugs, which "close" the repository hydraulically.

Thus:

- The distances of several hundred meters between repository zones are greater (and in some cases very much greater) than the extensions of the aforementioned major processes, i.e. thermal (several decameters), mechanical (several meters), chemical (one metre to several meters) and hydraulic (several meters to several decameters) (Inset 4.1). Owing to these distances, the phenomenological evolutions of the various repository zones and surrounding Callovo-Oxfordian clay are almost totally independent;
- The adjacent disposal modules within a particular repository zone are a few decameters apart. As with repository zones, any non-adjacent disposal modules are far enough apart to prevent phenomenological interactions. Consequently, all disposal modules have the same phenomenological evolutions. The same principle applies to the various disposal cells in a module.

Disposal cells and disposal modules constitute basic phenomenological templates that are repeated spatially to form the overall phenomenological evolution of a repository zone and the surrounding section of the Callovo-Oxfordian layer.

Inset 4.1 ***Phenomenological interactions in the Callovo-Oxfordian layer: Estimated times and distances relating to thermal, hydraulic and chemical interactions***

Heat and solute transfers, and the propagation of hydraulic pressure variations in a porous medium such as the Callovo-Oxfordian layer, tend to be diffusive in nature. Such phenomena are characterised by a diffusion coefficient, expressed $m^2.s^{-1}$. This coefficient represents the porous medium's ability to transfer a quantity of heat, pressure or solute created by a source. For example, thermal diffusivity is the ratio of thermal conductivity (which represents the medium's ability to transfer heat by conduction) over heat capacity (which represents the medium's ability to accumulate heat). In transition conditions, the smaller the diffusion coefficient, the slower the transfer of the quantity in question.

The orders of magnitude of the diffusion coefficients in the Callovo-Oxfordian layer are given in the table below:

Thermal diffusivity	**Hydraulic diffusivity**	**Apparent solute diffusivity**
10^{-6} $m^2.s^{-1}$	10^{-8} $m^2.s^{-1}$	10^{-10} $m^2.s^{-1}$

By convention, the following two quantities are estimated:

- The ***characteristic distance*** L_c beyond which a constant heat, pressure or solute source is felt after a period of time t_c,
- Conversely, the ***characteristic time*** t_c required for the aforementioned constant source to be felt at a distance L_c

…using the formula $t_c = \frac{L_c^2}{2D}$, where D is the diffusion coefficient.

When applied to heat transfers, for example, this formula corresponds to the case of an infinite medium at a initial homogeneous temperature (e.g. 0 °C) that contains an infinite planar source. At a given point in time ($t = 0$), this source is assumed to be brought to a temperature (T) other than the initial temperature, and then maintained at that temperature. Under the effect of the planar source, the medium gradually increases in temperature until temperature T is reached. The above formula gives the time required for a point located at a distance L from the planar source to reach a temperature of T/2.

Note that:

- This formula is not linear: the characteristic time increases as the square of the distance from the source, highlighting the fact that interaction periods increase exponentially as one moves further from the source;
- The characteristic time varies in a linear relation with the diffusion coefficient. Comparing the values of the diffusion coefficients listed in the above table clearly shows that heat transfer is the fastest transfer process. The characteristic times for hydraulic transfer and solute transport are respectively two and four orders of magnitude longer than the characteristic thermal transfer time. This reflects the Callovo-Oxfordian layer's ability to act as a hydraulic barrier and solute diffusion barrier.

With the repository, the sources might be:

- Heat sources: heat release from waste packages.
- Pressure sources: hydraulic head discharge accompanying the creation of the structures, or over pressure created by thermal expansion of water caused by heat released from waste packages.
- Solute sources: Radionuclide releases by waste packages or cement water from concrete structures.

These sources are not constant over time: **i)** the heating power of packages decays over time, **ii)** the hydraulic head discharge generated when the repository is created is limited by the operating period of one or several centuries, and **iii)** radionuclide and solute sources become exhausted either through radioactive decay and gradual release by the waste packages (in the case of radionuclides), or because the masses of the repository's materials are finite (in the case of solutes).

Furthermore, the Callovo-Oxfordian layer is not an infinite medium. Regarding the transfer of the radionuclides released by the repository, the overlying and underlying geological formations form zero-concentration boundary conditions, such that the transfer times given by the formula for a planar source in an infinite medium are higher than those for transfers from the repository to surrounding formations. The same also applies to the hydraulic head discharge around the repository, as the surrounding formations act as hydraulic head boundary conditions. Nevertheless, the formula for a planar source in an infinite medium is useful for estimating the interaction distances involved, as shown in the table below (in order to allow for the finite thickness of the Callovo-Oxfordian layer, the exercise was limited to a 100,000-year period, and "Not applicable" has been entered for any meaningless time/space combinations).

Theoretical characteristic distance (planar source in an infinite medium)	**1 year**	**10 years**	**100 years**	**1,000 years**	**10,000 years**	**100,000 years**
Heat transfer	7.7 m	24 m	77 m	245 m	Not applicable	Not applicable
Water pressure transfer	0.77 m	0.24 m	7.7 m	Not applicable	Not applicable	Not applicable
Solute transfer	0.07 m	0.24 m	0.77 m	2.45 m	7.74 m	24 m

It can be seen that:

- Heat transfer occurs rapidly, but between 100 and 1,000 years are required for a heat source to generate a temperature rise of more than a few degrees at distances of approximately 100 and 250 meters, respectively. Over such lengths of time, the heating power of the waste packages decays considerably, meaning that their thermal influence is small even at the relevant characteristic distances;

- The same applies to water pressure if the repository is only open for a period of around a century. In this case, the hydraulic head discharge is imperceptible further than a few meters from the structures;

- Solute transfer occurs even more slowly. In broad terms, it takes more than a million years for a solute to travel a minimum of 80 m by diffusion. For example, the distance of more than 250 m between the concrete B waste disposal cells and the C waste and spent fuel repository zones ensures that cement fluids from the B waste disposal cells cannot interact with the other zones (even when the relative chemical buffer effect of the Callovo-Oxfordian layer, which further inhibits the cement fluid transfer process, is not taken into consideration).

5

Thermal load

5.1 Introduction 187

5.2 The modes of heat transfer given off by waste packages in the repository and the surrounding geological formations 187

5.3 Spatial organisation of the thermal load 191

5.4 Thermal loads of C waste and spent fuel repository zones..............................194

5.5 Thermal load of the B waste repository zone..199

5.6 Summary of the thermal load of the repository 203

5.1 Introduction

As soon as C waste packages and spent fuel packages have been emplaced in the disposal cells, the heat given off by these packages triggers a gradual and transient temperature rise in the corresponding repository zones and in the surrounding geological medium. This is known as the "thermal load" (cf. § 2.3.4.6–(Andra, 2005e)). For B waste packages, this phenomenon only affects disposal cells containing reference packages B1 and B5 which have low exothermicity and therefore a more limited thermal load.

The hydraulic, chemical and mechanical processes affecting the repository during the same period have little or no impact on the thermal load. On the other hand, the thermal load does affect all of these processes. It therefore provides important information on hydraulic, chemical and mechanical evolutions and, ultimately, on the release and migration of radionuclides.

In order to describe the thermal load in this chapter, we firstly reiterate the modes of heat transfer in the repository and geological formations. We then generally describe the time/space organisation of the thermal load in the repository on a macroscopic scale and in the geological medium. Finally, the thermal loads of the various repository zones are described in detail on various scales from the disposal cell to the repository zone and surrounding geological formations.

The description of the thermal load is mainly based on numerical modelling (finite element) work which help to provide an understanding of the various scales of time and space (Inset 5.1). Using modern computing tools, reliable numerical calculations regarding temperature changes can be achieved, thanks especially to precise meshing and adequate time step definitions. For example, evaluations of temperature changes by numerical modelling carried out while preparing various heating experiments in underground research laboratories, such as FEBEX in Grimsel (Switzerland) (Rutqvist & Tsang, 2003) and HE-D (Kull *et al.*, 2005) at Mont Terri, are consistent with the measurements taken in situ.

5.2 The modes of heat transfer given off by waste packages in the repository and the surrounding geological formations

Generally, the heat given off by exothermic waste packages in the various components of the repository, in the Callovo-Oxfordian layer and in the underlying and overlying geological formations is mainly propagated by conduction (Inset 5.2).

5.2.1 Within the geological medium

Owing to the very low permeability of the Callovo-Oxfordian argillites, the proportion of heat conveyed by advection with the interstitial water flow (natural or disturbed by the repository) is low. Similarly, the low permeability of the Callovo-Oxfordian layer and the thermal gradients limited by the criterion of a 90 °C maximum admissible temperature in argillites (Inset 2.5, (Andra, 2005n)) allow for little (if any) heat transfer by thermoadvection (Coelho, 2005).

The surrounding geological formations have higher permeabilities than the Callovo-Oxfordian argillites, but the thermal gradients created by the repository in the far field are low (less than one degree Celsius per metre) and diminish with distance from the repository, such that heat is transferred in these formations by conduction (Inset 5.2). Therefore, at the Meuse/Haute-Marne site, conduction is the primary mode of heat transfer. This analysis, also adopted by NAGRA for the clay "Zurich Weinland" site in the north of Switzerland (Johnson *et al.*, 2002) is applicable to any repository site in a low-permeability clayey formation under sedimentary cover.

Inset 5.1 **Evaluations of the thermal load of the repository**

The repository represents a sum of heat sources – the waste packages – distributed in space on scales ranging from a disposal cell to a repository zone. In addition to this diversity in space scales, we also find diversity in the components in which the heat is propagated: the repository components and all site's geological formations. Finally, owing to the decrease in the heat released by the waste packages, the time required to reach the maximum temperature rises varies from one year to hundreds or thousands of years and the maximum temperature values vary from zero to tens of degrees Celsius according to the location considered (for example, within a disposal cell, in the centre of a module or a repository zone, in the Callovo-Oxfordian layer or in the surrounding formations above and below the repository zone).

Numerical modelling (two or three-dimensional finite-element calculations) is therefore necessary to evaluate the thermal load (Bauer, 2005). This is done by:

- adopting geometric simplifications of all or part of the repository for the purpose of homogenisation;
- modelling the modes of heat transfer by conduction in all materials of the model and by radiation between all parts separated by air (functional clearances, etc.) where represented. The evolution in the clearances over time and the variations in thermal conductivity of the repository components with the degree of saturation (such as engineered swelling clay barriers) are taken into consideration.

Owing to the high ratio between the characteristic dimensions of the disposal cell components (e.g. a matter of centimeters for functional clearances or the lining) and the zone thermally affected by the repository (up to a few hundred meters), the approach used is a breakdown into models of different scales, each with its own area of validity:

- the **local model** on a disposal cell scale is used to assess the history of temperatures in a disposal cell and in its near field. The disposal cell is represented in detail and complex phenomenology, such as the coupling between heat transfer and saturation, can be used;

- the **medium model** on a repository module scale includes the structures surrounding the disposal cell (access grabens, seals, etc.) and is used to evaluate the thermal load on a module scale. It requires a less detailed representation of the disposal cells and a heat transfer phenomenology limited to pure conduction without coupling with hydraulics;

- the **global model** on a site scale provides information on the temperatures reached in the various geological formations taking account of their thermal characteristics. It is built on a highly simplified representation of the repository, generally a homogenised volume heat source. As in the case of the medium model, only heat transfer by pure conduction not coupled with other processes is adopted.

These models as a whole lead to uncertainties regarding the evaluations of the temperature rises which are estimated at a few degrees at most.

Inset 5.2 ***The modes of heat transfer***

There are three main modes of heat transfer: conduction, advection and radiation.

- **Conduction** corresponds to the transmission of heat by the cumulative vibration of atoms in all directions in space.
- **Radiation** is the propagation of heat in the form of electromagnetic vibrations (vibration-animated photons) which move in a straight line without transfer of matter.
- **Advection** corresponds to heat transfer through the transfer of matter, generally liquids and gases.

In geological media, and natural porous media in general, conduction and advection are the main modes of heat transfer. Advection is observed in powerful water-bearing formations where water flow rates can convey the geothermal heat given off by the earth's core. In the majority of geological formations, the water flow is too slow for it to be able to entrain a significant quantity of heat and conduction is the dominant mode of heat transfer.

As far as radiation is concerned, all solid bodies radiate heat. However, transfer by radiation between two bodies is only significant if there is a sufficiently large air gap between them and if their emissivity levels are high. As every effort is made to keep such gaps to a minimum in the disposal concepts, such concepts and the natural media are only slightly affected by this, if at all.

Fourier's law

Conduction in a given medium is described by Fourier's law which links the heat flux ϕ transmitted to the temperature gradient grad(T) applied to this medium: $\phi = -\lambda.\ \mathrm{grad}(T)$ where λ is the thermal conductivity of the medium ($W.m^{-1}.°C^{-1}$).

The ratio of the thermal conductivity (λ) of the medium to its volumetric heat capacity (ρC_p) is thermal diffusivity ($D_{thermal}$):

$$D_{\mathrm{thermal}} = \frac{\lambda}{\rho C_{\mathrm{p}}} \quad (m^2.s^{-1})$$

where ρ is the density ($kg.m^{-3}$) and C_p the specific heat ($J.kg^{-1}.°C^{-1}$).

Physically, thermal diffusivity ($D_{thermal}$) represents the capacity of the medium to evacuate heat in relation to its capacity to store it. The higher the thermal diffusivity, the less the medium subjected to a heat flow heats up, and conversely, the lower the thermal diffusivity, the greater the temperature rise in the medium. While natural media generally have similar thermal diffusivity levels (approximately 10^{-6} $m^2.s^{-1}$), their thermal conductivity values may be very different (around 6 $W.m^{-1}.°C^{-1}$ for a salt and 1 to 2 $W.m^{-1}.C^{-1}$ for argillites).

5.2.2 In the repository

The engineered repository structures consist of various materials, which, for the most part, are put into place in an unsaturated state (such as the engineered barrier of the spent fuel disposal cells, concretes after setting and graben backfill), and functional clearances. Furthermore, the grabens and B waste disposal cells are ventilated during the operating phase. These arrangements create conditions which can have a local influence on heat transfer within the structures.

5.2.2.1 The effect of emplacement clearances

The emplacement clearances and residual spaces within the disposal cells make heat transfer by radiation and natural advection possible. These are minimised by design. In C waste disposal cells and spent fuel disposal cells, they are a few centimeters thick at most. Their thermal insulating effect is therefore limited and the increase in temperature that they induce compared with perfect contact is around ten degrees on the temperature of the waste package skin. On the other hand, the influence of the clearances on the temperatures reached in the argillites and/or in the engineered barrier diminishes with the distance of the disposal packages to less than a few degrees. In B waste disposal cells, such clearances are larger (measured in tens of centimeters). Not until ventilation is stopped – and it may be maintained for a period ranging from a few years to several tens of years – will these clearances influence the temperature of the waste packages (cf. below).

5.2.2.2 The effect of ventilation in exothermic B waste disposal cells and grabens

B waste disposal cells are ventilated throughout their entire operating phase and until they are closed. The ventilation period after emplacement in the repository may vary from the time required to fill the disposal cell (immediate closure) to a few years, several tens of years, or more depending on the choices made in terms of the reversible management of the repository. Ventilation air can remove by advection 80 to 90 % of the heat released by all of the packages. When ventilation is maintained in the disposal cell following waste package emplacement, the thermal load within the disposal cell and in the near-field argillites is less than that of a non-ventilated disposal cell (cf. § 5.5). Once ventilation has been stopped, the temperature in the various disposal cell components increases and the thermal load is almost equivalent to that obtained with disposal packages which are stored prior to emplacement for periods equivalent to the ventilation periods (Bauer, 2005).

On a repository module and repository zone level, ventilation of the connecting and access grabens during the operating phase is designed to guarantee working conditions which are compatible with human presence. It prevents the air temperature from rising in the engineered structures but only plays a minor part in dissipating heat (a few percent) and does not therefore alter the thermal load around the disposal cells. Once ventilation has been stopped and the grabens backfilled, the temperatures increase gradually in the backfill.

5.2.2.3 Coupling with repository resaturation

The hydraulic evolution of the components of the engineered structures, especially their saturation level, influences the thermal load. The thermal conductivity of components such as the swelling clays of the plugs or engineered barriers, the argillites of the disposal cell wall or the backfill indeed depends on their saturation level. The thermal conductivity of the other disposal cell components has little influence on the thermal load due to their low volume (steel coverings and linings for instance) or their presence in engineered structures where little heat is released (for example, the concretes in B waste cells). The hydraulic evolution of the repository shows that no desaturation of the argillites occurs around the C waste disposal cells and the spent fuel disposal cells (cf. § 6). Furthermore, the transfer of heat is faster than the resaturation of the plugs of these disposal cells and the engineered barrier specifically in the spent fuel disposal cells. The maximum temperatures of the thermal load are therefore little affected by hydraulic evolution. On the other hand, the thermal load is influenced by hydraulic evolution as soon as the degree of saturation of the disposal cell plugs, engineered barriers, concretes and backfill increases (as thermal conductivity increases with the degree of saturation, the heat transfer becomes greater). However, this occurs either when the thermal phase has decreased considerably, or after the thermal phase. Consequently, the effect of hydraulics on heat transfer is limited to a few degrees Celsius.

5.3 Spatial organisation of the thermal load

5.3.1 On the scale of the repository and surrounding geological medium

5.3.1.1 Thermal independence of the repository zones

Due to the decrease in the heat given off by the waste packages and spent fuel packages over time, and the high kinetics of this decrease compared with the propagation kinetics of heat, the thermal influence of a repository zone is no longer felt beyond a distance of a few hundred meters, either vertically or horizontally (Bauer, 2005). Therefore, given the distances between repository zones (≥ 250 m), thermal interaction between the various repository zones is limited to a temperature rise of a few degrees Celsius at most.

5.3.1.2 A thermal load affecting mainly the repository and Callovo-Oxfordian argillites

For a constant heat source, the heat transfer time from the repository level to the top and bottom of the Callovo-Oxfordian layer is of the order of several hundred years to over a thousand years. This duration is much greater than the time required for the heat released by the waste packages to decrease significantly. Indeed, as a first approximation, during the first hundred years, the heat ratings of C waste packages and spent fuel packages decrease by a factor of two every thirty years (corresponding to the half-life of ^{137}C which is the main contributor to the heat rating). The thermal interaction distance corresponding to a period of thirty years is of the order of forty meters – less than the distance between the repository and the top or bottom of the Callovo-Oxfordian layer (50 meters in the reference scenario at the underground research laboratory). As a result, the temperature rise linked to the repository does not increase indefinitely over time, but reaches a maximum which decreases with distance from the repository in the Callovo-Oxfordian layer, and especially towards the underlying Dogger and towards the surface through the whole of the overlying formations (Figure 5.3.1). The thermal load therefore affects mainly the repository and the Callovo-Oxfordian layer.

Moreover, owing to the planar structures of the geological formations and the repository, and the constant temperature condition imposed on the surface, the thermal load remains localised in a direct line with the repository zones. However, as the argillites have greater horizontal thermal conductivity than vertical thermal conductivity, heat removal is significantly better in the horizontal direction than in the vertical direction (the horizontal thermal conductivity of argillites is 1.9 $W.m^{-1}.°C^{-1}$ while their vertical conductivity is 1.3 $W.m^{-1}.°C^{-1}$ (Andra, 2005h, chapitre 27). The outcome is a slight deformation (anisotropy) of the thermal field in a line with the repository. Finally, the low vertical variability of thermal conductivity within the Callovo-Oxfordian layer does not cause any significant variations in the thermal load, especially as distance from the engineered structures increases. In the formations surrounding the Callovo-Oxfordian layer, as distance from the engineered structures increases, the variations in thermal conductivity have little if any effect on the thermal load and this dissipates in a homogeneous manner.

5.3.2 On a repository zone scale

5.3.2.1 The effect of gradual thermal loading linked to the gradual operation of a zone

A repository zone is operated gradually by module and by disposal cell within a module. Therefore the thermal loading of a repository zone, on a module scale and on a disposal cell scale, is gradual. The distances between C waste package disposal cells or between spent fuel package disposal cells vary from 8 to 25 m depending on the type of package in question. The distances between disposal modules are of the order of 50 to 60 m. The thermal interaction times for these distances vary respectively from a few years to over a hundred years. Such times are long compared with the times to load a module or compared with the periods between the loading of two adjacent disposal modules. As a result, the "lags" linked to a gradual operation of a repository zone have little effect on the overall thermal load of a module, and subsequently of a repository zone.

5.3.2.2 Similar thermal behaviour between disposal modules and between disposal cells of the same module

Within a given repository zone, only immediately neighbouring disposal modules interact thermally due to the 50 to 60 m distances between two adjacent disposal modules. Given the spatial organisation of the repository and its gradual operation (and, therfore, gradual thermal loading), each repository module has an identical thermal evolution which repeats itself in the space to form the overall thermal evolution of a repository zone and the surrounding geological medium. This also applies to the disposal cells within the same module.

5.3.2.3 Homogenisation of the thermal load in module level, and subsequently in a repository zone level

Within a repository module, each disposal cell quickly reaches its maximum temperature independants of the other disposal cells. Then, the heat released by the disposal cells combine and lower, but relatively uniform, temperature rises gradually affect the entire module. The temperature field therefore gradually moves from a sum of independent hot spots, corresponding to the disposal cells, to a single hot spot corresponding to the repository module (Figure 5.4.4 and Figure 5.4.5).

Initially, the thermal load affects the disposal cells into which the waste packages are introduced. The maintenance of ventilation in the access drifts during module operation, solely designed to guarantee working conditions compatible with human presence, prevents temperature increases in the access drifts. The homogenisation of the thermal load within a module cannot occur until it has been closed. Similarly, the homogenisation of the thermal load on a repository zone scale only begins once it has been closed.

5.3.2.4 The effect of repository positioning on the transposition zone

The thermal load on a cell, module and repository zone scale is specific to the type of waste and the disposal concept in question. Indeed, the temperature levels, the dates on which maximum temperatures are reached, the kinetics of the temperature rise and fall and the thermal gradients depend on the evolutions in the heat released from the waste packages (and, consequently, the period of storage prior to disposal) and the thermal properties of the disposal cell components. On the other hand, the thermal load of the repository depends little on the position of the repository in the transposition zone. The depth of the repository level varying from 500 to 630 m in the transposition zone (cf. § 3.3.1.1) the initial temperature of the argillites only increases by 2 – 3 °C with depth. In the following, the thermal load is described for a repository located in the reference scenario at a depth of 500 m, corresponding to the position of the underground research laboratory. At this point, the initial temperature of the argillites is 22 °C (cf. § 3.2.4 and (Andra, 2005h, chapitre 8)).

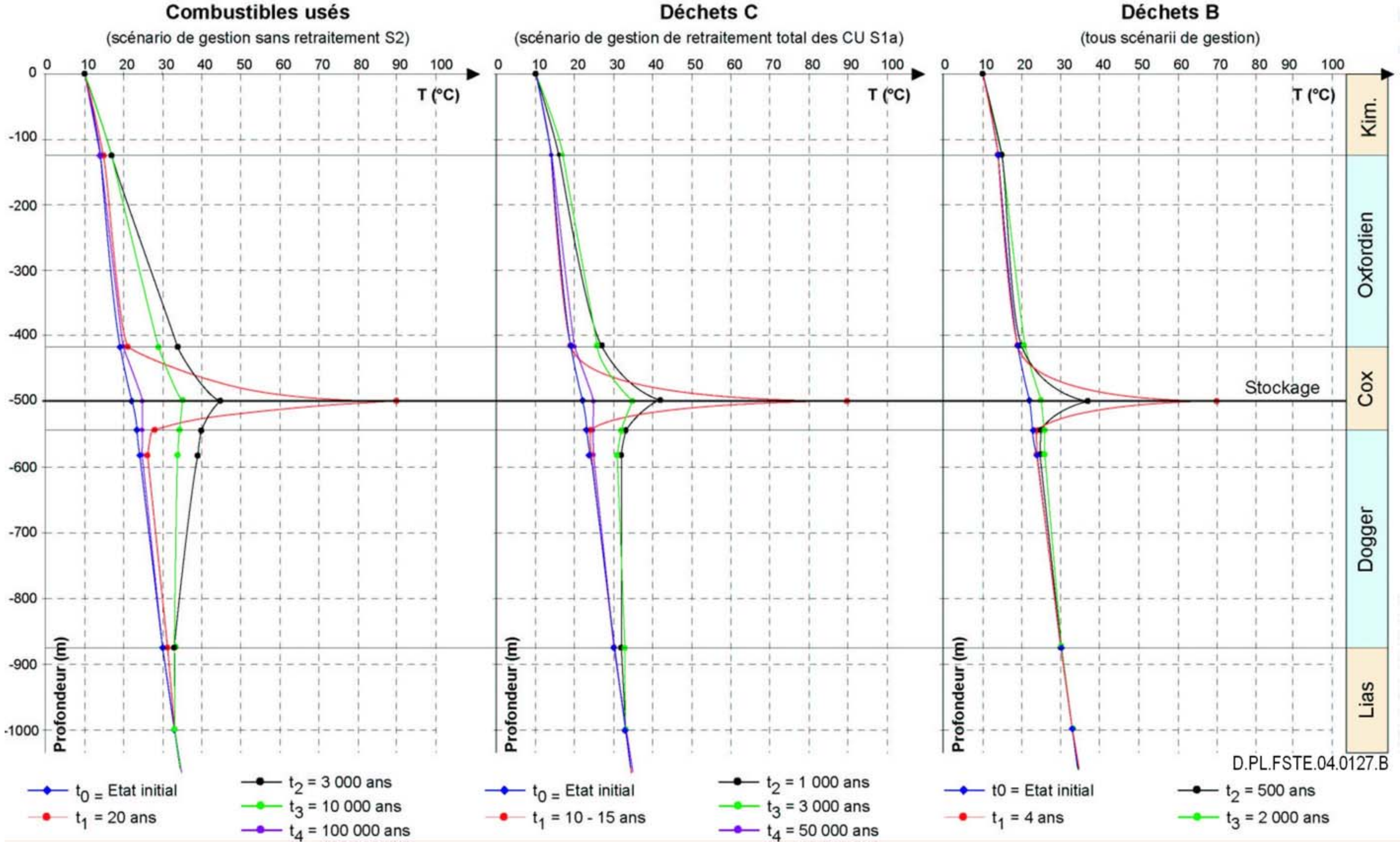

Figure 5.3.1 Thermal load of the various repository zones on a site scale

5.4 Thermal loads of C waste and spent fuel repository zones

As the disposal concept (the number of packages and spacers per cell, the distances between disposal cells and the preliminary storage period for the packages) is adapted to each type of package (and to each concept) and based on compliance with the same criterion of a maximum admissible temperature of 90 °C in clay (argillites and swelling clay – Inset 2.5), the temperature levels reached within and around the C waste and spent fuel disposal cells are similar for the various types of package. Differences are essentially found in the temperature rise times and, more clearly, in the heat discharge times which are longer for spent fuels than for C waste.

The number of C waste or spent fuel reference packages varies according to the waste management scenario envisaged (Table 2.3.4). The thermal load of C waste zones is evaluated for a scenario involving full reprocessing of spent UOX and MOX fuel (scenario S1a) where the number of C waste reference packages is maximal. The thermal load of spent fuel zones is evaluated for a scenario with no spent fuel reprocessing (scenario S2) and with direct disposal of spent UOX and MOX fuel.

5.4.1 On a disposal cell scale

The 90 °C maximum temperature at the lining/argillite interface is reached around 10-15 years after emplacing the packages in the C waste disposal cells. In the spent fuel disposal cells, this maximum is reached a little later (20 years after emplacing the packages) at the lining/engineered swelling clay barrier interface.

The maximum temperatures in the various disposal cell components, which decrease with distance from the packages, are reached after a few tens of years near to the packages and a hundred or two hundred years at the periphery of the disposal cells.

The temperature of the argillites half-way between two disposal cells does not exceed 60-65 °C. This maximum is reached after a period of 30-50 years for C waste reference packages C1 and C2, 100 years for reference packages C3 and C4, and 100-200 years for spent fuel. The maximum temperature on the inner surface of the disposal cell plug is 70-75 °C and is reached after 15-20 years for C waste and spent fuel type CU1 and 50-100 years for spent fuel type CU2. It is just 50-55 °C on the outer surface of the disposal cell plug, reached after 50-100 years for C waste and 150-200 years for spent fuel (Figure 5.4.1 and Figure 5.4.2).

The core temperature of reference packages C3 or C4 or spent fuel packages drops below 50 °C after 1,000-1,500 years. For C waste reference packages C0 and C1/C2, the package core temperature returns to 50 °C after 150 and 650 years respectively.

These changes in temperature over time and the dates when maximum temperatures are reached in the various components of the C waste disposal cells and spent fuel disposal cells are consistent with the evaluations made with similar concepts for a repository in the Opalinus clay studied by NAGRA (Johnson *et al.*, 2002).

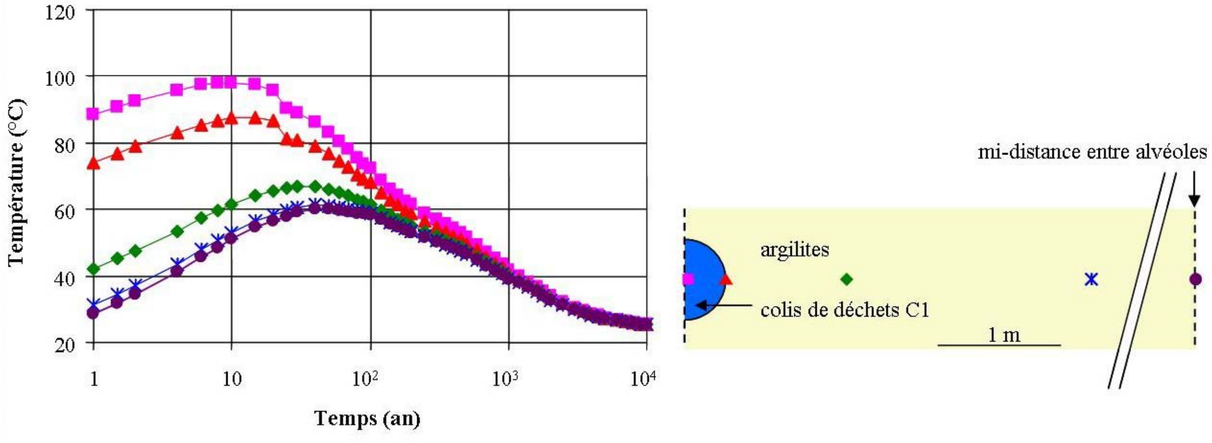

Figure 5.4.1 *Temperature evolution in and around a C1 waste disposal cell emplaced in a repository after a 60-year storage period*

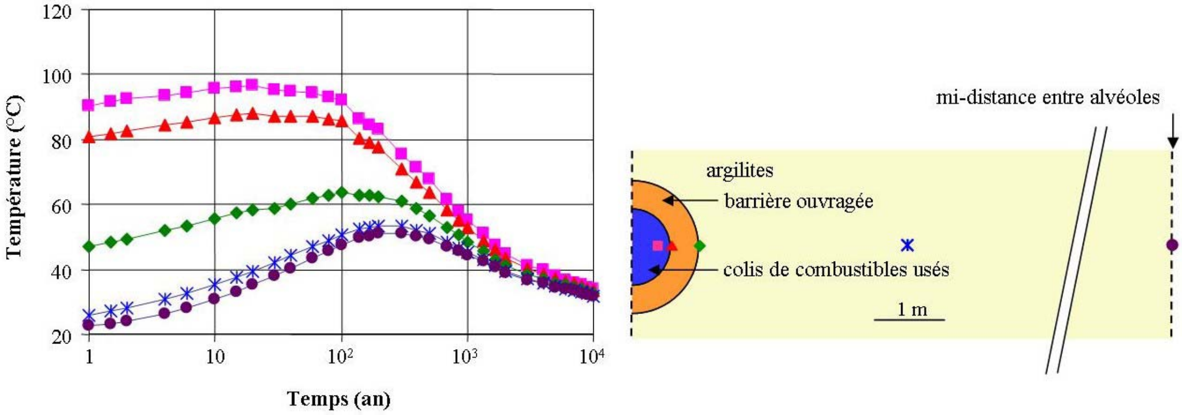

Figure 5.4.2 *Temperature evolution in and around a CU2 spent fuel disposal cell emplaced in a repository after a 90-year storage period*

5.4.2 On a repository module scale

Thermal interaction between the disposal cells within the same module and between two adjacent disposal modules becomes significant after a few tens of years for C waste zones and a few hundred years for spent fuel zones.

Temperature homogenisation times are also longer for spent fuel than for C waste: a uniform temperature of the order of 45-50 °C is reached after 1,000 years within a C waste module. Within a spent fuel module, it is only attained after some 3,000 years. Temperature homogenisation and cooling are quicker at the module accommodating reference packages C0 which release less heat than the other C waste reference packages (Figure 5.4.4 and Figure 5.4.5).

The maximum temperature reached in the access drifts is 50-55 °C. It is reached after 50 to 100 years for C waste and after 200 years for spent fuel, assuming that the access drifts are quickly backfilled once the packages have been emplaced in the disposal cells (Figure 5.4.3). Depending on the choices made in terms of the reversible management of the repository, the drifts may remain open over longer periods. In this case, ventilation prevents the air temperature from rising in the drifts and the temperatures reached in immediate proximity to the drifts are lower.

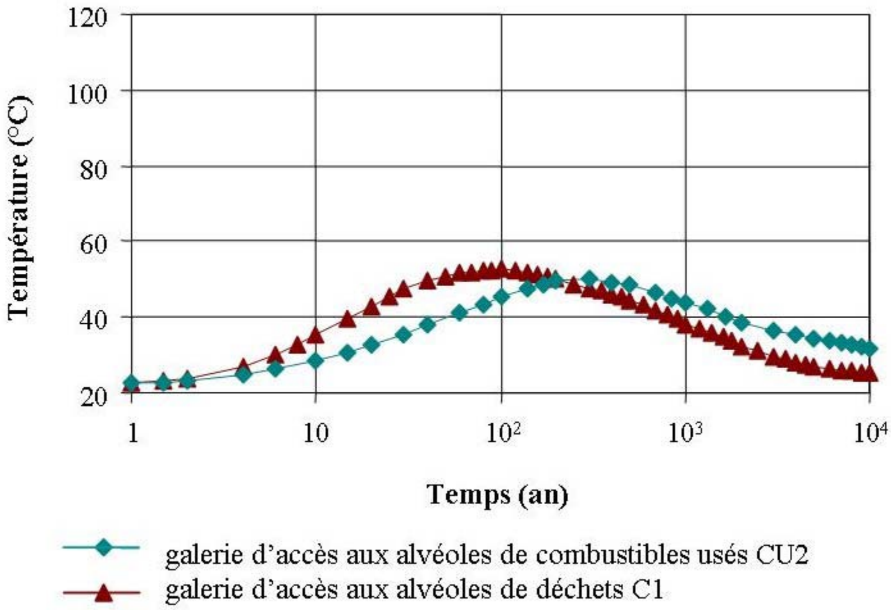

Figure 5.4.3 *Temperature evolution in the centre of the access drifts to CU2 spent fuel disposal cells (90-year storage period) and to C1 waste disposal cells (60-year storage period) assuming rapid backfilling of the access drifts (30 years after package emplacement)*

5.4.3 On a repository zone scale

On a repository zone scale, a uniform temperature of the order of 30-35 °C is reached after 3,000 years for C waste and 10,000 years for spent fuel. The connecting drifts where the zone seals are located are subjected to a maximum temperature of the order of 30-35 °C (after 700 years for C waste and 1,500-2,000 years for spent fuel). At a distance of 250 m from the various repository zones, the temperature rise is no more than a few degrees Celsius (Figure 5.4.4 and Figure 5.4.5).

5.4.4 On a site scale

The entire thickness of the Callovo-Oxfordian layer straight above the repository zones rises in temperature following the emplacement of spent fuel and C waste packages. The maximum temperatures are reached within the repository zones (the maximum temperature of 90 °C being reached at the wall of the C waste disposal cells and in the engineered barrier of the spent fuel disposal cells). At the bottom of the Callovo-Oxfordian formation, the temperature reaches a maximum of 45 °C after around 500 years (equivalent to a temperature rise of 22 °C). At the top of the Callovo-Oxfordian formation, the maximum temperature of 35 °C is reached after around 1,000 years (equivalent to a temperature rise of 16 °C). At the calcareous Oxfordian/Kimmeridgian interface, the maximum temperature is 20 °C (a temperature rise of 5 °C). The repository does not cause any significant increase in temperature at the ground surface (Figure 5.3.1).

After 10,000 years, the temperature rise within the Callovo-Oxfordian layer straight above the repository zones is relatively uniform and does not exceed 10 °C. The return to the initial geothermal field (± 5 °C) occurs after some 50,000 years for C waste zones and 100,000 years for spent fuel zones.

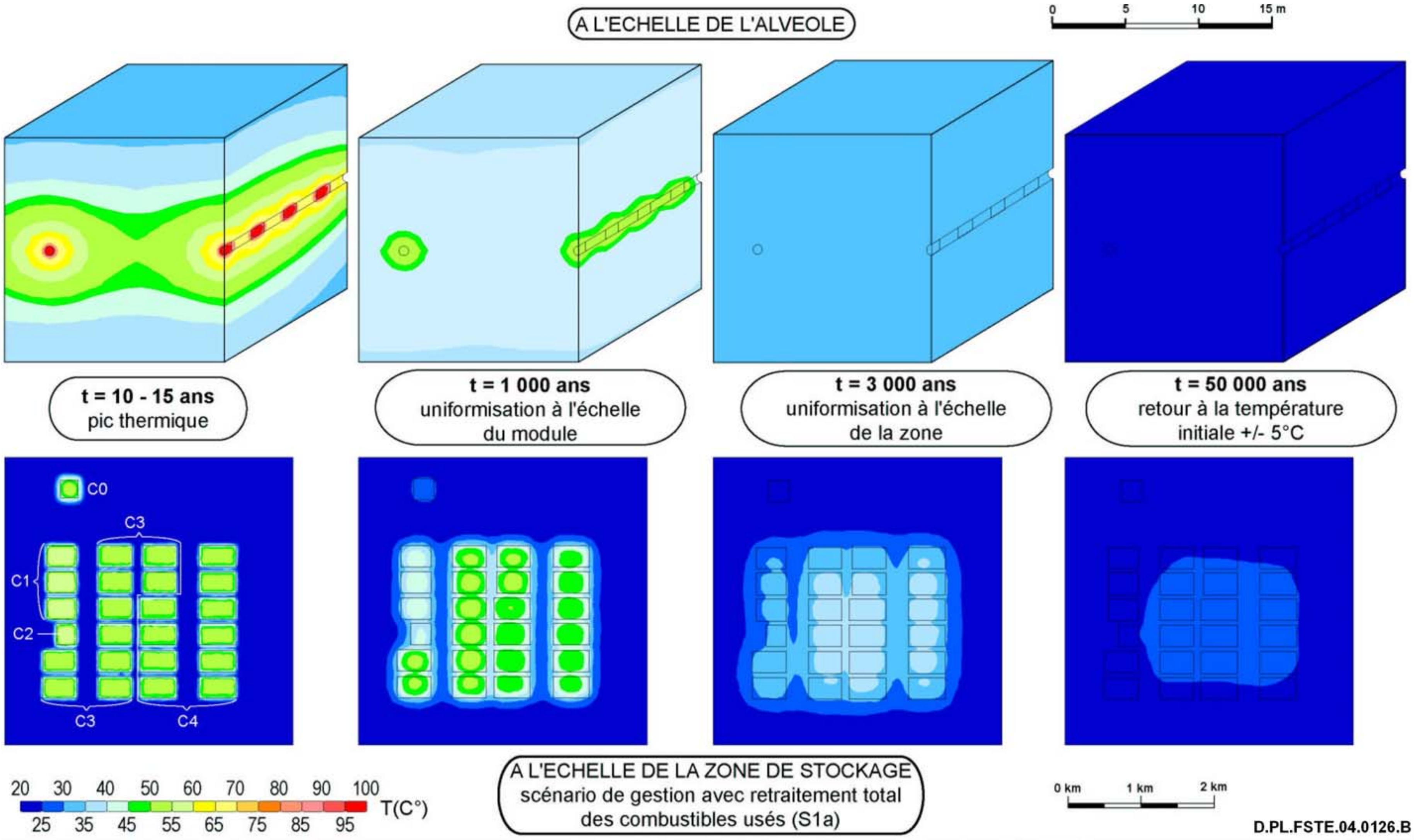

Figure 5.4.4 *Representation of the thermal load of C waste repository zones at various times (scenario S1a – total reprocessing of spent UOX and MOX fuels)*

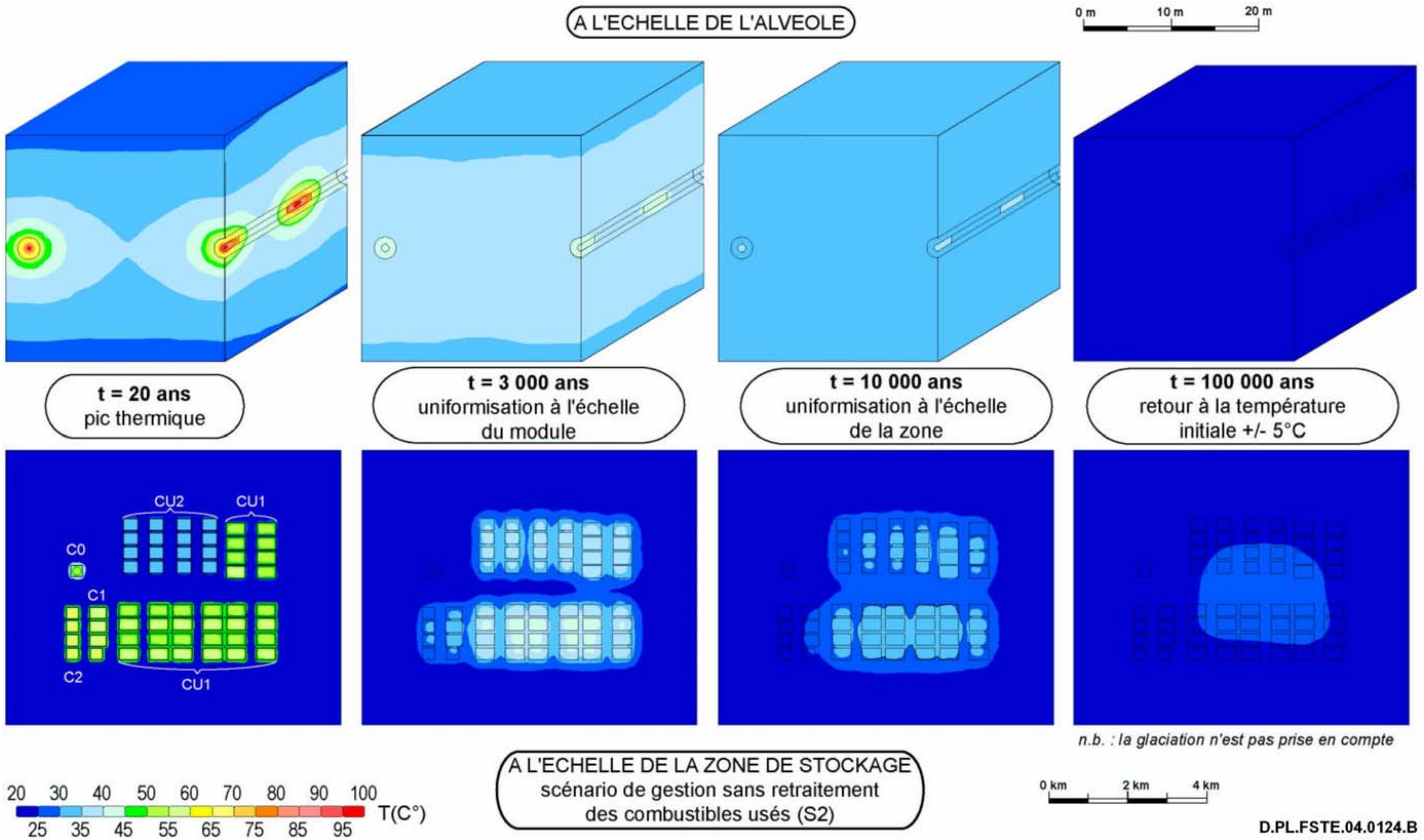

Figure 5.4.5 *Representation of the thermal load of spent fuel repository zones at various times (scenario S2 with direct disposal of spent UOX and MOX fuels)*

5.5 Thermal load of the B waste repository zone

Owing to the fact that less heat is released by B waste, the temperature levels are lower and characteristic thermal load times shorter than for C waste and spent fuels.

From the point of view of distribution of the various B waste reference packages, the disposal cells containing mainly exothermic waste are grouped together into a sub-zone of the B waste repository zone. The disposal cells containing bituminised, non-exothermic or slightly exothermic waste are grouped together in another sub-zone at a distance of around 100 meters from the one with cells containing exothermic waste disposal (Figure 5.5.3).

The B waste thermal load presented assumes that the disposal cells are closed immediately, i.e. without a period of ventilation following emplacement of the waste packages. The consequence of ventilating these disposal cells for a few years (or a few tens of years) is lower disposal cell components and near-field argillites temperatures (cf. § 5.2.2.2). By way of an illustration, the thermal load of a disposal cell containing reference packages B5.2 with a ventilation period of ten years following emplacement in the repository is also presented.

As far as a disposal cell containing reference packages B5.2 – the most exothermic B waste – is concerned, in the absence of disposal cell ventilation, the maximum temperature is reached in the concrete lining during the first years following package emplacement (60 °C). The disposal cell wall argillites are subjected to a maximum temperature of the order of 50 °C (around ten years after package emplacement). The homogenisation of the temperature on a disposal cell scale is achieved around 500 years after package emplacement (temperature less than 30 °C) (Figure 5.5.1).

When ventilation is maintained in the disposal cell (air flow rate of 3 $m^3.s^{-1}$), the ventilation air removes 80 to 90 % of the heat released by the packages. At the centre of the cell, the maximum temperature is also reached during the first years following package emplacement but does not exceed 40 °C. The temperature reached in the disposal cell wall argillites is then lower than 35 °C. Once the ventilation has been stopped, the temperature at the centre of the disposal cell increases to 55 °C, the disposal cell wall argillites reach a maximum temperature of approximately 45 °C. Disposal cell ventilation for around ten years therefore results in a maximum temperature 15 °C lower at the centre of the disposal cell and 5 °C lower in the disposal cell wall argillites. The temperatures of the various disposal cell components after reaching the maxima are slightly higher (approximately 5 °C) than those evaluated without a ventilation period (Figure 5.5.2).

Around a disposal cell containing bituminised waste packages (reference packages B2), the temperature remains below 25 °C irrespective of the point considered in and around the disposal cell (corresponding to a temperature rise of less than 3 °C). At the centre of the cell, the peak temperature is reached three or four years after package emplacement. Elsewhere, this is not reached until after a period of 700 years and is due to the neighbouring disposal cells. The influence of the neighbouring disposal cells of reference packages B3 is felt after 100 years and the resulting additional temperature increase (3 °C at most) occurs in the long term and, therefore, after the thermal peak (Figure 5.5.1). The C waste and spent fuel repository zones have a later influence (over 10,000 years) and the resulting temperature increase is 1 to 2 °C.

Due to splitting B waste into two sub-zones, the thermal load is specific to each sub-zone. The temperature within the bituminised waste sub-zone only increases by a few degrees and remains homogeneous at around 25 °C. The temperature within the exothermic waste sub-zone homogenises after around 2,000 years at 25 °C (Figure 5.5.3).

The temperature of the Callovo-Oxfordian layer straight above the B waste repository zone (50 °C maximum in the immediate vicinity of the disposal cells) rises by 2 °C at most at the bottom and top of the Callovo-Oxfordian formation (after 1,000 and 1,700 years respectively). The return to the initial geothermal field (±5 °C) occurs after 2,000 years (Figure 5.3.1).

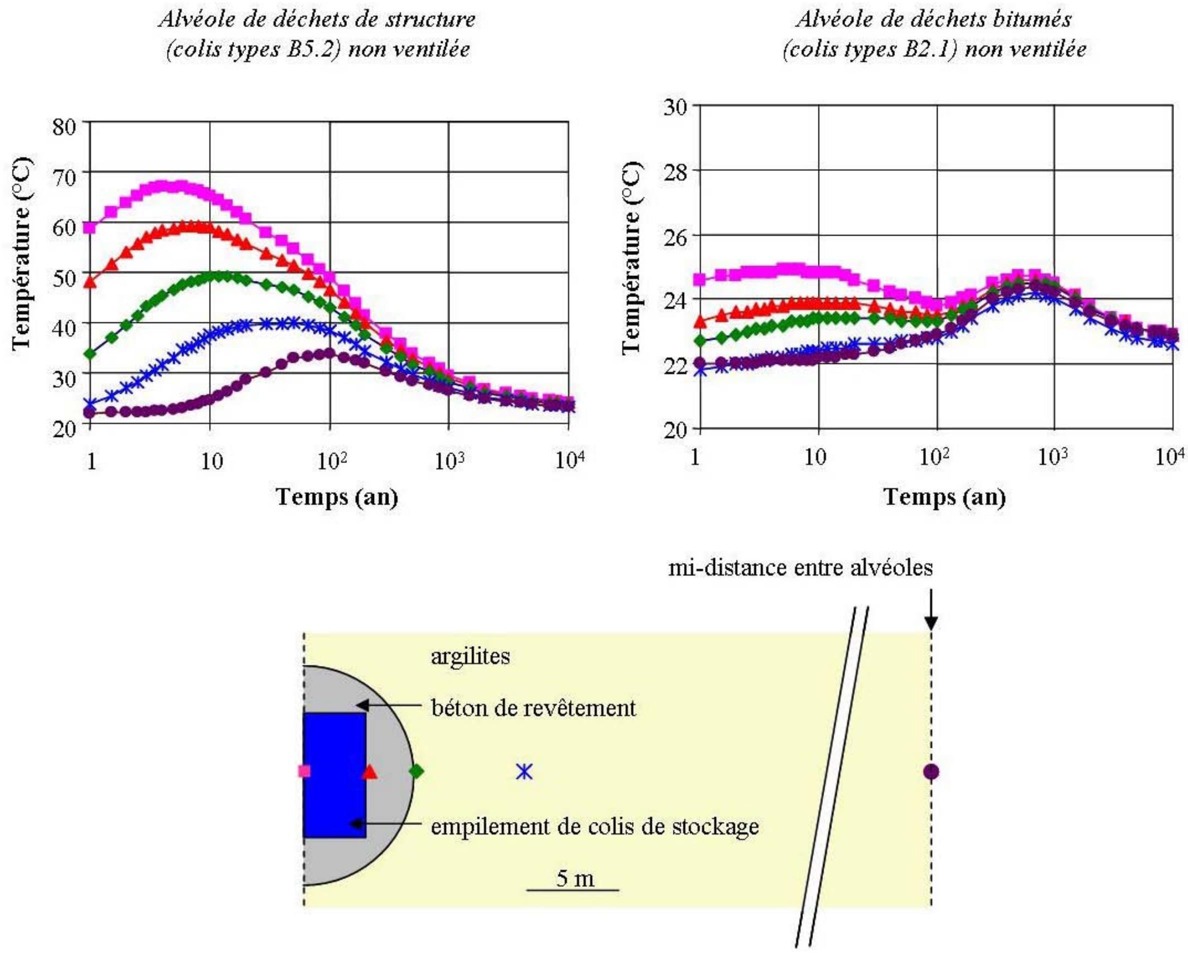

Figure 5.5.1 *Temperature evolution in and around a disposal cell of cladding waste (reference packages B5.2 emplaced in the repository after a ten-year storage period) and a disposal cell of bituminised waste (reference packages B2.1 emplaced in the repository after a one-year storage period) with no ventilation period following package emplacement*

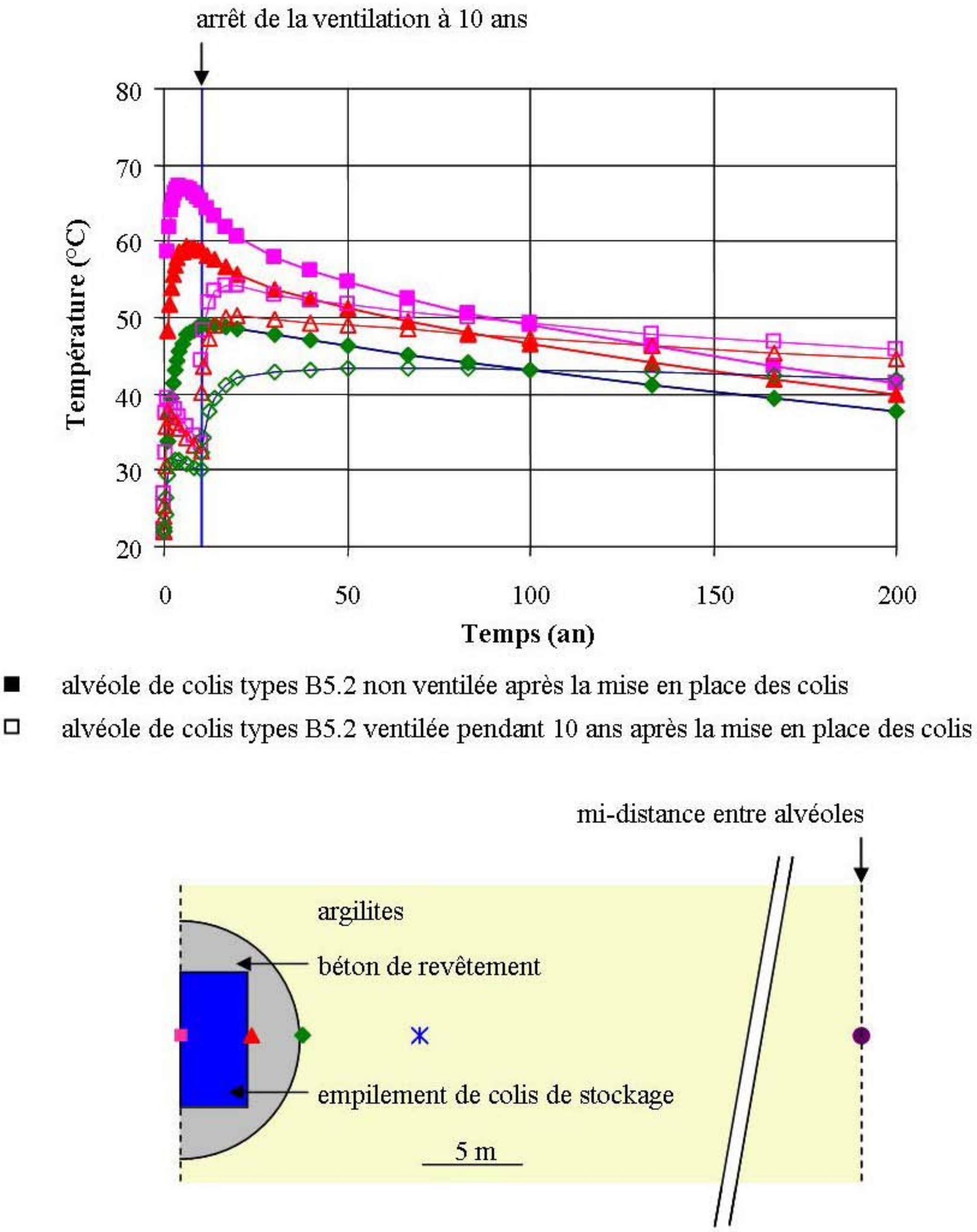

Figure 5.5.2 *Temperature evolution in and around a cladding waste disposal cell (reference packages B5.2 emplaced in a repository after a ten-year storage period) with no ventilation period following package emplacement and with ventilation maintained for ten years*

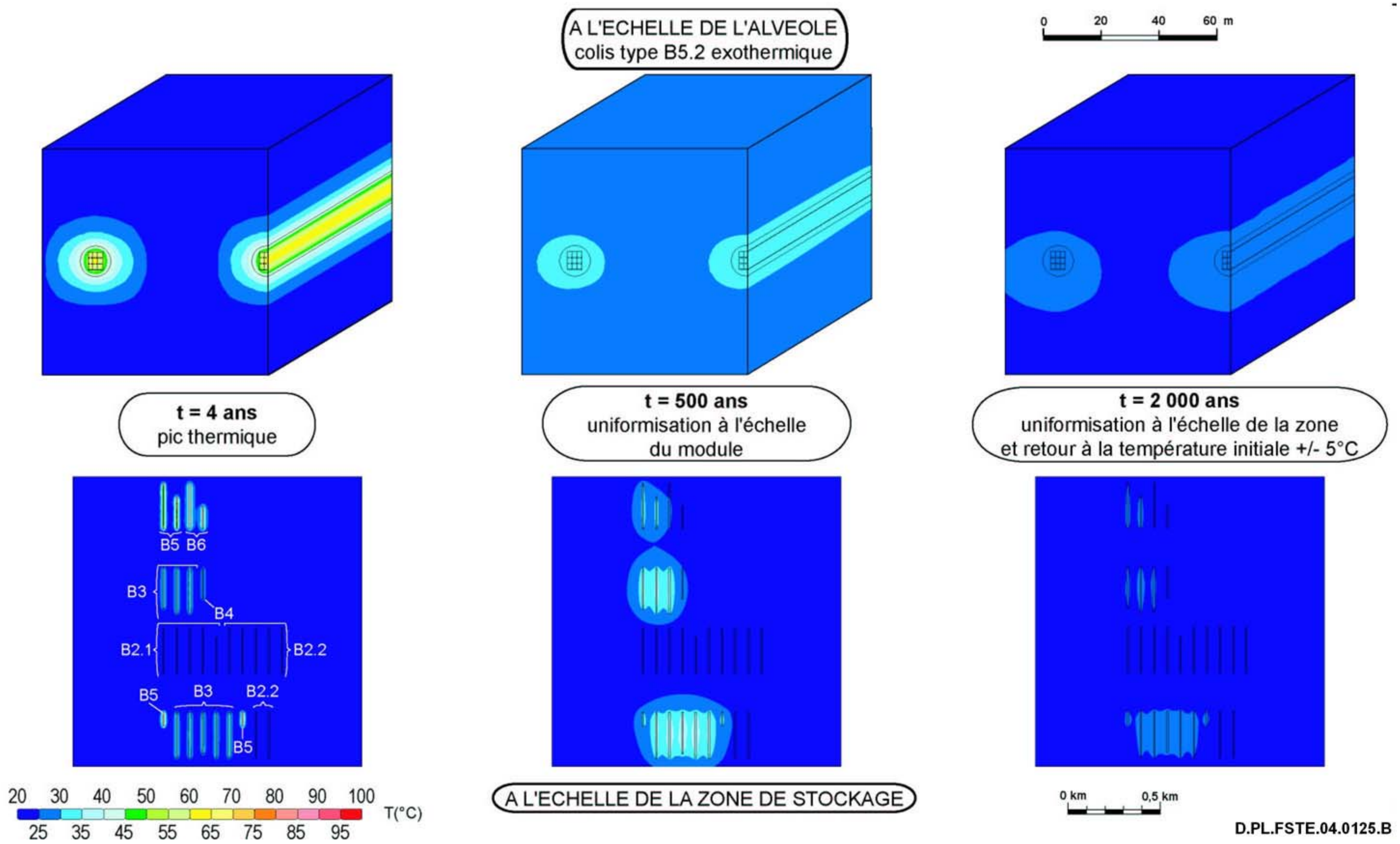

Figure 5.5.3 *Representation of the thermal load of the B waste repository zone at various times under the assumption that the disposal cells are closed immediately after emplacing the packages*

5.6 Summary of the thermal load of the repository

A few elements of the thermal evolution affecting the repository and the repository zones can be identified with a view to the descriptions of hydraulic, chemical and mechanical evolutions and, ultimately, the release and migration of radionuclides (Table 5.6.1 and Figure 5.6.1).

5.6.1 Thermal independence of the repository zones

From a thermal viewpoint, the various repository zones (250 m apart) are (quasi-)independent. Owing to the fact that the heat given off by waste packages decreases over time, the thermal effect of the various repository zones is negligible beyond a distance of 100 to 250 m, both in a vertical direction (towards the surrounding formations) and in a horizontal direction (mid-plane of the Callovo-Oxfordian layer where the various repository zones would be located). The thermal load of the repository appears as a sum of the thermal loads centred on the various repository zones and affecting each of the geological medium volumes centred on these zones.

5.6.2 Maximum temperatures reached in the short term in the disposal cells

Maximum temperatures are reached within the disposal cells. The times required to reach these temperatures are short: a few years for the most exothermic B waste (60 °C) and from 10 to 20 years for C waste and spent fuel (90 °C).

5.6.3 Homogenisation of temperatures in the disposal modules and zones

The temperatures homogeneise on a B waste repository module scale after around 500 years (temperature of the order of 35 °C). On a C waste module scale, they harmonise after approximately 1,000 years and on a spent fuel module scale after around 3,000 years (at similar temperatures for C waste and spent fuel, of the order of 40 to 45 °C).

On a repository zone scale, homogeneisation of temperatures is achieved later: after approximately 2,000 years for B waste (25 °C), 3,000 years for C waste and 10,000 years for spent fuel (at similar temperatures for C waste and spent fuel of the order of 30 to 35 °C).

Moreover, homogeneisations are achieved when the temperatures are decreasing.

5.6.4 Generally moderate thermal gradients

As in the case of the temperature rises, the thermal load is characterised by thermal gradients which change with time.

The maximum thermal gradients are reached inside the C waste disposal cells and spent fuel disposal cells during the first years following waste package emplacement. They are then of the order of a few tens of degrees Celsius per metre ($°C.m^{-1}$). Beyond a hundred years, they are less than ten degree Celsius per metre and then diminish quickly as the temperature homogeneises.

In the Callovo-Oxfordian layer, the maximum temperature gradients are very low (a few $°C.m^{-1}$) and concern the immediate vicinity of the disposal cells (a few decimeters to a few meters) over a period of approximately 100 years.

The temperature gradients in the repository and near field decline rapidly (after approximately 100 years) as the temperatures homogeneises on the scale of the repository zones and the Callovo-Oxfordian layer.

In the vertical plane of the repository zones, from a few meters in the Callovo-Oxfordian layer then in the surrounding formations, the temperature gradients created are low – less than 1 °C.m^{-1} and generally less than 0.1 °C.m^{-1}.

In the horizontal plane, the thermal influence between repository zones remains limited to a few degrees Celsius and only takes effect after approximately one hundred years. The associated horizontal thermal gradients are also low to very low (less than 0.1 °C.m^{-1}).

5.6.5 Limited duration of the thermal load

The return to the initial geothermal field in the repository (taking a temperature deviation with the geothermal field of less than 5 °C as a reference) occurs after around 2,000 years for B waste, 50,000 years for C waste and 100,000 years for spent fuel.

Although this return occurs relatively slowly, the temperatures drop quickly and the majority of the thermal load in the repository and the Callovo-Oxfordian layer only lasts a few thousand years. The temperature at the centre of the C waste disposal cells and the spent fuel disposal cells is of the order of 50 °C after 500 years and 1,000 years respectively. In exothermic B waste disposal cells (B5.2 reference packages), the temperature is less than 35 °C after 500 years (Table 5.6.1).

This duration is minor compared with (i) the hundred thousand years or so for surface climate changes (glacial/interglacial cycles) and (ii) the millions to tens of millions of years (or even more) for the main thermal dependant processes which are the driving the natural evolution of sedimentary formations (mineralogical transformations and transformations of organic matter) (cf. § 3.3.1.3).

Consequently, the phenomenological evolution of the repository and its geological environment occurs essentially under natural geothermal conditions. More particularly, as we shall see in the chemical and mechanical evolutions, the leaktightness periods of C waste over-packs and spent fuel containers relating to corrosion and mechanical behavior (at least 4,000 years and 10,000 years respectively) are such that the thermal load has little or no effect on the release and migration of radionuclides.

5.6.6 Low thermal loads on the Callovo-Oxfordien layer on a macroscopic scale and on the surrounding formations

The temperature rise in the formations surrounding the Callovo-Oxfordian layer remains limited: it is approximately 20 °C at most at the top and bottom of the Callovo-Oxfordian, 5 °C at the top of the calcareous Oxfordian and less than 1 °C for the Kimmeridgian and Calcaire du Barrois (Tithonian) formations.

Consequently, if its limited duration is also taken into account, the thermal load is not a decisive parameter of the macroscopic phenomenological evolutions of the Callovo-Oxfordian layer and the surrounding formations. In particular, the temperature levels (less than 90 °C in the clay materials) and the heating periods (generally less than 10,000 years) do not cause any significant mineralogical transformations to the argillites and swelling clays.

5.6.7 Sensitivity of the analysis with regard to the reversible management process

The evaluation of reversibility is conducted in relation to the temperature conditions liable to be encountered in the repository and in the surrounding geological medium, for an operating period of a hundred to several hundred years.

The temperature conditions in the various components of the repository with respect to possible future retrieval of the waste packages when the repository is operated over a century-long period (reference used in this analysis) are presented in this chapter.

Depending on the choices of management, repository operation over a period of several centuries may be envisaged. This paragraph examines the possible consequences for thermal phenomena. In particular, the effect of extending the duration before closing a repository zone or the duration between the realisation of disposal modules within the same repository zone is considered.

5.6.7.1 Extending the duration before realisation of a zone or a module of a repository zone

The design of the repository into dedicated repository zones several hundred meters apart renders the zones quasi-independent from a thermal aspect. Therefore, any lag in the realisation, operation or closure of a zone compared with another would have no effect on the thermal load of the zones and their surrounding geological medium.

On the other hand, with constant architecture, this would mean a de facto increase in the preliminary storage time for C waste and spent fuel and, consequently, a reduction in the heat rating of the packages on emplacing in the repository. As an initial approximation, the heat ratings of C waste and spent fuel decreasing by a factor of two every thirty years for the first hundred or so years, preliminary storage of the disposal packages extended by 30 years would result in a thermal load of half the size.

Distances between the disposal modules are shorter than the distances between the repository zones but they are still sufficient for the maximum temperature of a module to be independent of the other disposal modules, especially adjacent disposal modules. On the other hand, the homogenisation temperatures of the C waste and spent fuel repository zones, and the time required to reach such homogenisation, depend on interactions between disposal modules. An increase in the time between the realisation of the disposal modules in a repository zone would result in a longer preliminary storage time for the disposal packages. With constant architecture, this would result in a reduction in the homogenisation temperature of the repository zone. These phenomena do not significantly affect the conclusions presented above.

5.6.7.2 Increase in the duration before closing a repository zone or a module of the repository zones for C waste or spent fuel

The C waste repository zones and the spent fuel repository zones are designed so that the thermal load does not depend on drift ventilation. Any increase in the duration before the closure of a module or a repository zone would therefore have no effect on the thermal load in the disposal cells or the neighbouring geological medium. On the other hand, it would lead to lower backfill and seal temperatures.

5.6.7.3 Increase in the duration before closure of a B waste cell

Ventilating a B waste disposal cell removes a large part of the heat released by the packages and therefore plays an important role in the thermal load in the disposal cell and the surrounding geological medium. Any increase in the duration before closure of a B waste disposal cell while maintaining ventilation reduces this thermal load.

The decrease in the heat rating of the most exothermic B waste packages is particularly significant during the first hundred years after waste conditioning. For example, it is reduced by a factor of four to seven between ten years and several hundred years for reference packages B5; beyond this, reduction is slower. Consequently, an increase of several tens of years in the duration before closure of an exothermic B waste disposal cell would significantly lower the thermal load of this cell, reducing it to within a few degrees Celsius of the thermal load of a disposal cell for slightly exothermic B waste packages such as reference packages B2.

Consequently, the thermal model remains generally valid for longer opening periods. Their main effect would be to lower the thermal load to a greater or lesser extent, further reinforcing the general conclusions on its limited impact.

Table 5.6.1 Thermal load of the various repository zones (repository located at a depth of 500 m)

			B waste zone	**C waste zones (scenario S1a – full reprocessing of spent UOX and MOX fuels)**	**Spent fuel zones (scenario S2 – direct disposal of spent UOX and MOX fuels)**
Thermal peak (temperature and date)			*Example of the exothermic cladding waste cell reference packages B5.2:* T_{max}= 60 °C after 4 years (in the concrete lining)	T_{max}= 90 °C after 10-15 years (at the lining/argillites interface)	T_{max}= 90 °C after 20 years (at the lining/engineered barrier interface)
			T_{max}= 50 °C after approx 10 years (in the disposal cell wall argillites)		T_{max}= 70 °C after 20-150 years (at the engineered barrier/argillites interface)
Thermal homogenisation (temperature and date)	***On a repository scale***	cell	$T_{500years}$ = 35 °C (reference packages B5.2)	$T_{500years}$ = 45 – 55 °C	$T_{1,000years}$ = 45 – 50 °C
		module	(same as cell)	$T_{1,000years}$ = 40 – 45 °C	$T_{3,000years}$ = 40 – 45 °C
		zone	$T_{2,000years}$ = 25 °C	$T_{3,000years}$ = 30 – 35 °C	$T_{10,000years}$ = 30 – 35 °C
	On a Callovo-Oxfordian scale	top	T_{max}= 21 °C after 1,700 years $T_{10,000\ years}$ = 20 °C	T_{max}= 35 °C after 700 – 1,000 years $T_{10,000\ years}$ = 27 °C	T_{max}= 35 °C after 1,000 years $T_{10,000\ years}$ = 30 °C
		wall	T_{max}= 25 °C after 1,000 years $T_{10,000\ years}$ = 24 °C	T_{max}= 45 °C after 500 years $T_{10,000\ years}$ = 31 °C	T_{max}= 45 °C after 500 years $T_{10,000\ years}$ = 34 °C
Duration of the thermal phase	$\Delta T \leq 10$ °C*		700 years	5,000 years	10,000 years
	$\Delta T \leq 5$ °C**		2,000 years	50,000 years	100,000 years

Definition criterion :* definition criterion: temperature within the repository zone ≤ initial geothermal temperature + 10 °C

** definition criterion: temperature within the repository zone ≤ initial geothermal temperature + 5 °C

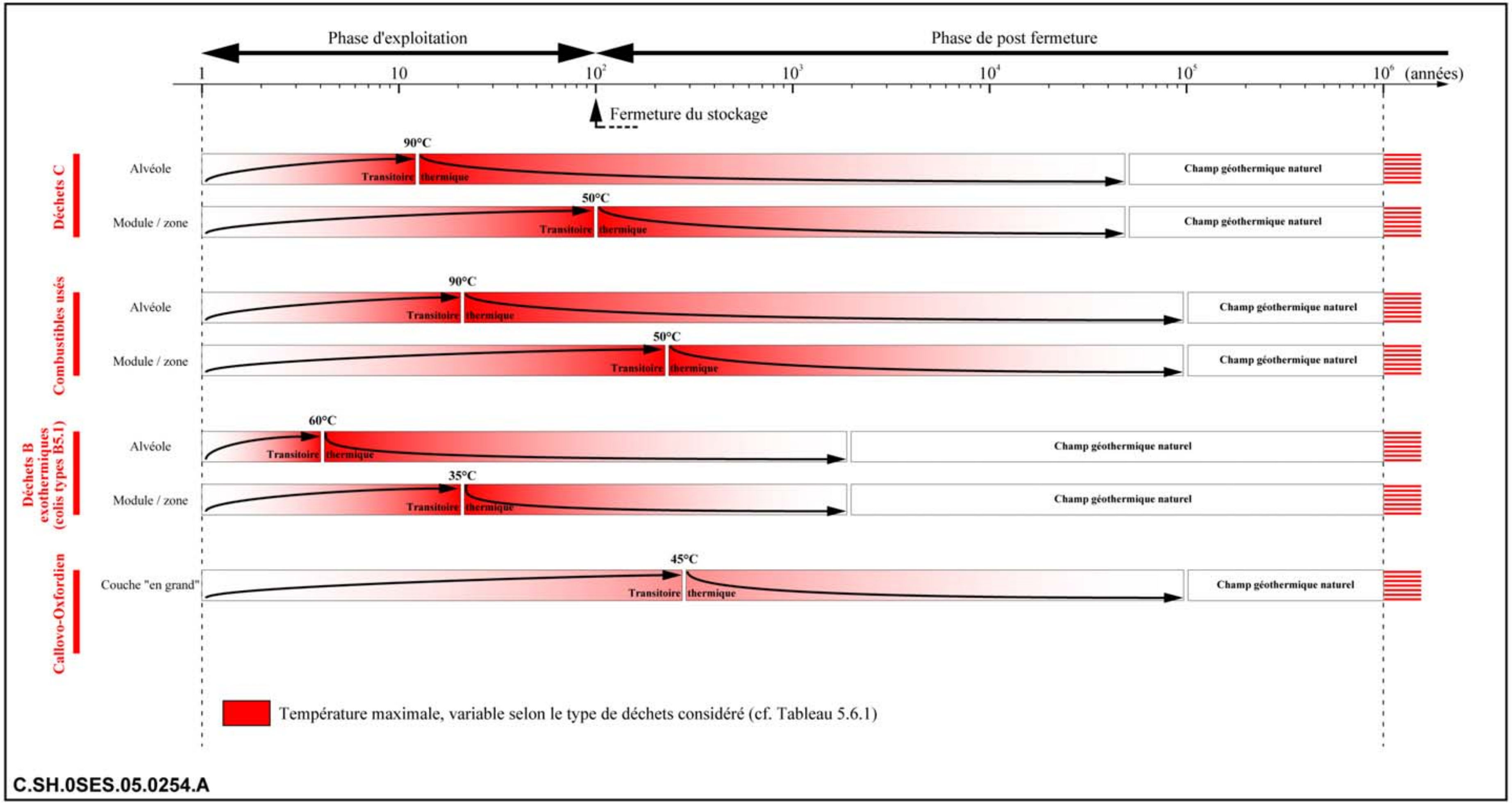

Figure 5.6.1 *Time chart of the thermal load in the various repository zones and the Callovo-Oxfordian layer on a macroscopic scale (on the basis of the conventional 100-year repository creation/operation/closure time chart)*

6

Flow and transfer in solution and as gas

6.1 Introduction 211

6.2 The hydraulic behaviour of the surrounding formations under the effect of the repository 217

6.3 The hydraulic behaviour of the Callovo-Oxfordian under the effect of the repository 223

6.4 Summary on flows and the transfer in dissolved and gaseous form 263

6.1 Introduction

6.1.1 The implications of water flows on other phenomena

The presence of water, its chemical composition and its circulation in the repository and the surrounding environment have major consequences on the other processes that come into play during the phenomenological evolution.

- From a chemical perspective, water flows determine the nature as well as spatial and time limits of reactions. This is particularly true of metal container corrosion, chemical attack of concrete, dissolution of glass matrix or spent fuel and the chemical interactions between the repository materials and the Callovo-Oxfordian layer, such as alkaline disturbance caused by concrete structures.
- They take part in the mechanical evolution of the repository during the operating and observation periods followed by the post-closure period by virtue of their effects on the chemical processes. This is particularly true of concrete structures, such as the B waste disposal cells, whose mechanical properties change as the concrete degrades chemically.
- In the final analysis they determine the release of radionuclides by the waste packages, and their transfer from the waste packages to the biosphere, through the repository, the Callovo-Oxfordian layer and finally the surrounding formations.

6.1.2 The driving forces behind water flow evolution

The geological formations are at hydraulic equilibrium prior to construction of the repository. Starting from that current reference state, the hydraulic evolution of the repository and its geological environment is due to:

- the repository itself,
- geodynamic evolution.

The low permeability and transmissivity coefficients of the Callovo-Oxfordian are mainly responsible for determining the kinetics and durations of the hydraulic processes. The repository construction and operating periods, the thermal, chemical and lastly mechanical processes intervene to a lesser extent. The repository makes its effects on the water flows felt for an overall timescale of the order of a hundred millenia.

Geodynamic evolution and its effects layers extend throughout one million years, the period of interest. They mainly involve the surrounding, primarily the overlying formations, whereas the hydraulic effects of the repository are restricted to the repository and the Callovo-Oxfordian.

6.1.3 Spatial organisation of the processes as determined by the repository design: independence and similarity

The compartmentalised architecture of the repository, its phased management and the conventional century-long operating period contribute to simplifying the organisation and limiting the interactions of repository-related hydraulic disturbances just as they do for thermal processes. For instance this is true for the repository zones that are several hundred meters apart. The distances between disposal modules and between disposal cells inside a repository zone enable hydraulic interactions to take place. However the phasing of module construction leads to similar hydraulic changes between these various structures.

6.1.4 Chapter outline

All the above-mentioned general considerations lead to the following format used for description of the hydraulic evolution of the repository and the surrounding geological medium:

- the first section only covers the hydraulic evolution of the repository and the surrounding geological formations, primarily the Callovo-Oxfordian layer and the overlying rocks surrounding the shafts. Large-scale hydraulic evolution of the geological medium, particularly that of the surrounding formations over the next million years is covered in the section on geodynamic changes;
- the description is firstly made in terms of water flow and gas transfer. Then once the hydraulic framework has been established, solute transport in and around the repository throughout the hydraulic evolution is discussed;
- the evolution of water flows is first considered for the overlying formations surrounding the shafts followed by the repository and the Callovo-Oxfordian;
- in the latter instance, description of the water flows starts at the scale of the repository (disposal modules, zones) and the surrounding Callovo-Oxfordian, further broken down depending on the type of the structure (B, C and spent fuel waste disposal cells);
- the hydraulic processes are presented in chronological order making the overall distinction between:
    - the hydraulic head drop and desaturation of the geological formations surrounding the repository structures during the operating phase,
    - the production of gas and the resaturation of the repository, and
    - the return to a new state of saturated hydraulic equilibrium in the repository and the Callovo-Oxfordian.

The effects of the thermal, chemical and mechanical processes on the water flows are discussed whenever required indicating their relevant time and space scales. Two processes, described further down in the volume are particularly mentioned.

- Mechanical: the formation of a damaged zone in the argillites surrounding the repository structures (known as "EDZ") (cf. § 8.2) with initially higher permeability levels than those of the pristine argillites. Its evolution over time contributes to the hydraulic evolution both in terms of water flows and gas transfers in and around the repository and in terms of solute transport.
- Chemical: the corrosion of the repository’s metal components leads to the formation of hydrogen. The descriptions presented in *Inset 6.1* enable us to get a perception of the volumes of hydrogen produced and the characteristic timescales of the phenomenon.

For the purposes of this chronological description, distinction is made between the shafts, drifts and B waste disposal cells that are ventilated during the operating phase and the C disposal cells and spent fuel disposal cells that have no ventilation.

The description of solute transport in and around the repository during the hydraulic evolution follows the same general chronology as given for the water flow and gas transfer descriptions. In concluding section are singled out the key hydraulic evolution facts that are needed to describe the chemical and mechanical evolutions and finally the analysis of radionuclide release and transfer.

The description of the hydraulic processes that mark the phenomenological evolution of the repository and its geological environment draws on field data produced essentially from the exploratory boreholes on the Meuse/Haute-Marne site. It also results from the numerical modelling that throws light on the spatial and temporal scales that characterise the processes at work (Inset 6.2).

Inset 6.1 ***Hydrogen production in the repository (1/2)***

Metal corrosion leads to hydrogen formation by water reduction under the anoxic conditions that prevail in the repository. The quantities of gas formed by other processes such as radiolysis of water and organic compounds are always low and amount to less than 10 % of the total production regardless of the scenario chosen for waste estimation.

The metals are mainly found in the disposal cells, in the form of structural components (such as the linings of C waste and spent fuel disposal cells), containers (for example C waste over-packs or the primary containers of many B waste primary packages) or waste itself (for example B5 waste hulls and end caps) This amounts to a mass of several hundreds of thousands of tonnes and a surface of several hundreds of thousands of m^2. These masses and surface areas lead to the production of the hydrogen volumes indicated in the following table.

Magnitude of masses of iron, moles of hydrogen produced and volumes taken up in physical and chemical conditions representative of a repository, for a representative disposal cell of the different types of waste (reproduced from (Talandier, 2005)*).*

	Mass of iron (kg)	**Moles of Hydrogen produced**	**Volume of Hydrogen (m^3)***
C0 cell	50,000	$1.2\cdot10^6$	600
C1, C2, C3 and C4 cell	28,000	$0.6\cdot10^6$	330
CU1 spent fuel cell	260,000	$6.3\cdot10^6$	3,100
CU2 spent fuel cell	110,000	$2.6\cdot10^6$	1,300
B waste cell	Variable depending on the type of B waste		
	20,000 – 90,000	$2.5\cdot10^6$ - 10^7	1,400 – 5,000

*: estimate of volumes on the basis of a pressure of 5 MPa and temperature at 30 °C.

The production kinetics of hydrogen depends on the surface available for corrosion and on corrosion cinetics, independant of any considerations considering the presence of water or the coupling between water and H_2 transfert.

Given the variety of metal components inside a structure, these kinetics are not constant over time. They depend on the timing at which the components are affected by the phenomenon.

Hydrogen production in the repository (2/2)

The following figure illustrates the evolution of the hydrogen flow over time for a spent fuel cell, obtained on the basis of a corrosion rate of 2-3 Nm.yr^{-1} and assuming that corrosion begins as soon as the disposal cell is closed. From this figure one can observe that

(i) hydrogen production may extend over a period of about 100,000 years,

(ii) about 50 % of the hydrogen is produced during the first 4,000-5,000 years and

(iii) after this initial period, hydrogen production generally decreases by one order of magnitude every 10,000 years.

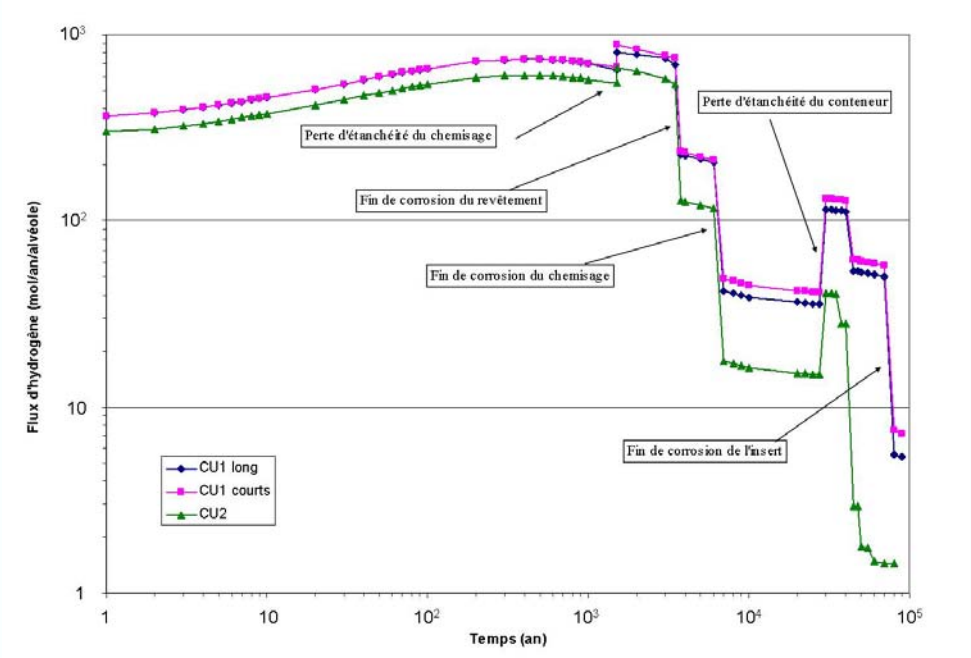

Schematic representation of the evolution of the corrosion-induced H_2 production flux as a function of time inside a spent fuel disposal cell (excerpt from (Talandier, 2005))

The hydrogen production flows presented in the figure above are based on corrosion rates depending only on temperature. Values of corrosion rates mainly correspond to total water saturation conditions on contact with metal components ((Talandier, 2005)) (Inset 7.3).

Inset 6.2 ***Modelling of hydraulic phenomena (1/2)***

General framework

Numerical modelling is a tool traditionally used for the research and exploitation of water or hydrocarbon resources. In the context of the repository feasibility study it is used to assess a) the behaviour of large dimension objects, such as formations of the Meuse/Haute Marne site geological on a regional scale of several tens of kilometers for example, or objects that because of their geometry and/or composition are complex, such as disposal cells, b) evolution at major temporal scales, such as geodynamic evolution whose effects on the hydrogeology of the surrounding formations run to a million years, and c) phenomenologies that tend to be complex, such as coupling between hydraulics and mechanics or coupling between hydraulics and gas generation and transfer.

Examples of modelling

Numerical modelling brings into play specific problem-related computing tools combined with a more or less complex representation of the objects involved. This is illustrated in the following figures relating to the study of two hydraulic processes, one of which refers to the water flows at the scale of the Paris basin up to the Meuse/Haute-Marne sector, the other refers to the resaturation of a repository structure (on the scale of a few tens of meters).

- The following figure represents the 3D geometry adopted for the study of the current equilibrium water flows in the Callovo-Oxfordian and surrounding formations at the regional scale, namely a mesh of several million mesh disposal cells for an object a few kilometers thick and a surface area of about one hundred thousand square kilometers (IFP, 2004).

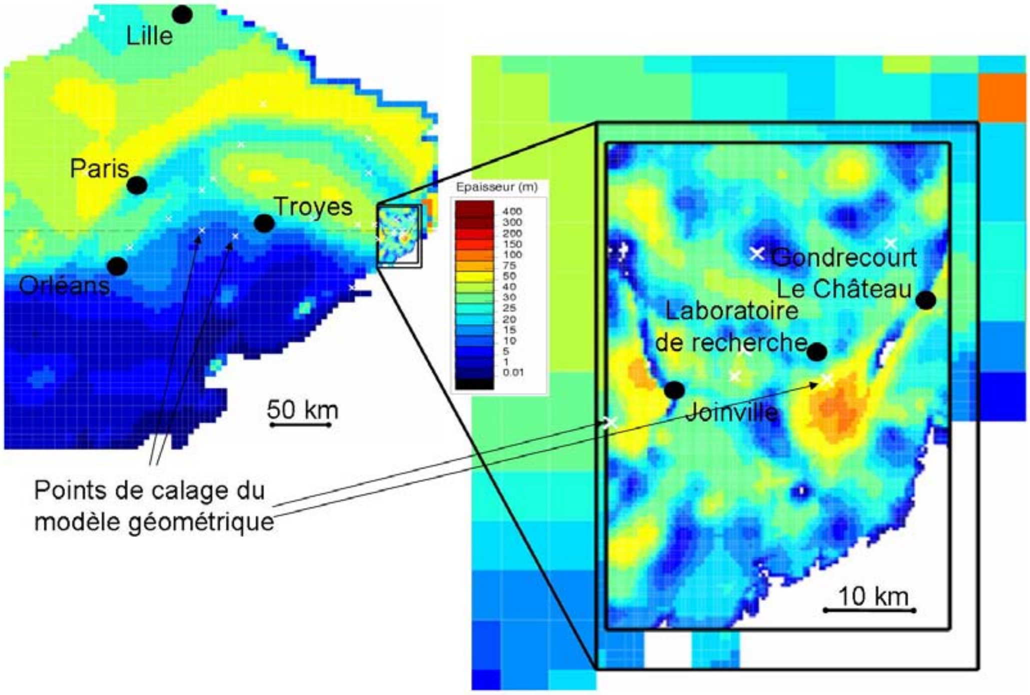

Extract of the meshing used for the numerical estimate of the current water flows, from the scale of the Paris basin to the scale of the Meuse/Haute Marne site: representation of the thickness of the upper Rauracian (from (IFP, 2004))

Modelling of hydraulic phenomena (2/2)

- The following figure represents the 3D mesh of several in tens of meters used for the study of the water flows in and around a B waste disposal cell and its access drift, coupled to corrosion-induced H_2 production. The study covered a time scale of several millennia following the closure of the disposal cell and the “galerie” (Colenco Power Engineering, 2004).

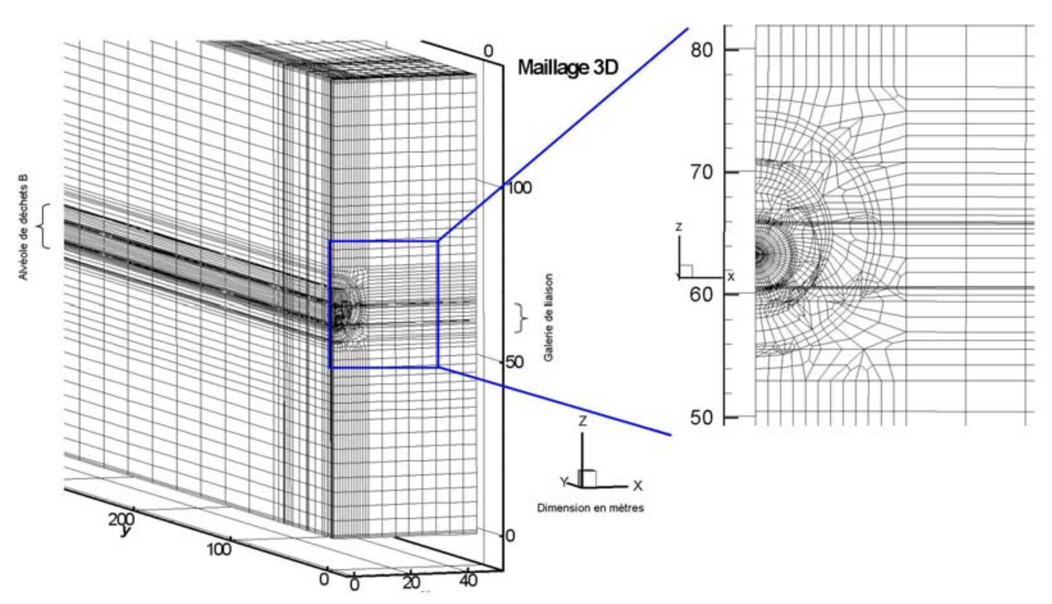

Representation of the mesh used for the numerical estimate of the water and gas flows in a B waste disposal cell (from (Colenco Power Engineering, 2004))

6.2 The hydraulic behaviour of the surrounding formations under the effect of the repository

The hydraulic impact of the repository on the surrounding formations can be disassociated from that of the Callovo-Oxfordian layer because of the repository's general architecture and in particular the very low permeability of the Callovo-Oxfordian.

The arrangement of the overlying surrounding formations is a succession of aquiferous and semi-permeable deposits (Figure 6.2.1). For this reason hydraulic interactions are minor. Their hydraulic behaviour under the effect of the repository depend on their intrinsic characteristics and construction details of the shafts traversing them (impermeability or non-impermeability).

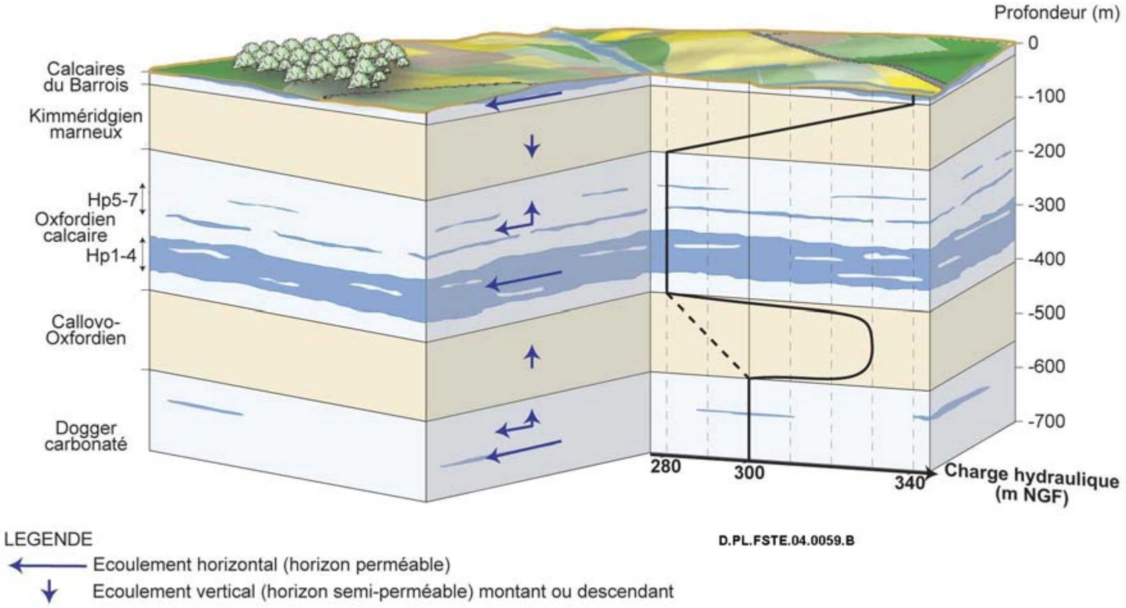

Figure 6.2.1 Diagram showing flow diections and a profile of the initial hydraulic head in the Callovo-Oxfordian and its surrounding rocks

6.2.1 The initial hydraulic head drop

The excavation of shafts leads to an rapid drop in the hydraulic pressures of the geological formations in the immediate periphery of the shafts (commonly known as the "hydraulic head drop"). The shaft wall is instantly vented, that is submitted to a lower pression than the initial hydraulic pressure inside the formations: on the order of some tenths of a MPa[7] in the Kimmeridgian marls and about 5 MPa in the case of the Callovo-Oxfordian argillites. A radial convergent flow from the formation to the shaft wall thus appears immediately in each formation crossed. If the latter is not leak tight, the flow continues until the end of the repository operating period (shaft closure prior to sealing), while at the same time the drop in hydraulic pressure spreads radially inside the formation (Figure 6.2.2). On the basis of this general pattern, hydraulic characteristics specific to each overlying surrounding formation and the design of the shafts crossing them (impermeable or not) lead to specific hydraulic evolutions.

---

[7] The hight of the column of freshwater is commonly used as the unit of pressure in hydrogeology. This volume uses SI units for reasons of consistency with the other phenomenologies, in particular geomechanics. Thus all pressures will be expressed in MPa. As a result of the residual uncertainties surrounding estimated pressure values, one MPa is approximated to a 100-metre column of freshwater. This approximation allows easy conversion between the two units and does not misrepresent the phenomena described.

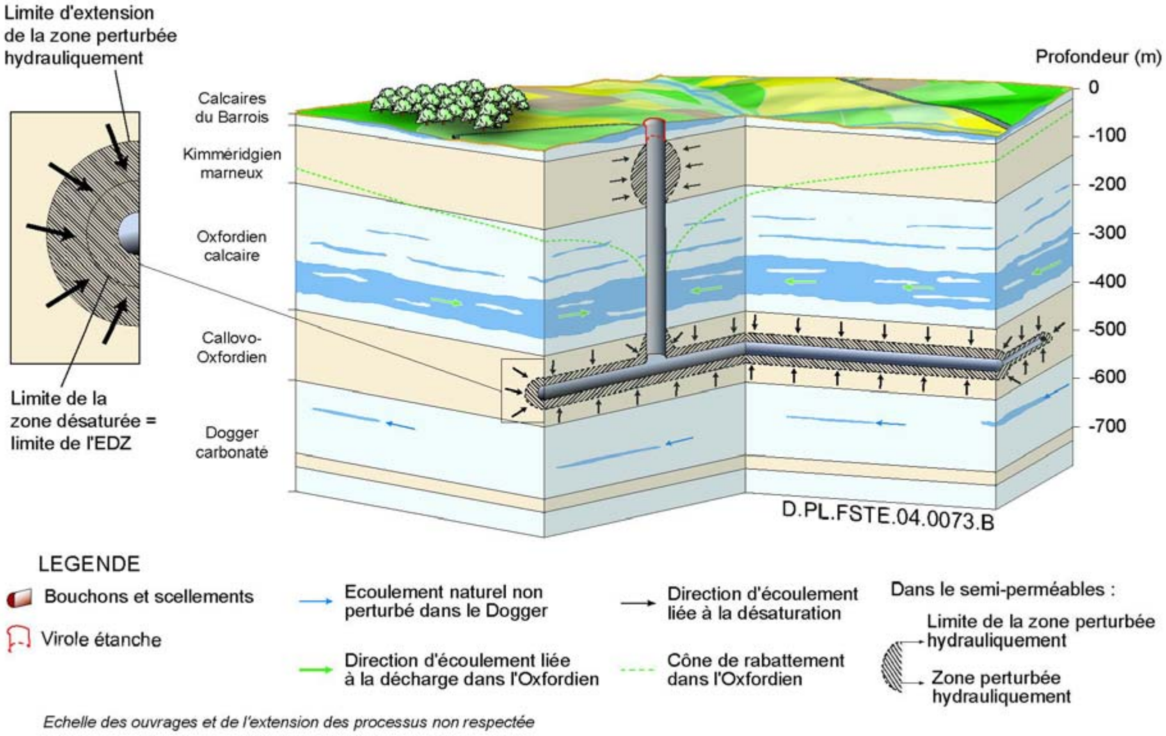

Figure 6.2.2 *Diagram of hydraulic disturbances caused by the repository in the Callovo-Oxfordian and surrounding rocks during the operating phase.*

6.2.2 The Tithonian limestone: rapid return to hydraulic equilibrium

The high permeability of the Tithonian limestones potentially leads to a significant flux of water (Trouiller & Benabderrahmane, 2005) into the shaft. As a consequence, it may be considered to make the shaft walls of the Tithonian limestones impermeable for their entire length (a few tens of meters in the region of the Meuse/Haute-Marne laboratory). Impermeability is achieved using metal flanges. The flanges are inserted before the excavation has had time (a few months at the most) to allow the hydraulic head drop to have reached a significant amplitude (the drop is only a few hundredths of one MPa) and extent (a few tens of meters or a hundred meters at the most). The measure of impermeabilising the shaft walls thus prevents the hydraulic head drop from spreading during the operating phase, so the Tithonian limestones return to their natural initial hydraulic head field around the shaft a few months after flange insertion.

6.2.3 The Kimmeridgian and the carbonated Oxfordian: hydraulic head drop and desaturation

As shaft construction crosses these formations, the shafts will not be impermeabilised. This enables the hydraulic head drop to continue throughout the repository operating phase (Andra, 2005a, situation G_0.4). Desaturation may potentially occur around the periphery of the shafts depending on the permeability of the formation in question.

6.2.3.1 The Kimmeridgian

During the repository operation phase the hydraulic head drop spreads around the shafts to a radial extent on the order of a few hundred meters per century. The low permeability of the Kimmeridgian also limits the interactions of the hydraulic head drop with the overlying Tithonian limestones and the underlying carbonated Oxfordian. In contrast the hydraulic head drop produced by the sinking of the shafts in the carbonated Oxfordian is gradually transmitted upwards and in the space of a few decades affects the hydraulic heads of the Kimmeridgian. It will overlap with the direct hydraulic head drop of the Kimmeridgian. At the end of a century-long operating period, the hydraulic head drop affects a surface area several kilometers in radius. The magnitudes of hydraulic head drop values are a few tenths of a MPa at a hundred or so meters from the shafts and less than one hundredth of one MPa beyond a few hundred meters or so.

The low permeability of the Kimmeridgian marls causes desaturation around the shafts through the effect of air ventilation parallel to the hydraulic head drop. This desaturation, in the same way as the hydraulic head drop, initially spreads slowly outwards to the shaft walls at around one metre per year, then at the rate of a few tens of meters per year after 10 years.

6.2.3.2 The carbonated Oxfordian

The carbonated Oxfordian is made up of alternating horizons with contrasting levels of permeability. Two sets of porous horizons (named Hp1-4 and Hp5-7) which levels of permeability on the order of 10^{-8} m.s^{-1} and of higher magnitude than the rest of the formation (c.f. § 3.3.2.2), have been distinguished.

The existence of lower permeability levels between the two sets of porous horizons implies that the initial hydraulic head drops of each set are independent (Wendling, 2005). The hydraulic head drop also spreads into the less permeable horizons.

The hydraulic head drop in the porous horizons is initially greater in the upper set (Hp5 - Hp7) because it was the first to be crossed by the shafts. Subsequently the hydraulic head drop also increases in the lower set of permeable horizons (Hp1 - Hp4), gradually exceeding the drop created in the upper permeable horizons.

The hydraulic heads even out throughout the carbonated Oxfordian several decades after sinking the shafts at a distance of about a kilometre from the shaft. This is because the permeability contrasts between the permeable and less permeable horizons are too small to maintain significant differences in hydraulic head at these scales of space and time.

The overall rate of water influx into each shaft is several tens of litres per minute immediately after excavation. After a few years it reduces and stabilises at an almost stationary level of a few tens of litres per minute.

In the proposed design the shafts are grouped together in a zone that extends to only about one kilometre in contrast to the distances of hydraulic interaction in the carbonated Oxfordian. Thus after a few months, the hydraulic disturbances related to each of the shafts will influence each other (Figure 6.2.3). After several years, the interactions are so great than the hydraulic head drop a long way from the shafts can be treated the same way as the hydraulic head drop produced by a single central large-diameter shaft (on the order of one hundred meters). The advance of the hydraulic head drop is several kilometers from the shafts after a decade or so. At that time, the hydraulic head drop is in over of 1 MPa in an area of several hundred meters around the shafts. Thereafter the kinetics of migration of the shaft impact zone is curbed by the presence of carbonated Oxfordian outcrops that provide sufficient flow without significant discharge of hydraulic head, as the level of permeability is greater there than when buried. The zone of hydraulic head drop becomes almost stationary after, about thirty years.

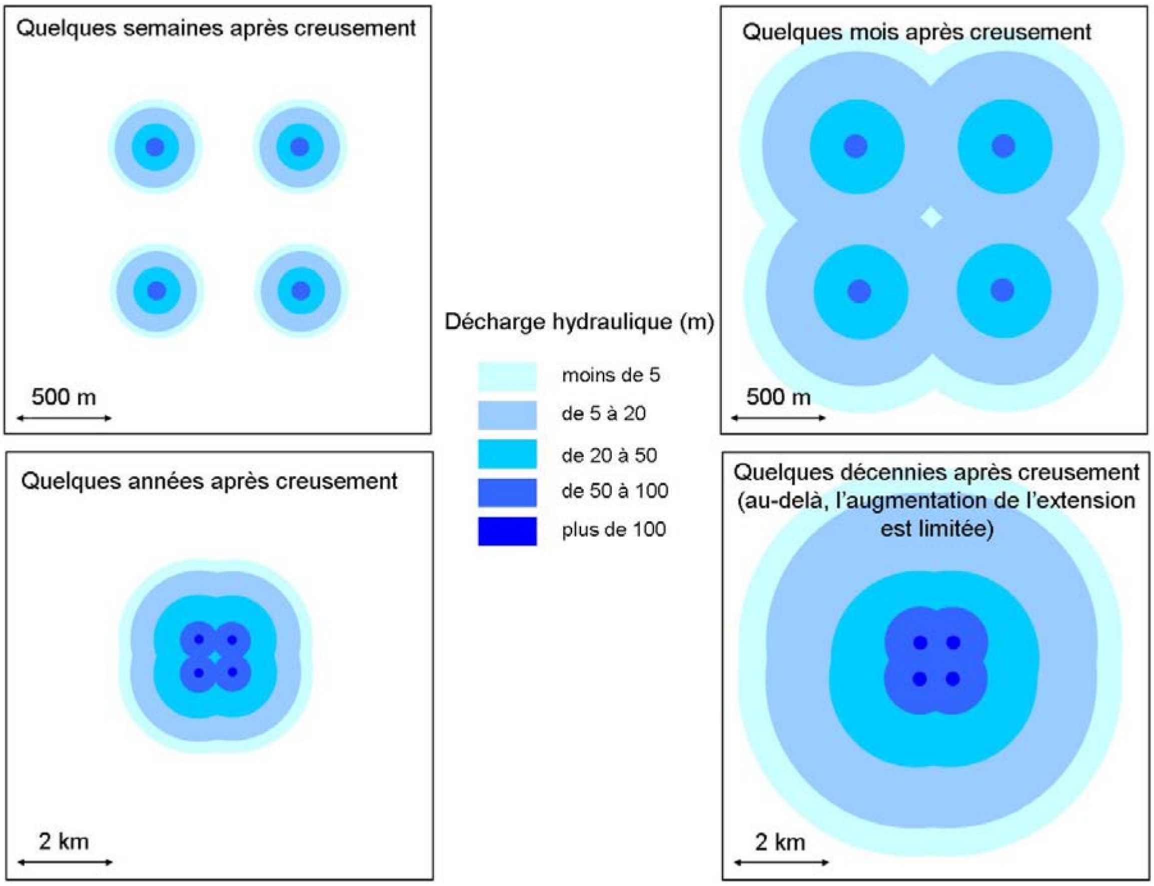

Figure 6.2.3 *Schematic representation of the hydraulic head drop by the shafts created in the Hp1-4 horizon of the carbonated Oxfordian*

The carbonated Oxfordian is part of the hydraulic boundary condition for the top of the Callovo-Oxfordian. Consequently when the shafts are opened, a hydraulic head drop occurs in the Callovo-Oxfordian in relation to the hydraulic head drop in the carbonated Oxfordian. As the permeability levels of the Callovo-Oxfordian are very low, the vertical propagation rate of the hydraulic head drop is very limited in comparison to the horizontal spreading rate within the carbonated Oxfordian. It takes several centuries for the zone of hydraulic head drop to reach the central part of the Callovo-Oxfordian layer and to become superimposed on the repository-related hydraulic head drop. However this superposition phenomenon is only recognizable a few hundred meters around the shafts and thus will not affect the repository zones.

Inset 6.3 ***Notion on the degree of water saturation***

The degree of water saturation is the relative proportion of porosity filled up with water (the degree of saturation may be referred to in the rest of this document by the abbreviation, capital S). In theory it varies between 100 % when the entire pore volume it filled with water, and 0 % when the porous medium is totally dry (moisture-free). The term of non-saturated is used for porous media a degrees of saturation below 100 %.

The degree of water saturation is generally determined on the basis of the dry density of the medium, the mass-related water content (defined as the radio of the mass of water over the mass of solid) and the grain density (density of the solid constituants of the porus medium). These three parameters may be determined by experiment. However clays are multi domain porous environments with complex pore structure and made up of different solids. The uncertainties on water content and grain density, as determined experimentally are so great that this approach can only be seen as an estimate of water saturation.

The degree of water saturation does not consider the distribution of the water within the individual pores nor the thermodynamic nature of the water (free, adsorbed, or structural). It is a macroscopic parameter to be applied delicately in the description of thermal, hydraulic and geochemical behaviour in a porous medium. All these behaviour patterns partly depend on the quantity of water present in the porosity. We talk of a quasi-saturated state when referring to a given behaviour pattern below the theoretical total water saturation (S = 100 %), but with a behaviour nonetheless similar to that at total saturation.

Water flows in clay environments constitute a prime example: for a degree of water saturation above 95-97 %, the hydraulic parameters of the water, primarily permeability and kinetic porosity, are almost identical to those at total saturation. For a degree of saturation below this limit, the water permeability of the medium diminishes progressively up to several orders of magnitude if the degree of saturation drops below 20-30 %.

It is reasonable to adopt a similar almost saturated state for mechanical behaviour. However it is when the degree of saturation is below 80% that the evolution of mechanical properties is particularly influenced.

It is harder to define this notion of quasi-saturated state for chemical behaviour patterns. It depends on the process in question. When considering steel corrosion in non-saturated porous environments and under anoxic conditions a linear increase in corrosion kinetics as a function of water saturation can be applied to a maximum saturation level of 95-97 %. In contrast, in an oxidising environment, bell shaped curve behaviour is observed: the corrosion rate peaks at a saturation degree within the range of 80-90 %. It drops on either side, through lack of water (lower saturation degree) or because of the difficulty of oxygen transfer in the porous medium (higher saturation degrees).

6.2.3.3 The Dogger limestone and underlying surrounding formations

Following construction design, the geological formations underlying the Callovo-Oxfordian do not have shafts or any other repository structure crossing them. The hydraulic head drop in the Callovo-Oxfordian caused by the repository slowly transfers to the Dogger limestone but the clearance distance of about 60 meters between the repository and the top of the Dogger limestone limits its progress over the conventional century-long repository operating phase. Even if the intention was to keep the repository open over several centuries, the high permeability levels of the Dogger limestone would absorb any repository-originated hydraulic effect. No significant impact on the hydraulic heads is thus to be expected. Therefore all the formations underlying the Callovo-Oxfordian are expected to remain unaffected by repository-induced hydraulic head drop.

6.2.4 Repository closure and return to a new hydraulic equilibrium

Once the repository has been closed (and shafts sealed), the water flows in the overlying formations will eventually allow a return to equilibrium of the hydraulic head field at with boundary conditions imposed by the surface aquifers in the outcrop zones. As flanges are inserted in the region of the Tithonian during the operating phase this formation will have returned to hydraulic equilibrium during the exploitation phase, hence the following paragraphs only refer to the Kimmeridgian and the Oxfordian.

6.2.4.1 The Kimmeridgian

The desaturated zone extends a few tens of meters around each shaft at the time of their closure. There is no hydraulic interaction by way of desaturation because of the several hundred-metre clearances between these structures.

Shaft closure triggers the gradual resaturation of the desaturated zone. It takes several thousand years to achieve total resaturation. This return to resaturation does not affect the layers directly in contact with the Kimmeridgian.

The influence of the shafts on the evolution of the hydraulic head drop is restricted to their immediate vicinity. Beyond a distance of a few hundred meters from the shaft, the hydraulic head drop in the Kimmeridgian is governed by the hydraulic head drop in the carbonated Oxfordian.

The time required to return to a new hydraulic equilibrium in the carbonated Oxfordian is similar to the length of the operating phase (cf. below). Thus the carbonated Oxfordian ceases to have any hydraulic influence on the hydraulic heads at the wall of the Kimmeridgian one to several centuries after the repository has been closed. However it takes several additional decades for this change to reach the top of the Kimmeridgian. Therefore the carbonated Oxfordian ceases to have any hydraulic influence on the hydraulic head drop in the Kimmeridgian a few centuries after closure. The shafts will continue to exercise an influence on the hydraulic head drop only in a very limited zone where desaturation dominates. Hence the build-up will continue gradually over several thousand years.

6.2.4.2 The carbonated Oxfordian

The time taken to return to hydraulic equilibrium is of a similar magnitude to the shaft opening time given the hydraulic characteristics of the carbonated Oxfordian. The hydraulic head drop will have spread to a radius of several kilometers by the time the shafts close. Thus the hydraulic interaction between the various shafts is strong. The overall hydraulic head drop is radial as it builds up from the periphery of the disturbed zone. In a presentation of hydraulic heads for a situation a few months prior to the return to hydraulic equilibrium the overall hydraulic disturbance clusters around each individual shaft. Thus the hydraulic head drop associated with each of these structures gradually reduces independently of the neighbouring shafts. Once the hydraulic head drop has disappeared in the carbonated Oxfordian, its effect is felt for a further few decades in the Kimmeridgian and for several centuries to a thousand years in the Callovo-Oxfordian.

6.2.5 The hydraulic evolution of the surrounding rocks following repository-induced hydraulic disturbance

The shaft-induced hydraulic head drop influences the water flows for several centuries in the carbonated Oxfordian and for several thousand years in the Kimmeridgian. These timescales are short compared with the characteristic timescales of climate change-induced geomorphological alterations (c.f. § 9) The new state of hydraulic equilibrium closely resembles that of the initial state particularly in the case of the general pattern of water flows in the surrounding formations. Additionally, geodynamic evolutions (c.f. § 9) will have no significant effect until several hundreds of thousands of years later and will thus govern the evolution of water flows in the surrounding formations at the scale of the Meuse/Haute-Marne site and its transposition zone (c.f. § 3).

6.3 The hydraulic behaviour of the Callovo-Oxfordian under the effect of the repository

6.3.1 Hydraulic head drop and desaturation during the operating phase

The venting of the walls of the various repository structures during excavation leads to a hydraulic head drop in the same way as it does for the surrounding formations. Furthermore, because of the very low level of permeability presented by the Callovo-Oxfordian argillites, desaturation caused by ventilation air not saturated in water vapour spreads from the excavation walls to the rock but at a very much slower rate than the hydraulic head drop.

6.3.1.1 At the scale of the layer as a whole

Because the construction of the various repository structures is in phases, the hydraulic head drop in the Callovo-Oxfordian is firstly driven by the shafts then by all the main connecting drifts and lastly by the repository zones. Thus it takes place earlier for the shafts than for the C waste and spent fuel disposal cells. Hence the hydraulic head drop at the repository scale is gradual. As the repository structures are not impermeable in the Callovo-Oxfordian, this drop can spread for as long as they remain open.

As pointed out in time section on mechanical behaviour (c.f. § 8), the mechanical discharge of confinement of the argillites around the structures, creates an initially damaged zone, during the excavation works (c.f. § 8.2) whose permeability level is higher than that of the undisturbed argillites (Altmann & Coelho, 2005 ; Ozanam & Su, 2004). The impact of this damaged zone on the hydraulic head drop is to drive it rapidly towards the undisturbed argillites. The hydraulic head drop spreads slowly outside the damaged zone.

Based on the assumption of anisotropy in the permeability (Kh = 10 Kv) in the mechanically undamaged argillites, the horizontal and vertical spread of the hydraulic head drop in the repository will differ.

- In the vertical plane the hydraulic head drop for a conventional century-long operating phase would neither reach the top nor the wall of the Callovo-Oxfordian. The two kinds of hydraulic head drops are likely to overlap after 100-200 years a few hundred meters around the shafts where the hydraulic head drop created in the carbonated Oxfordian spreads downwards inside the Callovo-Oxfordian layer. At the centre of the layer this overlap would produce total negative pressures just a few hundredths of a MPa higher than those created by two drops in hydraulic head taken individually.

- In the horizontal plane, the front of the hydraulic head drop extends faster: it spreads 50-60 meters within a century or so.

At the scale of the Callovo-Oxfordian, the hydraulic head drop interacts with the initial overpressure whose origin is attributed to a phenomenon comparable to chemical osmosis (cf. § 3 on the initial state). In a steady state hydraulic regime, which applies to the Callovo-Oxfordian, this phenomenon does not create water flows, the overpressures are stable over time and identical almost throughout the thickness of the Callovo-Oxfordian. They are linked to the solute concentration in the waters of the Callovo-Oxfordian and the mineralogical composition of the rock. The hydraulic head drop generates water flows that are too weak to alter the chemistry of the interstitial water at the scale of the layer, disturb the chemical equilibrium or the osmotic equilibrium. Therefore the repository-induced hydraulic head drop spreads without affecting osmotic overpressure.

6.3.1.2 At the scale of the repository

The different repository zones are several hundreds of meters apart from one another so that their individual hydraulic head drops do not interact during the century of operation. Thus each repository zone is hydraulically independent.

The general description of desaturation evolution in the Callovo-Oxfordian is broken down by structure type. The operating phase is explicitly considered for ventilated structures (drifts and B waste disposal cells). On the other hand the insertion of leak tight covers on unventilated C waste disposal cells and spent fuel disposal cells a few years after they are constructed, restricts the horizontal spread of the hydraulic head discharge to a few meters and so enabling resaturation to be initiated. Consequently there is no need to consider this phase explicitly. However a transient hydraulic evolution will be considered in the description of the post-closure phase (§ 6.3.2)

Minor hydraulic interaction may occur between two adjacent B waste disposal cells if they are kept ventilated for several decades. However the phenomenon is negligible.

Hydraulic interactions are more significant between two connecting drifts kept open for about a century. At the peak of the hydraulic interaction, the hydraulic head drops are of a few 0.01 MPa to a few 0.1 MPa. These values are low compared with the initial hydraulic pressure prior to excavation (about 5 MPa). The hydraulic interactions between structures are greater when a repository is operated for several centuries, yet remain low, on the order of a few tenths of a MPa.

6.3.1.3 Desaturation in ventilated structures: shafts, drifts and B waste disposal cells

The shafts, drifts and B waste disposal cells are ventilated throughout their operation using air that is not water vapour-saturated. This causes negative water pressures at the walls of the structures (commonly known as suctions) (Inset 6.4). The air flow and significant suction thus created may lead to desaturation in the immediate periphery of the structures because of the low permeability of the argillites.

● Ventilation air hygrometry inside the repository

The considerable length of the drifts implies that the relative hygrometry of the ventilation air varies according to their position in the repository (Wendling, 2005).

The relative hygrometry of the air at the Meuse/Haute-Marne site varies from 75 % in the summer at a mean temperature of 17 °C (which is equivalent to about 11 g of water vapour per kg of air or alternatively a partial water vapour pressure of about 1700 Pa) to 84 % in the winter at a mean temperature of 3 °C (that is 4 $g.kg^{-1}$ or 600 Pa). The mean relative hygrometry of the air over the year is 80 % and a mean temperature of 10 °C (that is 7 $g.kg^{-1}$ or 1100 Pa) (cf. § 3.5.1).

As the ventilation air descends inside the shafts, its hydrological conditions change influenced by two factors:

- the temperature of the geological formations increase with depth reaching 22-23 °C at the centre of the Callovo-Oxfordian layer;
- water influx or dischargees along the walls, particularly as when crossing the carbonated Oxfordian which have relatively high permeability levels.

Thus on average over a year, the hydrological parameters of the ventilation air at the bottom of the shafts are equivalent to a relative hygrometry of 90 % at a temperature of 12 °C (that is 8.5 $g.kg^{-1}$ or 1300 Pa) (Figure 6.3.1).

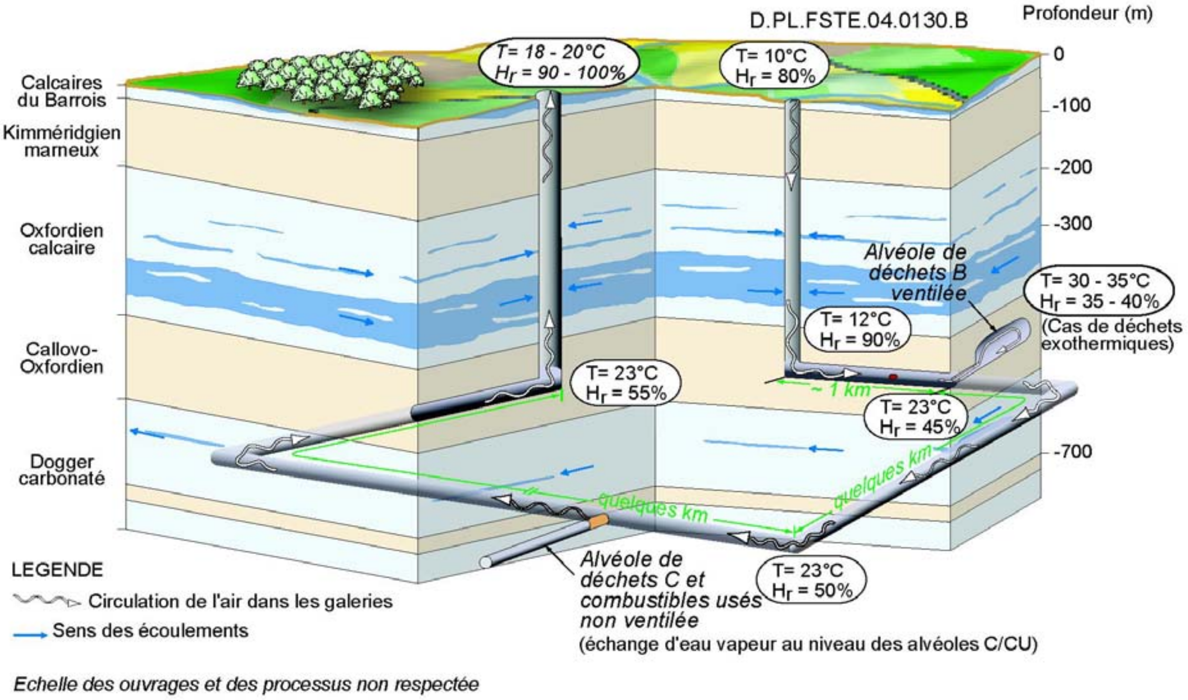

Figure 6.3.1 Representation of the evolution of temperature and relative hygrometry of air along a schematical ventilation path

Once the air reaches the bottom of the shafts it continues to circulate along the drifts. The hydrological parameters of the ventilation air gradually change as the distance from the shafts increases, mainly by readjustment to the natural geothermal temperature of 22-23 °C. Equilibrium is reached approximately 1 km away and the mean relative hygrometry over the year is then nearly 50 % (13.5 $g.kg^{-1}$ or 2100 Pa). Beyond that, over greater transit distances (at least several kilometers), the hygrometry may increase by a few % because of the intake of water from the Callovo-Oxfordian via the drift walls (on the order of 10^{-11} $m^3.s^{-1}$ per linear metre of drift).

Relative hygrometry of the air at the base of the return air supply shafts may be comparable with that of a connecting drift, that is about 50-55 %. During the ascend, temperatures drop yearly-averaged air. This temperature drop combined with water intake through the walls significantly increases the relative hygrometry of the air. The air expelled to the surface by the repository over the year has a relative hygrometry in the mean range of 90-100 % and a temperature of around 19 °C.

The ventilation air in the exothermic B waste and ventilated disposal cells may reach around 50 °C, whereas its hygrometry may drop below 50 %. The relative hygrometry of the air varies inside the disposal cells and approaches 40 % at the dead end of exothermic B waste disposal cells as the length of these disposal cells (about 250 m) is too short to implement a steady state thermal regime (the estimated length for reaching a steady state regime is one kilometre by analogy with the drifts).

The annual variations in the relative hygrometry of the surface air influence the hydrological conditions of the air in the repository. However mean annual hygrometry can be used to make allowance made for behaviour over the repository operating phase. Seasonal variations only affect thicknesses of tens of meters in the argillites from the walls of the ventilated structures.

Five reference configurations can be distinguished from this global pattern:

- the shafts through which the air arrives and in which the ventilation air is close to saturation,
- the first few hundreds of meters of drifts, the transient zone in which hygrometric variations are significant,
- the drifts located far away from the shafts and ventilated B waste disposal cells whose air hygrometry is low and constant during the ventilation period,
- the C waste disposal cells and spent fuel disposal cells that are not ventilated once the waste packages are emplaced and that do not exchange air with the drifts because the leak tight covers put into place,

the return air supply shafts that have dry air at the bottom and are heavily laden with humidity at the surface.

Inset 6.4 ***The relative hygrometry of the air and the suction in a porous medium at equilibrium***

Hygrometry of the air

The hygrometry of the air (i.e. air humidity) expresses the water vapour content in the air. It is expressed in g.m^{-3} of air or in g.kg^{-1} of air at a given temperature and total air pressure. The notion of relative hygrometry is more commonly used, which is the ratio of partial water vapour pressure to saturated vapour pressure at the temperature and pressure in question. Saturated vapour pressure is equivalent to the water vapour pressure beyond which water in the air can no longer be maintained in the vapour phase but condenses. The notion of relative hygrometry is generally used in the air but is independent of the composition of gas containing water vapour.

At atmospheric pressure (about 10^5 Pa or about 10 m of water column), the saturated vapour pressure in the air is 600 Pa at 0 °C, 1200 Pa at 10 °C and 2400 Pa at 20 °C (Lide, 2002).

The capillary pressure of a porous medium at equilibrium with an atmosphere at a given relative humidity

There are interfaces between water and air in a partially water-saturated porous medium. The pressure is not the same on either side of these interfaces. This difference in pressure is known as the capillary pressure:

$$P_{capillaire} = P_{air} - P_{eau}$$

When Kelvin's law is applied (Wendling, 2005), the relative hygrometry (i.e. relative humidity) of the air is the main variable used to determine the capillary pressure at the wall in a porous medium at equilibrium with that air. Kelvin's law stipulates that:

$$P_c = -\frac{RT\rho_w}{M}\ln(H_r)$$

Where

P_c: capillary pressure at the drift wall (Pa)
ρ_w: volume mass of water (kg.m^{-3})
R: ideal gases constant: 8.3 (J.°K^{-1}.mol^{-1})
M: molar mass of water (kg.mol^{-1})
T: temperature (°K)
H_r: relative hygrometry of the air (-)

When the relative hygrometry of the air is much lower than 100 %, capillary pressure may be very high (several MPa). If the air is at atmospheric pressure (about 0.1 MPa), water pressure becomes (very) negative, a phenomenon known as water suction.

The hydraulic implications of high capillary pressures on the saturation of media are discussed in Inset 6.5.

- **General description of the desaturation-resaturation process**

These boundary conditions on suction forced by the ventilation air induce gradual desaturation of the materials present in these structures and the near-field argillites (Inset 6.3). This desaturation in the argillites happens at the same time as the process of hydraulic head reduction. The general process at the scale of a structure is illustrated by the various diagrams in Figure 6.3.2:

- **prior to excavation**, the water flows are vertical as dictated by the gradient imposed by the surrounding rocks of the Callovo-Oxfordian layer;
- **immediately after excavation**, an EDZ forms induced by mechanical disturbance. A hydraulic head drop is induced when the walls of the excavations are vented. It spreads through the medium and causes water to flow that converges on the repository structures. This flow is weaker in intensity than the flows generated by desaturation;
- **while the ventilated structures are operating**, the argillites desaturate at their periphery affected by hydrological exchanges with the ventilation air. The size of the desaturated zone increases throughout the excavation opening period, although a pseudo state of equilibrium is established after a decade or so. After that the desaturated zone tends to extend very slowly. The saturation profiles in the ground support, the lining concrete and the argillites are governed by the suction imposed by the ventilation air and also the porosity structure and permeability of each of these porous media (Inset 6.5). Desaturation creates flows of water that converge on the structures gradually diminishing over time. These albeit weak flows are several magnitudes higher that the flows in saturated conditions (of the order of 10^{-11} $m^3.s^{-1}$ per m^2 of wall surface at maximum desaturated conditions, as against about 10^{-14} $m^3.s^{-1}$ per m^2 of wall surface following return to hydraulic equilibrium).

  At the end of the operating period, the ground support concrete and fractured zone of the EDZ in the drifts are highly desaturated (10 %<S<30 %). After that, the saturation degree rises rapidly to over 90 % at the limit of the microfissured zone of the EDZ. The undisturbed argillites are hardly affected by desaturation and their saturation degree in contact with the microfissured zone remains over 97 %. The B waste disposal cells present a similar pattern of desaturation profiles, however the extensions are proportional to the diameter of these structures and their associated EDZ;

- **after closure**, and particularly once the drifts have been back-filled, the near-field argillites and repository structures (mainly the drifts and B waste disposal cells) start to resaturate. Resaturation is influenced by gas production (metal component induced corrosion hydrogen), that for a transient period of some ten thousand years at the most, creates water flows that run towards the geological medium from the repository. Thereafter the water flows generally revert to convergent behaviour. By that time, the argillites will have returned to a state approaching total saturation (S>97 % in the EDZ; S>99 % in the undisturbed argillites). It takes a hundred thousand years or so for the back-filled drifts to reach a saturation degree in over of 90 %. A quasi-saturated state (S>97 %) is reached in the drifts when all the produced hydrogen is dissolved, that is roughly 200,000 years after closure. **Return to hydraulic equilibrium** coincides with reaching saturation in the repository and surrounding Callovo-Oxfordian. The water flows are then determined by natural hydraulic conditions and the permeability levels of the repository components, primarily the seals.

The distances between the structures are designed so that the desaturated zones at the walls of each individual structure never interact.

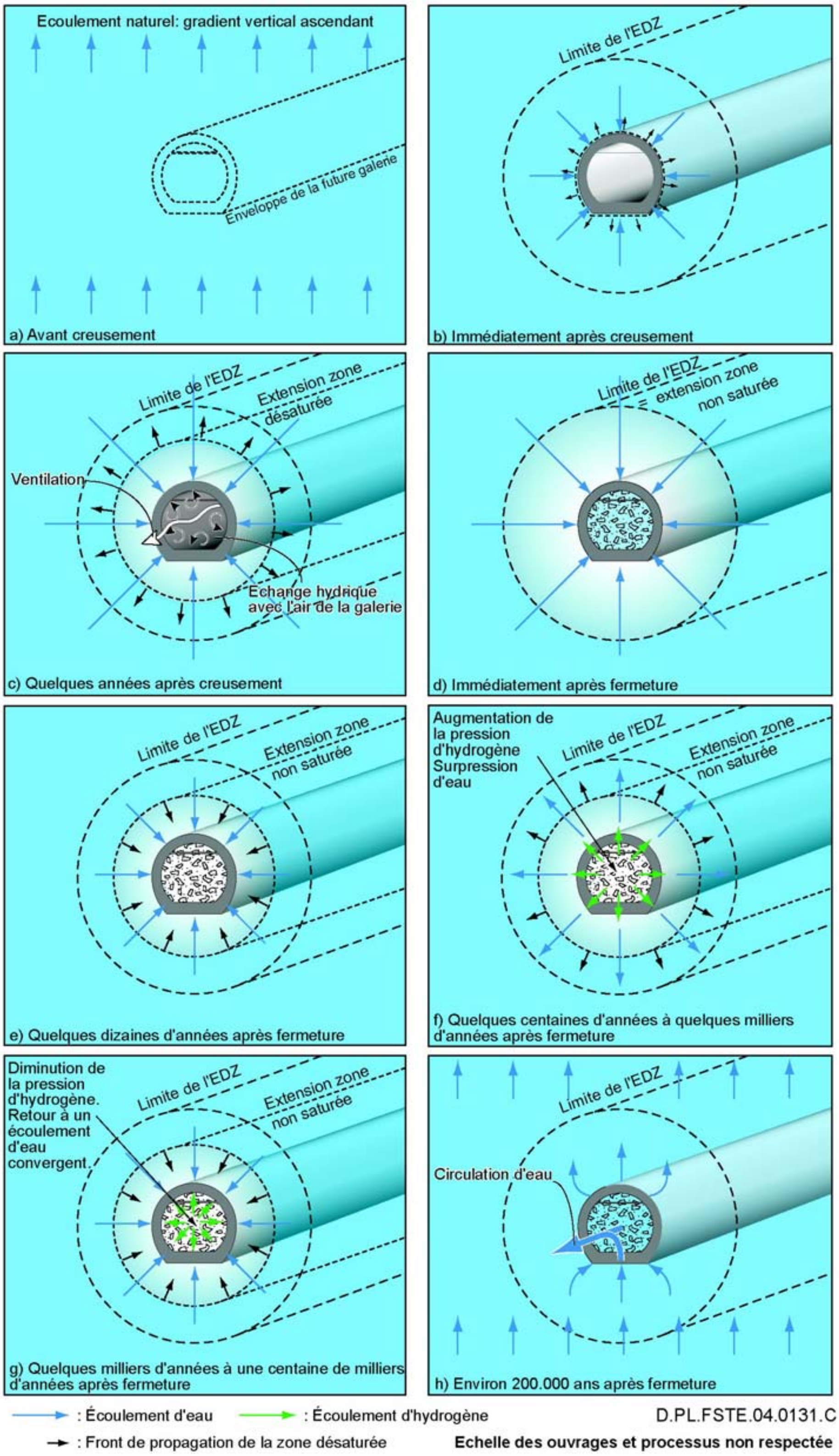

Figure 6.3.2 *General diagram of the ventilation-induced desaturation process during the operating phase and the generation of hydrogen in the post-closure phase. (Not to scale are the structure dimensions and the significance of phenomena)*

Inset 6.5 ***The sorption - desorption curves of porous environments***

Sorption-desorption curves (also commonly known as "capillary pressure curves" or "retention curves") express water's affinity to the solid skeleton that forms the porous media. Clays, when compared with other porous media generally present a distinctive feature resulting from the fact that water adsorption on the solids alters the arrangement of the solid skeleton. Thus the pattern of porosity varies with water content. The following figure presents the sorption-desorption curves of four standard porous media: the Callovo-Oxfordian argillites, bentonite (swelling clay), concrete and sand.

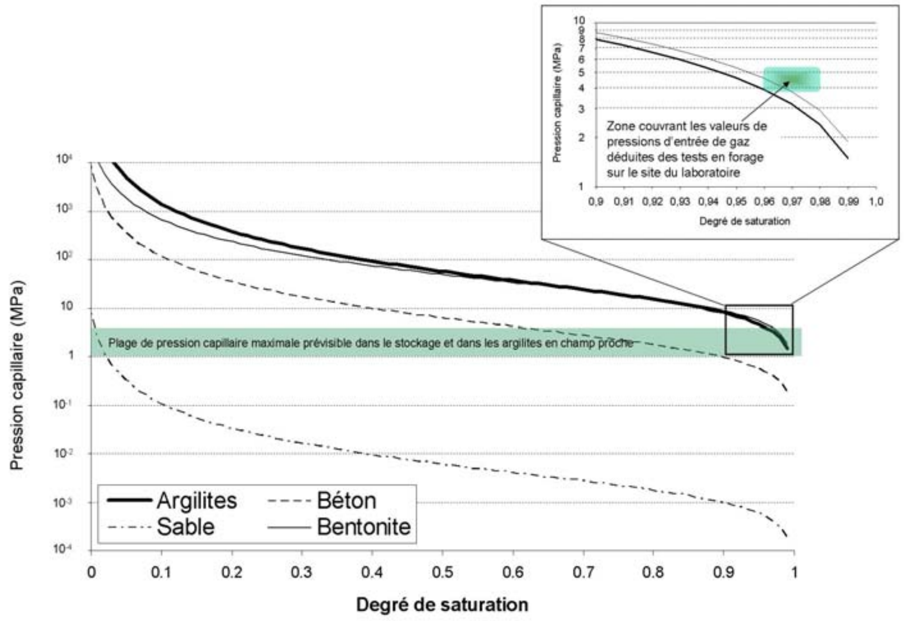

Sorption-desorption curve (capillary pressure as by a function of the degree of saturation) in different porous media. Inset for a degrees saturation in over of 90 % shows the area covered by the gas input pressure measurements deduced from bore-holes on the Meuse/Haute Marne laboratory site.

The shape of these curves reveals a major element that clarifies our understanding of the transfer of water and gases in these different porous media. The clays present (very) strong affinity for water. That means that they retain significant amounts of water even when suctions are very high (i.e. low relative humidity levels). Therefore in practice, low relative humidity levels must be imposed so that the clays can start desaturating. In contrast, sand is already highly desaturated for high relative humidity levels (i.e. low suction levels). Capillary pressures on the order of a few MPa are needed to start argillite or bentonite (swelling clay) desaturation. This same range of values is conceivable in the repository (Talandier, 2005). This means that in this pressure range, the gaseous hydrogen produced in the repository can not significantly desaturate the argillites or swelling clay (S>97 %).

The sorption-desorption curves present two curved zones, one around total water saturation (S>90 %) corresponding to the gas input pressure field and the other for much lower (S<20 %) degrees of water saturation corresponding to the gradual disappearance of water from the outside.

The sorption – desorption curves can show hysteresis. For bentonite and argillites,these hystereses are only significant for low degrees of water saturation and are mostly related todeformation of the porous skeleton with the degree of saturation. Lastly, givenclose links between interstitial water and solid phases of argillites and bentonite, temperature has no significant impact on sorption – desorption curves in the range of temperaturesbelow 100 °C.

Inset 6.6 ***The sorption - desorption curves of porous media***

Definition

The gas input pressure in a porous media is defined as the pressure needed to overcome the capillary forces binding the water to the mineral skeleton that makes up that porous media and allow the gas to penetrate the porosity of the media that was initially saturated. The intensity of these capillary forces depends on pore size, the smaller the pore size the greater the intensity. Gas input pressure is defined in reference to the interstitial water pressure in the saturated porous media corresponding to atmospheric pressure. When the interstitial water of the porous medium is under pressure, the effective pressure required by the gas to penetrate the porous media is equal to the sum of the gas input pressure and the water pressure.

Porous medias may display a distribution of pore sizes. Thus applying strict logic and independently of any consideration as to the connectivity of the various pores, gas input pressure corresponds to that of the largest pores.

Characteristics of the Callovo-Oxfordian argillites

The gas injection tests carried out in the bore-holes on the Meuse/Haute Marne laboratory site indicate gas input pressures on the order of 2-3 MPa probably corresponding to the damaged zone in the bore-hole periphery, and 4-5 MPa for the undisturbed argillites. No direct measurement is available in these tests to gauge the quantity of gas that has penetrated the argillites and the resulting degree of saturation. However, these bore-hole test values and others determined from samples, are sufficient to define a sorption-desorption curve. Its curved zone near water saturation is at a capillary pressure of a few MPa.

These experimental data give the same order of magnitude as the theoretical gas input pressure calculations in pores measuring a few nm to a few tens of nm, according to Jurin’s law. This law gives capillary pressures as a function of the surface tension at the liquid-solid-gas interface and the pore size (approximated to a cylinder).

The Callovo-Oxfordian argillites present pore size distributions ranging from a few nm to 100 nm, averaging at around 20 nm. It is very likely that the gas penetrates the largest pores of the argillites during the various gas injection tests, and thus at a lower pressure than indicated by the threshold values of the sorption-desorption curve shown above. The amounts of gas involved are very small and very difficult to measure experimentally given the limited contribution of large pores to the total porosity of the argillites.

Application to two-phase gas transfer modelling

The dependency of the gas input pressure value on the porosity pattern of a porous medium generally leads to dispensing with a threshold value when modelling two-phase transfers in favour of using the sorption-desorption curve continuously with a first curve field consistent with the experimental gas input pressure measurements. Thus the sorption desorption curve accounts for gas penetration even at low pressures (less than one MPa) continuously (without a threshold) from total water saturation, but with water saturation degrees of over 97 % corresponding to the fraction of gas that penetrates the macropores.

This is the approach that was adopted for the modelling to support the description of gas transfer presented in the following paragraphs. Accordingly with this approach, a gas can enter the argillites once its pressure exceeds hydrostatic pressure of 5 MPa in the Callovo-Oxfordian layer at equilibrium. Because of the hydraulic head drop, interstitial water pressures in the near-field structure argillites may be much lower than 5 MPa, enabling the gas to enter at lower pressures, as low as atmospheric pressure. However the thresholds are useful indicators for appraising the possible effects of certain gas pressures and their associated transport mechanisms.

Drifts and shafts

There is a brief transient period that lasts a few weeks to a few months before the desaturation process can commence fully. It is related to the concrete ground support is made up of shotcrete (nearly saturated). It slows down the desaturation process in the argillites until the concrete has set and its saturation level has equilibrated with the hydrological conditions imposed on its external surface by the ventilation air.

The extent and scale of desaturation are similar for all the drifts regardless of their use as access or connecting drifts.

Desaturation extends to the boundary of the EDZ fractured zone after about one year. Because of the lower level of permeability of the microfissured zone of the EDZ (about $5\cdot10^{-11}$ m.s^{-1} as against $5\cdot10^{-9}$ m.s^{-1} in the fractured zone), spreading within this zone takes longer. It takes a few years for the desaturated zone to reach the outer boundary of the damaged zone. Spreading within the undisturbed argillites takes even longer because of the much lower level of permeability (of the order of $5\cdot10^{-14}$ to $5\cdot10^{-13}$ m.s^{-1}). After about a decade, a pseudo permanent pattern is reached, characterised by a very slow evolution of the desaturation profile.

After 100 years, the degree of saturation is on the order of 20-30 % in the ground support concrete, 30 % throughout the fractured zone, it rises rapidly to about 90 % in the microfissured zone and is always in over of 97 % in the mechanically undisturbed argillites where it reaches 100 % within a few meters (Figure 6.3.3). This profile would hardly change if the drift was to remain open for several centuries.

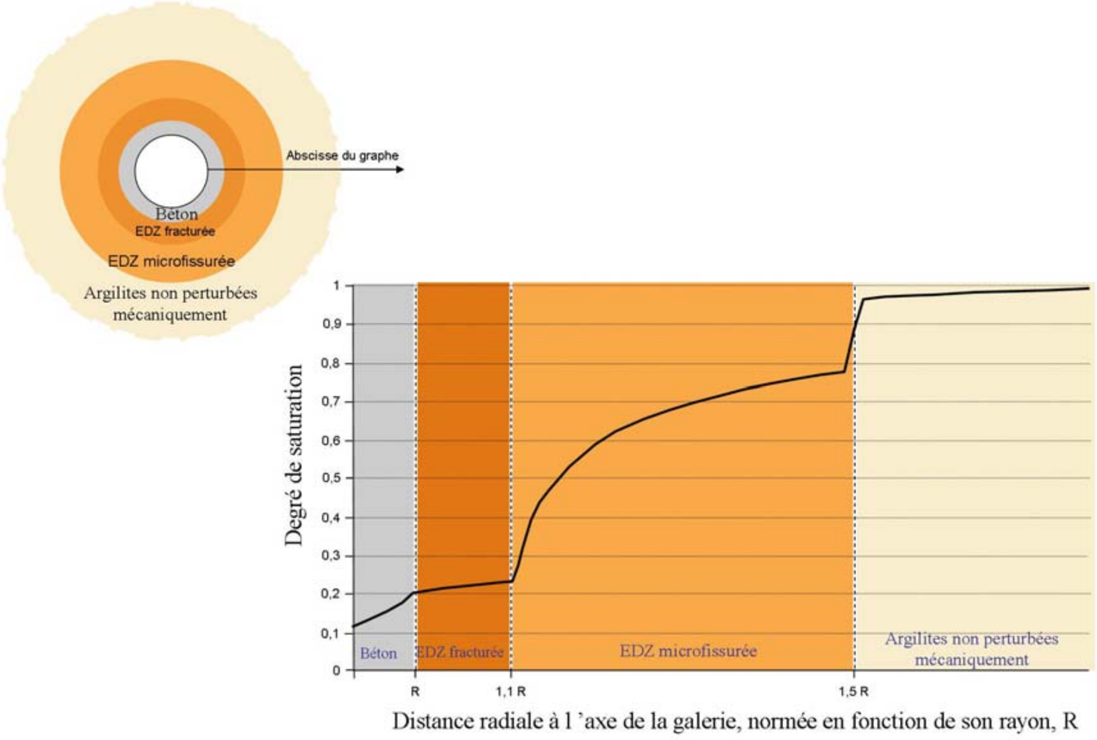

Figure 6.3.3 *Schematic representation of the quasi-stationary saturation profile obtained in a drift that remained open for at least a decade*

As the relative hygrometry of the ventilation air is higher in the shafts through which it arrives, desaturation of the ground support concrete is less significant here. The saturation degree of concrete is on the order of 40-50 %, and is 50 % in the over all fractured zone of the EDZ. The remainder of the saturation profile follows the preceding description

- **B waste disposal cells**

The B waste disposal cells behave in a similar way to the drifts during the operating period. The differences arise primarily from:

- the thicker coat of concrete lining;
- the orientation of the disposal cells parallel to the major horizontal geomechanical constraint, that results in the absence of any fractured zone being created when these structures are excavated at a depth of 500 meters (c.f. § 8.2.3).

The lining concrete occupies a significant part of the excavated volume, which implies that thicknesses may be as much as several meters. Once it has set (a few weeks to a few months), the hydraulic conditions imposed by the ventilation air causes significant desaturation in the concrete that starts at the disposal cell walls. This desaturation spreads outwards to reach the microfissured zone of the argillites at the excavation wall within a few months to one year. The degree of saturation in the concrete is close to 30 %.

The desaturation phenomenon spreads within the argillites thereafter. After a few decades the degree of saturation the concrete is in the range of 20-30 %. It rapidly increases to the 90 % mark in the microfissured zone to reach 100 % a few meters into the mechanically undisturbed argillites.

- **The special case of exothermic waste disposal cells and drifts subject to thermal load**

The temperature rise in low permeability porous media tends to result in the volumetric expansion of the water. This can in theory produce an overpressure. However this is possible only when water saturation and temperature rise are concomitant.

Now this concomitance does not exist in exothermic B waste disposal cells or drifts subject to thermal load because the temperature rise timescale (about a decade in the B waste disposal cells and a few centuries in the drifts) is much shorter than the time it required to return to saturation inside these structures.

In contrast, the thermal expansion of water in the argillites causes overpressures of a few MPa (Wendling, 2005) that peak after one to several centuries at radial distances on the order of ten to several tens of meters from the structure walls (Figure 6.3.4). Yet the convergent water flows created by these overpressures in a low permeability media are too weak to make a significant impact on desaturation during the operating phase or even thereafter.

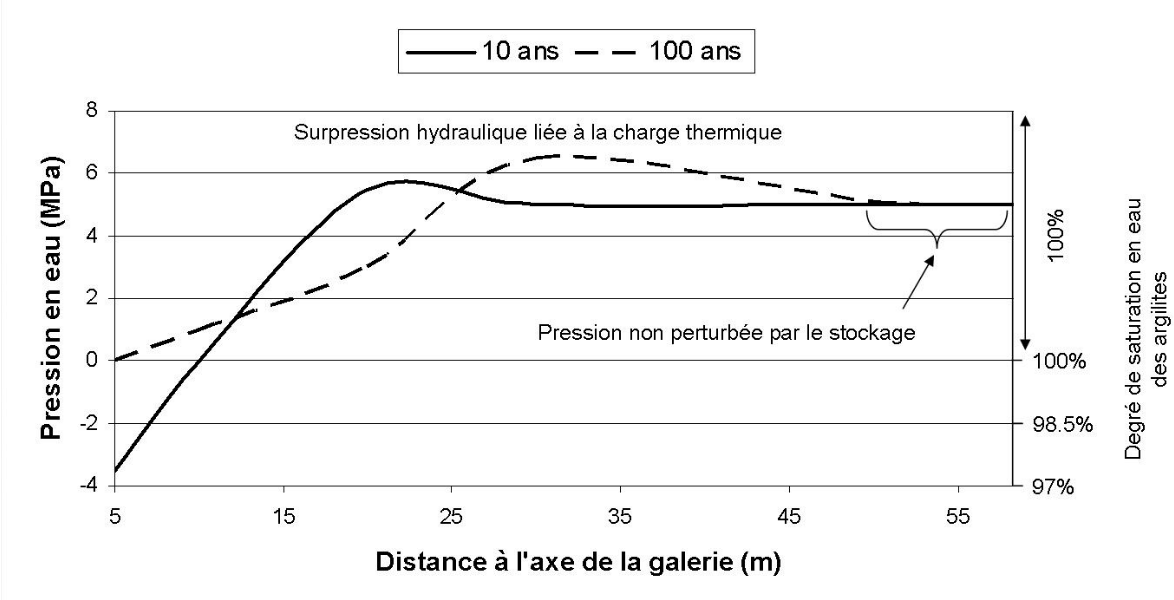

Figure 6.3.4 *Evolution with time of the hydraulic pressure profile in the argilites radially surrounding the centre line of a drift open for several decades and subject to thermal loading*

In the C waste and spent fuel disposal cells the argilites are close to saturation after cell closure, and thus during the thermal phase. A thermal load-induced hydraulic overpressure may thus be produced in the argillites around the disposal cells. In the case of C waste, it causes a divergent water flow because the overpressure is at its maximum at the disposal cell walls. In the case of spent fuel, **(i)** emplacement of the swelling clay engineered barrier at about 80 % saturation implies slight desaturation of the argillites at the walls, which delays the pressure build-up at the disposal cell walls by several decades **(ii)** the maximum point of the overpressure is sited far from the disposal cell walls during this period (Figure 6.3.5) and **(iii)** the water flow created by thermally-induced hydraulic overpressure converges towards the disposal cells. These overpressures last for a few centuries at the most. The created flows decrease more rapidly, within a few decades, as the temperature in the argillites evens out.

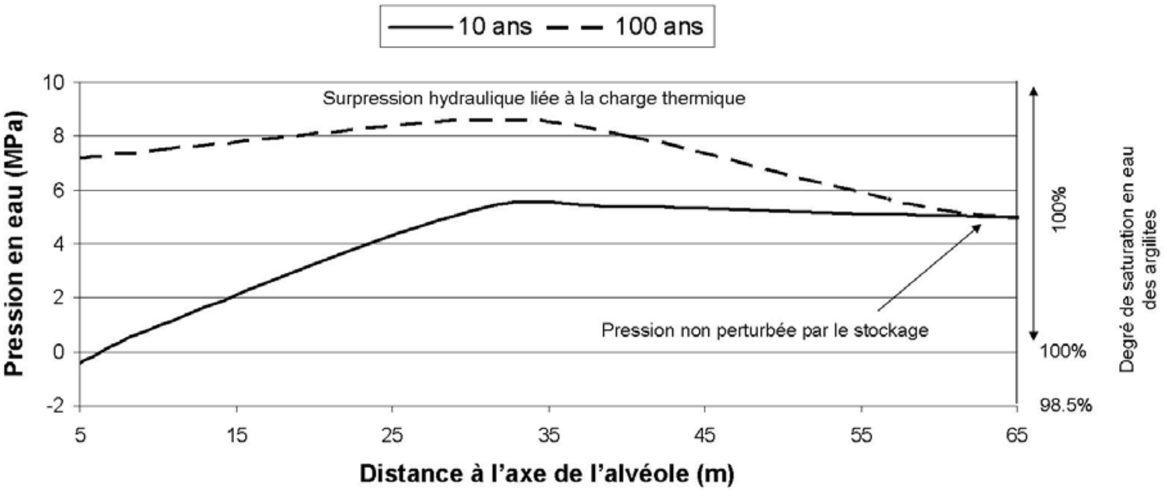

Figure 6.3.5 *Evolution with time the hydraulic pressure profile in the argilites radially surrounding to the centre line of a spent fuel cell*

6.3.2 Repository resaturation during post-closure and the effect of the hydrogen produced by metal corrosion

The progressive closure of the repository from disposal cell to shafts sealing, halts the hydraulic head drop and desaturation processes. A new phase of hydraulic evolution sets in, namely resaturation of the repository and any desaturated argillites in the periphery until a new state of hydraulic equilibrium is reached in the repository and the surrounding Callovo-Oxfordian layer. This phase is influenced by the production and migration of hydrogen released by corrosion.

The following paragraphs will describe the main hydrogen production phases, the general pattern of hydrogen migration through the repository and Callovo-Oxfordian and a more detailed approach for the various types of structure.

6.3.2.1 Hydrogen production by corrosion: characteristic timescales and quantities produced.

Air will be trapped in the repository after closure, primarily in the back-fill of the drifts. Furthermore, the repository is a source of gas, because of the chemical decay of a number of its components. Various mechanisms in the repository will produce gases (mainly hydrogen): the corrosion of metal components, microbial activity, radiolysis of water and organic matter, and alpha decay. Anaerobic metal corrosion is by far the most important process with over 90 % of the gases produced (Talandier, 2005).

The source of hydrogen produced in the C waste and spent fuel zones is essentially related to corroding metal containers, linings and ground supports (the latter goes for spent fuel disposal cells).

Hydrogen production occurs during two phases: the first relates to corrosion of ground support and lining. It lasts about 4,000-5,000 years, with an annual production[8] of approximately 250 m^3 for C waste and 1,400 m^3 for spent fuel (this volume is estimated at a pressure of 5 MPa and a temperature of 30 °C. All the other volumes of gas expressed in the rest of the document are also estimated at this pressure and temperature unless otherwise stated). The second phase extends up to a hundred thousand years or so during which the amount of hydrogen released by the corrosion of (overpacks) containers and inserts (in the case of spent fuel) gradually decreases.

Production drops by about one order of magnitude after 5,000 years (c.f Inset 6.1). The total quantities of hydrogen produced during these two phases are almost identical.

In the case of B waste, the production of hydrogen takes place during two phases of different lengths: about 500 years for the first phase and again up to about one hundred thousand years for the second. B wastes are heterogeneous and are conditioned in different forms, which multiplies the number of hydrogen production processes. Two of these types of waste package are responsible for most of the hydrogen production, namely packages of compacted hulls and end caps (reference package B5) and bitumen-embedded packages (reference package B2).

- Gas production in the case of reference packages B5 essentially stems from the corrosion of the metal envelopes and the waste itself. Gas production is significantly reduced after a 500-year period of attacking the non-alloy steels, and is sustained at a constant level of about 18 m^3 per annum per disposal cell for approximately 100,000 years.
- Hydrogen production in the case of reference packages B2 essentially stems from bitumen radiolysis over roughly 50,000 years. Between year 500 and year 50,000 gas production (all sources taken together) stabilises around a value on the order of 14 m^3 per annum per cell.

---

[8] This volume is estimated for a pressure of 5 MPa and a temperature of 30°C. Except an opposite mention, all other volumes of gas noted in the text are also estimated for these pressure and temperature.

The various evaluations presented have been obtained on the assumption of an annual corrosion rate of about 2-3 $\mu m.yr^{-1}$ in the non-stainless steel, but neither the potential effects of the changins degree of saturation of the surroundings of the metal components on the corrosion rate nor water consumption through corrosion were taken into consideration.

Current evaluations (experimentation and modelling) tend to suggest that corrosion rates could be significantly lower, as low as 0.1 to 1 µm per year, thus extending the production curve over a longer period.

While it is reasonable to assume that the degree of saturation in C waste disposal cells and spent fuel disposal cells could rapidly exceed 97 % in the near-field argillites and swelling clay (with reference to spent fuel) (cf. Inset 6.4), in contrast it appears that very low saturation rates could be maintained over long periods in the B waste disposal cells given the hydrological characteristics of the concrete and the presence of residual gaps. Under these conditions the kinetics of corrosion could be strongly influenced and the initial production period of hydrogen prolonged.

Moreover the water re-injection capacities of the Callovo-Oxfordian argillites could limit the amounts of water available for corroding metal components, particularly in C waste disposal cells and spent fuel disposal cells.

Current modelling methods allow for the consideration of various gas transfer processes but are incapable of representing the various couplings mentioned above.

The evaluations of hydrogen transfer and its effects on water flow and solute transport presented in the following paragraphs have to be conservative in the light of these observations. Therefore the outline presented is an envelope of possible evolutions to adopt a conservative approach to the phenomena.

6.3.2.2 Radioactive gases

A number of radionuclides are gaseous or may potentially be in a gaseous state under repository conditions: ^{3}H, ^{39}Ar, ^{85}Kr, ^{14}C, ^{129}I and ^{36}Cl. They occur in marginal amounts by comparison with corrosion-induced hydrogen.

Given their short half-life (12 and 11 years respectively for ^{3}H and ^{85}Kr), by the time the repository closes the ^{3}H and ^{85}Kr will have largely disappeared through radioactive decay.

^{129}I is gaseous under the temperature, pressure and radiation conditions of the nuclear reactor where it combines with cesium to form CsI, which is partly volatile under these conditions. Under repository conditions, ^{129}I will dissolve in the form of iodide I^{-} when water arrives. It appears highly improbable that it will convert to a gaseous form (CH_3I or I_2) as these compounds are very reactive or are quickly rehydrolyse in the form of iodide (Nagra, 2003a). The same is true of ^{36}Cl (Giffaut, 2005).

The ^{14}C in the wastes may be both in inorganic and organic form (C^{-IV}-C^{-VI}). Over 98 % of the inventory of organic ^{14}C occurs in the zircaloy cladding sections (reference packages B5, B4 and spent fuel). A minute fraction of ^{14}C from spent fuel, less than 0.01 %, would be directly in gaseous form (CO_2). The total inventory of ^{14}C (B, C wastes and spent fuel) is on the order of 500-600 moles. Only organic ^{14}C can lead to a gaseous form, (i.e. CH_4) if bacterial activity is present. Thus this phenomenon would only apply to reference packages B5.1, through the presence of organic matter with the potential for bacterial development (Libert, 2005). In the absence of bacterial activity, the dissolution of iron carbide (Fe_3C) or zirconium carbide (ZrC) should lead to the formation of non-gaseous and soluble organic species (acetic acid, formic acid, acetaldehyde, formaldehyde, ethanol, methanol, propanol,…). The inventory of ^{14}C of the B5.1 packages would account for about 6-20 % of the total inventory of ^{14}C, that is 20-75 moles respectively. In standard conditions that would amount to a low volume of CH_4 between 1.7 and 0.5 m^3. Furthermore only 55-85 % of this total (^{14}C of the zircaloy) would be in organic form. The inorganic carbon (C^{+IV}) released by the matrices of oxide and C wastes would dissolve in the form of carbonates (Johnson & Schwyn, 2004).

Consequently it may be considered to ignore radioactive gases in the hydraulic evolution over the long term.

6.3.2.3 Hydrogen transfer mechanisms

There are four mechanisms that should be mentioned for hydrogen migration in and around the repository (cf. Inset 6.7):

- dissolution in water and diffusion,
- two-phase water flow,
- transfer along microfissurs,
- transfer along fractures, both formed as a consequence of pressure build up.

Hydrogen solubility in water is on the order of 37 moles.m^{-3} at a pressure of 5 MPa and a temperature of 30 °C. During the first intensive phase of production, hydrogen dissolution and diffusion in the repository and the Callovo-Oxfordian layer would prevent significant evacuation of the hydrogen produced. From then on the hydrogen will occur in gaseous form and only the lower three processes mentioned above will be capable of evacuating hydrogen, at least in the beginning.

It should be mentioned here (i) that data obtained from a bore-hole dedicated to measuring gas input pressures in the Callovo-Oxfordian argillites suggest that gas pressure of at least 12 MPa (Andra, 2005h) the value of the natural vertical stress, would be required to induce fracturing, and that (ii) the hydrogen pressures developed in the repository would never rise to such values. Thus transfer along fractures formed via pressure build-up does not come into play.

However the two migration mechanisms of two-phase water flow and along induced microfissurs may come into play particularly during the first phase of hydrogen production when the flows are at maximum. Their respective importance in hydrogen transfer depends on the hydrogen pressures reached in the repository and the saturation level of the various components. Transfer along induced microfissurs requires higher pressures of hydrogen to be developed than those built up by two-phase water flow (Inset 6.7).

6.3.2.4 The global pattern of hydrogen transfer and of repository resaturation

Broadly, hydrogen has several potential transfer paths open to it from the disposal cells:

- the mechanically undisturbed argillites and the whole of the Calllovo-Oxfordian layer;
- the damaged zone around various repository structures, the disposal cell plugs, the drifts (back-fill and/or ground support/lining/slab) and the seals.

Given the low permeability levels combined with the sharp sorption-desorption profiles described in Inset 6.5, the mechanically undisturbed argillites, disposal cell plugs and seals (if saturated) are intrinsically the most difficult transfer path ways for the hydrogen.

Nevertheless the repository offers an exchange surface area of several million m^2 with the Callovo-Oxfordian (as against a surface area of around 400-500 m^2 for the cumulated centre line surface area of the shafts that would give direct access to the carbonated Oxfordian by short-circuiting the Callovo-Oxfordian). This large exchange surface area lends itself to being the preferred hydrogen transfer path through the Callovo-Oxfordian.

When analysing potential transfer path ways allowance must also be made for the relative evolutions in time of the degree of saturation of the disposal cell plugs, the EDZ around the drifts, the drifts themselves and the seals, particularly the shaft seals. This is because gas migration is easier in non-saturated media. Some of the potential transfer paths, in particular the seals, will be non-saturated at the time the repository closes.

The hydrogen transfer and repository resaturation processes can be described from these various considerations using a time breakdown that makes allowance for the successive timescales taken to reach almost total saturation of the disposal cell plugs (10 years for C waste, 100 years for spent fuel, 1,000 years for B waste) and seals (1,000 years for drifts and a few decades for the upper part of shaft seals) and the characteristic hydrogen production timescales already mentioned (*Inset 6.1*). Particular attention will be paid to the transition between the two production phases timed at about year 5000 for C waste and spent fuel zones and year 500 for the B waste zone. This description is based on a "time 0" that equates to the closure of the disposal cells and plug fitting, and on an analysis that makes allowance for the disposal of spent fuel.

- **From year 0 to 100: preferential migration from the disposal cells to the repository drifts during the time that the C waste disposal cell and spent fuel cell plugs are not resaturated.**

The engineered barrier and the disposal plugs are installed at a saturation degree of nearly 80 %, which enables the produced hydrogen to migrate without obstruction towards the access drift. Accordingly, the structures act as the preferred transfer path for the hydrogen until the degree of saturation of the disposal cell plugs and subsequently the module seals exceeds 95-97 %. The hydrogen that has been mainly produced inside the disposal cells, therefore simply flows across the disposal cell plugs then across the module seals (Figure 6.3.6). The 100-year value is representative for a spent fuel disposal cell and resaturation of the swelling clay (engineered barrier and disposal cell plug). The timescale for disposal cell plug resaturation is about ten years shorter for C waste disposal cells. An equivalent process affects B waste disposal cells whose seals behave like drift seals in that they take about 1,000 years to achieve saturation in over of 95-97 %.

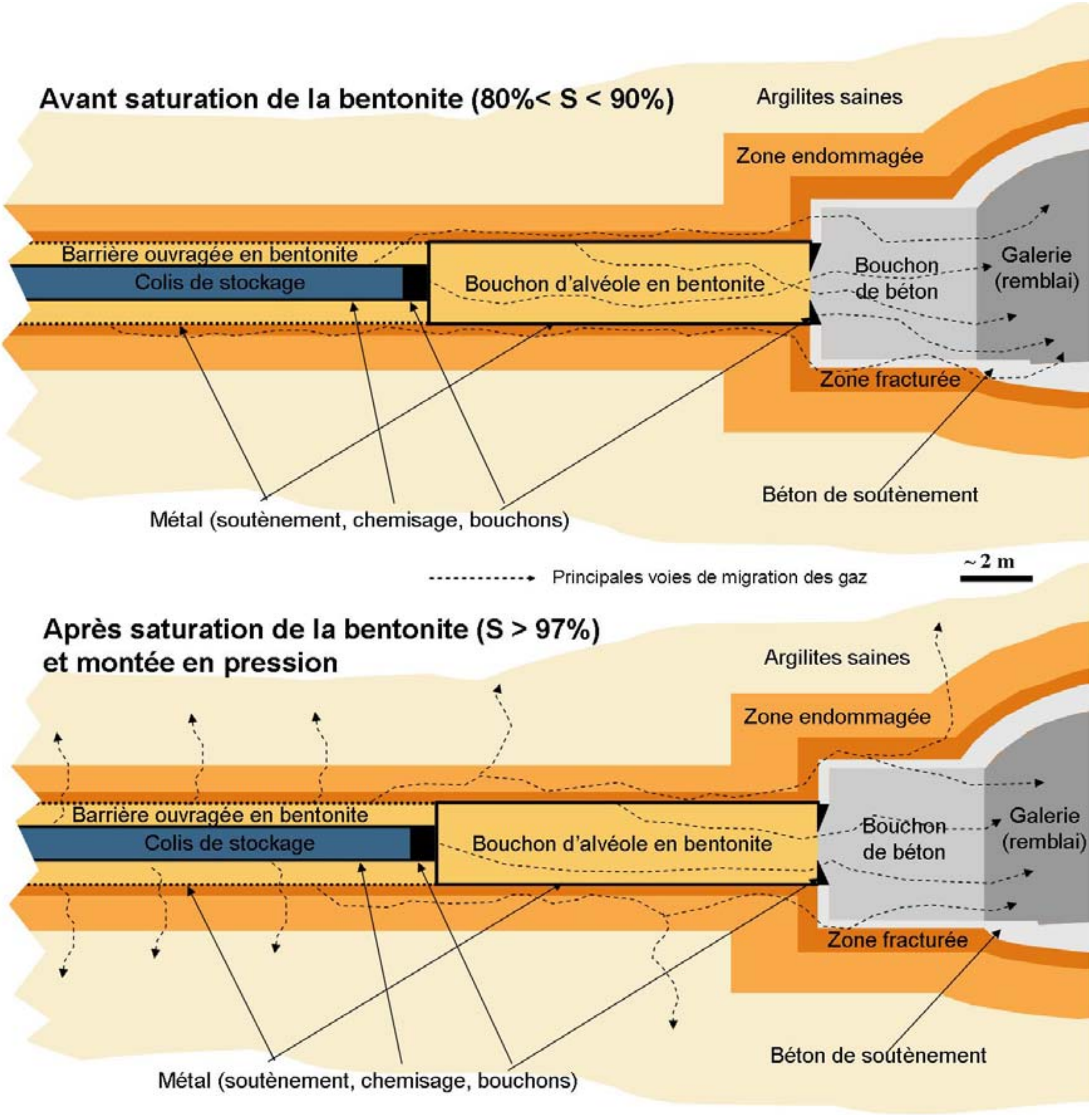

Figure 6.3.6 *Diagram of the main hydrogen migration paths to the access drift before and after resaturation of the ways from a spent fuel disposal cell plug*

Furthermore the waters of the carbonated Oxfordian resaturate the upper part of the shaft seals and that of the argillites within their periphery in less than a decade (Figure 6.3.7). In this way they rapidly limit the two-phase flow of hydrogen transfer to the carbonated Oxfordian (Inset 6.5). During this first phase, hydrogen production in the repository is very low and accounts for about 1 % of the total production. Under these conditions and given the volume offered by the drifts, the hydrogen pressure reached inside the repository is a few tenths of a MPa lower. In view of the sorption-desorption characteristics of the swelling clay, this sort of production rate does not prevent disposal cell resaturation and in particular that of the swelling clay structures.

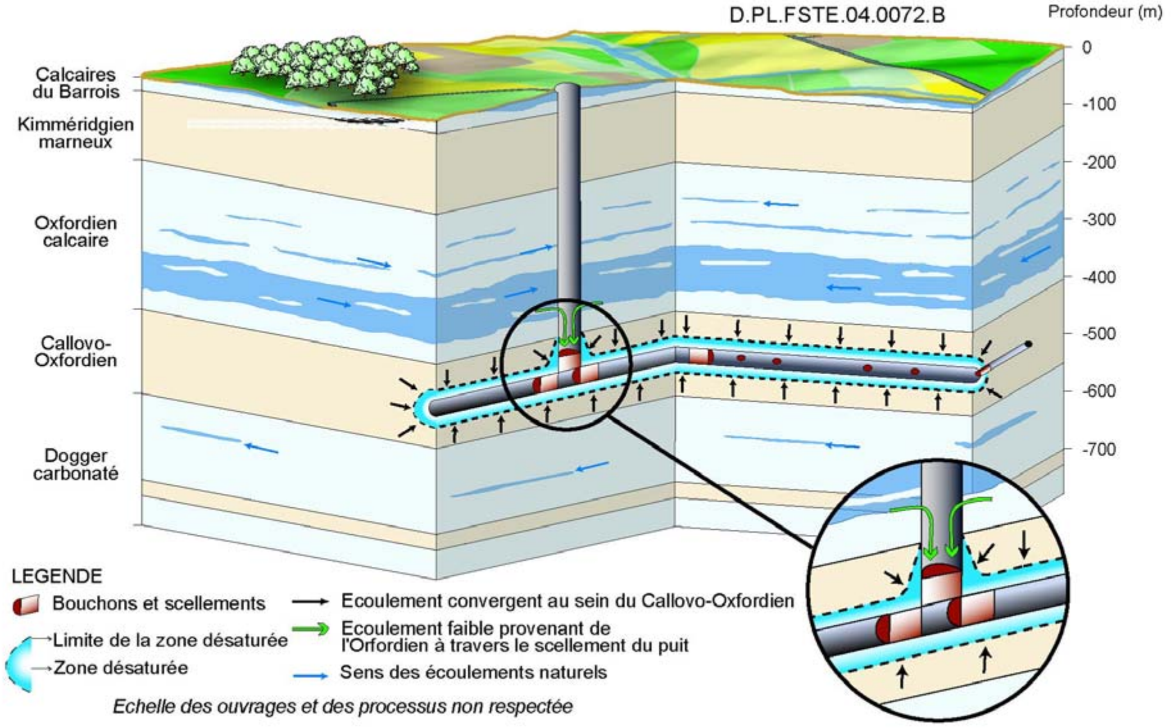

Figure 6.3.7 *General resaturation pattern at the scale of the repository. The upper part of the shaft seal is resaturated by water from the carbonated Oxfordian. The rest of the repository is resaturated with water from the Callovo-Oxfordian.*

Beyond year 100 the passage of hydrogen by two-phase flow is significantly restricted because of the >97 % saturation of the plugs of the C waste and spent fuel disposal cells that is equivalent to a swelling pressure approaching 7 MPa at geostatic equilibrium. Subsequently transfer pressure starts to build up in the disposal cells.

- **From year 100 to years 2,000-3,000: pressure build-up in the disposal cells and in the drifts, a two-phase flow is initiated in the Callovo-Oxfordian**

Hydrogen behaviour depends mostly on the two-phase flow characteristics (permeability levels, sorption-desorption curves) and the geometry (surface) of the various materials at the water-gas interface in the cell. The hydrogen migrates via two-phase flow through all the components (swelling clay plugs, EDZ, engineered barrier in the spent fuel disposal cells and undisturbed argillites) (Figure 6.3.6). The path that offers the least resistance is the initial EDZ. However the build-up of swelling pressure in the vicinity of the plugs should lead to EDZ healing in the damaged argillites. Observations suggest an initial return to water permeability but as yet they cannot demonstrate an equivalent phenomenon for gas transfer. Nonetheless the mechanisms involved in healing (swelling, reduction of porosity through the effect of mechanical loading) should also lead at least partially to restoration of the properties of two-phase flow.

As the profiles of the argillite and swelling clay sorption-desorption curves are similar, the distribution of gas flows will essentially depend on the permeability ratios between swelling clay (disposal cell plug and/or engineered barrier) and argillites (Callovo-Oxfordian) and the ratios of the surface areas offered for gas migration by these two components.

Calculations indicate that in the centre line of the C waste disposal cells transfer through the plug to the drifts predominates. Incomplete healing of the EDZ would accentuate this preferential transfer to the drifts.

The hydrogen produced on the ground support level of the spent fuel disposal cells follows the same pathway as described above for C waste disposal cells. The hydrogen produced at the lining crosses the engineered barrier then follows the centre line path as described above. Transfer via this centre line may be accentuated by ground support corrosion products that may provide an imperfect interface between the argillites and the swelling clay (engineered barrier and plug).

Once the seals are saturated (year 1,000) in B waste disposal cells, the ratio of centre line to radial surfaces favors hydrogen transfer towards the drifts.

Under these conditions and given the surface areas offered, calculations demonstrate that most of the gas produced in the disposal cells travels towards the drifts by crossing or bypassing the seals. Never the less although the Callovo-Oxfordian remains a potential path for two-phase hydrogen transfer (Figure 6.3.8).

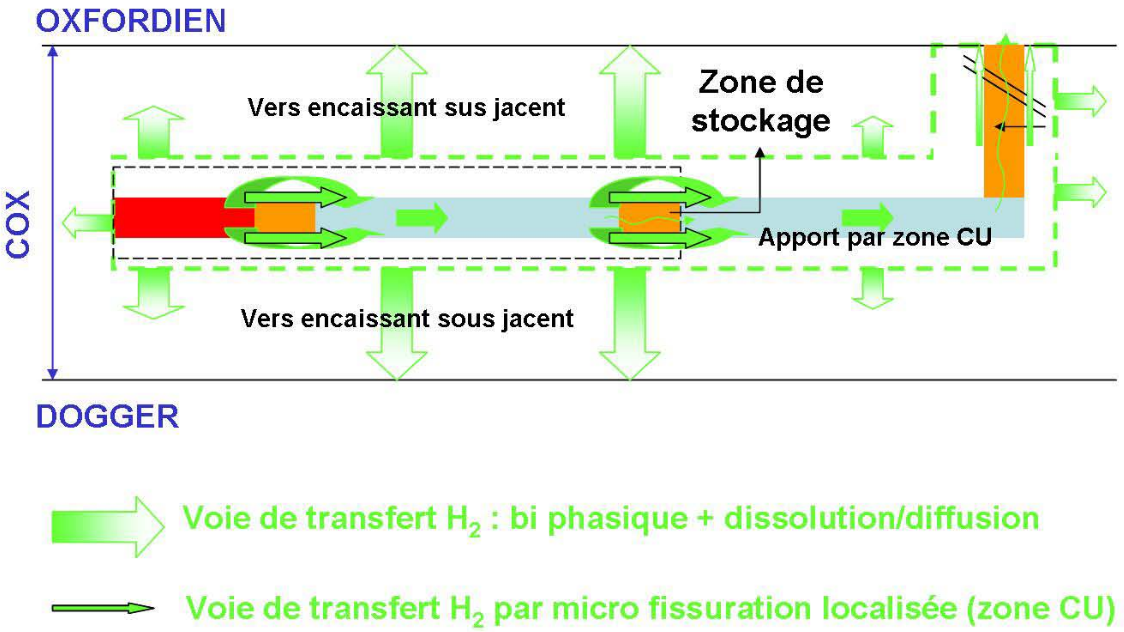

Figure 6.3.8 *Diagram of the hydrogen transfer path ways in the repository and the surrounding Callovo-Oxfordian*

Inset 6.7 ***The conceptual model of gas transport in dense clay environments (1/2)***

The current conceptual model developed to represent gas transport in deep clays (argillites, Opalinus Clay) and dense, initially saturated, swelling clays, comprises 4 successive phases each of which corresponds to a specific mechanism (Talandier, 2005). The sequence of these mechanisms depends on the gas pressure and flow:

- The first mechanism is that of **gas dissolution** in water, and its **transport by advection - dispersion and/or diffusion** in the dissolved state (Diagram A, below).

This mechanism is not conducive to transporting significant amounts of gas as the diffusion coefficients of the dissolved gases in the clays and the permeability levels of the clays are low. Therefore the second mechanism is triggered as soon as the gas flux exceeds the capabilities related to dissolution and dissolved gas transport.

- The second mechanism is **two-phase flow** (Diagram B, below). The flux of gas produced remains in gaseous form and migrates into the porosity following a Darcy type flow, partially desaturating the environment depending on the gas pressure attained (Inset 6.5).

This transfer mechanism is independent of the mechanical stress field applied to clay. The clay porosity is not modified as the gas flows through. As the term two-phase indicates, this mechanism brings water and gas into joint motion. Thus water permeability and gas permeability (in the Darcy sense) are defined according to the degree of saturation of the clay.

- The third mechanism initiates if the flux of gas production cannot be evacuated by the first two mechanisms. Gas migration is thus coupled to mechanical behaviour. More to the point it depends on the contact forces between the solids of the clay skeleton. Gas pressure builds up until it locally overcomes the contact forces (cohesion), it "relaxes" the porosity and the gas can then migrate onwards in the larger porosity domain that it has created (Diagram C, below) At the microscopic scale, this porosity dilation is equivalent to the formation of localised **microfissures**. Given the low viscosity of the gases and their low affinity to the solids (as against those of water), this microfissuring-based transfer mechanism enables large amounts of gas to be transferred even though only locally occuring microfissures are involved.

During this purely mechanical mechanism, water is not carried ahead of the gas penetration front this in contrast to two-phase transfer. Strictly speaking the Darcy type flow concept is no longer applicable.

If the gas pressure drops, the microfissures cannot be kept open. The microporosity initially created contracts mechanically and the water can again reoccupy the entire porosity. When combined with the swelling of the clay minerals near the microfissures, self-healing of the clay enables their closure and a return to total saturation. The argilite regains its initial permeability to water.

The mechanism of microfissuring can be initiated in the swelling clay as soon as gas pressure exceeds swelling pressure. The swelling pressure of the swelling clay at mechanical equilibrium with the argillites in the repository is around 7 MPa.
The effective gas pressure in the argillites leading to microfissuring has been set to a lower value than for the fracturing pressure (12 MPa, cf. below). A value of about 9 MPa has been retained by comparing the results obtained on Opalinus Clay and considering the threshold value of the gas input pressure obtained in the bore-hole of the Meuse/Haute-Marne site.

The conceptual model for gas transport (2/2)

- The fourth mechanism initiates if the gas production flux is still too high to be evacuated by the previous three mechanisms. In this case gas pressure continues to build up beyond the mechanical stress field and reaches the clay **breakdown** threshold of this stress field. A fracture is created as opposed to microfissures (Diagram D, below).

It takes a direction perpendicular to the direction of the minor stress.

As the bore-hole test results suggest, effective gas pressures in over of 12 MPa are required to trigger this mechanism for argillites.

As in the case of microfissures, (i) the extent and opening of a fracture are in part a function of the gas pressure and associated gas flux, (ii) there is no significant water displacement, as the water only moves locally and while the fracture is opening up: only the gas can flow there without causing water to flow, and (iii) self-healing after return to total saturation brings permeability back to its original level.

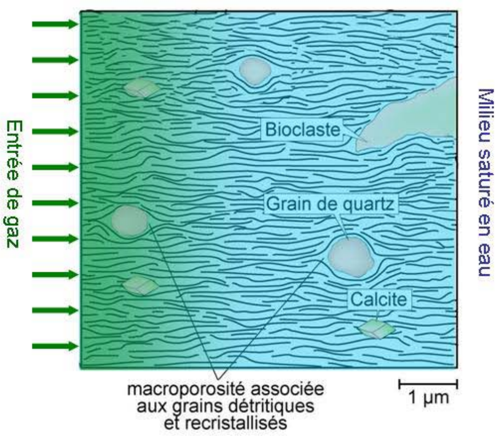

Schéma A : Dissolution et convection/diffusion

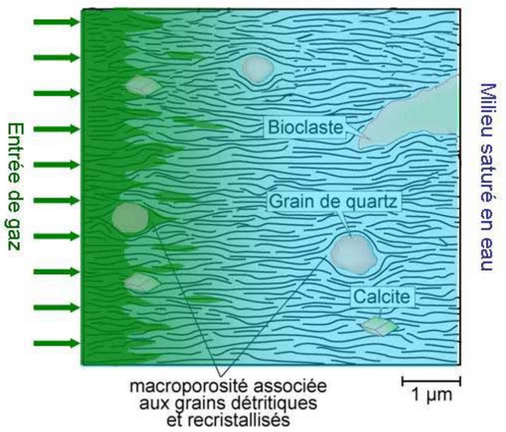

Schéma B : Écoulement bi-phasique

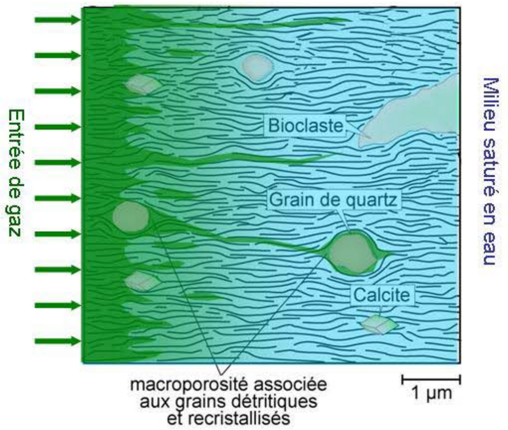

Schéma C : micro-fissuration

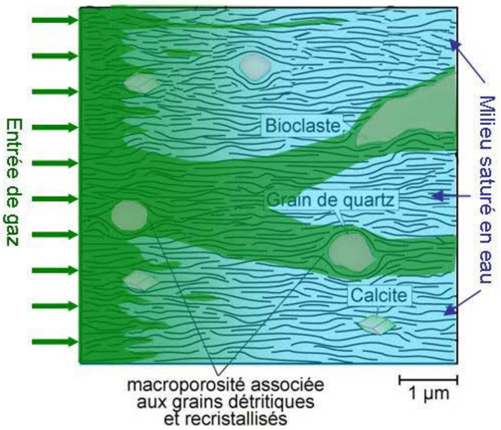

Schéma D : Fracturation

The fraction of hydrogen reaching the drifts moves in them provided the drift seals have not been resaturated to a level in over of 95-97 %. This saturation degree is reached around year 1,000. Thereafter the gas pressure builds up and becomes almost uniform inside a module (module drifts and disposal cells).

This pressure peaks between year 2,000 and 3,000 in the C waste and spent fuel waste repository zones. It is then on the order of 6-7 MPa in the C waste repository zones and 9 MPa for the spent fuel zones because of larger production. In the B waste repository zone the maximum hydrogen pressure (about 7 MPa) will be reached towards year 500.

For the spent fuel zones the value of 9 MPa equals the adopted pressure for microfissuring within the argillites (Inset 6.7). It is higher than the swelling clay pressure reached at the seals and plugs. Thus a network of connected microfissures appears in the module seals (in the EDZ and/or swelling clay) through which the hydrogen from the spent fuel repository zones migrates to the connecting drifts. The latter offer enough room for expansion for the pressure to drop to values of 5-6 MPa and to prevent an impact of hydrogen production in the spent fuel zone on the B and C waste repository zones.

Parallel to this local transient process that only affects the spent fuel zones, the two-phase transfer continues in the Callovo-Oxfordian (towards the Dogger limestones and carbonated Oxfordian) using the significant repository exchange surface area with the Callovo-Oxfordian offered for hydrogen migration. This two-phase flow affects a maximum area of 40 m of Callovo-Oxfordian either side of the repository around the B and C waste zones and the connecting drifts and shafts (when the gas pressure peaks in the repository zones). The two-phase hydrogen migration front around the spent fuel repository zones will reach the surrounding rocks. This two-phase flow only involves a very low fraction of the porosity and produces only negligible desaturation in the argillites, the degree of saturation remaining above 97 % in the near-field and 99 % in the far-field.

In view of the hydrogen and water fluxes in these surrounding rocks, no significant hydraulic disturbance will be generated in the system and the gaseous hydrogen will rapidly travel in dissolved form into the carbonated Oxfordian and the Dogger limestone (Talandier, 2005). The hydrogen fraction reaching the surrounding rocks in dissolved form around the whole of the repository, will remain in this physical state. All the hydrogen dissolved in this way in the surrounding rocks is mobilized and diluted by advection-dispersion.

- **From years 2,000-3,000 to year 100,000: hydrogen pressure drops**

After 2,000-3,000 years, the volume for hydrogen expansion offered by the Callovo-Oxfordian with two-phase flow promotes hydrogen dissolution diffusion.

These two processes explain with the gas pressure drops at this point in time in the repository although production fluxes are still high and continue to be until years 4,000-5,000.

Beyond that point, the production fluxes in C waste disposal cells and spent fuel disposal cells drops sharply (Inset 6.1). By this time the hydrogen pressures have dropped by 0.5-1 MPa in the C waste repository zones and spent fuel disposal cells.

The drop in hydrogen production around year 5,000 in the C waste and spent fuel disposal cells and year 500 in the B waste disposal cells halts the two-phase advance of the hydrogen in the Callovo-Oxfordian towards the surrounding rocks and marks the start of return to total saturation of the repository. Beyond that date, the dissolution-diffusion takes over as the dominant mechanism of hydrogen migration towards the surrounding rocks.

It then takes a few tens of thousand years for the whole of the Callovo-Oxfordian to return to a degree of saturation in over of 99 %.

- **Beyond the year 100,000: the repository is totally resaturated and reaches a new state of hydraulic equilibrium**

It takes a hundred thousand years or so for the drifts to reach a water saturation in over of 90 %. It is estimated that it takes an additional few tens of thousands of years for the saturation to reach 95-97 %. Thereafter a new hydraulic state of quasi equilibrium is established in the repository and the surrounding Callovo-Oxfordian layer. During this period the hydrogen continues to evacuate by dissolution-diffusion. It is only after several hundred thousand years after the repository closure that all the hydrogen will have been evacuated to the surrounding rocks.

6.3.2.5 General pattern of the water flows during hydrogen transfer

The above paragraphs have described the mechanisms that lead to hydrogen transfer in the repository and the Callovo-Oxfordian layer. These transfers have implications for the water flows in and around the repository and for the resaturation kinetics of the various structures and the Callovo-Oxfordian formation. It is possible to construct a time series for water fluxes that broadly affirms the time series for hydrogen transfer as presented above.

- **During the operating phase**

In the case of the drifts and B waste disposal cells the flow pattern is generally convergent from the Callovo-Oxfordian to the structures because of the hydraulic head drop and ventilation-induced desaturation. During that time, the "negligible" fraction of hydrogen produced in the disposal cells migrates towards the drifts and is evacuated by ventilation.

- **After repository closure and until hydrogen pressure peaks in the repository: years 2,000-3,000 for C waste and spent fuel zones and year 500 for the B waste zone.**

In the repository near-field the interstitial water pressure of the Callovo-Oxfordian evolves with the hydrogen pressure: at the disposal cell walls it reaches a maximum value of about 6 MPa for C waste by year 3,000, 8 MPa for spent fuel by year 2,000 (Figure 6.3.9), and 6.5 MPa for B waste by year 500. Subsequently it decreases in the same way as the hydrogen pressure. During that phase, flows are divergent around the disposal cells but remain very slow. The hydraulic gradients created in the Callovo-Oxfordian layer in very near-field (for a few meters) may reach maximum values on the order of 20 m/m in spent fuel zones and 6 m/m in B and C waste zones. Low overpressures are created in the Callovo-Oxfordian further away than these first few meters, they are always less than 0.5 MPa and, in most cases (particularly zones B and C), below 0.1 MPa.

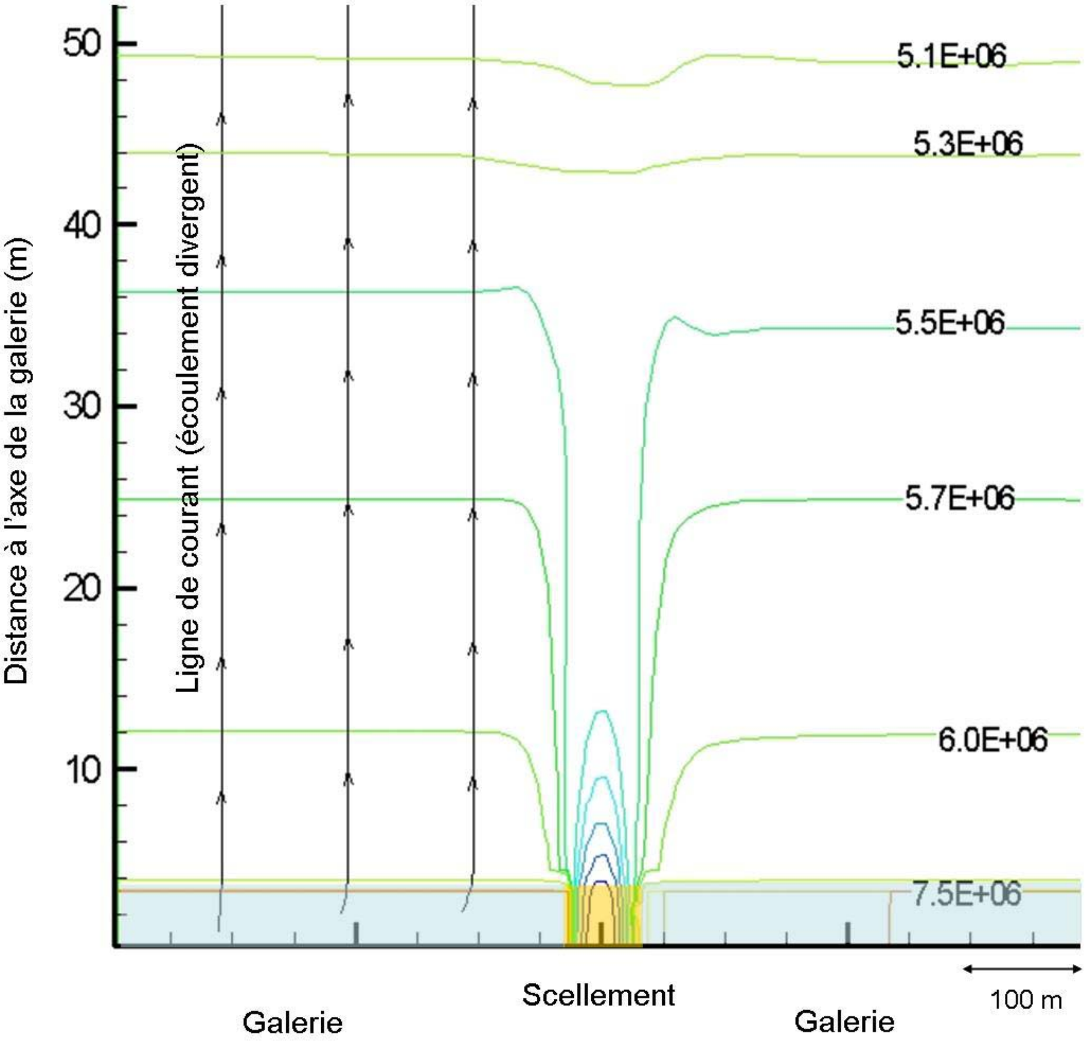

Figure 6.3.9 *Isopressure curves at peack pressure (about year 2,000) of water in the Callovo-Oxfordian around the drift of a spent fuel repository module. The water flows are divergent from the drift to the argillites. The ordinates scale in this figure is expanded by a factor of 15*

The hydrogen does not prevent resaturation of the seals and plugs inside the repository. When it migrates inside the drifts the hydrogen is likely to temporarily cause the back-fill water to move along the drift centre lines. However, given the elongated design of the drifts and the presence of seals, this will be of minor importance compared with the flows in the direction of the Callovo-Oxfordian.

The C waste disposal cells and spent fuel disposal cells are resaturated after the first hundred years or so.

Because of the hydrological characteristics of the argillites and swelling clays the production of hydrogen has no influence on how their saturation evolves (Inset 6.5).

At the end of this period all the repository seals are resaturated and the saturation degree of the Callovo-Oxfordian is in over of 97 % in the near-field and 99 % in the far-field.

- **After years 2,000-3,000 and up to year 10,000: the removal of hydraulic overpressure linked to hydrogen**

The hydraulic overpressures due to gas in the Callovo-Oxfordian and around each repository zone gradually reduce as hydrogen pressures drop. They will have disappeared for the spent fuel, C waste and B waste zones by year 9,000 (Figure 6.3.10), year 7,000 and a few thousand years respectively. From then on the flows will converge towards the repository and the generalised full repository resaturation process can begin. It will primarily involve the B waste disposal cells and the drifts. At the end of this period, the degree of saturation in the argillites (including near-field) will have exceeded 99 %.

It is recalled that during this period, the hydrogen is rapidly moving towards equal pressure inside each repository zone and no longer drives the displacement of water inside the repository.

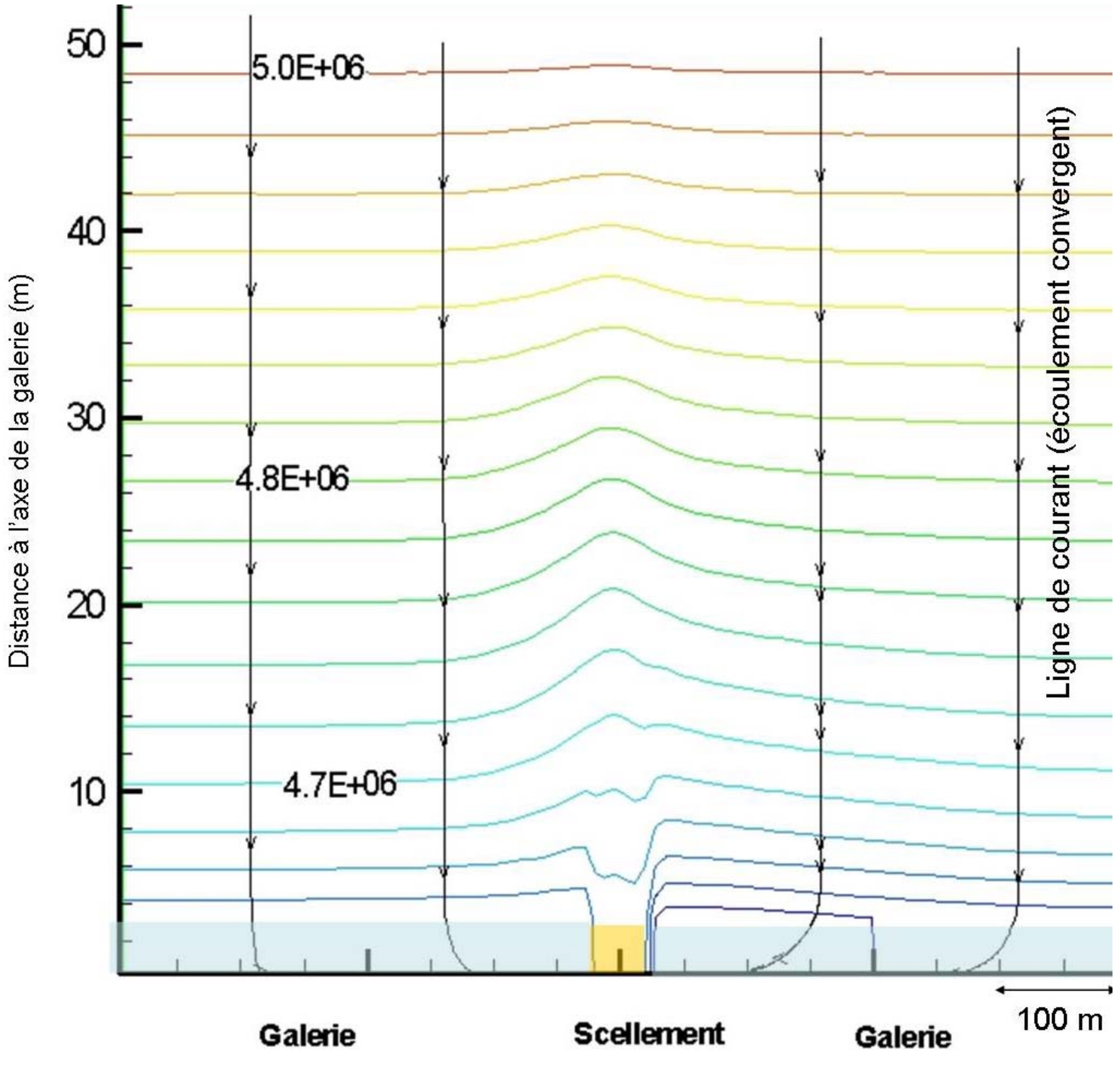

Figure 6.3.10 *Isopressure curves of water in the Callovo-Oxfordian around a drift of a spent fuel repository module (at about year 9,000). The water flows are convergent towards the drift. The ordinates scale in this figure is expanded by a factor of 15*

- **Beyond the year 10,000: a new hydraulic equilibrium is reached**

General pattern

The flows converge from the Callovo-Oxfordian towards the repository until a degree of saturation in over of 97 % is reached in the back-fill and B waste disposal cell components. (Figure 6.3.7). The water flows are weak because of the low permeability in the Callovo-Oxfordian and amount to one litre per year per linear metre of drift at the most. This slow kinetics combined with the effect of the hydrogen imposes resaturation timescales (S>97 %) in the drifts of the order of 200,000 years after repository closure. In the case of B waste disposal cells, similar characteristic resaturation timescales are retained.

Return to hydraulic equilibrium is almost concomitant with this resaturation process. Thus it is reached approximately 200,000 years after repository closure. Thereafter the flow patterns in the repository and Callovo-Oxfordian in the region of the repository are directly above (i) the hydraulic conditions at the limits imposed by the surrounding rocks and (ii) the permeability levels of the repository components, primarily the plugs and seals.

These boundary conditions impose an ascending vertical gradient from the Dogger limestone to the carbonated Oxfordian for most of the transposition zone. The repository drains part of the ascending water flow created by the natural gradient estimated at a few m^3 per year. The horizontal flows in the repository are limited by the presence of seals, with their low permeability (about 10^{-11} $m.s^{-1}$ and a maximum of 10^{-10} $m.s^{-1}$), so that only roughly one hundred litres of water at the most travel towards the carbonated Oxfordian via the shafts (Figure 6.3.11). Most of the flow drained by the repository is restored to the carbonated Oxfordian through the Callovo-Oxfordian layer (Figure 6.3.12).

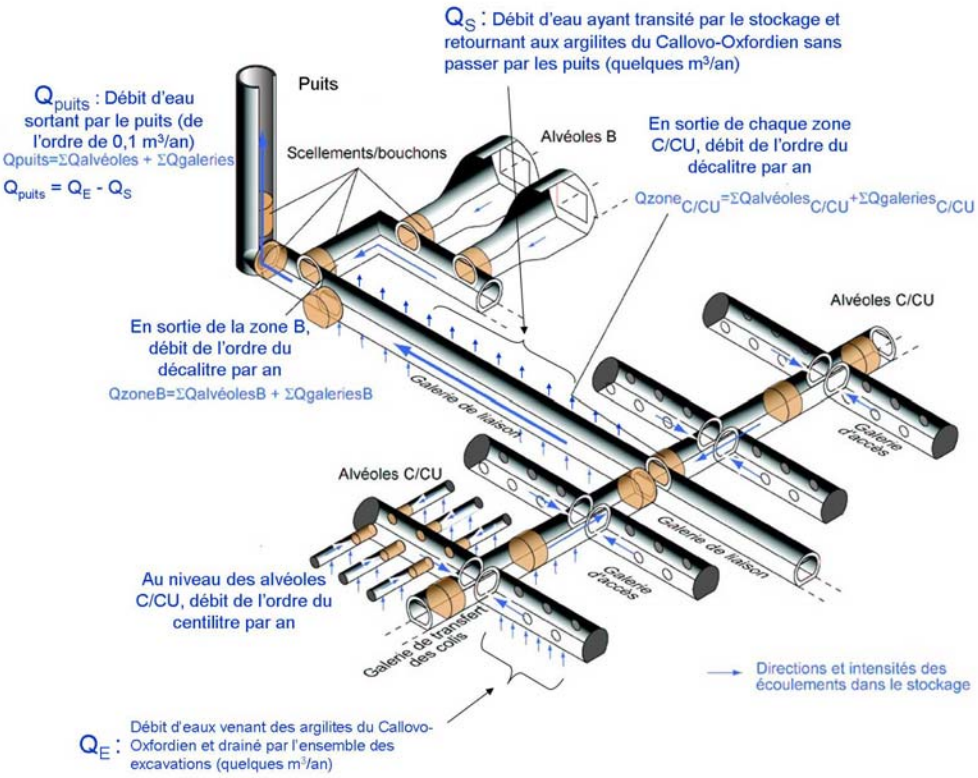

Figure 6.3.11 *Diagram of the water flow at the scale of the repository following its total resaturation*

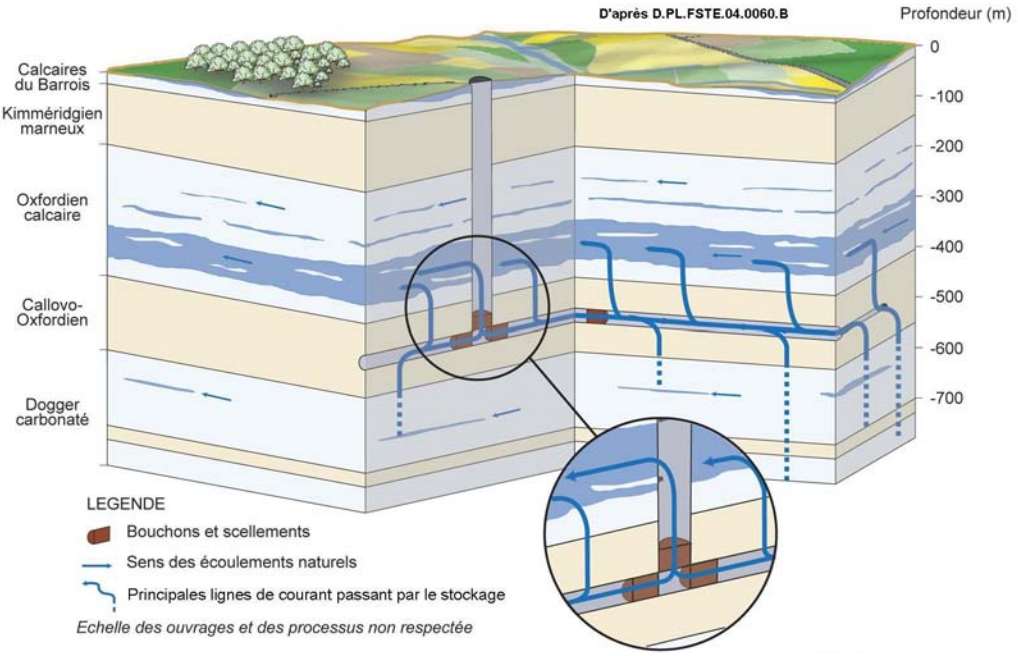

Figure 6.3.12 *Example of water flow lines crossing the repository after return to hydraulic equilibrium: Most of the flow lines travelling through the repository join the Callovo-Oxfordian argillites and do not end up in the shaft.*

The influence of geomorphological evolution and creep on achieving a new hydraulic equilibrium (cf. § 9)

The hydraulic heads in the surrounding rocks of the Callovo-Oxfordian will be influenced by geomorphological evolutions and particularly by erosion. During this evolution, the absolute values of vertical hydraulic head gradients across the Callovo-Oxfordian will gradually rise from a maximum value of about 0.1-0.2 $m.m^{-1}$ to a maximum value of about 0.3-0.4 $m.m^{-1}$ over the transposition zone. This modification of hydraulic head loads will not be felt until after 300,000 years have elapsed, that is at a date later than the expected return to hydraulic equilibrium. Thus they will have no effect on any of the phenomena described above, particularly that of reaching hydraulic equilibrium.

The back-fill will have reached a quasi-saturated state (S>97 %) after about 200,000 years. At that date, the rate of creep will have become very slow (about 10^{-15} s^{-1}), creep of the argillites will thus not be sufficient to create significant overpressures inside the drifts. Overpressures will be less than 0.01 MPa and thus have a very minor influence on the flows in the repository and at the scale of the layer (Wendling, 2005).

Interactions between the hydraulic transients and the natural overpressure in the Callovo-Oxfordian

Initially there is an overpressure of a few tenths of a MPa in the Callovo-Oxfordian attributable to an osmotic effect. This overpressure exists throughout the thickness of the Callovo-Oxfordian (Figure 3.2.1). None of the processes that come into play during the hydraulic transients is likely to alter the water-rock balances of the Callovo-Oxfordian, particularly beyond the first few meters from the repository, and thus the initial overpressure is unlikely to change in profile, but remain constant over time.

The latter will generally present a weaker osmotic potential than that of the Callovo-Oxfordian by virtue of the materials that make up the repository (Figure 6.3.13). However as the osmotic pressure remains constant in the Callovo-Oxfordian, the osmotic discontinuity thus created will have no impact on the water flows and in particular on those than come into play during the hydraulic transient.

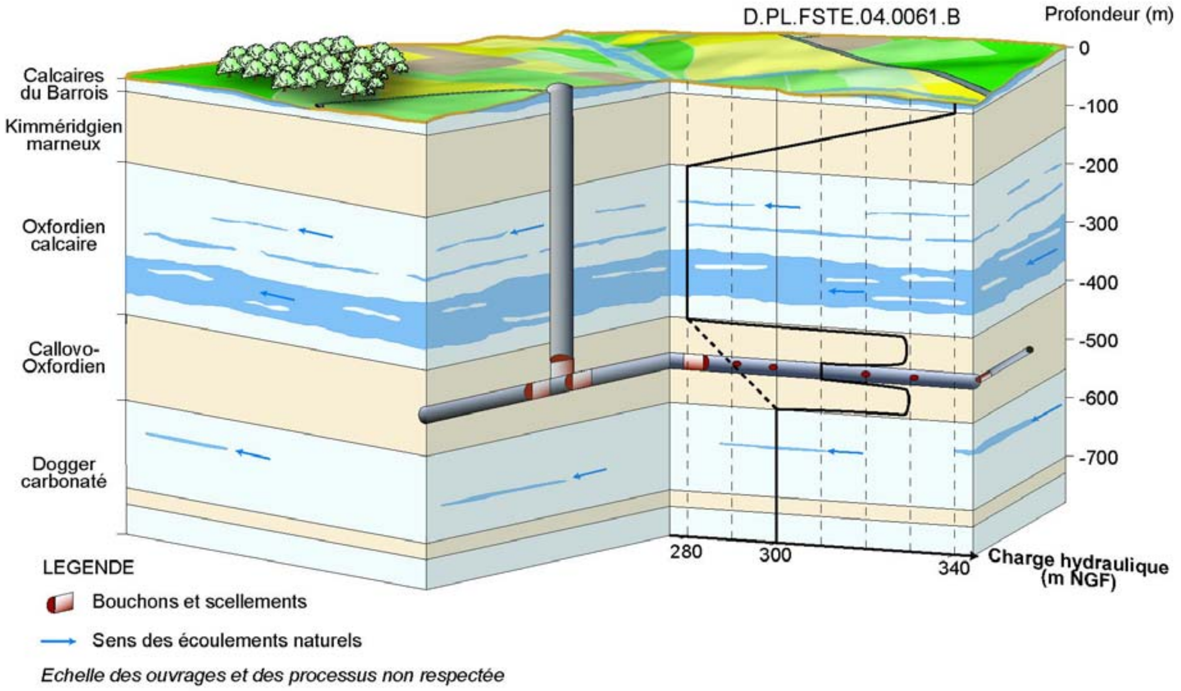

Figure 6.3.13 *Diagram of the hydraulic heads in the geological layers after return to hydraulic equilibrium following the impact of the repository*

6.3.2.6 Special elements in the hydraulic evolution of the disposal cells

The general description of both the hydraulic transient in the Callovo-Oxfordian argillites at the scale of the repository and the influence of hydrogen can be developed in more detail at the scale of various structures to take allowance of their specific characteristics (emplacement clearance, characteristic dimension, filling material).

- **B waste disposal cells**

The analysis of the corrosion-induced hydrogen production did not consider the explicit coupling between the corrosion kinetics and the water degree of saturation. As previously stated, where environments are highly desaturated (S<30-40 %), the corrosion rate is significantly lower (by a factor of 4-5 for S = 30-40 % as against S>90 %). When the B waste disposal cells are closed they are highly desaturated. However, as modelling indicates (Talandier, 2005), hydrogen production in the disposal cells in these water saturation conditions would be low but sufficient to sustain these desaturation conditions. Thereafter the general pattern of hydraulic evolution in the disposal cells as previously described would broadly hold true, but the timescales involved would be longer.

There are emplacement clearances between and inside the repository packages in the B waste disposal cells, although they are minimised by design. With dimensions in the centimetre to several centimetre range, they represent macroporosity in which liquid water cannot start to appear unless the relative hygrometry is around 100 %. The existing macroporosity in specific primary waste packages such as those containing compacted waste (reference package B5) as opposed to cemented packages (reference package B3) has to be added to these gaps.

In view of the existence of this macroporosity, resaturation will not be uniform at the scale of the cell. Capillary forces are weak in the macropores, thus gravity dominates, forcing the liquid water to concentrate at the bottom of the waste packages and disposal cells. Water saturation remains very low in the gaps throughout the hydrogen production phase and until most of the hydrogen has been evacuated by dissolution and diffusion at around a hundred thousand years. Thus the internal part of the B waste disposal cell generally saturates from bottom to top, as illustrated in Figure 6.3.14. Depending on the existence or otherwise of macroporosity in the primary waste packages, this same phenomenon may be found in disposal and primary waste packages. Thus by way of example, the primary packages inside B5 disposal packages, are at a low water saturation degree of about 20-30 % for several tens of thousand years. This contrasts with the primary packages containing cemented waste held in B3 disposal packages, which are at a higher water saturation degree of about 80 % for the same period. These differences in the evolution of the saturation degree of B waste disposal packages are illustrated on the time chart in Figure 6.3.15. The water saturation of the various macroporosities will thus be obtained at a later stage as soon as the lining concrete or the concrete of the disposal packages have reached a degree of saturation of almost 100 %, enabling the water to seep into these macroporosities and gradually fill them with water.

The different characteristic hydraulic evolution timescales of the B waste disposal cell components are represented on the time chart in Figure 6.3.15 and in Figure 6.3.16.

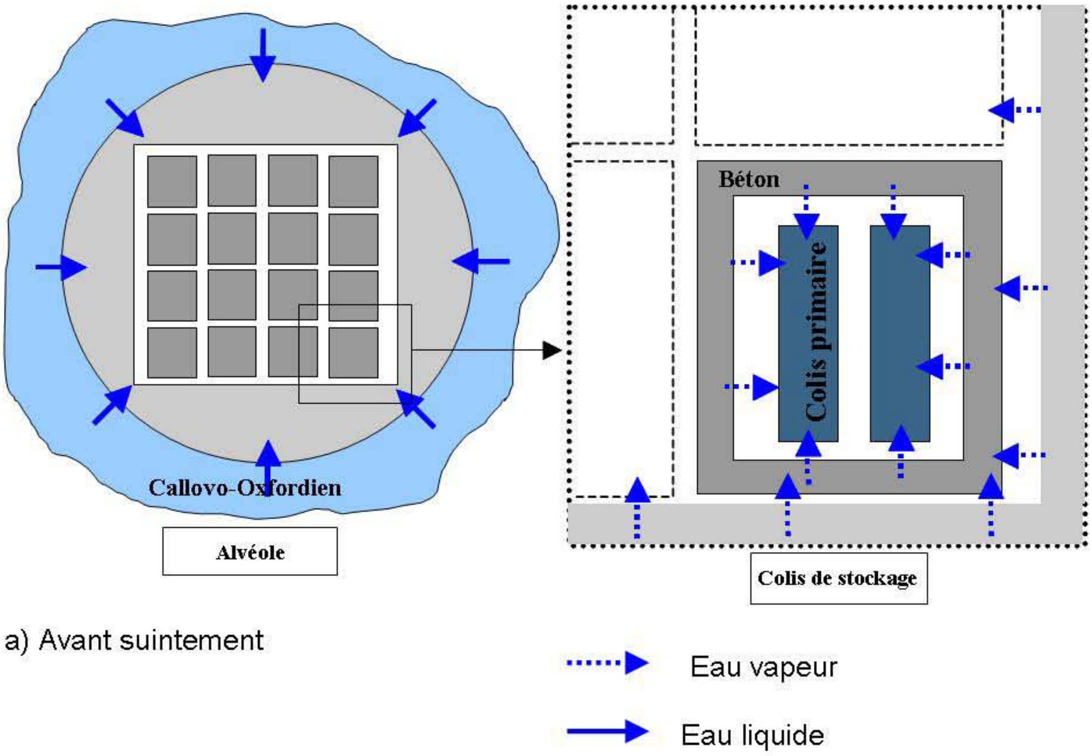

a) Avant suintement

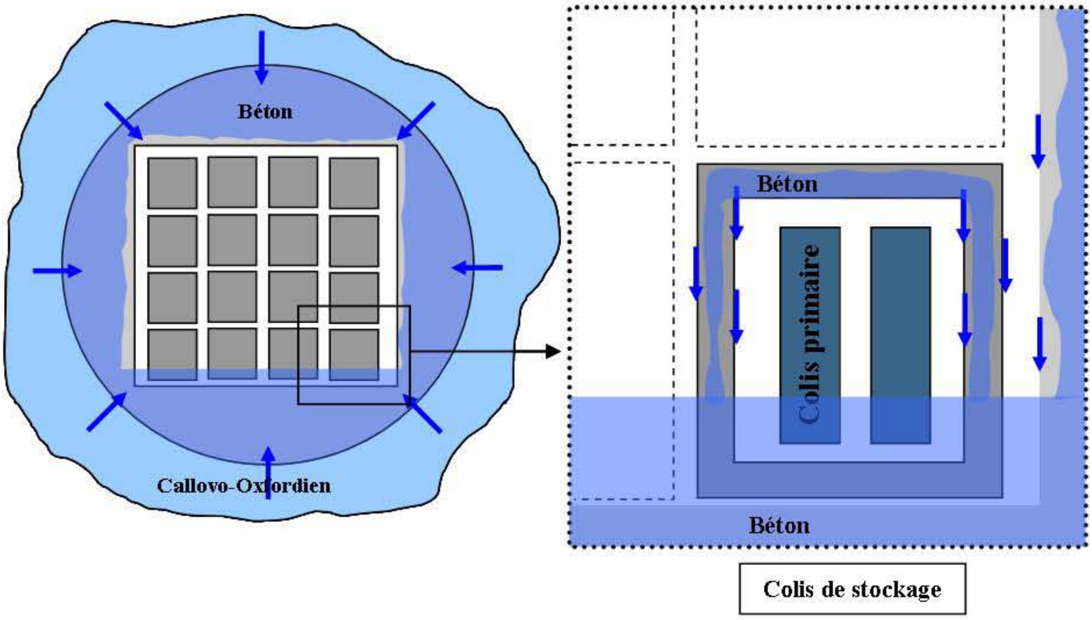

b) Après apparition d'eau liquide dans les jeux (suintement)

Figure 6.3.14 *Diagram of the resaturation of a B waste cell. Evolution of the type of water flow before and after seepage into the emplacement gaps. Zoom is on the individual stacks of waste packages*

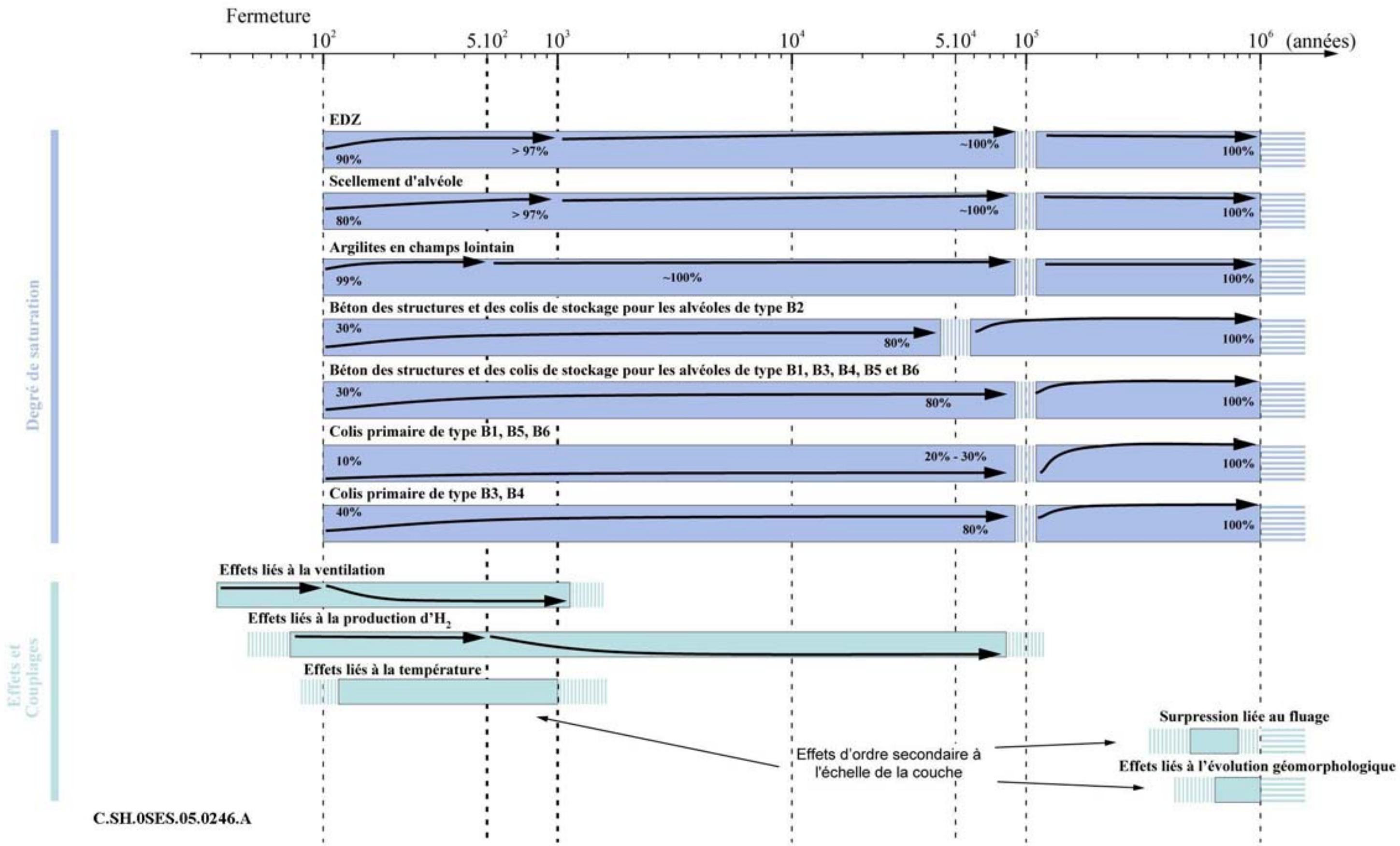

Figure 6.3.15 *Time chart giving the degree of saturation in the various components of a B waste repository module and the associated effects and couplings (on the basis of the conventional century-long construction/operating/repository closure time chart)*

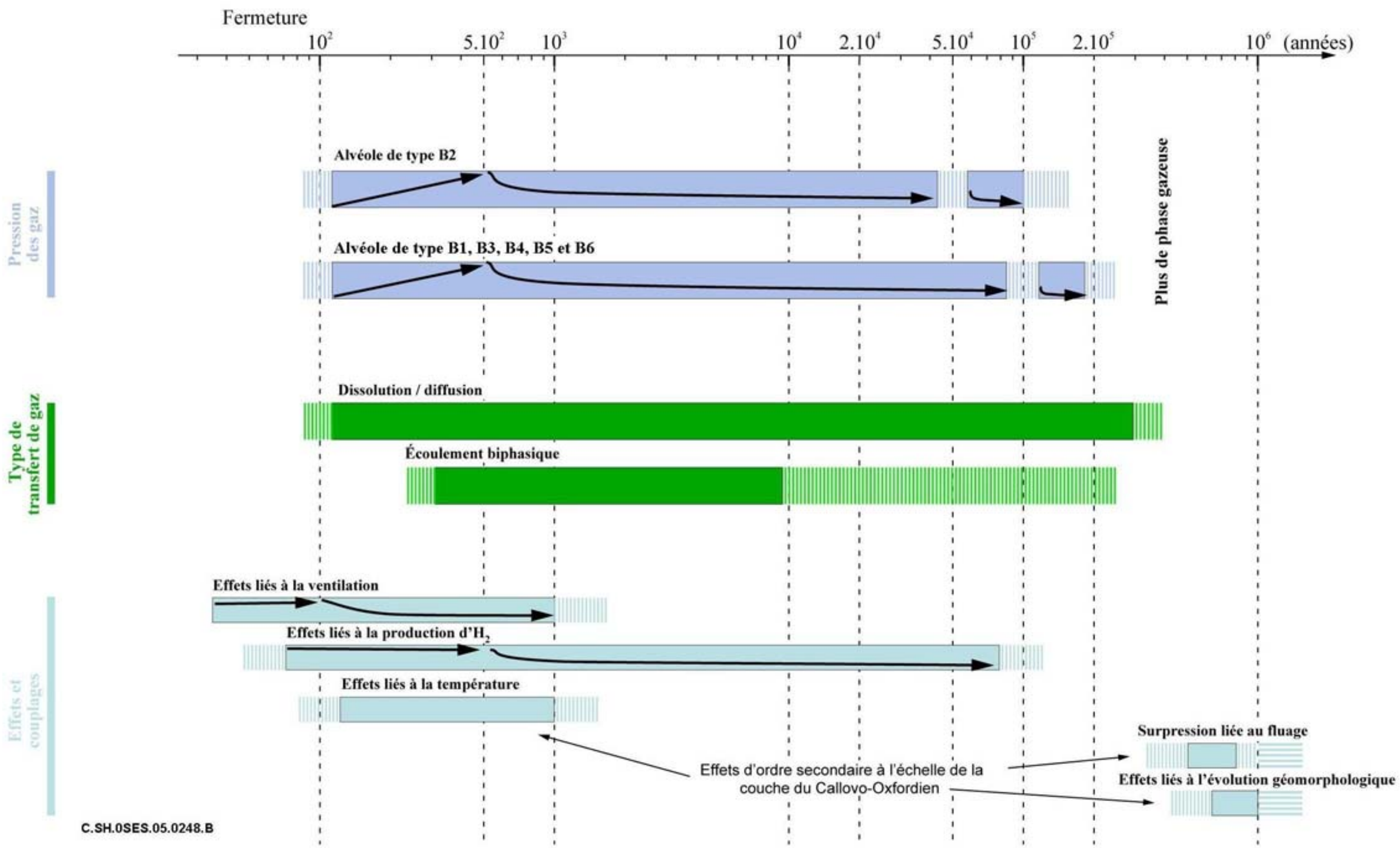

Figure 6.3.16 *Time chart giving the hydrogen gas pressure in the various components of a B waste repository module and the associated effects and couplings (on the basis of the conventional century-long construction/operating/repository closure time chart)*

- **C waste disposal cells and spent fuel disposal cells**

The inside of the lining does not corrode as long as it remains leak tight, that is for about 1,000-1,500 years (cf. § 8). During that period the internal part of the lining and the metal containers are subject to very little corrosion. Metal container corrosion is initiated once the lining breaks. Their discharge of impermeability is specified at 4,000 years for C waste and 10,000 years for spent fuel. The expanding products of corrosion gradually fill the voids in the packages. However these voids are not totally saturated with water because of the production of hydrogen. Water saturation inside the packages gradually increases over a few thousand years. This state remains constant for about ten thousand years until hydrogen production has reduced sufficiently for hydrogen dissolution and diffusion to predominate. Thereafter the gas pressure gradually drops inside the cell. The return to total resaturation inside the packages (S=100 %) is initiated and takes at least several tens of thousand years to complete.

The different characteristic timescales of hydraulic evolution the spent fuel disposal cell components are given in the time charts in Figure 6.3.17 and in Figure 6.3.18.

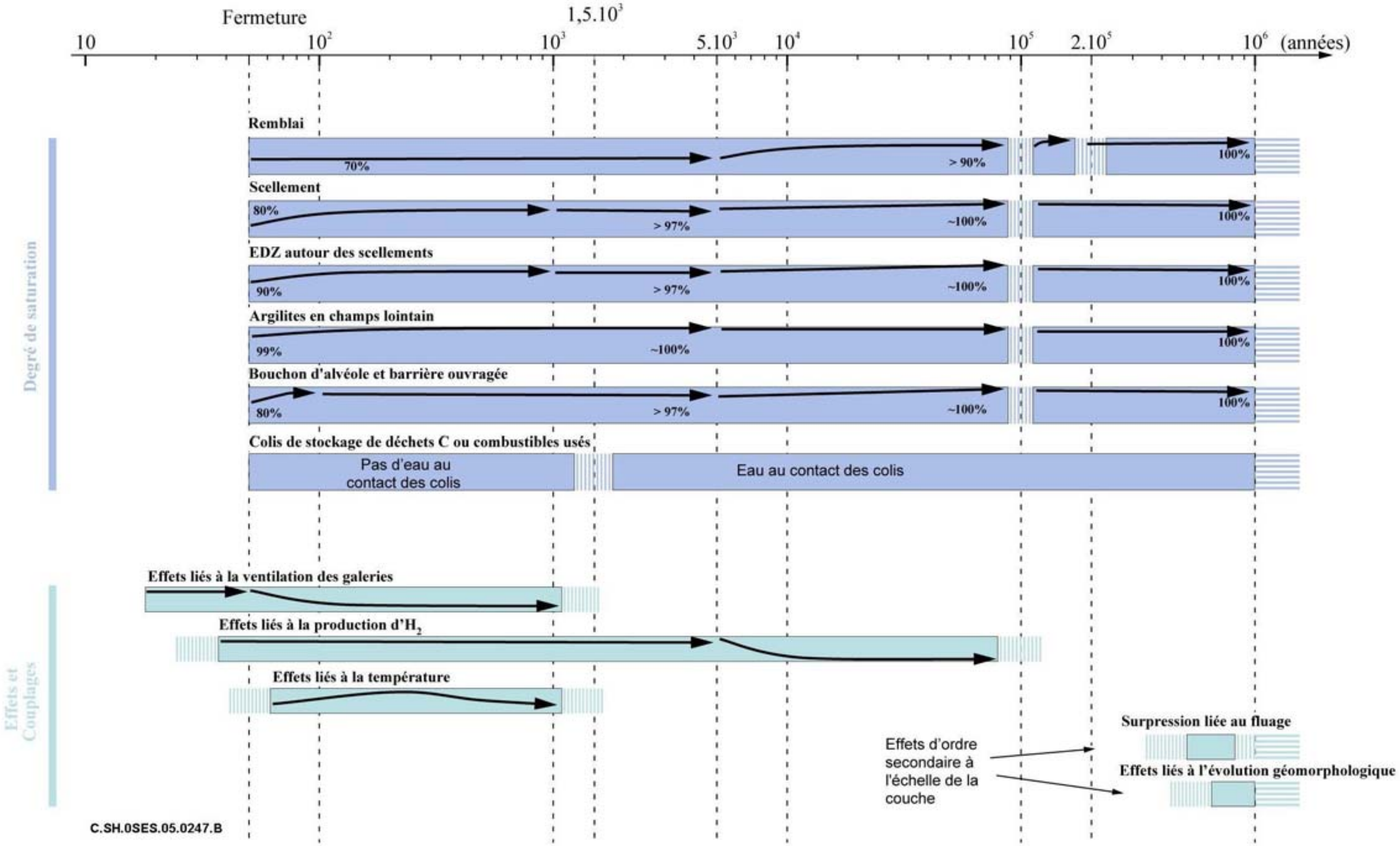

Figure 6.3.17 Time chart giving the water saturation in the various components of a C waste or spent fuel repository module (on the basis of the conventional century-long construction/operating/repository closure time chart)

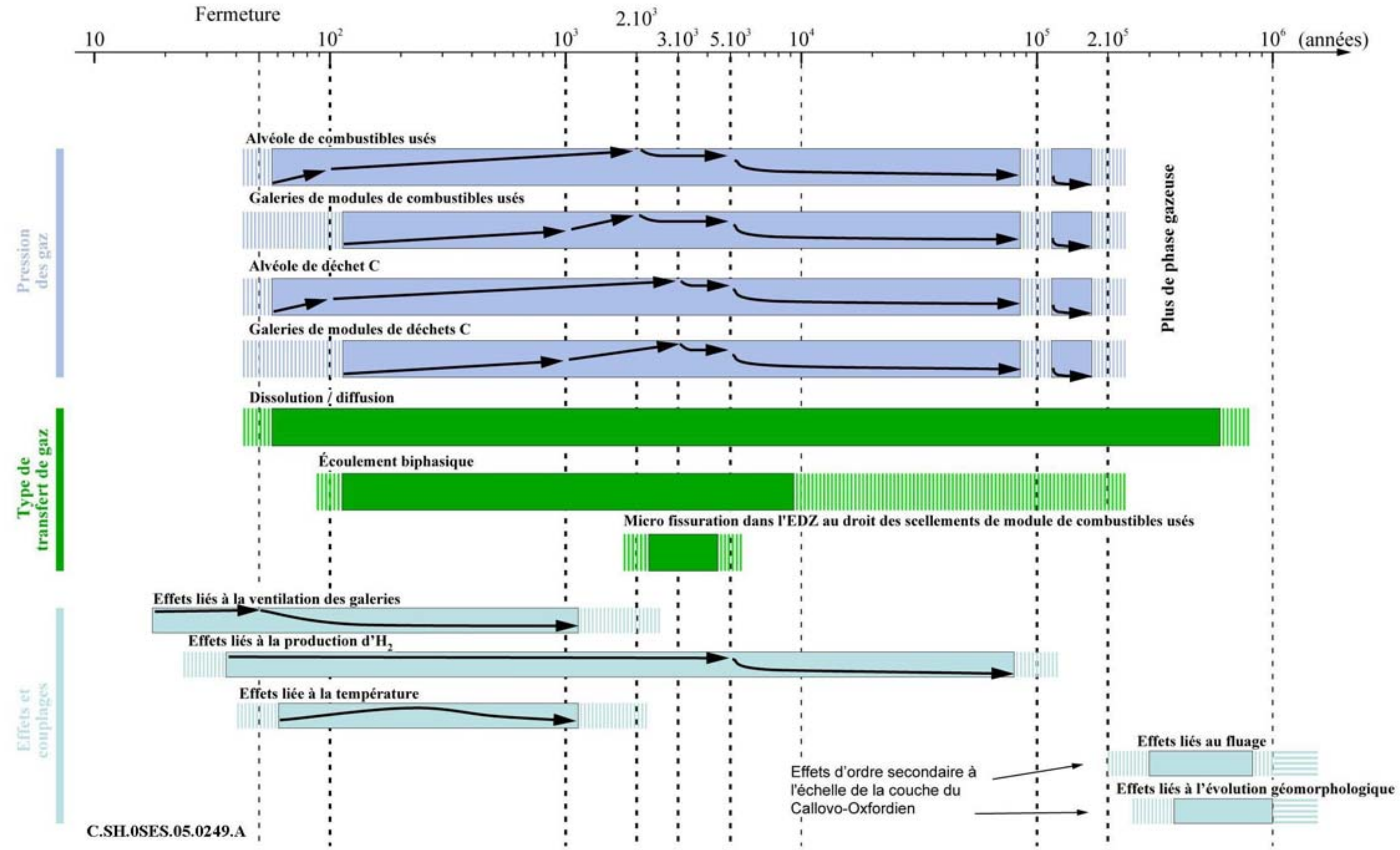

Figure 6.3.18 *Time chart giving the gas pressure in the various components of a C waste or spent fuel repository module (on the basis of the conventional century-long construction/operating/repository closure time chart)*

6.3.3 Solute transport in the repository and Callovo-Oxfordian until the return to a new hydraulic equilibrium

Initially, diffusion is the dominant solute transfer mode in the Callovo-Oxfordian (§ 3.3.1.7). The previous chapters show that the flows in the repository reach a state of equilibrium after 200,000 years. There are transient phenomena that induce variations in the water flows and their direction in the repository and Callovo-Oxfordian in the interim. These modifications are likely to influence the solute transport conditions and directions in and around the repository.

Four time stages can be identified to describe the hydraulic influence of the repository at the scale of the Callovo-Oxfordian geological layer.

- A first stage when the hydrogen produced by corrosion has no significant effect on the flows. This stage includes the operating period and a few centuries at the most after repository closure. When this stage starts, the argillites of the drifts and B waste disposal cells are highly desaturated in the EDZ fractured zone and hence the flows broadly converge towards these structures. The induced hydraulic head gradient values may be very much higher than those of natural gradients. In the case of C waste disposal cells and spent fuel disposal cells, this phase is marked by the saturation of the engineered barriers.
- A second stage that covers the pressure build-up phase (up to 2,000 years) and that results in the dissipation of the overpressure in the Callovo-Oxfordian. This stage lasts a maximum of 10,000 years. It is characterised by the near-field pressure build-up in the Callovo-Oxfordian. For about 4,000-5,000 years the divergent flows of the repository set in. The hydraulic gradients created in the Callovo-Oxfordian layer in the near-field may reach maximum values on the order of 20 $m.m^{-1}$ in the very near-field (4-5 m) of the spent fuel zones and 6 $m.m^{-1}$ in B and C waste zones. Low overpressures are created in the Callovo-Oxfordian further away than these few meters, and are always less than 0.5 MPa and for zones B and C in particular, are less than 0.1 MPa. The mean Peclet number for solute transfer - calculated between the repository and the top of the Callovo-Oxfordian - is 1.6 at the maximum for anions (for spent fuel), hence diffusion and advection are codominant. The mean Peclet numbers calculated for cations are always less than 1. The Peclet numbers calculated for anions for the B and C waste zones are equal to 1 at the most (Inset 3.9). However the hydrogen-related hydraulic gradients fall to such an extent within a few hundred years that diffusion soon becomes the dominant process again. These gradients disappear completely after 9,000 years for spent fuel, 7,000 years for C waste and a few thousand years for B waste. The hydrogen-related hydraulic overpressure will thus have no effect on the radionuclides released in solution by the spent fuel waste packages because the containers remain leak tight for at least 10,000 years. A 4,000-year period of impermeability is specified for the C waste overpacks. However the phenomenological analysis (cf. § 7 and 8) demonstrates that overpack integrity could be maintained for over 10,000 years. Under these conditions, and as in the case of spent fuel, no radionuclides would be released during the period marked by the existence of hydraulic overpressure. If a 4,000-year long leak tight period is considered, the hydrogen-related hydraulic overpressure will already have started to drop by the time the radionuclides are released and the drop will be even more pronounced after 5,000 years. The transfer of radionuclides released by C waste packages at year 4,000 in these conditions would be affected by hydrogen overpressure. However, over the maximum period of 3,000 years between the beginning of release (after year 4,000) and the end of the overpressure (before year 7,000), the increase in the transfer distance of the released radionuclides would only be into the tens of centimeters at the most.

Solute transport would thus generally remain diffusion dominanted at the scale of the whole Callovo-Oxfordian layer, and the repository would not act as a significant transfer path for radionuclides in solution. More specifically in the case of B waste disposal cells, which would not be fully saturated, any radionuclide release and transfer in solution throughout that period would be limited or prevented.

- A third phase, corresponding to the gradual evacuation of hydrogen by dissolution and diffusion. Until total saturation is achieved (200,000 years for S>97 % in the back-fill), the flows are convergent towards the repository and very limited. The hydraulic gradient values are generally low.
- The fourth phase is characterised by the establishment of a new state of hydraulic equilibrium with similar hydraulic gradients in the repository and Callovo-Oxfordian to compared those that initially prevailed. It is during this phase that the effects of geodynamic evolution start to make themselves felt. Through erosion and the incision of the valleys, the vertical hydraulic gradients across the Callovo-Oxfordian can double at some points in the transposition zone. Nonetheless diffusion broadly remains dominant in the Callovo-Oxfordian argillites.

A transient effect related to the thermal load may also have an impact on the conditions of solute transfer.

- The temperature rise results in a drop of the water density which implies hydraulic overpressure around the exothermic waste zones in the Callovo-Oxfordian. The induced load gradient values may exceed those of natural flows considerably, particularly in the region of the spent fuel disposal cells. However this overpressure is limited in time, that is a few centuries, while temperature rises in the argillites. Because of their respective leak tight periods of at least 4,000 years and 10,000 years, no radionuclides are released by the C waste and spent fuel packages during this time. For the record the additional distance travelled by the solutes subjected to this effect in the Callovo-Oxfordian would be on the order of one centimetre at the most. Furthermore, the hydraulic overpressure caused by the thermal load would not overlap the overpressures created by the hydrogen because it will have disappeared by the time the latter becomes significant.
- For several decades the high thermal gradients in the near-field of the repository imply a significant Soret effect at the walls of the spent fuel disposal cells. As in the case of the hydraulic overpressure relating to temperature rise, the radionuclides would not be affected as they will not be released by the waste packages until at least year 4,000 for the C waste and year 10,000 for the spent fuel. Furthermore this effect would not increase the solute transport distance significantly over that travelled in pure diffusion (Coelho, 2005).
- The thermal load that prevails for several tens of thousand years in the region of the C waste disposal cells and spent fuel disposal cells, induces joint increases in the diffusion coefficient and permeability to water. Nonetheless diffusion remains the dominant process. Because of the increase in the diffusion coefficient during this period, the distance travelled by diffusion is higher than that at the initial geothermal temperature, but the increase in distance would be a few meters at the most.

Lastly, in addition to transport in the form of elements dissolved in water, radionuclides can be transported through advection by colloids. However, the dominant nature of diffusion compared to advection and the role of colloid filter ensured by the Callovo-Oxfordian and bentonite-based structures (cell plugs, drift and shaft seals and EB cores) result in highly restricting the possibilities of radionuclide transfer by colloids.

6.3.4 Conclusion

The following points are relevant to our conclusion:

- Neither the thermal nor the hydraulic influences of the repository modify the dominance of diffusion over the other transport modes at the Callovo-Oxfordian scale (Figure 6.3.19). Codominances shared by diffusion and advection originating from the various processes mentioned above could exist over periods no longer than a few thousand years and mainly in the near-field. They would primarily affect the C waste and spent fuel zones, and they would peak before the impermeability of the metal containers is compromised.

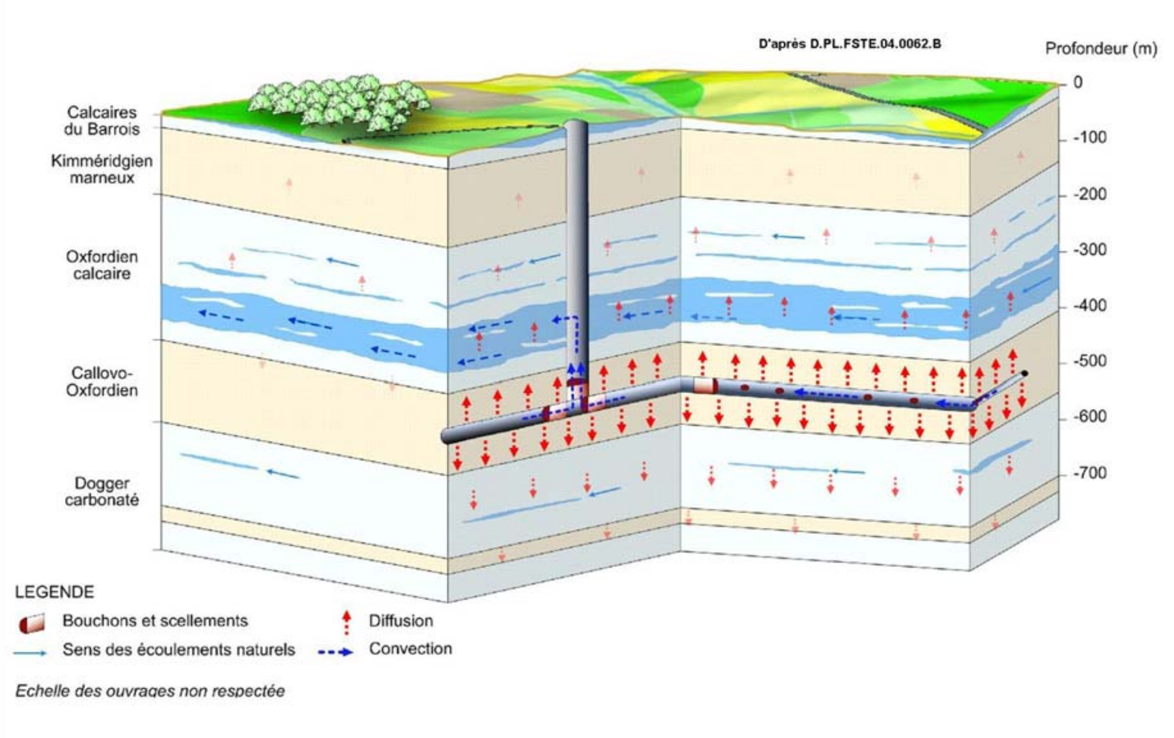

Figure 6.3.19 *Diagram of the solute transport modes from the repository, at the scale of the Callovo-Oxfordian and its surrounding rocks on the Meuse/Haute-Marne site, and after return to hydraulic equilibrium*

- Diffusion broadly remains dominant inside the repository regardless of the phases quoted above. When the hydrogen pressure builds up inside the drifts, a very transient convective transport component could be established. However this convective component would remain fairly low in comparison with the diffusion and radial dispersion towards the Callovo-Oxfordian (Figure 6.3.20) because the back-fill would not be fully saturated (S = 70-80 %) and because of the drift design (elongated and narrow diameter).
- With specific reference to the inside of the disposal cells:

In the case of B waste disposal cells the non-saturated state of the concrete (S<80 %) and waste packages, some of which might even reach degrees of saturation of around 20-30 % is to be noted (for example B5 packages). This would be compounded by the effect of emplacement gaps, which would remain in a state of low saturation (20-30 %). As total waste package saturation generally occurs after 100,000 years, this non-saturated state caused by the corrosion-induced hydrogen could last in some cases for tens of thousands of years. Solute transport out of the waste packages and disposal cells would be very limited over this period under these conditions.

In the case of slightly exothermic B waste (B5 and B2), the temperature field created is too low to produce a significant Soret effect. Similarly the dominance of diffusion over advection would not be weakened by the hydraulic gradient created by the thermal load overpressure in the Callovo-Oxfordian in the region of the disposal cells containing this waste. Furthermore some decades after repository closure diffusion is increased by a factor of 3 at the highest end of the thermal field. The influence of the thermal field decreases over time to become negligible a few centuries after repository closure. The additional distance travelled is about one metre for anions in comparison with diffusion at geothermal temperature at the scale of this time period.

Despite of the production of hydrogen, a high saturation degree is reach in about a century in the C waste disposal cells and spent fuel disposal cells (S>97 % at the plugs and in the engineered barrier in the case of spent fuel). Hydrogen pressure is uniform inside the disposal cells and thus does not influence solute transport within them. Moreover in the case of spent fuel, radionuclides would not be released until after the end of the period during which hydrogen has a significant influence on the water flows and solute transport in and around the disposal cells. As the waste packages are highly exothermic they induce both a Soret effect and hydraulic overpressure that lengthens the convective transport period. A few years after waste package emplacement diffusion increases by a factor of 6-7 at the highest end of the thermal field, which compounds these two effects. Thus diffusion remains dominant throughout this period despite the Soret effect and hydraulic overpressure. The Soret effect diminishes as the temperatures inside the disposal cell even out after a few decades. Hydraulic overpressure lasts a few centuries and the significant influence of the thermal field on diffusion continues for one thousand years at the most for C waste and a few thousand years at the most for spent fuel.

- Water may be displaced in the drifts throughout the very first 2,000 to 3,000-year period of hydrogen migration inside these structures. The longitudinal element of this phenomenon will be very limited given the presence of seals and the design of the drifts. Later on the gas pressure field inside the drifts will be almost uniform and will not permit such displacements. Lastly as the drift back-fill will not be totally saturated (S=70 %) during this early phenomenon (2,000-3,000 years after closure), the convective solute transport rates will remain low particularly compared to diffusion.

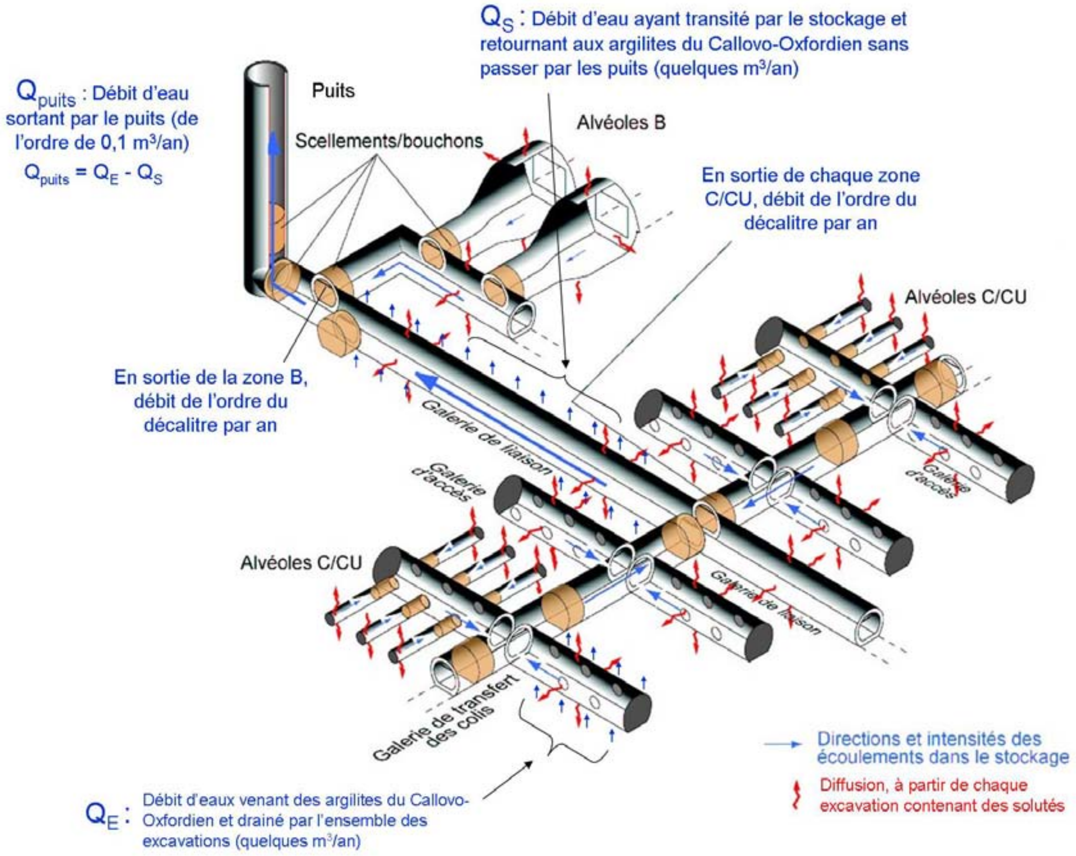

Figure 6.3.20 Schematic representation of water flow rates across the repository and solute migration modes within the repository, after return to hydraulic equilibrium

6.4 Summary on flows and the transfer in dissolved and gaseous form

6.4.1 A framework for chemical and mechanical evolutions in the repository followed by radionuclide release and transfer

The evolution of the flows in the repository and its geological environment contribute to define the framework of chemical and mechanical evolutions and thus that of waste package decay and at least that of the release of radionuclides by the waste packages. When associated with the chemical evolution it determines the mobility of the released radionuclides and their transfer into the biosphere.

1. The presence of water is required to initiate chemical processes. Therefore their propagation over time and space is dependent on hydrodynamics (i.e. water flows) and on the quantities of reagents likely to be transported by the water flows or to be displaced by diffusion in water.
2. The mechanical behaviour of the repository components and argillites also depends on water. This dependence may be direct, as in the case of argillites (particularly the EDZ), disposal cell plugs or seals, whose plasticity and behaviour when ruptured depends on their state of saturation. Alternatively it may be indirect via the chemical processes, as in the case of corrosion that alters the mechanical strength of the steel components of the repository.
3. Radionuclide release primarily results from the chemical and mechanical degradation of the waste packages, and thus indirectly from the hydraulics of the repository. Once they have been released, the future of the radionuclides partly depends on the water flow and solute transport conditions firstly in the repository, then in the Callovo-Oxfordian layer and lastly in the surrounding formations.

The following paragraphs single out the key hydraulic evolution facts that are needed to describe the chemical and mechanical evolutions and in the final analysis radionuclide release and transfer.

6.4.2 Two specific driving factors behind the flows

At the current time (i.e. prior to repository construction), the geological formations at the Meuse/Haute-Marne site and further afield throughout the transposition zone, are at hydraulic equilibrium. The flow over most of this zone ascends from the Dogger limestone towards the carbonated Oxfordian with maximum gradients of the order of 0.2 $m.m^{-1}$. This configuration has been adopted as the reference for the entire water flow analysis. However the water flow is vertical descending directly above the reference position of the laboratory and also to the South-East of the transposition zone. velocity rate of some tens of meters per million years. Solute transport is primarily via diffusion in this very weak flow context and at the scale of the Callovo-Oxfordian layer.

The water flows upstream of the laboratory reference position are primarily horizontal in the carbonated Oxfordian and the Dogger limestone. The permeability levels of these formations are higher than that of the Callovo-Oxfordian, on the order of 10^{-10} $m.s^{-1}$ to 10^{-8} $m.s^{-1}$, so that advection plays a significant role in solute transport as far as the local outlets in the valleys where the surrounding rocks crop out. However downstream of the laboratory reference point part of the flows follows a regional route broadly North-West in orientation.

Starting from the current state of hydraulic equilibrium, the evolution of the water flows in the repository and its geological environment over the next million years is marked by two successive major phases respectively originating from:

- ***hydraulic disturbances engendered by the repository itself***, in particular the desaturation of the argillites in the near-field of the repository during the operating phase and the production of hydrogen through the corrosion of the metals once the disposal disposal cells have been closed;

- ***geodynamic evolutions*** whose effects will become significant after a few hundred thousand years. These primarily take the form of gradual changes to the morphology of the surface, resulting in modification to the water flows in the surrounding rocks of the Callovo-Oxfordian, primarily in the carbonated Oxfordian.

6.4.2.1 Hydraulic disturbances engendered by the repository: a transient that primarily affects the repository and the Callovo-Oxfordian

The considerable thickness of the Callovo-Oxfordian layer and its very low level of permeability contribute to limiting the spatial extent of the hydraulic disturbances engendered by the repository. The latter are mainly restricted to the repository and the Callovo-Oxfordian layer in the near-field, and cover a period on the order of 200,000 years at the end of which a new hydraulic equilibrium is established. At that point the repository is totally saturated (S>97 % in the drifts).

The hydraulic disturbances engendered by the repository last for a timescale comparable with that of other processes such as:

- solute transfer by diffusion that on average lasts several hundreds of thousands of years in the Callovo-Oxfordian layer,
- the chemical degradation of the concrete that lasts several hundreds of thousands of years,
- the evolution of water flows in the surrounding rocks through the geodynamic effect that sets in over one million years and does not become significant until after 300,000 years have elapsed.

6.4.2.2 Hydraulic effects related to geodynamics: continuing evolution over one million years that primarily affects the surrounding formations of the Callovo-Oxfordian

The geodynamic evolutions over the next million years will broadly take the form of gradual erosion of the surface terrain. Their hydraulic effects mainly involve the geological formations overlying the Callovo-Oxfordian layer. They become significant from 300,000 to 500,000 years, namely once the hydraulic disturbances engendered by the repository in the Callovo-Oxfordian layer have diminished. The geodynamic evolutions and their hydraulic effects then continue over the next million years.

6.4.3 Hydraulic evolution of the repository: the involvement of various processes until the return to a new state of hydraulic equilibrium

The repository generates many hydraulic disturbances. They are linked chronologically over time to the sequence of repository construction, operation and closure, then to the hydrogen production through the corrosion of the repository's metal components and finally by the mechanical behaviour of the argillites (creep) vis-à-vis the repository structures.

The modular operation and architecture of the repository combined with a timescale on the order of one to several centuries during which the structures are open (which is short in comparison with the period of hydraulic interaction inside the Callovo-Oxfordian (Inset 4.1)), makes the repository zones almost independent in their hydraulic evolutions, and similar to those of the disposal modules and disposal cells of a single zone. Subsequently the hydraulic history of the repository and the surrounding Callovo-Oxfordian layer can be summarized chronologically for the whole of the repository as follows:

1. The hydraulic head drop around all the structures in the geological formations crossed (overlying surrounding rocks and Callovo-Oxfordian) throughout the construction and operation of the repository.
2. The permanent introduction of air and thus O_2 and CO_2, into the ventilated structures (drifts, shafts, and part of the B waste disposal cells) throughout the construction and operation of the repository.

3. The desaturation of the Callovo-Oxfordian in the immediate periphery of the ventilated structures throughout the construction and operation of the repository giving oxygen access to the argillites (initially reducing prior to the repository construction).
4. Outside the desaturated zone, the transient pressure build-up of the Callovo-Oxfordian around the exothermic waste repository zones (C waste, spent fuel and part of the B waste) because of the temperature rise.
5. After closure of the structures (i.e. of the repository), gradual resaturation of the latter and the Callovo-Oxfordian argillites on their periphery that will have been desaturated during the operating phase. This resaturation is coupled with the production and transfer of hydrogen resulting from the corrosion of metal components (mainly present in the disposal cells), which in contrast to gasless resaturation postpones the return to full saturation.
6. The return to saturation of the whole repository accompanied by gradual evacuation of the hydrogen through the Callovo-Oxfordian layer and/or the repository to the carbonated Oxfordian.
7. The low hydraulic transient build-up in the structures, once saturated, because of the slow creep in the argillites on their periphery.
8. The return to a new state of hydraulic equilibrium in the repository and Callovo-Oxfordian layer. This state is controlled by the hydraulic head fields in the carbonated Oxfordian and Dogger limestone, and the permeability levels of the various repository structures, primarily the drift and shaft seals.

6.4.3.1 Hydraulic impact of the repository on the upper surrounding rocks: a local phenomenon limited to a few centuries or millennia.

The shafts are leak tight as they cross the Tithonian, and thus have no hydraulic impact on that formation. The water flows in the other surrounding formations, Kimmeridgian marls and carbonated Oxfordian formations are so weak that the shafts crossing them do not need to be leak tight during the operating phase. A hydraulic head drop is thus induced in these formations by the absence of impermeability, possibly coupled with desaturation depending on their hydraulic properties.

- The hydraulic head drop is limited in the Kimmeridgian marls. The low water flow rates in this formation enable it to be partially desaturated, by about 10-20 %, and gradually around the shafts by the ventilation air. The desaturated zone extends to some tens of meters radially to the shaft centre line at the most. The saturation degree of the concrete ground support is of the order of 30-40 %.
- The hydraulic head drop is greater in the carbonated Oxfordian. The decrease in water pressures is on the order of a few MPa over radial distances running into several hundreds of meters from the shafts. During the century-long repository operating phase, the hydraulic head drops around each of the shafts join up creating an overall hydraulic head drop that extends for several kilometers after a few decades and that increases very little thereafter. The water flows in the various porous horizons are high enough to prevent desaturation by the ventilation air circulating in the shafts.

After the repository closure, the sealing of the shafts in the Callovo-Oxfordian layer and the water flows in the porous horizons restore hydraulic equilibrium to the carbonated Oxfordian within a few centuries. This return takes a little longer, several millennia, to achieve in the Kimmeridgian marls.

The hydraulic disturbance caused by the shafts on the overlying surrounding rocks is thus a local, reversible and very transient phenomenon.

6.4.3.2 Desaturation of the Callovo-Oxfordian on the periphery of the ventilated structures during the operation of the repository: a process that limits the chemical evolutions and the creep of the near-field argillites

The drifts, shafts and B waste disposal cells are ventilated during all or part of the operation of the repository. The ventilation air, which is not saturated with water vapour, induces the desaturation of the peripheral argillites, which combines with hydraulic head drop (which advances in the argillites to a few tens of meters at the most). In contrast, the lack of ventilation and rapid insertion of a leak tight cover at the hydraulic head of the C waste disposal cells and spent fuel disposal cells prevents their peripheral argillites from desaturating.

Within a few years desaturation in the drifts and shafts will affect all the concrete infrastructures and the initial EDZ. A pseudo-stationary system is established with water flowing at very low rates converging on the structures. Desaturation then spreads very slowly and reaches the undisturbed argillites (S=97 % a few meters beyond the EDZ) by the end of the operating phase. The saturation degrees of the concrete infrastructures and the fractured zone of the EDZ are established at about 20-30 % and 30-40 % respectively. The degree of saturation gradually increases in the microfissured zone towards the undisturbed argillites that remain saturated a few meters beyond the EDZ. Desaturation remains limited to the EDZ around the B waste disposal cells. The B waste disposal packages are heavily desaturated, like the concrete infrastructures.

Therefore the operating period can be considered as a "dry" period for the ventilated structures. The chemical processes are thus (very) limited, in particular the degradation of infrastructure concrete and B waste disposal packages. In mechanical terms, the non-saturated state of all or part of the damaged zone of the argillites tends to slow down or stop argillite creep. These points are developed in chapters 7 and 8.

6.4.3.3 Resaturation of the repository after closure, corrosion-induced hydrogen production and transfer: coupled processes

Closure of the repository structures initiates the repository resaturation process by the waters of the argillites. The seals on the main shafts and access drifts prevent the repository zones and connecting drifts from being resaturated by the waters of the carbonated Oxfordian or other overlying formations. Resaturation is an intrinsically slow process because of the low permeability of the argillites. The process competes with the production of hydrogen through corrosion, which in turn is dependent on water.

Corrosion rates are low, at the most on the order of a few $\mu m.yr^{-1}$ (more likely to be one to a few tenths of a $\mu m.yr^{-1}$). Despite these low corrosion rates, hydrogen transfer by dissolution and diffusion may not be enough to evacuate the hydrogen continuously during the first thousand years. Experiments carried out to date on argillite and borehole samples have resulted in an appraisal of the gas transfer properties in the argillites and in a proposed representation of the future of the hydrogen produced in the disposal cells.

Hydrogen evacuation is slow and gradual and dominated by the following transfers: (i) two-phase flow from the repository towards the Callovo-Oxfordian layer and inside the repository from the disposal cells towards the drifts and (ii) by dissolution-diffusion in the Callovo-Oxfordian layer. In the case of spent fuel, a transient transfer by localised microfissuring in the disposal cell plugs and module seals is envisaged.

Two-phase hydrogen transfer in the undisturbed Callovo-Oxfordian does not lead to desaturation (S>97 % in the near-field and S>99 % in the far-field). The hydrogen is pressurised to a few MPa in the repository during the production phase (up to 4,000-5,000 years). That implies a transient increase in the interstitial water pressure of the argillites at the excavation walls, which could locally create divergent water flows in the near-field argillites (for a few meters). The properties of the argillites would tend to make the water fluxes in question very weak and the processes very slow. These phenomena would disappear after 10,000 years.

The proposed representation results in a timescale on the order of 200,000 years to reach total repository saturation (S>97 % in the back-fill). More specifically in the case of B waste disposal cells, hydrogen production would result in maintaining the infrastructures and disposal packages in a non-saturated state, with degrees of saturation in the range 50-80 % in the infrastructure concretes and even lower for some of the B waste packages. In contrast, the hydrological properties of the argillites and the swelling clay would keep the C waste disposal cells and spent fuel disposal cells in a state close to saturation (S>97 %).

The non-saturated state of the B waste disposal cells and drifts would limit all the chemical processes. In mechanical terms, recommencement of creep in the argillites around the structures would be constrained by the gradual resaturation of the damaged zone.

6.4.3.4 Once the repository is totally resaturated a new state of hydraulic equilibrium is reached: the period of chemical and mechanical process development inside the repository

Once the repository is totally saturated, mechanical loading of the drifts through argillite creep creates transient overpressures that remain low because of the low prevailing creep rates (after 100,000 years). They do not induce a significant flow of water in the repository and quickly dissipate.

Once total resaturation of the repository is achieved, hydraulic equilibrium establishes itself in the repository and surrounding Callovo-Oxfordian. Laterally and over a few hundred meters from the repository, the hydraulic head field in the Callovo-Oxfordian layer is never affected by the repository but corresponds to the natural hydraulic head field that evolves under the effect of geodynamic evolution.

In the repository and surrounding Callovo-Oxfordian, the hydraulic head field at equilibrium and the flows are determined by the permeability levels of the various repository components, particularly the seals. Although these permeability levels are low, they are higher than those of the Callovo-Oxfordian layer, resulting in the repository functioning as a drain. Given the natural ascending vertical gradient in the Callovo-Oxfordian from the Dogger limestone to the carbonated Oxfordian, the repository drains part of the ascending water flow originating in the Dogger limestone: a flow of water is established along the repository structures and flows towards the shafts. This water drained by the repository towards the shafts flows at a very low rate, on the order of a few tens of litres per year given the low level of permeability in the Callovo-Oxfordian and the seals.

The chemical and mechanical evolutions take place in this hydraulic context, and in the final analysis the release and transfer of radionuclides, in the repository and the Callovo-Oxfordian layer for up to one million years.

6.4.4 Solute transport that is dominated by diffusion in the Callovo-Oxfordian

Until a new state of hydraulic equilibrium is established, the hydraulic transient of the repository is marked by a significant evolution in the water flows. However the flows are very weak and at the scale of the layer diffusion remains the prevalent transport mode except for a short transient during which overpressures caused by hydrogen production are likely to create gradients significant enough to establish codominance of advection-diffusion. This transient effect would intervene at a very early stage (at the most up to 5,000 years after repository closure) and would not have any significant effect. In addition, this phenomenon is likely to be less pronounced if less conservative hypotheses are adopted.

6.4.5 The production and migration of very small quantities of radionuclides in gaseous form

Of all the radionuclides and provided there is bacterial activity in the repository, organic ^{14}C alone can result in a gaseous form, as it happens CH_4. Thus this phenomenon would only apply to reference packages B5.1, through the presence of organic matter with the potential for bacterial development. The inventory of ^{14}C of the B5.1 packages would account for a range of about 19 % to 5.7 % of the total inventory of ^{14}C, that is 75 to 20 moles respectively. Furthermore only 55-85 % of this total (^{14}C of the zircaloy) would be in organic form. In standard conditions, this would represent a volume of less than one m^3 of CH_4, thus very low in comparison with the volume of hydrogen present in the repository. The impact of radionuclide transfer in gaseous form can be considered to be negligible all the more because the transfer times to the outlets of several tens of thousands of year would significantly contribute to their radioactive decay.

6.4.6 Geodynamic evolution causes significant modification to the water flow and transport in the surrounding rocks over the million years

Studies made of future climate changes in the Northern hemisphere demonstrate the existence of a succession of glacial cycles roughly every 100,000 years for the next million years. The date of the next glacial maximum will occur within 100,000 to 600,000 years, varying according to whether or not a man-made effect is allowed for, and thus after the repository is totally resaturated. Glaciers will not form at the latitudes of the Meuse/Haute-Marne site during the glacial maxima. A continuous permafrost will set in without reaching the Callovo-Oxfordian, but it may block the reloading of the surrounding formations and decrease the water flow rates inside them, particularly the carbonated Oxfordian. Over the next million years, glacial cycles and tectonic emergence will lead to gradual erosion that will become significant in 300,000-500,000 years' time, with the valleys sinking lower and locally cutting into the sedimentary series down to the carbonated Oxfordian, and plateau levels lowering. These changes to the topography to the East and South of the sector will force the outcrop zones that serve as reloading areas for the formations to recede to the West and North-West, and lower the hydraulic heads in the surrounding rocks of the Callovo-Oxfordian, in particular the carbonated Oxfordian.

Thus geodynamic evolutions will gradually alter the directions of the flows in the overlying surrounding formations from 300,000 to 500,000 and to a lesser extent in the Dogger limestones. The initial regional flow direction in particular gradually disappears while local directions emerge with new local outlets in the valleys as they deepen. Nonetheless the water flow rates in the Dogger limestones and carbonated Oxfordian will remain similar to those currently observed in the transposition zone.

Given the depth of the Callovo-Oxfordian layer, it is not directly affected by the erosion. The water flow will remain similar to the current flow, generally ascending vertical over the transposition zone. The hydraulic head gradient will increase to 0.3-0.4 $m.m^{-1}$, because of the hydraulic head drops in the carbonated Oxfordian, whereas the hydraulic heads in the Dogger limestones will evolve less but more evenly because the outcrops are at a greater distance from the repository. This increase in hydraulic head gradient in the Callovo-Oxfordian layer will not alter solute transport, which will remain predominantly diffusive.

The timescales of the hydraulic effects due to geodynamic evolutions are similar to those of the radionuclide transfer from the Callovo-Oxfordian layer to the surrounding rocks. Thus the period of 300,000-500,000 years by the end of which significant concentrations in solution of mobile radionuclides such as ^{129}I, start to appear in the permeable horizons of the carbonated Oxfordian, also corresponds to the period by the end of which the influences of geomorphological evolution will start to make themselves felt on the water flow routes in this same carbonate layer. As soon as these radionuclides appear in the carbonated Oxfordian, their transfer will thus be influenced by the modifications in the water flow directions and by the emergence of local outlets.

6.4.7 Phenomenological elements that are important for reversibility

Reversibility evaluation is carried out in relation to the hydraulic and hydrological conditions. Firstly we will recall the main results in relation to reversibility then we will analyse the potential consequences of repository operation over several centuries.

6.4.7.1 The state of the repository at the end of the conventional reference repository operating period

At the end of the century-long operating period (at the time of closure), corrosion of metal components and the chemical processes are generally limited. This is true for C waste disposal cells and spent fuel disposal cells: they are close to total saturation, but the corrosion rates are low (at most a few μm.yr^{-1})) so that the corrosion thicknesses are a few millimeters. More to the point, their mechanical strength and thus their impermeability are maintained as a result of the minor corrosion of linings during this period, . Hence the waste packages in a "dry" environment are not affected by significant corrosion. In the case of B waste disposal cells and the drifts, the curbing of chemical processes (concrete degrading and metal component corrosion) in conjunction with that of mechanical processes (argillite seepage) is related to the non-saturated state of these structures, either through ventilation, or because the time needed to fully resaturate them after closure runs to several tens of thousands of years to 200,000 years. Therefore, even if the B waste disposal cells are closed after the century-long period, they will still be in a non-saturated state by the end of that period.

6.4.7.2 The influence of repository operation over several centuries on reversibility

- **Drifts**

The maintenance of ventilation over a period spanning several centuries would not have an influence on the water flows and state of saturation of the concrete infrastructures and argillites in the near-field. This is because a pseudo permanent state is established after a decade of repository operation. The flows of drained water and the saturation degree profile (in the argillites) from the walls of these structures evolves very slowly from then onwards: A few additional centuries later, the saturation degree profile will only have increased by a few centimeters. Furthermore the lack of significant evolution in the state of saturation of these structures contributes to curbing the chemical degradation processes (primarily concrete degradation), and also to their mechanical withstand.

- **B waste disposal cells**

Similar conclusions to those on the drifts can be drawn if these disposal cells were to be kept open and ventilated over a period spanning several centuries. More specifically, there would be an interaction between the hydraulic head of two neighbouring disposal cells after a few decades of ventilation, but this influence would be limited to a few tenths of a MPa at the most at the end of period spanning several centuries and would not have a significant effect on disposal cell desaturation and saturation state. Furthermore it is noted that maintaining ventilation over several centuries would lead to the evacuation of the hydrogen produced by corrosion.

If the disposal cells were to be closed as in the conventional reference time chart but the repository remained open over several centuries, the hydraulic state of the disposal cells would not evolve much over this period. However, the quantity of hydrogen present inside some disposal cells would represent almost ¾ of the hydrogen produced in the course of the first 500 years.

- **C waste disposal cells and spent fuel disposal cells**

Prolonging repository operations over several centuries would not lead to any significant change in the evolution of the various processes that would take place over that time. Primarily corrosion rates would remain low and would have no bearing on the mechanical withstand of the metal components (ground support and lining). The impermeability of the lining would be maintained, and thus the waste packages would not be subject to corrosion, which would preserve their physical integrity.

The desaturated zone of argillites around the access drifts in the region of the disposal cells would spread beyond the disposal cell plugs, thus within the first metre of the useful part of the disposal cells (that holds the waste packages). Most of the useful part would remain saturated and in anoxic conditions. The quantity of hydrogen produced over a period spanning several centuries would still be limited (a few percent of production over the first 5,000-year phase). However hydrogen pressure would have started to build up after 100 years, to reach a few tenths of one MPa by the end of the period spanning several centuries.

- **The Callovo-Oxfordian and the overlying surrounding rocks**

At the end of the period spanning several centuries, hydraulic head drop would reach the top and wall, but the value of the hydraulic head drop at these Callovo-Oxfordian boundaries would be less than a tenth of one MPa. Around the shafts the hydraulic head drops would overlap, but the total negative pressure would be a few tenths of one MPa at the most.

Thus the history of the repository presented in this section remains valid for a reversibility period spanning several centuries.

7

Chemical phenomena

7.1 **Introduction** **273**

7.2 **Chemical evolution of structures ventilated during the repository operational period: Type B waste disposal cells, drifts and shafts** **275**

7.3 **Chemical evolution of disposal cells of type C waste and spent fuel** **287**

7.4 **Chemical Evolution of B waste disposal cells in Post-Closure Status** **312**

7.5 **Chemical evolution of drift and shaft seals in the post-closure phase** **328**

7.6 **Chemical evolution of drifts and shafts in the post-closure phase** **331**

7.7 **Chemical evolution of Callovo-Oxfordian argillites in the far field** **332**

7.8 **Chemical evolution of the surrounding formations (Dogger and carbonated Oxfordian)** **332**

7.9 **Summary of the chemical evolution of the repository and its geological environment** **333**

7.1 Introduction

Chemical evolution effects several aspects of the overall phenomenological evolution of the repository and its geological environment.

- associated with hydraulic and thermal evolution, it is the main source of the release of radioactive nuclides by the deterioration of waste packages such as, for example, the dissolution of the glass matrix of type C waste or the corrosion of the metal containers of type C waste or spent fuels. It further determines the mobility of the radioactive nuclides released, via its impact on solubility and retention;
- it is a driving force behind physical change through the deterioration of the mechanical properties of the repository components combined with chemical deterioration. This is the case, for example, for the chemical attack of the concretes used in infrastructure works by water originating from the argillites or the corrosion of the metal linings and coatings of type C waste and spent fuel disposal cells. For this reason, chemical evolution is also an important factor when operating and monitoring the repository in the context of reversibility.

7.1.1 The result of desequilibria

Chemical evolution is primarily the result of the interfacing of different materials, chemical compounds or chemical fluids. It is also influenced both kinetically and in the initiation of reactions by natural thermal and hydraulic phenomena. More particularly, on a hydraulic level, water is required for the development of chemical reactions. Furthermore, the spatial and temporal extension of these reactions depends essentially (as in the case of thermodynamically balanced systems) on the water fluxes and solute exchanges involved in these reactions (i.e. transport conditions of species in solution).

Before building the repository, the geological medium and, more particularly, the Callovo-Oxfordian layers are in a state of chemical equilibrium. Building the repository involves placing various materials which constitute the various repository components into the Callovo-Oxfordian ; they are placed in contact with the argillites and/or with each other. The materials involved are essentially:

- metals, for example type C waste and spent fuel over-packs and containers or type B metal waste (hulls and end caps, metal technological waste etc.),
- concrete, for example for infrastructures (supports etc.) or type B waste disposal packages,
- re-worked engineered clays, for example swelling clays for disposal cell seals and plugs or argillites excavated for back-filling drifts,
- to which should be added the special materials forming the waste packages, for example the glass matrix in type C waste, the uranium/plutonium oxide pellets in spent fuels or the organic substances in bituminised sludge packages.

The chemical processes are influenced in particular by:

- the temperature increase transient produced by exothermic waste packages, which principally affect the repository and the Callovo-Oxfordian (see § 5),
- the hydraulic transient created by the repository (cf. § 6). One notable feature of this transient is the existence of a period when part or all of the repository is in an unsaturated state, particularly in structures which are ventilated during the operational life of the repository (type B waste disposal cells and drifts). The presence and renewal of oxygen are liable to initiate processes (oxidation etc.) that will not occur in unventilated structures (type C waste and spent fuel disposal cells).

7.1.2 Evolution principally concerning the repository and the near-field Callovo-Oxfordian layer

The chemical processes involved are above all those occurring on interface and thus apply essentially to the repository and the Callovo-Oxfordian layer. In fact, the surrounding formations are sufficiently remote from the repository so as not to be chemically affected by it. Their physico-chemical evolution is mainly governed by climatic changes and internal geodynamics (see § 9).

7.1.3 Independence and similarities of chemical evolution

As already highlighted in the description of thermal and hydraulic evolution (see § 5 and 6), the compartmentalised design of the repository into distinct repository zones for each major HAVL waste category and into disposal modules within a given zone leads to chemical evolutions that are (i) independent for each zone and (ii) similar for the disposal modules and disposal cells within a given zone.

7.1.4 Two categories of structure in terms of chemical evolution

During the operational life of the repository, ventilation is the main driving force behind chemical processes and makes it possible to distinguish between type B waste disposal cells, drifts and shafts (ventilated during the operational period), type C waste disposal cells and spent fuel disposal cells, which rapidly become isolated from the ventilation air by a sealing cap.

In the post-closing phase and in the absence of oxygen in the chemical system, it is the nature of the materials introduced into the repository and the thermal and hydraulic evolution described in chapters 5 and 6 that make it possible to distinguish between two major categories of structure from the point of view of chemical evolution:

- one characterised by the presence of metals and /or swelling clay (type C waste and spent fuel disposal cells, seals of drifts and shafts),
- the other, whose major ingredient is cement-based (type B waste disposal cells, drifts and galleries),

Structures in the first category may present a high level of thermicity (type C waste and spent fuel disposal cells) and are characterised by reaching a saturated state in less than a thousand years. The second category has a low level of thermicity (see § 5) and retains a de-saturated state for at least several tens of thousands of years.

7.1.5 Organisation of the chapter

Based on the considerations outlined above, the description of the chemical evolution of the repository and its geological environment is structured, on the one hand, according to the management of the repository (operation, post-closing) and, on the other, according to the category of the structures. We are primarily interested in the repository and the Callovo-Oxfordian layer. The surrounding formations are dealt with at the end of the chapter (see § 7.8). This chapter is organised into 7 parts:

§ 7.2 The chemical evolution of structures which are ventilated during the operational phase: type B waste disposal cells, drifts and shafts.

In this part, the problems discussed are the oxidation of argillites, the atmospheric carbonation of concretes, the atmospheric corrosion or corrosion in an unsaturated porous medium of steels, and the radiolysis of organic components in type B waste.

§ 7.3 The chemical evolution of type C waste disposal cells and spent fuel disposal cells during the operational and post-closing phases. In fact, for these structures, the fitting of a sealing cap during the operational phase makes it possible to consider that chemical evolution is a continuous process over these two periods.

The main chemical processes involved are, for the inside of disposal cells, the corrosion of coatings, linings and over-packs and containers under anaerobic conditions, the interactions of the swelling clay of the engineered barrier of spent fuel disposal cells and near-field argillites of type C waste disposal cells and iron and the dissolution of the glass and assemblies in spent fuel. In disposal cell ends, the principal chemical process is the alkaline disturbance of swelling clay plugs and near-field argillites in contact with cement-based water seeping from support bases.

§ 7.4 The chemical evolution of type B waste disposal cells during the post-closing phase.

This evolution essentially occurs under anaerobic conditions. The principal processes involved are deterioration of cement-based materials by re-saturation water, an alkaline disturbance in the argillites and back-filling materials due to water from the concretes, corrosion of type B metal waste (zircaloy in hulls, steel in end caps and technological waste) and the deterioration of bituminised sludge.

§ 7.5 The evolution of drift and shaft seals in the post-closing phase.

§ 7.6 The evolution of drifts during the post-closing phase.

The seals and drifts are essentially subjected to chemical phenomena associated with the deterioration of cement-based components and alkaline disturbance in clay-based materials (swelling clay and argillites) situated in contact with concrete.

§ 7.7 The chemical evolution of the near-field of the Callovo-Oxfordian layer.

§ 7.8 The chemical evolution of the surrounding formations.

It should be pointed out that bacterial activity (especially that introduced during repository operation) does not significantly develop over the long term given environmental conditions (for example, dry medium and basic medium, (Libert *et al.*, 1996 ; Libert *et al.*, 1998) and the absence or finite quantity of energy-providing substrates within the repository (Andra, 2005k ; Andra, 2005l ; Libert, 2004 ; Nagra, 1999b ; Nagra, 2003c). It therefore has no significant impact on other chemical processes and is not developed in any of the following paragraphs.

7.2 Chemical evolution of structures ventilated during the repository operational period: Type B waste disposal cells, drifts and shafts.

During its construction, air enters the repository. Until they are closed, the air in shafts, drifts and type B waste disposal cells is continuously renewed by ventilation. As indicated in chapter 6 the relative humidity of the ventilation air in the drifts and type B waste disposal cells settles at a level of around 50 %, causing to the concrete in the structures and waste packages to become highly de-saturated. De-saturation also affects the argillites at the periphery of the structures. Only the air in air inlet shafts and the first few hundred meters of galleries downstream of these shafts have a higher relative humidity

The ventilation conditions cause specific chemical changes in the constituent materials of the various components of the repository. The argillites in the walls of ventilated structures undergo oxidation by oxygen in the air. Furthermore, concrete structures react with the carbon dioxide in the ventilation air and undergo superficial carbonation. The metal materials are subjected to corrosion processes whose intensity depends on the repository's saturation conditions. Moreover, the fitting of fresh cement-based materials causes slight alkaline disturbance of the argillites in the walls.

The highly de-saturated conditions in type B waste disposal cells during the operational period greatly limit the chemical evolution of the waste packages. The near absence of free water limits or prevents the corrosion or dissolution processes. However, the waste remains subjected to irradiation processes, such as radiolytic oxidation of bituminised sludge. These processes are dealt with in a final section (see § 7.2.5).

7.2.1 Oxidising disturbance in argillites in structure walls due to desaturation

During the operational period, the ventilation air gradually penetrates the argillites in the near-field of ventilated structures as they de-saturate, with a maximum level in the microfissured area of the EDZ (Excavation Damaged Zone, Inset 7.1), notably in the access drifts which remain open throughout the repository operational period (see § 6).

The Callovo-Oxfordian argillites are initially in a state of chemical equilibrium under reducing conditions. The latter are imposed by the sulphide / sulphate redox couple, the sulphide contents in solution being determined by the solubility of the pyrites and that of sulphates by the solubility of the celestine (see § 3.3.1.8) (Altmann & Jacquot, 2005 ; Andra, 2005h ; Andra, 2005k). The penetration of the oxygen in the air disturbs this balance and causes oxidation of the pyrites and of the organic material (Andra, 2005k). The temporal and physical extent of the oxidising transformations in the argillites depends entirely on the penetration of the oxygen into the argillites and not on the intrinsic kinetics of each of the transformations involved. The argillite oxidation processes are instantaneous in the ventilation timescales considered. Furthermore, oxidation of the pyrites requires the simultaneous presence of oxygen and water (Inset 7.1). It therefore occurs essentially along the de-saturation front, which progresses through the EDZ, whereas it is slower and limited in the area already de-saturated. On the other hand, the oxygen in the organic material develops more readily in de-saturated areas. The extent of the oxidation corresponds very closely to that of the de-saturated area, i.e. to 2 or 3 meters over an operating period of a hundred years. It is therefore limited to the EDZ and, in its mass, principally concerns the vicinity of fractures and micro-fissures (Charpentier, 2001 ; Mäder & Mazurek, 1998), see § 8.

In access structures, only the walls of shafts in Callovo-Oxfordian argillites and Kimmeridgian marls are susceptible, due to their mineralogical structure, to be subjected to oxidation processes. The relative humidity in shafts is higher than in other repository structures (~ 90 %) (Wendling, 2005). However, it is insufficient to prevent penetration of oxygen into the highly de-saturated area of the EDZ (essentially the fractured area) (see § 6). Thus, the oxidising disturbance in access structures principally extends to this part of the EDZ.

7.2.1.1 Oxidation of pyrites

The oxidation of pyrites, whose content within the Callovo-Oxfordian argillites is between 2 and 3 % (Table 3.3.1), by the oxygen in the ventilation air, eventually results in the formation of sulphates and ferrous iron (Inset 7.1). It also leads to the release of protons, causing a local drop in the pH of the interstitial fluids. However, the buffer effect exerted on the pH of the interstitial fluids by the dissolution of the calcite present in the argillites(Andra, 2005k), has the effect of preventing the interstitial fluids in the argillite during oxidation from reaching acidic pH levels (< 7).

The oxidation is probably catalysed and accelerated by the development of bacterial activity introduced into the repository due to human activity (Andra, 2005k). The bacteria that catalyse the oxidation of the pyrites are acidophile. However, the buffer effect of the calcite limits the effective development of bacterial populations. Consequently, their catalytic effect on the oxidation kinetics of the pyrites in the argillites remains limited.

The oxidising disturbance results in a change in the composition of the pore water with an increase in the calcium and sulphate contents. Cationic Na / Ca exchanges with the clay-based materials occur, the sodic smectite phases becoming calcic. Furthermore, secondary phases then speed up the rate of de-saturation in the medium: gypsum ($CaSO_4$, $2H_2O$), jarosite ($KFe_3(SO_4)_2(OH)_6$), iron oxides and hydroxides such as haematite (Fe_2O_3) and goethite ($FeO(OH)$).

Inset 7.1 **Oxidation of pyrites (FeS_2)**

The presence of pyrite causes acidification in rivers. For that reason, it's oxidation has been widely studied, such that the entire process is today fully understood (Andra, 2005f, Tome 3 ; Rimstidt & Vaughan, 2003).

The oxidation process

The oxidation of pyrites requires the simultaneous presence of oxygen and water. It breaks down into numerous basic stages which result in the following overall reaction (Rimstidt & Vaughan, 2003):

$$FeS_2 + 7/2O_2 + H_2O \leftrightarrows Fe^{2+} + 2SO_4^{2+} + 2H^+$$

The degree of oxidation of the iron remains blocked at +II, the oxidation by oxygen to +III being thermodynamically possible but kinematically slow (Andra, 2005f, Tome 3 ; Andra, 2005k ; Crusset, 2005 ; Gras, 2001), except when the reaction is catalysed by the presence of the *Thioalcools Ferrooxidans* bacteria. The overall pyrite oxidation reaction is then written (Panin *et al.*, 1985):

$$2FeS_2 + 15/2\,O_2 + H_2O \xrightarrow{bacterialactivity} 2Fe^{3+} + 4SO_4^{2-} + 2H^+$$

The ferric iron thus produced is itself a powerful oxidising agent that accelerates the oxidation of the pyrite. The establishment of the cycle "pyrites oxidation → formation of ferrous ions → formation of ferric ions → pyrites oxidation" cycle gradually amplifies the existing chemical reactions and accelerates the pyrite oxidation process:

$$FeS_2 + 8H_2O + 14Fe^{3+} \leftrightarrows 15Fe^{2+} + 2SO_4^{2-} + 16H^+$$

The bacteria, by regenerating the ferric iron produced in the previous reaction in its ferric form, gradually amplify the existing chemical reactions and accelerate the pyrite oxidation process.

In the absence of bacterial activity, the Fe^{II} released by chemical oxidation of the pyrites is incorporated into solid carbonate solutions (ankerite $CaFe(CO_3)_2$) or into the structure of the clay-based minerals in octahedric sites.

The Fe^{III} precipitates in the form of an oxide (haematite Fe_2O_3) or oxyhydroxide (goethite $FeO(OH)$) (Charpentier, 2001 ; Pokrovski *et al.*, 2003).

Extent of pyrite oxidation into the argillites around the repository structures

The spatial extent of pyrites oxidation is determined by the penetration of oxygen into the argillites around the repository. This therefore principally concerns the ventilated structures around which argillites de-saturation occurs. This de-saturation allows a significant quantity of oxygen to enter and the extent of the oxidation is determined by that of the de-saturation. In saturated argillites, the diffusion or convective transport of the dissolved oxygen is too slow to allow a significant entry of oxygen and oxidation remains a surface phenomenon.

7.2.1.2 Oxidation of organic matter

The study of oxidation processes of the organic matter contained in geological formations concentrates mainly on coals and oils, and less on kerogen type organic phases rich in immature organic matter, like those contained in the Callovo-Oxfordian argillites. However, several series of experiments have been conducted in order to characterise these processes, in particular depending on the temperature conditions(Andra, 2005a) (Andra, 2005k) (Elie *et al.*, 2000) (Faure *et al.*, 1999). These experiments have made it possible to characterise fairly accurately the oxidation processes involved.

The oxidation of immature organic matter contained in Callovo-Oxfordian argillites leads to oxygen being incorporated in the structure of the kerogen and the formation of oxygenated functions (acids, ketones etc.). The progression of the oxidation of organic matter can be monitored by means of various phenomena: the deterioration of biological markers in the organic matter (hopanes, hopenes, steranes, sterenes), the displacement of the distribution of n-alcanes towards low molecular weights and the production of polar compounds with low molecular weights with a high proportion of carboxylic acids. Some of these compounds, placed in solution by the re-saturation of the argillites, have complexing properties with respect to radioactive nuclides (Andra, 2005k). However, given the quantities that can be mobilised, their influence on the transport of radioactive nuclides is not significant.

7.2.2 Atmospheric carbonation of structural concretes

The ventilation, and the de-saturated state of the infrastructure components made from concrete, contribute to the atmospheric carbonation processes, namely the reaction of the concrete with the carbon dioxide (CO_2) contained in the air (Inset 7.2). However, in type B waste disposal cells, drifts and air return shafts, the low relative humidity (~ 50 %) cause a de-saturation of cement-based materials, between 20 % and 30 % saturation, which greatly restricts atmospheric carbonation due to the absence of liquid water (Andra, 2005f, Tome 2). Thus, even if the ventilation is maintained for a hundred years, the carbonation does not exceed a centimeter (Bourbon, 2005) and remains diffuse. The temperature increases in the repository during this period, as described in Chapter 5, do not influence these processes.

The higher relative humidity in air inlet shafts, (up to ~90 %) compared to the drifts and type B waste disposal cells (see § 6) causes greater saturation of cement-based materials (degree of saturation between 40 % and 50 %). This concrete saturation limits the transfer of CO_2 within them (principally in dissolved phase) such that the extent of carbonation in these shafts does not exceed a centimetre either (Bourbon, 2005).

In the first few hundred meters of drifts, the relative humidity varies between 90 % and 50 %. It is within this range scale that the optimum relative humidity for the development of carbonation occurs (55 % to 65 %) (Andra, 2005f, Tome 2), (Inset 7.2) its extension is then a maximum of a decimetre throughout the structures' operational period.

Inset 7.2 ***Atmospheric carbonation of cement-based materials (1/2)***

Due to their mineralogy (Inset 2.8), cement-based materials are very reactive in the presence of gaseous CO_2 or water rich in carbonates. The reaction with gaseous CO_2, known as atmospheric carbonation, is well known in the civil engineering field because of its consequences for the corrosion of reinforcements and, eventually, on the mechanical behaviour of reinforced concrete. It has been the subject of numerous studies, the results of which have contributed, notably, to the specifications of the formulae of concretes and the definition of reinforcing rules. The knowledge acquired, supplemented by monitoring of the evolution of atmospheric carbonation on structures over periods of several decades, give confidence in the models developed and in their application to the assessment of atmospheric carbonation in the context of repositories over the conventional hundred-year reference period and over a longer period on the order of several centuries (Andra, 2005f, Tome 2).

Chemical reactions

Atmospheric carbonation can be broken down into the following three stages (Andra, 2005f, Tome 2), (Bourbon, 2005). Stages 2 and 3 are identical for carbonation in water:

1. the transfer as a gas phase of atmospheric CO_2 within the material via the associated non-saturated porosity;

2. the dissolution of the CO_2 in the interstitial aqueous phase:

$$CO_{2(g)} \leftrightarrows CO_{2(sol)} \text{ and } CO_{2(ground)} + 2OH^- \leftrightarrows CO_3^{2-} + H_2O$$

3. the neutralisation of the cement hydrates (portlandite $Ca(OH)_2$; hydrated calcium silicates CSH) by CO_3^{2-} and their gradual dissolution at the same time as the precipitation of calcium carbonate (Andra, 2005f, Tome 2):

$$Ca(OH)_2 + CO_3^{2-} \leftrightarrows CaCO_3 + 2OH^-$$

This reaction leads to a gradual reduction in the pH of the interstitial waters due to the disappearance of the portlandite and the CSH. This reduction in the pH is responsible for the de-passivation of the stiffereners, causing an increase in the corrosion kinetics, the formation of expanding corrosion products and, eventually, formation of fissures or even fracturing of the concrete.

Temporal and physical extension

The physical extent of the atmospheric carbonation is determined by the transfer of CO_2 into the concrete. It therefore depends on the degree of saturation. Close to saturation, the extent of the carbonation is constrained by the transport of CO_2 in the dissolved phase in the water. In the very highly desaturated state, the gaseous CO_2 can rapidly migrate but it is then the quantity of water available which limits carbonation. We therefore generally observe a maximum carbonation propagation depending on the degree of saturation in water (*i.e.* relative humidity) as illustrated in the figure below.

Atmospheric carbonation of cement-based materials (2/2)

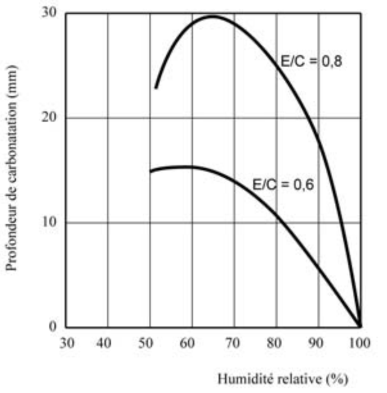

Influence of the relative humidity on the extent of carbonation of a concrete depending on its initial composition (E / C: ratio of initial water / mixing cement)

Atmospheric carbonation propagates along fronts inside cement-based materials. Directly above the reaction front, the carbonation reactions cause a reduction in the porosity (clogging) on the one hand, by precipitation of calcite, and *de facto* a larger degree of saturation (formation of water by carbonation and reduction in the porosity) on the other. The combination of these two phenomena then considerably slows down the propagation kinetics by limiting the transfer of CO_2 within the material.

7.2.3 Corrosion of metal structural components

7.2.3.1 Shaft rings

In air inlet shafts, the ventilation air being close to saturation, the corrosion processes of metal materials enclosed within cement-based materials are important. However, during the operational period, monitoring of structures makes it possible to replace corroded components.

The case of rings placed vertically in front of the Barrois limestones is a special case due to their contact at one outside with a saturated concrete in chemical interaction with the waters of the Barrois limestones and at the other side with an unsaturated concrete interacting chemically with the ventilated air in the shafts. They are thus subjected on both sides to generalised corrosion in a undisturbed oxidising cement-based medium, saturated on the outside and partially saturated on the inside (degree of saturation between 40 % and 50 %). On the outside, under conditions of Barrois limestone water containing chlorides (Andra, 2003c), the generalised corrosion rate is around ten µm per year due to the simultaneous presence of O_2 and Cl^- (Andra, 2005f, Tome 3). The progression of the degradation of cement-based materials by water from the Barrois limestones causes a reduction in the pH of the interstitial water (see § 7.4.2) and leads to an increase in the corrosion kinetics (Inset 7.3) up to a hundred µm per year. On the inside, the corrosion is limited by the flow of oxygen through the partially saturated concrete. Its speed should be approximately a µm per year due to the unsaturated state of the concrete and the absence of chlorides (Andra, 2005f, Tome 3).

The corrosion of the rings is thus approximately a centimetre over the repository's hundred year operational life. It does not affect the total thickness (several centimeters) of the rings and its consequences for their mechanical behaviour are limited.

7.2.3.2 Other metal components

The very small quantities of water available during the ventilation period (relative humidity of around 50 %) almost completely inhibit the corrosion processes susceptible to affect the other metal components encased in cement-based materials (seal arches, metal fibres of type B waste disposal package containers etc.). Due to the low saturation state of the concretes (degree of saturation from 20 to 30 %, cf. § 6.3), their level of corrosion is very low during the hundred year operational period.

Inset 7.3 ***Corrosion of non or lightly alloyed steels (1/3) (Andra, 2005f, Tome 3)***

Introduction

Knowledge on the corrosion of steels over periods of several thousand years has been developed in numerous European projects on the study of geological repositories (CONTAINER CORROSION, COBECOMA,…). The corrosion mechanisms and speeds have been studied thanks to many experiments and modelling activities. They highlight the role of corrosion protection layers.

The extrapolation of the corrosion process in both time and space is based on the study of a number of archaeological analogues (David, 2003) which, though often representative of different conditions from those within a repository (essentially oxidising conditions), confirm the role of protective layers.

Generally speaking, two sets of environmental conditions can be identified with respect to corrosion: (i) an atmospheric type media and (ii) an aqueous media either in contact or not with a saturated or partially de-saturated porous medium. The kinetics and sometimes the products formed via corrosion, vary according to these different conditions. For these different conditions, corrosion depends on the presence or absence of oxygen.

Corrosion under the presence of oxygen

Corrosion under atmospheric conditions is similar to that in an aqueous phase as it occurs in the liquid water thin layer on the surface of the steels. In aerated water, corrosion is controlled by reducing cathodic reaction of dissolved oxygen and corresponds to the stability ranges of oxides and oxyhydroxides of Fe^{III} (ferrihydrite $Fe_2O_3.0.5H_2O$, lepidocrocite γ-FeOOH, goethite α-FeOOH, haematite α-Fe_2O_3,…) (Andra, 2005f, Tomes 1 et 3). For example: $O_2 + 2H_2O + 4e^- \leftrightarrows 4OH^-$

$$4/3\,Fe + 4OH^- \leftrightarrows 2/3\,Fe_2O_3 + 2H_2O + 4e^-$$

For solid compounds of $iron^{III}$, the stability of goethite is limited to temperatures below 100 °C, whereas that of haematite is improved by increasing the temperature.

In contact with clay-based materials, the presence of phyllosilicates and montmorillonite slows down or blocks the transformation of ferrihydrite into crystallised haematite and goethite. The $Iron^{III}$ remains present in the form of oxyhydroxides.

The presence of soluble species (carbonates, sulphides,…) may cause the formation of other compounds: siderite ($FeCO_3$), ferrosilite ($FeSiO_3$), pyrites (FeS_2), vivianite ($Fe_3(PO_4)_2,8H_2O$),…,.

Corrosion under anoxic conditions

In the absence of oxygen or other oxidising species, the only possible cathodic reaction of the iron-water system is the reduction of the water and the formation of hydrogen. Under these conditions, the metal iron oxidises, forming magnetite (Fe_3O_4). This reaction is the result of two simultaneous processes:

- The oxidation of iron coupled with the reduction of water:

$$2H_2O + 2e \leftrightarrows H_2\uparrow + 2OH^- \text{ and } Fe + 2OH^- \leftrightarrows Fe(OH)_2 + 2e$$

- Then the formation of magnetite from ferrous hydroxide (Schikorr reaction):

$$3Fe(OH)_2 \leftrightarrows Fe_3O_4 + H_2\uparrow + 2H_2O$$

$$\text{whence } 3Fe + 4H_2O \leftrightarrows Fe_3O_4 + 4H_2\uparrow$$

Most corrosion products have significantly lower densities than that of iron, hence the fact that corrosion is accompanied by volumic expansion, which can in theory (without considering dissolution of part of these corrosion products) reach 130 % for magnetite and 320 % for siderite. However, corrosion experiments in porous medium under mechanical stress seem to indicate that corrosion products can ultimately be only slightly expansive probably due to mechanical consolidation combined with slow corrosion rates.

Corrosion of non or lightly alloyed steels (2/3)

The thermodynamics and kinetics of corrosion

The thermodynamics and kinetics of the corrosion of iron in the presence of oxygen or under anoxic, conditions are influenced by a certain number of parameters, in particular, saturation, the medium in contact, the pH and the presence of chlorides. The Eh/pH conditions in the medium in contact with the iron impose variable corrosion conditions: general corrosion, pitting, passivation, immunity (see Figure below) (Andra, 2005f, Tome 3 ; Pourbaix, 1972).

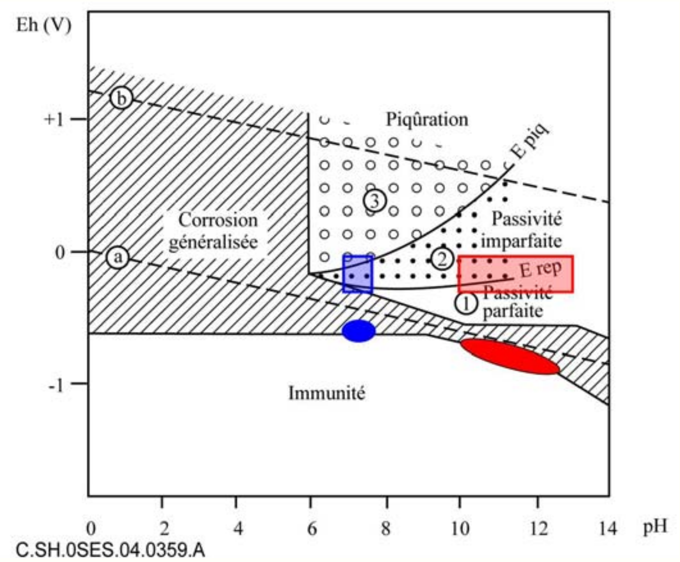

Iron behaviour in water in the presence of chloride ions (355 ppm Cl^-) for various experimental conditions: immunity, generalised corrosion, complete ① and incomplete ② passivation and pitting ③

***Blue** rectangle: instability range of water in Callovo-Oxfordian argillites; **Red** rectangle: stability range of water in concrete ; **Blue** and **red** ovals: metal potentials; a) line corresponding to the hydrogen release reaction, b) line corresponding to the oxygen release reaction. The water is stable between lines a) and b)*

The average kinetics of corrosion thus evolve according to the conditions in the surrounding medium (see Figure and Table below) (Andra, 2005f, Tome 3), (Gras, 2001). The figures are generally valid at temperatures of 25 – 50 °C for cement-based media and 25 – 80 °C for clay-based media. A few values are given as an example in the table below.

Order of magnitude of the spread of corrosion of black or lightly alloyed steel under various conditions in the medium term (a few years)

	Cement-based medium	Clay-based medium
Oxygen present	• ≤ 1 µm.year^{-1} with passivation • > a few µm.year^{-1} to a few 10 µm.year^{-1} with de-passivation	a few 10 µm.year^{-1}
Oxygen absent	≤ 1 µm.year^{-1}	a few µm.year^{-1} maximum

A number of factors influence these speeds, in particular the pH, the dissolved oxygen content, the formation of corrosion products and the saturation in the water of the medium. In the absence of oxygen and in a clay-based medium, the reference speed is considered to be 2-5 µm.year^{-1}. However, experiments strongly suggest that these speeds could be much slower (around a µm.year^{-1} or less).

Corrosion of non or lightly alloyed steels (3/3)

An example of the effects of saturation of the porous medium on corrosion is given in the graphs below. They show that the corrosion rate significantly decreases below 80 % of the degree of saturation. Such low degrees of saturation are not expected in argillites and bentonite (saturation always more than 97 %), so that the effects of saturation on corrosion kinetics of metal components in the repository in contact with argillites and bentonite should be weak or nil.

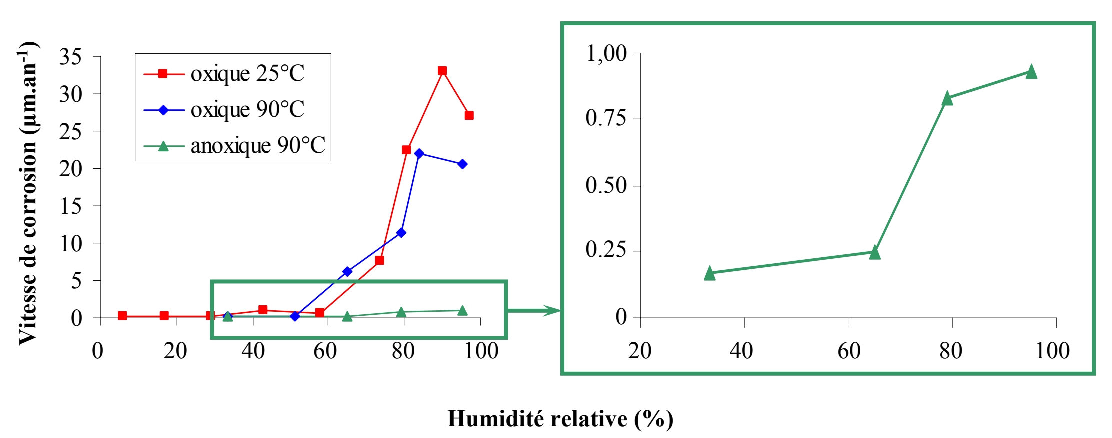

Influence of the relative humidity on the speed of generalised corrosion of a non or lightly alloyed carbon steel in contact with an MX80 bentonite (Andra, 2005f, Tome 3)

7.2.4 Alkaline disturbance of argillites by the concrete in infrastructure components

During excavation of the various repository structures, the use of fresh shotcrete as a temporary support on argillite walls leads to a contact between the highly alkaline fluids in the concrete (pH ~ 13.5) and the argillites. This causes the development of an alkaline disturbance on the surface of the argillites. The disturbance remains limited to the surface in contact with the concrete, because the setting of the concrete (which takes from a few days to a few weeks, see § 6), and its de-saturation by the ventilation limits or even prevents the availability of cement-based water in contact with the argillites.

7.2.5 Alteration processes of type B waste disposal packages

7.2.5.1 Atmospheric carbonation of concrete components of disposal packages

Like the disposal cell support and coating, type B waste disposal packages are in a highly de-saturated state. All the concrete components of disposal packages (envelope, embedding matrix of certain types of waste and the envelope of certain primary packages) are subjected to very weak atmospheric carbonation.

7.2.5.2 Chemical deterioration of waste

As indicated in chapter 2.3.4, the contents and structure of type B waste disposal packages covers a wide range of materials and, thus, of chemical deterioration processes in the broadest sense. However, the low availability of water renders these deterioration processes, such as corrosion of metal components (for example stainless steel or carbon steel primary package containers) or the waste itself (type B1, B3, B4, B5 and B6 packages) practically non-existent.

The dissolution processes of bituminised sludge (types B2 packages) by water are also practically non-existent because the low relative humidity (≤ 50 %) (see § 6) does not encourage condensation of water on the surface of the packages (Andra, 2005d).

As far as other types of waste are concerned (for example AIC alloys, boron carbide, glasses (pyrex, nuclear glass etc.), organic compounds, the various sealed sources, lead sulphates, waste containing radium, debris, filtration sludge or graphite), they also undergo almost zero chemical change due to the lack of water.

7.2.5.3 Radiolytic effects in type B waste disposal packages (Andra, 2005d)

During the ventilation period, type B waste is subjected to radiation by radioactive nuclides. This radiation does not affect metal waste, however it does affect waste containing organic compounds: in particular the bitumen matrix of type B2 packages and organic compounds in type B5, B6 and B3 packages (PVC, polyurethane, cellulose etc.).

On the surface of bituminised sludge packages, the combination of oxidation (ventilation air) and radiolysis (radio-oxidation) due to the effects of radiation from the embedded radioactive salts, results in the formation of CO, CO_2 and oxygenated organic species and a reduction in the viscosity of the bitumen (Inset 7.4). Over the hundred year ventilation period of type B waste disposal cells, the oxygen has only diffused over a distance of about a centimetre within the bitumen. The radiolysis of the bitumen thus affects only a limited thickness of the packages and remains a surface phenomena.

The remainder of the matrix is subjected to radiolysis processes under unsaturated conditions and without oxygen. It principally causes the production of hydrogen by radiolysis of the bitumen matrix. Other gases, such as CH_4, C_2H_6 or C_2H_2, are also produced, but in small quantities. The irradiation of the bitumen under anoxic conditions, and the discharge of hydrogen, lead to an increase in the condensation of the bitumen and, therefore, an increase in its viscosity.

Salts do not participate in the radiolysis processes, except for cobalt salts used for the bituminised sludge of type B2.1 packages (STE2 and STE3 families). They consume some of the hydrogen produced. The production of hydrogen within the bitumen matrix causes swelling of the coating. Initially, the hydrogen produced is evacuated by diffusion. Subsequently, when the hydrogen content exceeds its solubility threshold, it forms a gas bubble which migrates out of the coating.

For example, the production of hydrogen by type STE2 packages is approximately 1 to 2 $L.year^{-1}.package^{-1}$ between 10 and 100 years after manufacture, which leads to a maximum swelling of the coating occurring after approximately 50 years.

Thus, throughout the operational period, the chemical deterioration of bituminised sludge only affects the bitumen matrix (essentially a production of gases).

The radiolysis of plastics (type B5.1, B3.1.3, B3.1.2 packages) leads to the formation of gases such as H_2, CO_2, CH_4 and HCl (Talandier, 2005). The production of HCl by PVC occurs over a short period (~ 8 years) after the production of a type B5.1 package and, thus, ends when the packages are taken under control in the repository. The total production of CO_2 by the polyurethane is low. It does not exceed 10 moles per B5.1 package over its entire deterioration period. The assessment of hydrogen production by type B5.1 packages leads to a production of approximately 22 $L.year^{-1}.package^{-1}$ (or approximately 1 mole of H_2 per year per package) during the operational period. All of these gases are evacuated by the ventilation.

Inset 7.4 **Radiolysis of the bitumen matrix**

Generally speaking, the deterioration mechanisms of a bitumen matrix are similar to those of all organic polymers. In the presence of oxygen, self-irradiation of the bitumen matrix causes it to oxidise (Andra, 2005d). This process occurs in several stages.

- Firstly, the irradiation of the bitumen leads to ruptures of homolytic links and the formation of free, so-called primary radicals (R°). This is the first stage, or initiation, of the radio-chemical ageing process:

$$\text{polymer} \xrightarrow{Irradiation} R^{\circ}$$

- In the presence of oxygen, the bitumen radiolysis process proceeds by means of a chain reaction in which propagation causes the addition of oxygen to a radical (R_1°) and the removal of an atom of hydrogen from the substrate (R_2H) leading to the formation of a hydrogen peroxide and another radical:

$$R_1^{\circ} + O_2 \longrightarrow R_1OO^{\circ}$$

$$R_1OO^{\circ} + R_2H \longrightarrow R_1OOH + R_2^{\circ}$$

The kinetics of the reaction depend on the concentration of free radicals and the oxygen content. It therefore depends, for a given material, on the dose rate, the oxygen penetration into the matrix (which is a slow process) and on the evolution mode of the peroxide radicals formed. In fact, these radicals maintain (propagation) or limit (termination) the oxidation reaction; propagation stops when two radicals inter-react to produce non-reactive species by re-combination:

$$R_1^{\circ} + R_2^{\circ} \longrightarrow R_1R_2$$

$$R_1OO^{\circ} + R_2^{\circ} \longrightarrow R_1OOR_2$$

$$R_1OO^{\circ} + R_2OO^{\circ} \longrightarrow R_1OOR_2 + O_2$$

The radiolysis of bitumen causes the formation of numerous oxidised organic compounds (formic and acetic acids, carbonyl compounds, alcohols, nitrogenous compounds etc.), susceptible to be consumed by bacterial activity and to migrate into the disposal cells as they dissolve (Andra, 2005d ; Bourbon, 2005). These organic compounds are thus generally more soluble than those released during irradiation without oxygen.

7.2.6 Summary of information concerning the chemical evolution of ventilated structures during the operational phase

This stage is marked by the highly de-saturated state of all the ventilated structures. Chemical interactions are thus limited by the small quantities of water available. The oxidation of argillites on the walls of these structures is restricted to the EDZ and the immediate vicinity of fractures and micro-fissures within the damaged area. The corrosion of metal components and the atmospheric carbonation of concretes are minor phenomena that do not affect the properties of these components. The radiolysis of the organic components present in the various type B waste packages is a phenomenon that leads to the production of gases (principally hydrogen) and to very superficial alteration by radiolysis of bituminised sludge. The gases produced during the operational period are evacuated by the ventilation. Finally, given the relative humidity inside type B waste disposal cells, the level of radiolysis of the ventilation air (water vapour and nitrogen) is low.

7.3 Chemical evolution of disposal cells of type C waste and spent fuel

The fitting of the sealing caps shortly after placing the packages in type C waste and spent fuel disposal cells makes it possible to greatly limit any exchanges with the adjacent access drifts. Under these conditions, it can be considered that the chemical evolution of these unventilated structures during the operational phase differs only very slightly from that in the post-closing phase, which really starts after emplacement of the swelling clay plug. The task of removing the sealing cap and fitting the disposal cell end plug takes at maximum of a few days. The oxidising transient associated with this short operation can be ignored in the chemical evolution of these disposal cells.

Type C waste package disposal cells differ from those holding spent fuel packages by the absence of a swelling clay based engineered barrier fitted between the packages and the argillites. More precisely, the engineered barrier is fitted between the lining and the metal coating of spent fuel disposal cells. However, both types of disposal cell have very similar ends, namely a swelling clay plug and a concrete plug.

The design of these disposal cells in two distinct parts with different dimensions leads to considering that their chemical evolution also has two distinct components, one related to the inside of the disposal cell and the other to the disposal cell end. In fact, other than the indirect chemical effects associated with the release of heat by the packages inside the disposal cell or the transfer of hydrogen, the chemical evolutions of both parts of the disposal cell have little influence on each other and can be considered as practically independent.

- Beyond the chemical behaviour of the spent fuel assemblies and glass matrices themselves, the chemical evolution of the inside of the disposal cell is marked by the presence of metal components (coating, lining, over-pack or container) and of clay-based materials in the broadest sense (argillites and/or the swelling clay of the engineered barrier). Corrosion, interactions between clays in the broadest sense and iron, and chemical balancing between argillites and swelling clays are thus the main chemical processes involved.
- The chemical evolution of the disposal cell end is principally marked by interactions between clays in the broadest sense (argillites and the swelling clays of the plug) and concrete: The alkaline disturbance of clays and the chemical deterioration of concretes.

The chemical evolution of both parts of the disposal cell is influenced by hydraulic processes and by the thermal load. The former determines a set of parameters on which the nature and spatial and temporal extent of the chemical processes depend: the presence of water, water flows, organisation of the flows, solute transport conditions. The thermal load comes in as a conventional parameter in chemical reactions. In particular, it should be noted that:

- the 90 °C thermal peak in the disposal cells is reached after a few decades and, thus, before the disposal cells become completely saturated, particularly the engineered barrier of the spent fuel disposal cells. The temperature has already dropped back to around 30 °C-35 °C after a few thousand years;
- the hydraulic evolution is characterised by the production of hydrogen due to the corrosion of the lining and metal coating. This production does not prevent the disposal cell plugs and engineered barrier of spent fuel disposal cells from reaching a state of near total saturation ($S > 95\ \%$) in approximately a hundred years.

In view of all the considerations outlined above, the presentation of the chemical evolution of the disposal cells is structured by separating the inside of the disposal cell and the disposal cell end.

- As far as the inside of the disposal cell is concerned, we will deal in succession (in roughly chronological order) with the arrival of water inside the disposal cell until it reaches the inside of the packages:
    - corrosion of metal components: coating, lining and over-packs and containers,
    - chemical evolution of the engineered barrier and near-field argillites,

  - the dissolution of type C waste matrices and the chemical behaviour of spent waste assemblies (dissolution of Uox and Mox pellets, corrosion of sheaths and structural components)
- As far as the disposal cell end is concerned, the following will be discussed:
  - the alkaline disturbance of the swelling clay plug and argillites in the near-field by the concrete of the plug,
  - the chemical deterioration of the concrete in the plug

7.3.1 Corrosion of the coating, lining and containers inside disposal cells

7.3.1.1 The phenomenological conditions of corrosion hydraulic: temperature and redox

As shown in chapter 6, the relative humidity of the air in type C waste and spent fuel disposal cells, after placement of packages and plugs, rapidly becomes very high (~ 100 %). These conditions contribute to the premature development of corrosion processes in coatings and linings.

Fitting the sealing cap after inserting the packages will trap air, and thus oxygen, inside the disposal cells. This oxygen is consumed by corrosion after a maximum of a few years, such that the redox conditions within the disposal cells become anoxic (Andra, 2005k). The corrosion then produces hydrogen. In detail, the redox conditions evolve along the length of the disposal cell during the operational period: they remain oxidising at the start of the disposal cell end due to the proximity of the open, ventilated access drifts and gradually become reducing farther away from the drift. The redox conditions also rapidly become reducing on the inside of the disposal cells. The closing of the access drifts rapidly removes this oxidising component at the end of the disposal cell and the entire disposal cell then evolves under anoxic conditions.

The quantities of oxygen trapped in the disposal cell when the sealing cap and plug are fitted are small. The thicknesses of metal corroded (less than a millimetre) are negligible compared with the thickness (several centimeters) of the metal components.

During the thermal period, the corrosion kinetics under anoxic conditions are increased by a factor of 4 at 90 °C and a factor of 2 at 60 °C compared with those at the natural geothermal temperature of 22 °C. Given the decrease in temperature in the disposal cells after a few decades, the effects of the thermal load on the corrosion kinetics are limited.

7.3.1.2 Corrosion sequence of metal components over time

Generally speaking, the corrosion of the various metal components over time depends on their successive discharge of sealing integrity: (i) firstly, corrosion of the coating in spent fuel disposal cells (internal and external faces) and of the lining (external face), (ii) then, after the discharge of the lining's sealing integrity[9], corrosion of the lining on both faces and on the outside of the containers, and (iii) finally, after the discharge of the containers' sealing integrity, corrosion of its internal face, of the type C waste primary package's stainless steel envelope and of the insert of spent fuel packages.

The discharge of the sealing integrity of linings, coatings and containers is mainly mechanical in origin: corrosion gradually reduces the thickness of the metal components until they can no longer withstand the mechanical stresses to which they are subjected. At this stage, they distort and locally fracture (see § 8).

Generalised corrosion in a reducing medium (Inset 7.3) leads to the formation of expanding corrosion products on the interfaces of metal components, notably: (i) at the point of contact between the Callovo-Oxfordian argillites and the coating of spent fuel disposal cells and the lining of type C waste

---

[9] The lining's seal is not specified. However, as the various sections of the lining are welded together, it is considered to be sealed for the analysis the phenomenological evolution of type C waste and spent fuel disposal cells.

disposal cells, (ii) at the point of contact between the swelling clay engineered barrier and the coating of spent fuel disposal cells, and (iii) at the point of contact between the lining and the packages. Associated with the flow of the argillites and the swelling of the engineered barrier of spent fuel disposal cells during its re-saturation (see § 6), the formation of these corrosion products contributes to the establishment of a direct contact between the metal components and between these components and clay-based media (argillites and engineered barrier of spent fuel disposal cells). This encourages the establishment of weak corrosion kinetics at an approximated maximum rate of 2 to 5 μm.year^{-1} (Crusset, 2005).

The 30 mm thick coating of spent fuel disposal cells corrodes on both sides. The estimated time required for it to fully corrode is a few thousand years.

Whether it is in type C waste disposal cells or spent fuel disposal cells, the outside of the lining takes at least 1,000 years to corrode (Crusset, 2005) (Figure 7.3.1 and Figure 7.3.2) before it loses its sealing integrity by distortion and mechanical fracture (see § 8). Thenceforth, the inside of the lining can also corrode, as can the containers of type C waste and spent fuel packages. The re-saturation of the lining's internal clearances is initially limited by the production of hydrogen by corrosion in a reducing medium. Compressive mechanical distortion and the formation of expanding corrosion products (magnetite (Fe_2O_3), siderite ($FeCO_3$) etc.), contribute to the resorption of the gaps. Saturation inside the lining increases and significant corrosion of the inside of the lining and outside of the package containers may begin. A few thousand years are required to fully corrode the lining. It therefore takes approximately 4,000 to 5,000 years for the coating and lining to be fully corroded.

The thicknesses of the containers of type C waste and spent fuel packages are specified in order for their sealing integrity to remain intact for 4,000 and 10,000 years, respectively. By design, the total thickness of containers has been determined using a conservative approach concerning both the kinetics of corrosion and mechanical strength in view of the stresses involved. The 55 mm thickness of type C waste over-packs was thus calculated to allow for a corrosion thickness of 27 mm and a mechanical strength thickness of 28 mm. The phenomenological approach developed in this document, concerning both corrosion and mechanical changes, results in the achievement of longer intact sealing integrity being achieved than that specified: it is approximately 15,000 years for the over-pack of type C waste packages and 30,000 years for spent fuel containers, whose initial thickness is greater (110 mm for type CU1 spent fuels and 120 mm for type CU2) (Crusset, 2005). In the remainder of the document, the 4,000 and 10,000 year figures will be taken as the reference and the phenomenological figures will be used exceptionally when justified. The evolution of the inside of containers is described below for type C waste (see § 7.3.4) and for spent fuels (see § 7.3.5).

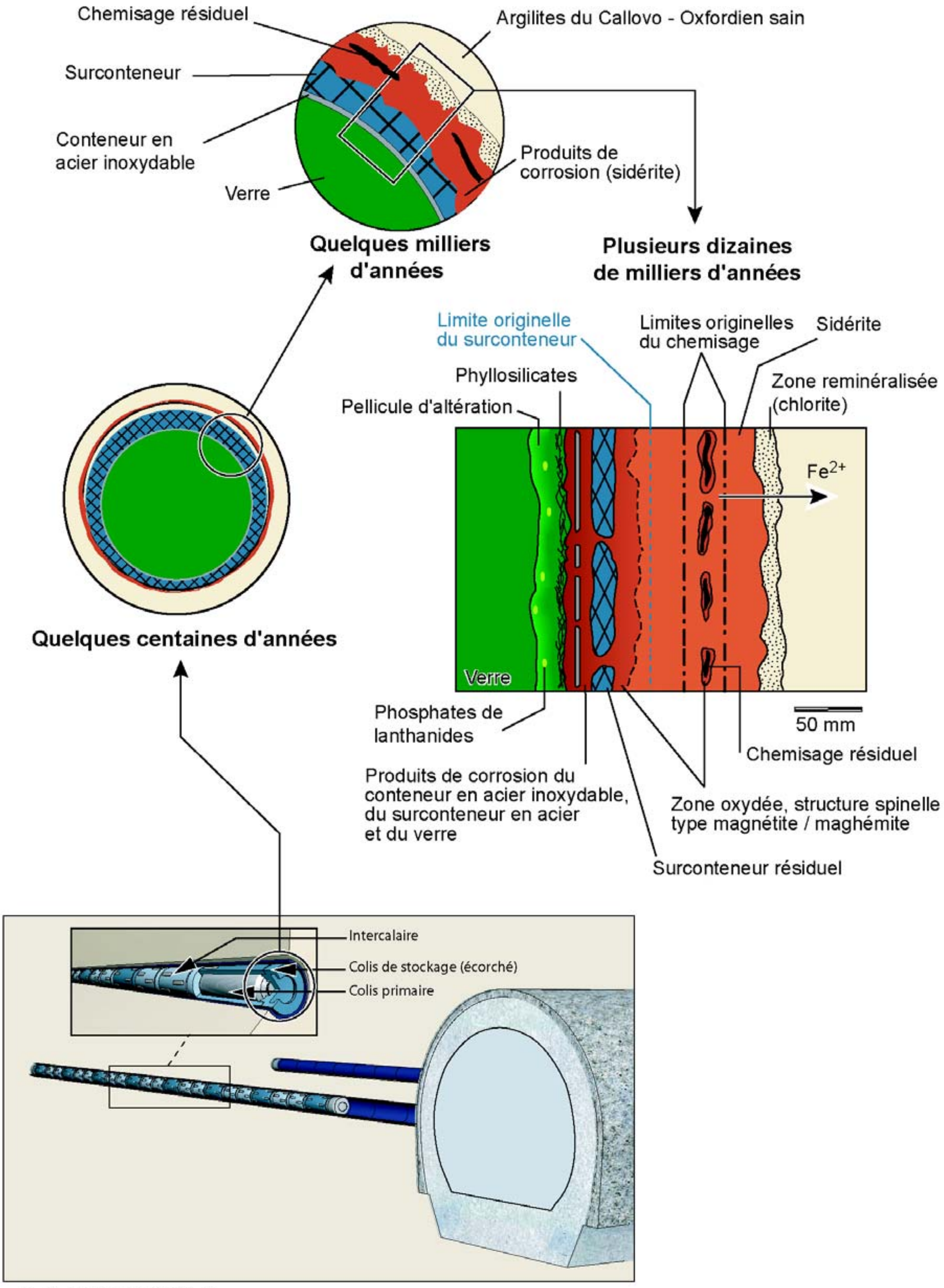

D.PL.FSTE.04.0091.B

Figure 7.3.1 *Schematical representation of the progression of corrosion of the lining and over-pack in a type C waste cell, from several hundred, several thousands and tens of thousands of years*

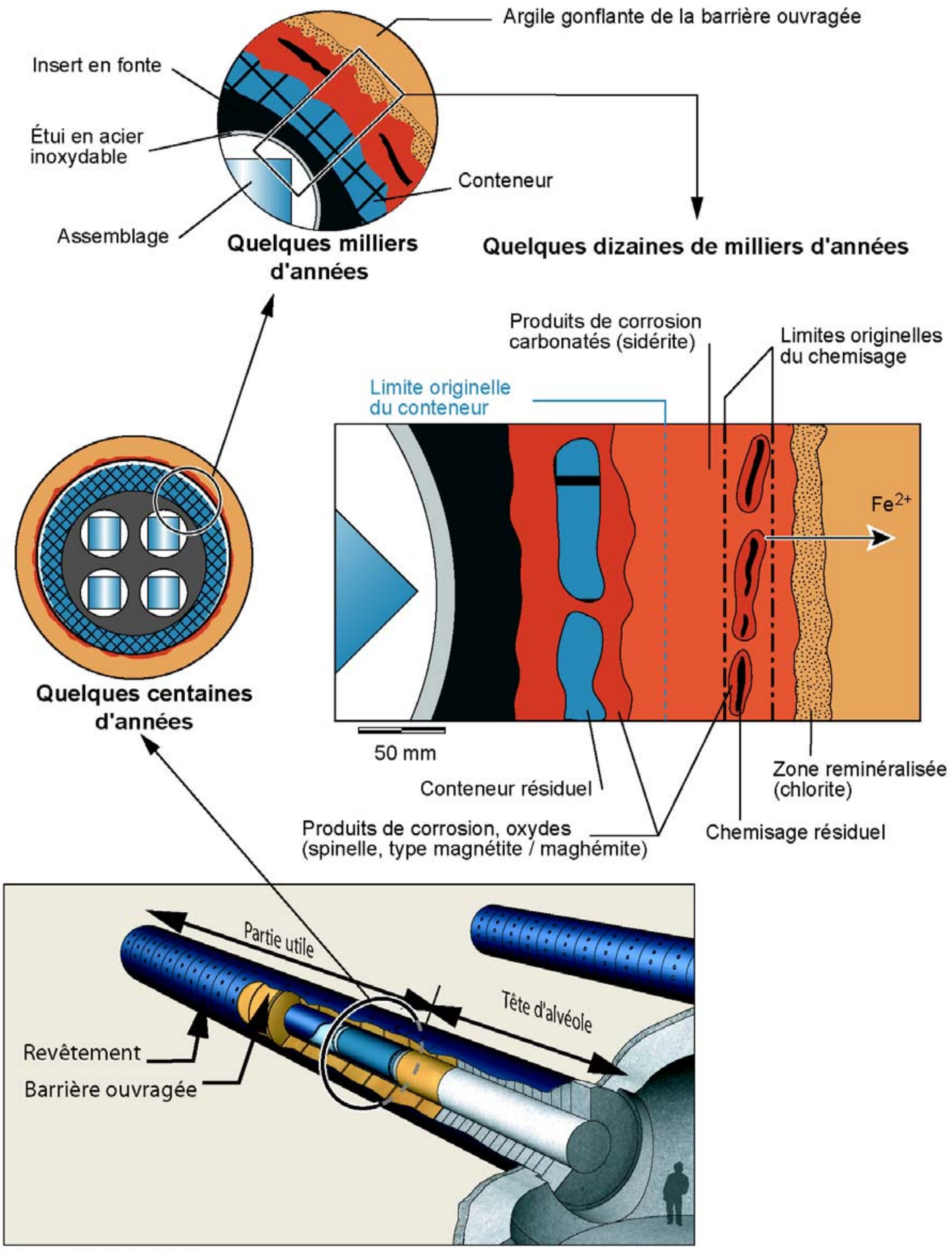

D.PL.FSTE.04.0092.B

Figure 7.3.2 *Schematical representation of the progression of corrosion of the lining, container and insert in a spent fuel disposal cell after several hundred, several thousand and tens of thousands of years*

7.3.2 Chemical evolution of the engineered barrier of spent fuel disposal cells

From re-saturation onwards, the clay engineered barrier of spent fuel disposal cells interacts with the water from the Callovo-Oxfordian layer and metal components (coating and lining).

7.3.2.1 Achieving a state of equilibrium with water from the Callovo-Oxfordian argillites and the effect of temperature

The engineered barrier gradually achieves a state of chemical equilibrium with the water from the argillites. That occurs principally by ionic exchange and protonation / deprotonation processes. In fact, both types of clay-based materials (swelling clay and argillites) consist of similar mineral phases (Inset 2.6, Table 3.3.1) and have similar balanced water chemistries. Thus the achievement of equilibrium between the swelling clay of the engineered barrier and the water in the argillites does not produce any major changes to its crystal chemistry or to the chemistry of the interstitial waters.

This balancing process occurs over a period of approximately ten thousand years, notably linked to the solute transfer kinetics in the near-field argillites and in the swelling clay. However, the changes to the major chemical parameters of the water in the swelling clay (pH, Eh, carbonates, sodium, calcium…) associated with this process are limited (Giffaut & Coelho, 2005 ; Nagra, 2002b). The mineralogical changes concern the dissolution of the secondary minerals in swelling clay (calcite, gypsum, siderite) and the Na / Ca ionic exchange causes some of the initial sodic montmorillonite in the swelling clay to change into a calcic montmorillonite, the former however remaining largely preponderant in the swelling clay when chemical equilibrium is achieved (Nagra, 2002b).

The thermal load can cause precipitation of gypsum and dissolution of quartz contained in the swelling clay, but these processes remain localised (interface with the lining) and limited, notably given the small quantity of quartz in swelling clays (< 3 %) (Andra, 2005f, Tome 1). Generally speaking, temperature is an important parameter in the illitisation process, the consequence of which is the gradual dissolution of the minerals within the swelling clay and, therefore, the discharge of its swelling properties. However, the small concentration of potassium in argillites and the temperatures reached in disposal cells during the first thousand years (always below 65 °C on the outside of the engineered barrier and between 85 °C and 55 °C in contact with the containers, see 5) are insufficient to allow illitisation of the engineered barrier in its mass. In fact, the numerous studies of the illitisation process in sedimentary basins demonstrate that it only starts at temperatures in over of 80 °C and does not become significant until beyond 100 °C, as long as there is a potassium source (see § 3.3.1.3). Illitisation of the engineered barrier therefore remains localised at the interface between the coating and the argillites. Modelling leads to an estimate of the illitised thickness of the engineered barrier of less than a centimetre (Michau, 2005b). It is accompanied by iron/clay disturbance developing in swelling clay in contact with the coating (see below). The influence of iron/clay disturbance on illitisation has so far not been assessed, but is almost certainly negligible due to the mechanisms involved in the two disturbances respectively.

Thus, under repository conditions, the engineered barrier, when in equilibrium with the interstitial waters of the Callovo-Oxfordian argillites, generally retains its initial mineralogical structure and an interstitial water chemistry moving towards that of the argillites, thus maintaining their hydraulic, swelling and retention properties.

7.3.2.2 Iron/clay interaction

An iron/clay disturbance develops at the point of contact with the coating and lining (Figure 7.3.3). This process is closely linked to the corrosion kinetics of the steel components. In fact, the corrosion of the metal causes gradual release of iron in the disposal cell saturation water. This iron may spread in the swelling clay and react with the minerals in the clay, notably smectites.

The iron/clay disturbance (Inset 7.5) in clay-based material is characterised by ionic exchange and dissolution / precipitation processes (Michau, 2005b). It progresses by means of concentric fronts, starting at the interfaces: coating/swelling clay and swelling clay/lining. Experiments, combined with the recent modelling activities, demonstrate that the disturbance takes the form of the formation of an initial highly re-mineralised area, a centimetre or so thick, in contact with the metal components, consisting mainly of ferric chloride and ankerite. This gradually moves into a second, less disturbed area, characterised only by the smectite being iron-enriched and the formation of secondary minerals (particularly quartz, feldspar and zeolites). This enrichment does not change the swelling or retention properties of smectite (Giffaut & Coelho, 2005). This second mechanism affects the entire thickness of the engineered barrier over a period of a few tens of thousands of years.

The reaction processes are only really effective when the engineered barrier is re-saturated (after about a hundred years, § 6) and are more intense at higher temperatures. Thus, the iron/clay disturbance develops mainly when favourable temperature and saturation conditions occur simultaneously, i.e. during the first few thousand years. It develops more slowly after the thermal transient.

Taking into account the effects of the lining and coating, the total extent of the re-mineralised areas has been assessed by chemical/transport modelling at a maximum of ten centimeters, or 15 % of the thickness of the swelling clay. This result, and the limited mineralogical transformations in the remainder of the swelling clay, do not lead to a change in the hydraulic, retention or swelling properties of the entire engineered barrier for a period of a million years.

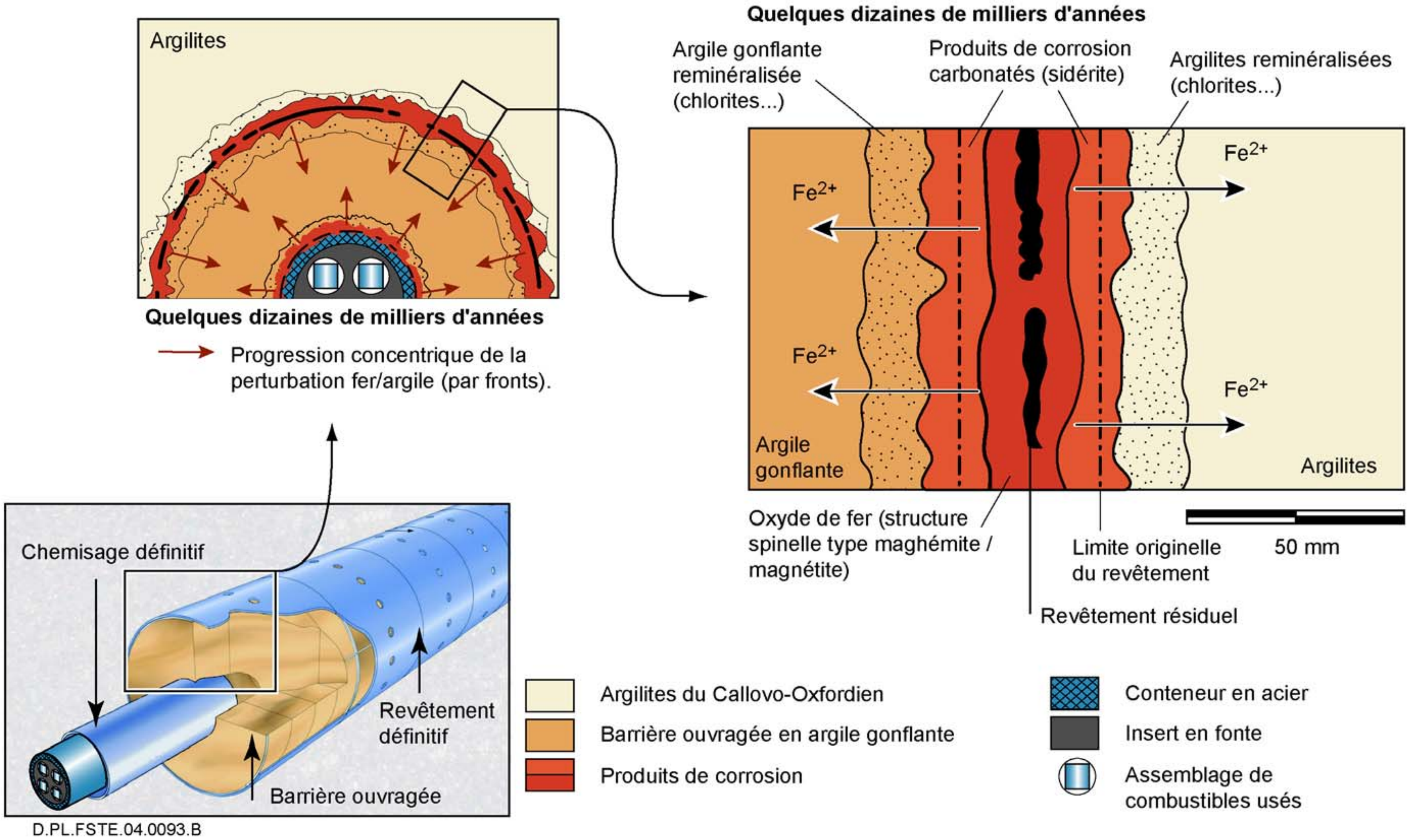

Figure 7.3.3 *Schematical representation of the perturbation of the iron/swelling clay engineered barrier of a spent fuel disposal cell, after a few tens of thousands of years*

Inset 7.5 Iron (metal) /clay (argillites and swelling clay) disturbance

There are few archaeological analogies concerning the chemical interaction between iron (metal) and clay media in the broadest sense. However, advantage has been taken of the work carried out into natural diagentic chloritisation processes (Chamley, 1989). The assessment of iron/clay interactions carried out by ANDRA, combined an experimental approach in a surface laboratory and the development of thermodynamic and kinetic reactional models (Michau, 2005b).

The process

The deterioration of the clay in contact with metal iron under saturated, reducing conditions is characterised by ionic exchange processes, the transformation of the mineral species forming the original clay (Inset 2.6) and the precipitation of secondary phases.

- The ionic exchange processes on the surface of the initial smectites lead to the adsorption of iron which can lead to the surface precipitation of Fe^{III} (Giffaut & Coelho, 2005 ; Tournassat, 2003). This stage is perhaps a transient phase before mineralogical changes.

- The mineralogical transformations firstly involve the dissolution of the montmorillonite (clay 2:1 dioctahedric) present in the original swelling clay in contact with the metal material.

  In parallel, experimental studies indicate the formation initially of *nontronites* (clays 2:1 dioctahedric, $(SiAl)_4Fe_2O_{10}(OH)_2Na_{0,3}.4H_2O$) still corresponding to a partially oxidised state, then of *berthierines* (clays 1:1 trioctahedric, $(SiAl)Fe_2^{II}AlO_5(OH)_4$) precursors of ferro-magnesian *chlorites* (clays 2:1, $(FeMgAl)_6(SiAl)_4O_{10}(OH)_8$) (Andra, 2005f, Tome 1 ; Michau, 2005b).

  Due to the temperatures to be considered in the repository and the slow kinetics of the mineralogical transformations susceptible to occur in the longest term, they can only be the subject of a short-term experimental approach at high temperatures (300 °C). In the presence of corrosion products or the absence of the addition of metal iron, they indicate that the montmorillonite evolves into a ferro-magnesian *saporite* type smectite (clay 2:1 trioctahedric, $(NaCa_{0.5})_{0.3}(MgFe^{II})_3(SiAl)_4O_{10}(OH)_2.4H_2O$). With a metal iron source, *chlorites* form close to the source containing more and more iron (Guillaume, 2002 ; Guillaume *et al.*, 2003).

With water rich in carbonates and calcium, as in the Callovo-Oxfordian argillites, ankerite type mixed Fe/Ca carbonates form in contact with the iron source ($Ca(FeMgMn)(CO_3)_2$). The neo-formation of quartz, feldspar and zeolites are also noted, whilst the clay carbonates and phosphates dissolve (Michau, 2005b).

Spatial organisation of the disturbance

Under conditions of solute transfer by dominant diffusion, the iron/clay disturbance process spreads along fronts in contact with the metal. The ionic exchange processes are very rapid with the arrival of the ferriferous outer zone in the clays. However, the kinetics of the mineralogical transformations are slow, particularly at temperatures below 100 °C, which limits the extent of the disturbance to the interface with the metal.

7.3.3 Chemical evolution of near-field argillites of type C waste and spent fuel disposal cells

As for the engineered barrier of spent fuel disposal cells, an iron/argillite disturbance develops in contact with metal components (lining of type C waste disposal cells and coating of spent fuel disposal cells).

The reactional and kinetic mechanisms involved in the iron/argillite disturbance are similar to those described for the engineered barrier of spent fuel disposal cells: formation of a highly re-mineralised area in contact with the metal components, then of a second, lightly affected area until reaching a zone totally unaffected by the iron.

The disturbance begins as soon as the metal components are placed in position, notably because the disposal cell near-field argillites are saturated and remain close to the fully saturated state throughout the hydrogen production and migration period (see § 6). It continues (i) until the coating is fully corroded, i.e. several thousand years, in spent fuel disposal cells, and (ii) until complete corrosion not only of the lining but also of the over-pack, i.e. beyond ten thousand years, in type C waste disposal cells.

As for the engineered barrier of spent fuel disposal cells, the iron/argillite disturbance develops essentially during the thermal period (several thousand to ten thousand years). Beyond this period, they evolve very slowly. Furthermore, they cease after several thousand years with the total corrosion of the metal components involved (see above). It can therefore be considered that, over a million years, the extent of the disturbance remains close to that achieved at the end of the thermal period.

Given the mineralogical similarities between argillites and swelling clays it is reasonable to assume that the extent of the disturbance associated with the interactions with iron are similar for both media. The extent of the highly re-mineralised area is around a centimetre and that of the slightly disturbed area, a few centimeters. The extent of the highly re-mineralised area is therefore considerably smaller than that of the initial EDZ. The mechanisms involved beyond the highly re-mineralised area make it possible to consider that the disturbance does not affect the hydraulic, chemical and mechanical properties of micro-fissured or undisturbed Callovo-Oxfordian argillites.

7.3.4 Dissolution of the glass matrix

Type C waste packages consist of a sodic alumino-borosilicated glass matrix and waste materials. The latter consist of fines resulting essentially from insoluble matter from dissolution processes (RuO_2, Rh and Pd), concentrated fission products and actinide residues. During fusion, they become an integral part of the glass structure.

The principal components of the glasses are SiO_2, B_2O_3, Al_2O_3 and Na_2O (Inset 7.6). Depending on the chemical composition of the solutions of the fission products and the origin of the reprocessed fuel, the other principal oxides are CaO, Fe_2O_3, NiO and MgO. C0.2 (UMo) glasses are molybdenum enriched and C4 glasses richer in plutonium. The waste content incorporated into the glasses is less than 18.5 %, with a mean content of ~ 12.8 % for R7T7 glasses (Andra, 2005d).

7.3.4.1 Behaviour of the glass matrix before over-pack rupture

Before the over-pack loses its sealing integrity, the glass matrixes are in a closed, dry atmosphere. The only deterioration then possible in the absence of water is α and $\beta\gamma$ self-irradiation.

For type R7T7 glasses (type C1 and C2 packages), $\beta\gamma$, principal irradiation during the operational period has little effect (no significant production of helium, no significant diffusion of mobile elements). For type C0 packages (PIVER, UMo R7 and AVM waste), the radiological content is lower than for type C1 and C2 packages and the self-irradiation effects are practically zero. For type C3 and C4 packages (vitrified UOx / MOx waste and vitrified Pu waste), the effects of self-irradiation are currently under study.

As far as α self-irradiation is concerned, the mean helium production for the various types of C waste packages is approximately 1 mole per package per 15,000 years (Talandier, 2005). For type C1 and C2 glasses the production of helium does not cause mechanical fracturing of the glass. For type C3 and C4 glasses which have not yet been produced (vitrified UOx / MOx waste incorporating a small quantity of Pu), the effects of self-irradiation are currently under study (Andra, 2005d).

Inset 7.6 ***The structure of (boro)silicated glass***

Introduction

The structure of silicated vitreous materials has been the subject of studies for almost a century (Zachariensen, 1932 ; Zachariensen, 1933), particularly by the glass and nuclear industries, in order to better understand and optimise the chemical durability properties. From a physico-chemical point of view, a glass is a fixed super-cooled liquid with, thus, an amorphous structure (Scholze, 1991 ; Zarzycki, 1982). Furthermore, the development of high-powered analysis tools (neutron diffraction (Wright, 1994), reflective infrared spectroscopy (Geotti-Bianchini & De Riu, 1995 ; Geotti-Bianchini *et al.*, 1991), molecular dynamic modelling (Aertsens & Van Iseghem, 1996 ; Ganster, 2004 ; Ledieu, 2004),…) has made it possible over the years to refine observations to the point of proposing a general structural model. This model is essential to the understanding of the dissolution processes.

Structure

The three-dimensional framework of silicated glasses consists of SiO_4 tetrahedra. It is modified by the introduction of alkaline or alkaline-earth elements. A silicated glass thus has three different types of cations: network-forming cations (Si, B, P,…), network-modifying cations (Li, Na, K, Mg, Ca, Ba,...) and intermediate cations which may be network-formers or modifiers, depending on the composition of the glass (Al, Pb, Zn, Ti, Fe,...).

Generally speaking, vitreous network-forming cations are cations that can adopt a tetrahedric environment and are interconnected by bridging oxygen. Modifying cations cause the breaking of the network's tetrahedric chain with the appearance of non-bridging oxygens, connecting a network forming atom and a network modifying atom. It is not always possible to assign one or other of these types to all cations and certain can adopt mixed configurations whilst others can change type according to the composition of the glass. These are then said to be "mixed".

In nuclear glasses, the radioactive nuclides and chemical toxins are incorporated into the structure of the glass as forming or modifying elements, depending on their electronic structure (see Figure below, (Andra, 2005d)).

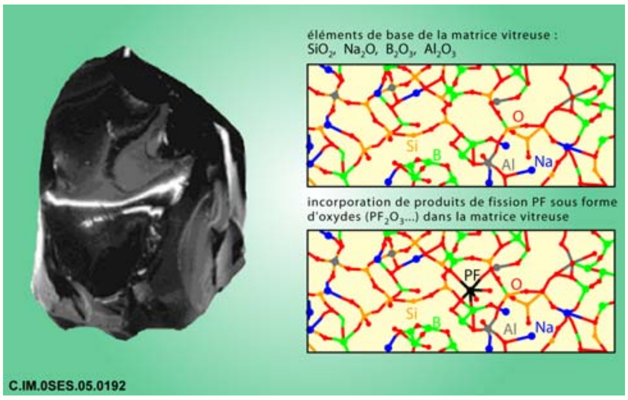

Photograph of a piece of R7T7 glass and diagram of the vitreous structure

7.3.4.2 Type C waste after rupture of the over-pack

The discharge of the over-pack's sealing integrity of type C waste container's (see § 7.3.1) allows gradual re-saturation of the internal gaps to take place and initiates corrosion of the inside of the over-pack and the primary stainless steel envelope of the type C waste package. The primary envelope's sealing integrity is rapidly lost due to mechanical stresses, so that water is then able to come into contact with the waste almost as soon as the over-pack ruptures.

However, due to the continued production of hydrogen over several tens of thousands of years, total saturation (S = 100 %) of the inside of the over-pack does not occur until beyond this timescale. Nevertheless, the drop in hydrogen production after 10,000 years leads to a saturation level in over of 90 % inside the package.

The dissolution kinetics of vitrified packages is controlled by the thermal and chemical conditions of the water in contact with the glass. It also depends on the chemical composition of the glass. However, the αβγ self-irradiation processes which begin from the moment that the vitrified packages are manufactured, do not influence the dissolution kinetics of the glasses, essentially due to the high self-healing ability of the glass matrix (Andra, 2005d).

In type C waste disposal cells, when water comes into contact with the glass (at least 4,000 years), the temperature has dropped sufficiently, below 50 °C; dissolution kinetics will not be significantly altered (Bauer, 2005). Beyond this time, the temperature rapidly decreases and is between 25 and 30 °C after approximately 10,000 years.

The dissolution kinetics of the glass matrix are also influenced by materials located in direct contact with the glasses and, therefore, by the presence of corrosion products from the primary container, over-pack and lining. Only the outside (surface) of the glass is subjected to this influence. These materials affect the chemistry of the water in contact with the waste due to the retention properties of the silica. The chemistry of the interstitial water at the heart of the glass is only very slightly sensitive to the immediate environment around the packages (steel deterioration products) due to their distance (Andra, 2005d).

Dissolution of the glass matrix (Inset 7.7) occurs in three successive stages: (1) selective dissolution of the most soluble elements (boron, alkaline elements). This stage is short, roughly a few days; (2) dissolution of the glass is at a linear speed of V_0. This phase can last for several years to several decades; (3) a rapid reduction in the speed until it reaches a very low residual speed (V_r). The sequence of stages 2 and 3 is denoted as V_0➠V_r. The transition phase between these two stages is very short and can be ignored in describing the glass matrix dissolution process over time.

The dissolution kinetics of the different glasses (see § 2.3) and their evolution have been assessed based on numerous experiments, some of which have been going on for several years, and models developed from these experiments. The total dissolution periods for PIVER, UMo R7 and AVM glasses (type C0.1, C0.2 and C0.3 packages respectively) are currently estimated at around a few thousand years. For type R7T7 glasses (type C1 and C2 packages) and vitrified UOx / MOx and Pu waste (type C3 and C4 packages), the dissolution of the glass based on the V_0➠V_r model indicates that total dissolution of the glass will take at least 300,000 years. Recent studies seem to indicate that V_r reduces over time and as the temperature falls (Andra, 2005d) (Figure 7.3.4).

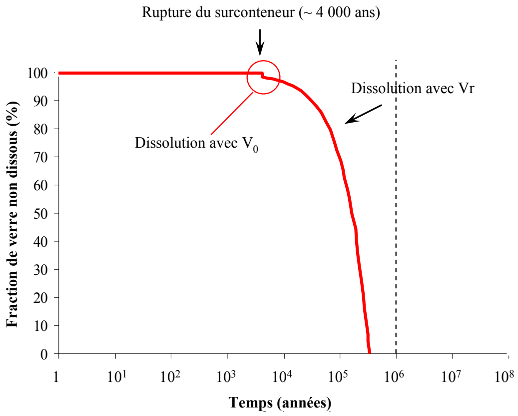

Figure 7.3.4 *Simplified curve for the dissolution of the glass matrix over time for a generic type R7T7 glass (type C2 packages) (Andra, 2005m)*

Inset 7.7 ***Dissolution phases of silicated glasses***

Introduction

The question of understanding the behaviour of silicated glasses in an aqueous medium has been within the scientific community for many years now. Various approaches have been proposed in order to characterise the dissolution processes of borosilicated nuclear glasses (Advocat *et al.*, 1990 ; Advocat *et al.*, 2001 ; Andra, 2005d ; Bourcier *et al.*, 1990 ; Grambow, 1985 ; Grambow & Müller, 2001 ; Jégou *et al.*, 2000) and studies of natural analogues of nuclear glasses (basaltic glasses) have been used to check these approaches. European programmes have also investigated the question of the dissolution of nuclear glasses, including GLASTAB (Andra, 2005d), CORALUS and GLAMOR. Generally speaking, a concensus has been reached at international level concerning the evolution of the dissolution kinetics of glasses, however the phenomena controlling these kinetics are still the subject of debate.

The process and its kinetics

The dissolution of a nuclear glass (Inset 7.6) occurs in two successive stages (see Figure):

- Firstly, **the phenomenon of inter-diffusion** corresponds to an ionic exchange between the hydrogenated species present in the solution and the elements least linked to the network, the network modifying cations. During these reactions, the silicated network remains intact (incongruent dissolution). The kinetics of inter-diffusion progress at the square root of time (process controlled by the diffusion). This process is rapid and is then marked by **hydrolysis of the silicated network**. This process causes congruent dissolution of the glass at a linear speed V_0. The change from the first to the second of these processes corresponds to a competition between the ionic exchange processes and, with the increase of the hydrated and dealcalinised glass and the slowing down of this process, the hydrolysis process. The duration of this first stage depends, in particular on the presence of container corrosion products close to the glass packages (Andra, 2005d ; Nagra, 2003b) and is estimated to be between several years and several decades.
- The second stage corresponds to the **formation of glass alteration products** (Inset 7.8). During this stage, the dissolution kinetics reduce with the accumulation of alteration products, tending rapidly towards a residual speed. This transient corresponds to (i) the modification of the composition of the solution causing an increase in the silica content in solution and thus a change in the affinity between the glass and the solution and (ii) the formation of secondary products, including the alteration thin layer. These two processes lead to the slowing down of the exchanges between the surface of the glass and the solution and enable a very low, but never zero, residual dissolution speed (V_r) to be reached rapidly.

The fraction of glass altered over time depends on the dissolution rate of glass and also on the reactional surface of glass in contact with water and therefore on the state of glass fracturing. Nevertheless, dissolution experiments, especially under V_0 conditions, show that only a fraction of the fissures/fractures actually contributes to dissolution, so that the actual dissolution surface is smaller than the theoretical surface offered by fissuring/fracturing (Andra, 2005d).

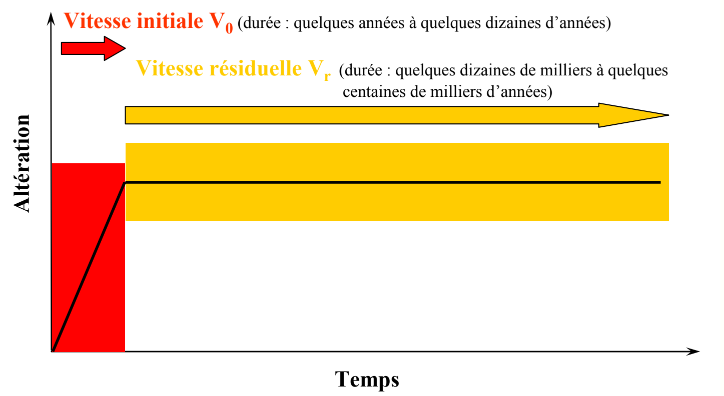

Diagram of the evolution of the alteration kinetics of a nuclear glass (Andra, 2005d)

Inset 7.8 ***The dissolution products of silicated glasses***

Introduction

The alteration products of nuclear glasses, and their evolution, have also been the subject of studies based on the analysis of the deterioration products of basaltic glasses, considered as natural analogues (Grambow *et al.*, 1985 ; Lutze *et al.*, 1985 ; Malow & Ewing, 1981 ; Techer *et al.*, 2000). In parallel with the study of natural analogues, models have been developed that have made it possible to satisfactorily represent the formation of these alteration products (Advocat, 1991 ; Advocat *et al.*, 2001 ; Bourcier *et al.*, 1990 ; Caurel *et al.*, 1990 ; Crovisier *et al.*, 1989 ; Grambow *et al.*, 1985 ; Michaux *et al.*, 1992 ; Munier *et al.*, 2004).

Alteration products

Alteration products consist of an amorphous phase, known as the "alteration thin layer" and external, more or less crystalline, compounds.

The **alteration thin layer** forms very rapidly once water has come into contact with the nuclear glass and initiated glass dissolution. The formation of alteration film consists either of the recombination *in situ* of some of the less soluble elements in the glass after hydrolysis of the glass at the interface between the undisturbed glass and the alteration thin layer, or by precipitation of an amorphous compound that in solution has reached the solubility product. Whether these two mechanisms develop more or less rapidly depends on the nature of the elements retained in the thin layer and on the alteration conditions.

All the chemical and hydraulic characteristics of the alteration thin layer (texture, porosity, chemical composition, diffusion properties etc.) are directly influenced by the composition of the glass, its formation conditions and the environment of the package (Andra, 2005d). A certain number of external factors influence the protective character of the alteration thin layer: the pH, the increase in which tends to influence the dissolution of the glass, the increase in the S / V ratio (glass surface area / volume of the solution), the fracturing rate, the varying water flow rate and the physico-chemical reactivity of the materials in contact with the glass. The varying composition of the solution has little effect, other than for example on the silica or magnesium content.

In addition to the alteration thin layer, generally speaking the **first more or less crystalline alteration products** observed during the alteration of a nuclear glass in aqueous phase and at a higher temperature **are smectite type silicates** (Caurel *et al.*, 1990). This composition changes according to the duration of the alteration process and is similar to that of silicates. High temperature experiments on the dissolution of type R7T7 glass (~ 250 °C) also demonstrated the formation of analcite ($NaAlSi_2O_6.H_2O$), zeolites and hydrated calcium silicates (tobermorite ($Ca_5Si_6O_{16}(OH)_2.4H_2O$) or gyrolite ($Ca_2Si_3O_7(OH)_2.H_2O$)). For more advanced alteration states, the deterioration products of nuclear glasses approach those of basaltic glasses (Grambow *et al.*, 1985 ; Lutze *et al.*, 1985 ; Malow & Ewing, 1981).

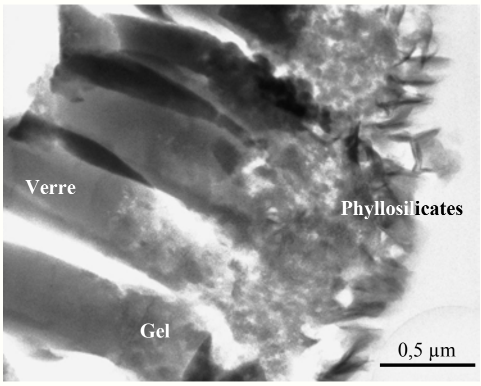

Transmitting electron microscope image of a SON68glass (i.e. non-active R7T7) altered in static mode for 5.7 years at 90 °C in pure water (Ribet et al., 2003)

7.3.5 Spent fuel assemblies

Type CU1 and CU2 spent fuel assemblies (UOx and Mox respectively) consist principally of pellets formed from grains of oxides $(U\text{-}Pu)O_2$ (Inset 7.9). In the case of type CU2 spent fuels, clusters of Pu (8.65 % Pu) are embedded in grains of depleted UO_2 (0.225 % ^{235}U).

The assemblies also contain various structural components: reactor positioning end caps (zircaloy, inconel), guide tubes for guiding pencils (zircaloy), spacing grills (stainless steel), pencil sheaves (zircaloy) (Andra, 2005d).

7.3.5.1 Condition of spent fuels before discharge of container sealing integrity

As long as the container remains sealed, the oxide pellet changes little. In fact, inside the containers, the assemblies are in a confined atmosphere with very small or zero quantities of oxygen and water vapour. There can therefore be no significant oxidation of the oxide pellets, nor even corrosion of the metal components of the assemblies' structure. In addition, the reduction in the temperature after removal from the reactor does not cause any change in the oxidation state of the oxide pellets nor the amorphisation (Andra, 2005d). The α decay (Andra, 2005k) causes the production of helium up to the point of seal discharge. This helium, produced principally in the oxide grains, can be diffused by Alpha self-irradiation by accelerated diffusion (D3AI) to the grain boundaries. Oxides can then be released in the pencils, notably at the interface between the grains and the oxide pellets at the top of the pencils. As the pencils cool after removal from the reactor, the sheaths fissure, which allows helium to be released from the pencils into the clearances within the container. The temperature and pressure exerted inside the containers by the release of helium at the moment that the seal is lost, after 10,000 years are approximately 0.15 MPa for type CU1 and 0.78 MPa for type CU2. Throughout the duration of the phenomenological seal, estimated at 30,000 years, this helium pressure will be approximately 0.25 MPa for type CU1 and approximately 1.2 MPa for type CU2 (Talandier, 2005). Such pressures have no affect on the mechanical behaviour of the insert or the container.

Inset 7.9 ***Structure of oxide pellets and assembly sheaths of spent fuels (Andra, 2005d)***

The characterisation and study of the behaviour of spent fuels are the subject of research programmes both in France (Precci programme conducted jointly by the CEA and EDF), and at European level (SFS programme).

Oxide pellets

The pencils which form a spent fuel assembly consist of a zircaloy sheath in which uranium oxide pellets (UOx fuel) or mixed uranium and plutonium oxide pellets (MOx fuel) are stacked. These pellets consist of grains of uranium oxide UO_2 (type CU1 packages: UOx / URE assembly) or mixed oxide grains $(U\text{-}Pu)O_2$ (type CU2 packages: MOX assembly).

For UOX (CU1) fuel, when used in reactors, with high burn-up rates (> 40 GWj.t$_{-1}$), the microstructure of pellets changes. A rim, several hundred µm thick, forms around the edge of the pellets. Within this rim, the size of the oxide grains has been reduced (< 1 µm) compared with their initial size before use in the reactor (around 9 µm) (see figure below). In the centre of the pellets, the size of the grains has, on the contrary, increased. In addition, due to thermo-mechanical stress in the reactor, fissures and fractures, mainly of a radial nature, appear at the local level. Pellet restructuring is then likely to develop once unloaded from the reactor mainly due to the formation of helium bubbles caused by α activity.

In the case of MOx fuels (CU2), passing through the reactor does not cause the formation of a rim type microstructure within the clusters of mixed oxides. The size of the Pu clusters can reach 20 µm; they are embedded in a uranium oxide pellet, the grains of which are approximately 7 µm in size.

The sheath

The sheath and structural materials (grills, springs, spider etc.) are essentially made from zircaloy. Their passage through the reactor causes a layer of zirconium to form on their surface.

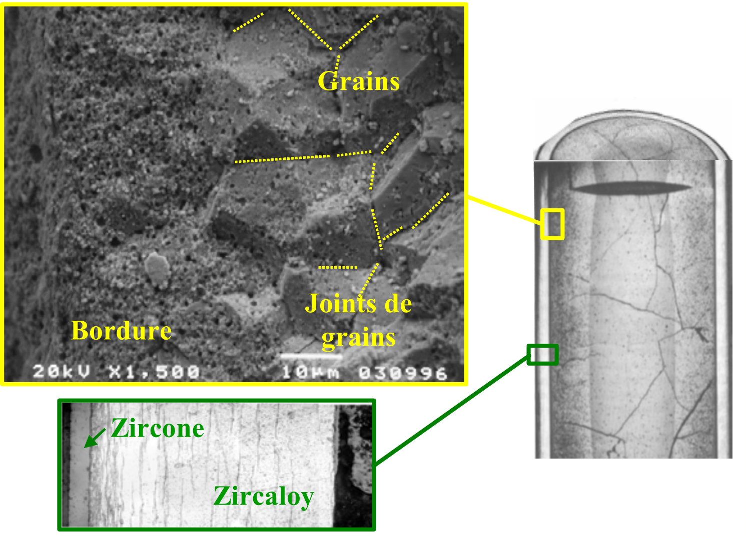

Structure of a UOx type spent fuel pencil (vertical section, on the right): a)scanning electron microscope image of an area close to the sheath (top left) ; b) sectional view of the sheath through an optical microscope (bottom left)

7.3.5.2 Spent fuels after rupture of a container

After about ten thousand years, the rupture of the container caused by corrosion (see § 7.3.1) initiates the immediate release of the gases contained in the assemblies (helium, volatile radioactive nuclides) (Andra, 2005d ; Nagra, 2003a ; Talandier, 2005). These gases accumulate before the arrival of water in the spaces within the pencil, following the filling of the pencil before being placed in the reactor, following irradiation within the reactor and following radioactive decay.

After the container has ruptured, due to the production of hydrogen by corrosion, another ten thousand years is still needed for the saturation level within the container and, in particular, in contact with the assemblies, to be greater than 90 %. In fact, the forward movement of the water until it reaches the assemblies, is slowed by the high level of de-saturation in the internal gaps within the insert, maintained by localised production of hydrogen. Contact between free water and the assemblies is facilitated by the closing of the gaps associated with the formation of corrosion products. The fissuration of the sheaths, or even the local rupture of the pencils (by dry creep before discharge of seal or distortion when the container ruptures) allows liquid water to enter the pencils and come into contact with the oxide pellets. The U-Pu oxide pellets, zircaloy sheaths (zirconium-tin alloy) and stainless steel and inconel structural materials then begin to deteriorate.

When water comes into contact with the oxide pellets, radioactive nuclides (fission products, rare gases etc.) localised around the oxide pellet grain boundaries, in fissures and fractures, or in the spaces within the pencils can immediately be placed in solution. This so-called “labile” activity varies according to the radioactive nuclides in question: it can thus represent up to approximately 35 % of the ^{36}Cl or $^{135\text{-}137}$Cs for type CU2 packages (Andra, 2005d).

After discharge of sealing integrity, the $\beta\gamma$ radiation has greatly decreased (Andra, 2005a, Situation Zu1_1). The oxide pellets are then essentially affected by α radiation (Andra, 2005k). This α radiation leads, very locally out to a distance of a few tens of micrometers from the surface of the oxide grains (Andra, 2005d ; SKB, 1999), to radiolysis of the water, causing the formation of oxidising species (essentially H_2O_2, Inset 7.10). These species cause oxidation of the uranium from valence IV to the much more soluble valence VI. The kinetics of uranium oxidation is thus linked to α decay and the quantity of oxidising species formed by radiolysis of water (Inset 7.11). Beyond a few tens of micrometers, the conditions are again reducing and cause precipitation of stable uranium solid phases.

Radiolytic dissolution is a surface process which depends on the specific surface of the pellets offered to the water (grain boundaries, fissures, fractures etc.). However, it is not affected by temperature. Radiolytic oxidation may be inhibited by the presence of hydrogen produced principally by the corrosion of the disposal cell’s metal components. This hydrogen has the ability to reduce, by surface catalysis, the U^{VI} species formed by radiolytic dissolution (Spahiu et al., 2004).

The radiolytic dissolution mechanism leads to total dissolution of the oxide pellets after 80,000 to 100,000 years (depending on the combustion rate). Allowing for the fact that only a fraction of the actinides may be labile, this gives total dissolution after 50,000 years (Figure 7.3.5).

In the absence of the radiolytic dissolution mechanism, the oxide pellets deteriorate by slow conventional dissolution in a reducing medium (solubilisation) (Andra, 2005d ; SKB, 2004). The total dissolution of the oxide pellets then requires at least a million years. In the absence of radiolysis, the conditions are reducing, even in contact with the oxide pellets and the uranium IV released by the dissolution of the uranium oxide precipitates in the form of stable phases in the immediate vicinity of the packages (Andra, 2005d ; Giffaut & Coelho, 2005).

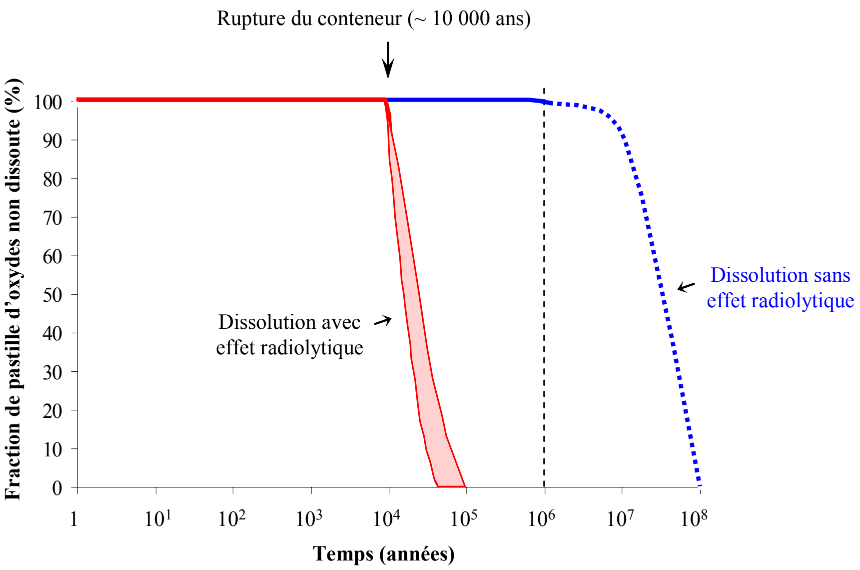

Figure 7.3.5 *Simplified representation of the evolution of the dissolution of oxide pellets with time for the long type CU, UOx3 spent fuel (Andra, 2005d ; Andra, 2005m)*

Corrosion of the other materials present in the assemblies (stainless steels, inconel and zircaloy) occurs after the container has ruptured and water has entered. During the loss of the container's sealing integrity is lost, the redox conditions in the disposal cell are reducing, due to the chemistry of the waters and the presence of hydrogen produced by corrosion. Moreover, the metal components in the assemblies are located sufficiently far from the oxide pellets (at least several millimeters) so as not to be affected by the water radiolysis processes.

In addition, when water comes into contact with the assemblies, the temperature has reduced sufficiently (T < 50 °C) (Bauer, 2005) for its influence on the alteration processes to be limited.

Under these reducing, slightly thermal conditions, the corrosion level of stainless steels and inconel are low due to the formation of a layer of passivating oxides; the corrosion speeds are approximately 10^{-2} µm.year^{-1}. Under these same conditions, the zircaloy sheaths corrode at a speed of around 10^{-3} µm.year^{-1} (Andra, 2005d). Given the dimensions of these various components, those made from inconel become fully corroded after approximately 500 years, those made from stainless steel after several thousand years, and the zircaloy sheaths after approximately 20,000 years. These corrosion times are almost identical for both types of spent fuel, CU1 (UOx) and CU2 (MOx), their geometries being similar.

Inset 7.10 **Radiolysis of water**

Radiolysis of water is due to the interaction of α and βγ radiation with the water molecules. It produces free radicals that rapidly react to form oxidising species and gases such as hydrogen (Andra, 2005j) (Andra, 2005d).

Firstly, the radiation destabilises the water molecule, causing the formation of OH° and H° radicals along its path. In areas adjacent to its path, or in "clusters", the high concentration of radicals allows them to recombine and form H_2O_2 and H_2 (primary species) which are powerful oxidants.

1st stage: ionisation or excitation of the water molecule:

$$H_2O \xrightarrow{radiation} H_2O^+ + e_{aq}^- \text{ and } H_2O \xrightarrow{radiation} H_2O^*$$

2nd stage: formation of free radicals:

$$H_2O^+ \rightarrow OH^\circ + H^+ \text{ and } H_2O^* \rightarrow OH^\circ + H^\circ \text{ (homolytic dissociation)}$$

3rd stage: recombination of free radicals:

$$OH^\circ + OH^\circ \rightarrow H_2O_2\,,\ H^\circ + H^\circ \rightarrow H_2\,,\ e_{aq}^- + e_{aq}^- \rightarrow H_2 + 2OH^-\,,\ OH^\circ + H^+ \rightarrow H_2O\,,$$

$$OH^\circ + e_{aq}^- \rightarrow OH^- + H_2O\,,\ H^\circ + e_{aq}^- \rightarrow H_2 + OH^-$$

The various primary species migrate out of the clusters and continue to react. The probability of these species reacting with each other reduces significantly, whereas the reactions with solutes in the aqueous medium intensify:

$$OH^\circ + H_2 \rightarrow H^\circ + H_2O\,,\ H^\circ + H_2O_2 \rightarrow H_2O + OH^\circ\,,\ H_2 + H_2O_2 \rightarrow 2H_2O\,,$$

$$H_2O_2 + e_{aq}^- \rightarrow OH^\circ + OH^-\,,\ H_2O_2 + OH^\circ \rightarrow HO_2 + H_2O\,,\ 2HO_2 \rightarrow O_2 + H_2O_2 \ldots$$

The total quantity of oxidoreducing species produced by radiolysis depends on the chemistry of the solution, the compounds present (steel, radioactive nuclides sensitive to redox…) the kinetics of the formation and consumption of oxidising species and the nature of the α or βγ radiation (SKB, 1999). Depending on the nature of the solutes, either active (nitrates, carbonates, chlorides, iron, fuel pellet etc.) or otherwise, the final species in solution differ but, for the most part are H_2, H_2O_2 and O_2. These species are liable to combine with each other, which essentially corresponds to the neutralisation of oxidising species by the hydrogen.

In the case of α radiolysis, the point aspect of the radiation causes a very localised increase in the H_2 and H_2O_2 content and favours the formation of molecular species. The area of the species formed extends for a few tens of micrometers around the irradiating source (SKB, 1999).

Moreover, βγ radiolysis in a de-aerated medium leads principally to the formation of radicals. Experiments in fact show that βγ radiolysis, by essentially forming radical compounds that can recombine, allows the establishment of a stationary state, with partial destruction of the molecular compounds formed, whereas α radiolysis mainly produces molecular compounds that can only accumulate (Andra, 2005f, Tome 2). The molecular species, nevertheless formed by βγ irradiation, are rapidly consumed in the medium by the radicals also produced.

Inset 7.11 ***Radiolytic dissolution of a UO_2 / PuO_2 pellet (1/2)***

Introduction

The dissolution mechanisms of a spent fuel oxide pellet have been studied worldwide, particularly through a number of national and international research programmes such as the European SFS programme, or the CEA / EDF Precci research programme (Andra, 2005d). This type of research combines experimental approaches with the study of natural analogues such as Oklo (Gabon) (European Oklo Natural Analogue programmes (I and II) (Del Nero *et al.*, 1999 ; Horie *et al.*, 2004 ; Salah *et al.*, 2000) and modelling (Andra, 2005d ; SKB, 2004).

The process

The dissolution of a UO_2 or UO_2 / PuO_2 oxide pellet is due to the solubilisation of the pellet followed by local attacks of species produced by the radiolysis of water (radiolytic dissolution) caused by the effect of α and βγ radiation (see Figure below). Radiolytic dissolution itself breaks down into several stages:

① the production of oxidising species by radiolysis of water:

$$H_2O + \text{radiation} \rightarrow \text{oxidising species } (H_2O_2,\ O_2,\ \text{radicals...}) + \text{reducing agents } (H_2)$$

② the oxidising species formed react with the surface of the UO_2, causing the formation of UO_{2+x}:

$$(UO_2)_n \equiv UO_2 + 0.33H_2O_2 \leftrightarrows (UO_2)_n \equiv (UO_2) \equiv U^{IV}_{0.67}U^{VI}_{0.33}O_{2.33} + 0.33H_2O$$

③ the oxidation of the uranium pellet can also lead to the formation of highly soluble U_3O_7 due to the +VI valency of the uranium. The uranium oxides then dissolve depending on their solubility in the medium:

$$(UO_2) \equiv U^{IV}_{0.67}U^{VI}_{0.33}O_{2.33} + 0.67H^+ \leftrightarrows (UO_2) \equiv (UO_2)_{0.67} + 0.33UO_2^{2+} + 0.33H_2O$$

The uranium VI can be reduced by hydrogen or the other reducing species present to form solid phases of uranium IV which precipitate *in situ*.

A fuel pellet emits α and βγ radiation. The latter rapidly diminish and the α radiation becomes predominant after a few hundred years. After this period, the speed of radiolytic dissolution increases with the α dose rate due to its effect on the concentration of oxidants produced by radiolysis of the water (Andra, 2005d). α radiolysis then leads to an increase in the speed of dissolution of the fuel of several orders of magnitude compared with dissolution without radiolysis. This kinetic of radiolytic dissolution is also greatly influenced by the hydrogen produced: tests show that hydrogen can prevent the radiolytic dissolution process, but its exact role is not entirely clear at the present time. The kinetics of radiolytic dissolution also depend on the pellets' surface and, as a consequence, their fracturing rates. However, all the fractures are not involved in pellet dissolution, because of their reduced accesibilty to the water, especially the clogging of grain boundaries during secondary phase precipitation (Andra, 2005d).

Radiolytic dissolution of a UO_2 / PuO_2 pellet (2/2)

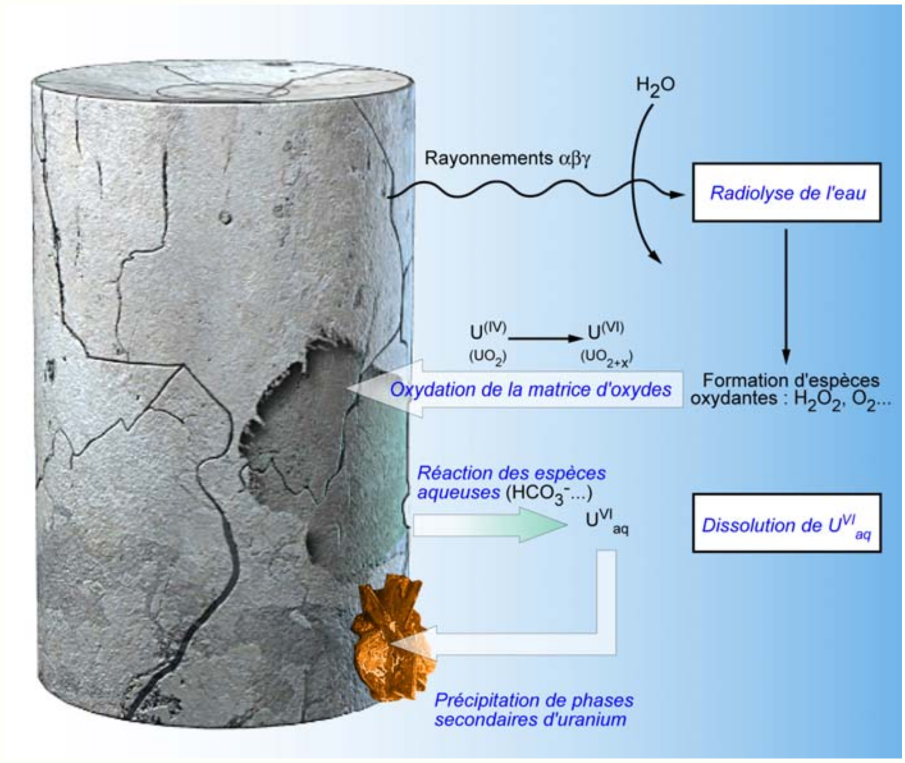

Simplified schematic of the various dissolution processes of an oxide pellet

7.3.6 Alkaline Disturbance at the Disposal cell Hydraulic head

The concrete plug on C waste and spent fuel disposal cells has created an alkaline disturbance in the swelling clay core and the Callovo-Oxfordian argillites (Jacquot & Michau, 2005) (Figure 7.3.6). At the same time, the concrete plug undergoes degradation, mainly when interacting with the water flowing from the argillites. This item will be discussed in the paragraphs dealing with the chemical evolution of B waste disposal cells (see § 7.4.2). The development of the alkaline disturbance requires that a concrete saturation ratio greater than 80 % be attained. This ratio is attained throughout the plug a few thousand years after the repository has been closed.

The hydraulic and transport conditions of the solutes set out in chapter 6 dealing with runoffs demonstrate that, overall, diffusion remains the dominant process. On a temporary basis, during hydraulic overpressure phases, especially the hydrogen migration phase, a advection/diffusion codominance may occur at the hydraulic head of the disposal cell for a few thousand years. However, the low water flows involved and the partially saturated condition of the concrete during that time mitigate concrete degradation and the spread of alkaline disturbance. As a result, these mainly occur under conditions of dominant diffusion.

7.3.6.1 Alkaline Disturbance of the Swelling Clay Plug

In C waste disposal cells, the clay and cement-based components are in direct contact; therefore, alkaline disturbance does not appear simultaneously with other types of degradation. In spent fuel disposal cells, the concrete and clay plugs are also in contact. The steel coating is held in place, especially at the concrete plug and may, at a very local level, promote the superimposition of alkaline disturbance over iron-clay disturbance. On account of the contact surfaces provided, such superimposition may be more significant in way of the concrete plug in the argillites.

The experiments and modelling exercises carried out–among others–as part of the European programs ECOCLAY and ECOCLAY II (Gaucher *et al.*, 2004 ; Savage *et al.*, 2002) demonstrate that alkaline disturbance corresponds to ion exchange and dissolution/precipitation processes within swelling clay. This results in the formation of an zone profoundly remineralized in contact with concrete; it corresponds to the dissolution of smectites and to the precipitation of cement-based phases, of zeolites and of a lightly disturbed zone, mainly characterized by the transformation of sodic montmorillonite into calcic montmorillonite (Gaucher *et al.*, 2004 ; Jacquot & Michau, 2005 ; Mosser-Ruck & Cathelineau, 2004 ; Savage *et al.*, 2002). These disturbances also correspond to an increased pH in the interstitial water.

Regarding spent fuel disposal cells, alkaline and iron-clay disturbances occur simultaneously. The risk factors related to the superimposition of both disturbances have not been assessed to date. However, given the fact that the cement-based and ferriferous phases are weakly reactive to one another, the development of the iron-clay disturbance will probably not modify the reactivity of the clays to cement-based water. In this way, alkaline disturbance is similar to that which develops without iron-clay disturbance. In contrast, the iron-clay disturbance is probably different under alkaline conditions from that occurring under argillaceous conditions, and should demonstrate more limited extensions especially in light of the corrosion kinetics of the metallic components in a basic medium.

Alkaline disturbance will continue until the concrete plug is completely degraded, i.e. at least several hundred thousand years. The current models, which do not take account of the depletion of the concrete source (Jacquot & Michau, 2005), show that the extent of the highly remineralized zone will reach about 20 centimeters in 100,000 years and about 60 centimeters in 1 million years. The model for the weakly disturbed zone is multi-decimetric over a 100,000-year period (approx. 60-70 cm) and remains less than 2 meters after a million years (Jacquot & Michau, 2005). Given the fact that the increased pH in the swelling clay plug is limited to the highly mineralized zone, the waste packages are assumed not to be affected by this local pH increase.

The mineralogical changes in the disposal cell plug are limited in scope so that the plug retains its hydraulic and swelling properties over most of its length (> 80 %) for a 1 million-year time window. On the other hand, the plug also keeps its retention properties over this thickness.

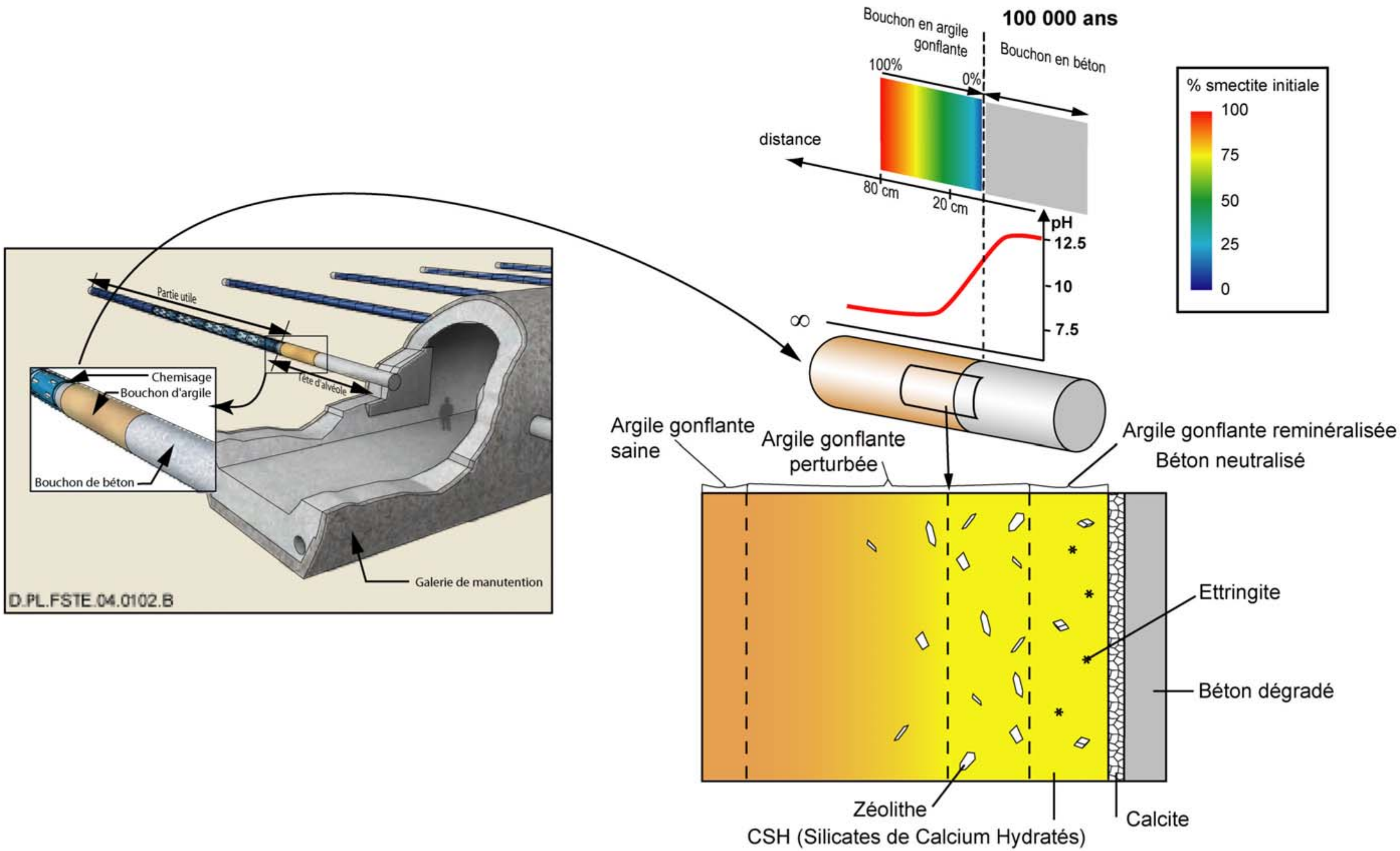

Figure 7.3.6 *Schematic representation of the alkaline disturbance of swelling clay plugs in C waste disposal cells over 100,000 years*

7.3.6.2 Alkaline Disturbance of Argillites Around the Concrete Plug

The alkaline disturbance in near-field argillites will start as soon as the disposal cell plug is degraded and the alkaline plume migrates to the wall argillites. In a spent fuel cell, the contact between the concrete and the argillites is not direct. The coating left on the head of the disposal cell is not punctured at the hight of the concrete plug. However, its corrosion is significant after a few hundred to a few thousand years, meaning at the time when the saturation in the core of the concrete is sufficient to cause an alkaline perturbation in the argilites. Hence, the alkaline perturbation is not affected by the presence of the impermeabile coating. However, given the fact that the coating left on the hydraulic head of the disposal cell is punctured at the concrete plug, alkaline disturbance is unaffected.

In C waste disposal cells, the progression of alkaline disturbance (Inset 7.12) is similar to that described for B waste disposal cells (see § 7.4.4) with the formation of a highly remineralized zone and a more weakly disturbed zone. In the remineralized zone, the dissolution and precipitation processes make up a more plastic, less porous zone than the undisturbed argillites, with hydraulic properties close to those of undisturbed argillites–particularly low permeability. Alkaline disturbance leads to the significant "hydraulic scarring" of the EDZ fractured zone. The weakly disturbed zone retains the hydraulic and mechanical properties similar to those of the undisturbed argillites.

In spent fuel disposal cells, the alkaline disturbance overlaps the iron-argillite disturbance. The risk factors related to the overlap of both disturbances have not been specified to date. However, they are probably similar to those described for the swelling clay in the previous paragraph.

Alkaline disturbance will continue until the concrete plug is completely degraded, i.e. at least several hundred thousand years. Over a 1 million-year period, the extent of the alkaline disturbance in the argillites at the hydraulic head of the C waste and spent fuel disposal cells is limited to that of the initial EDZ. Model results (Jacquot & Michau, 2005 ; Michau, 2005a) indicate that the extent of the highly remineralized zone is approximately 10 cm after 100,000 years and 30 cm over a 1 million-year time window; and the extent of the weakly disturbed zone reaches about 50 cm after 100,000 years and remains less than 3 m over a 1 million-year time window.

Inset 7.12 ***Alkaline disturbance in clays (argillites and swelling clay)***

Introduction

Alkaline disturbance of the clays by cement-based fluids has been under extensive research both in France and overseas for several years, mainly regarding the study of geological repositories. Following a parallel approach, this research combines experiments performed in day and underground research laboratories, the study of natural analogues, particularly at the Maqarin and Khushaym Matruck, Jordan, sites and model exercises (Jacquot & Michau, 2005).). The research was conducted as part of the European ECOCLAY I and II bringing together international agencies and university or national research laboratories (ENRESA, NAGRA, PSI, SCK-CEN, AB SKB, BRGM, etc.), and as part of the CNRS / Andra (FORPRO… (Andra, 2005d)) research group. For argillaceous rocks, we particularly benefit from the underground experiments conducted at Mount Terri (Adler, 2001 ; Andra, 2005d). In this way, the main reactive mechanisms of alkaline disturbance and mineralogical evolutions are well known (Chermak, 1992a ; Chermak, 1992b ; De Windt *et al.*, 2004 ; Gaucher *et al.*, 2004 ; Hlavacek M., 1995 ; Jacquot & Michau, 2005 ; Mosser-Ruck & Cathelineau, 2004 ; Savage *et al.*, 2002 ; Taubald *et al.*, 2000 ; Vieillard *et al.*, 2004).

The Reactive Process

The cement-based (Inset 2.8) and argillaceous (Inset 2.6) materials have different thermodynamic stabilities. Alkaline disturbance in clays in a broad sense (swelling clays and argillites) develops either when in contact with a cement-based fluid or during percolation by a cement-based fluid. This fluid results from the degradation of cement-based materials which essentially leads to the release of hydroxyl ions and alkaline / alkaline-earth cations. These elements react with the argillaceous phases either via ion exchange processes with the clay surfaces, or via dissolution/precipitation processes.

The exchange of ions in clays mainly occurs for Na, Ca and Sr ions. This instantaneous process helps to reduce the pH and alkaline / alkaline-earth concentrations in clay interstitial fluids thereby buffering the alkaline disturbance in the clays.

The concurrent dissolution/precipitation processes for the exchange of ions principally involves the dissolution of the argillaceous phases (smectites, etc.) and certain accessory minerals such as quartz; and the precipitation of secondary cement-based phases such as CSH (hydrated calcium silicates), CASH (hydrated aluminosilicates) and zeolites as well (De Windt *et al.*, 2004 ; Jacquot & Michau, 2005). The CSH and CASH phases evolve toward zeolites in time.

Extension (Time – Space) and Organization of Alkaline Disturbance

Assuming a diffusive transfer of solutes, the alkaline disturbance advances in steps along two successive zones; firstly, a highly remineralized zone in contact with the cement-based water or concrete (disappearance of argillaceous minerals, precipitation of cement-based minerals), then beyond a weakly disturbed zone (partial dissolution of the argillaceous minerals, 5 % maximum dissolution of the smectites). The pH decreases dramatically in the remineralized zone, then gradually tends toward the initial pH of the argillites (7.5) (Jacquot & Michau, 2005).

Advance Kinetics of Alkaline Disturbance

The advance rate of the alkaline disturbance (i.e. steps) through the clays is contingent upon their diffusion properties. In addition, it tends to decrease over time because of the clogging occurring at the interface between the two types of cement-based and argillaceous materials through the formation of the remineralized zone.

Recent models have given an account on the couplings of reactions for porosity and diffusion. Codes such as Phreeqc or Hightec provide an opportunity to assess the orders of magnitude of the extend of alkaline disturbance extension (Jacquot & Michau, 2005).

7.3.7 Other Chemical Processes at the Hydraulic head of C waste & Spent Fuel Disposal cells

The different disposal cell hydraulic head materials (swelling clay core, concrete plug and metallic components: metallic plug and spent fuel disposal cell coatings) also react with one another and with the surrounding argillaceous environment. As a result, the metallic components (coating, metallic plug) on the disposal cell hydraulic heads become corroded. In addition to the alkaline disturbance resulting from the concrete plug, the swelling clay core of the plug also reacts to the water in the Callovo-Oxfordian argillites and to the metallic materials (coating and metallic plug). Similarly, in addition to alkaline disturbance, the argillites in contact with the cement plug interact with the metallic coating at the hydraulic head of the disposal cells.

Processes identical to those described for the storage part are encountered at the hydraulic head of the disposal cell (see § 7.3.1, 7.3.2 et 7.3.3), but with lower temperatures.

Therefore, similar conclusions may be drawn: (i) the plug re-equilibrates itself with the water from the Callovo-Oxfordian argillites without disturbance of its mineral content; (ii) the extent of the highly remineralized zone related to the iron-clay disturbance remains centimetric. Thus, the plug retains its hydraulic and transport properties; (iii) the interactions between the metallic coating and the argillites remain limited: the extent of the disturbance-related, highly remineralized zone remains centimetric and the weakly disturbed approximately multi-decimetric.In spent fuel disposal cells, the corrosion affecting the coating above the plug is similar to that described for the storage part of the disposal cells. In contact with the concrete plug, the alkalinity of the water leads to weaker corrosion kinetics than in an argillaceous medium. As a result, total coating corrosion in this zone should not occur until about 10,000 years. However, it should be noted that during the operating phase, desaturation of the argillites around the access drift can reach the outermost section of the coating. At this stage and on a very temporary basis, corrosion may develop in an oxidizing environment (Crusset, 2005) (Inset 7.3) but its kinetics will be mitigated by the unsaturated condition of the argillites. As soon as the disposal cell is closed, anoxic conditions are rapidly re-established.

7.4 Chemical Evolution of B waste disposal cells in Post-Closure Status

The presence of concrete within B waste disposal cells (support / coating, filling, slab, disposal package) impacts their chemical evolution, particularly that of B waste disposal packages and near-field argillites (Inset 2.6, Inset 2.7).

Chapter 6 indicated the existence of a significant hydraulic transient in the B waste disposal cells, related to the dimensions of these structures, to the ventilation phase and to the production of hydrogen by corrosion of the metallic components (waste and primary containers). Although specific differences may appear between the various disposal cells depending on the disposal packages they contain, the hydraulic history of the B waste disposal cells is marked by a long period during which the disposal cells are not completely saturated. The saturation ratio of concretes reaches 80 % in a few thousand years, but near-total saturation of (S > 95 %) of the most hydrogen-effective disposal cells is only reached after 100,000 years. Near-field argillites regain a saturation ratio greater than 99 % after 10,000 years. The saturation condition of the concretes and primary packages, values and organization of the water flows in and around the disposal cells for that resaturation period determine the chemical evolution of the disposal cells.

Current simulation tools do not provide an account of the chemical evolutions under unsaturated conditions. However, it can be assumed that the unsaturated condition period for B waste disposal cells should be characterized by slower chemical evolutions and with a more limited extent than those occurring in a saturated environment such as that reached after 100,000 years in these structures. This qualitative analysis is based upon the water quantities involved and the slower diffusion process in unsaturated environments. In the extreme case, it may be considered that the chemical evolutions over the first 100,000 years are short enough for the actual beginning of most chemical processes to be postponed to later time. This would particularly concern concrete degradation and alkaline disturbance of the argillites associated therewith. On the other hand, other processes such as corrosion or water uptable via bituminized sludges may be initiated well before a high saturation ratio is attained. Numerical simulations, particularly on concrete degradation, were assumed to be carried out in a saturated environment. Therefore, they do not take account of this unsaturated phase and provide increasing time elements (e.g. service life of components). As will be pointed out in the following paragraphs, the degradation processes of concretes and alkaline disturbance in B waste disposal cells span several hundred thousand years, which is far longer than what is applicable to the non-saturation phase (100,000 years). Thus, this puts into perspective the significance of the possible shift which may induce the non-saturation phase in the sequence of chemical degradations within B waste disposal cells.

Beyond 100,000 years, after a near-saturated condition is reached in the disposal cell or throughout the repository and a new hydraulic equilibrium condition occurs, the chemical evolution is determined by the water flows involved and the diffusion conditions of the solutes. Given the fact that B waste is little or not exothermic, temperature only marginally affects the chemical evolution of such disposal cells. Furthermore, the thermal load is short-lived and only concerns the period during which the disposal cells are highly desaturated (see § 5).

The chemical evolutions of the storage part and disposal cell hydraulic head may be considered similar. In fact, the disposal cell hydraulic head only consists of a concrete filling. The seal of the B waste disposal cell is located in the access drift and behaves in the same way as a drift seal (see § 7.5).

The description of the hydraulic evolution of a B waste disposal cell shows that its resaturation is organized locally in a complex fashion, especially because of the installation clearances and macropores within certain primary packages. After total resaturation, diffusion remains the dominant mode of transport and the effect of the vacuum on the transport of solutes in the disposal cell may be disregarded. At this stage, it can be reasonably admitted that chemical degradation in a B waste disposal cell generally occurs in an isotropic manner from its walls in contact with the water flowing from the argillites and from its core out (for disposal cells whose packages release species that may be aggressive to concretes).

The following will be successively discussed in the description of the chemical evolution of the B waste disposal cells according to the hydraulic evolution of the disposal cells:

- return to anoxic redox conditions, then to reducing conditions;
- degradation of cementitious components (support / coating, slab and disposal package) cause by the presence of argillite water and degradation products of certain B waste materials;
- the chemical evolution of primary packages. The hull and end cap waste packages (B4 and B5 reference packages) and bituminized sludge packages (B2 reference packages) will be mainly discussed as they make up the main bulk of the radiological and quantitative inventories of B packages;
- alkaline disturbance of the argillites in the near-field of the disposal cells.

7.4.1 Transition to anoxic redox conditions, then to reducing conditions

Closing a disposal cell stops oxygen and CO_2 supply. The oxygen is consumed, either by corrosion of the metallic materials, or by pyrite oxidation in the desaturated argillites around the perimeter of the cell, or by bacterial activity. At the beginning of resaturation, the redox conditions in the disposal cell are essentially imposed by the water flowing from the argillites. The redox potential is imposed by the S^{II} / S^{IV} pair controlled by pyrite and sulphate contents in the interstitial water, which leads to redox potential values close to -200 mV (Andra, 2005k). Inside the cell, the presence of hydrogen and metal iron may impose control of the redox potential and lead to more reducing conditions in all the disposal cells. The degradation process of the waste packages are likely to lead to locally oxidizing conditions near the waste packages. These processes are detailed below (see § 7.4.3).

After closing a B waste cell, the resaturation water percolates the oxidized argillites on the structure's walls and leads to changing mineralogical balances resulting from argillite oxidation during the operating phase (particularly, dissolution of sulphated minerals). This does not significantly modify the composition of the already sulphated resaturation water (Altmann & Jacquot, 2005). Dissolved sulphates cause a decrease in the Na / Ca ratio of the resaturation fluids, which leads to an exchange of cations, sodium with calcium, in the interlayer site in the argillite smectites. These phenomena are transient and given the water-to-rock ratios involved, the near-field water chemistry remains comparable to that of the undisturbed argillites. In this way, on a macroscopic scale, the argillite swelling properties are unchanged (Andra, 2005k).

7.4.2 Chemical degradation of cementitious materials in B waste disposal cells

The cement-based materials of a B waste disposal cell are subjected to a variety of disturbances mainly related to the water flowing from the Callovo-Oxfordian argillites (hydrolysis, water carbonation, sulphate attack; (Inset 7.13)) but also to chemical, especially acidic, compounds released by certain waste packages. This mainly concerns bituminized sludge B2 packages and those packages containing organic components such as B5.1 reference packages.

Inset 7.13 ***Water reactivity of cement-based materials***

Introduction

Concrete chemical degradation phenomena have been studied for several decades in the field of civil engineering (dams, power plants, etc.). The study of concrete chemical degradation in the configuration of a repository in a deep geological formation falls into that general approach, but it was also the subject of scientific programs, especially within the framework of the European Community like RADWASTOM 3C and 4C. The entire spectrum of research has provided the opportunity to develop chemical degradation models for concretes and degradation processes are well understood today. The residual uncertainties mainly concern the impact of the degradation reactions on the water flow and solute transport properties. Dissolution and precipitation phenomena related to chemical degradation lead to changes in porosity, permeability and diffusion coefficients. In return, such changes may cause the extension of the degradation processes to vary over time and in space (Bourbon, 2005).

Process

Carbonated water, lightly alkaline and more or less rich in sulphates from Callovo-Oxfordian argillites, results in three concurrent concrete degradation reactions: hydrolysis, water carbonation and sulphate attack.

Hydrolysis: concrete lixiviation and opening of its porosity

Hydrolysis consists in the successive dissolution of different minerals composing the cement-based materials (Inset 2.8) and leads to their gradual neutralization. The first stage is the dissolution of alkaline (Na_2O and K_2O) and alkaline-earth (MgO and CaO) oxides, with formation of strong bases. At the initial balance, the pH of the cement-based water is greater than 13. When the oxides have dissolved, the pH decreases to a value of 12.5 controlled by portlandite ($Ca(OH)_2$). Then, the portlandite, in turn, is dissolved:

$$Ca(OH)_2 + 2H^+ \leftrightarrows Ca^{2+} + 2H_2O$$

When all the portalandite has been consumed, the hydrated calcium silicates (CSH, e.g.: afwillite ($Ca_3Si_2O_4(OH)_6$ or in the abbreviated form ($C_3S_2H_3$) which are gradually neutralized with a gradual decrease of the calcium-silicon ratio (C / S).

$$C_3S_2H_3 + 6H^+ \leftrightarrows 3Ca^{2+} + 2H_4SiO_4 + 2H_2O$$

The pH decreases from 12.5 to 10.5, with the lower value and is controlled by tobermorite which is more stable and the last to become calcium-depleted. The last stage of hydrolysis corresponds to the neutralization of brucite ($Mg(OH)_2$). The sulphoaluminates (e.g: calcium monosulpho-aluminate ($3CaO,Al_2O_3,CaSO_4,12H_2O$ or in the abbreviated form $C_3A,Cs,12H$)) jointly dissolve into the CSH:

$$C_3A, Cs, 12H + 12H^+ \leftrightarrows 4Ca^{2+} + 2Al^{3+} + SO_4^{2-} + 18H_2O$$

Carbonation: Porosity clogging

Water carbonation is identical to the atmospheric carbonation described in Inset 7.2. It corresponds to portlandite dissolution and calcite $CaCO_3$ precipitation, which leads to a reduction in porosity that may result in clogging:

$$Ca(OH)_2 + CO_3^{2-} \leftrightarrows CaCO_3 + 2OH^-$$

Attack by sulphates: Material cracking

Attack by sulphates corresponds to the formation of sulphated compounds (essentially ettringite) from aluminates. These sulphated compounds are highly expanding, which leads to local material cracking. The first stage corresponds to the formation of gypsum which reacts with calcium aluminates to form ettringite:

$$Ca(OH)_2 + SO_4^{2-} \leftrightarrows CaSO_4, 2H_2O$$

$$4CaO, Al_2O_3, 19H_2O + 3(CaSO_4, 2H_2O) + 16H_2O \leftrightarrows 3CaO, Al_2O_3, 3CaSO_4, 32H_2O + Ca(OH)_2$$

7.4.2.1 Hydrolysis of cement-based materials

The coming into contact of the water with the cement-based materials initiates their hydrolysis. The conditions of this hydrolysis depend directly on the hydraulic conditions. Hydrolysis is controlled by percolation of the concrete by the interstitial water from the Callovo-Oxfordian argillites and by diffusion of the concrete OH towards the argillites.

The first process only becomes significant after the cementitious structures have been fully resaturated (i.e. about 50,000 years for the disposal cells containing the B2 reference packages and about 100,000 years for the other B waste disposal cells). During the hydrogen production period, the cementitious materials–in direct contact with the saturated argillites–are subjected to a hydrolysis by inter-diffusion from the alkaline plume to the argillites, and from the clay solutes to the concretes. After resaturation, hydrolysis is maintained both through percolation of the interstitial water from the Callovo-Oxfordian argillites in the structures of the waste B disposal cells and through diffusion. Hydrolysis progresses in fronts within the disposal cell from the wall to the core (Figure 7.4.1).

In both cases, the hydrolysis processes are identical and correspond to the successive dissolution of the concrete minerals: alkaline and alkaline-earth oxides, portlandite ($Ca(OH)_2$), then the CSH (hydrated calcium silicates) (Inset 2.8, Inset 7.13).

This dissolution is broken down into four successive phases characterized by different pH and mineral phase stability conditions. Thus, the concrete is characterized in a simplified manner by a “undisturbed”, then “altered”, “degraded” and lastly “neutralized” condition (Bourbon, 2005). These 4 phases are preceded by the initial, transient condition of concrete, i.e. the fresh condition:

- fresh cement is characterized by the presence of alkaline and alkaline-earth oxides. The pH of the interstitial solutions is greater than 13. The bases resulting from these oxides are initially neutralized by the percolating water;
- after this initial transient condition, the cement is called “undisturbed”. It retains this condition until all of the portlandite has dissolved. The pH of the interstitial water is then buffered to about 12.5;
- after the portlandite has dissolved, the altered concrete degrades by dissolution-precipitation of the CSH with a decrease in the calcium / silicon (C / S) ratio and by release of calcium hydroxide. The pH drops from 12.5 to 10.5 approximately. This last value corresponds to the pH for which the tobermorite is stable;
- Tobermorite decalcification corresponds to the degraded condition of the cement. The pH remains stable at 10.5;
- beyond this point, the cement is considered neutralized, which is the final stage of degradation at which it is regarded as comparable to a consolidated, granular material.

The concrete hydrolysis models based only upon diffusion (Bourbon, 2005) lead to an enhanced of degradation of about 7 cm over 10,000 years and about 30 cm over a 100,000-year period. These models do not take into account the carbonation-induced clogging effect (see below).

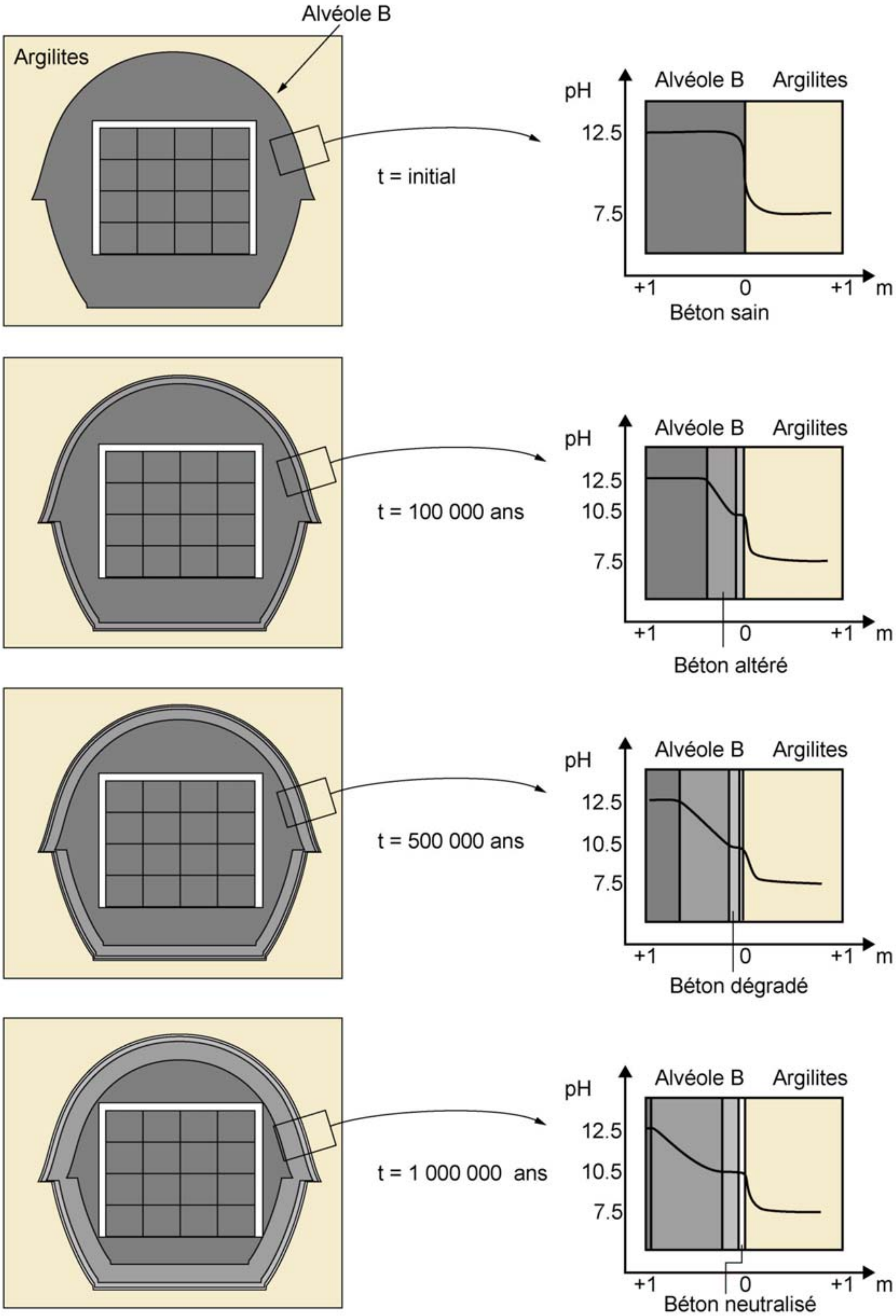

Figure 7.4.1 *Schematic representation of the progressive degradation of type CEM V concrete coating / support of a B waste disposal cell (Bourbon, 2005)*

In the case of assessments involving argillite water percolation, the speed of concrete degradation by hydrolysis depends on the water renewal flow in the pores of the materials and the formulation of concretes (Inset 2.8). The hydraulic disposal conditions detailed in § 6, are characterized by low water fluxes within the Callovo-Oxfordian and within the structures. These lead to a slow chemical degradation of the cement-based materials occurring over hundreds of thousands of years. The propagation of the front relating to the altered condition of the concrete would reach less than one metre in one million years for a CEM V concrete. This means the disposal packages would remain in a undisturbed concrete environment and, would not be chemically degraded over that period.

7.4.2.2 Water carbonation

Diffusion, then percolation of the interstitial water in the Callovo-Oxfordian argillites into the cementitious structures of a B waste disposal cell also leads to water carbonation processes. Such processes are similar to those described previously for atmospheric carbonation (see § 7.2.2). It corresponds to the formation of a highly zone calcified limited to the concrete interface with the argillites and with a multi-decimetric extent over the 1 million-year time window (Inset 7.13).

The kinetics of carbonation progression is controlled by the diffusive transport properties of the cement-based material. Thus, progression within the cement-based material does not occur by fronts as it was the case for hydrolysis in a homogeneous chemical system on either side of the front, nor does it occur constantly over time (Bourbon, 2005). Water carbonation leads to gradual clogging of porosity, which induces decreased permeability and material diffusion coefficients. These coefficients become significantly weaker than those in the undisturbed material and lead to slower hydrolysis processes by dramatically limiting exchanges on either side of the carbonated interface. Two zones–whose transport properties are modified–occur successively from the interface with the argillites: the carbonated zone whose permeability is decreased with respect to that of the undisturbed concrete and the hydrolyzed zone whose permeability is increased with respect to that of the undisturbed concrete.

According to model exercises, the extent of the altered zone of a concrete both by hydrolysis and water carbonation is estimated at less than 4 cm over 7,500 years under saturated conditions.

7.4.2.3 Attack by argillite water sulphates

The cementatious materials, in contact with percolation waters from the argilites are also subject to a chemical attack by sulfates (Inset 7.13). This attack probably remains a secondary phenomenon, particularly considering the choice of the composition (adapted to expected sulphate contents) of the concretes used in the structures.

However, based on the quantities of sulphates brought in by the argillite water (Altmann & Jacquot, 2005), a sulphate attack may occur on their interface. This phenomenon is likely to affect only about 10 centimeters of concrete in 10,000 years (Bourbon, 2005). Also, this phenomenon will only have a minor effect on the consumption of portlandite which controls the pH of concrete.

7.4.2.4 Degradation by waste

Closing and resaturating a B waste disposal cell may, in addition to initiating and maintaining the degradation of cement-based structures, bring the water into contact with the disposal packages then with the primary waste packages. Previous paragraphs showed that concrete degradation by argillite water was limited to a few tens of centimeters over a 1-million year period. Under such conditions, the water coming into contact with the disposal packages is that of a undisturbed concrete and is not aggressive, so that the disposal cell core, and particularly the disposal packages, will only be degraded by elements coming from the waste itself.

Near-total saturation inside the primary packages occurs after 100,000 years. A degree of saturation in the primary packages sufficient to initiate the waste alteration processes is reached in a few thousand years, except however for packages with macroporosities (e.g. compacted waste packages).

Waste packages whose contents are likely to release some species which may be aggressive to concrete are essentially bituminized sludge B2 reference packages. These release organic acids and sulphates (see § 7.4.3). A balance performed over all the acids likely to be released by the bituminized sludges–independently of any kinetics–leads to a degradation of the concrete of the disposal packages only. Coating and filling concretes are unaffected (Bourbon, 2005). The sulphate release kinetics (10^{-4} year^{-1}) leads to a sulphate attack in the disposal package and does not massively affect the cell.

7.4.2.5 Degradation of metallic components of disposal packages

The B waste disposal packages are reinforced with stainless steel metallic fibres. Their degradation starts a few hundred to a few thousand years after the disposal cells have been closed because the saturation ratios of the disposal packages during the hydrogen production transient are approximately 80 %, which makes room for corrosion processes to occur. Under these conditions, the corrosion rate is less than 10^{-2} µm.year^{-1} (Andra, 2005d).

Based on this, the reinforcement fibres, average diameter: 0.5 mm, become corroded in about 25,000 years. Corroded fibres lead to a discharge of mechanical, particularly tensile, resistance of the disposal packages that may cause rupture (see § 8).

7.4.3 B waste packages

Like B waste disposal cells, disposal packages are in an environment which becomes resaturated progressively. However, the organization of the disposal cell resaturation depends on the nature of the waste they contain and on the amounts of hydrogen produced. The degradation of B waste packages is intimately controlled by the organization of resaturation in the disposal cells (see § 6) and relative by the humidity conditions.

Differences appear according to the nature of the waste. In disposal cells containing compacted, but not cemented, metallic waste (B1, B5 and B6 reference packages), the coming into contact of the liquid water with the primary packages only occurs after about 100,000 years on account of the hydrogen production by corrosion and the presence of macroporosity. However, during this time, the relative humidity conditions are sufficient to allow the metallic waste to become corroded shortly after the disposal cells have been closed.

In the case of a disposal cell containing compacted and/or cemented metallic waste (B3 and B4 reference packages), a saturation ratio sufficient for liquid water to appear and come into contact with the waste is reached in a few hundred thousand years. In the case of bituminized sludge packages (B2 reference packages), water recovery is initiated as soon as relative humidity is greater than 70 %, i.e. shortly after the disposal cell has been closed (see § 6).

Degradation of the waste packages is intimately related to the physical/chemical conditions in contact with them. In particular, after the disposal cells have become resaturated, B waste degrades in a buffered water by the cement-based materials of the disposal cells. In addition, the water irradiation and radiolysis processes may locally modify the redox conditions in contact with the packages. In this way, waste degradation is influenced by the capability of the waste to be irradiating or not and by the oxidation-reduction characteristics of the released compounds (e.g.: nitrates in B2 reference packages).

During the degradation of any kind of B waste the thermal conditions are moderate (< 30 °C) (see § 5). They do not affect the package degradation processes.

7.4.3.1 Radiolysis processes in B waste packages

Water radiolysis processes occur when two conditions are satisfied: on the one hand, the saturation conditions shall allow the presence of free water, and on the other hand the packages shall be irradiating.

In the case of irradiating packages, as long as the hydric conditions within the packages remain significantly desaturated, water radiolysis (Inset 7.10) is negligible. However, over the period in which these packages have become desaturated, water condensation within the non-tight primary packages cannot be completely excluded, but remains a marginal occurrence.

Water radiolysis in contact with the primary packages depends directly on the dose rate values. They become significant beyond 1 Gray per hour ($Gy.h^{-1}$). The dose rates decrease after the manufacturing of the packages (Figure 7.4.2) during their installation in the repository, during the post-closure period (Andra, 2005a, Situations Zb1x_1/2, Zb2_1/2 et Zb1h_1/2), (Andra, 2005d ; Andra, 2005e) and become lower than 1 $Gy.h^{-1}$ after about 500 years, regardless of the nature of the waste. Therefore, these are essentially non-irradiating when water comes into contact with them. In the event that a small number of packages should remain irradiating, this condition would only last for a few dozen to a hundred years and would be inconsequential.

Under these conditions, water radiolysis is a negligible process and has no effect whatsoever on the chemical evolution of the waste.

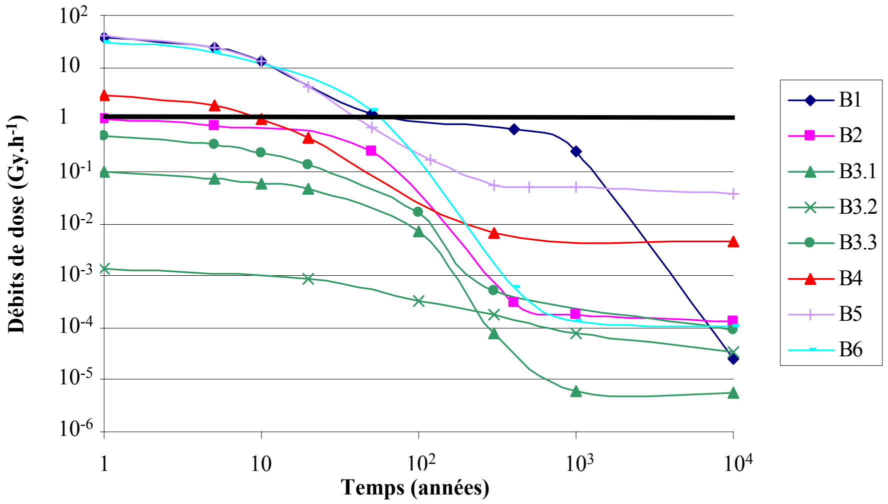

Figure 7.4.2 *Evolution of dose rates ($Gy.h^{-1}$) in contact with primary B reference packages (evaluation on the side of the package) (Andra, 2005a)*

7.4.3.2 Hull and end cap waste degradation (B4 and B5 reference packages)

Hull packages and end caps essentially consist of stainless (and Inconel) steels and zircaloy. After the disposal cell has been closed and during the oxidizing transient, the desaturated conditions of the disposal cells significantly mitigate corrosion to the metallic waste, like during the operating period (see § 7.2.5). The redox conditions become anoxic very rapidly.

With resaturation and during the hydrogen production transient, the B4 and B5 waste start becoming degraded: either in contact with free water for B4 waste packages, or by a water thin layer forming at the surface for B5 waste packages.

Compacted B5 waste packages have significant empty spaces and gaps. During the hydrogen production episode, the humidity in these gaps increases by about 50 % to approximately 90 % after of few dozen years. In this way, the corrosion processes are controlled by the formation of a thin layer of water in contact with the metal. On the other hand, the B4 waste packages are cemented which, during the hydrogen production transient, leads to saturation ratios of the filling concrete in the primary packages on the order of 80 %, whereby the metallic B waste comes corroded. In both cases, the waste packages start becoming degraded shortly after the disposal cells have been closed.

However, the corrosion kinetics of the B4 and B5 metallic wastes are comparable on account of the anoxic conditions reached over a few dozen years at most in all B waste disposal cells. Moreover, the liquid water in all the disposal cells is typical of a fluid which is balanced with a undisturbed cement-based material.

The corrosion of the stainless steels and Inconel mainly occurs by corrosion to the metal and dissolution of the passivating oxide. The cement-based water in contact with the cemented packages or that reaches the waste packages after resaturation has a high pH (~ 12.5). Under these pH conditions, the corrosion rate is less than 10^{-2} µm.year^{-1} (Andra, 2005d). During the resaturation transient, the corrosion kinetics of the compacted waste are slower, but remain roughly comparable. The corrosion kinetics could only increase if the pH decreased (towards 10) as a result of the degradation of the cement-based structures. However, these pHs are reached in degraded concrete only (Bourbon, 2005) which would occur within the disposal cells far later than the time required for the stainless steel waste to become totally corroded.

The chlorides in the interstitial water flowing from the Callovo-Oxfordian argillites do not modify the corrosion kinetics under the anoxic conditions which are rapidly reached within the disposal cells (Andra, 2005f, Tome 3). The development of locally oxidizing redox conditions in contact with the packages may be conceivable before 500 years (Figure 10.6.3), which is the maximum irradiating period for waste packages. Under these conditions, the corrosion kinetics may be faster (on the order of a few 0.1 µm.year^{-1}) in the presence of chlorides. However, the arrival of chlorides from the Callovo-Oxfordian water is not conceivable and such kinetics is highly unlikely. Lastly, over a 500-year time window, the corroded thickness would be negligible.

Zircaloy (and M5 alloy) degradation also occurs as a result of metal corrosion with formation of zirconium (or zirconia) oxide, then zirconium dissolution. The M5 alloy corrosion kinetics is similar to that of the zircaloy. The corrosion kinetics under saturated alkaline conditions remains very weak, approximately 10^{-4} to $2 \cdot 10^{-3}$ µm.an^{-1}(Andra, 2005d). For the reasons given earlier, an oxidizing transient, if any, coming into contact with the waste is inconsequential.

Complete corrosion of the metallic waste of B disposal cells depends on upon the geometry and the thickness of the waste materials, which vary according to the reference packages. For B4 and B5 waste, corrosion time for the stainless steel waste materials is approximately 70,000 years, approximately 15,000 years for Inconel waste and approximately 100,000 years for zircaloy waste.

7.4.3.3 Degradation of bituminized sludge packages (B2 reference packages)

Right after the disposal cells have been closed and during the short oxidizing transient, degradation of the bitumen matrix by irradiation/oxidation continues (see § 7.1.3), until all of the oxygen has been consumed. Radio-oxidation of the bitumen only affects a thin layer of the package (a few centimeters), regardless of the bituminized sludge packages. The salts are unaffected by such oxidation (Andra, 2005d).

During resaturation of the disposal cells and during the hydrogen production transient, internal radiolysis of the organic matrix continues with hydrogen production in the same way as during disposal cell operation (see § 7.1.3). The swelling related to the production of hydrogen (see § 7.2.5) tends to decrease firstly because of the drop in radiolysis intensity with radioactive decay and, secondly, on account of the migration and release of the hydrogen bubbles formed. Thus, it passes through a maximum value, levels off at about 5 % of the embedded volume (i.e. approx. 10 litres of stored gas), then slowly decreases after about 100 years. The gas bubbles disappear after a few thousand years. The presence of cobalt salts in certain embeddings (ST2 and ST3) allows consumption of a few hundred litres of hydrogen, which remains low in comparison to the accumulated production, approx. 10 m^3 per package after 10^5 years, regardless of the package family.

The resaturation transient continues for about 50,000 years (see § 6). At the beginning of this period, the humidity conditions in the type B2 waste disposal cells change by about 50 % to approximately 90 % in a few dozen years. At this rate of relative humidity, the bitumen matrix of the B2 waste packages starts degrading. Water recovery by the bitumen is initiated at relative humidity rates greater than 70 %.

Degradation of the bituminized sludge packages in contact with liquid water is characterized by the dissolution of mineral salts embedded by it and by the release of organic compounds (Figure 7.4.4) (Inset 7.14).

Degradation of bituminized sludges in aqueous solution initially corresponds to the adsorption of the water at the surface of the bitumen matrix. Subsequently, the front of water penetration into the bitumen matrix slowly moves inside of the bitumen matrix and leads to the solubilization of soluble and non-soluble salts which diffuse in the reverse direction toward the surface of the embedding.

The degradation time of the bituminized sludges is intimately related to the water uptake rate of the bitumen matrix. It is at least equal to the release time of the soluble salts. According to the current models of bituminized sludge degradation, the time required to fully recover the water is estimated at about 1 million years. Regarding radionuclide release, a reliable assessment leads to a salt release time of about 10,000 years (Figure 7.4.3) (Inset 7.14).

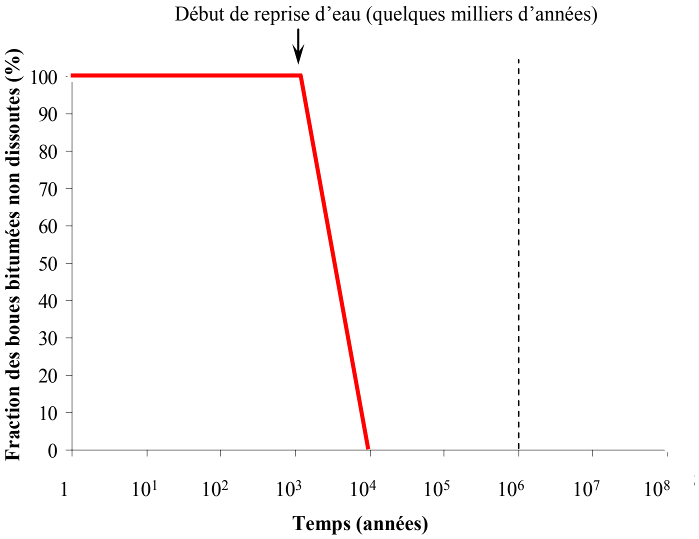

Figure 7.4.3 *Simplified representation of the degradation of bituminized sludges over time (Andra, 2005d)*

This degradation time is similar for all bitumen sludge packages, except those containing less than 2 % of salts. For these packages, the extrapolation of the experimental data available leads to release kinetics similar to the all enclosing value kinetics selected for the other waste packages, corresponding to a total dissolution in 10,000 years.

These assessments are not significantly modified by an evolution of the package geometry due to corrosion to the primary package. Creep of the bituminized sludges is unlikely to occur as long as the metallic shell of the primary package is intact, i.e. for several thousand years after the package is installed. After corrosion, the embedding may become deformed. However, the contact between the bitumen and a low-porosity environment, such as the filling materials of the disposal package, should confine the bitumen within the disposal package.

As far as degradation of the bitumen matrix is concerned, maximising assessments lead to estimate that less than 20 % of the bitumen could be solubilized over a 1 million-year period (Andra, 2005k). The impact of the released organic products will be discussed in the paragraph dealing with radionuclide transfer to B waste disposal cells (see § 10).

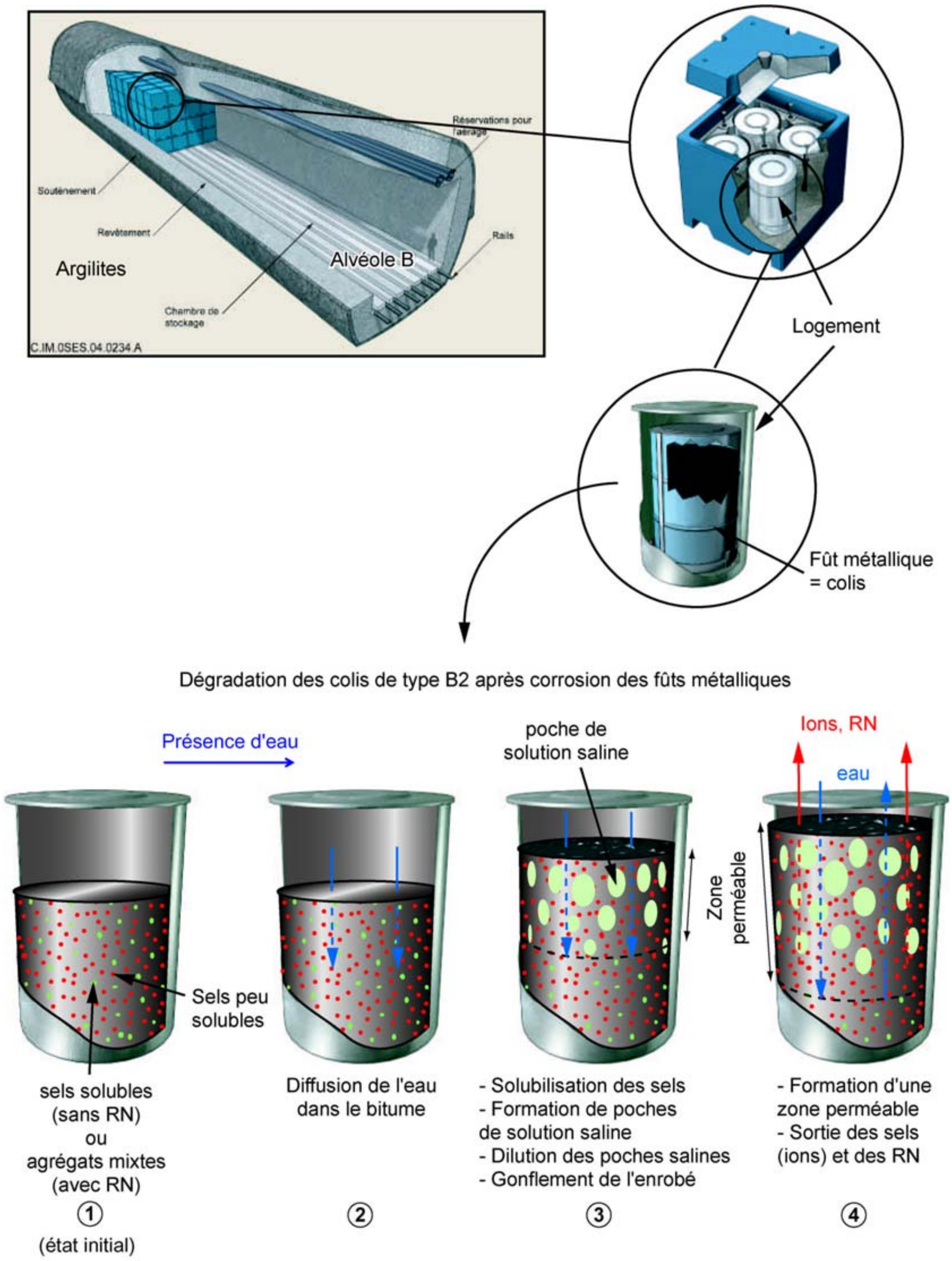

Figure 7.4.4 *Schematic representation of the degradation stages of bituminized sludges*

Inset 7.14 ***Aqueous degradation of bituminized sludges (B2 reference packages)***

Introduction

The use of a bitumen matrix for the purpose of coating waste dates back to the mid-1960s. In order to explain the evolution processes of the matrix in repository conditions, extensive research has been conducted (Nagra, 2002b ; ONDRAF, 2001a ; ONDRAF, 2001b ; RWMC, 2002) to provide an understanding of the processes governing the long-term behaviour of bitumen (Andra, 2005d ; Bernat, 1994 ; Brodersen, 1999 ; Camaro *et al.*, 1999 ; Conrad *et al.*, 1983 ; Dejonghe, 1999 ; Gwinner, 2004 ; Libert, 1999 ; Sercombe *et al.*, 2004 ; Van Iseghem & Sneyers, 1981). This research led to a better understanding of the degradation mechanisms of bituminized sludges.

The process and Associated Extent

Bituminized sludges consist of a bitumen matrix embedding mineral salts resulting from the treatment by selective co-precipitation of low- and medium-activity effluents with long half-lifes: These are salts called “soluble” mainly consisting of $NaNO_3$ and weakly soluble salts called “insoluble”, the main one being $BaSO_4$ (Andra, 2005d).

Degradation of the embedded material occurs in a wet or atmospheric environment when relative humidity is greater than that imposed by an $NaNO_3$ saline solution, the most abundant salt (74 %). The degradation processes are identical. The first degradation stages of the bituminized sludges in an aqueous solution are initially characterized by the adsorption of water at the surface of the bitumen matrix and saturation at the surface. The front along which water penetrates into the embedded material then slowly diffuses inside the bitumen matrix and leads to the solubilisation of soluble and non-soluble salts. (Figure 7.4.4). The pockets of saline solution thus formed continue recovering water (dilution) until water activity is equal to that of the external medium. This leads to local bitumen deformation, which as a result modifies the diffusion barrier formed by the bitumen and creates a permeable zone enhancing salt migration by diffusion.

The diffusion process observed on samples is generally Fickian, regardless of the salt types. There is continuing uncertainty regarding the salt-releasing kinetics, which depend on many factors: the chemical composition of the water in contact with the bitumen, solution activity, amount of salt in the waste package, transport conditions in the disposal cells, bitumen type and expansion.

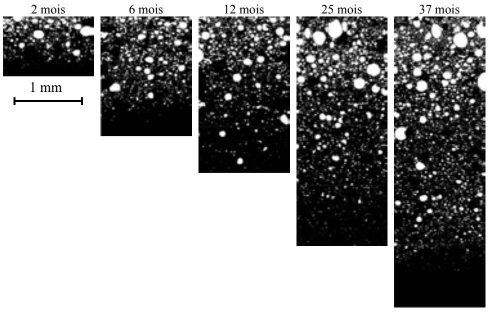

Binary electron microscopy image of lixiviated embeddings ST3 0.5N for 2, 6, 12, 25 and 37 months with pure water (Andra, 2005d)

The bitumen matrix also becomes degraded and causes release of organic compounds (formic and acetic acids, etc.). The quantity, type and solubility of the organic species available in the bitumen matrix depend on the bitumen oxidation condition and the composition of the solution in contact (Andra, 2005d ; Bourbon, 2005).

The presence of micro-organisms (Andra, 2005d ; Nagra, 2003c) also impacts this process. In fact, embeddings are a potential source of nutrients. However, bitumen is hardly biodegradable and only 0.3 % of the bulk can be consumed by the micro-organisms under anaerobic conditions (Libert, 1999). Bitumen biodegradation leads to gas production (CO_2, N_2), hydrogen consumption and release of complexing compounds. It does not significantly affect the release of salts (Andra, 2005d).

7.4.3.4 Degradation of other waste packages

The other materials composing the B wastes mainly consist of metals and organic compounds. These wastes only make up a fraction of the total B waste inventory (see § 2.3.4). In all cases, the wastes start degrading shortly after the disposal cells have been closed.

In the case of metallic wastes, the assessments and behaviours set out in the previous paragraphs apply. Only the corrosion time differs on account of the specific waste geometries (Andra, 2005d). Thus, for B1 reference packages, corrosion time for stainless steel wastes is a little over 20,000 years, and for Inconel wastes it is approximately 200,000 years. Zircaloy components become corroded in about 100,000 years regardless of the wastes.

Corrosion to unalloyed or low-alloy steels occurs in partially saturated or cement based media with kinetics in the order of 0.1 to 1 $\mu m.year^{-1}$ (Andra, 2005f, Tome 3), (Guillaume *et al.*, 2003) (Inset 7.3). These kinetics are similar after the disposal cells become saturated. The temperature in the disposal cells–lower than 30 °C in B1 and B3 disposal cells–or the contents in chlorides from the Callovo-Oxfordian argillite interstitial water do not alter these values. As indicated previously, an oxidizing, radiolysis-related transient, if any, is assumed to have no incidence on corrosion rates. In this way, unalloyed steel wastes are totally consumed after a few tens of thousand years.

The other metallic wastes provided in smaller amounts (magnesium, copper, aluminium, etc. alloys) also become corroded. Corrosion kinetics vary depending on their composition. Current assessments show a high corrosion rate in magnesium wastes (approx. 1 $mm.year^{-1}$ (Talandier, 2005)). However, such significant reactivity requires high water availability to allow corrosion spreading. They become degraded in this way only when the package is fully resaturated, in which case corrosion is quick, of the order of a few years as soon as the disposal cells are resaturated. As far as copper is concerned, it is thermodynamically stable in reducing environments. The presence of complexing agents (chloride ions, sulphide ions, etc.) and pitting corrosion may, however, lead to its destabilization (Andra, 2005f, Tome 3). For conservative purposes, an immediate alteration of all these wastes (magnesium, copper, aluminium, etc. alloys) is retained.

Additionally, a number of B waste packages (B3.1.2, B3.1.3, B5.1, etc. reference packages), not including bituminized sludge packages, contain a variety of organic compounds such as polymers (PVC, polyurethane, Viton, etc.), cellulose, resins, etc. (Inset 10.8). Under the cement based conditions of the B waste disposal cells, these organic compounds decompose under the effect of cement based water and by radiolysis. Thus ethylene glycol and phtalic acid are formed from PVC, amines, alcohols, olefins, etc. from polyurethane, fluorinated polymers from Viton; isosaccharinic and carboxylic acids (acetic, formic, etc.) from cellulose, oxalates, sulphates and amines from resins (Andra, 2005d). Cellulose degradation is a slow process (Inset 10.8).

7.4.4 Argillite alkaline disturbance in near-field B waste disposal cells

As in the case of C waste and spent fuel disposal cell plugs (see § 7.3.6), degradation of cement based materials in B waste disposal cells by the Callovo-Oxfordian water during or after the disposal cells have been resaturated, leads to the migration of an alkaline plume towards the argillites (Jacquot & Michau, 2005) (Inset 7.12).

Alkaline disturbance in the argillites corresponds to the formation of a disturbed front which diffuses from the B waste disposal cell wall (Figure 7.4.5) to the undisturbed Callovo-Oxfordian argillites via the EDZ. The progression of alkaline disturbance over one million years remains limited to that of the initial EDZ at the periphery of the B waste disposal cells. Current alkaline disturbance models predict that the extension of the highly remineralized zone changes by about 10 cm over 100,000 years up to approximately 30 cm over one million years. The extent of the disturbed zone progresses by about 50 cm after 100,000 years up to less than 3 meters over one million years (Jacquot & Michau, 2005).

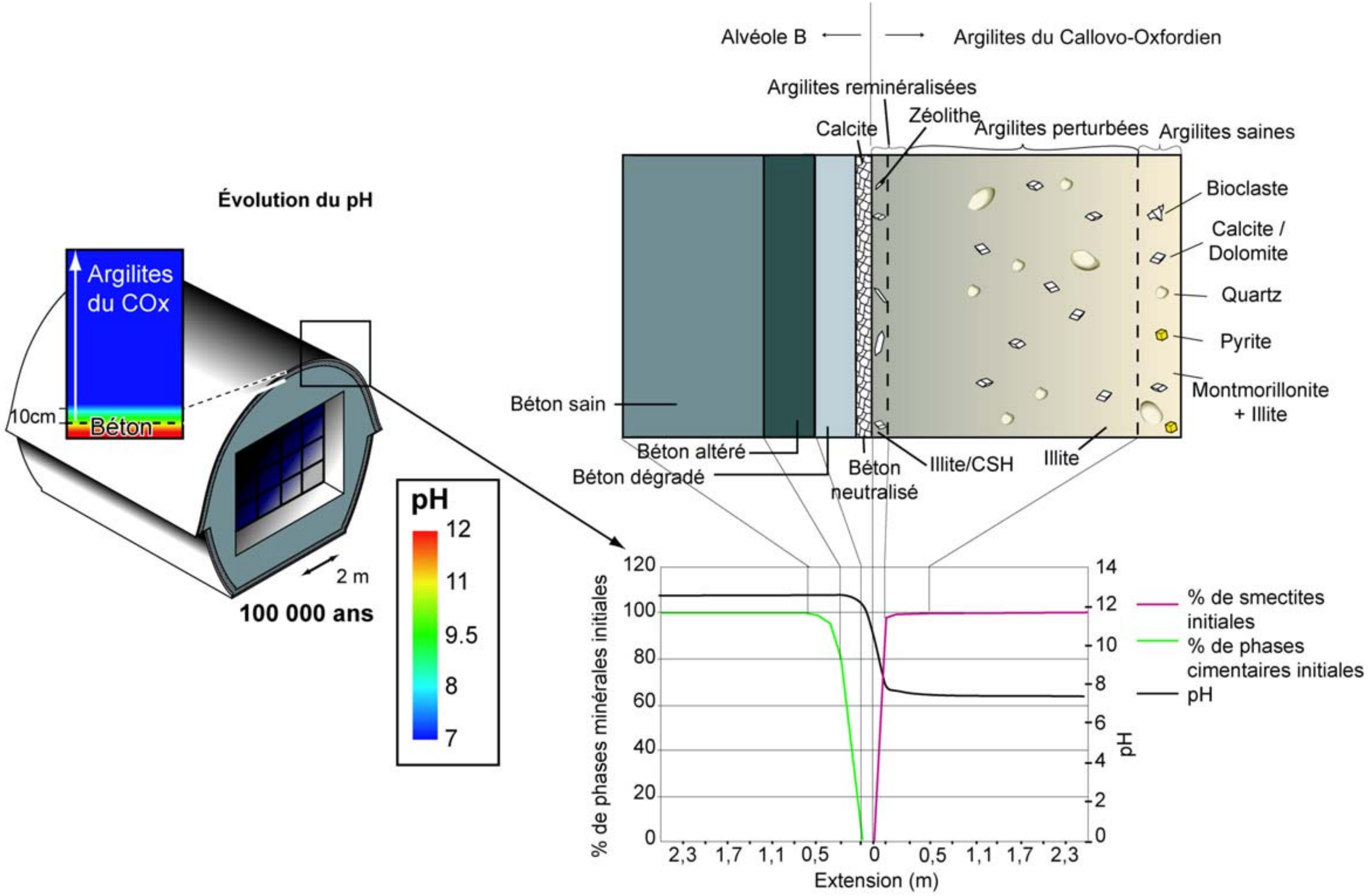

Figure 7.4.5 *Schematic representation of alkaline disturbance in clays of B waste disposal cells and degradation of support / coating concrete over 100,000 years (Jacquot & Dimier, 2005)*

7.5 Chemical evolution of drift and shaft seals in the post-closure phase

The installation of drift seals corresponds to the progressive closing of the access and connecting drifts of the disposal cells for B waste, C waste and spent fuel. During this period, seals installed while the repository was still operating are only affected at the level of the concrete support bases in contact with drifts that are still open. These support bases undergo slight carbonation. The remainder of the seal starts to resaturate. Thus, during the operating period, drift seals evolve very little.

The seals (swelling clay core and hydraulic keys) reach chemical equilibrium with the water in the Callovo-Oxfordian argillites during their resaturation. As is the case for the swelling clay cores in the C waste and spent fuel disposal cells, the fact that the seals reach equilibrium does not change the initial properties of the swelling clay. The low temperatures at the level of the seals (see section 5) do not allow illitisation to develop.

At the same time, cement based materials in the drift seals (linings, slab and support bases, Figure 2.4.12) and shaft seals (linings and confinement blocks, (Figure 2.4.14) deteriorate due to the effects of the water in the Callovo-Oxfordian argillites. The chemical evolution of these cement based materials is similar to that described above for cement based materials in B waste disposal cells (see section 7.4.2). They undergo deterioration processes due to the effects of percolation of the interstitial waters from the Callovo-Oxfordian argillites (hydrolysis, wet carbonation, attack by sulphates (see section 7.4.2, Inset 7.13). Their deterioration continues for several hundred thousand years (Bourbon, 2005).

This deterioration causes the development of an alkaline perturbation in the swelling clay core in contact with the support bases and linings, and in the hydraulic keys near linings and slabs that have not been removed. Bentonite drift and shaft seal cores are not in direct contact with metal components, as the arches are embedded in the liner concrete. They do not, therefore, undergo iron/clay deterioration.

Argillites in contact with support bases, confinement supports, liners and slabs also undergo alkaline perturbation.

The metal components, which are used only as arches in drift seals, undergo corrosion in a cement based environment.

7.5.1 Alkaline perturbation of seal cores and hydraulic keys due to concrete components

The deterioration of the shaft seals' confinement supports, of the support bases, liners and of the concrete slabs at the level of drift seals is identical to that of the cement based structures in the B waste disposal cells (see below, section 7.4.2). This causes the diffusion of an alkaline plume in clay materials in contact, and the development of an alkaline perturbation (Jacquot & Michau, 2005) (Figure 7.3.6). In the shaft and drift seals, clay and cement based components are directly in contact. The alkaline perturbation does not therefore enter into competition with other sorts of deterioration.

In contact with support bases and liners, the alkaline perturbation in the swelling clay core is of a similar nature to that described above for the C waste and spent fuel disposal cell plugs (see section 7.3.6).

The alkaline perturbation continues until complete deterioration of the liners, slabs and support bases, i.e. for a minimum of several hundred thousand years. The specific geometries of the different structures lead to different extents of the alkaline perturbation. In contact with the support bases, the extent of the perturbation is similar to that described above for the C waste and spent fuel disposal cells (see section 7.3.6): between 100,000 and one million years. The extent of the strongly remineralized zone varies between about twenty and sixty centimeters, that of the weakly perturbed zone between about 60-70 cm and less than two meters. In contact with the liners and slabs, the total perturbation is more limited; it propagates over a distance of several tens of centimeters at 100,000 years to a distance of about a metre at 500,000 years (Jacquot & Michau, 2005).

At the level of the hydraulic keys (Figure 7.5.1), the perturbation is less pronounced due to removal of the liner and slab concrete over a distance of 50 cm around the hydraulic cut-off. This explains with the strongly remineralized zone does not reach the hydraulic cut-off. The alkaline perturbation is mainly marked by an increase in pH to about 10 and by ion exchange processes that lead to the almost complete transformation of the sodium smectite in the hydraulic cut-off into calcium smectite over a period of about a million years. This mineralogical modification does not, however, significantly change the swelling properties of the swelling clay at the level of the hydraulic cut-off. In addition, the clay core conserves its initial properties over most of its thickness, so its swelling properties are not modified. The hydraulic role of the seal is therefore conserved.

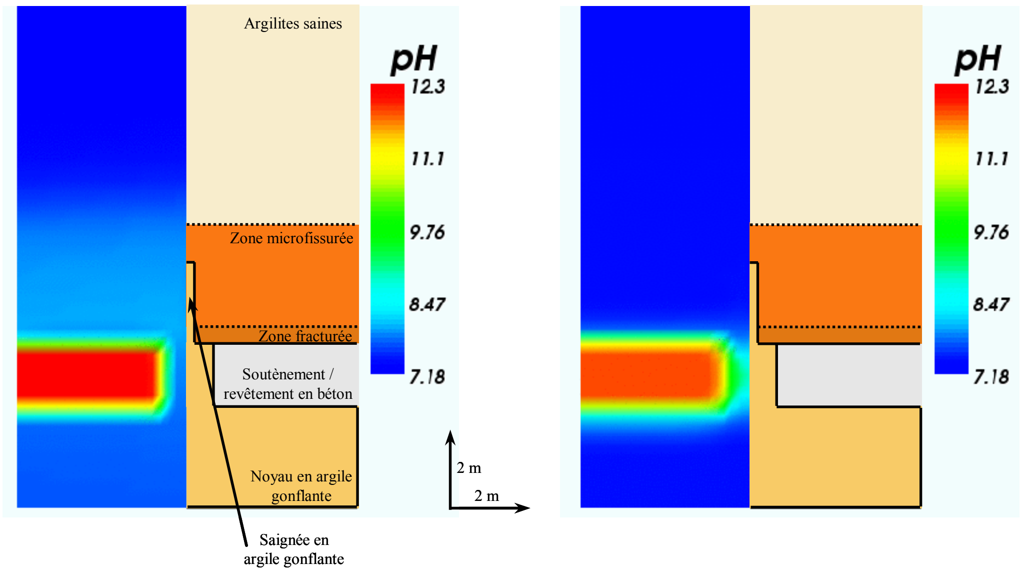

(a) 20 000 ans

(b) 500 000 ans

Figure 7.5.1 *Diagram of the alkaline perturbation of a drift seal around the hydraulic cut-off: pH field a) at 20,000 years and b) at 500,000 years (Jacquot & Michau, 2005)*

At the same time, the chemical deterioration of the concrete plug is a slow process. The plug conserves significant mechanical strength, thus ensuring the mechanical confinement of the seal (see section 8).

7.5.2 Alkaline perturbation of argillites in the near field close to drift and shaft seals

The progression of the alkaline perturbation (Inset 7.12) is similar to that described for the B waste disposal cells (see section 7.4.4). In the remineralized zone, the hydraulic properties are close to those of undisturbed argillites, notably with low permeability. The alkaline perturbation contributes to significant "hydraulic healing" of the fractured zone in the EDZ. The weakly perturbed zone, whose mineral phases are little altered, conserves hydraulic, mechanical and retention properties similar to those of undisturbed argillites.

The alkaline perturbation continues until the complete deterioration of the cement based components, i.e. over a minimum of several hundred thousand years. On support base walls, the maximum extent of the perturbation over one million years is similar to that assessed for the B waste disposal cells: 30 cm for the strongly remineralized zone and less than three meters for the weakly perturbed zone. In contact with the liner, the extent of the perturbation is less. It is about one metre maximum at 500,000 years (Jacquot & Michau, 2005).

7.5.3 Corrosion of metal components of drift and shaft seals

The metal arches present in the parts of the liner left in position corrode in a cement based environment in the same way as the metal components of the same type in the B waste disposal cells.

During the short oxidising transient (a maximum of several tens of years (Andra, 2005k), the presence of chlorides is likely to lead to corrosion rates of about 10 µm per year. However, as the oxidising transient is of short duration, the chlorides only have a limited effect on the corrosion of the arches.

As soon as the conditions become anoxic, then reducing, corrosion depends on the chemical evolution of the concretes due to the effects of the weakly alkaline waters of the Callovo-Oxfordian. In a undisturbed cement based environment, corrosion speeds are about 0.1 – 1 µm per year. As demonstrated in the § 7.4.2, the chemical deterioration of liner concretes lasts for a minimum period of several hundred thousand years. This means that the corrosion of the arches takes place mainly in a undisturbed to weakly deteriorated cement based environment. This leads to corrosion durations of at least several thousand years.

7.6 Chemical evolution of drifts and shafts in the post-closure phase

The chemical evolution of the drifts and shafts in the post closure period corresponds mainly to the deterioration of their cement based components (liner, slab, confinement supports) and to the alkaline perturbation developed on the argillites of the Callovo-Oxfordian in the near field and on backfill.

7.6.1 Chemical deterioration of cement based shaft components

Generally speaking, the evolution of the cement based components is similar to that described above for the cement based components of the B waste disposal cells (see section 7.4.2) (Figure 7.4.1).

In the shafts, the deterioration of the cement based liner in contact with the Kimmeridgian marls is slow due to the low water flow (see section 6) and extends over several tens to hundreds of thousands of years (Bourbon, 2005).

At the level of the Barrois limestones and the calcareous Oxfordian, the water flows are greater, so leading to faster deterioration of the concretes. The concrete located outside the rings is therefore subjected to water flows of about a m^3 per year coming from the Barrois limestones. Considering the quantity of the concrete (a maximum of a few m^3), the external liner should be completely deteriorated after a few hundred years. The cement based materials placed on the internal surface of the rings are percolated by rainwater that has passed through the backfill. Their deterioration is slower than that of the concretes on the external surface of the rings, but has not yet been assessed. The complete deterioration of the liner concretes located in contact with the calcareous Oxfordian is also swift, and probably takes place in a few thousand years.

In a similar way, the support bases of the separation seal for the porous layers of the calcareous Oxfordian (Hp) deteriorate progressively, depending on the water flow passing through them. This deterioration could extend over a period of about a thousand years, with limited mechanical consequences.

The cement based materials affected by percolating water from the argillites, marls or the calcareous Oxfordian are also attacked by the sulphates. This attack remains a minor phenomenon, due notably to the composition chosen for the concretes, resistant to the sulphate levels encountered.

7.6.2 Alkaline perturbation in the near field geological environment close to the shafts

In the same way as for the drift seals (see section 7.5.2), the deterioration of the cement based materials of the shaft seals and liners by water from the Callovo-Oxfordian and the overlying host rocks causes the migration of the alkaline plume towards the formations located next to the concrete structures (Jacquot & Michau, 2005).

Concerning the argillites, refer to the section dealing with the B waste disposal cells. As the hydraulic properties and the mineralogical composition of the Kimmeridgian marls are close to those of the Callovo-Oxfordian argillites (see section 3.3.2.3), the progression of the alkaline perturbation is probably similar and should extend for about one metre. The alkaline perturbation therefore has no effect on the hydraulic properties of this formation.

The extent of the alkaline perturbation is not assessed at the level of the calcareous Oxfordian and Barrois limestones. However, in these carbonate formations, it is highly probable that the alkaline plume would be quickly buffered by dissolution of calcite. At the level of the aquifers, the high water flows present should quickly dilute the effects of the perturbation.

7.6.3 Alkaline perturbation of drift and shaft backfill in the post-closure phase

The closure of the drifts and shafts in the repository includes backfilling with material based on the excavated argillites that have been reworked (crushing, compaction). These argillites, excavated and placed in spoil heaps during operation of the repository, undergo oxidation that has similar effects to that described for the desaturated argillites in the walls of the ventilated structures (Andra, 2005l).

The backfill is brought to saturation by cement based water coming from the percolation of water in the argillites through the structure concretes. Backfill is put into place in a desaturated condition, with a saturation level that should be about 70 %. As a consequence, the water volume required to achieve saturation represents about 30 % of the backfill's pore space. This volume of water is small compared to the volume of the backfill argillites, so the cement based water for saturation is quickly buffered by the argillites. The alkaline perturbation associated with resaturation therefore remains very limited.

After nearly complete saturation has been reached (S > 90 % at 100,000 years), an alkaline perturbation develops, due to the deterioration of the liners and the slab. By comparison with the Callovo-Oxfordian argillites making up most of the backfill, the extent of the strongly remineralized zone should be at maximum of about one metre at one million years.

7.7 Chemical evolution of Callovo-Oxfordian argillites in the far field

The physico-chemical interactions between the Callovo-Oxfordian argillites and the repository materials (alkaline perturbation, iron / argillites perturbation, oxidising perturbation) are interface phenomena whose extent is limited to the initial EDZ.

The only perturbation that could possibly have chemical consequences (for water and mineral chemistry) and that could have a widespread effect on the Callovo-Oxfordian strata is linked to the thermal loading next to C waste repository zones and spent fuel repository zones (Bauer, 2005) (Figure 5.3.1). It has been demonstrated that the temperature increase in the near field close to the exothermic waste disposal cells should not have any mineralogical consequences (see section 7.3.2.1).

Next to these repository zones, the thermal profiles in the Callovo-Oxfordian show a rapid decrease in the temperature a few meters away from the repository. After the first few meters, the temperature does not exceed 60 °C. At the roof of the Callovo-Oxfordian, it reaches a maximum of 35 °C at about 1,000 years and descends to less than 30 °C again at about 10,000 years. Between 50,000 and 100,000 years are required to return to the geothermal temperature (Figure 5.3.1).

The time-temperature pairs corresponding to the thermal evolution of the layer are not of a type likely to modify the mineralogy of the argillites either in the far field or in the near field. The chemistry of the interstitial fluid also changes very little (Altmann & Jacquot, 2005 ; Cathelineau & Mosser, 1998).

7.8 Chemical evolution of the surrounding formations (Dogger and carbonated Oxfordian)

The chemical influence of the repository on the host rock formations is minimal. It only takes place during the first few tens of thousand years via a moderate temperature increase (< 15 °C, Figure 5.3.1) and only next to C waste repository zones and spent fuel repository zones. At 100,000 years, the temperature of the host rocks has returned to the initial geothermal temperature.

The intensity and duration of this thermal transient have a negligible effect on the properties of the host rocks. The host rocks are mainly composed of carbonates that are not very sensitive to this level of temperature increase (Buschaert & Giffaut, 2005).

7.9 Summary of the chemical evolution of the repository and its geological environment

7.9.1 An important component of the phenomenological evolution of the repository

The chapters on the thermal and hydraulic evolutions of the repository and its geological environment have defined the framework in which the chemical evolution is described (Figure 7.9.1). Together, these components of the phenomenological evolution of the repository define the framework of the mechanical evolution of the repository (see section 8). Finally, they determine the release, then the transfer of radionuclides within and outside the repository over time (see section 10).

The mechanical behaviour of repository components is partly determined by their chemical evolution, for example the corrosion of metals, which causes the progressive discharge of their mechanical strength and of the sealing of C waste and spent fuel containers. The chemical deterioration of the concretes by water from the Callovo-Oxfordian influences their mechanical properties by modification of the cementation and the porosity due to dissolution and precipitation processes.

- Release of radionuclides from the waste packages is mainly due to chemical processes, such as the aqueous solution of the glass matrix.
- The solubility and the retention of the radionuclides depend on the chemical environments they encounter once they have been released. In association with the conditions of transport in solution, they determine the complete immobilisation of the majority of the radionuclides or, for some, their mobility within the repository, then possibly their transfer into the Callovo-Oxfordian strata, and finally into the host rocks.

7.9.2 Slow chemical evolution mainly affecting the repository and the Callovo-Oxfordian in the very near field

The water fluxes involved in the repository and in the Callovo-Oxfordian strata during the hydraulic evolution of the repository are low. Overall, diffusion remains the dominant mode of transport for solutes within and around the repository. The Callovo-Oxfordian strata have chemical characteristics that contribute to limiting any chemical perturbation:

- the pH increase, due to the alkaline perturbation and the progression of the alkaline plume, is limited by the cationic exchange capability of the Callovo-Oxfordian clays,
- the oxidising perturbation, linked to the ventilation oxygen during operation of the repository, is buffered by the solution of the carbonates,
- the reduction potential of the Callovo-Oxfordian is due to the presence of pyrite and organic matter.

In addition, the significant thermal periods of the C waste and spent fuel repository zones (this applies partly to the B waste zone, but is less important as this waste is not exothermic or only weakly exothermic) are short, about a few thousand years, compared with the scale of a minimum of a million years for the phenomenological evolution of the repository. The temperatures reached in the repository (and therefore in the Callovo-Oxfordian strata) do not exceed 90 °C due to the design arrangements retained. In the far field, in the Callovo-Oxfordian strata, the thermal period is longer, several tens of thousand years, but the temperatures reached are lower (< 60 °C) than those reached in the repository.

This set of characteristics means that (i) the Callovo-Oxfordian layer is only slightly perturbed by the repository, (ii) the chemical evolution is globally restricted to the repository, and (iii) the chemical processes involved are slow (mostly from a few thousand years to a minimum of several hundred thousand years).

The chemical perturbations in the Callovo-Oxfordian strata linked to interactions with the repository materials, notably the concretes, only develop in the repository's very near field, over a maximum distance of 2 to 3 m (perturbed zone). This is low compared to the minimum thickness of 60 meters of the Callovo-Oxfordian between the repository and the host rocks.

The overall chemical properties of the Callovo-Oxfordian strata therefore remain unchanged. In particular, the chemistry of the interstitial water stays identical to the initial state. The repository does not have any chemical effect on the host rock formations, both because they are kept far enough away and because of the capability of the Callovo-Oxfordian to quickly limit the progression of these perturbations.

7.9.3 A limited number of major processes

Overall, the chemical evolution of the repository and its geological environment is marked by a limited number of processes.

(i) The deterioration of the concrete based repository components. This particularly concerns the concretes in the B waste disposal cells (support / liner and disposal package).
(ii) The alkaline perturbation created by the concrete components on the argillites and on the swelling clay based repository components, with which they are in contact. This concerns particularly the hydraulic structures of the repository: the disposal cell plugs and the drift access shaft seals.
(iii) The corrosion of metal components. This concerns notably the C waste and spent fuel containers, but also waste such as the cladding and the structural components of spent fuel assemblies.
(iv) The iron / clay and iron / argillites perturbation in contact with the metal components. This is mainly the case for the engineered barrier of the spent fuel disposal cells or for the argillites with the lining and the metal liner of the C waste and spent fuel disposal cells.
(v) The solution of the glass matrix of vitrified waste.
(vi) The solution of spent fuel oxide pellets.

The redox processes of the repository can be added to this list, particularly those occurring after the structures have been closed, notably the passage from oxidising conditions during the operation of the repository to anoxic, then reducing conditions after closure of the repository. The nature of the corrosion reactions of the metal components and the mobility of many of the radionuclides depend on these processes.

7.9.3.1 Deterioration of concretes: a process that takes several hundred thousand years

Because of their chemical buffer capability and the drainage and solute transfer conditions imposed by the Callovo-Oxfordian strata, the chemical deterioration of the concretes of the repository lasts for a minimum of several hundred thousand years. So, for the B waste disposal cells, a undisturbed concrete chemical environment persists around and within the B waste packages. This slow chemical deterioration of the concretes leads in practice to slow evolution of their overall mechanical properties.

7.9.3.2 Alkaline perturbation: an interface process

The alkaline perturbation is characterised by two mineralogical zones: one zone strongly remineralized by the cement based water and one perturbed zone. Over a million years, the extent of the strongly remineralized zone reaches a maximum of several tens of centimeters (60 / 70 cm), that of the weakly perturbed zone several meters (2 to 3 meters).

For the argillites, the extent of the alkaline perturbation therefore remains restricted to that of the initial EDZ. The solution and precipitation processes involved should contribute to the healing of the EDZ. It is probable that the strongly remineralized zone corresponds to a plastic zone with hydraulic properties that are close to those of undisturbed argillites. In addition, due to the mineral species formed (zeolites…), it is also probable that this zone has high radionuclide retention properties.

The C waste and spent fuel disposal cell plugs and the seals have dimensions of several meters to several tens of meters. This means that the extent of the alkaline perturbation appears limited when the scale of these structures is considered. In particular, the total extent of the alkaline perturbation does not reach the waste packages. If the swelling properties of the strongly remineralized zone are (very) low, the mass of unaffected swelling clay allows the overall hydraulic performance of these structures to be maintained. More precisely, the design arrangements retained at the level of the drift seal hydraulic keys (removal of the liner around the keys) avoid the inclusion of the hydraulic keys in the strongly remineralized zone.

7.9.3.3 Stability of repository components based on swelling clays

The repository components based on swelling clay are globally little affected by the chemical processes. Thus the chemical interactions of the spent fuel disposal cells engineered barrier with the iron in the liner, the lining, or the container are restricted to the zones in direct contact with these components. The iron / clay perturbation entails the apparition of a strongly remineralized zone (chloritised) whose extent corresponds to less than 15 % of the total thickness of the engineered barrier. Outside this zone, the swelling clay is little affected. The mass of the engineered barrier therefore comes into chemical equilibrium with the water in the argillites and remains stable over time, particularly during the thermal loading. The overall hydraulic, swelling and retention properties of the engineered barrier do not therefore change over time. This is also the case for the disposal cell plugs and the seals.

7.9.3.4 Corrosion of C waste and spent fuel containers: a process that takes at least several thousand years

The corrosion rates of the metal components of the C waste disposal cells and the spent fuel disposal cells (lining, liner, overpack, container) are low, a maximum of about a few micrometer per year under anoxic conditions. This therefore leads to durations for the sealing of the containers of several thousand years at minimum, corresponding to the required specifications. Less conservative durations can, however, be estimated on a phenomenological basis; 15,000 years for the C waste overpack and 30,000 years for spent fuels.

7.9.3.5 Release of radionuclides: a slow processes

- **B waste packages**

The deterioration of B waste primary packages takes place in a undisturbed perennial cement based environment. This leads to deterioration durations of at least ten thousand years (for B2 bituminised sludge type packages), to several tens of thousands of years to about a hundred thousand years (for B4 and B5 type compacted or cemented packages). In correlation, the release of radionuclides occurs over these time scales. In addition, the radionuclides released encounter a cement based environment only weakly perturbed compared with the initial condition of the concretes within the disposal cells.

- **Solution of the glass matrix of C waste and of the oxide pellets in spent fuel assemblies**

The solution of the C waste glass matrix takes a few thousand years for C0 glass and several hundred thousand years for C1, C2, C3 and C4 glass, after the discharge of sealing of the overpacks.

The solution of the spent fuel oxide pellets takes place over a time scale from several tens of thousands of years to about 100,000 years after the discharge of sealing of the containers, if the process of radiolytic solution is taken into account. An absence of the radiolytic effect would lead to a time scale for solution of at least a million years.

7.9.4 Important phenomenological elements for reversibility

The assessment of reversibility is carried out by reference to the chemical condition of the repository components. We will start by summarising the main results concerning reversibility, and follow by considering the analysis of the potential consequences of an operation over several centuries.

7.9.4.1 Repository condition at the term of the 100 year conventional reference period set by convention for operation of the repository

At the term of the 100 year operation period (at the time of closure), the chemical processes remain limited. This is the case in the C waste and spent fuel disposal cells: they are close to total saturation, but corrosion speeds are low (a maximum of a few micrometer per year), so corrosion thicknesses are of the order of a few millimeters. More precisely, the low corrosion of the linings during this period leads to their mechanical strength, and therefore their sealing, being maintained, so that the packages are in a dry environment and are unaffected by any significant corrosion. The dry desaturated condition of the B waste disposal cells and the drifts strongly limits the processes of concrete deterioration and corrosion of metal components and, in correlation, limits the mechanical processes (argillite creep).

7.9.4.2 Influence of an operating period of several centuries on reversibility

- **For the drifts**

Maintaining the ventilation for a period of several hundred years (i.e. a dry environment) would not have an influence on the chemical evolution of the concrete infrastructures and the argillites in the near field. A pseudo permanent condition is already established after about ten years of operation of the repository. The water fluxer are drained and the profile of the degree of saturation (in the argillites) from the structure walls then evolves very slowly: after another few hundred years, the profile of the degree of saturation would only have progressed by a few centimeters. The conditions of low atmospheric carbonation of the concretes and of low corrosion of the metal components are therefore maintained.

- **For B waste disposal cells**

Conclusions similar to those for the drifts can be made if these disposal cells were to be kept open and ventilated for a period of several hundred years. If the disposal cells were closed as planned in the chronogram set by convention for the operation of the repository, and if the repository were to remain open for a period of several hundred years, the hydraulic condition of the disposal cells would evolve very little during this time. The evolution would not be sufficient to cause deterioration of the concretes and corrosion of the metal components.

- **For C waste and spent fuel disposal cells**

Extending the operation of the repository for a period of several hundred years would not lead to significant modification of the evolution of the different chemical processes taking place during this period. In particular, the corrosion speeds would stay low and would not have any effects on the mechanical strength of the metal components (supports and lining). The sealing of the lining would be maintained, ensuring the absence of corrosion of the disposal packages, thus maintaining their physical integrity.

It should however be pointed out that the desaturated zone of argillites around the access drifts right above the cells stretches over a distance of about a metre beyond the EDZ, thus in the first metre of the useful part of the cells. Saturation of the useful part of the cell thus always remains above 97 % and anoxic conditions are maintained at the level of the packages.

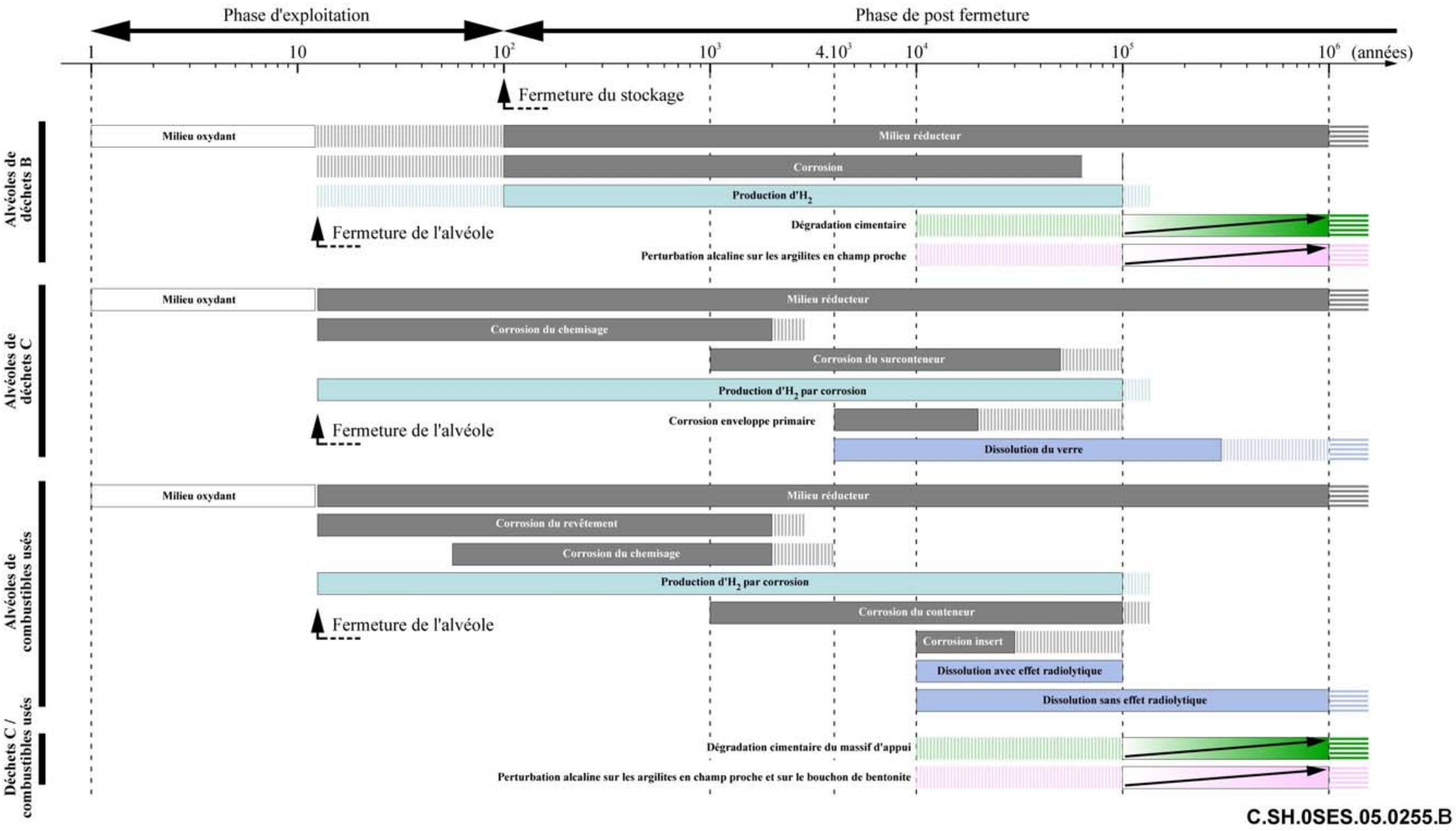

Figure 7.9.1 *Chronogram for the main chemical processes in the B waste, C waste and spent fuel disposal cells (based on the chronogram for the 100 year period set by convention for building / operation / closure of the repository)*

8

Mechanical evolution of the repository and the surrounding geological medium

8.1 Introduction 341

8.2 Creation of an initial excavation damaged zone (EDZ): excavating the engineered structures and instantaneous mechanical relaxation 343

8.3 Mechanical evolution of ventilated engineered structures during repository operating phase: drifts, B waste disposal cells and shafts 357

8.4 Mechanical evolution of B waste disposal cells and drifts in post-closure phase 363

8.5 Mechanical evolution of C waste disposal cells and spent fuel disposal cells..369

8.6 Mechanical evolution of seals 386

8.7 Large-scale mechanical evolution 399

8.8 Summary of mechanical evolution...401

8.1 Introduction

8.1.1 A component in the phenomenological evolution of the repository

Mechanical evolution within the overall phenomenological evolution of the repository and its geological environment concern three aspects.

- It provides data for operating and observing the repository with respect to the protection of workers exposed to the hazards of working underground and to the recovery conditions for the waste packages under repository reversibility.
- The mechanical degradation of the waste packages is a factor to take into account in the release of the radionuclides, even when mainly driven by chemical processes.
- The mechanical evolution of seals, disposal cell plugs and argillites in the near-field contributes to the organisation of the water flows and transfer paths of solutes in and around the repository. Ultimately, mechanical evolution thus plays a role in radionuclide transfer after their release.

8.1.2 Effect of intrinsic mechanical behaviour of the argillites and thermal, hydraulic and chemical evolutions of the repository

Before the repository is created, the Callovo-Oxfordian layer and geological medium are at mechanical equilibrium under a stable stress state for many millions of years, as indicated in § 3.2.5. Creating the repository creates mechanical desiquilibrium. A new mechanical evolution is initiated, firstly by the excavation of the engineered structures in the repository, causing the rock to lose strenght at their periphery, then under the effect of all the thermal, hydraulic and chemical processes brought into play in the repository and the surrounding geological medium. Mechanical evolution of the repository therefore results in:

- purely mechanical stresses, like the excavation operation that is a major mechnical stress affecting the argillites in the near-field of the engineered structures, with the creation of a damaged zone;
- hydro-mechanical couplings. The repository creates a hydraulic transient, described in Chapter 6. It is marked by a period of non-saturated state of all or part of the repository, particularly during its operational phase, during which the chemical degradation processes of the repository components are limited and the deferred behaviour of the argillites around the engineered structures is restrained by the non-saturated damaged zone. Once the repository has been closed, while hydrogen produced by the metals corroding keeps the concretes in infrastructures (ground supports/liners and waste B disposal packages) and the backfill in a non-saturated state ($S \approx 80$ %), it does not influence the saturation of the argillites and the swelling clay (plugs, seals and engineered barriers in spent fuel disposal cells) up to degrees of saturation of over 97 %. Return to a totally saturated state after closure of the repository takes place after a period in the order of 200,000 years ($S > 95$ % in the entire repository). The saturation state of the repository components, and in particular the argillites or swelling clay, influences numerous mechanical processes like the deferred behaviour of the argillites or the development of the swelling pressure of the swelling clay;
- thermo-mechanical couplings. Emplacing the C waste packages and spent fuel packages creates a thermal load that mainly affects the repository zones and the surrounding Callovo-Oxfordian layer (see § 5). Rises in temperature generate deformations and stress in the repository components and argillites. The evolution of the mechanical behaviour of the repository engineered structures and surrounding argillites is then coupled to temperature evolutions in and around the engineered structures;
- chemical-mechanical couplings. Hydraulic and thermal repository conditions influence the mechanical evolution of the repository engineered structures through the corrosion and chemical degradation of their components. The existence of a non-saturated state of the waste B repository disposal cells and the drifts over a period in the order of 100,000 to 200,000 years limits the

chemical degradation of the components of these engineered structures (particularly the concretes) and, therefore, the modification to their mechanical properties. After return to the saturated state, given the low water flows in and around the repository, the chemical degradation process, and therefore the modifications to the mechanical properties of the repository components, are slow and limited in space.

8.1.3 An evolution mainly concerning the repository and the Callovo-Oxfordian layer in the near-field

The mechanical processes brought into play mainly concern the repository and the Callovo-Oxfordian layer. Apart from the shaft near-field, the surrounding formations are sufficiently distant from the repository to avoid being affected mechanically. Their phenomenological evolution, and particularly the mechanical component, is mainly governed by climatic changes and internal geodynamics (see § 9).

8.1.4 Independence and similarity of the mechanical evolution

As for the thermal, hydraulic and chemical processes, the compartmentalised design of the repository, the distances between engineered structures and the method of managing the repository operation converge on a simplified organisation of the mechanical processes and a limitation of mechanical interactions within the repository, and therefore at the scale of the Callovo-Oxfordian layer and the surrounding formations.

Thus (i) each repository zone follows its own mechanical evolution independently from the other zones and (ii) every repository module and disposal cell shows similar evolutions. A large part of the mechanical evolution of the repository and the surrounding geological medium can therefore be dealt with at the scale of characteristic engineered structures as so many elementary mechanical patterns: disposal cells (B waste, C waste and spent fuels), drifts, seals and shafts, both during repository creation and operation and after closure up to a million years.

8.1.5 Three categories of engineered structure in terms of mechanical evolution

The type of materials introduced into the repository and the thermal, hydraulic and chemical evolutions described in Chapters 5, 6 and 7 can be used to distinguish three major categories of engineered structure in terms of mechanical evolution:

- C waste disposal cells and spent fuel disposal cells. They are characterised by the presence of metals and swelling clay (disposal cell plugs and engineering barriers for spent fuel), high thermal load (see § 5.4), the lack of ventilation and a return to a state close to rapid saturation after closure.
- B waste disposal cells, drifts and shafts. These engineered structures are mainly built of concrete. They have little or no thermal load (see § 5.5). They are ventilated during the operating period. In post-closure phase, the hydrogen produced by corrosion of the metallic components keeps them in a non-saturated state ($S < 80$ %) for about 100,000 years (see § 6) ;
- seals. These engineered structures combine the presence of different clays (swelling clay and argillites) and concrete. They may have a moderate or nil thermal load depending on whether or not they are located near disposal cells containing exothermic waste (see § 5). To a certain extent they are a combination of the two previous categories of engineered structure.

8.1.6 Organisation of the chapter on mechanical behaviour

Given the general elements above, the description of the mechanical evolution of the repository and its geological environment is structured as follows.

- Firstly, the repository and the Callovo-Oxfordian layer are dealt with. The mechanical behaviour on a large scale of the repository and the surrounding formations is addressed at the end of the chapter (§ 8.7).
- Excavating the engineered structure, the initial mechanical load in the mechanical evolution, is dealt with specifically in a first section (§ 8.2).
- Then, in conjunction with the thermal load and the hydraulic and chemical evolutions, the mechanical evolution per standard engineered structure is addressed, with distinction, if necessary, between the operating phase and the repository post-closure phase:
    - B waste disposal cells, drifts and shafts ventilated during the operating phase (§ 8.3),
    - B waste disposal cells and drifts after closure (§ 8.4),
    - C waste and spent fuel disposal cells used from the operating phase onwards (§8.5),
    - B waste disposal cell seals, drift seals and shaft seals (§ 8.6).

8.2 Creation of an initial excavation damaged zone (EDZ): excavating the engineered structures and instantaneous mechanical relaxation

Creating a repository engineered structure causes the rock to lose containment at its periphery, resulting in an immediate redistribution of stresses, deformations and possibly the creation of a mechnically damaged zone with respect to the initial rock called EDZ (Excavation Damaged Zone) (Inset 8.1), (European commission, 2003). In this zone, fracturing and/or microfissuring, and in general terms, rearrangement of the rock poral structure can result in localised and generalised increase in rock permeability compared with its initial permeability.

Within the context of a radioactive waste repository and independently of its evolution over time, all or part of this initial mechanical EDZ is therefore likely to constitute a pathway fostering water flows and solute transfers thus adversely affecting repository performance. Consequently, by extension of hydraulic properties, the EDZ is ultimately defined as “the zone of the rock where hydromechanical and geochemical modifications result in significant variations in transport and water flow properties” (European commission, 2003), (Tsang *et al.*, 2005).

Geometry, extent and intensity of the initial EDZ depend on the mechanical behaviour of the rock and also on the initial stress state which varies according to structure orientation compared to stresses within the massif and the depth under consideration.The EDZ also depends on a number of parameters relating to engineered structure design, like the excavation method, phasing of the installation and type of ground support/liner, and the shape and dimensions of the engineered structure. Thus, the conceptual measures adopted to create the engineered structure can be used to limit their influence (excavation method using mechanical working or soft blasting, pseudo-circular engineered structures, etc.).

Inset 8.1 ***EDZ or damaged zone around the engineered structures***

Excavating an underground structure may create a damaged zone, called **EDZ**, on the wall of the excavation, which is represented in different ways (European commission, 2003).

Thus, the usual conceptual model, established from the observations carried out in the foreign underground laboratories and more particularly in the underground laboratory of the Mont Terri distinguishes two zones (Figure below):

- a **fractured zone** in the immediate vicinity of the engineered structure is produced if the rupture threshold, corresponding to the maximum mechanical strength of the rock, is exceeded; this is characterised by the appearance of more or less connected fractures, parallel with the axis of the drift and which may induce increased permeability of the rock;
- a **microfissured zone,** which is produced when the fissuring threshold is exceeded in the vicinity of the engineered structure (if the fractured zone is not formed) or behind the fractured zone. Mechanical relaxation from the engineered structure excavation causes deformations that manifest themselves as barely-connected, diffuse microfissuring. This low connectivity limits the increase in permeability. Nevertheless, the fractures not or very little connected may locally exist within this microfissured zone

The fractures and cracks of the fractured and microfissured zones such as above defined are preferentially oriented parallel with the axis of the structures.

In the experimental drift located at the -490 m level in the Meuse/Haute-Marne underground research laboratory, the observations show that shearing fractures appear in front of the working face. These fractures are oblique compared to the axis of the drift. The conditions of their creation and geometry seem to depend on the conditions of excavating (speed and regularity of the excavating and the installation of the lining). With the excavating, only the ends of these fractures persist in wall of the structures, thus forming a network in "rafters". Their extension is close to the microfissured zone. Only the part of these fractures nearest to the wall has a greater permeability than undamaged argillites, because of a lower constraint on their surface.

The EDZ does not include the **so-called "influenced" zone** (ou “disturbed zone”- EDZ) which extends beyond the microfissured zone. This is the seat of limited modifications to the field of stresses and deformations, without effect on the properties of the rock (particularly permeability).

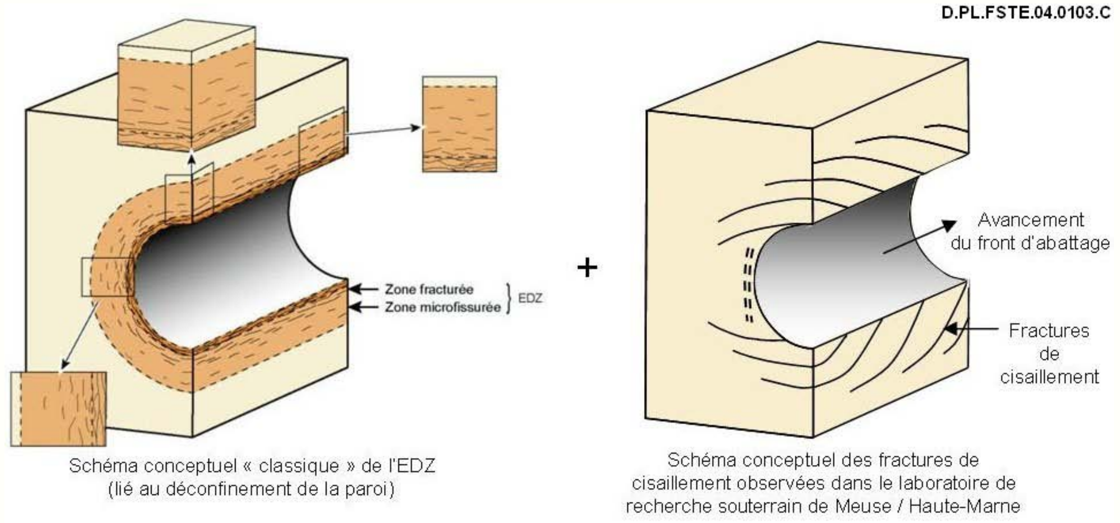

EDZ conceptual scheme
(hypothesis of an initial, isotropic stress state perpendicular to the axis of the engineered structure)

8.2.1 Various mechanical behaviours according to the geological formations crossed

Shafts cross the surrounding formations overlying the Callovo-Oxfordian layer and its upper part up to the repository level. The repository engineered structures (disposal cells, drifts) are all installed at the same stratigraphic level (zone C) in the middle of the Callovo-Oxfordian layer.

The surrounding formations and the Callovo-Oxfordian layer have different mechanical behaviours. The calcareous Oxfordian has relatively high mechanical properties (strength and modulus of deformation); the Kimmeridgian marls and the Callovo-Oxfordian argillites may be deformed more easily (Inset 8.2).

In addition, vertical variability in the mechanical properties is noted within the Callovo-Oxfordian layer, particularly in the part crossed by the shafts. There are thus three distinctive mechanical zones. The upper zone, called zone A, with a higher carbonate content, has higher mechanical properties (strength, modulus of deformation) than the underlying zones B and C and alternates between varying degress of carbonates that induces a dispersion of mechanical properties. Zone C, where the repository engineered structures are installed, is characterised by a maximum clay content, resulting in mechanical behaviour more easily deformed than in zone B and greater homogeneity of the mechanical properties (see § 3.3.1.4).

In the Meuse/Haute-Marne underground research laboratory, the experimental drift located at the -445 m level is installed in the zone B and experimental drifts located at the -490 m level are installed in the zone C.

Inset 8.2 ***The law of short-term mechanical behaviour of the argillites (1/2)***

The mechanical properties of the rocks are divided into two categories:

- resistance to mechanical loadings (compression, traction) defining the rupture thresholds or criteria,
- deformabilities under mechanical loadings.

The term "**law of behaviour**" normally designates the mathematical equation of the relationship between the stresses (σ), the deformations (ε) and the deformation rates. The behaviour and mechanical properties of rocks are studied in the laboratory on samples, with basic tests bringing stress or traction loads into play.

Under unixial, the most common test, the macroscopic mechanical behavior of the argillites can be summarised in four fields (Figure below).

- field I: the relationship between the deformations and the stress is linear for a low load. This virtually reversible field is called "elastic". The slope of the curve (deformation; stress) is called the modulus of deformation (or Young's modulus - E).
- field II: from a certain stress level, called damage initiation (σ_{end}), a discrepancy appears with respect to the linearity on the curve (σ–ε), with a faster increase in deformations than in the elastic field. The deformations cease to be linear up to the compression strength (σ_c) and become irreversible. They are linked to the appearance of microfissuring of the rock which is accompanied by a degradation in the mechanical properties and an increase in the permeability of the rock. It corresponds to the "field with microfissuring".
- field III: the postpeak field results in the unstable, uncontrolled development of the fissuring network which in turn causes increasing damage to the rock. This is combined with increased permeability of the rock, with it gradually losing cohesion and reaching a residual strength (σ_r) lower than the initial strength. It is called "post-rupture or with fracturing field".
- field IV: beyond a certain deformation level, field of significantly constant residual strength.

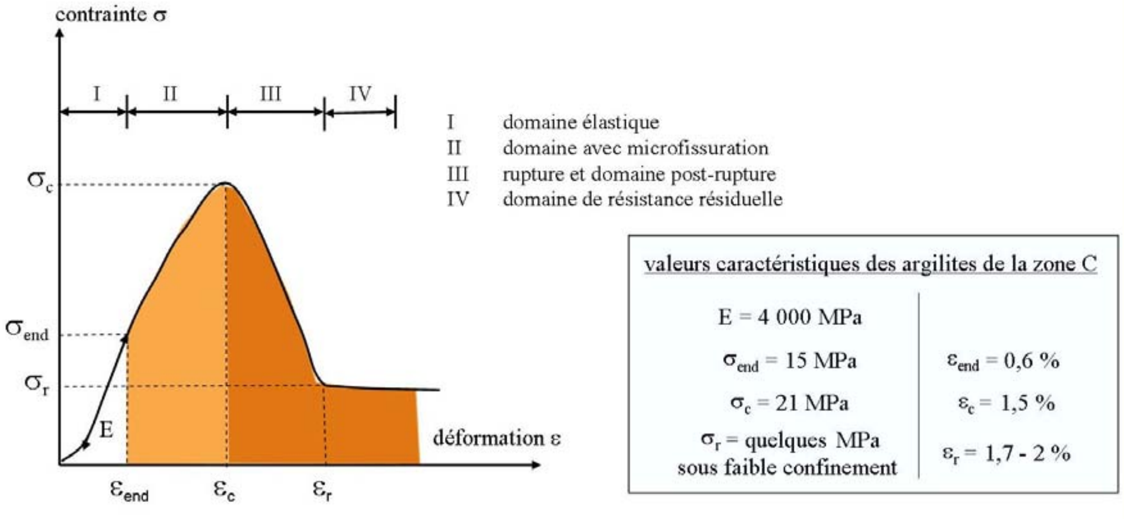

valeurs caractéristiques des argilites de la zone C

E = 4 000 MPa	
σ_{end} = 15 MPa	ε_{end} = 0,6 %
σ_c = 21 MPa	ε_c = 1,5 %
σ_r = quelques MPa sous faible confinement	ε_r = 1,7 - 2 %

Diagram of a unixial compression test illustrating the short-term mechanical behaviour of the argillites and characteristic values of the mechanical properties of the argillites in the locality of the repository (Andra, 2005m, Chapter 25)

The law of short-term mechanical behaviour of the argillites (2/2)

The short-term mechanical behaviour of the clay formations brings several phenomena into play:

- **elasticity**, corresponding to modifications to interatomic distances based on distances of equilibrium at rest, is characteristic of the carbonate fraction,
- **plasticity,** linked to the existence of permanent deformations and the non-linearity of the curve ($\sigma-\varepsilon$), is characteristic of the clay fraction,
- **damage** is the gradual deterioration from microfissuring of the material cohesion, with a variation in the physical and mechanical properties as a result.

Establishing a law of short-term behaviour is used to reproduce the behaviour of the argillites under mechanical loading such as excavating an engineered structure. It must be able to estimate the extents of the fractured and microfissured zones created during construction of the engineered structure, the reproduction of the greatest deformability of the microfissured rock before rupture and the discharge of mechanical strength of the fractured rock after rupture. It must also involve variables, called "hardening", which are used to reproduce the non-linear and irreversible behaviour of the rock.

The behaviour of the argillites is said to be "damageable elastoplastic". The model used for the EDZ evaluations is the Hoek & Brown elastoplastic model with hardening, developed under the MODEX-REP project (Hoek & Brown, 1980 ; Su, 2003). This is a purely mechanical model used only to assess the hydraulic properties (geometry of the fracturing/fissuring and permeability) of the fractured and microfissured zones.

8.2.2 An initial, variable EDZ according to the depth under consideration and the orientation of the engineered structure

On the site and the transposition zone the state of mechanical stress is slightly anisotropic (see § 3.2.5):

- the vertical stress (σ_v) relates to the weight of the overlying terrain, i.e. about 12 MPa at 500 m deep,
- the minor horizontal stress (σ_h), oriented N65°, is close to the vertical stress,
- and the major horizontal stress (σ_H), oriented N155°, is in the order of 1 to 1.2 times the minor horizontal stress, i.e. 12 to 14.5 MPa.

When the engineered structure is oriented according to the major horizontal stress, the state of initial stress in the perpendicular plane of the engineered structure axis is isotropic, and the EDZ develops in circular fashion. Depending on this orientation, the stress applied to the engineered structure is also weak and therefore limits the extent of the EDZ. By design, the disposal cells and the drifts receiving the seals are oriented according to the axis of the major horizontal stress, to minimise the extent of the initial EDZ.

Conversely, when the engineered structure is oriented according to the axis of the minor horizontal stress or the vertical stress (for shafts), it is subjected to an initial, anisotropic stress state which produces an elliptically-shaped EDZ. The EDZ develops more easily at the top and the bottom than on the walls for a horizontal engineered structure and following the direction of the minor horizontal stress for the shafts (see § 3.3.1.4).

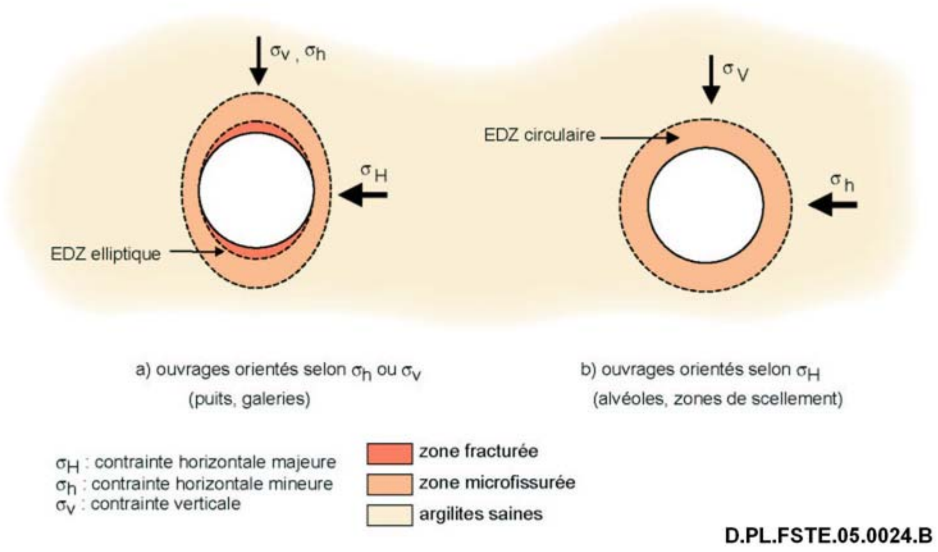

Figure 8.2.1 *Geometry of the initial EDZ based on the orientation of the engineered structures with respect to the state of natural stress*

8.2.3 Extent of the initial EDZ around the various repository engineered structures

The extent of the initial EDZ around the repository engineered structures is assessed mainly by numerical modelling. Some measurements taken in the Kimmeridgian marls and zone A of the Callovo-Oxfordian layer during sinking of the main shaft in the Meuse/Haute-Marne underground research laboratory are also available.

8.2.3.1 Repository engineered structures in the argillites

- **Assessment of the extent of the initial EDZ**

An assessment of the extent of the initial EDZ was modelled numerically:

- using the mechanical properties of the saturated argillites (determined from samples) for all the geomechanical zones. Representative parameters of the behaviour of the least-resistant samples were adopted to take account of uncertainties on the mechanical properties of the rock at the scale of the engineered structure;
- based on the hypothesis of total decontainment without ground support (circular section engineered structures);
- with a law of short-term behaviour of damageable elastoplastic argillites. Developed under the international MODEX-REP project (Su, 2003), the model adopted is controlled both theoretically (relatively simple model incorporating significant mechanical phenomena in the initial EDZ assessment) and for parameter adjustments (Inset 8.1) ;
- by considering a significantly greater anisotropy of the horizontal stresses than assessed on the laboratory site, a ratio equal to 1.4 between the two horizontal stresses (see § 3.2.5) ;
- by taking influence of the repository depth into account (repository engineered structures located at depths varying between 500 m and 630 m in the tranposition zone - see § 3.3.1.1) with respect to the amplitude of the initial stresses.

The hypotheses of minimum mechanical properties and marked anisotropy of stresses adopted for the models tends towards a maximum estimation of the extent of the initial EDZ around the repository engineered structures. The influence of engineered structure design-related factors, such as excavation method, the geometry of the engineered structures and ground support conditions has not been taken into account.

Based on the depth of the engineered structure and its orientation, the extent of the fractured zone is thus assessed at 0 to 0.3 times the radius of the engineered structure and that of the microfissured zone at 0.3 to 1.2 times the radius of the engineered structure (Table 8.2.1). The extent of the reversible disturbances (stresses, deformations) is around 3 times the radius of the engineered structure, if it is considered that the influenced zone relates to a stress variation higher than 10 % compared with the initial stresses.

The fractured zone does not develop around a repository disposal cell or drift section designed to receive a seal (still oriented according to the major horizontal stress) and the isotropic microfissured zone extends 0.5 times beyond the radius of the engineered structure in a repository 500 m deep. At the maximum depth in the transposition zone (around 630 m), excavating an engineered structure oriented according to the major horizontal stress cases a fractured zone with 0.1 radius and a microfissured zone of 0.7 radius.

Thus, around a B waste disposal cell 12 m in diameter, located 500 m deep in the repository, the fractured zone does not develop and the microfissured zone extends isotropically for around 3 m. In a repository 630 m deep, the fractured zone develops, extending isotropically to 0.6 m. The microfissured zone extends for 4 m.

In a repository 500 m deep, the microfissured zone extends for less than 20 cm around a C waste disposal cell (excavated diameter of 0.7 m) and 75 cm around a spent fuel disposal cell (excavated diameter in the order of 3 m). If a repository 630 m deep is considered, a fractured zone of 3-4 cm for a C waste disposal cell and 15 cm for a spent fuel disposal cell develops around the cell. The microfissured zone extends 25 cm for a C waste disposal cell and over a metre for a spent fuel cell.

An engineered structure oriented according to the minor horizontal stress develops a fractured zone extending up to 0.1 radius at the top and bottom and a microfissured zone of 0.3 to 0.7 radius at a depth of 500 m. At a depth of 630 m, the maximum extent of the fractured zone is 0.3 radius and that of the microfissured zone 1.2 radius. Thus, at a depth of 500 m, an access drift oriented perpendicularly to the disposal cells and 8 m in diameter has a fractured zone extending up to 40 cm and a microfissured zone extending from 1.2 m to 2.8 m.

The fractured and microfissured zones extend more at the galleries connections zones (up to twice more than in the standard section). Thus, only the first part of the cell disposal gallerie head is influenced mechanically by the access drift. Beyond, particularly in the section of the disposal cell receiving the packages and the swelling clay plug, there is no mechnical influence from the access drift.

Given the distances between the engineered structures (around 5 diameters), there is no mechanical interaction between neighbouring engineered structures. Thus, the initial state of the Callovo-Oxfordian argillites when the various engineered structures are being excavated is not disturbed mechanically by the neighbouring engineered structures, apart from at the inter-structure connections and intersections.

- **Observations and measurements in the experimental drifts of the Meuse/Haute-Marne underground research laboratory**

Excavation of experimental drifts at the – 490 m level in the underground research laboratory of Meuse/Haute-Marne has provided further information for this modelling. This information takes into account narrower architecture of these drifts than that envisaged for the repository (inter-axial distances between two drifts about four times the diameter of the drifts, pillars of 12 m alongside), which results in a stress state around the laboratory drifts being higher than in the repository where the drifts are further apart (for example, inter-axial distance of 5 times the structure diameter).

Observations *in situ* confirm the existence of a fractured zone due to loss of rock confinement in the wall of structures orientated towards the minor horizontal stress such as suggested by 2D modelling (cf. Table 8.2.1). This is partly attributed to the excavation method (hydraulic rock breaker) and its maximum extension is estimated at around 0.2 times the drift radius, i.e. the same order of magnitude as that given by 2D modelling (0.1 radius).

Observations also show that shear fractures diagonal to the drift axis can appear at a local level in front of the working face. With the advance of excavation, only the ends of these fractures remain in the structure wall, thus forming a herringbone pattern. The maximum radial extension of these fractures can reach one times the drift radius. These shear fractures are well replicated by 3D digital modelling of the drift excavation taking into account the advance of the working face.

Water permeability measurements carried out in the radial boreholes show that argillite permeability in the fractured zone is significantly increased compared to that of undisturbed argillites (values estimated at between 10^{-10} and 10^{-8} m.s^{-1}, i.e. an increase of 3 to 5 orders of magnitude). On the other hand, beyond the fractured zone, permeability values measured below 10^{-12} m.s^{-1}. These results indicate that microfissuring is limited or nil and that shear fractures possibly encountered show an increase in permeability of two orders of magnitude at the most compared to that of undisturbed argillites (cf. § 3.3.1.6). These measurements are consistent with the fact that the mechanical stress state applied to shear fractures beyond the fractured zone is sufficient to maintain the latter closed thus limiting the increase in permeability. It is therefore only in the wall vicinity in the fractured zone, where mechanical stress is weak or nil that argillite permeability rises sharply.

The initial EDZ thus observed on the first structures of the Meuse/Haute-Marne laboratory, consistent with conventional EDZ representation (cf. Inset 8.1), can thus be compared to two successive zones: a fractured zone where argillite permeability increases by 3 to 5 orders of magnitude compared to that of undisturbed argillites and then a zone where permeability is modified by a maximum of 2 orders of magnitude compared to that of undisturbed argillites.

Table 8.2.1 *Numerical modelling assessments of geometries and extensions of the initial EDZ in the Callovo-Oxfordian argillites for the various repository engineered structures (Barnichon & Su, 2005a) (Barnichon & Su, 2005c) (Su & Barnichon, 2005)*

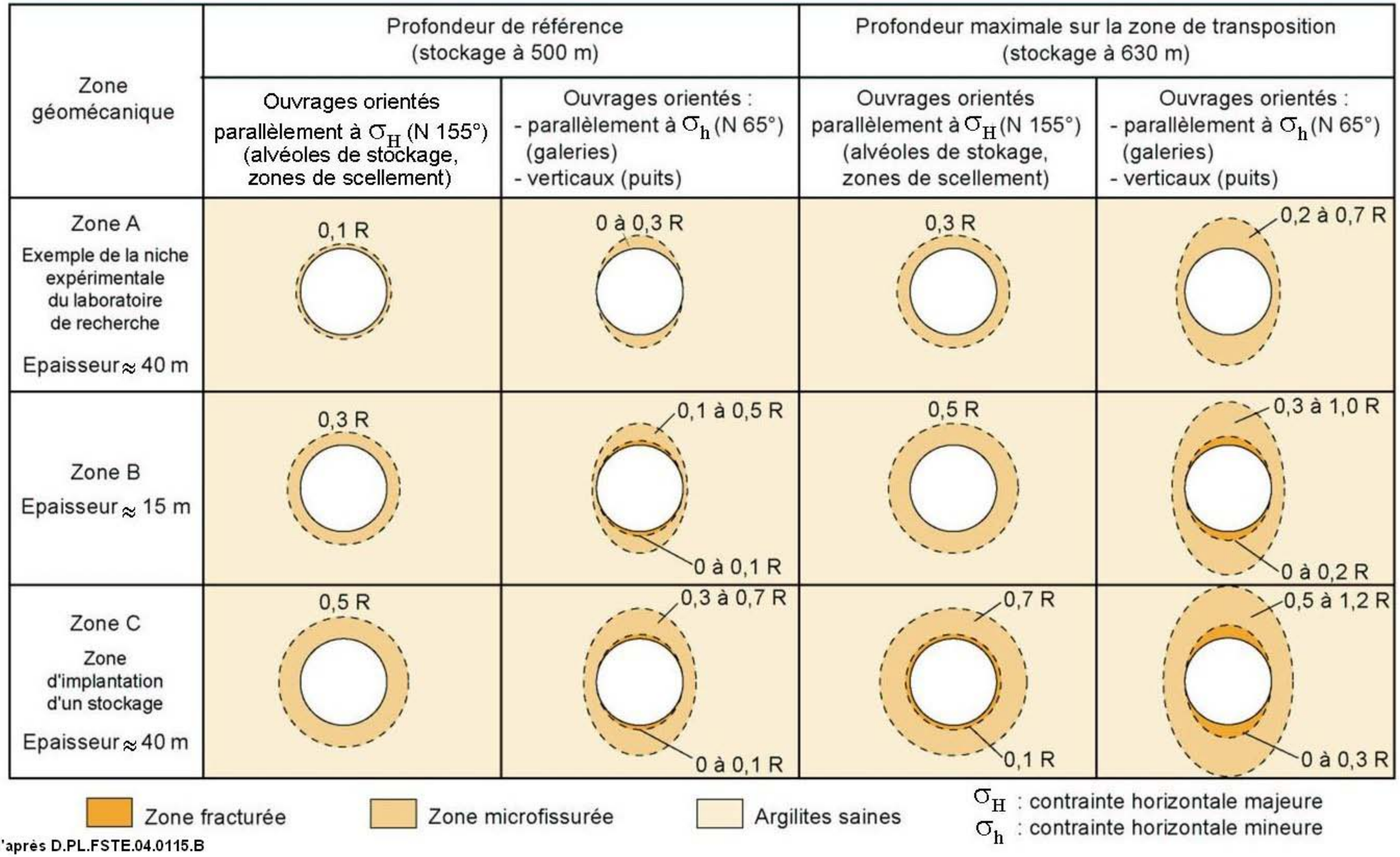

Zone géomécanique	Profondeur de référence (stockage à 500 m)		Profondeur maximale sur la zone de transposition (stockage à 630 m)	
	Ouvrages orientés parallèlement à σ_H (N 155°) (alvéoles de stockage, zones de scellement)	Ouvrages orientés : - parallèlement à σ_h (N 65°) (galeries) - verticaux (puits)	Ouvrages orientés parallèlement à σ_H (N 155°) (alvéoles de stokage, zones de scellement)	Ouvrages orientés : - parallèlement à σ_h (N 65°) (galeries) - verticaux (puits)
Zone A Exemple de la niche expérimentale du laboratoire de recherche Epaisseur ≈ 40 m	0,1 R	0 à 0,3 R	0,3 R	0,2 à 0,7 R
Zone B Epaisseur ≈ 15 m	0,3 R	0,1 à 0,5 R 0 à 0,1 R	0,5 R	0,3 à 1,0 R 0 à 0,2 R
Zone C Zone d'implantation d'un stockage Epaisseur ≈ 40 m	0,5 R	0,3 à 0,7 R 0 à 0,1 R	0,7 R 0,1 R	0,5 à 1,2 R 0 à 0,3 R

🟧 Zone fracturée 🟧 Zone microfissurée ☐ Argilites saines

σ_H : contrainte horizontale majeure
σ_h : contrainte horizontale mineure

d'après D.PL.FSTE.04.0115.B

8.2.3.2 Repository access drifts in the Callovo-Oxfordian argillites

Before the underground research laboratory is excavated, 2D models indicated that, however deep the repository is, a fractured zone does not appear around the shafts in the upper, more calcareous, levels of the Callovo-Oxfordian (more resistant and a little less deep than in the middle, more clayey, area of the formation). A fractured zone can appear in the middle levels of the Callovo-Oxfordian layer, particularly in the deepest zones of the transposition zone (-630 m), where natural stresses are at their strongest. Its maximum extent would be roughly 0.1 to 0.3 times the shaft radius, depending on the depth. A microfissured zone develops beyond the fractured zone according to these models. Its extent can vary from roughly 0.3 times the shaft radius in the upper, more calcareous, levels of the Callovo-Oxfordien, to roughly 0.7 times the radius in the more clayey levels, where the underground laboratory is located. At the maximum depth of the Callavo-Oxfordian layer in the transposition zone (-630 m), the maximum extent of the microfissured zone can vary from 0.7 times the radius to 1.2 times the radius along the shaft depeding on the depth (Table 8.2.1).

Observations and measurements were carried out in the core boreholes radially to the shafts at different levels, in both the upper, more calcareous, levels of the Callovo-Oxfordian (in particular next to the experimental drift at -445 m) and in the middle levels. The measurements were mainly:

- geophysics measurements (microseismic velocities) and permeability measurements in the experimental drift at – 445 m ;
- geophysics measurements, deformation and permeability measurements at different depths of the main access shaft.

Results of observations and measurements have been compared with those of modelling. In the upper levels of the Callovo-Oxfordian, observations prove the absence of a fractured zone around the structure. In zone A, the measurements made show a microfissured zone from 0.1 to 0.2 times the shaft radius. In zone B, microseismic measurements highlight the very slight changes in rock density around the excavation area (microfissured zone). This slight modification to density noticeable up to 1-1.5 m from the shaft wall, i.e. an extension of the microfissured zone of between 0.3 and 0.5 times the shaft radius. Permeability measured around the main shaft indicates a very slight modification of values up to a distance of 2 metres from the wall (in all cases permeability lower than 10^{-11} m.s^{-1}) and beyond that permeability remains unchanged. All the experimental results confirm the initial EDZ representation from digital modelling, mainly depending on the depth.

8.2.3.3 Shafts in the overlying, surrounding formations

The extent of the initial EDZ measured *in situ* in the Kimmeridgian marls during excavation of the main shaft for the underground research laboratory is around 0.5 times the shaft radius. The evolution in permeability, measured at the wall is low and in the order of magnitude of variations in permeability in the formation (Bauer *et al.*, 2003).

No assessment or measurement of the extent of the initial EDZ is available in the calcareous Oxfordian, but its mechanical properties determined from samples are such that there should be no fissuring of the rock on the wall of the shaft given the discharge of containment, and the damage should remain limited in the immediate vicinity of the shaft (Barnichon & Su, 2005c).

8.2.4 Convergence relating to the initial mechnical relaxation

Modifying the stress state in the rocks as a result of excavating an engineered structure is accompanied by convergence. The convergence is produced partly in front of the working face and before the ground support is installed. However, the resultant convergence after the ground support/liner is in place reduces the clearances between the natural rock and the ground support/liner.

- In the Callovo-Oxfordian argillites, the "instantaneous" convergence accompanying the excavation is estimated at 0.5-0.8 % (Barnichon & Su, 2005a).
    - For a C waste disposal cell or a spent fuel cell, the convergence from excavation is thus a few millimeters. Given the clearances in the order of a few centimeters between the lining (or liner for a spent fuel cell) and the disposal cell wall, this convergence is not enough to close the installation clearances totally. The more discrete, deferred convergence (creep) thus contributes gradually to the continued closing of the voids (Inset 8.3).
    - For a B waste cell, drift or shaft, the temporary ground support is constructed using sprayed concrete (possibly with added anchoring bolts) and/or by arches interfacing directly with the argillites. The convergence of the argillites then starts to place load on the ground support. The pressure applied to the sprayed concrete and/or the arches is less than 1 MPa (Barnichon & Su, 2005a). The convergence rate decreases rapidly over time, and delaying the installation of the final liner by a few weeks to a few months once the engineered structure has been created (like for a B waste disposal cell or a drift) limits the pressure applied on the liner by the terrains. According to feedback from instrumentation tunnels excavated in similar rock formations, the pressure applied on the liner after a few years is in the order of a few MPa (Leger et al., 1999).
- The convergence of the Kimmeridgian marls reaches less than 0.1 %, i.e. 5 mm movement at the wall for a 6 m-diameter shaft during the unsupported phase (a few days) (Bauer et al., 2003). Installing the ground support/liner as excavation advances then stops the marls converging at the wall and starts the loading on the liner.
- As for the Kimmeridgian marls, when sinking the shaft, the installation of the ground support/liner as excavation progresses in the calcareous Oxfordian halts the convergence at the wall (Barnichon & Su, 2005c). In addition, the calcareous Oxfordian shows little or no aptitude for deferred convergence.

Inset 8.3 ***Deferred mechanical behaviour of the argillites***

Apart from their instantaneous (or short-term) behaviour, the argillites show deferred behaviour, in other words there is an evolution over time in the stresses and/or deformations with no direct relationship with an evolution in mechanical loadings. For the argillites, the deferred behaviour is controlled by the clay fraction, the carbonate fraction normally not showing deferred effects. In the context of an underground engineered structure, this results in convergence on the wall and deformations of the argillites.

The deferred effects are revealed by creep tests on samples (and less frequently by relaxation tests). The creep test involves uniaxial or triaxial compression with deferred deformations measured over time for a given stress.

Creep tests on argillites show that (Andra, 2005h, chapitre 25) (Figure below):

- deferred deformations are of insignificant amplitude. The order of magnitude of the creep rate is 10^{-2} to 10^{-3} year^{-1} for tests lasting a few weeks to a few months;
- under a constant stress state, the creep rate is gradually reduced over time: after a few years, the creep rate is in the order of 10^{-4} year^{-1};
- the creep speed increases with the applied stress and the temperature (red curve in the figure): under the same stress, the creep rate is tripled at 80 °C compared with the rate measured at ambient temperature;
- desaturation brakes the creep, however (blue curve in the figure). In particular, considerable desaturation (degree of saturation of 40 %) halt the creep.

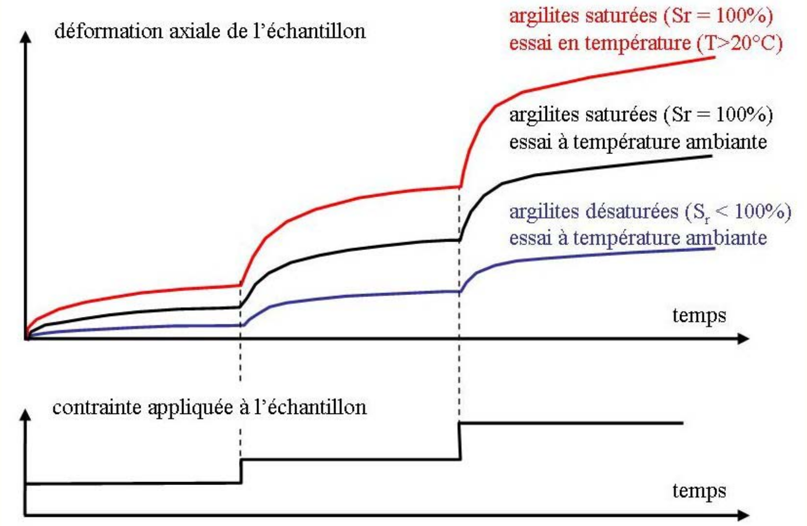

Diagram of a creep test illustrating the deferred mechanical behaviour of the argillites based on the degree of saturation and the temperature

The relaxation test, which involves blocking the axial deformation during uniaxial or triaxial loading, simulates the behaviour of the argillites around a lined engineered structure. The reduction in creep rate over time is accompanied by a reduction in the stress deviator.

The deferred behaviour of the argillites may be described by a long-term behaviour model such as the Lemaître (or modified Norton) model, describing the relationship between the deferred deformation rate and the stress plus the accumulated deferred deformation (Andra, 2005h, chapitre 25).
The deferred deformation rates of the argillites based on stresses and time, their evolution with temperature or desaturation are, at this stage, only obtained from samples and for short test periods (a few weeks to a few years). Predicting the long-term behaviour of the argillites at several tens, hundreds or thousands of years assumes extrapolation.

8.2.5 Permeability of the initial EDZ

The first *in situ* measurements of permeabilities around structures of the Meuse/Haute-Marne underground research laboratory are comparable with permeabilities measured in other indurated clays at Mont Terri and Tournemire (Boisson, 1998 ; Bossart *et al.*, 2002). These measurements taken in boreholes cover small quantities of rock and are used to assess permeability selectively (measurement chamber of a few centimeters). The increases in permeability at fractures identified in the first tens of centimeters in the fractured zone are of 5 to 6 orders of magnitude at most and of 2 to 3 orders of magnitude in the microfissured zone. At a larger scale (several tens of centimeters to several meters), with reduced fissure connectivity the further away from the wall, the equivalent permeability of the fractured and microfissured zones is less than the permeability obtained by selective measurement.

The development of fissuring immediately after excavation has been modelled numerically using the PFC code, where the relationship between the fissure geometry (opening and connectivity) and permeability is assessed using special models. These models for an engineered structure 500 m deep have shown the development of connected microfissures up to depths of 0.2 times the radius of the engineered structure and related increased permeability of 2 to 3 orders of magnitude (Figure 8.2.2, (Barnichon & Su, 2005a)).

The conclusions corroborate:

- the maximum increase in permeability can be estimated at approximately 3 to 5 orders of magnitude in the fractured zone, in the case where this zone exists;
- the maximum increase of 2 to 3 orders of magnitude of the permeability in the microfissured zone;

At the scale of all the fractures, the fracture connectivity (even partial) suggests isotropic permeability on the fractured zone. In the microfissured zone, the excavation may cause favoured orientations for the microfissures, it difficult to predict the effect on the anistropy of permeability.

The initial EDZ created immediately after an engineered structure has been evolves (in extent and intensity) under the effect of the various mechanisms based on thermal and hydraulic conditions applied to it during the operating and post-closure phases (see § 8.3 to 8.6 for the various types of engineered structure).

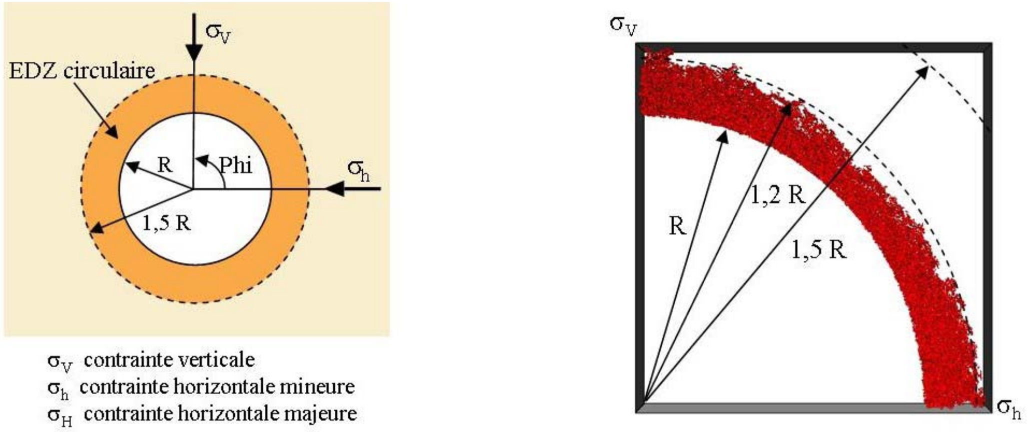

a) Extension de l'EDZ (zone microfissurée) évaluée à 0,5 fois le rayon de l'ouvrage

b) Développement de microfissures connectées jusqu'à des profondeurs de 0,2 fois le rayon de l'ouvrage

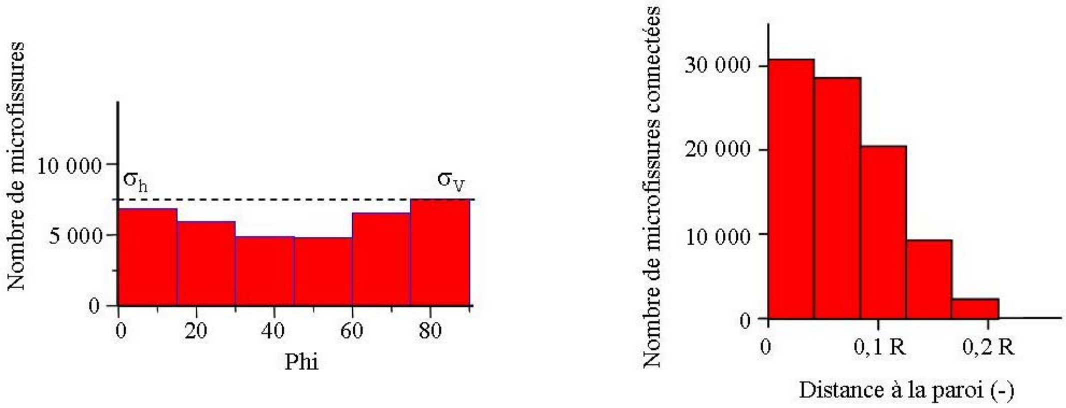

c) Répartition quasi-isotrope des microfissures autour de l'ouvrage orienté selon σ_H

d) Diminution de la connectivité des fissures avec la distance à la paroi

Figure 8.2.2 *Sample network of connected microfissures obtained by simulating the excavation of an engineered structure oriented* s_H *using the PFC code*

8.3 Mechanical evolution of ventilated engineered structures during repository operating phase: drifts, B waste disposal cells and shafts

8.3.1 Thermal, hydraulic and chemical contexts

During their operation, the shafts, drifts and B waste disposal cells are ventilated, which causes the concrete infrastructures and the argillites in the initial EDZ to desaturate in a few years. This desaturation, described in § 6, then propagates very slowly, reaching the undisturbed argillites at the end of the operating phase. Given the hygrometry conditions in these engineered structures, the degree of saturation of the concretes in the ground support/liner and the argillites in the fractured zone is homogenous and less than 30-40 %. Beyond that, it increases rapidly up to over 90 % at the limit of the EDZ microfissured zone. The undisturbed argillites maintain a degree of saturation of over 97 % a few meters beyond the EDZ (Figure 8.3.1).

As indicated in § 5 the argillites and ground support/liner in a C waste module or spent fuel drift experience a rise in temperature, whereas the ventilation keeps the air temperature constant in the drift. The maximum temperature in the argillites and the ground support/liner is in the order of 50 °C one hundred years after emplacement of the disposal packages (see § 5.4). The B waste disposal cell containing exothermic waste is not subjected to this phenomenon, for the ventilation evacuates virtually all the calories emitted by the wastes; the thermal load only intervenes after the disposal cell is closed (Figure 8.3.1).

The hydraulic and thermal contexts of the operating phase cause that chemical degradation of the ground support/liner concretes and the B waste disposal packages, as the corrosion of the metallic components is limited (see § 7.2). They therefore have no influence on the mechanical evolution of the engineered structure. This is mainly driven by the effects of the desaturation of the argillites in the near-field (Inset 8.4) and, to a lesser extent, by the effects of rises in temperature where appropriate (Inset 8.5).

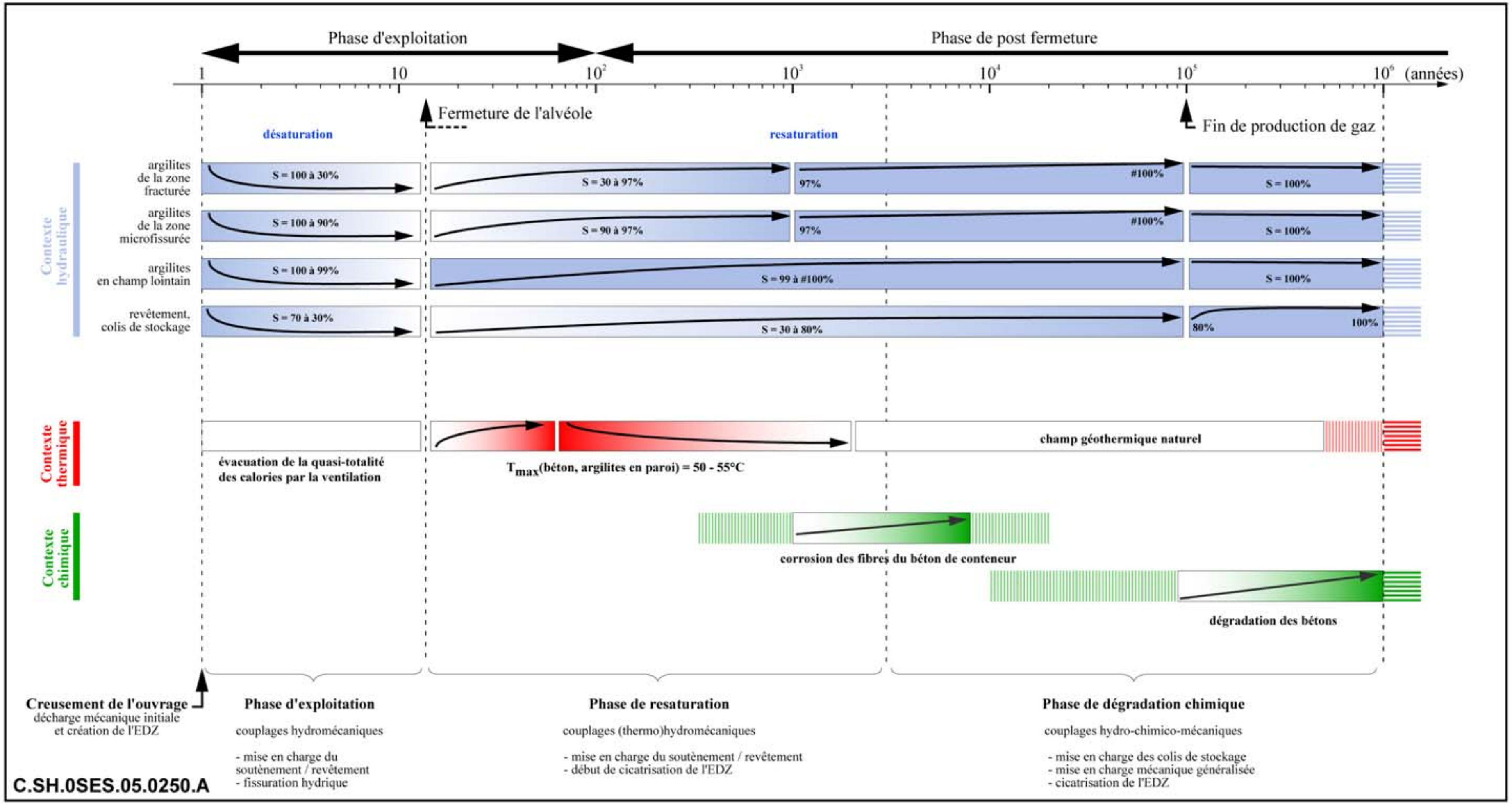

Figure 8.3.1 *Time chart of the mechanical evolution of a B waste cell: thermal, hydraulic and chemical contexts during construction, operating and post-closure phases (based on a conventional, hundred-year time chart of the construction/operation/closure of a repository)*

Inset 8.4 ***Hydromechanical coupling in the argillites***

In saturated state

The mechanical behaviour of the saturated argillites or the "stress-deformation" relationship may be described using the principle of effective stresses: deformations caused by stresses that are actually applied between the solids making up the skeleton. These stresses known as "effective" (σ') are defined as the difference between the total stresses applied to the skeleton (σ) and all or part of the interstititial water pressure (p):

$$\sigma' = \sigma - bp$$

Biot's coefficient (b) describes the ability of the skeleton to recover the interstitial water pressure. For sandy granular media, Biot's coefficient is equal to 1. For the argillites, it will in the order of 0.6 given their very small pore structure (Andra, 2005h, chapitre 25).

In non-saturated state

Non-saturation is characterised by the existence of water menisci in the pores. These menisci create tensile stresses at the solid/liquid water/gas interfaces that produce contact stresses between the skeleton solids comparable to effective stresses. The result is rigidification of the argillites (increase in cohesion and stress at rupture). The strength at the unixial compression of the argillites increases by a factor of 3 to 6 between a saturated sample and a totally dry sample (Andra, 2005h, chapitre 25). and the argillite creep rate is reduced (Inset 8.3).

When there is extensive and/or heterogeneous desaturation, the tensile stresses linked to a contraction of any smectite minerals through discharge of water may produce fissuring. The contracting deformations caused by the desaturation of the argillites are in the order of 0.5 % when the relative humidity drops from 100 % to 66 %. They are similar to the mechanical deformations created at the wall of the engineered structure during excavation (Andra, 2005h, chapitre 25), (Ata *et al.*, 2002).

Swelling of the argillites

The argillites have a smectite content of a few percents to ten percents. These minerals give the argilites a swelling potential and swelling pressure, as for the swelling clays adopted for the seals and disposal cell plugs (Inset 2.7): swelling is estimated at a few percents and the swelling pressure, defined as the pressure that must be applied to a sample to counteract any swelling, at 1-3 MPa (Andra, 2005h, chapitre 25).

Inset 8.5 ***Coupled thermo-hydro-mechanical behaviour of the argillites***

In saturated state

Variations in temperature with respect to the natural geothermal temperature generate two types of effect.

They modify ***the mechnical behaviour*** of the argillites quantitatively (deformability, strength, damage, creep rate) or even qualitatively (cooling makes the rocks more fragile, heating makes them more ductile).

- The work on the Callovo-Oxfordian argillites reveals no significant influence from temperature, up to 100 °C, on the characteristics of the **short-term mechanical behaviour** of the argillites (deformability, strength and damage).
- In **deferred behaviour**, a rise in temperature in the argillites increases their creep rate. For a temperature of 80 °C, the creep rate triples compared with the creep rate at ambient temperature (Inset 8.3).

They generate ***elastic thermal expansions***, which in turn may create stresses. Cooling creates tensile stresses, heating creates compression stresses. The order of magnitude of these stresses, frequently referred to as "thermal stresses" is:

$$\sigma \approx -E\,\alpha\,\Delta T$$

where:		
	E	modulus of deformation (MPa)
	α	thermal expansion (°C^{-1})
	ΔT	temperature variation (°C)

The thermal expansion of the Callovo-Oxfordian argillites is equal to 10^{-5}°C^{-1}, the modulus of deformation is 4,500 MPa. A rise in temperature of 20 °C thus creates a thermo-mechanical stress in the order of 1 MPa.

In non-saturated state

The rise in temperature has an antagonistic effect on the effect of desaturation, namely activating the argillite creep (Inset 8.3). Little is currently understood on the combination of these opposing effects, but for limited rises in temperature the effects of desaturation should remain dominant, namely slowing down the creep.

A rise in temperature also cause thermo-mechanical stresses to develop in the argillites with the expansion of the argillites and the interstitial water.

8.3.2 Shafts, B waste disposal cells and drifts not subjected to a rise in temperature

Shafts, B waste disposal cells and sections of drifts away from the repository zones for C waste and spent fuel experience little or no rise in temperature during their operation. Their mechanical evolution is driven by the effects of desaturation on the geological formations, namely (i) slowing down of creep in the clay formations (argillites and Kimmeridgian marls), that limits the loading on ground supports/liners, and (ii) hydric fissuring at the wall of the engineered structures.

8.3.2.1 Loading on ground support/liner

The convergence of the argillites caused by modifying the stress state linked to excavation continues during the operation phase. Nevertheless, given the reduction in the argillite creep rate over time and through desaturation of the argillites (Inset 8.3), the loading on the ground support/liner by the argillites remains limited for the hundred- to several hundred-year lifetime of the operation.

The pressure applied to the ground support/liner by the argillites, assessed with the creep rate of the saturated argillites, is around 4 MPa after 100 years (Figure 8.3.2, (Barnichon & Su, 2005a)). The increase in pressure beyond a century is less than 0.5 MPa per century, with this increase slowing down over time (see § 8.4.2). The slowing down (or halting) of the argillite creep with their desaturation limits slightly the pressure applied by the argillites: the effect of reducing the creep rate by 25 % corresponds to a loading on the ground support/liner of less than 0.5 MPa at 100 years, i.e. around 3.5 MPa.

The same applies to the Kimmeridgian marls crossed by the shafts. The convergence of the marls is limited by their desaturation, the more so as they are located between 100 and 120 m deep and are therefore subject to a low stress state. The calcareous Oxfordian also has a limited creep potential.

The concrete adopted for the engineered structure liners has a strength of 60 MPa (at 28 days, i.e. taking into account the effects of shrinkage through drying), which corresponds to a maximum, acceptable radial pressure in the order of 8 MPa. Thus, regardless of the geological formation being considered, the stresses in the ground support/liner resulting from the pressure applied by the rocks are largely less than the liner concrete strength (not or only slightly degraded at this stage), which guarantees mechanical stability of the engineered structure for a period of several hundred years (Barnichon & Su, 2005a ; Barnichon & Su, 2005c).

8.3.2.2 Hydric fissuring of the clays in the near-field

If any desaturation causes hydric fissuring in the clay formations (Kimmeridgian marls and Callovo-Oxfordian argillites) (Inset 8.4). In the fractured zone, where the degree of saturation is in the order of 30 %, the fissuring caused by the hydro-mechanical coupling affects the entire zone. In the microfissured zone, the degree of saturation increases rapidly the further away from the wall and only a thin layer of rock a few tens of centimeters thick is affected by hydric fissuring. Beyond that, the degree of saturation remains high enough not to cause hydric fissuring (Barnichon & Su, 2005a), (Figure 8.3.2). Observations *in situ*, particularly in the Tournemire tunnel, have shown that this fissuring develops radially at the walls of the engineered structures when the relative humidity in the air drops and that an increase in relative humidity in the air causes these fissures to close (Ramambasoa, 2001).

In addition, improved mechanical properties and the slowing down of creep in the argillites with the desaturation of the microfissured zone (Inset 8.3 and Inset 8.4) and the containment of argillites by the ground support/liner prevents the EDZ from developing further. As long as the engineered structure is in operating phase (one hundred to several hundred years), the extent of the EDZ hardly alters from the initial EDZ.

8.3.2.3 B waste disposal packages subjected only to their weight

The disposal packages are stacked in a B waste disposal cell and thus must bear the weight of the packages stacked on top of them. The disposal cell slab also has to bear the weight of the stacked disposal packages. During the ventilated period, the chemical degradation of the ground support/liner concretes and the disposal packages is slight if not non-existent, and they retain their mechanical properties (see § 7.2). Additional loads linked to disposal packages therefore have no effect on the mechanical stability of the disposal packages, their stacking and the disposal cell (particularly the slab).

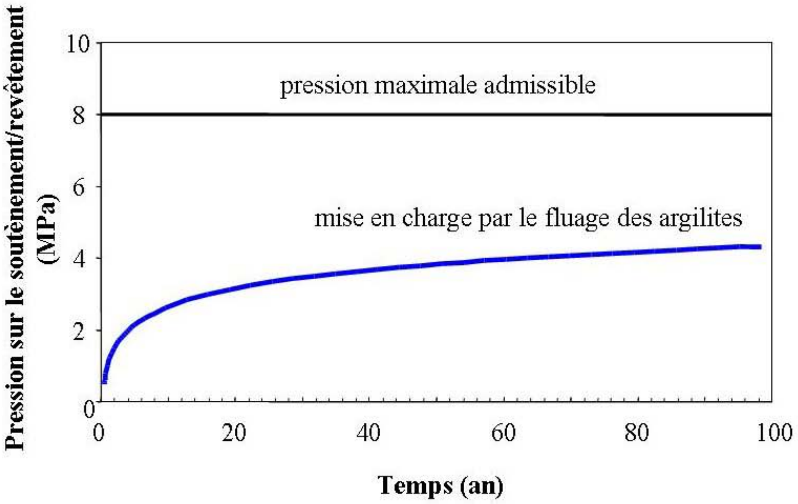

a) Mise en charge du soutènement/revêtement par le fluage des argilites

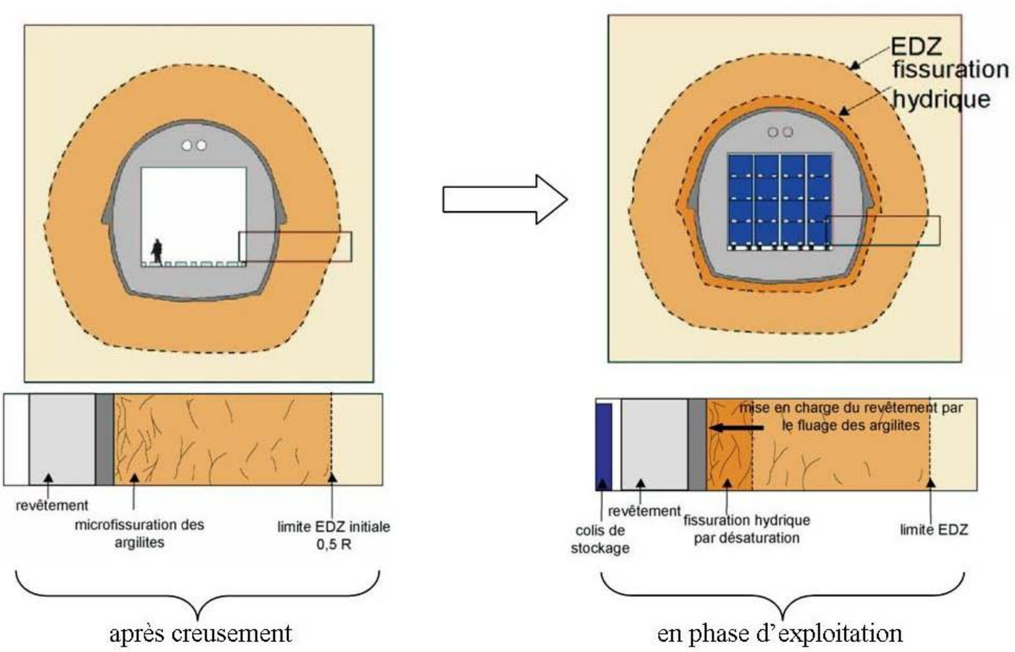

b) Schémas de l'évolution de l'EDZ autour d'une alvéole de déchets B au cours de la phase d'exploitation

Figure 8.3.2 *Loading on the ground support/liner from argillite creep and the evolution of the EDZ around a B waste disposal cell during the operating phase*

8.3.3 Drifts subjected to a rise in temperature

The access drifts to the C waste and spent fuel disposal cells are subjected to the effects of desaturation and thermal effects. The rise in temperature during the hundred-year period of the operation does not exceed 30 °C (see § 5.4). It causes thermo-mechanical stresses in the argillites and in the ground support/liner concrete.

8.3.3.1 Thermo-mechanical loading of the argillites in the near-field

In the argillites, such a rise in temperature creates thermo-mechanical compression constraints of less than 2 MPa. These constraint levels cause no perceptible damage in the argillites surrounding the engineered structures. As for the engineered structures not subjected to a rise in temperature, a thin layer of hydric fissuring a few tens of centimeters thick is formed around the engineered structures, without extending the EDZ further (Barnichon & Su, 2005a ; Barnichon & Su, 2005b).

8.3.3.2 Thermo-mechanical loading on the ground support/liner

The thermo-mechanical loading on the ground support/liner increases gradually with the rise in temperature, reaching a maximum value in the order of 1.5 MPa at around 100 years. This load is added to the pressure applied by the argillites. During the operating phase, the sum of the thermal load and the pressure applied by the argillites remains largely below the maximum acceptable load from the liner concrete that is not chemically degraded. The ground support/liner plays its containment role and guarantees the stability of the engineered structure.

8.4 Mechanical evolution of B waste disposal cells and drifts in post-closure phase

8.4.1 Closure of B waste disposal cells and drifts

Closing a B waste disposal cell or backfilling a drift does not cause specific, direct mechanical load. It corresponds to a move to different hydraulic conditions than during the ventilated phase, namely halting desaturation and the start of resatuation of the closed engineered structure.

The seal engineered structure for a B waste disposal cell is in principle identical as for a drift. It is installed in the disposal cell access drift. § 8.6 describes the mechanical evolution of a B waste disposal cell seal. Only the useful part of the B waste disposal cell is dealt with here.

8.4.1.1 Closure materials

At the hydraulic head of the B waste cell, a radiological protection screen made up of a double row of concrete blocks is installed upstream of the disposal packages. The rest of the disposal cell hydraulic head is backfilled with mass-poured concrete.

The basic material planned for use as drift backfill is the excavated argillites stored in the surface tip throughout the repository operation. It is ground and mixed, then put in place by being compacted at the Proctor optimum in successive, sloping layers so as to fill the entire volume and leave no installation clearances between the backfill and the upper part of the drift. This operation has been tested in the Aspö laboratory in Sweden (SKB, 2001), and should produce a backfill with an installed dry density of 1.6 that fills the drift volume completely. The backfill has no mechanical role when being installed. The argillites are contained by the ground support/liner.

8.4.1.2 Thermal, hydraulic and chemical contexts after closure

As indicated in § 6, the closure of a ventilated engineered structure triggers the gradual resaturation of the engineered structure components and the argillites at its periphery. The B waste disposal cells and backfilled drifts are only saturated (S > 90 %) after 100,000 years given the initial desaturation, then the production and transfer of hydrogen from corrosion after the engineered structures are closed. The resaturation of the argillites is not at first affected by the production of hydrogen. In the microfissured zone around the engineered structure, degrees of saturation higher than 97 % are achieved from the first thousand years. Beyond that, the hydrogen pressure produced by corrosion prevents 100 % saturation of a thin layer of EDZ around the engineered structure, but does not cause additional desaturation.

The hydrogen pressure increases until it reaches a maximum of 7 MPa in the B waste disposal cells at around 500 years, 6-7 MPa in the C waste repository zones at around 2,000-3,000 years and 9 MPa in the spent fuel zones also at around 2,000-3,000 years (see § 6).

The description of the thermal load of § 5 specifies that the temperature increases within and around an exothermic B waste disposal cell once ventilation is halted. The maximum temperature is achieved in the first years after closure, then thermal decay is initiated. The temperature in the argillites at the periphery of the disposal cell reaches approximately 45-50 °C about 20 years after closure and drops below 30 °C beyond 2,000 years. In an access drift to disposal cells containing C waste or spent fuel, the temperature continues to rise slightly for several decades (to around 55 °C), then drops gradually. It is below 40 °C after around 1,000 years (§ 5.4).

The saturation of the components in an engineered structure also triggers its chemical degradation (ground support/liner concretes, B waste disposal packages, etc.). § 7.3 underlines that the slow water flows limit strongly the chemical degradation of the ground support/liner concretes and the disposal packages through the water from the argillites extending for several hundreds of thousands of years. In particular, for at least several hundred to several thousand years, the ground support/liner is barely degraded chemically and retains its initial mechanical properties. Nevertheless, although the disposal packages remain in a stable cement-based material, the corrosion of the steel fibres in the disposal package concrete reduces the tensile strength of the concrete significantly in a few thousand years. In addition, the expansive corrosion products of the primary packages (particularly the B1 and B5 metallic reference packages), having initially plugged the handling clearances between the concrete jacket and the primary package housing, apply additional stresses within the disposal packages, thus contributing to the degradation of the global mechanical properties of the disposal packages.

In addition, the mechanical properties of the argillites around an engineered structure and the backfill in a drift are hardly affected by the alkaline disturbance from resaturation (see § 7.3). Moreover, the dissolution and precipitation of the alkaline disturbance contribute to a "hydraulic healing" of the fissures in the EDZ.

As regards the thermal, hydraulic and chemical contexts summarised above (Figure 8.3.1), the mechanical evolution of these engineered structures can be described based on two major, successive stages.

- A first stage relating to the resaturation of the argillites at the wall of the engineered structure. It causes (i) the reactivation of the argillite creep and swelling, accompanied by the commencement of the sealing of the EDZ fissures and (ii) the continuation of the loading on the ground support/liner until it reaches its breaking strength.
- As soon as the breaking strength of the ground support/liner is reached, the entire engineered structure is loaded by the argillites. The mechanical evolution is then mainly governed by the

deferred evolution of the argillites with the chemical degradation of the concretes (ground support/liner, disposal packages).

8.4.2 Loading of ground support/liner and commencement of EDZ healing

8.4.2.1 Ground support/liner

The argillites swell as they resaturate (Inset 8.4) applying a swelling pressure to the ground support. This pressure is assessed at 1-3 MPa (Andra, 2005h, chapitre 25).

In addition, the argillites achieve sufficiently high degrees of saturation to reactivate the creep from the first tens to a hundred years after closure of the engineered structure. This creep, possibly accelerated by the rise in temperature in certain sections of the engineered structures, reduces the deviator stress in the argillites and increases the radial stress which is applied to the ground support/liner concrete and the EDZ fissures.

The argillite creep and swelling thus increase the loading on the ground support/liner, resulting in an increase in stresses in the liner until the concrete strength is reached after several thousand to 10,000 years, whereas its mechanical properties are not reduced by chemical degradation (Barnichon & Su, 2005a). In the exothermic B waste disposal cells and the access drifts to the C waste or spent fuel disposal cells, the thermo-mechanical expansion stresses also contribute to loading on the ground support/liner. Whereas the extrados of the ground support/liner is subjected to high compression stresses (in the order of 45 MPa), tensile stresses appear at the intrados. This may result in tensile fissures appearing at the intrados of the ground support/liner concrete. The concrete retains residual strength, nevertheless, that prevents generalised rupture of the ground support/liner and remains sufficient to contain the argillites at their periphery.

Thus, at the heart of the engineered structures, the B waste disposal packages or the drift backfill is not loaded by the argillites at the timescale of around 10,000 years.

8.4.2.2 Callovo-Oxfordian argillites

As indicated above, the ground support/liner of the engineered structures continues to contain the argillites mechanically, thus preventing all free deformation.

The swelling pressure applied to the ground support/liner is also transmitted to the EDZ fissures, mainly oriented parallel to the engineered structures. They open less and therefore the permeability of the argillites in this zone is reduced. The "EH" experiments at Mont Terri on the evolution of permeability in the EDZ with resaturation show that resaturation and swelling in the clays reduce the transmissivity of the fissures by 2 to 3 orders of magnitude after three years (Meier *et al.*, 2000). Permeability measurements of water on fissured argillite samples confirm this evolution: the swelling of the argillites at a fracture can restore the permeability of the water in the undisturbed argillites after a few days (Barnichon & Su, 2005a).

As for the swelling pressure, the radial stress developed by the argillite creep, in the order of a few MPa after resaturation, is applied to the EDZ fissures and causes their compression with a reduction in permeability assessed at 2 orders of magnitude (Buehler *et al.*, 2003). As the stresses induced by the argillite creep are stronger than those caused by swelling, the reduction in permeability in the EDZ argillites is greater under the effect of the creep than the swelling. The permeability of the EDZ is thus reduced with the recompression of the fissures by one or several orders of magnitude, tending towards the permeability of the undisturbed argillites (Figure 8.4.1).

8.4.2.3 Disposal packages in the B waste cell

If there is no rupture of the ground support/liner, the stack of disposal packages within the disposal cell is not subjected to stresses other than from the specific weight of the packages and remains stable. In addition, deformations from expansion caused by the rise in temperature in a disposal cell initially containing exothermic waste, then from contraction through cooling, are absorbed by the functional clearances between the primary packages and the container and do not create thermo-mechanical stresses within these materials(Barnichon & Su, 2005a).

8.4.2.4 Drift backfill

At the scale of the first thousands of years, when full resaturation of the backfill is prevented by the production of hydrogen from corrosion, the backfill is likely to compact under its own weight and create a void in the key stone. As the argillites are always contained by the ground support/liner, the backfill is not subjected to loading from the argillites.

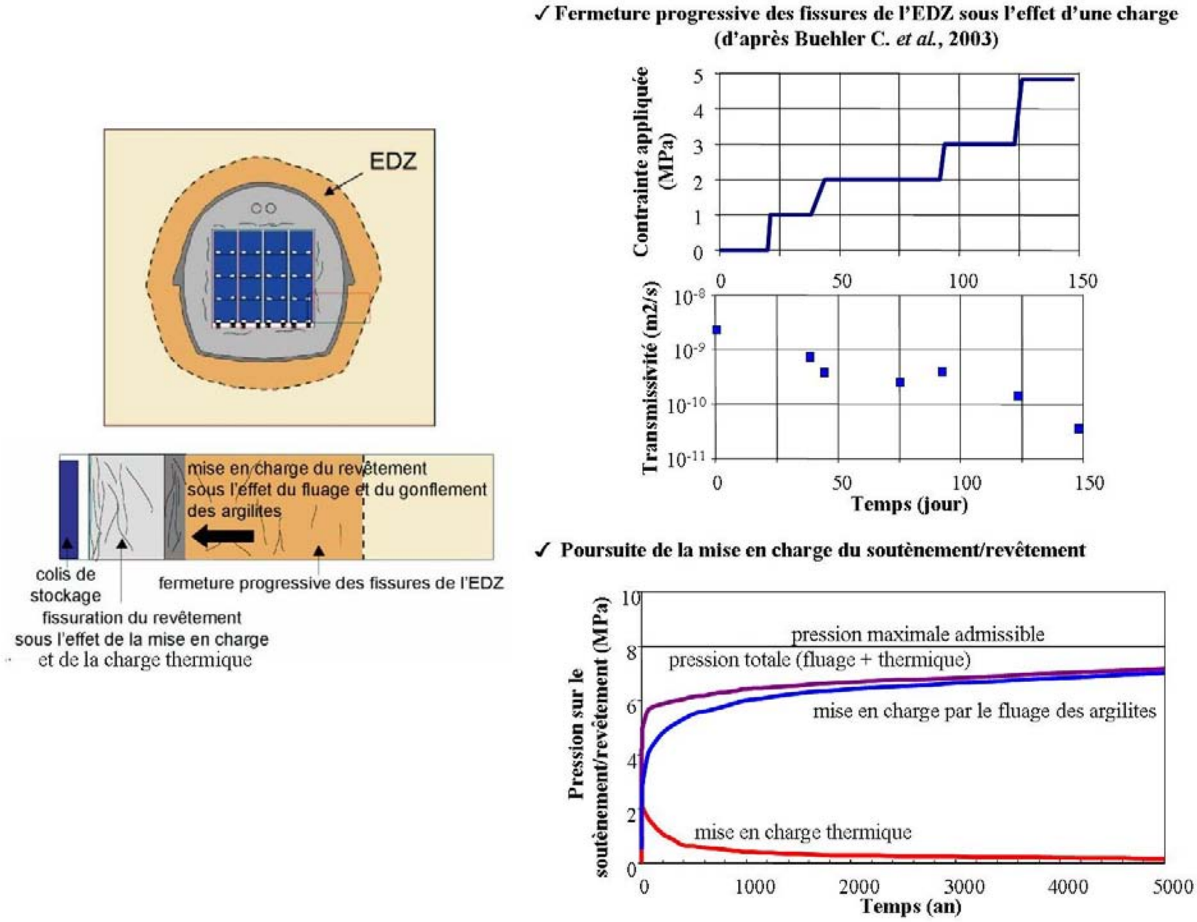

Figure 8.4.1 *Loading on ground support/liner and evolution of EDZ around an exothermic B waste disposal cell during hte first thousands of years after closure*

8.4.3 Mechanical evolution with the gradual chemico-mechanical degradation of the engineered structure components

Beyond the appearance of the first damage at the ground support/liner intrados a few thousand to 10,000 years after closure, the ground support/liner continues to be loaded by the argillites, but with a decreasing argillite creep rate. The mechanical properties of the ground support/liner are also reduced gradually with its chemical degradation.

Under the effect of the tensile stresses that are propagated from the intrados towards the liner centre and the compression stresses that increase and overtake the concrete strength over more than half of the liner thickness, the ground support/liner is damaged mechanically. Through fissures are produced from the intrados to the periphery and the behaviour of the ground support/liner can then be compared with a "drywall" engineered structure: the fitting of the concrete blocks and the dampening of loads by distortion between blocks give the ground support/liner a residual strength through friction. The load from the argillites emphasises this "tightening" effect and prevents generalised rupture of the ground support/liner.

As the concrete degrades chemically and mechanically, the amplitude of the deformations of the argillites and movements of the ground support/liner is dictated by the number of voids in the engineered structures. This is no more than a few percent, be it in the B waste disposal cells or the backfilled drifts. Mechanical forces from the argillite creep that are transmitted to the degraded ground support/liner produce convergence of the ground support/liner with the mobilisation of the voids (voids between the disposal packages for the B waste cell, voids in the key stone as the backfill settles in the drift). The resulting discharge of containment of the argillites is insignificant and causes no additional disturbances in the argillites.

In the *B waste cell*, the disposal packages are then gradually loaded mechanically by the argillites through the ground support/liner. At the same time, the corrosion of the steel fibres in the B waste disposal packages and the primary packages causes a reduction in strength of the disposal packages. In a few thousand years, the tensile strength of the fibre-reinforced concrete is reduced by around 25 % (see § 7.4.2.5). Loading on the disposal packages causes fissuring at the base of the packages and gradual compacting of the package stack with a new concentration of voids, mainly in the disposal cell key stone. As previously, the result is a further discharge of containment by the argillites that, based on the number of voids activated, may be accompanied by further damage to the argillites. In the least favourable case (significant number of internal voids in the disposal packages and sudden activation of these voids), the greatest damage thus produced is similar to the damage created during disposal cell excavation (a microfissured zone with an extent 0.5 times the radius of the engineered structure).

The mechanical evolution in the *drift* is similar to the B waste cell. The drift backfill is gradually resaturated with the reduction, then halt in the production of hydrogen from corrosion (a degree of saturation higher than 90 % is achieved beyond 100,000 years), and is accompanied by slight swelling. The swelling pressure is estimated at 0.1 MPa. Like the argillites, the backfill in contact with the ground support/liner concretes is also affected by an alkaline disturbance. The extent of the highly-remineralised zone of several tens of centimeters (see § 7.6.3), is slight compared with the diameter of the backfill. The mechanical properties of the backfill are scarcely affected. The rigidity of the backfill (initial modulus of deformation of 10 MPa) is enough to limit, then stabilise, the deformations of the argillites. As the alkaline disturbance extends in the backfill, the rigidity of the disturbed backfill zone is slightly reduced and allows slight deformation. However, with respect to the extent of the disturbed zone compared with the diameter of the drift, the maximum possible deformation of the disturbed backfill has a lower percentage (Andra, 2005l). The whole assembly, therefore, (argillites/concrete undergoing degradation/locally disturbed backfill) gradually becomes stable over time based on the reduced creep rate. The slow deformations caused by argillite creep "tighten" the drift with the loading on the backfill and its rigidification.

Limited, localised re-adjustments inside the engineered structure (local rupture, expansion, voids filled by creep) continue over a hundred to several hundreds of thousands of years until gradually reaching equilibrium. The deformations within the engineered structure become insignificant and are accompanied by a reduction in the stress deviator and in deformations (slowing down of creep) and an increase in the average stress. The EDZ fissures are closed gradually under the effect of all these mechanisms. Equilibrium is reached when the stress deviator induced by the construction and reactivated by the degradation of the engineered structure components is cancelled and the initial state of the lithostatic stresses in the geological medium is re-established.

The load from the geological medium on all the engineered structure components helps increase their rigidity and density. The engineered structure is gradually integrated mechanically with the geological medium. Having reached equilibrium, the creep of the argillites, and to a lesser extent the precipitation and dissolution of the alkaline disturbance, produce a virtually total recompression of the EDZ fissures.

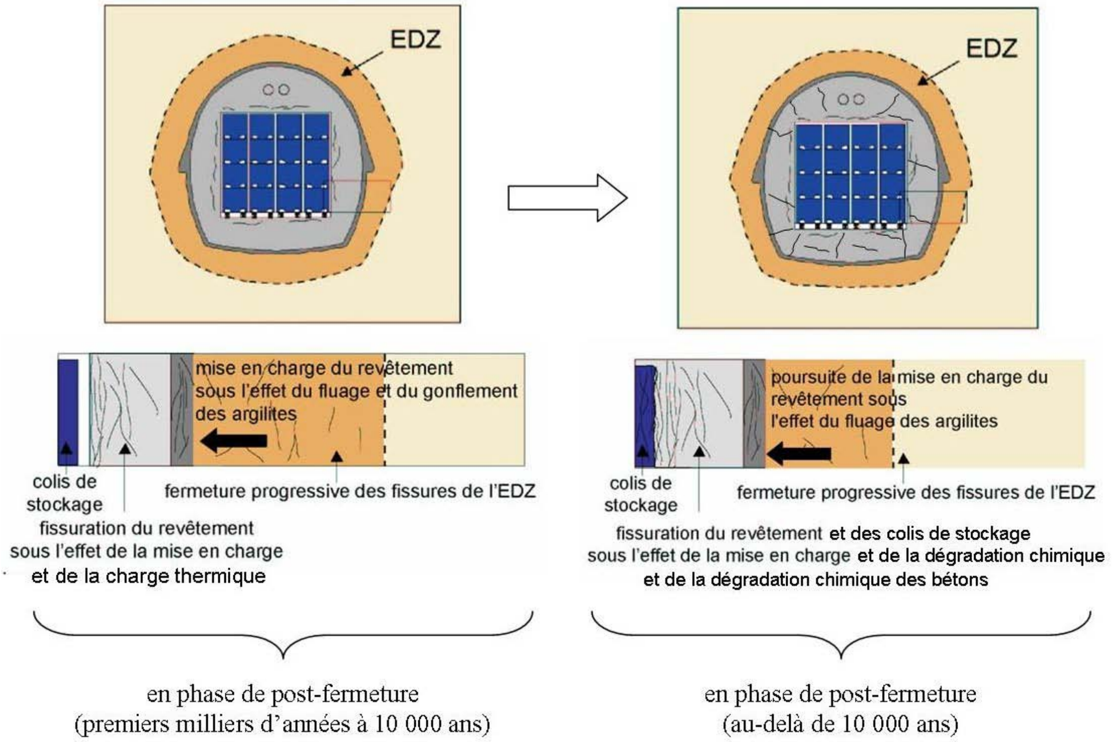

Figure 8.4.2 *Evolution of the EDZ around a B waste disposal cell with the chemical degradation of the concretes (beyond 10,000 years)*

8.5 Mechanical evolution of C waste disposal cells and spent fuel disposal cells

The C waste and spent fuel disposal cells are not ventilated after emplacement of the disposal packages. The disposal cells start to resaturate once the leak tight cover is installed shortly after emplacing the packages. Under these conditions, it may be assumed that the operating period for these unventilated engineered structures is only very slightly different in terms of mechanical evolution from the post-closure phase, which actually starts after the installation of the swelling clay disposal cell plug.

8.5.1 Mechanical behaviour of the useful part and the disposal cell hydraulic head

The disposal cell design comprises two distinct sections - the "useful part" and the disposal cell hydraulic head - given the nature of their components, their dimensions and their thermal, hydraulic and chemical evolutions. The mechanical evolution of the disposal cells can therefore be described as two distinct components relating to each section. Apart from the mechanical effects indirectly linked to the heat released by the packages and the transfer of the hydrogen produced from corrosion in the useful part, there is little mechanical influence between the two disposal cell sections and their evolution may be viewed as virtually independent.

- The useful part is characterised by the presence of metallic components (liner, lining, over-pack) and clay materials in the widest sense (argillites and swelling clay in the engineered barrier for the spent fuel disposal cells). The argillite creep, the swelling of the swelling clay with resaturation, the discharge of mechanical properties of the metallic components with corrosion and the generation of expansive corrosion products are the main elements in its mechanical evolution.
- The disposal cell hydraulic head is characterised by the presence of clay materials (argillites and the swelling clay of the plug) and the concrete support base. The argillite creep, the swelling of the swelling clay with resaturation and the chemical degradation of the concrete are the main elements in its mechanical evolution.

8.5.2 Thermal, hydraulic and chemical contexts

Chapters 5, 6 and 7 highlight the major processes in the thermal, hydraulic and chemical evolution of the C waste and spent fuel disposal cells (Figure 8.5.1 and Figure 8.5.2).

- The temperature field linked to the thermal load is rapidly uniform in the disposal cell and in the near-field (from a few hundred to a thousand years). Maximum temperatures (≤ 90 °C) are reached before the disposal cell is completely resaturated. Thermal decay is initiated during the saturation phase of the engineered barrier and the swelling clay plug.
- The hydraulic evolution is marked by the production of hydrogen from corrosion. This production does not delay the saturation of the disposal cell plug and the engineered barrier (of the spent fuel disposal cells) up to degrees of saturation in the order of 97 % (achieved in around ten years for the C waste disposal cell plug and around a hundred years for the plug and engineered barrier of a spent fuel cell). The totally saturated state of the plug and engineered barrier (of the spent fuel cell) ($S = 100$ %) is only achieved after around 100,000 years when hydrogen production is halted.
- Hydrogen pressure increases in the disposal cell up to 6-7 MPa in the C waste disposal cells and 9 MPa in the spent fuel disposal cells due to a higher production term towards 2,000-3,000 years (see § 6.3).
- The argillites and the swelling clay of the plug and engineered barrier do not undergo significant mineralogical transformations. In particular, interactions with the iron in the metallic components remain localised at the interfaces. The swelling clay plug undergoes an alkaline disturbance via the concrete support base: the extent of the highly-remineralised zone by the cement waters is low compared with the length of the plug. Beyond the remineralised zone, a basic pH front extends

more deeply into the plug, but does not reach the useful part of the cell. Overall, therefore, the disposal cell plug and engineered barrier retain their mechanical properties over time, particularly their swelling properties.
- The metallic components corrode gradually over a timescale of several tens of thousands of years. As will be seen later in the chapter, the result is the gradual discharge of strength in the lining and liner, then in the over-packs.

8.5.3 Organisation over time of the mechanical evolution of the disposal cells

8.5.3.1 Useful part of the cell

The linings of the C waste and spent fuel disposal cells guarantee the stability of the disposal cell by taking over the load from the geological medium (coupled or otherwise with the swelling pressure of the engineered barried of the spent fuel disposal cells) at least during the repository operating and reversibility phase lasting several hundred years. Their thickness is designed to take corrosion into account at this timescale.

Similarly, to maintain the leak tightness of the C waste package overpacks and the spent fuel containers for thousands and tens of thousands of years respectively, their thickness is designed to take into account a back-up corrosion thickness added to the thickness necessary to hold the lithostatic stresses of the geological medium.

The mechanical evolution of the useful part is therefore linked to corrosion: it is to be expected that this will reach a certain thickness of the lining, liner and containers, thus affecting their mechanical strength and causing deformation and rupture.

8.5.3.2 Disposal cell hydraulic head

The concrete support base degrades chemically over several hundreds of thousands of years, therefore well after saturation of the swelling clay plug and the mechanical equilibrium of the plug and the argillites.

Several phases stand out in the mechanical evolution of the cell:

- for the useful part:
    - the phase before the discharge of mechanical strength by the lining and the liner and, for the spent fuel disposal cells, the saturation of the engineered barrier,
    - the phase after the rupture of the lining and the liner and before the discharge of container strength,
    - the phase after rupture of the containers;
- for the disposal cell plug:
    - the saturation phase of the swelling clay plug,
    - the post-saturation phase and during the evolution of the mechanical properties of the support base caused by its chemical degradation.

The presentation of the mechanical evolution of the disposal cells is structured following an almost chronological logic, by separating the useful part and the disposal cell hydraulic head:

- thermo-mechanical loading once the packages are in place and the disposal cell plug is installed,
- the various phases described above.

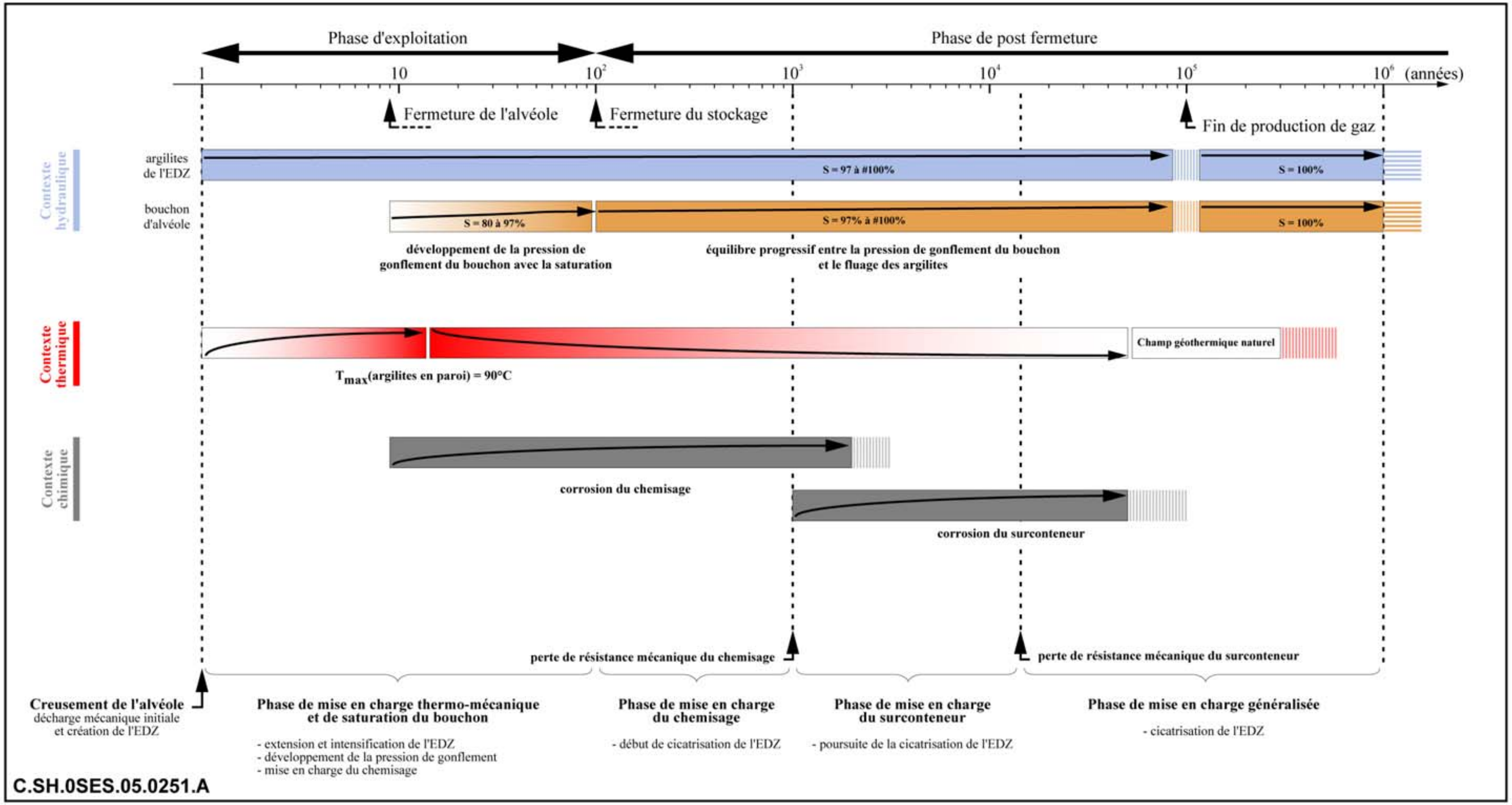

Figure 8.5.1 *Time chart of the mechanical evolution of a C waste cell: thermal, hydraulic and chemical contexts during construction, operating and post-closure phases (based on a conventional hundred-year time chart of the construction/operation/closure of a repository)*

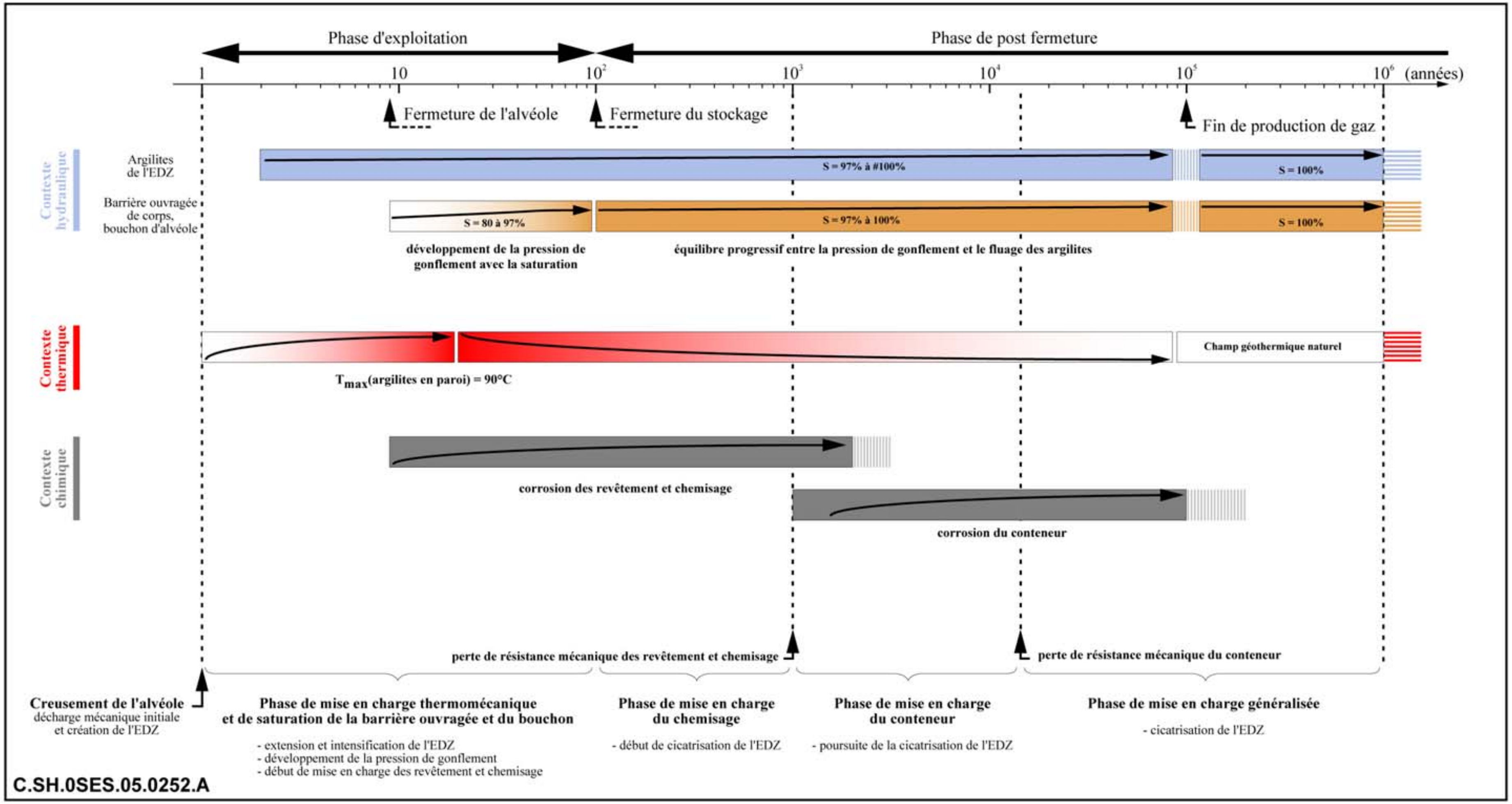

Figure 8.5.2 *Time chart of the mechanical evolution of a spent fuel cell: thermal, hydraulic and chemical contexts during construction, operating and post-closure phases (based on a conventional hundred-year time chart of the construction/operation/closure of a repository)*

8.5.4 Thermo-mechanical loading from emplacing the packages and installing the disposal cell plug

Emplacing the packages in the disposal cell causes heating inside the disposal cell and at its periphery. The temperature of the argillites (for C waste disposal cells) or the engineered barrier (for spent fuel disposal cells) at the disposal cell periphery increases up to 90 °C in the first tens of of years and remains in the order of 80 to 50° during the operating phase (Figure 8.5.1 and Figure 8.5.2). The rise in temperature causes the convergence of the argillites to accelerate and thermo-mechanical stresses to develop within the argillites. When the temperature increases, the differential thermal expansion between the solid matrix and the interstitial water in the argillites causes pore overpressure. This overpressure is at its maximum in a C waste disposal cell from the disposal cell wall over several meters, then decreases gradually. It reaches its maximum of 4 MPa in around ten years. The maximum thermal overpressure for a spent fuel disposal cell is not at the disposal cell wall but a few meters away. Its achieves the identical maximum of 4 MPa as reached on the wall of the C waste disposal cell (Su & Barnichon, 2005).

8.5.4.1 Convergence of argillites

The convergence of the argillites around a C waste or spent fuel cell, initiated when the disposal cell is created (see § 8.2.4), is highlighted by the rise in temperature following package emplacement. It contributes to the gradual reduction in functional clearances between the lining (C waste cell) or the liner (spent fuel cell) and the argillites at the disposal cell wall. After a few years, 50 to 60 % of the initial clearances are closed, with the total convergence of the argillites reaching 1.7 to 2.1 % (of the excavation radius) (Su & Barnichon, 2005).

The argillite creep rate is stabilised when thermal paroxysm is reached. After above 100 to 150 years, the clearances between the argillites and the lining (C waste cell) or between the argillites and the liner (spent fuel cell) are filled and the accumulated convergence of the argillites reaches 2.8 to 3.3 % (Figure 8.5.3). These assessments are based on the maximum values of the functional clearances (1 to 2 cm) normally recommended in mining engineering. The annulus space between the argillites and the lining (for the C waste cell) or between the argillites and the liner (for the spent fuel cell) could be reduced according to conditions observed *in situ*, thus limiting the extent of the EDZ around the cell.

8.5.4.2 Thermo-mechanical coupling and evolution of the EDZ in the useful part

The creep and thermal expansion mechanisms create deformations within the argillites that cause an escalation and propagation of the EDZ around the disposal cells (Figure 8.5.3).

- The EDZ increases and becomes slightly anisotropic under the thermo-mechanical interactions between neighbouring disposal cells: at the disposal cell top and wall, a fractured zone (extending less than 0.1 times beyond the disposal cell radius) develops and the extent of the microfissured zone increases slightly.
- The EDZ mainly evolves under the effect of deferred deformations relating to the argillte creep and the rise in temperature. In the hypothesis of maximum clearances, the deformations in the argillites reach 1.5 % a few years after emplacement of the disposal packages and culminate at 2.8 % at the abutments and 3.3 % at the disposal cell top and wall after around 100 to 150 years with closure of the clearances. These deformations are higher than the damage threshold (0.5 % in compression) and the rupture threshold of the argillites (1.5 % in compression - (Andra, 2005h, chapitre 25) -Inset 8.2).

Combining these processes in a disposal cell 500 m deep creates a fractured zone with a maximum extent equal to around 0.4 times the radius of the disposal cell (about 15 cm for a C waste cell). The microfissured zone also progresses until it reaches a maximum extent of around 1.4 times the radius of the disposal cell (about 50 cm for a C waste cell). The extents of the fractured and microfissured zones are greater at the top and wall of the disposal cell and at their minimum at the abutments due to the thermal interactions between the neighbouring disposal cells (Su & Barnichon, 2005), (Figure 8.5.5).

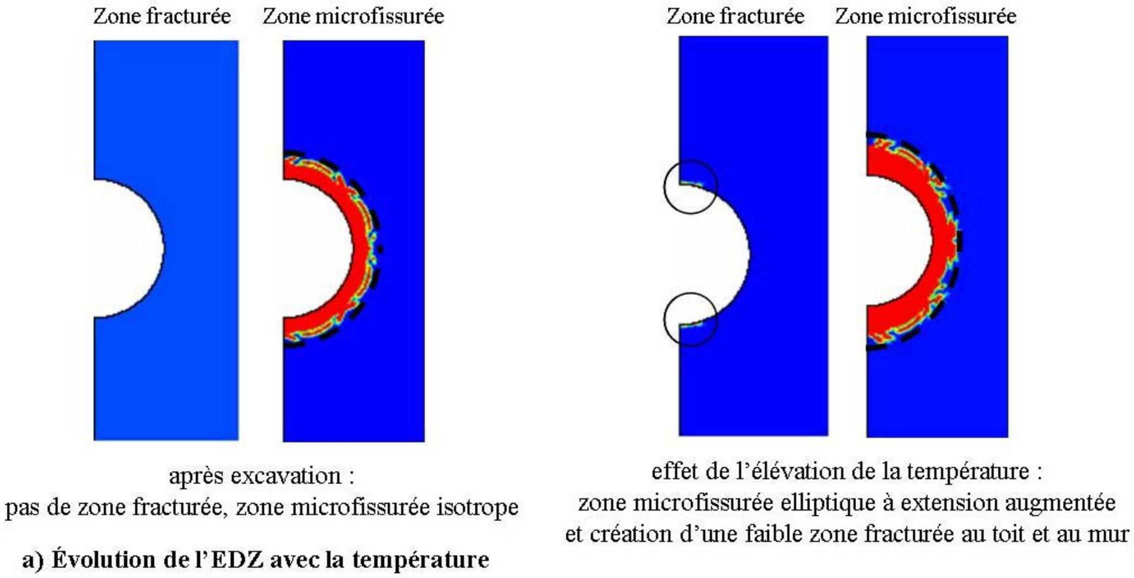

a) Évolution de l'EDZ avec la température

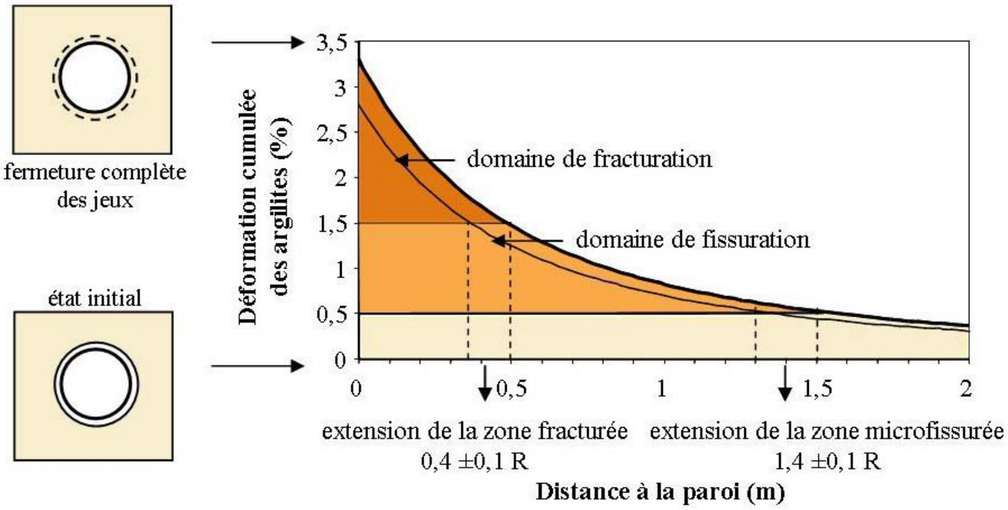

b) Évolution de l'EDZ avec la convergence

Figure 8.5.3 *Evolution of the EDZ under the effect of the rise in temperature and the deferred convergence aorund a C waste disposal cell (hypothesis of maximum clearances)*

8.5.4.3 Installation of the disposal cell plug and evolution of the EDZ directly above the plug

In the *spent fuel cell*, the removal of the lining and the simultaneous installation of swelling clay plug then the concrete support base does not affect the mechanical behaviour of the argillites in the near-field more, as the liner is supported (Su & Barnichon, 2005). The EDZ evolves in identical fashion as the useful part (Figure 8.5.3).

The EDZ evolves directly above the *C waste disposal cell* plug depending on the time taken to install this plug compared with the time required to recover the functional clearances between the argillites and the lining. The rapid installation of the plug thus limits the convergence of the argillites and the evolution of the EDZ under the effect of (i) thermo-mechanical interactions between neighbouring disposal cells (i.e. the creation of a small fractured zone and a slight extension to the microfissured zone at the top and wall of the disposal cells) and (ii) deferred deformations of the argillites. The prior removal of the lining to install the swelling clay and concrete plugs does not cause a new instantaneous relaxation of the argillites in this section of the disposal cell and has no further impact on the EDZ. Once the lining is removed, the swelling clay plug and the concrete plug are in contact with the argillites, which prevents additional free deformations of the argillites.

8.5.5 Saturation of the swelling clay in the plug and the engineered barrier (around 100 years)

The resaturation of the swelling clay in the disposal cell plug and the engineered barrier (spent fuel cell) starts immediately upon installation and continues up to degrees of saturation in the order of 97 % over approximately one hundred years. It affects firstly the periphery, forming a thin layer of saturated swelling clay. Saturation then continues by an inward flow within the swelling clay; this closes the residual clearances (swelling clay/argillites for C waste disposal cell and swelling clay/liner for the spent fuel cell) and develops the swelling pressure (Figure 8.5.4).

At saturation, the swelling pressure, lower than 7 MPa through the choice of swelling clay[10] (Andra, 2005i), Inset 2.7, is applied radially to the argillites (at the C waste disposal cell plug) or the lining and liner (for the spent fuel cell) and axially on the metallic plug and the overall disposal cell closing system, which contain the swelling clay plug, as they are not degraded at this stage.

Directly above the *useful part of the cell*, the functional clearance between the disposal packages and the non-degraded lining being held, the C waste or spent fuel packages are only subjected to their own weight and thermal expansion. This does not create significant thermo-mechanical stresses given the functional clearances within the cell.

Directly above the *C waste disposal cell hydraulic head*, as soon as the swelling clay is saturated, it applies radial stress on the argillites, which slows down their convergence (reduction in sheer stress). This encourages the fissures in the EDZ to recompress more or less parallel to the wall and therefore reduces the permeability around the disposal cell hydraulic head (Malama & Kulatilake, 2003). The Selfrac experiments at Mont Terri, that place the drift walls under a few MPa pressure representative of a swelling pressure, has demonstrated the reduction in permeability of 2 orders of magnitude (Buehler *et al.*, 2003), (Figure 8.4.1). The concrete plug, also in direct contact with the rock, halts the convergence of the argillites. The argillites are therefore subjected to radial pressure which encourges the EDZ fissures to recompress (Figure 8.5.5), thus healing this EDZ and in particular the disappearance of the additional damage from the thermo-mechanical deformations.

---

[10] The choice of swelling clay is based on the specification of a swelling pressure that does not exceed 7 MPa (effective stress). This is the pressure in equilibrium with the radial geostatic stresses of the site at 500 m deep. A higher swelling pressure would place needless load on the argillites or the support bases for the plugs before returning to this level of 7 MPa. A lower pressure is even preferable from this point of view.

Directly above the *spent fuel disposal cell hydraulic head*, with the liner maintained, the argillites behave in identical fashion to the standard section apart from the lesser effects of temperature (Figure 8.5.5).

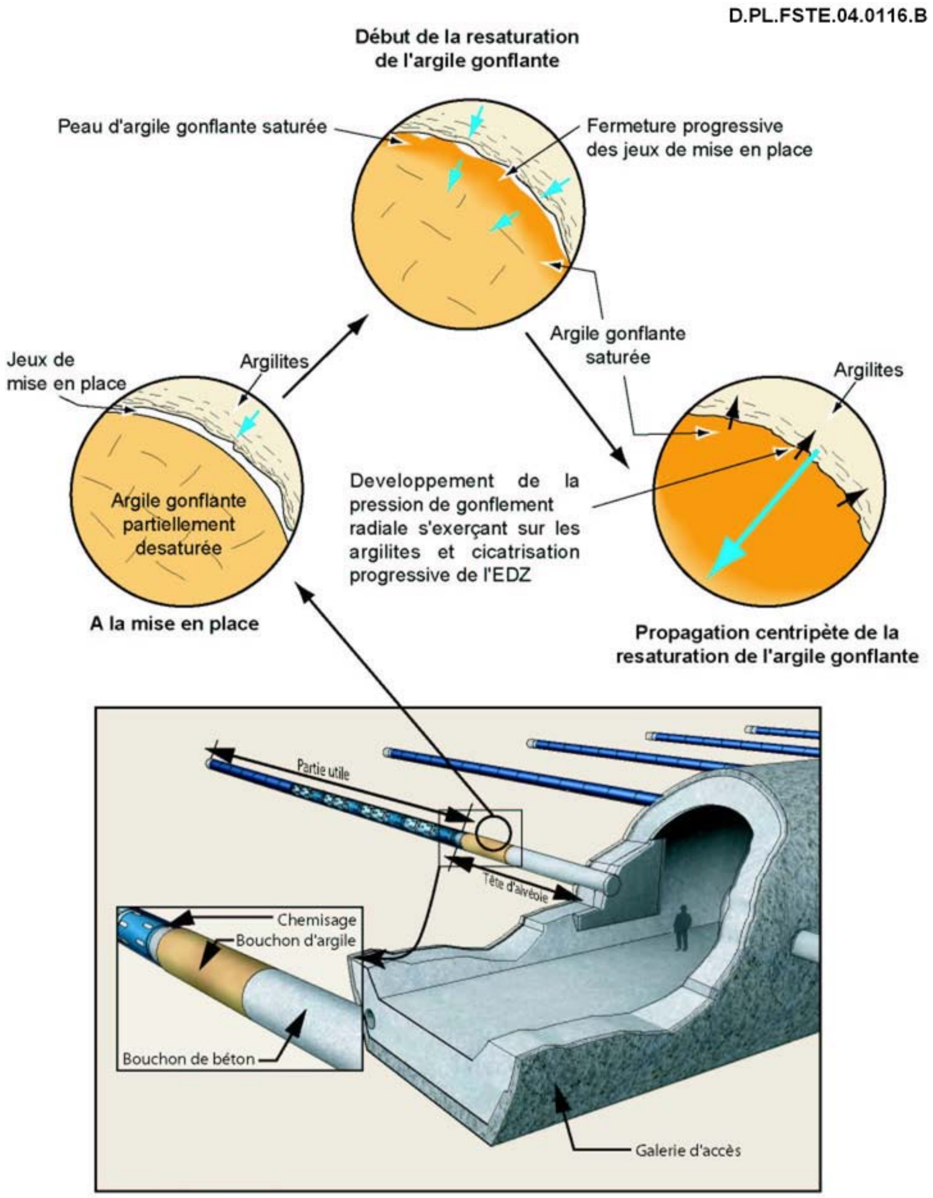

Figure 8.5.4 Resaturation process of the swelling clay - example of C waste disposal cell plug

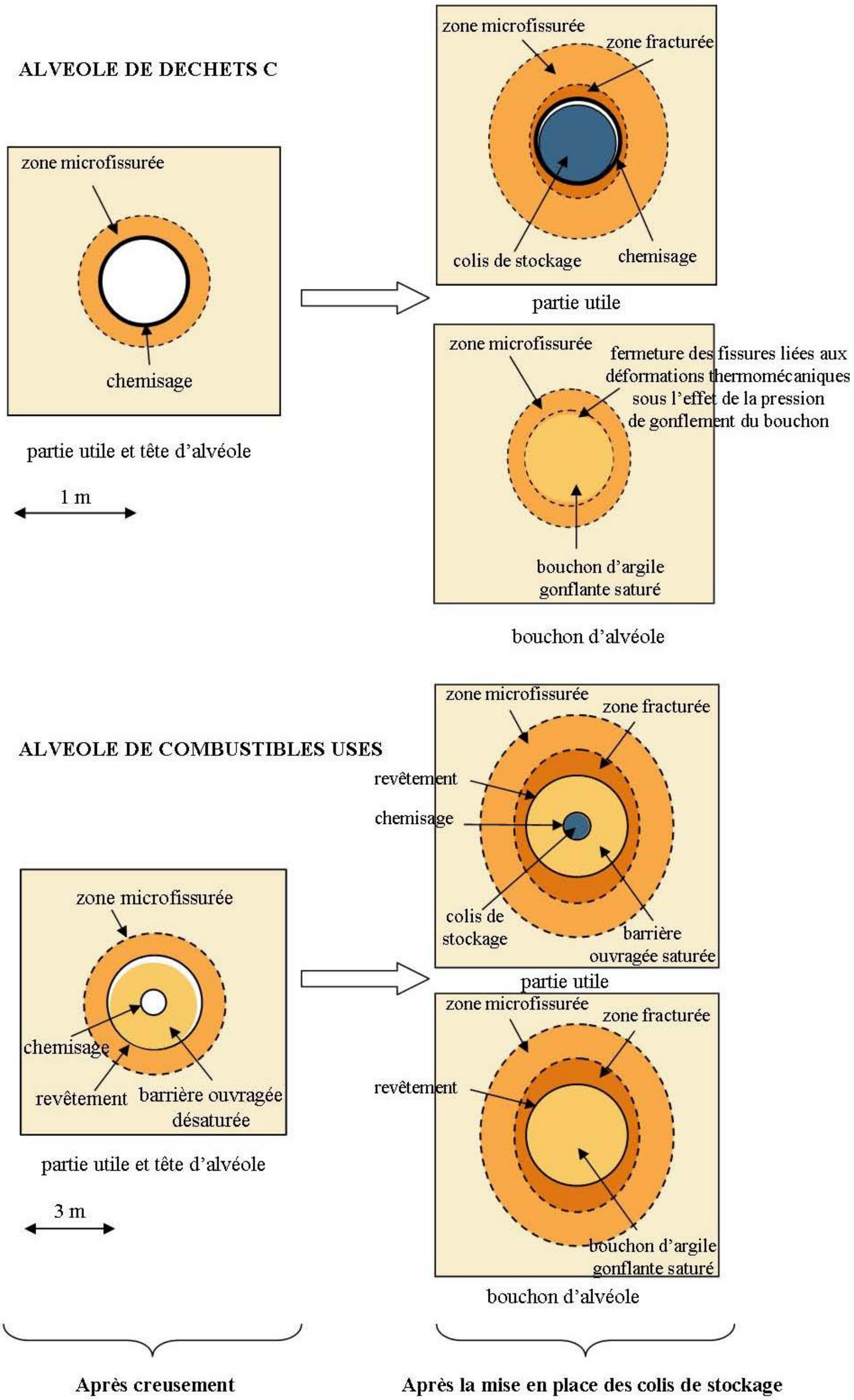

Figure 8.5.5 *Diagrams showing evolution of EDZ around a C waste disposal cell and a spent fuel disposal cell under thermo-mechanical coupling (timescale of 100 to 150 years)*

8.5.6 Mechanical evolution up to rupture of the lining and/or liner

8.5.6.1 Useful part

After closure of the residual clearances (lining/argillites in the C waste disposal cell and liner/argillites in the spent fuel cell), the lining and liner are loaded by the creep of the argillites, the swelling pressure of the engineered barrier (for the spent fuel cell) and the expansive corrosion products of the liner and lining. The radial pressure on the lining or liner increases gradually up to a pressure of 12 MPa, corresponding to the lithostatic stress at a depth of 500 m. This pressure is reached at about 1,000 years in the C waste disposal cell. In the spent fuel disposal cell with its perforated liner, the accumulation of swelling pressure of the swelling clay and the creep of the argillites accelerates the return to the state of initial stress. With an (effective) swelling pressure of 7 MPa, the pressure applied to the liner and on the lining is close to 12 MPa after a few hundred years.

In addition, the corrosion of the liner and the lining causes a gradual discharge in their tensile stress area. The assessment of the evolution of the loading by the argillites combined with the corrosion products and the evolution of the thickness of the liner and the lining is not yet accurately understood. However, given the design of the thickness of the lining and liner for a radial load of 12 MPa and a few millimeters of corrosion reserve, the liner and the lining is likely to rupture beyond 1,000 years (see § 7.3.1).

Before rupture of the liner or lining, under the combined effect of the radial stress from creep and the expansion of the corrosion products at the extrados of the liner or lining, the EDZ fissures, lying more or less parallel with the disposal cell walls, close up, thus containing the EDZ and limiting its extent and permeability (Malama & Kulatilake, 2003). In common with the results obtained at Mont Terri (Buehler *et al.*, 2003), the reduction in permeability is estimated at 2 to 3 orders of magnitude. The permeability of the fractured zone developed with the thermo-mechanical deformations during the first century (see § 8.5.4.2) evolves towards a similar permeability as in a microfissured zone (Figure 8.5.6).

For the *C waste cell*, the effect of the pressure linked to the corrosion products in the EDZ is likely to be reversed if this increases rapidly and exceeds the average initial stress prevailing in the argillites. Under this hypothesis, the pressure of the corrosion products produces fissuration by extension of the argillites at the disposal cell wall in the very long term. Nevertheless, given the slow progress of the corrosion, the creep by the argillites should be enough to counteract the effects of the corrosion products.

For the *spent fuel cell*, the argillite creep and the expansive corrosion products on the internal face of the liner and the external face of the lining result in the compacting of the saturated engineered barrier. Its swelling pressure increases until equilibrium is reached with the external stress state (an effective swelling pressure of 7 MPa for an equilibrium of 12 MPa). The deformations of the engineered barrier therefore prevent a deformation of the argillites up to rupture or damage (JNC, 2000). In addition, at the same time as the slow compacting of the engineered barrier, its porosity and therefore its permeability are reduced.

The lining (of the C waste disposal cell and the spent fuel cell) thus retains its mechanical properties for about 1,000 years, therefore preventing the water reaching the over-packs. Under these conditions, the disposal packages undergo no (or little) chemical degradation and retain their mechanical properties. Apart from the weight of the packages on the bottom section of the lining and possibly the load placed on the lining by the corrosion products, there is no mechanical interaction between the disposal packages and the other disposal cell components. Keeping the functional clearances in the lining and in the disposal packages limits the thermo-mechanical stresses at the heart of the cell.

8.5.6.2 Disposal cell hydraulic head

For the *C waste disposal cell hydraulic head*, the saturated swelling clay in the plug is compacted by the gradual load from the argillite creep. The swelling pressure of the swelling clay increases until reaching its maximum of 7 MPa and the deviator stress in the argillites decreases. Equilibrium between the swelling clay in the disposal cell plug and the argillites is established and prevents or limits gradually the convergence of the argillites. These processes contribute to the fissures created in the argillite closing at the swelling clay plug and the rapid return to a stress state in equilibruim (in the order of several hundred years) (Su & Barnichon, 2005). The permeability of the EDZ around the plug evolves gradually towards the permeability of the undisturbed argillites (Figure 8.5.6).

For the *spent fuel disposal cell hydraulic head*, as for the useful part, the swelling clay in the engineered barrier deforms under the effect of the argillite creep and the liner corrosion products. Permanent equilibrium is created. It prevents the EDZ developing further and encourages the EDZ fissures to close; this reduces the permeability of the argillites directly above the disposal cell hydraulic head (Figure 8.5.6).

The development of the swelling pressure in the clay plug also results in axial loading on the concrete support base, which retains its mechanical properties over several tens of thousands of years. This also guarantees the mechanical containment of the swelling clay plug during these periods.

The steel plug between the useful part and the disposal cell hydraulic head is degraded by corrosion similar to the other metallic components in the cell. As for the other disposal cell components, the swelling clay and the argillites take over the resultant deformations.

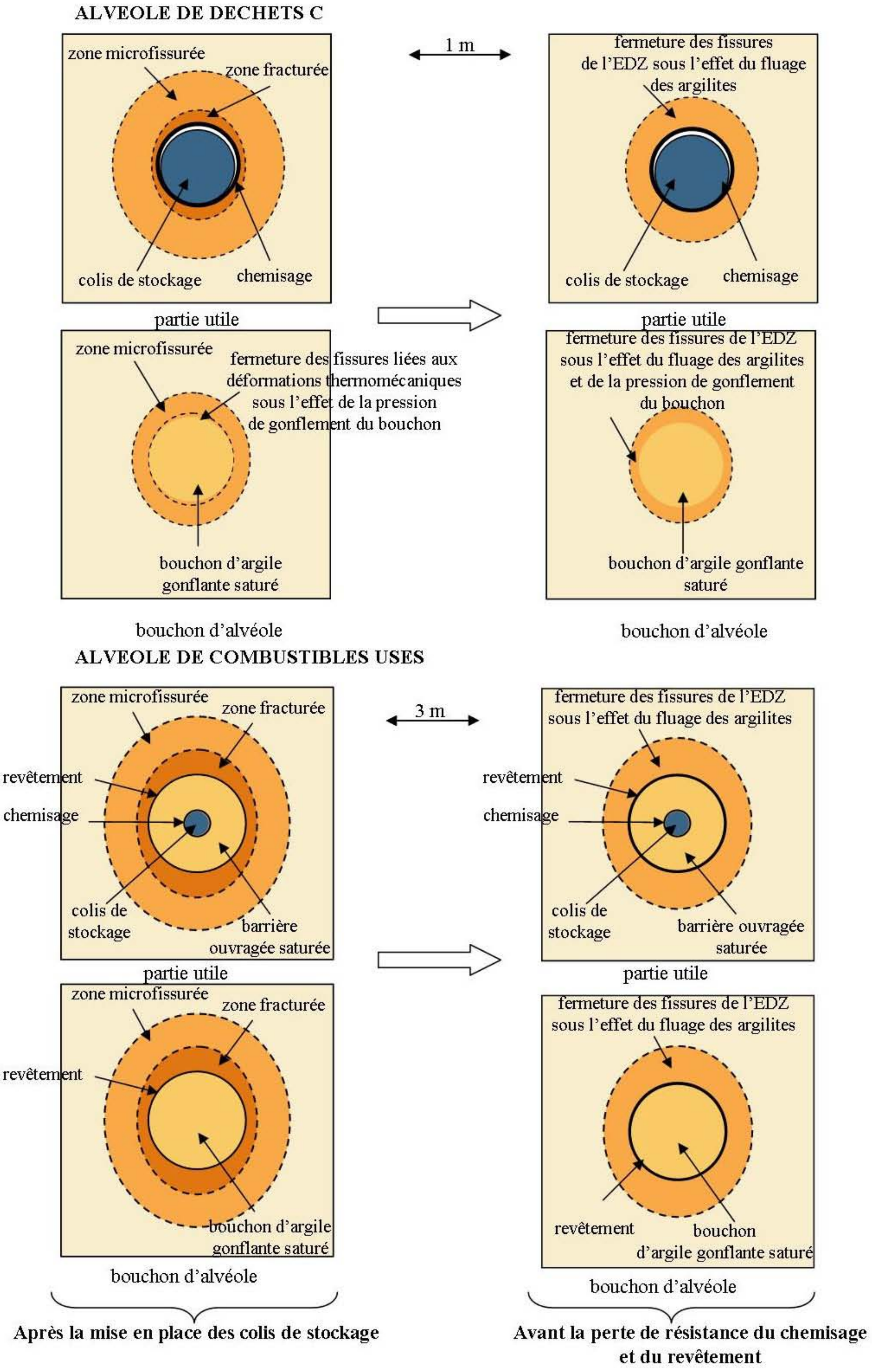

Figure 8.5.6 *Diagrams showing evolution of EDZ around a C waste disposal cell and a spent fuel disposal cell before rupture of the lining and liner (timescale of several hundred to thousands of years)*

8.5.7 Mechanical evolution after rupture of the lining and liner and before rupture of the over-packs

8.5.7.1 Useful part

Beyond 1,000 years, the loading of the liner and lining, consequential to their corrosion, exceeds their mechanical strength (see § 7.3.1). The deformation of the liner and the lining following their discharge of strength modifies the stress state (reduction in radial stress, increase in sheer stress) by mobilising the residual voids and gradual mechanical rearrangement between all the disposal cell components. Although the corrosion creates expansive products that fill the annulus voids and apply mechanical stresses to the other disposal cell components and on the argillites at their periphery, residual voids between the disposal packages and the lining may be left.

- **C waste disposal cells**

The increase in the stress deviator immediately after the deformation of the lining and the presence of residual voids reactivates the creep of the argillites. However, as these voids are slight, the argillites only suffer moderate discharge of containment and it is unlikely that the reactivation of the creep will reach the damage and rupture thresholds.

The slow deferred deformations continue until the voids are filled completely and results in a load being placed gradually on the over-packs. Damage is not reactivated; on the contrary, the creep of the argillites plays a part in the continued closing of the residual fissures. The extent and intensity of the EDZ continues to decrease to reach a permeability close to that of the undisturbed argillites (Figure 8.5.7).

The loads applied to the over-packs are the weight of the overlying formations, pressure from the interstitial pore, the residual thermal stresses and stresses linked to expansive corrosion products. All these stresses together ultimately establish an equilibrium corresponding to the lithostatic stresses in the geological medium (12 MPa).

The thickness of the over-pack is based on a useful thickness of strength with respect to stresses likely to affect the over-pack over a timescale of several thousand years and an additional thickness of discharge of substance through corrosion over the same timescale. Thus, although the corrosion of the over-pack becomes greater with the rupture of the lining, it remains sufficiently thick to resist this loading until the overthickness of corrosion has been entirely "consumed", i.e. beyond 15,000 years (see § 7.3.1).

- **Spent fuel disposal cells**

The liner is loaded by the argillites at the extrados and by the swelling clay of the engineered barrier at the intrados and is corroded on both its faces. It deforms, therefore, and loses its mechanical strength before the lining.

There is constant re-equilibrium during a first phase between the swelling clay in the engineered barrier, the expansive corrosion products in the liner and the external face of the lining and the argillites. The swelling clay controls this re-equilibrium: it absorbs the stresses from the corrosion products by deformation and limits the deformations inside the disposal cell (a process known as convergence-containment). The argillites are therefore only very slightly loaded and these processes prevent the argillites deforming up to damage or rupture.

Subsequently the loading of the lining and its corrosion make it lose its mechanical characteristics. The containers then come under load from the swelling pressure of the swelling clay in the engineered barrier. Initially, this gradually absorbs the functional clearances remaining between the lining and the containers through its potential for residual swelling. The same process of equilibrium between the swelling clay in the engineered barrier, the expansive corrosion products and the argillite creep as described above continues. The result is the gradual loading of the containers. The maximum pressure applied on the containers is estimated at 18 MPa. Ultimately, this is in equilibrium with the lithostatic stress of the geological medium (12 MPa). As the swelling potential of the swelling clay is higher than the creep potential of the argillites, this equilibrium process is, therefore, faster than for a C waste disposal cell (Figure 8.5.7).

In addition, the deferred convergence of the argillites and the compression of the swelling clay by the corrosion products compacts the engineered barrier, thus reducing its porosity and permeability.

The spent fuel containers, initially 110 mm and 120 mm thick respectively for the CU1 and CU2 spent fuels, remain sufficiently thick to resist this load up to around 30,000 years (after the corrosion thickness has been "consumed" - see § 7.3.1).

8.5.7.2 Disposal cell hydraulic head

At the *C waste disposal cell plug*, as there are no metallic components or modifications to the mecahnical properties of the argillites or the swelling clay, the stress state at equilibrium achieved in the first hundreds of years is maintained. The EDZ fissures around the swelling clay plug are closed and the EDZ permeability may be assimilated into that of the undisturbed argillites (Figure 8.5.7).

The mechanical evolution around the *spent fuel disposal cell plug* is similar to as described for the useful part of the cell. With equilibrium reached in the stress state, the EDZ fissures continue to close until the permeability of the EDZ is equivalent to that of the undisturbed argillites.

The chemical degradation of the concrete plug affects its periphery firstly, then continues towards its centre. Given the slow, gradual nature of this degradation and the absence of voids, the creep of the argillites is enough to recover the deformations caused by the peripheral chemical degradation. The concrete plug is gradually placed under load by the argillites on the periphery and by the swelling clay on its internal face and becomes rigid under the effect of this "tightening". The stiffened backfill in the access drift absorbs the deformations in the support base on its external face.

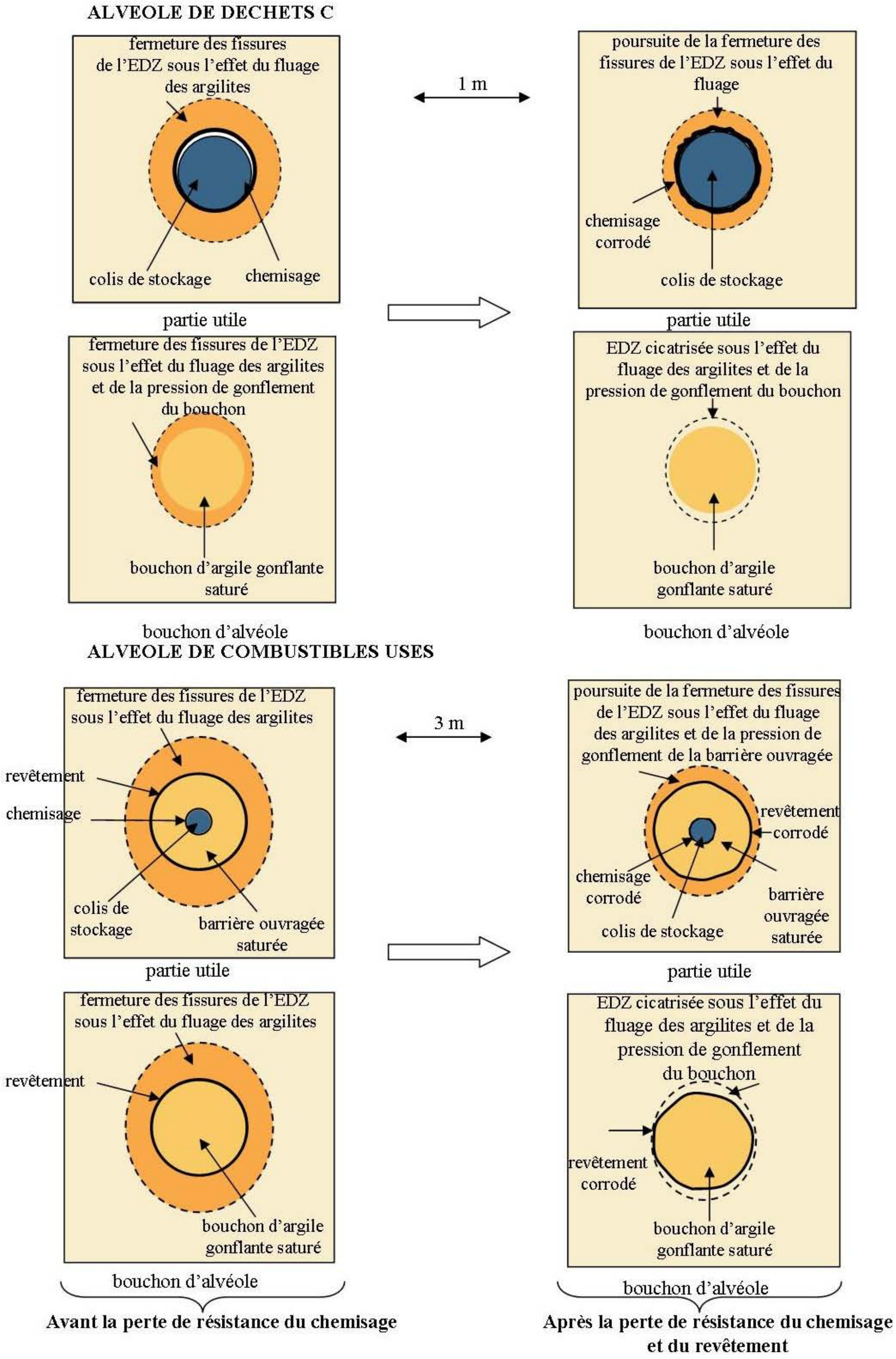

Figure 8.5.7 *Diagrams showing evolution of EDZ around a C waste disposal cell and a spent fuel disposal cell after rupture of the lining and before rupture of the over-pack (timescale of several thousands to several tens of thousands of years)*

8.5.8 Mechanical evolution with corrosion of over-packs

From a phenomenological viewpoint, the rupture of the over-packs by corrosion may be envisaged after around 15,000 years for C waste packages and 30,000 years for spent fuel packages (see § 7.3.1), in other words well beyond the specified leak tightness periods (4,000 years and 10,000 years respectively for the C waste over-packs and the spent fuel containers).

As for the rupture of the liner or lining, the rupture of the over-packs is caused by a modification to the stress state (mobilisation of internal voids at the disposal packages, reduction in radial stress, increase in sheer stress) and a gradual mechanical rearrangement between all the disposal cell components. These slow and gradual, local mechanical adjustments cause moderate reactivation of the creep of the argillites, but do not cause them damage. The low deformations of the argillites gradually fill the residual voids and compact the disposal cell components until a state of equilibrium is reached with parallel healing of the EDZ residual fissures. The permeability of the EDZ is close to the permeability of the undisturbed argillites (Figure 8.5.8).

The creep of the argillites at the disposal cell hydraulic heads accompanies the gradual degradation of the support bases which retain a residual strength without creating new disturbances in the argillites. Ultimately, the support base, like the other disposal cell components, becomes more dense under the effect of the argillite creep.

There is therefore a general loading of the disposal cells by the geological medium with a densification of the disposal cell components and mechanical "integration" in the geological medium.

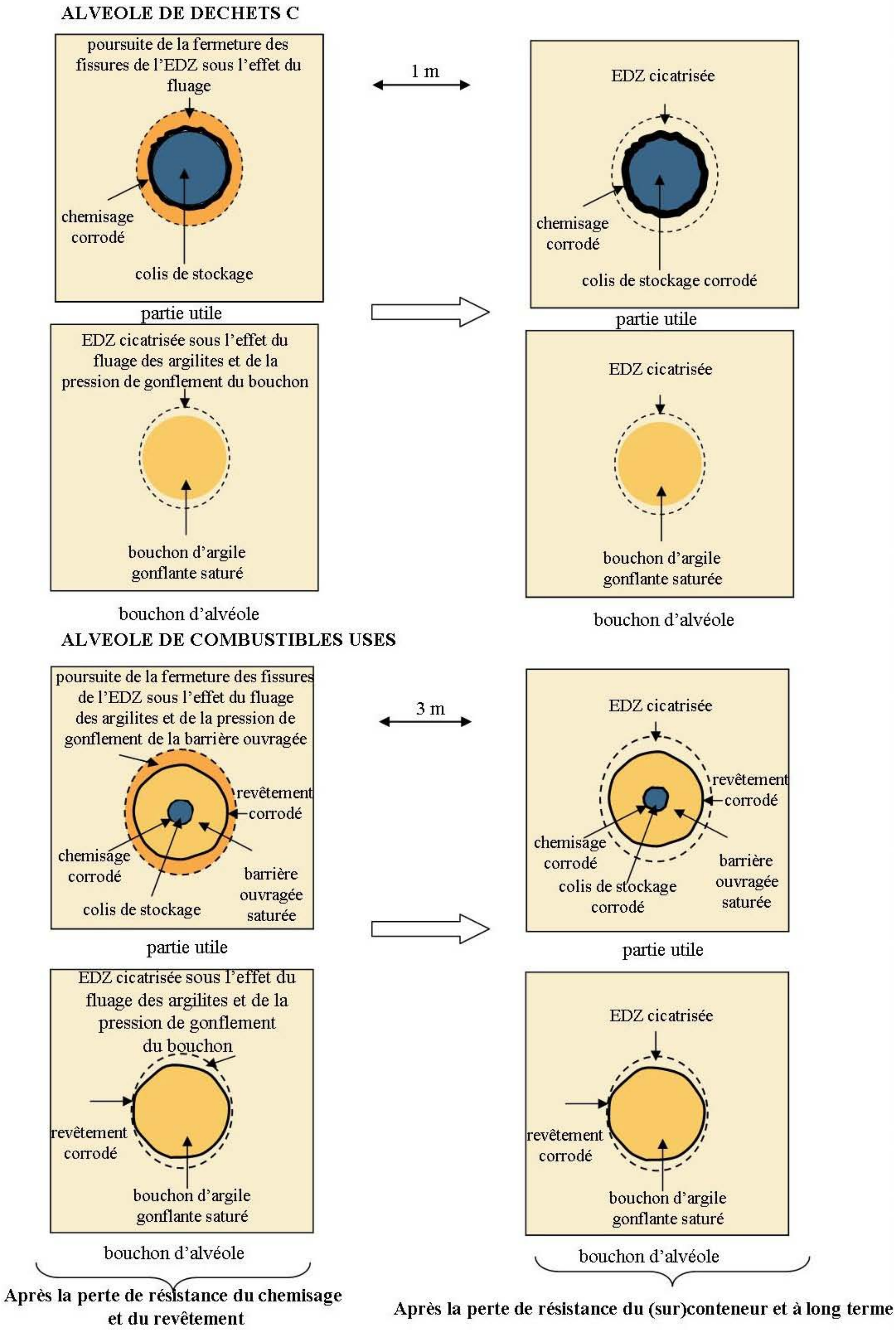

Figure 8.5.8 *Diagrams showing evolution of EDZ around a C waste disposal cell and a spent fuel disposal cell after discharge of strength of over-packs and in the long term (timescale of tens of thousands of years)*

8.6 Mechanical evolution of seals

The gradual closure of the repository corresponds to the installation of the seals in special sections of the drifts, and ultimately in the shafts.

The seals have the following in common:

- the principle adopted is based on the combination of a swelling clay core and two concrete support or containment bases either side of this core. Granular backfill bases keep the swelling clay core contained as the concrete bases degrade;
- to interrupt a preferential hydraulic path in the fractured zone (initial or immediately after mechanical evolution during the operating phase), any fractured zones in the argillites are removed by scraping when possible (as for shafts) or intercepted by creating thin hydraulic keys filled with swelling clay known as "hydraulic cutoffs" (as for drifts).
- the seals are several tens of meters long.

The seals have the following differences, however:

- the drifts intended to receive the seals are oriented according to the major horizontal stress. Their cross-section therefore undergoes an initial, isotropic stress field that encourages the minimisation of the EDZ during excavation (see § 8.2). As the shaft seals are vertical, their cross-section is subjected to an anistropic stress field;
- the drift seals are overall located at the same depth in zone C of the argillites. The shaft seals are located at different depths (and therefore subjected to various stress fields) and in different types of geological formation. The result is smaller EDZ extents (particularly the fractured zone in zone A of the argillites where the seals are installed), that negates the need to provide hydraulic cutoffs in the shaft seals;
- the scraping of any fractured zone at the shaft seals assumes the removal of the ground support/liner. Hydraulic cutoffs in the B waste disposal cell and drift seals hold the ground support/liner in place.

8.6.1 Creation of seals

8.6.1.1 B waste disposal cell seals and drift seals

The B waste disposal cell seals and drift seals are designed to favour limiting damage to the argillites. The drift sections receiving the seals are arranged according to the major horizontal stress, which minimises the initial EDZ immediately following excavation (see § 8.2). Removing the ground support/liner and scraping off the fractured zone by reboring to guarantee direct contact between the swelling clay of the seal and the argillites is likely to propagate damage around the seals and has not been adopted for this reason. Hydraulic keys were the preferred option to limit the damage and reduce the equivalent permeability of the EDZ around the seals by replacing the fractured argillites by swelling clay, a less permeable material.

The form and dimensions of these hydraulic keys, the distances between them and their method of excavation are defined so that they do not create a continuous fractured zone and that they effectively constitute an interruption of the fractured zone with greater permeability around these engineered structures. The reduction in axial permeability equivalent to the argillites at the wall of the seals is assessed at less than one order of magnitude. The permeability of the resaturated swelling clay in the hydraulic keys controls this equivalent permeability. Thus, under the hypothesis of a swelling clay permeability of 10^{-11} m.s^{-1}, the equivalent permeability around the seals is 10^{-10} m.s^{-1}. Experiments in foreign underground research laboratories have shown that a swelling clay permeability of 10^{-11} m.s^{-1}, even 10^{-12} m.s^{-1} can be obtained (Chandler & *et al.*, 2002).

This specification combined with technological constraints has dictated the choice of radial hydraulic keys 30 cm thick approximately at 8 m intervals for the B waste disposal cell and drift seals (Barnichon & Su, 2005b). The depth of the hydraulic keys is such that it crosses any fractured zone and reaches the microfissured zone, therefore in the order of 1 to 3 m. The technological feasibility of creating a hydraulic cut-off has been demonstrated at the Mont Terri laboratory (test EZ-A - (Barnichon & Su, 2005b) - Figure 8.6.1). A similar experiment has been performed in the Meuse/Haute Marne laboratory (KEY test).

Figure 8.6.1 *Creation of a radial hydraulic cut-off around a drift and filling with blocks of compacted swelling clay: feasibility test at Mont Terri*

The ground support/liner is maintained either side of the hydraulic keys. A 1.30 m-section of the ground support/liner is removed directly above each hydraulic cut-off to expose 50 cm either side of the hydraulic cut-off separating the ground support/liner concrete from the swelling clay in the hydraulic keys. This arrangement limits the alkaline disturbance in the swelling clay that thus retains its swelling capability (see § 7.5.1).

The hydraulic cut-off walls are loading mechanically in conjunction with the discharge of containment in the longitudinal stress of the engineered structure which is also the major horizontal stress. The damage from this new relaxation is moderate given the improved mechanical properties of the argillites through their desaturation (Inset 8.4). Creating the hydraulic keys nevertheless creates a new EDZ of slight extent and intensity. A fractured zone appears at the junction of the drift and the hydraulic cut-off and at the bottom of the hydraulic cut-off. This is discontinuous the length of the hydraulic cut-off which effectively represents a hydraulic cut-off (Figure 8.6.2 and Figure 8.6.3) (Barnichon & Su, 2005b ; Ozanam & Su, 2003).

The hydraulic keys are then filled by assembling blocks of compacted swelling clay. Swelling clay powder is injected to fill the interstices as required (Figure 8.6.1).

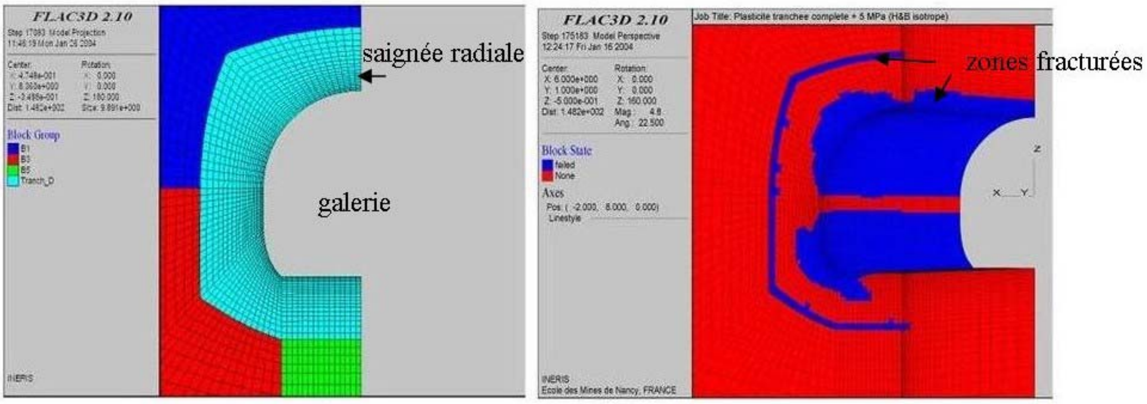

a) géométrie de la saignée

b) zone fracturée après la réalisation de la saignée (en bleu)

Figure 8.6.2 *Numerical modelling of the creation of a hydraulic cut-off around a drift: interruption of the fractured zone the length of the hydraulic cut-off*

The seal core, around 40 m long, whose task is to guaranteee low transmissivity, is based on swelling clay (Inset 2.7). To limit the loading on the support engineered structures either side of the core (concrete base and backfill), a swelling pressure of 3 MPa is sought. The swelling pressure of 3 MPa is achieved by assembling pre-compacted blocks of a swelling clay/sand mix (20 to 30 %) with a dry clay density of 1.4 to 1.5 approximately; a residual swelling pressure of 0.5 to 1 MPa is available after degradation of the support bases. The use of pre-compacted blocks has been full-scale tested in the Tunnel Sealing Experiment (TSX) in the Canadian Underground Research Laboratory. The peripheral voids were filled with swelling clay powder to improve the filling of the drift and obtain a more homogenous core (Chandler & *et al.*, 2002).

Two concrete support bases either side of the swelling clay core provide support for the mechanical containment fo the core and the development of its swelling pressure. High-performance, non-reinforced concrete, with low permeability, is chosen to delay its chemical degradation and prevent fissuring from expanding corrosion products.

A support backfill made up of a mix of excavation argillites (stored in a surface tip during repository operation) and sand is installed behind the support bases. This mix produces a modulus of deformation of 20 MPa and an angle of friction of 40°, enough to ensure rigidity and friction restricting the movement of the seal after the chemical degradation of the support bases. The length of the support backfill is around four times the excavated diameter, to allow friction between the backfill and the drift wall to balance the swelling pressure. In B waste disposal cells, the support base and the upstream backfill are positioned at the hydraulic head of the access drift. It is ground and mixed, then put in place by being compacted at the Proctor optimum (in non-saturated state) following the horizontal layers in the lower section, then, in the upper section, in successive, sloping layers so as to fill the entire volume and leave no installation clearances between the backfill and the upper part of the drifts. The backfill has no mechanical role when being installed. The argillites are contained by the ground support/liner.

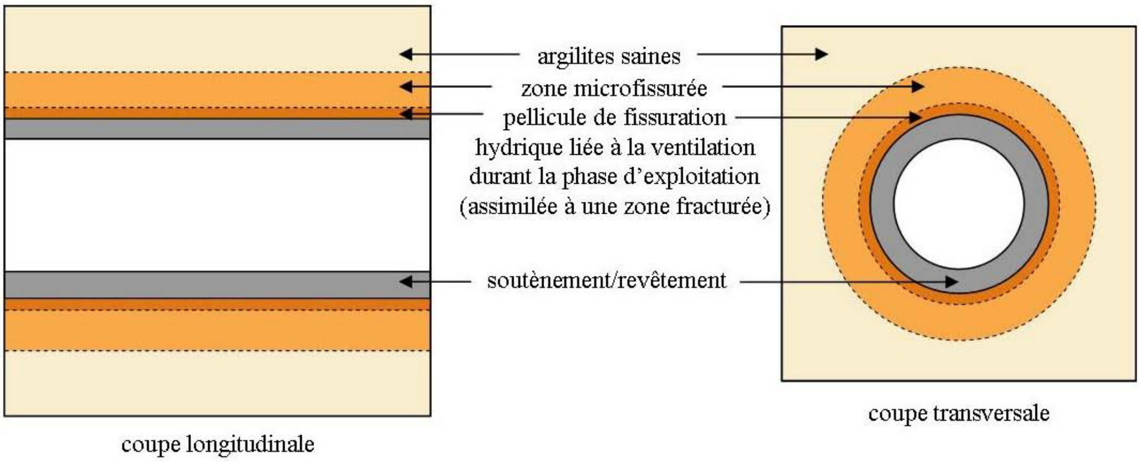

a) Avant la réalisation du scellement

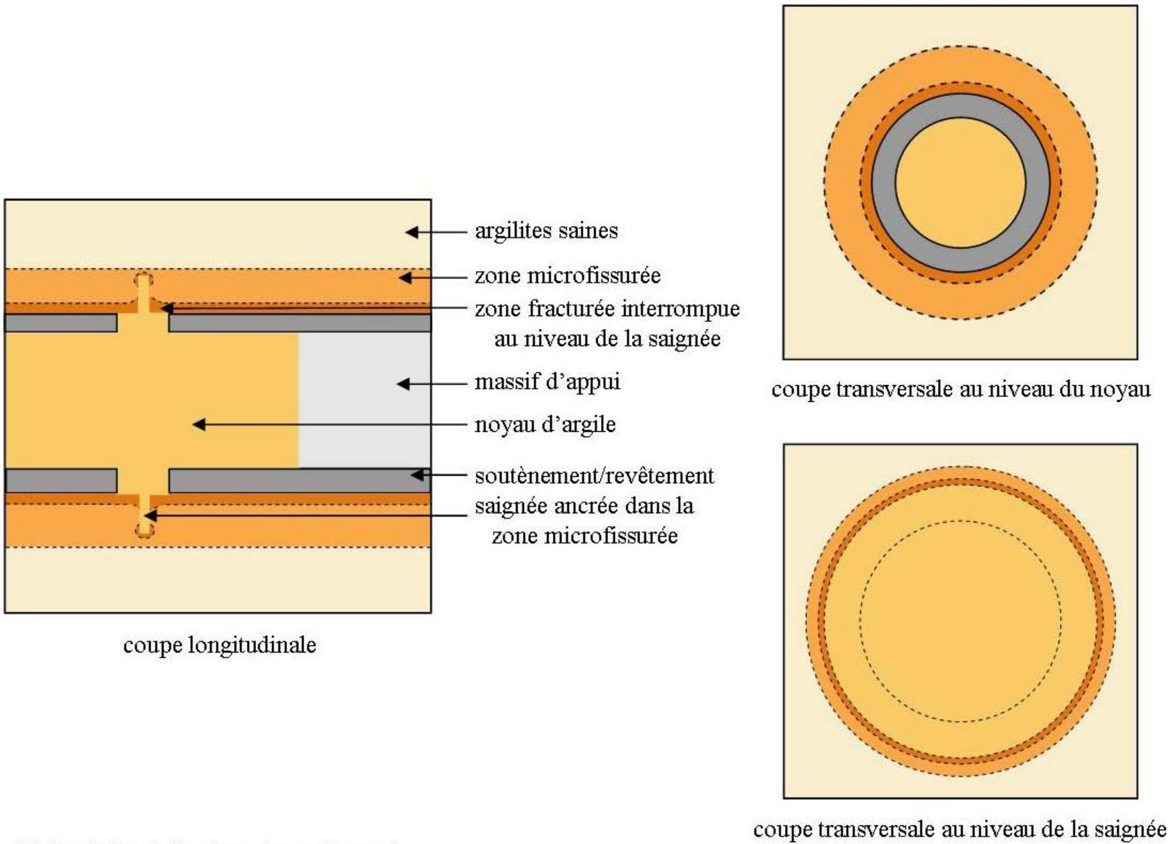

b) Après la réalisation du scellement

Figure 8.6.3 *Simplified diagrams illustrating the interruption of the fractured zone around the hydraulic cut-off in a drift seal*

8.6.1.2 Shaft seals

A shaft is closed with two seals and backfill.

A first seal installed in the upper section of the Callovo-Oxfordian layer (zone A), more calcareous than zone C containing the repository engineered structures, isolates the storage in the overlying geological formations. Its core is based on swelling clay, like the drift. The assessments of the initial EDZ in zone A do not provide for the formation of a fractured zone during excavation (see § 8.2.3). This assessment also applies to the removal of the ground support/liner. The new discharge of containment of the argillites takes places with a stress state lower than the initial stress state during the shaft excavation and causes no further damage to the argillites. In addition, the mechanical properties of the argillites are improved by their desaturation. Under these conditions, the microfissuring threshold is not reached. The concrete liner is therefore removed over the entire height of the seal (around 30 m): the swelling clay of the core is in direct contact with the argillites. Removing the liner and backfilling immediately the shaft section with swelling clay in successive studs limited in height are nevertheless envisaged to ensure site safety. A fractured zone is likely to develop at the shaft wall due to the desaturation of the argillites during the operating phase (mainly for the air outlet shafts which desaturate more than the air inlet shafts) (see § 8.3.2). In this hypothesis, the fractured zone will be scraped off.

The core lies on a concrete support base installed in shaft sections in zones B and C, sumps and shaft stations and extend into the drifts that are connected over several tens of meters. These arrangements provide the support base with enough mechanical robustness to guarantee the stability of all the overlying closure materials installed in the shaft. Unlike the drift seal, the risk of the core relaxing with the chemical degradation of the support base is ruled out and a swelling pressure of 7 MPa of the clay core, encouraging the return to a state of equilibrium, may be targeted. A support base, anchored in the calcareous Oxfordian, is built above the core to guarantee its mechanical containment during resaturation and the development of the swelling pressure.

As for the B waste disposal cell seals or the drift seals, the planned method of installing the swelling clay core is by assembling pre-compacted blocks that obtain directly the density required to produce a swelling pressure of 7 MPa (dry density of 1.8).

The upper shaft sections (calcareous Oxfordian, Kimmeridgian marls and Barrois limestones) are filled with compacted backfill.

A second compacted swelling clay seal similar to the repository isolation seal is installed to isolate the aquifers in the calcareous Oxfordian and Kimmeridgian (Figure 2.4.15).

8.6.2 The thermal, hydraulic and chemical contexts of the mechanical evolution of the seals after closure.

Chapters 5, 6 and 7 highlight the importance of the thermal, hydraulic and chemical evolution of the seals (Figure 8.6.4).

8.6.2.1 Hydraulic context

The resaturation of the seals in the Callovo-Oxfordian argillites is triggered immediately they are installed.

- In a first phase, the resaturation of the hydraulic keys of swelling clay, the clay core and the argillites around the seals is not delayed by the production of hydrogen from corrosion:
    - the thin hydraulic keys of swelling clay in direct contact with the argillites on their periphery are saturated up to degrees of saturation higher than 97 % in a few years;
    - the clay core and the argillites around the seals, including in the EDZ, reach this same degree of saturation after one or several thousand years.
- Subsequently, as the gas pressure increases, then reaches the pressure threshold that allows its extension beyond the seal, the passage of the gases prevents resaturation up to 100 %. Total saturation is reached once gas production is halted, i.e. beyond 100,000 years.
- In the backfills and support bases, the passage of the gases prevents their resaturation during the first thousands of years, when large quantities of gas are produced within the disposal cells (particularly the C waste and spent fuel disposal cells). The degrees of saturation of the backfills remaine close to 70 %. Beyond that, the production of gas decreases and the degrees of saturation of the backfills and the support bases increase up to values higher than 90 %. Total saturation is only reached, however, once gas production is halted, i.e. after 100,000 years.
- The upper shaft sections, above the repository isolation seal, is resaturated rapidly by the overlying calcareous Oxfordian. Subsequently, the permeability of the swelling clay controls the total resaturation of the clay core.
- The saturation of the isolation seal of the aquifers in the Kimmeridgian marls lasts several hundred to a thousand years.

8.6.2.2 Chemical context

The chemical degradation of the seal components (degradation of liner and support base concretes, alkaline disturbance in the swelling clay and the argillites, etc.) only becomes significant with total resaturation.

- In the argillites, the chemical degradation of the liner and support base concretes with modification to their mechanical properties only becomes significant beyond a period of 100,000 years. The mechanical properties of the liner and support base concretes in the calcareous Oxfordian decrease from a few tens of thousands of years.
- Only a fraction of the swelling clay of the core and the argillites, in contact with the liner or support base concrete, undergoes limited alkaline disturbance, without causing a discharge in their mechanical or hydraulic properties. In addition, the liner is removed 50 cm either side of the hydraulic keys, thereby preventing the alkalinisation of the swelling clay by the liner concrete. Lastly, as the arches are located over a metre from the hydraulic keys, their corrosion causes no disturbance at the hydraulic keys.

8.6.2.3 Thermal context

The closure of these engineered structures and the halting of ventilation is accompanied by a slow rise in temperature within the exothermic B waste disposal cell seals and the drift sales in the C waste repository zones and spent fuel repository zones. The temperature reached in these engineered structures does not however exceed 50 to 55 °C (see § 5) and the thermal gradients remain low (less than one degree Celsius per metre). The mechanical phenomena are therefore little influenced by the thermal load. The properties of the seal components, particularly the swelling properties of the swelling clay, are not modified by rises in temperatures of 30 – 35 °C (Chandler & *et al.*, 2002).

As the shaft zone is located at several hundred meters from the repository zones, there is no rise in temperature linked to the disposal of exothermic waste, but only a return to a state of equilibrium of the initial temperatures after the shafts are closed.

8.6.2.4 Assessment for mechanical evolution

There are two distinctive, major phases in the mechanical evolution of the seals:

- the saturation phase. This has the effect of (i) developing the swelling pressure of the swelling clay in the core and the hydraulic keys (in the drifts and B waste disposal cells), (ii) reactivating the argillite creep (Callovo-Oxfordian argillites and Kimmeridgian marls) and swelling which is accompanied by the commencement of the healing of the EDZ fissures and (iii) loading the ground support/liner and support bases gradually. During this period of several thousand years, the concretes degrade very little chemically and retain their intrinsic mechanical properties;
- as soon as they are saturated, the sealing system as a whole is placed under load by the argillites. Its mechanical evolution is then mainly governed by the deferred evolution of the argillites and swelling clays, with the chemical degradation of the concretes (ground support/liner, support bases).

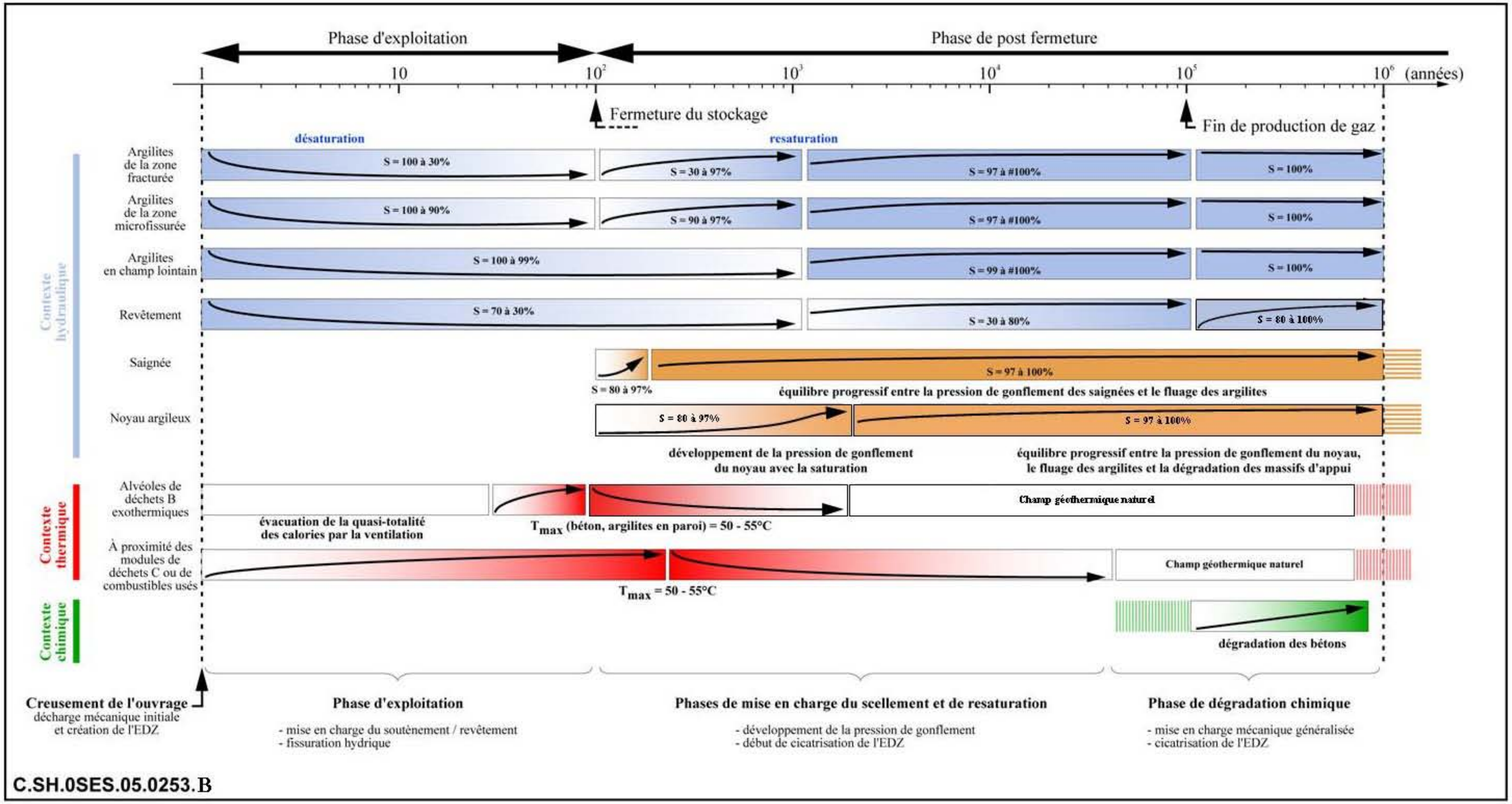

Figure 8.6.4 *Time chart of the mechanical evolution of a drift seal: thermal, hydraulic and chemical contexts during construction and post-closure phases (based on a conventional hundred-year time chart of the construction/operation/closure of a repository)*

8.6.3 Seal saturation phase and development of swelling pressure

8.6.3.1 Clay core and hydraulic keys

The swelling clay in the clay core and the hydraulic keys is installed in a desaturated state (80 % degree of saturation) at a dry density of around 1.5 for the drift seal and 1.8 for the shaft seal. The maximum swelling pressures thus achieved are 3 MPa and 7 MPa respectively.

In the drift or B waste disposal cell seal, the saturation state and swelling pressure developed by the swelling clay are heterogeneous over time and space given the very different resaturation times between the hydraulic keys and the clay core.

The hydraulic keys are saturated and the swelling pressure develops after a few years, well before the clay core, therefore. In the clay core, as for the engineered barrier in a spent fuel cell, the saturation affects the periphery first, then progresses inwardly towards the clay core, accompanied by the development of the swelling pressure (Figure 8.5.4). The differential saturation between the hydraulic keys and the clay core heart may generate shear forces at the base of the hydraulic keys. However, as the external thin layer of the clay core saturates at the same time as the hydraulic keys, the plastic behaviour of the swelling clay is sufficient to absorb any deformations and prevent the appearance of dislocations within the clay core. In addition, these processes become blurred, then disappear as the clay core continues to saturate.

The swelling pressure of the saturated swelling clay, in a shaft seal and around the hydraulic keys in a drift seal, is applied directly to the argillites. The saturated swelling clay interacts directly with the argillites under a process known as convergence-containment, similar to the one described for the clay plug in a C waste disposal cell (see § 8.5.5 - Figure 8.4.1): the argillite creep, reactivated by the saturation, their swelling and the swelling of the swelling clay reduces the stress deviator in the argillites and increases the normal stress at the walls. These processes gradually close the fissures in the argillites (Figure 8.6.5 and Figure 8.6.6, (Barnichon & Su, 2005b)). The resultant decrease in the permeability of the argillites is 2 to 3 orders of magnitude (Buehler *et al.*, 2003).

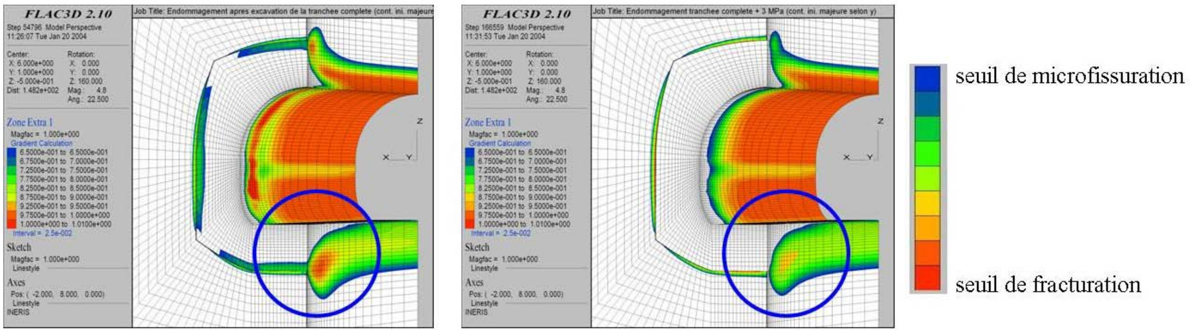

a) Après la réalisation de la saignée

b) Après développement de la pression de gonflement de l'argile gonflante dans la saignée

Figure 8.6.5 *Numerical modelling of the effects of the load applied by swelling pressure of the swelling clay in the hydraulic cut-off in the argillites: recompression of EDZ fissures*

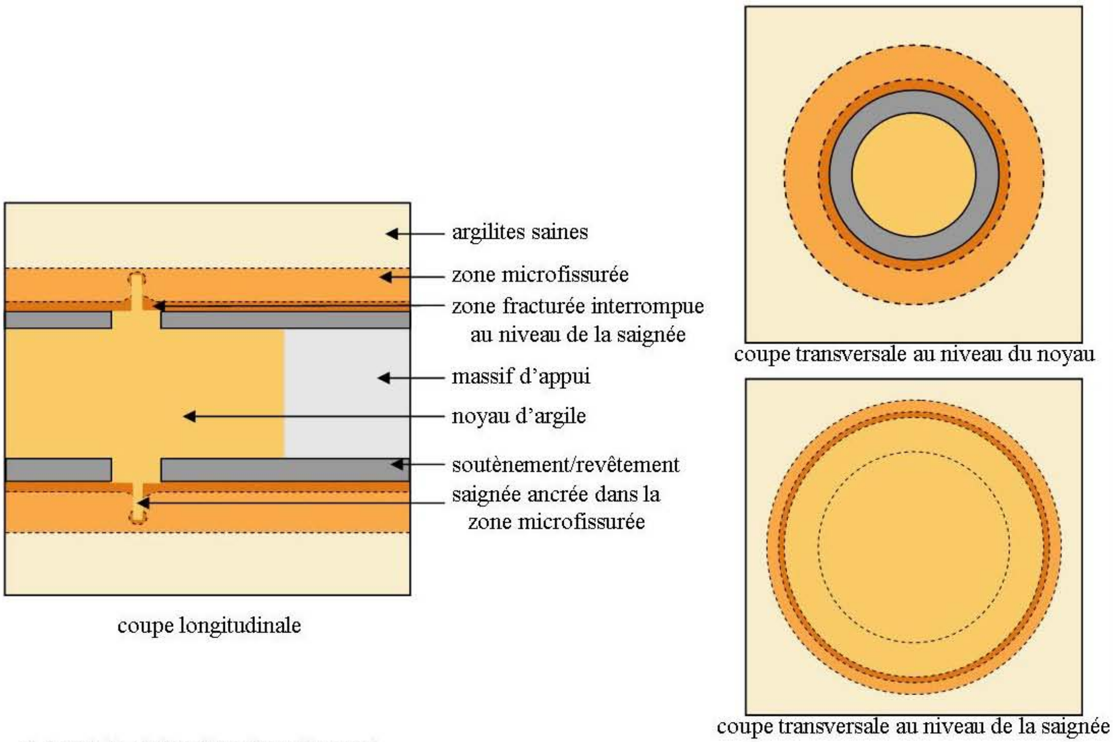

a) Après la réalisation du scellement

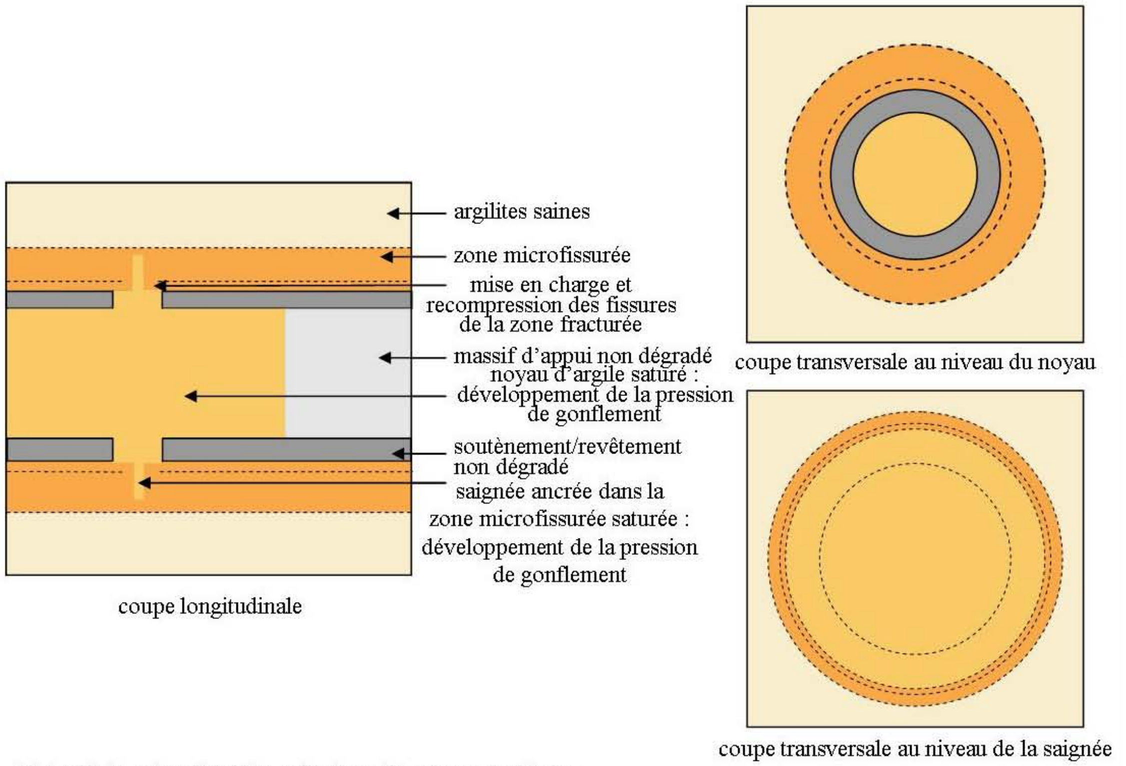

b) Après la saturation des saignées et du noyau argileux (échelle de temps millénaire)

Figure 8.6.6 *Simplified diagrams illustrating the recompression of the EDZ fissures under the load applied by the swelling pressure of the swelling clay and by argillite creep and swelling around a drift seal (timescale of a thousand years)*

8.6.3.2 Support bases and ground supports/liners

For the support bases, the inwards saturation of the clay core is accompanied by heterogenous loading of their face in contact with the swelling clay core. It affects the periphery firstly before extending gradually over the entire contact surface area. The dimensioning and design of these support bases takes these heterogeneous loading conditions into account, particularly the anchoring in the intrados of the maintained coating. The support bases last longer than the total resaturation time of the clay core. As the support bases are not degraded chemically, or only slightly, there is no "piston" effect by the clay core.

The ground support/liner concretes in the drifts, support bases and shaft stations are also loaded by the argillites on their external face. The argillite creep and swelling activated by the resaturation produces radial pressure applied to the extrados of the ground supports/liners, support bases and shaft stations. As they have not been degraded chemically at this stage, like the B waste disposal cells or backfilled drifts, they contain the argillites mechanically and prevent all free deformation. The swelling pressure and the radial stress resulting from the creep are transmitted to the EDZ fissures, reducing their opening and therefore the permeability of the argillites at the seal walls (see § 8.4.2).

The load placed on the concretes by the argillite creep and swelling produces stresses in the ground supports/liners and, to a lesser degree, in the support bases, that are higher than their strength after several thousand to 10,000 years, therefore well before they are degraded chemically. It is likely, therefore, that fissures will appear in the concretes, which nevertheless retain a residual strength. In addition, all the internal voids in the engineered structures are filled by the swelling clay (clay core) or support backfill. They are sufficiently rigid to keep the argillites contained at their periphery and prevent additional disturbances within them. In the shaft stations and support bases, given their great thickness (they cover the entire cross-section of the engineered structures), the stresses created by the argillites are less than those extending in the liner and rupture is therefore delayed.

8.6.4 After resaturation, as the mechanical properties of the support bases and ground supports/liners evolve

The gradual chemical degradation of the concretes in the ground support/liner, support bases and shaft stations and the deferred behaviour of the argillites controls the mechanical evolution of the seals after the resaturation phase.

8.6.4.1 Clay core and hydraulic keys

In the *clay core*, the deformations caused by the degradation of the concretes are limited due to the absence of voids, the argillite creep and the behaviour of the resaturated swelling clay. Equilibrium is gradually reinstated permanently between the swelling clay, the concrete and the argillites. The swelling clay accommodates this re-equilibrium: it absorbs the stresses linked to the degradation of the concrete by deformation and limits the deformations within the seal. It places little load on the argillites, therefore, and prevents deformation up to their rupture or damage.

Under loading by the argillites, the ground support/liner and support base concretes and the clay core become more dense and the residual EDZ fissures close. The deviator stress decreases then is canclled; the average stress increases and there is a gradual return to a state of equilibrium of the stress state and pore pressure. The engineered structure is gradually "integrated" mechanically with the geological medium.

At the *hydraulic keys*, the EDZ fissures continue to close due to equilibrium between the argillite creep and the swelling of the swelling clay. The extent and permeability of the EDZ decreases gradually towards the initial permeability of the argillites.

8.6.4.2 Support bases and ground supports/liners

In the support bases and ground supports/liners, at the interface between the concrete and argillites, given the slow, gradual chemical degradation and the absence of voids, the argillite creep compensates for the deformations produced by the degradation of the concrete. As the concretes degrade, the argillite creep and swelling stresses are transmitted to the swelling clay core and backfill as well as to the concrete filling the support bases and stations.

The result is a slight reactivation of the convergence of the argillites but, given the lack of voids and the slow, gradual degradation, this does not further extend the damage to the argillites. The deformations within the engineered structures reactivated by the degradation of the cement-based materials lessen and are accompanied by a reduction in the deviator stress and an increase in the average stress until the initial stress state is reestablished. All the seal components become dense under loading by the geological medium. The argillite creep, and to a lesser degree the partial clogging of the porosity of the argillites by their alkanisation in contact with the concretes, means that the EDZ fissures recompress.

The potential of residual swelling of the swelling clay at the interface with the clay core compensates for the discharge of concrete rigidity. The degradation of the concrete at the interface with the argillites nevertheless reduces the friction at the support base anchoring points and the load on the clay core is gradually transmitted to the backfill. As this load is transferred, the backfill behind the support base (made up of argillite and sand) becomes dense under the load applied by the argillites, acquires sufficient rigidity to support the support base and mobilises the friction with the remaining liner and the argillites (Figure 8.6.7).

In the shaft seal, the weight of the upper backfill is transmitted gradually to the clay core and may trigger shear movements at the clay core/rock and backfill/liner/rock interfaces. As the installed backfill is very dense and has no residual voids, it only settles slightly during saturation. The plastic behaviour of the swelling clay absorbs these deformations without causing disorders and therefore modifies the permeability of the clay core. In addition, the saturation of the backfill cause slight swelling of the argillites making up the backfill and the developing of a slight swelling pressure (in the order of 0.1 MPa (Barnichon & Su, 2005c)). This is applied radially to the ground support/liner concrete and axially to the support bases and increases the friction between the backfill and the ground support/liner and between the support bases and the backfill.

After the degradation of the concretes in the ground support/liner, support bases and shaft stations, the seals evolve mechanically in similar fashion to the other repository engineered structures, namely generalised loading by the geological medium. This loading is accompanied by the densification of the seal components which in turn contain the argillites. The result is the gradual decrease in creep accompanied by a reduction in the stress deviator and a return to a state of stationary equilibrium with the closure of the residual EDZ fissures at the same time.

Thus, as for the engineered structures already addressed above, the evolution of the stress state in the seals becomes homogenous and continuous. At the scale of several hundreds of thousands of years, the evolution of the geological context and erosion may be readjusted. They act homogenously on all the engineered structures in the repository (see § 8.7).

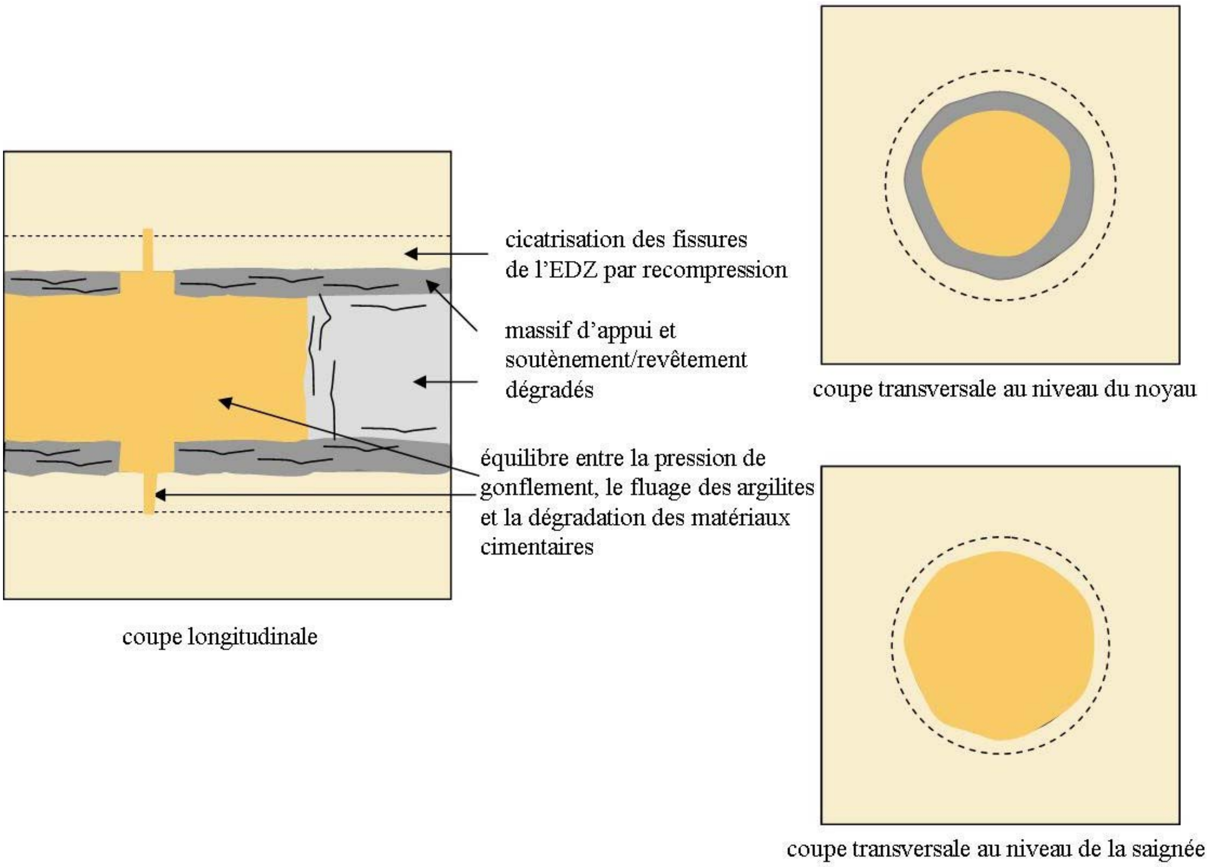

Figure 8.6.7 *Simplified diagrams illustrating the generalised loading of a drift seal as cement-based degradation takes place (beyond 100,000 years)*

8.6.5 In the overlying formations of the Callovo-Oxfordian layer

Directly above the *limestones* levels, the convergence of the formations and the resultant initial support for the liner (as long as this is not degraded chemically), then for the backfill, is negligible. The backfill is only subjected to the weight of the upper backfill column. With the appropriate density, it settles in limited fashion during saturation and does not create significant voids. As its deferred behaviour is negligible, the calcareous Oxfordian behaves in an elastic fashion and the gradual degradation of the liner concrete causes no damage to the shaft wall.

In the *Kimmeridgian marls*, whether or not the backfill is saturated by the underlying calcareous Oxfordian waters, the convergence does not exceed a few centimeters and the resultant stress is absorbed by the concrete ground support/liner and is not transmitted to the backfill. This loading is accompanied by continuing gradual closing of the EDZ fissures. Beyond 100,000 years, the concrete in the ground support/liner degrades chemically and loses its mechanical role. The creep in the Kimmeridgian marls is therefore reactivated. However, given the absence of voids, additional damage to the shaft wall is unlikely. In the continuity of the mechanical evolution during saturation, the mechanical phenomena produce balanced loads and an increase in friction between the various components.

The mechanical evolution of the *aquifer isolation seals* installed in the only slightly permeable levels of the cover formations to separate the aquifer porous levels is identical to the evolution described for the repository isolation seal installed in the Callovo-Oxfordian.

8.7 Large-scale mechanical evolution

At the large scale of the repository and the repository site, mechanical evolution is caused by:

- the creation of engineered structures with (i) excavation of the quantities of rock and introduction of the exogenous materials within the geological medium and (ii) the effects of the thermal load induced by the installation of exothermic waste;
- the evolution of the geological context and the erosion phenomena that may also give rise to mechanical readjustments with the repository engineered structures. These act homogeneously on the entire repository.

8.7.1 The effects of the repository

8.7.1.1 Excavation of engineered structures and modification of stress state

Creating the repository involves excavating quantities of rock and modifying the stress state in the vicinity of the engineered structures. The surface area of the repository is in the order of magnitude of about ten km^2. The excavated volume represents less than one percent of the volume of the Callovo-Oxfordian argillites corresponding to the repository surface area (for the Callovo-Oxfordian layer 130 m thick).

In addition, as the repository is operated, then closed, these excavated volumes are filled by materials close in chemical terms to the geological medium (backfill based on excavated argillites, swelling clay). Chapter 7 also showed that the introduction of other materials (concretes, steels) only produced limited chemical disturbances.

All the closure operations aim to limit the residual voids within the engineered structures as much as possible. The choice of materials and their installation method also aim towards an appropriate density of these materials so that mechanical integration of the engineered structures with the geological medium is rapid and allows a return to a homogeneous stress state (Su, 2005).

8.7.1.2 Thermal load

The rises in temperature in the various geological formations immediately after disposal do not induce special mechanical phenomena within these formations, other than those describted in the preceding paragraphs. Thermo-mechanical stress (lower than 1 MPa beyond the Callovo-Oxfordian argillites) does not lead to large-scale fracturing of the Callovo-Oxfordian, nor to thermo-mechanical damage as can be the case in a transient way in the near field of the C waste and spent fuel package cells. Thermo-mechanical damage is restricted to the near-field of the disposal cells containing the most exothermic waste and does not affect the Callovo-Oxfordian layer on a large scale (Su & Barnichon, 2005).

8.7.2 Effects of erosion and tectonics or seismicity

8.7.2.1 Surface erosion

Erosion phenomena are accompanied by the gradual relaxation of the terrains linked to the mass of eroded terrains. At the scale of several hundreds of thousands of years and on the repository plan area, the accumulation of the eroded terrains is limited (a few tens of meters above the Barrois limestones) and without significant consequence on the overall weight of the terrains at a depth of 500 m. This variation produces a decrease in the vertical stress in the order of 0.5 MPa and causes slight anisotropy of the stresses in the engineered structures section. This anisotropy remains negligible and has no effect on the mechanical evolution of the engineered structures.

Similarly, the slight modifications in stresses in the crust triggered by isostatic readjustments linked to climatic variations like the ice ages do not modify the site's morphological characteristics significantly (Su, 2005).

8.7.2.2 Earthquakes

Earthquakes can potentially produce additional loading on the engineered structure components and therefore the deferred activiation of the EDZ in the argillites. How the repository engineered structures respond to the dynamic loadings depends on the number of voids in the engineered structures, the type of structure and their ability to recover additional shear forces and interactions between them (connections, layout, density).

The Meuse/Haute Marne site is located in a very low earthquake hazard zone (Brulhet, 2005a). Historical seismicity, considered as representative of earthquake activity during the repository operating and observation phase, is used to estimate reference earthquakes during this phase (SSE (Safe Shutdown Earthquake) of magnitude 6 at a focal distance of 25 km). For the repository's post-closure period, the maximum possible earthquakes taken into account are linked to the faults near the site and have magnitudes of the same order as those of far-flung active zones (magnitude of 6.1 ± 0.4 for the Marne fault system 8 km away).

Simplified analytical studies considering the empty engineered structures (configuration representative of the operating phase) and earthquake loading representative of the seismicity of hte Meuse/Haute Marne site indicate that the engineered structures 500 m depth are only slightly sensitive to the seismic action. The dynamic effects are limited beyond 300 m deep for frequency ranges of spectra of the Safe Shutdown and Maximum Possible Earthquakes (under 15 Hz), regardless of the type of wave and their angle of incidence. Closing the engineered structures reduces the impedance contrasts and the effects of seismic loading are therefore less compared with the empty engineered structures. A risk of disturbance therefore only seems possible at the repository access shaft, less than 300 m deep, with no effect on the repository engineered structures and particularly the seals installed in the Callovo-Oxfordian (Brulhet, 2005a).

In the repository operating and observation phase, therefore, and subsequently in the post-closure period, when all the engineered structures will be backfilled, the repository engineered structures and the argillites at their walls are only slightly affected, if at all, by any seismic action and the propagation of fissures around the engineered structures from seismic actions seems highly unlikely. In addition, at the scale of the repository volume, the expected behaviour of the whole is that of the surrounding massif. The Callovo-Oxfordian layer in its current state must already have experienced earthquakes and will no longer be affected by potential seismic events in the future, at the scale of the next million years. An analysis of the effects of climatic variations and of seismicity suggest that they are not likely to modify the mechanical evolution of the repository engineered structures.

8.8 Summary of mechanical evolution

The thermal, hydraulic and chemical evolutions described in the previous chapters define the framework for mechanical evolution. Mechanical evolution is part of the overall phenomenological evolution of the repository and its geological environment.

The chapter on mechanical behaviour has attempted to provide as accurate a picture of mechanical evolution as possible. A few aspects of mechanical evolution may be highlighted, particularly with respect to safety in creating and operating a repository, waste package recovery conditions under reversibility and what becomes of the radionuclides after their release. Time charts for the mechanical evolution of the main engineered structures in the repository are summarised in Figure 8.3.1, Figure 8.5.1, Figure 8.5.2 and Figure 8.6.4.

8.8.1 Mechanical impact of the repository limited to the near-field in the Callovo-Oxfordian

The mechanical evolution of the Callovo-Oxfordian layer on a large scale and of the surrounding formations is limited.

- Climatic changes expected over a million years and the internal geodynamic processes (uplift and earthquakes) are unlikely to modify significantly the natural stress field on a large scale and induce generalised deformations in the geological medium. In zones subjected to erosion, the gradual relaxation of the eroded terrains reduces the vertical stress locally. This reduction has no effect on the mechanical behaviour of the geological formations, more particularly on the Callovo-Oxfordian layer and the repository, where it is less than 5 %.
- The mechanical effects of the repository are contained in the Callovo-Oxfordian in the near-field immediately next to the engineered structures. The following points stand out in particular.
    - The compartimentalised design of the repository and the distances between engineered structures limit or prevent inter-structure mechanical interferences from the repository cells to the repository zones, particularly in terms of mechanical relaxation during construction of the engineered structures.
    - The effects of the mechanical relaxation in the Callovo-Oxfordian layer around the repository engineered structures are limited to a zone of a few meters (EDZ), not very thick compared with keeping a minimum thickness of 60 meters of Callovo-Oxfordian between the repository and the calcareous Oxfordian or the Dogger.
    - The repository takes up little space compared with the surface area of the repository in the Callovo-Oxfordian layer. The repository engineered structures are filled so that the voids are kept to a minimum. The materials used, such as swelling clay, are not very compressible and/or capable of counteracting stresses from the geological medium. This backfilling of the repository is not affected by the chemical processes. This prevents large-scale deformations or fracturing of the Callovo-Oxfordian layer and allows mechanical healing of the geological medium and the return to a homogeneous mechanical stress state.
    - The thermal load on the repository makes itself felt in the surrounding formations, but it does not last long (a few thousand years) and the rises in temperature are homogeneous in space and limited to a few degrees. The thermal load does not therefore induce significant mechanical phenomena.
    - The thermal load of the repository mainly affects the repository and the Callovo-Oxfordian layer. Nevertheless, the kinetics of the rise in temperature are slow and the thermal gradients are weak beyond a few tens of centimeters to a few meters from the disposal cells containing exothermic waste. At the scale of the Callovo-Oxfordian

layer, the thermal load is therefore relatively homogeneous. For this reason it only induces a field of thermo-mechanical stresses in the near-field of the engineered structures and induces no effect on the large scale.

- The desaturation of the argillites from the ventilation air during repository operation, then from the hydrogen from corrosion after the repository is closed remains limited to the EDZ. Its mechanical consequences are also limited to the repository near-field.

8.8.2 No significant consequence on the hydraulic and chemical evolutions of the geological medium

The mechanical evolution of the Callovo-Oxfordian layer and the surrounding formations, particularly the Dogger and the calcareous Oxfordian, is not marked by the appearance of fracturing or deformations likely to modify the flows and transport of solutes, or the chemistry of the interstitial waters, locally or on a large scale. This helps maintain the initial properties of the Callovo-Oxfordian layer. As a mechanical phenomenon, only erosion caused by climatic changes and internal geodynamics has a significant impact on the flows in the surrounding formations, as described in the chapter on hydraulic evolution (see § 6).

8.8.3 Mechanical evolution of the repository and the Callovo-Oxfordian in the near-field marked by three major periods

8.8.3.1 In the very short term: excavation of the repository and initial damage to the argillites in the near-field

The redistribution of the stresses and deformations immediately following the construction of the engineered structures instantaneously forms a damaged zone (EDZ) in the argillites immediately next to the repository engineered structures. This initial EDZ is characterised by the appearance of fissures connected in varying degrees and whose density decreases the further away from the wall. This fissuring causes increased permeability of the argillites between one and several orders of magnitude compared with the undisturbed argillites.

The extent of the EDZ in the Callovo-Oxfordian argillites has been modelled numerically. These models, based on the minimum mechanical properties of the argillites, provides conservative estimations of the extent of the EDZ. The extent thus assessed is lower at the radius of the various engineered structures. The first observations and measurements in the Meuse/Haute Marne laboratory confirm the conservative nature of these assessments at this stage.

8.8.3.2 Over a hundred thousand years: the non-saturated state of the repository and the Callovo Oxfordian near-field linked to ventilation and the production of hydrogen from corrosion

The hydraulic evolution of the repository is marked by a period of non-saturated state of the engineered structures caused by the air from ventilation during repository operation, then by hydrogen from corrosion after the closure of the engineered structures and the repository as a whole.

- The B waste disposal cells, drifts and shafts only become totally saturated beyond around 200,000 years. The lack of saturation limits strongly the chemical degradation of the ground support/liner concretes by the argillite waters and results in the mechanical properties of the repository components being maintained. During the repository operating and observation period, the desaturation of the argillites around these engineered structures slows down or even halts the argillite creep and therefore places a limited load on the ground supports/liners not degraded chemically. The re-starting of the argillite creep with their gradual resaturation produces stresses within the ground supports/liners beyond their strength after a few thousand years. However, given the gradual nature of this loading and the low number of voids within the engineered structures, combined with the limited chemical degradation of their components, this does not cause an abrupt rupture of the engineered structures. The mechanical evolution of these engineered structures is gradual, with no propagation or intensification of the EDZ.

- In the C waste disposal cells and the spent fuel disposal cells, the argillites at the periphery of the disposal cells remain saturated overall and the saturation of the swelling clay in the plugs and, if appropriate, in the engineered barriers is achieved after about 100 years. The argillite creep and swelling of the swelling clay allows the recovery of the functional clearances from the first hundred years onwards. This closing of the clearances is accompanied by temporary propagation of the EDZ around the disposal cells. Nevertheless, at the scale of a few tens of years to a few hundred years, the EDZ is sealed by the argillite creep and the swelling pressure of the swelling clay (for the C waste disposal cell and spent fuel disposal cell plugs). Given the persistence of a non-saturated state at the heart of the disposal cells and the slow progress of the corrosion of the liners and metallic linings, the waste over-packs will not be loaded by major mechanical stresses before around ten thousand years.

8.8.3.3 Beyond a hundred thousand years, over the next million years: chemical evolution of the repository and large-scale creep of the Callovo-Oxfordian

Once the repository is totally saturated, its mechanical evolution is controlled by the slow chemical degradation processes of the repository components, the argillite creep and the swelling properties of the swelling clay.

The re-starting of the argillite creep with their resaturation, and to a lesser degree their swelling, accompanies the chemical degradation of the ground support/liner concretes in the B waste disposal cells and backfilled drifts, then the B waste disposal packages. Given the low number of voids in these engineered structures, the stress variations within the argillites caused by the chemical degradation of the concretes are moderate. The argillite creep reactivated by the gradual manifestation of voids ensures a return to a stress state in equilibrium with the geological medium.

Within the C waste and spent fuel disposal cells, the argillite creep and, if appropriate, the residual swelling potential of the swelling clay in the plugs and engineered barrier permit the recovery of the voids created by the chemical degradation of the liners, linings and over-packs. As for the B waste disposal cells or backfilled drifts, the low rates of chemical evolution of the disposal cell components allow the mechanical processes to guarantee a gradual return to stress equilibrium.

Consequently, the mechanical integration of the seal engineered structures (disposal cell plug, drift seal and shaft seal) within the geological medium is a result of the accumulation of the slow chemical degradation rates of the concretes, the maintained swelling potential of the swelling clay and the argillite creep.

8.8.4 Elements with respect to reversibility

Safety in constructing and operating the repository is based on the mechanical dimensioning of the repository engineered structures, like, for example, the design of the ground supports and liners for the shafts and drifts. This involves protecting the workers not just from risks of dissemination of radioactive substances, but also against risks from underground operation throughout the entire repository operating and observation period.

The mechanical dimensioning and design of the repository in general also integrates the repository ability to offer a choice in the management of the installations and the packages disposed of. The mechanical evolution of the repository engineered structures during the observation period of the state and evolution of the repository thus participates in the definition of the recovery conditions for the waste packages.

Throughout the repository operating and observation phase, in the order of a hundred to several hundred years, the non-saturated state of the repository is accompanied by the slowing down, or even the halting of the argillite creep and the absence of chemical degradation of the engineered structure components. The result is limited mechanical evolution of the repository engineered structures: the mecahnical stability of the engineered structures and the integrity of the disposal packages are maintained. A repository operation over several centuries under a reversible process has no effect on the phenomenological evolution of the repository in the long term.

8.8.4.1 C waste disposal cells and spent fuel disposal cells

The mechanical integrity of the C waste disposal cells and the spent fuel disposal cells is provided by the metallic liner and/or lining. They only rupture and are no longer leak tight after the closure of the installation clearances (in the order of centimeters) and their discharge of strength through corrosion. Given their thickness, the slow argillite creep rates and the slow corrosion rates, the disposal packages are only loaded after discharge of strength of the liners and linings after 1,000 years.

8.8.4.2 B waste disposal cells, drifts and shafts

Loading of the ground supports/liners of the B waste disposal cells, drifts and shafts until they rupture is a slow process. The slow argillite creep rates, the low temperatures and the absence of cement-based degradation results in the containment properties of the ground supports/liners being maintained, causing in turn stability of the engineered structures and no loading of the B waste disposal packages for periods at the scale of a thousand years or more. In addition, they undergo little if any chemical degradation in the desaturated hydraulic conditions prevailing within the disposal cells during this time.

8.8.5 Limited evolution of the initial EDZ from its creation to its healing

The choice of backfilling materials chemically compatible with the geological medium and their installation methods with maximum limitation of the residual voids within the engineered structures gives overall mechanical stability to the various engineered structures. This prevents propagation and/or intensification of the initial EDZ.

- During the repository non-saturation phase, particularly around the B waste disposal cells, the drifts and shafts where the argillites are highly desaturated, the chemical and mechanical processes like concrete degradation and argillite creep are slowed down, even halted. Desaturation causes the argillites to stiffen and may result in hydric fissuring of the argillites in a thin layer a few tens of centimeters around the engineered structures. With resaturation, the effect of the argillite creep and swelling is to heal this fissuring. The alkaline disturbance in the argillites also helps heal the EDZ hydraulically.
- Around the C waste and spent fuel disposal cells, the closure of the installation clearances in the liner and lining from argillite creep and, to a lesser degree, the rise in temperature in the argillites during the first tens of years after emplacement of the disposal packages cause the argillites to deform, resulting in a transient increase in the EDZ for a limited period (100 to 150 years). Beyond this closure phase of the installation clearances, the argillite creep, accelerated by temperatures remaining high, and the swelling pressure of the swelling clay in the engineered barriers and disposal cell plugs gradually close this fissuring. Once the installation clearances are closed, the EDZ around the C waste disposal cells and the spent fuel disposal cells heals during the first tens of years to first hundreds of years.
- Similarly, around the seal engineered structures (disposal cell plugs, drift seals and shaft seals), the swelling clay, which retains its swelling properties, and the argillite creep heals the EDZ.
- In the longer term, the extent of the EDZ around the various engineered structures does not extend beyond the initial EDZ and the permeability is increased by at least one order of magnitude compared with the undisturbed argillites.

8.8.6 Maintenance of the hydraulic properties of the disposal cell plugs and the seals over time

The disposal cell plugs, drift seals and shaft seals limit the transfer of the radionuclides via the engineered structures and their near-field.

The mechanical evolution of the disposal cell plugs and the seals are characterised by tremendous mechanical stability combined with healing of the EDZ around these engineered structures. In addition, the hydraulic keys, a design feature intended to interrupt the zones with the highest permeability, assist in achieving an overall permeability of these engineered structures that is increased by approximately one order of magnitude only compared with the permeability of the undisturbed argillites.

9

Geodynamic evolution of the Callovo-Oxfordian, the surrounding geological formations and the surface environment

9.1 **Introduction** 409

9.2 **Internal geodynamics** 409

9.3 **Climate change** 410

9.4 **Consequences of climate change** 416

9.5 **Topographic changes** 420

9.6 **Effects of the evolutions on geological formations and surface environments** 423

9.7 **Summary of the geodynamic evolutions of geological formations and surface environments** 427

9.1 Introduction

As seen in the preceding chapters (cf. § 5 to § 8) the phenomenological evolutions relating to the repository only concern the repository itself and the near-field geological medium. The characteristic times of these evolutions correspond to transients lasting a few tens of thousands of years at most.

The characteristic times of geodynamic evolutions are much longer: they concern time scales ranging from a hundred thousand years to a million years or more. Their potential consequences are limited to the formations close to the surface. They therefore essentially change the hydraulics of the surrounding formations and, consequently, the transfer of radionuclides and toxic chemical elements in these formations and their return to the biosphere.

This chapter firstly discusses in detail the causes of geodynamic evolutions: internal geodynamics (subsurface movements, especially vertical movements which, are the “driving forces” of erosion, § 9.2) and external geodynamics (climate variations, § 9.3).

The direct consequences of this evolution are then described on the scale of the sector (Brulhet, 2005b):

- the cyclical formation and disappearance of more or less continuous permafrost, over periods of the order of a hundred thousand years, associated with changes to the surface environment (soils, flora and fauna) (cf. § 9.4),
- change to surface morphology over the next million years (cf. § 9.5) according to a continuous process, resulting from the coupling between internal and external geodynamics.

Finally, the effects of these evolutions on the various geological formations and on the surface environment are presented in § 9.6.

A summary (cf. § 9.7) will focus more particularly on these effects with regard to the transfer of radionuclides and toxic chemical elements.

9.2 Internal geodynamics

Subsurface movements and the state of the natural stresses manifested therein are determined by the tectonics of the plates which move slowly: the present-day convergence between the European plate and the African plate is estimated at a few millimeters per year (Le Pichon, 2004).

The region has not been greatly deformed by the Alpine orogenic phases which have followed one another over the course of the last tens of million years (slight regional faults throws and acquisition of minor regional dips). The various data available both on the scale of the West European plate (Grellet et al., 1993) and on the scale of the sector (Brulhet, 2005a) show that tectonic stresses and the resulting deformations have evolved very little for five million years. Even if the mantle and crust mechanisms involved are not yet fully understood, almost all uncertainty regarding the probable evolution of the geological framework in the sector over the coming hundreds of thousands of years has been dispelled. Over this time scale, this framework will remain outside the active volcanic fields (located in the provinces of the French Massif Central and Eifel (Brulhet, 2005a ; Brulhet, 2005b) and the neighbounring areas currently subjected to moderately active tectonic deformations (West European rift, Ardennes border and Morvano-Vosgian sill) (Grellet et al., 1993). The present-day pattern of stresses and deformations in the sector will therefore last over the next million years.

The deformation rate is very slow on the scale of the sector and is likely to remain so in the future. Average annual displacement rates on the fault planes are estimated at 0.0001 to 0.001 mm (Brulhet, 2005b). The absence of quaternary signs of tectonic activity on the faults surrounding the sector confirms that possible tectonic movements are limited to very slight recurrences of pre-existing faults which structure the basement. In this context, the possibility of new faults being created in the sedimental cover, and subsequently in the Callovo-Oxfordian layer, is excluded in the transposition zone where such faults do not exist. This evaluation is confirmed by the stability of the zone throughout the entire history of the tertiary and quaternary periods which were however rich in tectonic events on a much greater scale than those expected during the next million years (Oligocene distension and Alpine compression notably). The maximum possible earthquakes in this context therefore show a moderate magnitude, of the order of 6.1 +/- 0.4 on the large faults surrounding the sector, with return periods of between 100,000 and 1,000,000 years (Brulhet, 2005a).

Vertical tectonic movements resulting from internal geodynamics determine, in association with sea level variations, the geomorphological evolution of continental regions. This evolution is generally controlled by erosion, sedimentation (filling) or alteration processes in the peneplain according to relative movements of uplift, collapse or stability respectively.

Over the entire Paris Basin, the observations made and the analyses conducted show tectonic uplift presenting spatial variability when examined in detail. This uplift would be more pronounced in the south-eastern part of the Paris basin where the cuesta morphology is particularly developed and would culminate on its border (prominent basement area in the Vosges and the Morvan) (Mégnien, 1980 ; Mercier & *al.*, 2004). The average values, calculated from observed altitude differentials and simulations of the stages of river incision (position of the paleoterraces) (Brulhet, 2005b ; Leroux & Harmand, 1998), are of the order of 50 to 70 $m.My^{-1}$ in the Paris basin, with a minimum of 10 to 20 $m.My^{-1}$ in the Loire Valley, and a maximum of the order of 100 $m.My^{-1}$ on the south-eastern border (Vosges-Morvan). These data are consistent with the more global estimations mentioned elsewhere (average uplift of the order of 100 $m.My^{-1}$) (Pomerol, 1978).

In this framework, the Meuse/Haute-Marne sector belongs to a region to which a uniform average uplift rate of the order of 80 $m.My^{-1}$ can be attributed. This tectonic stability is illustrated, on the sector scale, by various erosion indicators (paleosurfaces) which are all found at comparable altitudes (Brulhet, 2005b ; Mégnien, 1980).

In the tectonic context defined above, this uplift rate will remain constant for the next millions of years.

Furthermore, in the glacial maximum phase, the ice caps progress southwards as far as Germany and Southern England (see below § 9.3). The isostatic movements under the areas of the ice caps are the cause of an adjustment "ridge" which affects the site zone periodically. The corresponding variations in altitude, estimated by modelling (Brulhet, 2005b), are slight (10 to 20 m) and apply to the whole of the Northern France. The consequences of these periodic movements in terms of erosion are not detectable and are included in the erosion balances estimated by climate cycle from field data.

9.3 Climate change

The changes affecting the earth's climate during the Quaternary period – the last two million years – are explained by the astronomical theory of climate (Andersen & Borns, 1994 ; Berger, 1992 ; Joussaume, 1999): glacial and interglacial periods have succeeded one another, linked to variations in the orbital parameters characterising the earth's rotation around the sun. The duration of the cycles thus defined is of the order of 100,000 years. The most recent striking event in this history is the last glacial maximum 18,000 ± 2,000 years BP (Andra / CNF-INQUA, 1999). These cycles are perfectly illustrated, for example, by analyses of core samples of ice from the Antarctic providing a vision of climate change over the last 400,000 years (Petit et al., 1999) (Figure 9.3.1). By extrapolating this theory to the future for the Meuse/Haute-Marne site, we can assume that these quaternary climate cycles will continue in the absence of anthropic disturbance of the climate (see below) and given the slow rate of change in other factors (plate tectonics, major change in morphology, etc).

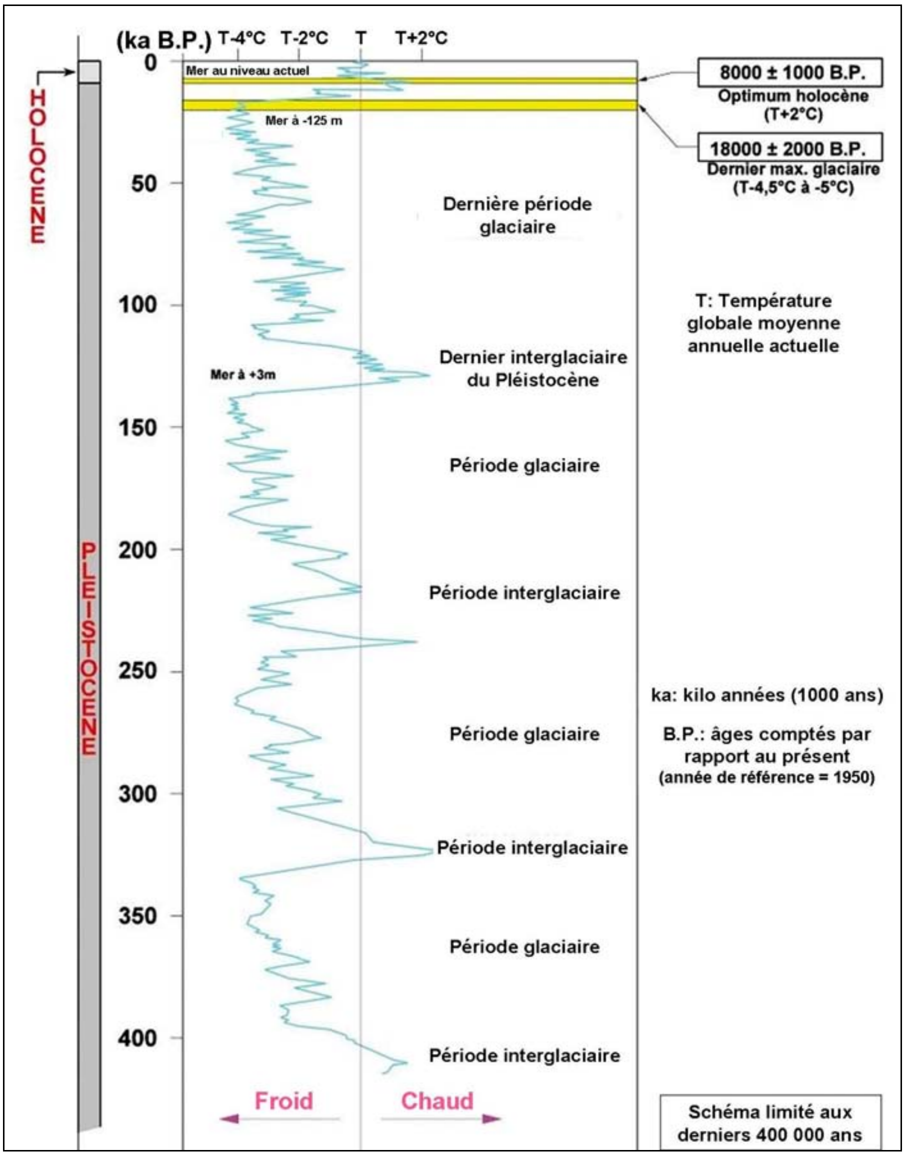

Figure 9.3.1 *Variations in temperature in the Antarctic (Vostok) over the last 400,000 years (from Petit et al., 1999)*

These glacial/interglacial cycles may contain internal fluctuations due to the superposition firstly of shorter cycles (20,000 years) and, secondly, of brief events (a few centuries to thousands of years), occasionally of high amplitude, which do not appear to be governed by the astronomic theory of climate (Brulhet, 2005b). In spite of such fluctuations, for a situation similar to that of the sector, each of these glacial/interglacial cycles presents a succession of climates, comparable from one cycle to another, which can be represented by three phases (Texier & Leclerc-Cessac, 2005) (Figure 9.3.2).

- The cycle begins with a period of temperate/oceanic climate (interglacial), such as the present-day climate (cf. § 3.5.1), with average annual temperatures of the order of 10 °C and annual precipitation of 800 to 1,100 mm. Within a cycle, this period is generally quite short, from 10,000 to 30,000 years approximately.
- The subsequent boreal climate is much cooler (average annual temperature of the order of 3 °C), with negative average temperatures from November to March causing a "deep" seasonal frost. Precipitation is significantly lower with an annual average of 600 to 700 mm.
- Finally, the establishment of an even colder tundra climate (negative annual average temperature of -2 to -3 °C, and temperatures below 0 °C for a large part of the year, from October to May) leads to the creation of permafrost. Average precipitation is of the order of 400 mm. On a European scale, this phase corresponds to the maximum extension of the ice caps. Reconstitutions of the last glacial maximum show that they covered the whole of the Nordic countries, to the centre of Germany and southern England (Figure 9.3.3). Following this phase, a new cycle begins with a rapid change to a temperate climate.

The last two climatic stages (boreal and tundra) represent the glacial stage which lasts much longer (70 to 90,000 years per cycle, on average) than the interglacial. The dynamics of the transition from one stage to another are also very different: the change from interglacial to glacial, and up to the glacial maximum, is a very gradual, continuous process (if we disregard the fluctuations mentioned earlier). The change from glacial to interglacial is however completed much more quickly – in a few thousand years (Brulhet, 2005b).

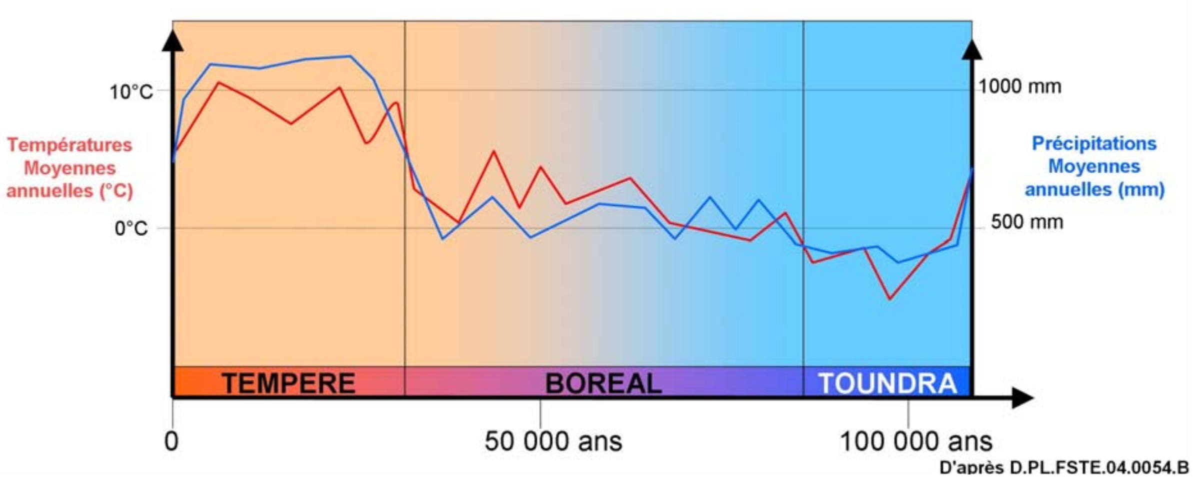

D'après D.PL.FSTE.04.0054.B

Figure 9.3.2 *Schematic representation of the main climatic phases during a glacial/interglacial cycle, for a situation comparable to that of the Meuse/Haute-Marne site*

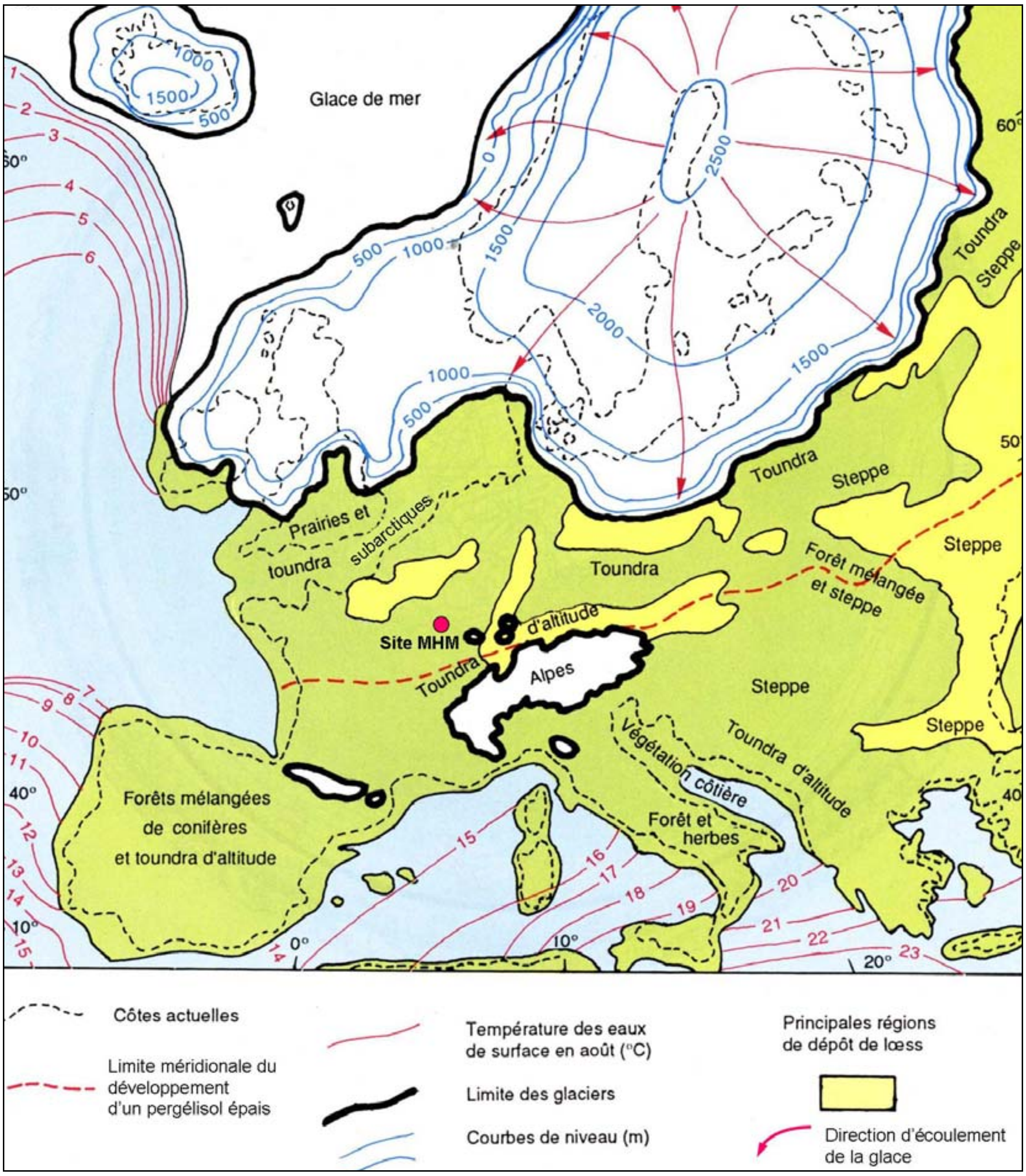

Figure 9.3.3 *Ice cap areas and principal environments during the last glacial maximum (Berger, 1992)*

Models (BIOCLIM, 2002 ; BIOCLIM, 2003b ; Loutre & Berger, 2000) produced on this basis predict the following evolution for the future.

- The current interglacial period is likely to last 50,000 years before entering a new ice age (Figure 9.3.4, curve n°1). The short, colder episode predicted at 20,000 years, especially sensitive at high latitudes, will have no notable impact at the level of the Meuse/Haute-Marne site. This interglacial period will be followed, from 50,000 years hence, by a sharp global cooling tendency and therefore by the extension of the ice caps. After a short milder period at around the 60,000-year mark, cooling will resume and the ice caps of the Northern hemisphere will reach their maximum volume after around 100,000 years. This maximum volume of ice will be less than the one reached during the last glacial maximum 18,000 years ago (34 million km^3 compared with 55 million km^3). Following this glacial maximum, the climate will warm and a new climate cycle with its internal fluctuations will begin after around 110,000 years.

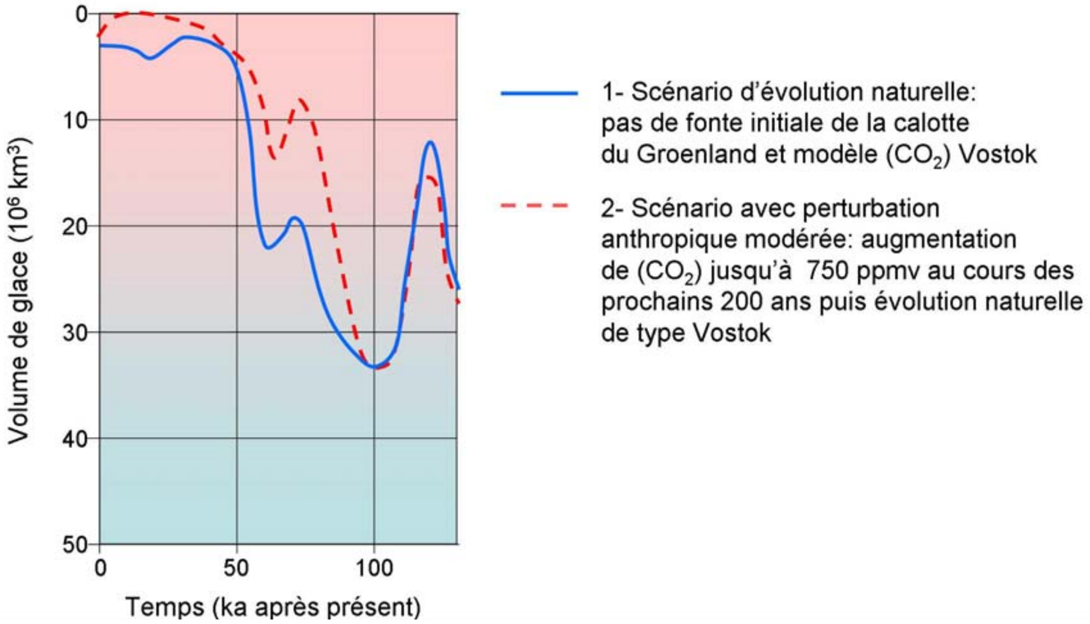

Figure 9.3.4 *Simulations of the volume of ice in the Northern hemisphere over the next 100,000 years (according to Loutre & Berger, 2000)*

- In the longer term, over 1 My, the models confirm the continuation of these cycles lasting 100,000 years on average with, however, longer cooler periods up to 500 / 600,000 years and significantly shorter cycles thereafter (Figure 9.3.5).

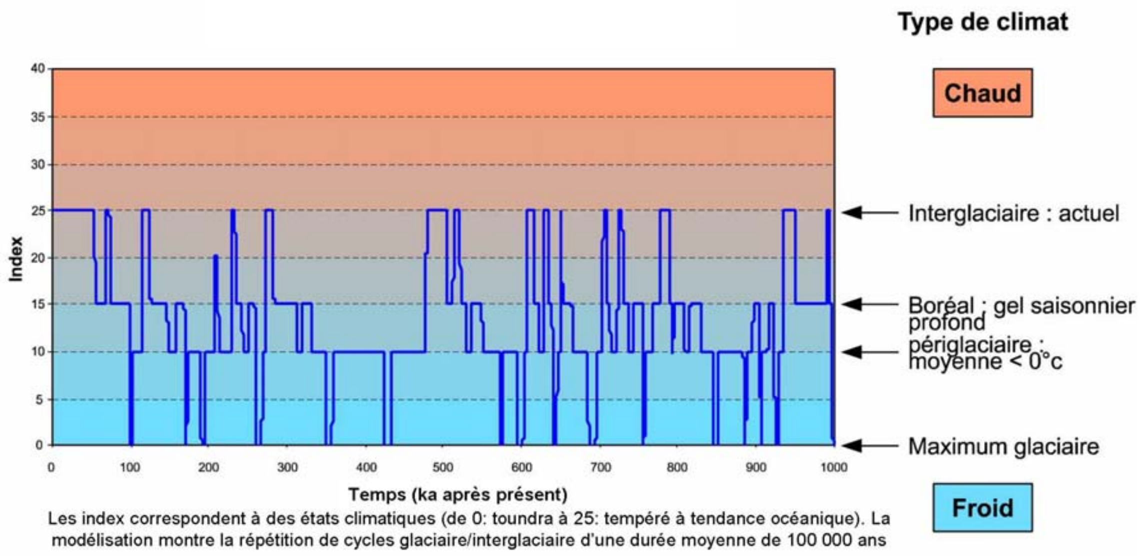

Les index correspondent à des états climatiques (de 0: toundra à 25: tempéré à tendance océanique). La modélisation montre la répétition de cycles glaciaire/interglaciaire d'une durée moyenne de 100 000 ans

Figure 9.3.5 *Natural climate change scenarios for the Meuse/Haute-Marne region (according to BIOCLIM, 2003a)*

This natural climate change may be disturbed on a long-term basis by human activities and notably by the massive emission of greenhouse gases (BIOCLIM, 2002 ; Texier & Leclerc-Cessac, 2005). Various modelling approaches, taking into account different greenhouse gas emission scenarios, have been attempted to quantify this disturbance. For "moderate" anthropic disturbance (curve n°2 of Figure 9.3.4), the models show the disturbed evolution reproducing the same tendencies over a cycle as the undisturbed evolution: the cooler episode at 20,000 years may be wiped out according to some hypotheses, the 60,000-year minimum is much less significant but the amplitude of the glacial maximum at 100,000 years remains unchanged (Loutre & Berger, 2000).

The approaches conducted in the scope of the BIOCLIM project (BIOCLIM, 2002 ; BIOCLIM, 2003a), more specific to the North-East of France, confirm this tendency. However, other scenarios with greater disturbance have also been tested (CO_2 increasing to approximately 1,150 ppm over the next 300 years and a subsequent exponential decrease up to 1 million years). The models all show, for disturbances of these magnitudes, a sharp decrease in the volume of ice in the Northern hemisphere and a lengthening of the current interglacial period by several tens of thousand years with the next installation of a periglacial climate pushed back to around 170 to 180,000 years, for the North-East of France (Figure 9.3.6). Its amplitude (volume of ice estimated at 17 million km^3) would be considerably less than that of the last glacial maximum and the volume modelled in the scope of a natural evolution (55 and 35 million km^3 respectively). Following this glacial episode, the natural climate cycles are not resumed immediately as they could be deferred to beyond 600,000 years (Figure 9.3.6). Up to 600,000 years, this scenario with anthropic disturbance shows interglacial periods with a significantly warmer climate than the present temperate period with oceanic tendency (index 30, Figure 9.3.6). This climate, similar to that found on the Atlantic coast of Spain or Portugal, shows a strong oceanic tendency with abundant precipitation, of the same order of magnitude as the present-day climate in the region of the site, but with average annual temperatures 4 to 5 °C higher (Texier & Leclerc-Cessac, 2005). Overall, the appearance of this climate over the next 600,000 years has little impact compared with the present-day climate. It can therefore be considered that, during this period, in the scope of a scenario with anthropic disturbance, the representative climate of the current interglacial will be the dominant climate.

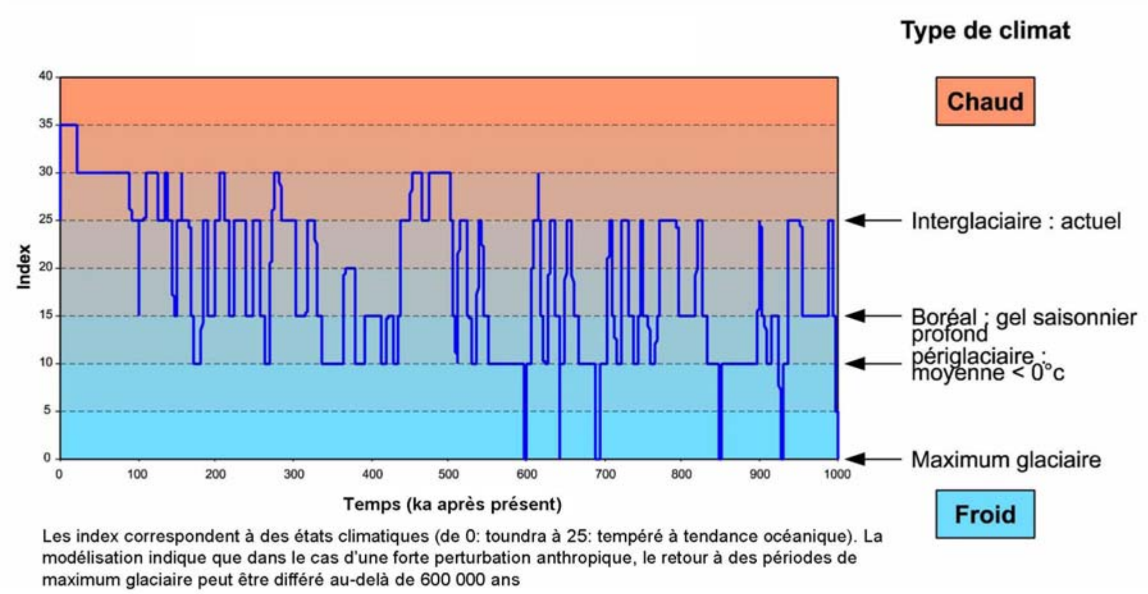

Les index correspondent à des états climatiques (de 0: toundra à 25: tempéré à tendance océanique). La modélisation indique que dans le cas d'une forte perturbation anthropique, le retour à des périodes de maximum glaciaire peut être différé au-delà de 600 000 ans

Figure 9.3.6 *Climate change according to a scenario with major anthropic disturbance for the next million years at the Meuse/Haute-Marne site (according to BIOCLIM, 2003a)*

As a general rule, these long-term climate change models are designed more to assess tendencies than to make fine predictions of these changes. They remain highly dependent on the scenarios selected, as shown by all of the simulations produced in the scope of the BIOCLIM project. However the multiplicity of the tested scenarios allow to propose the two evolutions described above (natural evolution and evolution affected by major anthropic disturbance) as extremes of the possible climatic situations over the next million years.

9.4 Consequences of climate change

9.4.1 Periodic formation and disappearance of permafrost

By definition, permafrost is the part of the earth in which water remains permanently frozen all year round. Generally, the formation of permafrost corresponds to a dynamic thickening and resorption process (Brulhet, 2005b). It can be illustrated by an increase in the frozen thickness, progressively or in stages, as soon as the average annual temperatures are negative over relatively long periods (tundra-type climate). At the end of the glacial period, it is resorbed from the top (from the surface due to climatic warming) and from the bottom (geothermal flux). Laterally, it may be continuous or discontinuous depending on the glaciation intensity and the surface conditions (presence or absence of snow cover, surface hydrology, slope exposure, etc.).

The analyses and reconstitutions conducted over the most recent climate cycles on the scale of the Paris Basin (Brulhet, 2005b) confirm the presence of thick, continuous permafrost over the whole of Eastern and Northern France throughout glacial maximum periods. For less extreme climatic situations, this continuity is affected by the major valleys in these regions.

On the site of the underground research laboratory, according to the information derived from the various reconstitutions (zero isotherm penetration curves over the last climate cycle, spread of permafrost according to morphology, etc.), the development of continuous permafrost over the entire zone during the glacial maximum period and also during long, cold periods (from 350,000 to 450,000 years, from 560,000 to 620,000 years and from 850,000 to 900,000 years, in a undisturbed situation) can be predicted for the next cycles.

On the basis of models produced from data from the last glacial cycle, this permafrost has the following structure (Brulhet, 2005b).

- Near the surface, the development of segregated ice, with ice lenses, obstructs all porosity. On the plateaux (limestone substratum), this zone is the seat of gelifraction phenomena. The maximum thickness of this zone, subjected to permanent freezing on each cycle, is of the order of 35 m, which is consistent with the observations of fractures in the upper terrains in the underground research laboratory shaft. For the Meuse / Haute-Marne site, this zone concerns the Calcaire du Barrois (Tithonian) and the upper part of the Kimmeridgian marls.
- Below, the frost only penetrates deeper, down to a depth of 100 to 200 m, through the networks of joints and fractures. These become less and less dense with increasing depth. Between these subvertical thin layers, the pores are occupied by increasingly salty water (salt expelled by the frost) in a cryotic state. At the site location, this zone only concerns the uppermost porous horizons of the calcareous Oxfordian.
- Lower down, as far as the 0 °C isotherm (approximately 300 m at most), ice is no longer found, but water in a cryotic state may be mixed with hydrates produced from gases dissolved in the aquifers or present in the rock. These hydrates are likely to form in the bracket of +5 to -5 °C, i.e. up to a maximum of 400 m deep, up to the deepest porous horizons of the carbonated Oxfordian right above the site. However, the formation of gas hydrates in this formation can be ruled out as this requires a quantity of methane much higher than that dissolved in the carbonated Oxfordian water (Cojan, 1999). Moreover, absence of natural gas resources around the site (mainly due to the absence of formation from the Westphalian era, cf. § 3.2) limits the possibility of formation of gas hydrates when permafrost is formed.

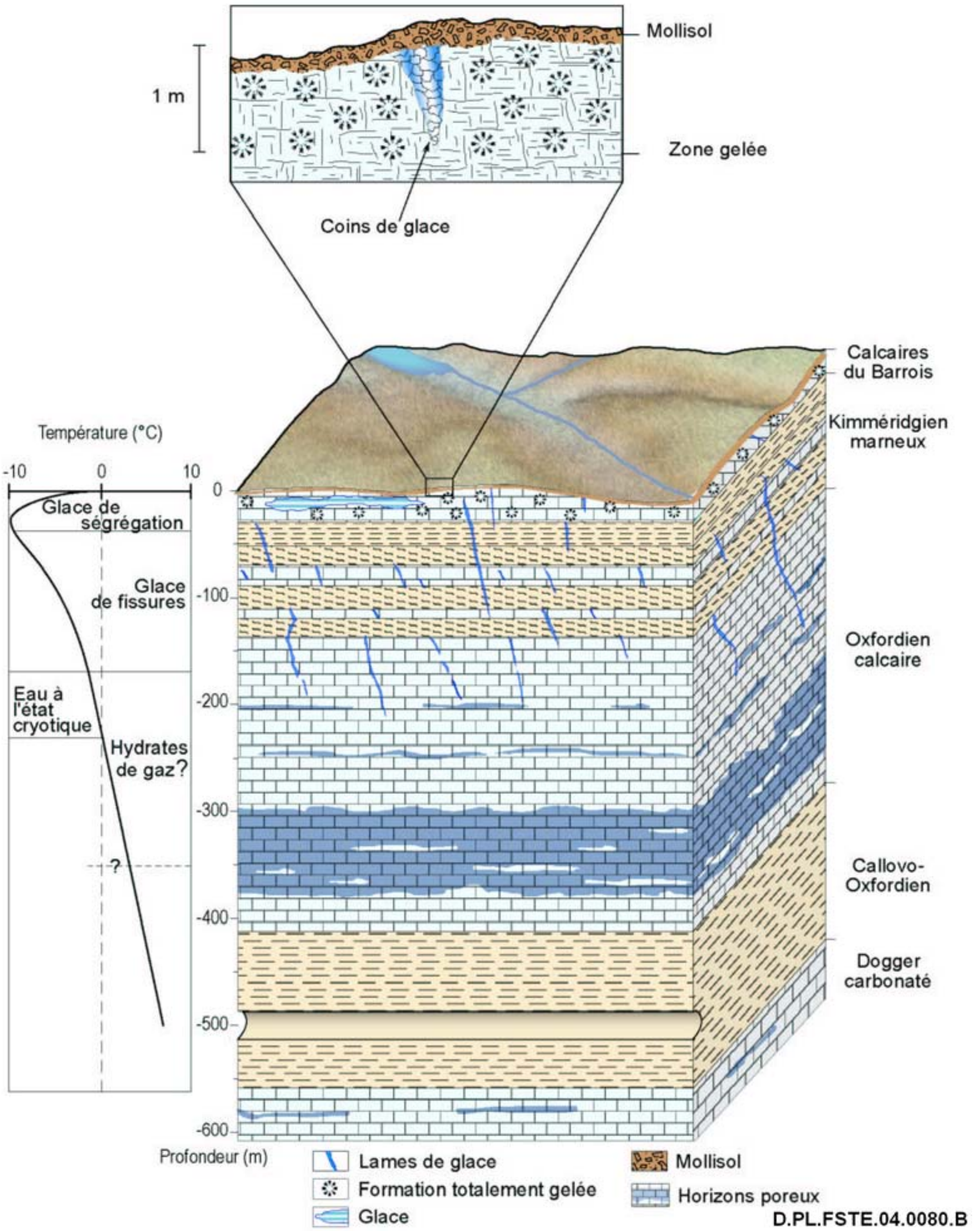

Figure 9.4.1 Conceptual model of future permafrost at the Meuse/Haute-Marne site

This permafrost is less thick under valleys. However, it does remain continuous during glacial maximum situations as seasonal flows do not provide the conditions for deep thaw. Nevertheless, at aquifer emergence points, water outlets can prevent the formation of permafrost on a very local scale. In this case, an unfrozen channel drain may subsist, marked in winter by a “tongue” of ice in the valley floors (talik).

For other, less intense, cold episodes, the permafrost is still continuous on the plateaux, but is not as thick as mentioned above. As the rivers continue to flow, the valleys form break lines.

In the case of major anthropic disturbance (massive greenhouse gas emissions according to the hypotheses mentioned above), the evaluations carried out show that the development of continuous permafrost does not appear possible before the return to undisturbed climate cycles, around 600,000 years (Brulhet, 2005b ; Texier & Leclerc-Cessac, 2005).

9.4.2 Biosphere evolution

Climate cycles also have a major impact on the surface environment. This environment, as described in chapter 4.4 in its present-day, progressively evolves with the change to a boreal climate (Texier & Leclerc-Cessac, 2005) (Figure 9.4.2). During the winter, the drop in temperatures causes seasonal freezing of rivers, lakes and the top meters of soil, causing a reduction in available surface water and stopping the infiltrations.

Nevertheless, water remains available locally all year round at groundwater outlets. In the spring, the thaw of snow and ice built up on the surface during the winter increases surface runoff, destabilise slopes and erode soils. In valley floors, rivers will swell (flow rate multiplied by four compared with the present-day state). Such flow rates begin to erode the alluvial valleys. On the plateaux, the natural vegetation evolves into a boreal forest adapted to the cold. Soil genesis slows down and the soils become charged with organic matter. Within a few thousand years, these soils turn to brown soils on the plateaux and gravelly soils in the valleys. Peat bogs develop in the marly depressions.

All of these factors condition human activity: the valley bottoms become more hostile and farmland is reduced. Farming is still possible, however, on the plateaux.

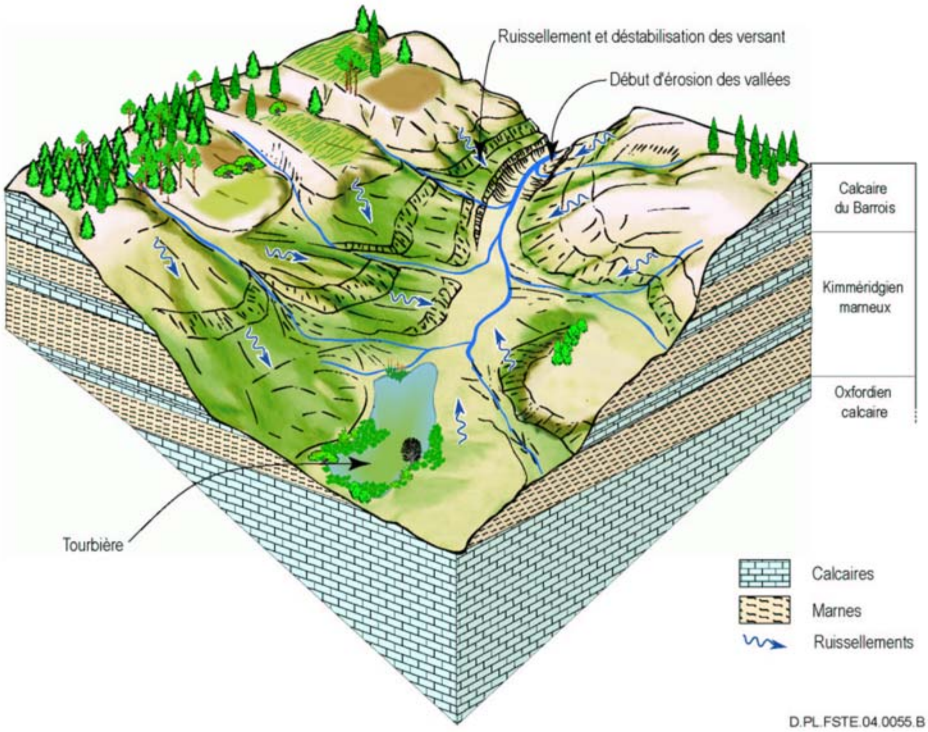

Figure 9.4.2 *Schematic representation of the "boreal" stage of the climate cycle - Vegetation and biosphere evolution around the underground research laboratory site*

The phenomena described above are continued with the change to a tundra type of climate and the additional cooling that it brings (Texier & Leclerc-Cessac, 2005) (Figure 9.4.3). The long winter freezes lakes and rivers for a large part of the year. Access to surface water is then extremely restricted and the presence of permafrost prevents the use of near-surface groundwater. Only a few springs are sustained (taliks). Only the top meters of soil thaw during the short summer. Erosive phenomena due to thawing ice and snow are amplified compared with the preceding climatic situation: the slopes are denuded (screes) and become unstable, increasing erosion still further. At the bottom of the valley, residual alluvial deposits are carried away by the floods (flow rates multiplied by eight compared with the present-day state), soils disappear and the rivers attack the substratum among gravels laterally transported. Peat bog and marshes develop in clay zones. On the plateaux, the soils turn into Arctic brown soils. The aridity, low temperatures and destructive action of the freeze/thaw cycles lead to the disappearance of trees and encourage the development of a low, herbaceous vegetation typical of tundra environments: dwarf birch and willow, juniper, lichens and fungi. Farming activities are further reduced compared with the boreal stage of the climate cycle. On the plateaux, these activities focus on rearing livestock in stables. Natural spaces increase with fauna adapting to the cold (reindeer, musk-ox, wolves, etc.) and becoming largely migratory.

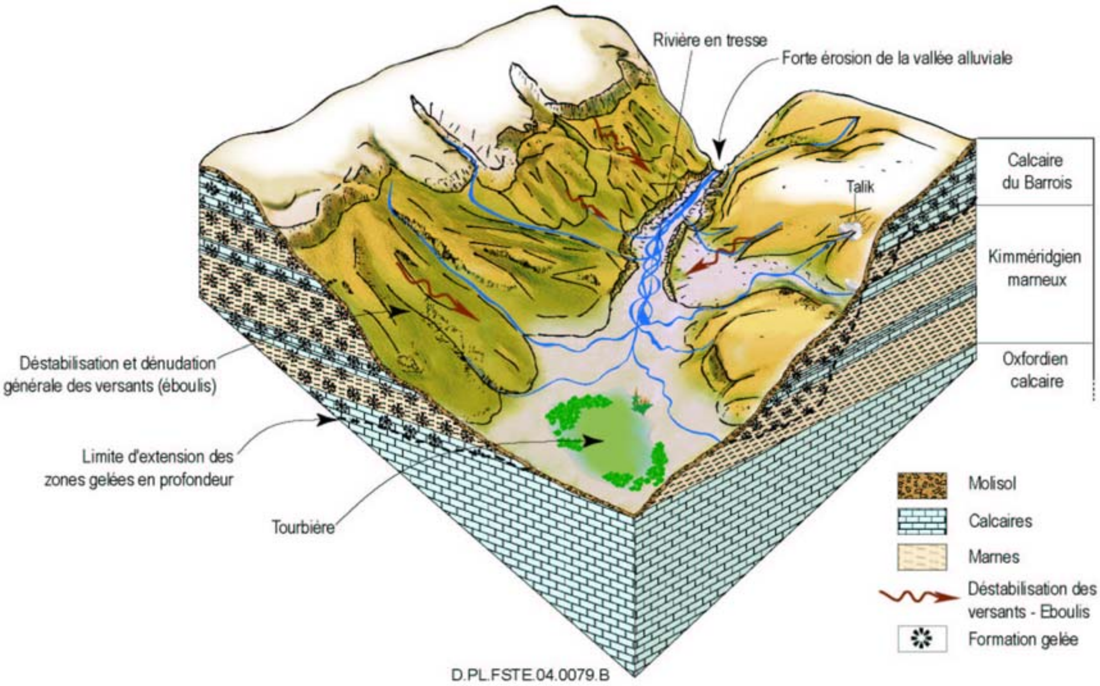

Figure 9.4.3 Schematic representation of the "tundra" stage of the climate cycle - Vegetation and biosphere evolution around the site

At the end of the glacial period, the relatively quick return to temperate conditions restores the present-day situation: reconstitution of the soils and alluvial plains following permafrost resorption (adjustment in the runoff and river flow rates), reformation of dense plant cover and diversification of fauna, year-round availability of water resources (increased precipitation and reduced winter freezing periods), development of farmland not only on the plateaux and in the valleys, but also on the peat bog and in the marsh areas inherited from the preceding cold period.

In the case of major anthropic disturbance of the climate, these cycles are disturbed over the next 600,000 years. Over this time, modelling shows a predominance of temperate climate, occasionally warmer than the present-day climate at the Meuse/Haute-Marne site, with a few short, colder intervals (boreal) (Brulhet, 2005b ; Texier & Leclerc-Cessac, 2005).

9.5 Topographic changes

The dynamics of the morphology evolutions are controlled by processes which interact according to very different time scales. We find:

- periodical changes, linked to the cyclic nature of climatic variations and notably glacial/interglacial cycles (runoff and surface erosion control, frost action, etc.), evaluated in the above paragraph,
- gradual changes, on the scale of a succession of several glacial/interglacial cycles, the effects of which cumulate over the long term and are controlled by tectonics.

Long-term phenomenological evolutions are evaluated on the basis of the consequences of several past cycles, extrapolated for the future by considering the internal geodynamic hypotheses already described: moderate uplift on the scale of the next million years (of the order of 100 meters.My^{-1}), in continuation of past uplift (Brulhet, 2005b).

These evolutions show dynamics specific to each geomorphological zone. On the scale of the sector, the dynamics of the topographic evolution are illustrated as follows (Brulhet, 2005b) (Figure 9.5.1).

- The valleys and flood plains evolve quickly, over a few millennia, on entering the glacial phase. Over the long term, the ranges of incision rate, integrated over several cycles, are dependent on the history of each section of valley (capture phenomena modifying flow rates, hydrographic conditions, etc.) and the nature of the locally incised substratum. The analyses conducted show that, over the long term, the incision rates in the floor of major valleys are of the same order of magnitude as the tectonic uplift – around a hundred meters per My (on the basis of uplift continuing with the same dynamics as at present). For the post-500,000 year period, a deceleration in uplift would result in a reduction of these incision rates. At the hydraulic head of the valley, erosion rates are of the same order of magnitude as on the plateaux (see below). Along the course of the valleys, the rates are therefore variable according to the sections in question and depend on the specific features of each river or stream (slope, nature of the substratum, etc.). Capture phenomena remain essentially local, at least over the first 500,000 years, therefore the incision rates proposed in the main valleys can be considered permanent.
- The evolution dynamics of limestone plateaux are weak. The values obtained from the reconstruction of the estimated initial surface positions show an ablation rate of a few meters per 100,000 years. Unlike the valleys, this evolution occurs essentially during interglacial periods, the predominant phenomenon being the dissolution of carbonates by meteoric waters.
- Located at the bottom of the cuestas, the clay and marly depressions corresponding to the Callovo-Oxfordian and Kimmeridgian formations show an evolution conditioned, in the long term, by the outcropping of the underlying limestone layers. The average ablation rates in these clay and marly depressions are of the order of 3 to 5 m per 100,000 years.

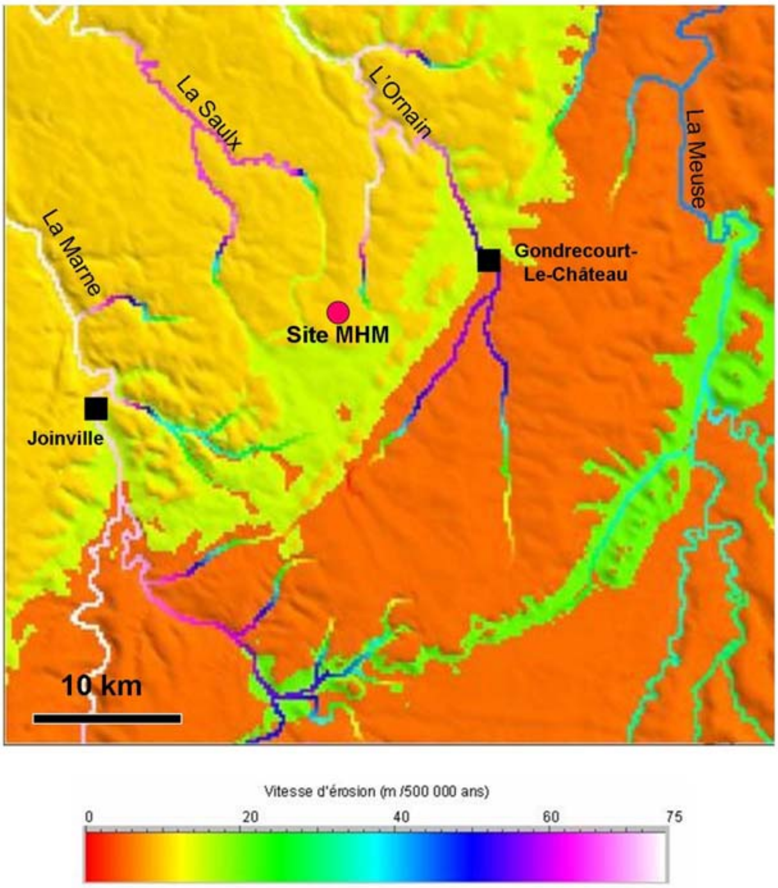

D'après D.PL.ASTE.05.0288.A

Figure 9.5.1 Spatial variability in long-term average erosion rates on the scale of the sector

The main long-term evolutions in the morphology of the sector are therefore (Brulhet, 2005b), (Andra, 2005h) (Figure 9.5.2):

- a retreat of the cuestas to the north-west (at a rate of 1 to 2 km.My^{-1}), initiated by the lowering of the surface of the plateaux and facilitated by slope destabilisation during the glacial phases. As a result, the Calcaire du Barrois (Tithonian) around the location of the underground research laboratory will completely disappear over the next million years. Generally, this retreat of the limestone formations is accompanied by the retreat of the karstified zones which are observed in these formations when outcropped (see § 3.3.2). Similarly, the outcropped Kimmeridgian marl zones, more permeable overall than the zones under cover, are displaced northwards ;
- a downcutting of the valleys due to the selective erosion between these valleys and the plateaux surfaces with outcropping of older geological formations in the valley floors (appearance of calcareous Oxfordian in the floor of the Ornain valley to the north of the site, northward displacement of the outcrop zones in the Marne valley and appearance of the Oxfordian limestones, upstream of the Saulx valley, to the west of the laboratory). However this downcutting will not cause major changes to the landscape or to the initial topographic conditions.

This evolution will remain largely identical in the case of a major disturbance to the climate cycles, notably due to anthropic activities.

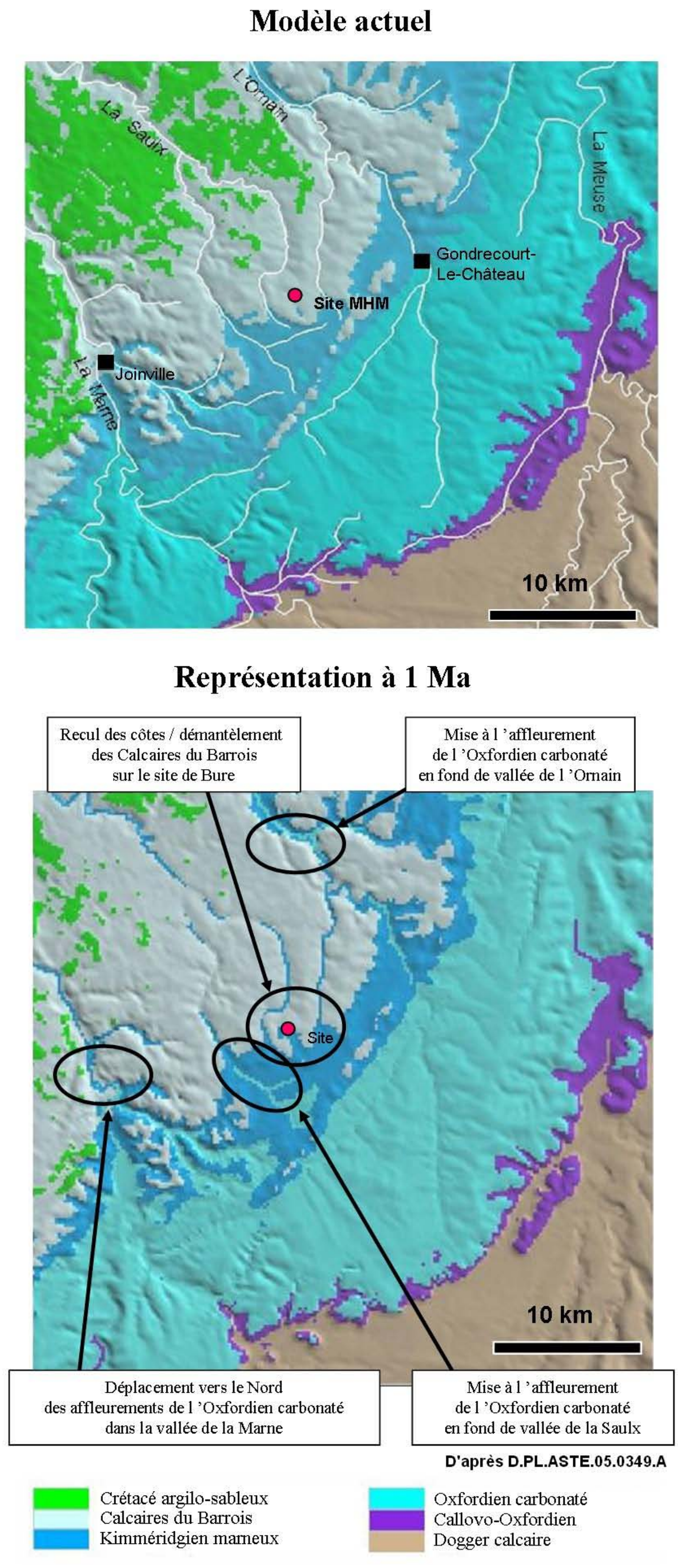

Recul des côtes / démantèlement des Calcaires du Barrois sur le site de Bure

Mise à l 'affleurement de l 'Oxfordien carbonaté en fond de vallée de l 'Ornain

Déplacement vers le Nord des affleurements de l 'Oxfordien carbonaté dans la vallée de la Marne

Mise à l 'affleurement de l 'Oxfordien carbonaté en fond de vallée de la Saulx

D'après D.PL.ASTE.05.0349.A

Figure 9.5.2 *Evolution in the morphology of the sector from the present day to one million years' time*

9.6 Effects of the evolutions on geological formations and surface environments

On the scale of the sector, the impact of the geodynamic evolution on the geological formations varies considerably depending on whether we consider the Callovo-Oxfordian, for which the consequences are slight, or the surrounding formations or surface environment which show periodical changes (linked to the climate cycles) and a long-term evolution (linked to topographic changes).

9.6.1 Callovo-Oxfordian

Over the long term, due to the depth of the layer and the location of the site, the Callovo-Oxfordian and the repository structures are barely sensitive to either internal (stress state variations, earthquakes, etc.) or external (climatic variations and surface effects) geodynamic phenomena over the transposition zone.

As far as the stress state is concerned, it has been acquired for over 20 million years and is not likely to change over the next million years. Only erosion phenomena will alter the vertical stress but such erosion will not exceed 40 to 60 m at most (Brulhet, 2005b). Indeed the laboratory site, considered in the reference scenario for the repository position in the scope of this analysis, corresponds to the Barrois plateau and is some distance away from the major valleys where rates of erosion are likely to be higher. The modification of the vertical stress resulting from erosion will therefore be negligible and not change the present-day stress state.

Analyses of the effects of possible earthquakes (and their return period) over the next million years show that earthquakes will have no deep impact either on the Callovo-Oxfordian or on the repository itself (Brulhet, 2005a) and (Andra, 2005h) as the zone is seismically calm, away from the major faults (cf. § 9.2).

The depth of the layer shelters it and the repository structures from the surface disturbances by climatic phenomena, notably the 100,000-year glacial/interglacial cycles (Brulhet, 2005b). Indeed, the layer is situated far below the maximum depth of permafrost liable to be created during glacial maximum episodes. Permafrost does however affect the temperature of the layer, temporarily, by a few degrees (minimum temperature of the order of 6 to 8 °C in the centre of the layer in a glacial maximum situation, compared with a present-day temperature of 22 °C – cf. § 3.2.3). Due to the absence of glaciers above the site, even in glacial maximum situations, vertical stress is not affected by climatic phenomena.

9.6.2 Surrounding formations

As for the Callovo-Oxfordian, internal geodynamic phenomena have little effect on the surrounding formations. Only earthquakes, due to their potential action on regional faults, can modify hydrogeological flows in the aquifers, by creating or reactivating fissure porosity. Such modifications only concern faults which are potentially the seat of tectonic movements on the scale of the sector: the Marne faults or Gondrecourt graben. In the range of possible earthquakes in the sector, by analogy with observations made elsewhere in the world, the forecast effects are essentially transient and reversible (Brulhet, 2005a) and (Andra, 2005h). Moreover, the latter remain essentially local, near to the faults, and do not modify the main directions of the hydraulic trajectories (Brulhet, 2005b).

On the other hand, external geodynamic phenomena, driven largely by climate change, have a more perceptible effect.

As far as the next hundreds of thousands of years are concerned, models show that massive greenhouse gas emissions can, in extreme scenarios, prevent the return of glacial conditions at the site over these time scales. After that, the climate cycles resume a “natural” pattern.

Irrespective of the scenario, the 100,000-year glacial/interglacial cycles have a significant influence on flows in the surrounding formations.

- The development of permafrost, which is more or less continuous in the glacial maximum period, stopps the infiltrations at the outcrops and is also liable, at site location, to limit the flows in the shallower aquifers (surface aquifers and the upper porous levels of the calcareous Oxfordian due to the presence of frozen water at depth in the fractures, or even gas hydrates). These cycles also have a transient effect on water chemistry in the surrounding layers: the phenomenon of salt exclusion on freezing implies a gradual concentration of salts at the permafrost front (Brulhet, 2005b). This phenomenon is of limited impact due to the shallow permafrost penetration (to a depth of approximately 35 meters, far above the calcareous Oxfordian in the transposition zone) and the periods over which it develops. In fact, this phenomenon only concerns short periods of time within a cycle (of the order of 20,000 years out of a total cycle of 100,000 years), which are minor compared with the characteristic transfer times into the surrounding formations (several hundred thousand years).
- On a million-year scale, the sequence of climate cycles conditions the geomorphological evolution of the landscape with, notably, the dismantling of limestone plateau formations and the downcutting of valleys. Such phenomena gradually modify the recharge areas of water-bearing formations and their outlets. Circulations in the formations are increasingly affected the nearer these formations are to the surface. Consequently, changes in the direction of flow or hydraulic hydraulic head gradient are only minor in the Dogger which, at the site location, is far from its outcrops (Brulhet, 2005b) and (Andra, 2005h). On the other hand, the evolution in the calcareous Oxfordian aquifer is more pronounced: the outcropping of certain parts of the formation in the valley floor in zones downstream of the flow determines the displacement of the present-day outlets (Marne Valley) or the creation of new ones (Ornain Valley). As a result of such disturbances to the hydraulic head field, the present-day regional flow direction from the site to the centre of the Paris basin will gradually disappear, in over of 500,000 years hence, in favour of flow directions to local natural outlets (Marne Valley, which will be sustained, and the Ornain Valley to the north of the site) (Brulhet, 2005b) and (Andra, 2005h) (Figure 9.6.1). Over the transposition zone, the average hydraulic head gradient of the calcareous Oxfordian will be doubled over the next million years, leading to convective transfer rates of a non-sorbed solute of a few kilometers per 100,000 years. At the million-year horizon, erosion will also lead to the direct outcropping of the calcareous Oxfordian, to the west of the site, in the upper Saulx valley (Figure 9.5.2). The topographic low point thus created will lead to the appearance of a local natural outlet in this valley. The trajectories from the site to this outlet will develop to the detriment of a part of the flows to the Marne valley. The hydraulic head gradients are high - of the order of 2 % - between the site and this low point (LSCE / CEA, 2004). The convective transfer times of a non-sorbed solute from the site to this outlet are of the order of tens of thousands of years. All of these evolutions are progressive between the present day and one million years' time. The changes described above will become perceptible from 500,000 years hence.

These changes on a million-year scale in the surrounding formations also condition the gradual evolution of the vertical hydraulic head gradient in the Callovo-Oxfordian over time. This gradient, which determines the flows over the transposition zone (essentially upflows at the present time), will become greater due to the reduction in hydraulic head in the calcareous Oxfordian. The maximum values over this zone will therefore increase from 0.2/0.3 $m.m^{-1}$ at the present time to values of the order of 0.4 $m.m^{-1}$ in a million years' time(Andra, 2005b), (Figure 9.6.2). This increase in the gradient will not however change the dominant mode of transfer in the layer which will still be diffusive.

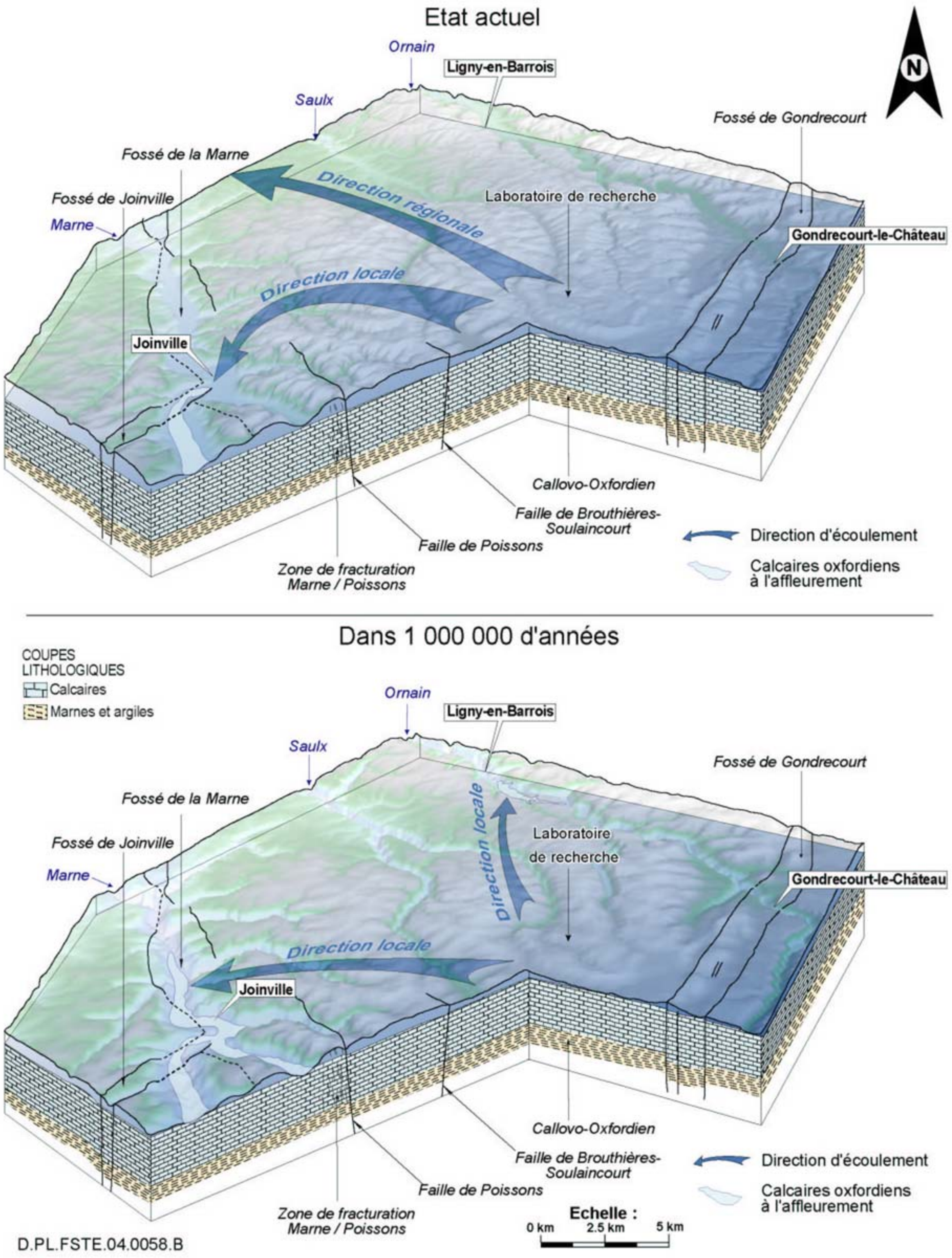

Figure 9.6.1 *Schematic representation of the change in flows in the calcareous Oxfordian between the present day and one million years' time*

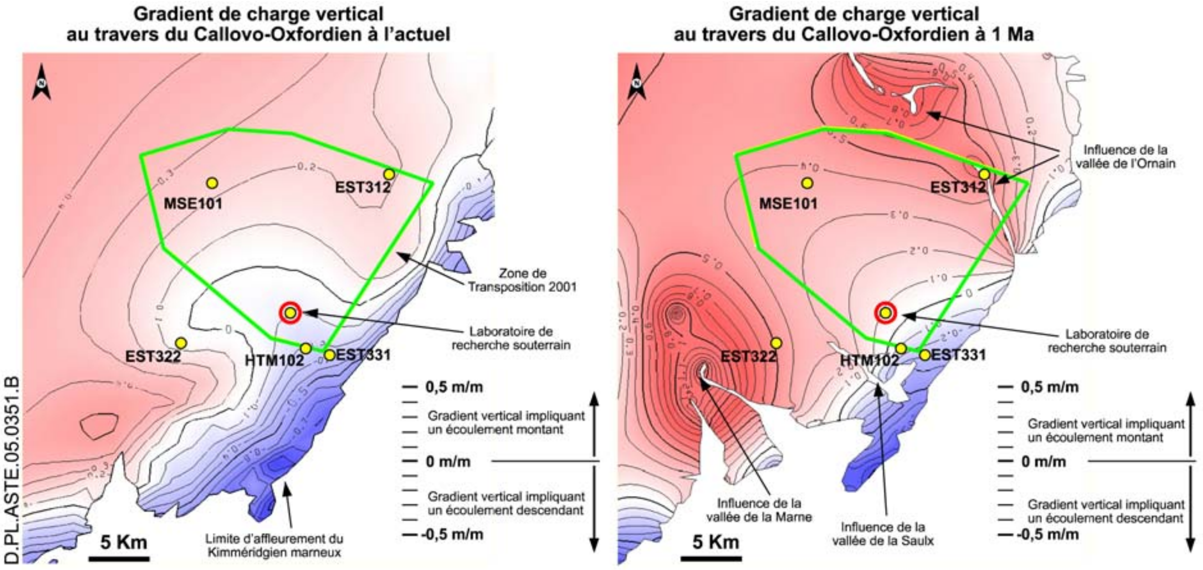

Au sein de la zone de transposition, les champs de charge dans les encaissants déterminent un gradient vertical responsable d'un écoulement essentiellement montant au travers du Callovo-Oxfordien (en moyenne de 0,1 à 0,2 m/m)

Sur le prochain million d'années, sur le secteur, l'érosion dans les vallées influence le gradient vertical au travers du Callovo-Oxfordien. Au sein de la zone de transposition, celui-ci détermine toujours un écoulement essentiellement montant mais il montre des valeurs plus fortes (en moyenne de 0,3 à 0,4 m/m)

Figure 9.6.2 Schematic representation of the vertical hydraulic head gradient in the Callovo-Oxfordian between the present day and one million years' time

9.6.3 Surface environment

The climate cycles disturb the surface environments periodically. Temperature and rainfall fluctuations lead to sequences of biospheres. Thus, across the sector, in the scope of a 100,000-years natural cycle, the temperate biosphere gradually gives way to a "boreal" biosphere, and subsequently to a colder, "tundra" biosphere.

On the scale of the next million years, a distinction needs to be made between the natural evolution of the site and an evolution disturbed by anthropic effects. These evolutions, as predicted by models, may be summarised as follows (Texier & Leclerc-Cessac, 2005):

- the natural evolution of the climate suggests the repetition of 100,000-year cycles with the clear predominance of periglacial biospheres over the first 500,000 years. Beyond this point, "cold" biospheres remain generally dominant but the sequencing of the cycles is faster (average periods of 50,000 to 70,000 years) ;
- over the next hundreds of thousands of years, major anthropic disturbance of the climate as a result of massive greenhouse gas emissions will prevent the creation of a "tundra" biosphere during the next cycles. The temperate biosphere will then become clearly predominant during this period. After the 600,000-year point, the cycles will resume a natural evolution.

9.7 Summary of the geodynamic evolutions of geological formations and surface environments

Section 9 describes the general framework, the driving forces and the effects of the future geodynamic evolution of the sector. The purpose of this summary is to extract from this, in connection with the chapter on the release and transfer of radionuclides and toxic chemical elements (cf. § 10), the structuring components of this evolution and its consequences on the Meuse/Haute-Marne site. Given the characteristic time frames of geodynamic phenomena (from 100,000 years for climate cycles to several hundred thousand years for the changes of surface morphology), this summary is oriented towards the effects of these evolutions in terms of consequences on the transfer of radionuclides and toxic chemical elements in the geological formations and surface environments.

9.7.1 For the Callovo-Oxfordian layer

Impacts are slight. The depth of the layer puts it out of reach of the thermal, mechanical or chemical phenomena induced by geodynamic evolutions. The physical and chemical characteristics of the Callovo-Oxfordian, notably with regard to the transport of radionuclides and toxic chemical elements, will therefore be sustained over time (Figure 9.7.1). From the hydraulic aspect, evolutions affecting the hydraulic head in the surrounding formations (see below) will gradually change the conditions at the limits of the layer over the next million years. The vertical hydraulic head gradient through this layer will therefore increase from a maximum value of 0.2-0.3 $m.m^{-1}$ in the transposition zone at the present time to 0.4-0.5 $m.m^{-1}$ in a million years' time This gradual change, which will only be perceptible from around the 500,000-year mark, will however remain minor and the diffusion phenomenon will still be the dominant mode of transfer in the Callovo-Oxfordian over the entire period.

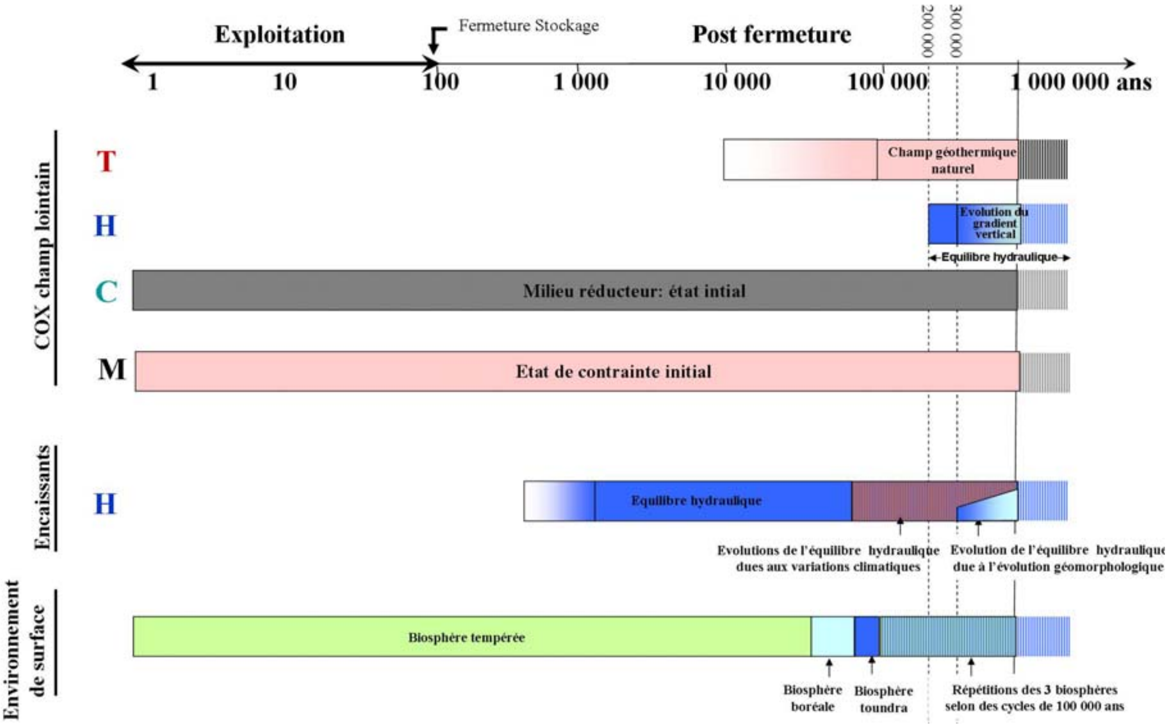

Figure 9.7.1 *Time chart of the effects of geodynamic evolutions on the geological medium and surface environment (on the basis of the conventional 100-year repository creation/operation/closure time chart)*

9.7.2 For the surrounding formations

Contrary to the Callovo-Oxfordian, the consequences of geodynamic phenomena on the transfer of solutes in the surrounding layers (Dogger and calcareous Oxfordian) are more pronounced (Figure 9.7.1).

Generally, the successive 100,000-year glacial cycles cause transient, reversible disturbance. During glacial maximum periods, more or less continuous permafrost develops on the surface and the 0 °C isotherm penetrates to a depth of approximately 300 m. This permafrost blocks infiltrations at the outcrops. At depth and at the site level, it is also likely to limit the flows in the more superficial aquifers (surface aquifers – Calcaire du Barrois (Tithonian) and Kimmeridgian carbonate intervals – and also the porous upper levels of the calcareous Oxfordian). The phenomenon of salt exclusion on freezing causes a gradual concentration of salt at the permafrost front, at an average depth of around 35 meters, much higher than the top of the calcareous Oxfordian in the transposition zone. These phenomena develop over short periods, approximately 20,000 years out of a 100,000-year cycle, which are minor compared with the transfer times in the surrounding formations (several hundred thousand years). Their impact is therefore limited.

The forthcoming glacial cycles may potentially be disrupted in terms of duration and amplitude by anthropic activities (massive greenhouse gas emissions) in extreme scenarios. This disturbance may prevent the return of glacial conditions to the site for the next 200,000 to 300,000 years and would disturb the amplitude of the following cycles up to 500,000 to 600,000 years hence. Over these periods, the transfer of radionuclides and toxic chemical elements is not likely to be disturbed by these transients in the case of anthropic disturbance. After the 600,000-year point, the effects of anthropic disturbance on the climate cycles would no longer be significant.

On a million-year scale, the sequence of climate cycles causes the geomorphological evolution of the landscape. This evolution leads to a significant change in the calcareous Oxfordian hydraulic head field. Indeed, the outcropping of certain parts of this formation in the valley floor in zones downstream of the flow causes the present-day outlets (Marne Valley) to migrate or new ones (Ornain Valley) to appear. Such disturbances to the hydraulic head field will therefore lead to the disappearance of the present-day regional direction of flow to the centre of the Paris basin. These gradual changes will become perceptible from the 500,000-year point. The Dogger carbonate is less sensitive to this evolution as it is more distant from the outcrops and, on the scale of the next million years, transfers in this formation will therefore remain similar to the present situation.

9.7.3 For the surface environments

Climate changes impose an alternation of temperate and cold (boreal, then tundra) biospheres over periods of the order of a hundred thousand years (Figure 9.7.1).

Compared with the initial state, the change to cold biospheres leads first of all to seasonal freezing (boreal climate), then permanent freezing (tundra climate) of the plateau subsurface. Due to the restriction of water resources, the development of vast farmed areas on these plateaux will no longer be possible. The transfer of radionuclides and toxic chemical elements from the Calcaire du Barrois (Tithonian) groundwater then becomes very limited.

During the cold periods, farming is concentrated especially in the valley areas or nearby. The outlets feeding the rivers may indeed be sustained here. The soils are neo-formed on each climate cycle in these zones, with the thaw at the back end of the cold season increasing the flow rates of the rivers and destabilising the alluvial terraces. The valleys therefore appear to be the only places where transfers to the biosphere remain possible in the cold period, especially in the boreal period.

In the marly depressions, the cold slows down the evolutions in the soils which become charged with organic matter. Peat bog and marshes then develop.

In the case of major anthropic disturbance to the climate cycles, the present-day temperate biosphere will remain predominant over the next 300,000 years, only allowing the significant development of boreal biospheres to occur beyond that time and glacial maximum conditions after 600,000 years.

10

Radionuclide release and transfer

10.1 Introduction 433

10.2 The Release of Radionuclides by Waste Packages..435

10.3 The Transfer of Radionuclides in the Repository Structure 446

10.4 Transfer of Radionuclides in Solution in the Callovo-Oxfordian Layer from the Repository and into the Surroundings..460

10.5 The Transfer of Radionuclides in the Surroundings..468

10.6 The Transfer of Radionuclides to the Biosphere and Humans 474

10.7 Summary 483

10.1 Introduction

The release and subsequent transfer of radionuclides are processes that take place over at least several hundreds of thousands of years. They are the subject of modelling and numerical simulation in the context of the safety analysis of a repository in deep geological formation. The parameters and models used are derived from the characteristics of the elements used (mainly diffusion, retention, solubility) but also within the framework of THM processes in which the release and transfer take place. In this chapter, these processes are essentially described for radionuclides. The behaviour of chemical toxins that may be important because of their content and toxicity will also be presented where applicable (Albrecht & Gallerand, 2005): boron, antimony, nickel, selenium and uranium, Inset 10.1).

10.1.1 The Release and Transfer of Radionuclides: Phenomena Governed by the Evolution of the Repository

The release and transfer of radionuclides are conditioned by the phenomenological evolution of the repository structure and their environment (near-field and far-field). This is the reason why they are dealt with after summarising the space-time evolution of all the phenomenological processes affecting the repository and its geological environment.

- The release is brought about by the degradation of the various B waste, C waste and spent fuel packages. This degradation is the result of the physical and chemical conditions in the disposal cells, in particular, the thermal and the hydraulic perturbations that in part the condition chemical phenomena such as corrosion of (on) containers or the degradation of concretes. In addition, these conditions govern the degradation of the waste matrices, like the aqueous dissolution of glass which causes the gradual release of radionuclides.
- Release and transport occurs once temperatures are below 50 °C in the case of C waste and spent fuel packages.
- In the case of C waste and spent fuel, the release of radionuclides begins after the failure of containers. The duration of design leak tightness is 4,000 years in the case of C waste and 10,000 years in the case of spent fuel. In the case of B waste, this release begins after several hundred to several thousand years depending on the type of waste and the saturation status of the packages.
- In the repository and in the Callovo-Oxfordian formation, the transfer of the radionuclides is governed by diffusion. The mobility of the radionuclides depends on their solubility and their retention within the repository and the argillites.
- In the surrounding under- and over-lying formations, the transfer of radionuclides – in the case of those that reach these formations - is mainly dominated by horizontal advection and to a lesser extent by vertical dispersion-diffusion.

10.1.2 The Organisation of the Chapter on the Release and Transfer of Radionuclides

The chapter is organised into two main parts.

- The first part concerns the release of radionuclides in relation to the evolution of waste packages and in particular the degradation of the waste and the conditioning matrix.

We will focus, in particular, on the processes of precipitation and coprecipitation in the vicinity of the waste such as in the degradation products of the vitreous matrices for example.

- The second part deals with the transfer of radionuclides and follows their migration from the waste packages into the repository, the argillites of the Callovo-Oxfordian formation and finally into the surroundings.

The transfer of radionuclides within the disposal cells is governed by the processes of solubilization in interstitial water and sorption on the different materials of the disposal cells. This transfer depends on the types of disposal cells considered and their physical and chemical characteristics.

In the far-field, the hydraulic, physical and chemical conditions of the argillite are stable and similar to those described in the chapter on the initial state. These conditions govern the transfer of radionuclides in the Callovo-Oxfordian layer. However, the evolution of the argillites in the near-field that are liable to influence the mechanisms and the kinetics of radionuclide transfer are dealt with. With respect to the radionuclides that reach the surrounding formations, the hydrogeological consequences of the geodynamic evolution are taken into account in the evaluation of their transfer.

Inset 10.1 ***Toxic Chemical***

The inventory of the chemical elements of the B waste, C waste and spent fuel packages reveals, on the one hand, the presence of radionuclides, but also non-radioactive elements that present a certain degree of toxicity for humans. A survey of the chemical toxins present in B waste, C waste and spent fuel yields the following compounds: As, B, Be, Cd, Cr_{total}, Cr (VI), CN^-, Hg, Ni, Pb, Sb, Se, U and antimony. In repository conditions, five chemical toxins are potentially important taking into account, in particular, their content and toxicity: boron , antimony, nickel, selenium and uranium. Three of these are also present as radionuclides; these are nickel, selenium and uranium.

The character of the chemical toxin is defined in accordance with several criteria corresponding to the evaluation of their potential danger: systematic carcinogenic effect for means of contamination by ingestion and inhalation. The study of these parameters in accordance with the approach recommended by INERIS (French National Institute for Industrial Environment and Risks) for Installations Classified for the Preservation of the Environment (ICPE) has led Andra to propose a basic list: As, B, Be, Cd, Cr_{total}, Cr (VI), CN^-, Hg, Ni, Pb, Sb, Se, U and antimony .

These elements are characterised by a toxicological reference value for the means of ingestion and/or inhalation, carcinogenic and/or non-carcinogenic effects. (Albrecht & Gallerand, 2005).

The total quantities (in metric tons) of some of these toxics chemical in all the B waste, C waste and spent fuel, depending on the various repository scenarios are summarized in the following table (Andra, 2005d). There are no Cr (VI), free cyanide ions or antimony in the repository waste packages or spent fuel assemblies.

Basic List of Toxics	S1a	S1b	S1c	S2
Antimony	10.58	10.7	10.78	8.85
Arsenic	0.16	0.17	0.17	0.17
Boron	656.35	665.33	771.20	311.31
Nickel	2,769.22	2,722.66	2,800.16	2,031.49
Selenium	3.15	3.4	4.01	3.52
Uranium	299.59	2,451.43	2,455.13	32,154.03

10.2 The Release of Radionuclides by Waste Packages

The release of radionuclides is associated with the nature of the waste and the immediate environment (chemistry of the water, redox conditions, corrosion products, etc.).

The evolution of the waste packages and the confinement matrices in particular, have been described in the chapters on the chemical evolution and the mechanical evolution. We will only cover general features here and we will focus on the link between the degradation of the packages and the release of radionuclides in order, in particular, to fix the typical time scales of the processes in question. The behaviour of radionuclides released in solution or in the form of a gas will be dealt with in the section on the repository structure (cf. § 1.3).

10.2.1 C Waste Packages

In C waste disposal cells, the release of radionuclides starts after the lining and the overpack lose their leak tightness which is approximately 4,000 years after the packages are placed in the repository. On the basis of purely phenomenological assessments and, more particularly, taking into account the rapid establishment of anoxic conditions in the C waste disposal cells, the duration of overpack leak tightness could reach 15,000 years. Consistent with the hypotheses used in the tomes on the repository architecture and the safety analysis, (Andra, 2005i ; Andra, 2005j) we have used a prudent leak tightness duration of 4,000 years in the following paragraphs.

The degradation of the vitreous matrices of C0 type packages takes place over a time scale of several thousand years and that of C1, C2, C3 and C4 type packages occurs over a time scale of several hundred thousand years (Figure 10.2.1). The radionuclides of the various C waste packages (Andra, 2005e) are distributed homogeneously in the structure of the vitreous matrices. The degradation of these matrices is characterised by the formation of alteration products, gel (*i.e.*alteration layer) and minerals (cf. § 7.3.4). which can bring about fixation by soprtion, precipitation and coprecipitation of part of the radionuclides released by the glass when it dissolves (Inset 10.2). This is the case for actinides in particular, which, unlike other elements such as technetium and boron, for example, are not released congruently with the dissolution of the glass.

Inset 10.2 ***Radionuclide Behaviour in Glass Alteration Products***

Research into glass dissolution processes (Inset 7.7, Inset 7.8) has revealed the retention processes of the elements released by the glass in its degradation products (Andra, 2005d ; Fillet, 1987).
The different elements released by the glass can therefore be classified on the basis of their retention in the alteration layer and other alteration products. (Andra, 2005d).

Elements that are not retained in the alteration layer are **mobile elements**. They comprise the alkalis (sodium, lithium), molybdenum and technetium. They are released congruently with the degradation of the vitreous matrix. (Andra, 2005d). Of the chemical toxins, boron corresponds to this category of elements.

  - In the case of molybdenum and technetium, their retention is possible and depends on the redox conditions in the alteration layer. In an oxidizing or mildly reducing medium, these two elements are only retained in the alteration layer in the case of an extremely advanced reaction (~ 10 %). However, under extremely reducing conditions (Eh < -400 mV), the change in the oxidation level of these elements leads to the formation of less soluble species that remain partially fixed in the alteration layer.

- Sodium and lithium are generally only retained by the alteration layer as charge compensators. (Munier *et al.*, 2004). This is also the case for boron.

So-called **intermediate** elements are partially retained in the alteration layer when the glass degrades. These elements are caesium, alkaline earth metals (calcium, strontium, barium), silicon and aluminium (Andra, 2005d).

- Caesium behaves more like an alkaline earth metal and when degradation is advanced, it is notably retained in the alteration layer (~ 30 % - 60 %) or in the layer silicates (Valle, 2001).

- The retention of alkaline earth metals in the alteration layer varies between 40 % and 60 %. They probably serve as charge compensators for aluminium or zirconium.

- The retention of silicon and aluminium in the alteration layer varies depending on the alteration conditions and, in static conditions with high surface / volume ratios, the retention of silicon can reach almost 95 %. Aluminium is better retained than silicon, perhaps on account of its lower solubility at basic pH.

Highly retained elements are insoluble at the basic pH imposed by the degradation of the glass. They include all the transition elements (iron, nickel, zinc, zirconium, etc.) and lanthanides and actinides (Andra, 2005d ; Fillet, 1987).

- As a general rule, La, Ce, Nd, Th, Am and Cm are present in +III form (Andra, 2005d) and this charge promotes a strong attraction with the negatively charged alteration layer. Actinides are retained to a greater or lesser extent depending on the elements. Almost 99.9 % of americium and curium are retained.

- Uranium and neptunium behave in a similar way to each other and are more mobile than the other actinides, especially in an oxidizing medium where they are in the forms U^{VI} and Np^{V}. In a reducing medium, neptunium IV is less mobile. It can be significantly retained (~ 35 %) depending on the type of glass (Andra, 2005d). In the presence of phosphates, the retention of neptunium in the alteration layer can reach 90 % (Andra, 2005d ; Andra, 2005g).

The behaviour of plutonium is intermediate between lanthanides and uranium. In some cases it is very highly retained (> 99 %) in the alteration layer by more stable phases than simple hydroxides or carbonates. (Andra, 2005d).

10.2.2 Spent Fuel Packages

The period of time during which spent fuel containers remain leak tight is specified at 10,000 years. As in the case of C waste over-packs, purely phenomenological assessment has yielded estimates that this period could reach 30,000 years. For the same reasons as those set out above, the behaviour of the spent fuel will be described in the following paragraphs on the basis of a specified leak tightness of 10,000 years. The arrival of water coming into contact with the oxide pellets in spent fuel rods means the discharge of leak tightness of the rod cladding. This discharge of leak tightness can occur from the moment water invades the packages as a result of cracking and/or by creep and rupture.

Spent fuel falls into two large categories of waste: structural materials (cladding, end caps, spacer grids and metal springs) and oxide pellets. The radionuclides are distributed between these two types. However, in the case of some radionuclides such as iodine, a fraction of their inventory is located outside the structural materials or the oxide grains that make up the spent fuel pellets. The release of this fraction of the radiological inventory is possible from the moment of the arrival of water ("labile" fraction). The release of other radionuclides is contingent upon the kinetics of corrosion and dissolution. They are considered to be homogeneously distributed between the oxide pellets, on the one hand, and structural elements on the other.

10.2.2.1 The Release of Radionuclides by Oxide Matrices

Schematically, two mechanisms can be distinguished that are of unequal importance and contribute to the release of radionuclides contained in oxide matrices: accelerated diffusion by alpha self-irradiation (D3AI) and dissolution with or without the radiolysis effect of the water. (Andra, 2005d).

The process of accelerated diffusion by alpha self-irradiation (D3AI) is initiated during the passage through the reactor and would only have significant consequences on the distribution of radionuclides for a few thousand years, i.e. before the containers fail. When the containers fail, this would correspond, at the maximum, to a migration beyond the grains of at least 5 % of the inventory initially present. However, this phenomenon would affect light, mobile radionuclides such as ^{129}I rather than heavy radionuclides like actinides, which would barely be affected.

The internal structure of oxide pellets is complex and comprises grains, cracks / fractures and seals. Radionuclides are distributed in the grains, on their surface or in the porosity of the pellets (grain boundaries, cracks, fractures). This distribution varies depending on the type of radionuclides. The total fraction of the inventory located outside the grains and in the empty spaces of the rods represents some 5 % in the case of spent fuel SF1 and 30 to 35 % in the case of spent fuel SF2.

Release will be highly dependent on location inside or on the periphery of the grains. It may begin from the moment the container fails, i.e. 10,000 years after emplacement in the disposal cell.

The release of radionuclides located in the empty spaces (gap and plenum) and on the surface of the grains (grain boundary, etc.) that is directly accessible when water reaches the package (*i.e.* the spent fuel rods) is instantaneous. The fraction varies depending on the radionuclides and the burnup.

The release of radionuclides situated on the surface of the grains not connected with the outer surface of the oxide pellet or at a distance from the cracks / fractures connected with the outer surface of the pellets, will depend on the gradual modification of the structure through the dissolution of the grains (gradual accessibility to water through the dissolution of the grains).

The release of radionuclides located inside the grains, the actinides in particular, is associated with the dissolution of the latter. On the basis of current understanding, this release is congruent with this dissolution.

Taking account of the radiolysis of the water by α radiation on the dissolution of the oxide grains gives a total pellet dissolution period, therefore radionuclide release period, of the order of several tens of thousands of years to a hundred thousand years depending on the burnup of the spent fuel (cf. § 10.2.3). This mode of release is not dependent on temperature. The reality of this process in repository conditions is the subject of scientific debate. Notably, radiation decay α and the presence of hydrogen (generated by the corrosion of steel) in direct contact with the packages are evoked to minimise the importance of this process in the dissolution of oxide pellets. (Spahiu *et al.*, 2004).

In the absence of the radiolysis effect of water on the dissolution of the oxide grains, the duration of the total pellet dissolution period would exceed a million years (Figure 10.2.1). It is then governed by (i) the low solubility of uranium and plutonium, determined by the stable solid phases of these two elements in the physical and chemical conditions of the disposal cells, (ii) the total masses of the uranium-plutonium oxide pellets, and (iii) the conditions of transport in solution of these two elements characterised by high sorptions and dominant diffusion. When the leak tightness of the container is lost, the surface temperature of the packages has decreased sufficiently not to significantly influence the dissolution of the oxide pellets.

10.2.2.2 The Release of Radionuclides by Structural Materials

As in the case of the oxide pellets, the distribution of radionuclides varies from one structural material to another. Their location within materials also varies. It is homogeneous for the structural elements of the fuels assemblies. However, in the cladding, while the activation products are homogeneously distributed, the fission products are embedded by fission recoil and are mainly located on the internal surface of the cladding several microns into the zirconia layer.

The radionuclides located on the surface of the zircaloy cladding and stainless steel and inconel structural materials are released immediately water arrives.

The radionuclides present in the zircaloy cladding and structural materials are released congruently with the corrosion of the cladding, stainless steel and inconels (cf. § 10.2.3) over maximum periods of the order of several tens of thousands of years (Figure 10.2.1) depending on the geometry of the parts. These evaluations take into account the temperature reached in the packages at the time of release.

Inset 10.3 ***The Location and the Distribution of Radionuclides in Spent Fuel Assemblies***

The radionuclides present in spent fuel (Inset 7.9, Inset 7.11) (Andra, 2005e) are distributed between the oxide pellets and structural materials (stainless steel and alloys). The fission products are mainly located in oxide pellets and activation products in the structural materials. However, the distribution of some activation products may be heterogeneous. For example, only a percentage of ^{93}Zr or ^{121m}Sn is found in structural material whereas this proportion exceeds 90 % in the case of ^{59}Ni or ^{63}Ni (Andra, 2005d).

Within the pellets, radionuclides are divided into five categories depending on their chemical form (Andra, 2005d):

- Radionuclides that are soluble in the oxide matrix (*i.e.* that form solid solutions): actinides, lanthanides, soluble fission products in the form of oxides (Zr, Nb, Sr),
- Radionuclides that form oxide precipitates: Cs, Zr, Nb, etc.,
- Radionuclides that form metal precipitates: Mo, Tc, Ru, Rh, etc.,
- Metalloids in the form of precipitates (Ge, As, Se),
- Fission gases: noble gases (Kr, Xe, He) and fission products that are volatile in the reactor (I, Cs, Se, Te, Br).

Most of the radionuclides (approximately 95 %) belong to the first category.

The process of accelerated diffusion by alpha self-irradiation (D3AI) brings about the migration of some mobile elements (mainly iodine, tellurium, bromine, noble gases and caesium), which can be released into the empty spaces of the rods, intergranular areas (grain boundaries and pores) or remain within oxide grains (Figure below, (Andra, 2005d)).

Mobile fission products are probably found in the porosity of the restructured areas ("rim" or clusters of Pu). Barely soluble elements such as actinides and lanthanides remain in the grains. The metal precipitates accumulate preferentially in the joint boundaries.

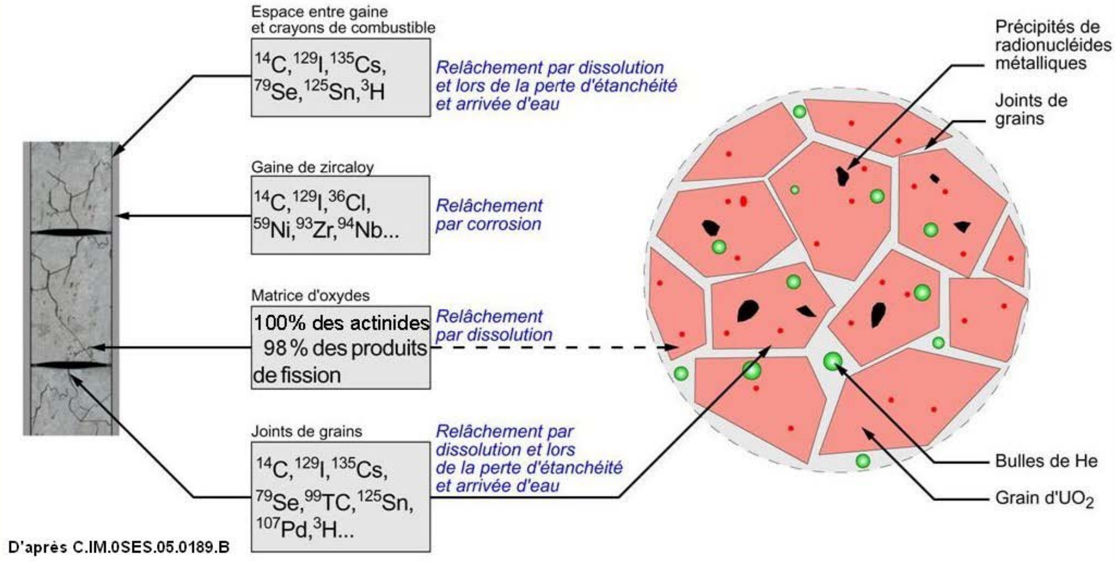

D'après C.IM.0SES.05.0189.B

Location of the Main Radionuclides in Oxide Pellets and the Cladding of Spent Fuel Assemblies

10.2.3 B Waste Packages

B Waste packages contain waste from various sources and of various shapes. They are conditioned in three main ways: cementation, bituminisation and compaction. Because of this, they have specific behaviour in respect of the release of radionuclides.

The resaturation of B waste packages depends highly on the conditioning of the waste in the primary packages. In addition to this, resaturation does not occur homogeneously within any one cell. Therefore, before full resaturation (S > 97 % at 200,000 years), the presence of condensed water in the cell, and within the primary packages, in particular, depends on the location of the package inside the disposal cell (cf. § 6.3.2.6 and Figure 6.3.14). Consequently, inside a cell, the point in time at which radionuclide release begins may vary depending on the location of the packages and the waste. The heterogeneous release should occur mainly when the disposal cell is close to total saturation. It is not likely to create significant differences in release by packages on the scale of the cell.

In terms of hygrometry, it is notable that the resaturation of B waste disposal cells corresponds to a rapid and homogeneous increase in hygrometry which reaches approximately 90 % over several hundred to several thousand years. Independently of the presence of condensed water, such a hygrometry is likely to allow corrosion of the metals and degradation of some waste (cf. § 7.4), and compacted waste (package types B1, B5 and B6) and B2 bituminised sludge packages in particular.

10.2.3.1 The Release of Radionuclides by B2 Type Waste Packages

Radionuclides are mainly located in soluble and mildly soluble salts (known as "insoluble") embedded in the bitumen matrix (Andra, 2005e). The distribution of radionuclides between different salts varies, although the latter are mostly associated with "insoluble" salts. The same is true for the chemical form of the radionuclides: sorbed to the surface of the salts, occluded in the salts, etc. Whatever the case, the release of radionuclides by bituminised sludge packages follows the arrival of water within the bitumen embedded waste.

Water can reach the embedded waste if it comes into contact with liquid water or is located in an atmosphere with a relative humidity of over 70 %. The hydraulic evolution of a B waste disposal cell shows that the latter condition would be reached in several hundred to several thousands of years' time. The release of radionuclides is therefore possible after this period. Water gradually penetrates the embedded waste by diffusion, permitting the progressive dissolution of the salts. Thus, schematically, it forms a water penetration front and a salt dissolution front, first the soluble salts then the so-called insoluble salts. The dissolution of salts therefore creates a so-called permeable zone behind the water penetration and salt dissolution fronts. The arrival of water and dissolution of the salts allows the dissolution of the corresponding radionuclides. They can then diffuse outside the embedded waste, in the reverse direction of water penetration and salt dissolution in the permeable zone, then reach the surface of the embedded waste and be released outside the primary package (Andra, 2005d) (Inset 7.14) (cf. § 7.4). The modelling of water penetration and salt dissolution shows that the period of time necessary for the complete theoretical uptake of water by the embedded waste is of the order of a million years. However, these models reveal uncertainties concerning the conditions of transfer of the salts dissolved in the permeable zone formed, in particular, and this gives rise to the more robust envelope evaluation of 10,000 years presented in § 7.4.3.3 in which the insolubilization of the salts is disregarded (Figure 10.2.1). The same is true for the release of radionuclides.

10.2.3.2 The Release of Radionuclides by B4 and B5 Type Packages

The release of radionuclides associated with B4 and B5 type waste packages depends on the location of each radionuclide in these types of waste (Andra, 2005d ; Andra, 2005e) and varies depending on the origin of the waste. So, for example, in the case of technological waste, contamination is generally on the surface whereas for structural waste, the radionuclides are more often inside the material.

Packages of hulls and end caps (B4 and B5 type packages) contain two types of waste: cladding waste (zircaloy hulls, springs and spacer grids made from inconel, stainless steel end caps) and various technological waste (made from stainless steel, zircaloy, etc.).

The release of radionuclides situated on the surface of the metal materials (contamination, residue, etc.) takes place by processes of dissolution / precipitation when liquid water arrives and comes into contact with the waste. It therefore depends directly on the physical and chemical state of the element and on the conditions of the environment the waste is in (undisturbed and reducing cement-based media).

The release of the radionuclides located in the mass of the materials (*i.e.* activation products) is governed by the degradation of the material that serves as a confinement matrix.

The corrosion of zircaloy is very slow in cement-based media on account of the formation of a passivating layer of zirconia. The radionuclides that it contains are essentially activation products, distributed homogeneously throughout the entire thickness of the hulls. However, their release is not necessarily congruent with the corrosion of the alloy because of the presence of the layer of zirconia on the internal and external surface of the hulls (Andra, 2005d). This layer of zirconia also contains radionuclides the release of which is not congruent with its dissolution (formation of secondary precipitates, formation of a passivating layer, diffusion, migration by preferential pathways, etc.). So, it is necessary to take into account the corrosion of the zircaloy on the one hand and the dissolution of the zirconium oxide (zirconia) and the migration of the radionuclides inside the zirconia on the other. Overall, the corrosion kinetics of zircaloy are slow in the cement-based conditions of a B waste cell, of the order of 10^{-4} at $2 \cdot 10^{-3}$ μm.year^{-1} (Andra, 2005d). In the event of an oxidant transient due to the irradiating packages, the latter is very short-lived (several decades to a few hundred years) and does not affect radionuclide release. The rate of inconel and stainless steel corrosion is 10^{-2} at 10^{-4} μm.year^{-1} (cf. § 7.4).

If the congruence of the release of radionuclides with the corrosion of the metals is accepted, (Andra, 2005d) the total release of radionuclides would take place over 15,000 years in the case of inconel, 70,000 years in the case of stainless steel and approximately 100,000 years in the case of zircaloy cladding (cf. § 7.4) (Figure 10.2.1).

10.2.3.3 The Release of Radionuclides by Other Metal Waste

Other B waste (other than B4 and B5) also contains numerous types of metal waste, in particular, activated cladding waste (package types B1, B6.2, B6.3, etc.) and technological waste (package types B3, B6.1, B6.4, B6.5, etc.) (Andra, 2005d). As in the case of B4 and B5 type waste packages, the radionuclides are located either on the surface, or in the metal mass.

This can be illustrated by the following three examples:

- the activity of activated waste from B1 type packages is located in the different components (poison clusters, control clusters and various metal waste) that comprise this type of waste. Activation products are, by nature, distributed uniformly through the mass of the materials (Andra, 2005d). The release of radionuclides takes place in the same way described above for the activation products of B4 and B5 waste;

- the activated waste of B6.2 and B6.3 packages are made from stainless steel, aluminium and magnesium. The activation products are distributed homogeneously throughout the mass of these types of waste. The release of those situated in stainless steel waste is similar to that described for hulls and end cap waste. Those located in aluminium and magnesium waste are most probably released with the corrosion of these materials;
- contamination is superficial in a very great number of cases and that of technological waste in carbon steel (package types B3, B6.1, B6.4, B6.5, etc.) in particular. The release of radionuclides takes place from the moment liquid water arrives.

In the case of most of this type of waste, time scales are similar to those described for B4 and B5 type waste packages.

Inset 10.4 ***The Location and the Distribution of Radionuclides in B4 and B5 Types of Waste***

B4 and B5 type packages contain two types of waste: cladding waste (zircaloy hulls, springs and spacer grids made from inconel, stainless steel end caps) and various technological waste (made from stainless steel, zirconium, zircaloy, inconel, molybdenum, etc.) (Andra, 2005d) (cf. (Figure below).

The activation products of cladding waste are distributed throughout the mass of the materials. The inventory depends on the impurity content and that of the elements of the alloys taken into account for the various materials. Where zircaloy components are concerned, approximately 20 % of the activation products are located in the zirconia layer. Part of the activation products of the fuel is also expressed in the form of surface contamination of the waste.

Fission products are found on the surface of cladding waste after dissolution of the fuel and flushing. Approximately 0.2 % of the inventory of fission products from the fuel is found in cladding waste, with the exception of special cases such as the ^{106}Ru + ^{106}Rh pair where 0.6 % is located in fines from shearing, and tritium where between 60 % and 80 % is retained on account of its diffusion in the zircaloy cladding. The majority of fission products are embedded in hulls by fission recoil in the zirconia. Only tritium is found in the zircaloy.

As regards **cladding waste actinides**, between 0.013 % and 0.03 % of the inventory of the fuel is retained in the hulls. Plutonium is the main radionuclide (70 % contained in the salt deposits and 30 % in the zirconia).

The fines produced by shearing structural elements are also contaminated by the dissolution solution. They contain almost 3 % of the α activity of the hulls (whereas they only represent 0.12 % by mass) and 4 to 6 % of the $\beta\gamma$ activity (fission products), mostly ^{106}Ru + ^{106}Rh. With regard to technological waste, the location of the radionuclides corresponds to surface contamination.

The actinides, in addition to ^{41}Ca and ^{65}Zn, are situated on the surface (deposits, fines); ^{3}H, ^{14}C, ^{36}Cl and ^{93}Zr are almost solely located in the hulls (zircaloy and zirconia); ^{57}Co, ^{63}Ni and ^{94}Nb are almost solely located in other structures (stainless steel and inconel); others (^{53}Mn, ^{60}Fe, ^{93}Mo) are distributed throughout the hulls and in cladding waste.

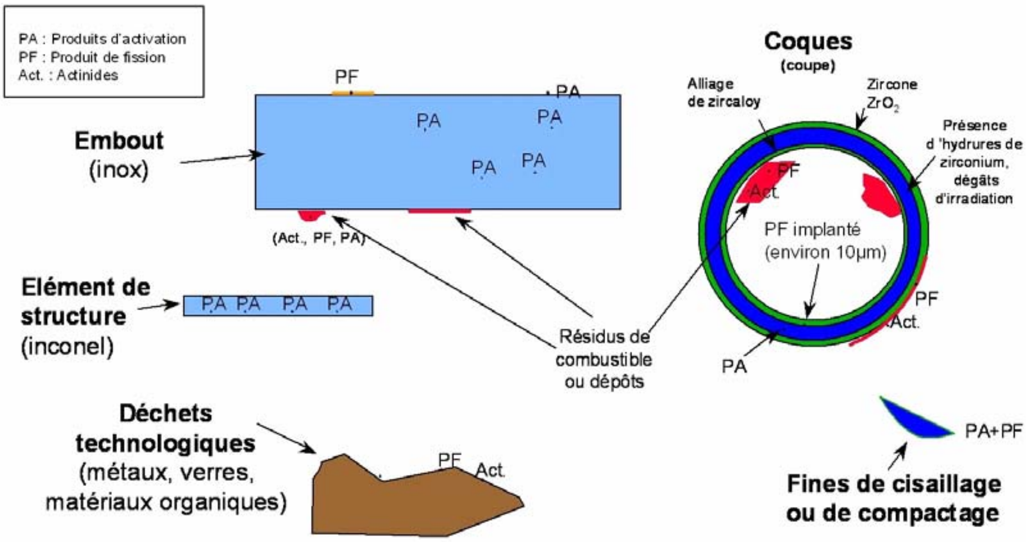

Diagram Showing the Location of the Radionuclides in Different B4 and B5 Type Waste Packages

10.2.3.4 The Release of Radionuclides by Other Types of Waste

The radionuclides present in other B waste materials (glass, organic compounds, etc.) are also situated on the surface of (contamination) or inside (activation) waste. This can be illustrated by the following three examples:

- Activation waste (B1 type package) in AIC *alloy*, (control clusters) and *boron carbide* (package types B1 and B6.5) are contaminated throughout their mass.
- Vitrified *waste* is either activation waste (pyrex of the poison clusters of B1 type packages), nuclear waste (nuclear glass of B6.1 type packages, vitrified sludge of B3.2.2 type packages), or surface contaminated waste (various glass from B3.1.3, B3.3.3, etc. type packages);
- In radiferous waste (B8 type packages), the radionuclides (mainly radium) are associated with lead sulphates.

The periods of time necessary for liquid water to come into contact with these types of waste are similar to those estimated for the metal waste above, i.e. several thousand years to one hundred thousand years depending on the characteristics of the reference package. A sufficient hygrometry rate for corrosion of them to begin is reached in several hundred to several thousand years' time.

As in the case of metal waste, the period of time during which radionuclides are released from these types of waste is very variable depending on whether they are located on the surface or inside the waste. The release of surface contaminants is rapid once liquid water comes into contact with the waste (independently of their retention set out below, cf. § 10.3.2). On the other hand, where radionuclides present in the structure of the materials are concerned, their release is slower since it is directly dependent on the degradation of the material itself. It continues until the complete degradation of the waste. The latter spans several thousand years, even several hundred thousand years in the case of vitrified waste (Figure 10.2.1).

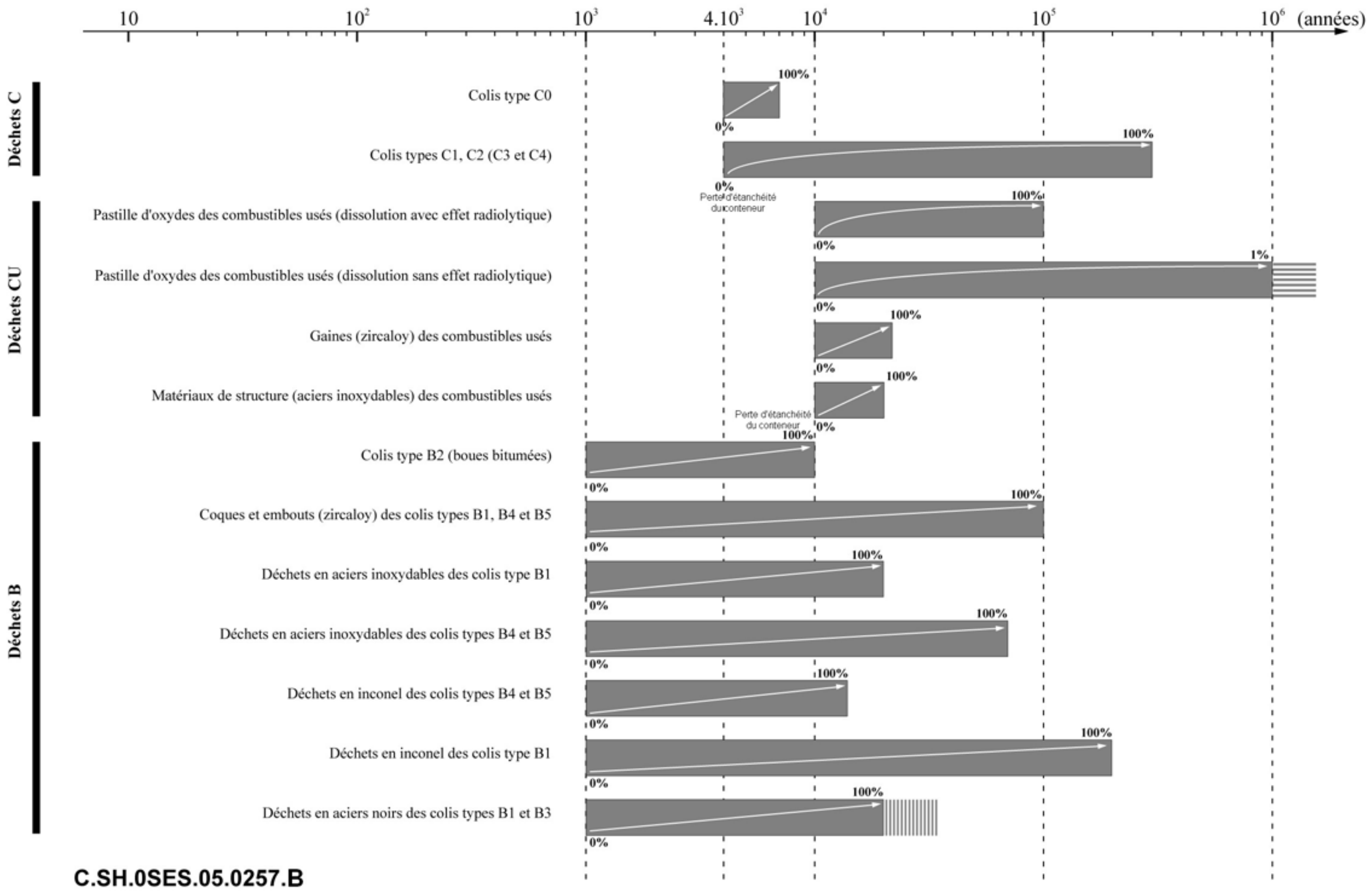

Figure 10.2.1 *Chronogram of the Degradation Processes of Reference Packages (Based on the Conventional Secular Chronogram for Manufacture / Operation / Closure of the Repository)*

10.3 The Transfer of Radionuclides in the Repository Structure

After being released by the waste, the mobility of the radionuclides in the repository depends on the water chemistry, the retentive properties of the materials and the flow conditions in the disposal cells and drifts (Inset 10.5, Inset 10.6 and Inset 10.7). These different factors are dealt with in the following paragraphs in accordance with the type of structure in question. The retention properties that, together with the chemistry in solution, condition the immobilisation of numerous radionuclides inside the disposal cells are dealt with separately. After defining all of these factors, we will describe the radionuclide transfer paths from the waste packages inside the disposal cells to the argillite and/or the drifts. The description of the transfer of radionuclides in the repository is based on information supplied in the chapters on water flow and the chemical evolution of the repository (cf. § 6 and § 7)

We will take into consideration that, not including very short-lived transients, the transfer of solutes and therefore radionuclides takes place principally by diffusion. The chemical environment is characterised by the slow evolution of the compounds and in particular by swelling clay and concrete, and by the extension of disturbances that are limited in space.

Inset 10.5 ***Sorption Properties of the Clay (1/2)***

Cation Exchange Capacity (CEC)

Clay has the capacity to reversibly (exchangeably) fix cations contained in its interstitial solutions. This is the cation exchange capacity (CEC in meq. $100g^{-1}$). These cations are retained by weak links either on the external surface of the crystals or in interfoliar areas (Bouchet *et al.*, 2000).

Cation fixation sites on external surfaces are sites on the edges of layers or defects emerging from the surfaces. The properties of the external sites depend on the pH. The internal CEC reflects the charge deficit of the layers (replacement of an Si^{4+} ion with an Al^{3+} ion in the tetrahedral layer of silica, replacement of an Al^{3+} ion with an Mg^{2+} ion in the octahedral layer of aluminium, etc.); it therefore depends on the permanent charge of the clay material.

The total CEC is equal to the sum of the external CEC (charges vary with the pH) and the internal CEC (fixed charges). The total CEC values of clay minerals vary depending on their structure (see table below).

Cation Exchange Capacity (CEC) of Some Clay Minerals

Minerals	CEC (meq. $100g^{-1}$)
Kaolinite	5 – 15
Illite	25 – 40
Montmorillonite	80 – 120
Chlorite	5 – 15

Sorption Properties of the Clay

The CEC does not, however, make the direct evaluation possible of the sorption properties of a material particularly because of the existence of different types of adsorption sites on the clay surfaces. Thus, on the scale of traces, the capacitative effects are secondary and the behaviour of radionuclides is governed by the type(s) of sites with which they have the greatest chemical affinity. By way of illustration, the work of (Gorgeon, 1994) shows similar Cs and Am adsorption capacities for a smectite from Wyoming and an illite from Puy (cf. Figure below). The model proposed accounts for a weaker concentration of sites for illite, compensated by higher adsorption constants than for smectite (Giffaut & Buschaert, 2005).

Sorption Properties of the Clay (2/2)

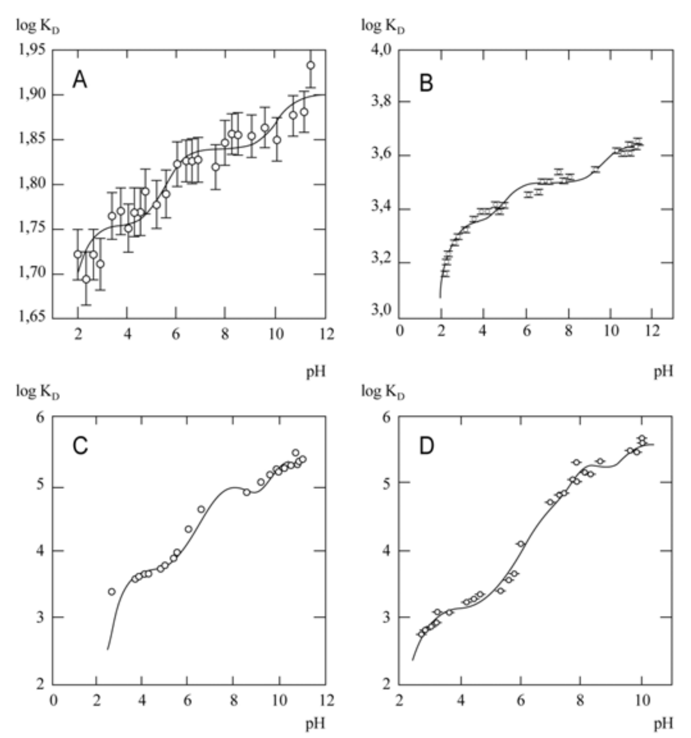

Comparison of the Sorption Isotherms of Cs and Am, Respectively on a Smectite and an Illite. A. Fixation of Cs(i) on a Smectite from Wyoming [NaCl] 1M. B. Fixation of Cs(i) on an Illite from Wyoming [NaCl] 1M. Fixation of Am(III) on a Smectite from Wyoming [NaCl] 0.1M, D. Fixation of Am(III) on an Illite from Wyoming [NaCl] 0.1M.

Inset 10.6 The Retention and Transport of Solutes (1/2)

The equation usually used to describe the transport of an inert solute in a porous medium is the advection-dispersion equation.

$$\frac{\partial \omega C_e}{\partial t} = -div(F)$$

Where: ω: porosity (-)
C_e: concentration of the solute in water ($kg.m^{-3}$)
div(F): divergence of the advective and diffusive flow ($kg.m^{-3}.s^{-1}$)

When the solute transported by water interacts with the porous matrix, the total concentration of the solute is distributed between the liquid phase, C_e and the solid phase, C_s, and the advection-dispersion equation becomes:

$$\frac{\partial \omega C_e}{\partial t} + \rho_d \frac{\partial C_s}{\partial t} = -div(F)$$

Where: ρ_d: dry density of the porous medium ($kg.m^{-3}$)
C_s: solute concentration in the solid ($kg.kg^{-1}$)

Several sorption models can be used to link the concentration in the liquid phase and the concentration in the existing solid phase. The Kd model expresses a linear relationship between these two magnitudes, valid at equilibrium in a range of concentrations and in given physical and chemical conditions.

$$C_s = K_d C_e$$

The Retention and Transport of Solutes (2/2)

The advection-dispersion equation can be re-written showing a delay coefficient (or factor) R as follows:

$$R\frac{\partial \omega C_e}{\partial t} = -div(F) \quad where \quad R = 1 + \frac{\rho_d K_d}{\omega}$$

This delay factor shows that the solute is displaced less quickly than the water. When Kd is nil, the delay coefficient is equal to 1 and the transport equation is reduced to that of an inert solute.

If the linear relationship defining Kd is as valid in the case of sorptions as in the case of desorptions, the process is reversible and the total mass of solute is found *in short* in solution after temporarily passing through the solid phase. The delay coefficient, R, therefore implies slower transport than in the absence of sorption. The rate diminution factor is equal to the delay coefficient, hence its name. The delay factor therefore also implies a reduction, by this same factor, of the maximum concentration in solution compared with a non-sorbed solute (see diagram).

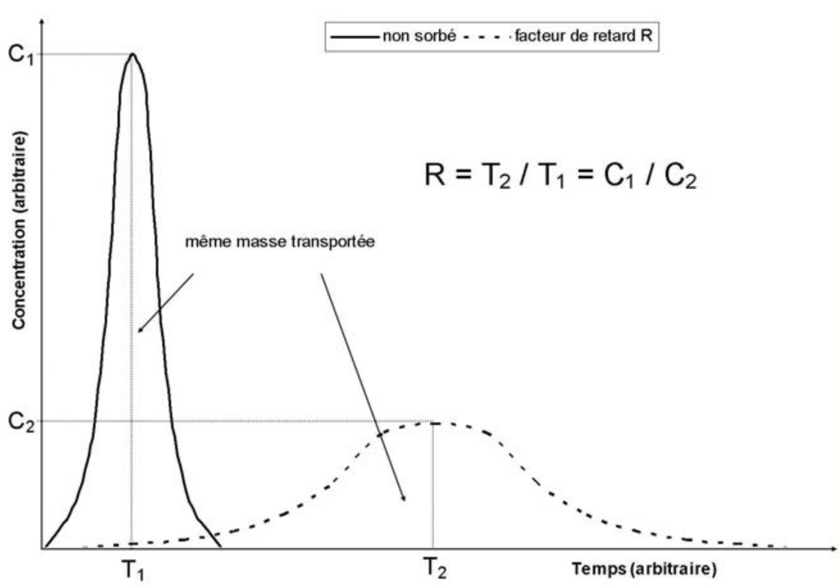

Diagram showing the differences between a peak concentration for a non-sorbed solute and a sorbed solute for the same abscissa during advective/dispersive transport downstream from a dirac of the stable tracer injection and for a sorption assumed to be linear and totally reversible sorption.

In the disposal cells and in the Callovo-Oxfordian argillites, the delay factor becomes significant once the Kd exceeds 10^{-4} $m^3.kg^{-1}$. Thus, a Kd of 10^{-3} $m^3.kg^{-1}$ corresponds to a delay coefficient of the order of 10.

10.3.1 The Physical and Chemical Conditions in the Repository Cells

The physical and chemical conditions in the disposal cells are characterised by the high degree of stability of the constituent materials (cement-based and clay materials) and by reducing redox conditions. As the chapter on the chemical evolution of the repository structure showed (cf. § 6.4.1), the constituent materials of the latter degrade slowly (degradation of the concrete, corrosion, etc.) or are chemically disturbed (stability of the engineered barrier made from swelling clay, etc.). The chemical characteristics of the disposal cells therefore remain almost stable over time.

10.3.1.1 The Chemistry of the Water in the Repository Cells

In C waste disposal cells and spent fuel disposal cells, the interstitial water is clayey water. In particular, the chemistry of the water in the spent fuel disposal cell engineered barrier can be compared to that of the argillites. In fact, most of the iron arising out of the corrosion of the steel components (cladding, lining, overpack, container, etc.) is mobilised in corrosion products and in iron /clay interaction so it is unlikely to modify the properties of the water as regards the radionuclides, the latter maintains a composition close to the interstitial water of the argillites for a period of a million years. Alkaline disturbance in the plug is liable to cause a increase in the pH ($8 \leq pH \leq 12.5$) over several decimeters after several hundred thousand years. This disturbance does not therefore affect the environment of the waste or spent fuel packages.

In the B waste disposal cells, the water from the argillites of the Callovo-Oxfordian formation is quickly buffered by the degradation of the cement-based materials of the disposal cell (cf. § 7.4). Thus, the water in contact with the primary B waste packages is unaltered cement-based water with a pH equal to 12.5. As the chemical degradation of the concrete components of the B waste disposal cell is slow (several hundred thousand years, cf. § 7.4), the composition of the interstitial water in the vicinity of the waste packages (pH, major elements) remains constant overall throughout the release of radionuclides. On the scale of the cell, the degradation of the structural concrete leads to the formation of an altered and degraded concrete zone in contact with the argillites over a period of a million years. The pH ranges from 10.5 to 12.5.

10.3.1.2 The Redox Conditions in the Repository Cells

- **C Waste and Spent fuel Disposal cells**

The redox conditions in these disposal cells are reducing long before liquid water comes into contact with C waste packages (4,000 years according to the reference scenario) and spent fuel (10,000 years according to the reference scenario). Radiation is stopped by the metal envelopes of the waste packages and cannot therefore cause radiolysis of the water in the cell. In the case of spent fuel and in the immediate vicinity of oxide grains, (Andra, 2005a, Situation Zu1_1 ; SKB, 2004) α radiolysis of the water can induce oxidizing conditions over several tens of micrometers (cf. § 7.3.5). Beyond that, the redox conditions are those prevailing in the disposal cell and are reducing.

The reducing conditions in C waste disposal cells and spent fuel disposal cells are controlled by the Fe^{II} / Fe^{III} pair and the different ferriferous phases present (metal iron, corrosion products (magnetite, anchorite), pyrite, ferriferous montmorillonite and siderite in the swelling clay, pyrite and ankerite in the Callovo-Oxfordian argillites) (Andra, 2005k). Pyrite / magnetite and pyrite / goethite assemblies form two reducing buffers (approximately -300 mV in the pH conditions of the disposal cells).

In the case of spent fuel disposal cells, the radiolytic dissolution of the oxide grains give rise to the release of uranium with a valence of +VI (cf. § 7.3.5). Soluble uranium +VI is reduced in contact with different reducing compounds present in the cell: metal iron and corrosion products associated with the containers and lining, pyrites and siderite present in the swelling clay and pyrites of the Callovo-Oxfordian argillites. The quantity of reducing compounds and their reactivity restricts the progress of uranium +VI inside the disposal cells (a few centimeters at most). Beyond this redox front, uranium has a valence of +IV, is barely soluble and the redox conditions are those imposed by the various components of the disposal cells (cf. above) (Andra, 2005k).

As regards the argillites, the redox potential is imposed by the S^{II} / S^{IV} pair determined by the pyrite and the sulphate content in the interstitial water. This yields values potentially close to -200 mV (Altmann & Jacquot, 2005). The presence of hydrogen, especially in high concentrations in the vicinity of steel components is likely to impose even more reducing conditions locally.

- **B Waste Disposal cells**

The irradiating character of industrial B waste packages is only significant for package types B1, B5 and B6 (Andra, 2005a, Situations Zb1x_1/2, Zb2_1/2 et Zb1h_1/2). Dose rates have largely decreased beyond 500 years after the emplacement of packages in the repository. Throughout almost the entire period, the slow resaturation of B waste disposal cells prevents liquid water from reaching the waste packages therefore limiting the radiolytic effects. Redox conditions quickly become anoxic. They endure for the duration of radionuclide release.

Specifically, in disposal cells containing B2 type waste packages (bituminised sludge), the release of nitrates (several kilograms to tens of kilograms of nitrates per package, (Andra, 2005k)) during their degradation can result in a modification of the redox conditions in the cell. In fact, nitrates can be reduced by bacterial activity and by the corrosion of the iron (Nagra, 2003c ; Pauwels *et al.*, 2000). Depending on the reduction kinetics of these nitrates, the consequences on the redox conditions in the disposal cell are variable. If reduction is slow (low reactivity), the nitrates migrate as far as the geological medium without interacting with the disposal cell components and therefore without significantly modifying the redox conditions as described above. On the other hand, if they are reactive, their reduction gives rise to the formation of a highly oxidizing zone in the vicinity of the packages (redox potential then imposed by the pair N^V / N^0). In this latter case, the reduction kinetics give rise to rapid consumption of the nitrates. The duration of the oxidizing transient is therefore dependent on the rate of the release of the salts by the waste packages and continues for approximately ten thousand years. The hypothetical scenario of high reactivity remains closely correlated to the evaluation of the associated biological activity. In fact, as in the case of sulphates, nitrate ions have a high degree of molecular stability which makes their reduction less probable if it is not catalysed by biological activity (Nagra, 1999b). As these conditions can only be found in the very near-field around the packages, the oxidizing transient related to the nitrates is only significant in this area. In the rest of the cell, it does not affect redox conditions.

The slag used to make the concrete used contains pyrite which imposes a radox potential in the concrete which is comparable to that of the argillites. In contact with the primary waste packages, the corrosion of steel gives rise to the formation of magnetite which forms a redox pair with the mineral species present in the argillites (gœthite, hematite) and buffers the potential between -200 mV and -300 mV (Andra, 2005k ; Nagra, 2003c).

Redox conditions therefore remain very largely reducing in B waste disposal cells and are buffered by the ferriferous species present in the cell (Andra, 2005k).

10.3.1.3 Hydraulic Conditions and Solute Transport in the Disposal cells and in the Repository Drifts

The chapter on water flow in and around the repository and the associated solute transport (cf.§ 6) has shown that, with the exception of very transient periods, diffusion is the dominant phenomenon for the transportation of solutes in and around the repository.

Because of their elongated shape, the disposal cells provide a large surface area for heat exchange to occur between them and the argillites as compared with the heat exchange area between the top of the disposal cells and the adjacent access drifts. Given the ratio of this surface area and the permeability ratio between the argillites and the disposal cell plug, the preferential solute transfer path is towards the argillites. Only a very small quantity of solutes migrate towards the disposal cell plug (C waste disposal cells and spent fuel disposal cells) or the concrete base slab (B waste disposal cells) towards the access drift (cf.§ 6). The access drift is very long (up to several hundred meters in the case of C waste disposal modules or spent fuel disposal modules) compared with its diameter. Because of the seals, the small advective component of transport in the access and connecting drifts means that the transport of solutes in the drifts takes place preferentially towards the argillites and not by advection towards the shafts.

10.3.2 Retention in the Repository Cells

Retention in the repository cells is mainly governed by the nature of the solid phases and the chemical characteristics of the interstitial water (Eh, pH, pCO_2 in particular) (Andra, 2005g).

10.3.2.1 Retention in C Waste Disposal cells and in Spent Fuel Disposal cells

Within these disposal cells, corrosion products (oxides and iron hydroxides) are likely to present retention properties in respect of the radionuclides (SKB, 1996). However, the retention capacities of these phases for the different radionuclides that may interact with them cannot be quantified on the basis of the level of knowledge available.

In the case of spent fuel disposal cells, the engineered barrier made of swelling clay has high retention properties for the majority of the radionuclides with the exception of chlorine, iodine and carbon (Inset 10.6). The part of the clay engineered barrier that is highly remineralised by iron / clay disturbance (a pluricentimetric extension) contains zeolites and chlorites that can present significant retention properties such as for caesium by zeolites for example (cf. § 7.3.2.2). Beyond the highly remineralised area, the retention properties of the clay are not affected. We can therefore consider the retention properties of the engineered barrier to be by and large preserved (Giffaut & Coelho, 2005).

Inset 10.7 ***The Retention Properties (Solubility and Sorption) of Radionuclides in Swelling Clay (1/2)***

The solubility of radionuclides in a swelling clay are very similar to those described for Callovo-Oxfordian argillites (Inset 10.11). They are widely dealt with in international literature. They are and have been the subject of numerous European (TRANCOM II, RADWASTOM 3C, NFS-2,…) and national research programmes (GdR Practis, etc.). The solubility data used by Andra are taken from numerous programmes, as well as specific Andra research through groups of laboratories. Schematically, we can differentiate between (Giffaut & Coelho, 2005):

So-called mobile elements such as Cl, I, C and B that have a high solubility and low retention

Chlorine and *iodine* have infinite solubility and no (or very poor) retention on clay. The solubility of *carbon* is not nil but presents no sorption property on clay. *Boron* is usually considered a mobile element (infinite solubility and poor retention between 2 and $5 \cdot 10^{-3}$ $m^3.kg^{-1}$).

Other elements, with a (very) low solubility and/or high retention on clay surfaces

- *Caesium* (Cs^+) has an infinite solubility in clay media but is adsorbed on the clay surfaces at two surface sites: an ion exchange site and a silanol site. A model is used to evaluate a shared constant in these conditions (~ 0.1 $m^3.kg^{-1}$).
- *Selenium* has a very low solubility, of the order $5 \cdot 10^{-10}$ – 10^{-14} $mol.^{-1}$, on account of its aptitude to coprecipitate with pyrite (Inset 10.11). In these very reducing conditions, it is probable that selenium would be in its -II oxidation level. Its sorption on clay in this form is low, of the order of 10^{-3} $m^3.kg^{-1}$.
- The behaviour in solution of the *trivalent lanthanides* (samarium, holmium and terbium) is similar overall for all these elements. Their solubility, governed by co-precipitation processes, is very low, (~ 10^{-12} $mol.L^{-1}$) (Inset 10.11). A sorption model is developed based on the sorption studies on clay of these elements, and europium in particular. An average value on the domain of interest of the exchange constant is thus evaluated (~ 12 $m^3.kg^{-1}$).
- The solubility of *plutonium* is approximately $2 \cdot 10^{-7}$ $mol.L^{-1}$ in the very reducing conditions of the spent fuel disposal cells (Inset 10.11); it reduces to approximately $4 \cdot 10^{-9}$ $mol.L^{-1}$ if conditions become less reducing (Eh > -200 mV) or more basic (pH > 7.5). Experimental studies indicate a retention of plutonium IV of approximately 1 $m^3.kg^{-1}$. No data is available for plutonium III, but its sorption is probably similar to that of the trivalent actinides such as americium.
- The solubility of *uranium* IV is of the order of $5 \cdot 10^{-8}$ $mol.L^{-1}$ (Inset 10.11). A surface complexing model has been developed which makes it possible to reproduce the high retention observed, of the order of $100 m^3.kg^{-1}$.
- *Americium* with a valence of +III is stable in spent fuel disposal cell conditions and has a solubility close to 10^{-10} $mol.^{-1}$ (Inset 10.11). The sorption of the americium on clay is considered analogous to that of europium (~ 12 $m^3.kg^{-1}$).

The Retention Properties (Solubility and Sorption) of Radionuclides in a Swelling Clay (2/2)

Summary of solubility and retention of certain radionuclides of interest in the engineered barrier of spent fuel disposal cells made from swelling clay

Element	Solubility ($mol.L^{-1}$)	Kd ($m^3.kg^{-1}$)
Cl^{-I}	infinite	0
B^{III}	infinite	$\sim 10^{-3}$
I^{-I}	infinite	0
Cs^{I}	infinite	$\sim 10^{-1}$
Tc^{IV}	$\sim 4\cdot10^{-9}$	~ 30
C^{IV}	$\sim 5\cdot10^{-5}$	0
Ni^{II}	10^{-5} - 10^{-6}	$\sim 5\cdot10^{-1}$
Se^{-II}	$5\cdot10^{-10} – 10^{-14}$	$\sim 10^{-3}$
Zr^{IV}	$10^{-11} – 3\cdot10^{-6}$	> 100
Nb^{V}	$< 5\cdot10^{-7}$	~ 10
U^{IV}	$\sim 5\cdot10^{-8}$	~ 100
Sm^{III}	$\sim 10^{-12}$	~ 12
Eu^{III}	$\sim 10^{-12}$	~ 12
Tb^{III}	$\sim 10^{-12}$	~ 12
Ho^{III}	$\sim 10^{-12}$	~ 12
Th^{IV}	$\sim 10^{-9}$	~ 3
Np^{IV}	$\sim 4\cdot10^{-9}$	~ 1
Pu^{IV} / Pu^{III}	$2\cdot10^{-7}$ - $4\cdot10^{-9}$	~ 1
Am^{III}	$\sim 10^{-10}$	~ 12

10.3.2.2 Radionuclide Retention in B Waste Disposal cells

Under anoxic conditions, concrete presents considerable retention properties for most radionuclides (Inset 10.9). However, as in the case of the clay, so-called mobile elements can be identified such as iodine, chlorine and technetium (depending on their valence). The retention properties of the concrete vary depending on its state of degradation, but it generally remains of the same order of magnitude for most of the radionuclides, between the unaltered and altered state in particular.

The chapter on chemical processes (cf.§ 6.4.1) demonstrated that the periphery of a B waste disposal cell became degraded in contact with the argillites over a time scale of several hundred thousand years. Schematically, over this period, it can be considered that, in the disposal cells, undisturbed concrete at the core of the disposal cells (in the disposal packages) and altered concrete around the periphery of the disposal cells alone coexist in the disposal cells. Overall, therefore, the general retention properties of B waste repository cells evolve little over a time scale of several hundred thousand years. Furthermore, this time scale is similar or greater than that of the release of radionuclides by different types of B waste.

The retention (and solubility) properties of B waste disposal cells could be influenced by the presence of complexing agents arising, in particular, from the degradation of organic waste. The organic admixtures of the concretes (plasticizers) are considered not to influence the behaviour in solution and the retention of the radionuclides on account of their weak concentrations in solution (Giffaut, 2005 ; Nagra, 2002a). Similarly, the impact of the organic compounds arising from the oxidation of the kerogen of the argillites in the disposal cell walls during ventilation while the repository is in operation is deemed to be low on account of the low kerogen content in the argillites.

Design provisions concerning the distribution of B waste packages in the disposal disposal cells aim not to mix waste containing organic compounds with waste that does not contain any. This is why packages of bituminised sludge (B2 type packages) or the technological waste in B3 type packages containing organic compounds (for example package types B3.12 or B3.31) are placed in specific disposal cells. Their degradation products cannot therefore influence the retention properties of B waste packages containing B5 or B4 type packages, for example.

Organic complexing agents produced by waste originating mainly from decontamination products used in reprocessing, degradation of bituminised sludge packaging and the degradation of cellulose (Inset 10.8) (Andra, 2005g ; Giffaut, 2005).

- Bituminised sludge packages (B2 type packages) mainly release carboxylic acids (formic and acetic acid) (Bourbon, 2005 ; Giffaut, 2005). The characteristics of the organic species released are influenced by the oxidation of the bitumen during the oxidizing transient. They are more oxygenated, more polar and hydrophilic (phenols, diols, ketones, acids) (Inset 7.14). Among them, oxalate ions are the main potential complexing agents (Giffaut, 2005) (Inset 10.8). Various studies have shown that these oxalate ions do not influence the behaviour of the radionuclides. Finally, bituminised sludge packages also contain tributylphosphate (TBP), but this has no notable effect on the retention of radionuclides, plutonium in particular, in disposal cell conditions (Inset 10.8). B2 type packages, therefore, do not significantly release organic complexing agents likely to modify radionuclide retention.
- B3 and B5.1 type packages have an organic compound inventory that is very variable in nature and quantity. (Giffaut, 2005). However, cellulose is the only compound that could give rise to a high complexing capacity in hyperalkaline conditions through one of its degradation products, isosaccharinic acid (ISA) (Inset 10.8). Concrete has ISA retention properties that limit its concentration in solution. Independently of this consideration, the evaluation of the ISA content in solution in B waste disposal cells (Giffaut, 2005 ; Nagra, 2002a) shows concentrations that are sufficiently low for the behaviour of radionuclides in solution and their retention not to be influenced.

Consequently, in general, radionuclide retention is not influenced by different organic compounds likely to be present in B waste disposal cells.

Inset 10.8 ***Organic Complexing Agents Contained in B waste or Originating from the Degradation of Organic B waste***

B waste has a fairly large inventory of organic compounds and cellulose in particular. The degradation of the latter gives rise to the subsequent formation of other organic compounds (Giffaut, 2005).

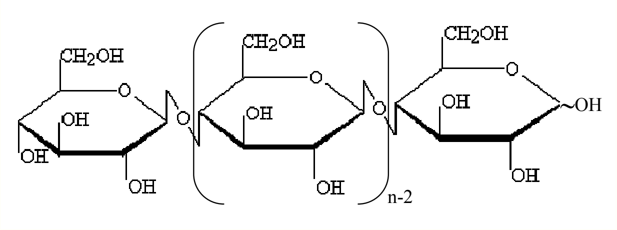

Formula of Cellulose

Of these initial organic products and their degradation products, only a few organic compounds are liable to have complexing properties: oxalates, tributylphosphate (TBP) and isosaccharinic acid (ISA).

Oxalates

The complexes formed by the oxalates are generally weak and in B waste disposal cell conditions, their concentration is limited by the solubility of calcium oxalates.

Tributylphosphate (TBP)

Tributylphosphate ($C_{12}H_{27}O_4P$) is present in bituminised sludge packages. The concentration of this powerful complexing agent of plutonium is, however, limited by its solubility in cement-based media. Its degradation products (monobutylphosphate $C_4H_{11}O_4P$ and dibutylphosphate $C_8H_{19}O_4P$) do not present significant complexing properties in respect of radionuclides in cement-based media.

Isosaccharinic acid (ISA)

Isosaccharinic (ISA) arises from the degradation of cellulose $(C_6H_{12}O_6)_n$, n ranging from 200 to 3,000 (cf. figure above). It is formed from a mixture of two isomers: αIsosaccharinic and β-isosaccharinic (cf. figure below) (Glaus & Van Loon, 2004).

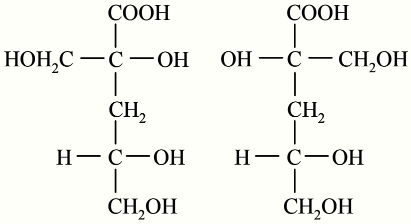

$$\begin{array}{rcl} & \mathrm{COOH} & \\ & | & \\ \mathrm{HOH_2C}- & \mathrm{C} & -\mathrm{OH} \\ & | & \\ & \mathrm{CH_2} & \\ & | & \\ \mathrm{H}- & \mathrm{C} & -\mathrm{OH} \\ & | & \\ & \mathrm{CH_2OH} & \end{array} \qquad \begin{array}{rcl} & \mathrm{COOH} & \\ & | & \\ \mathrm{OH}- & \mathrm{C} & -\mathrm{CH_2OH} \\ & | & \\ & \mathrm{CH_2} & \\ & | & \\ \mathrm{H}- & \mathrm{C} & -\mathrm{OH} \\ & | & \\ & \mathrm{CH_2OH} & \end{array}$$

Formula of the α-Isosaccharinic (left) and β-Isosaccharinic (right) Acids

The complexing capacity of isosaccharinic acids is related to their concentration in solution. The latter is related to the kinetics of cellulose degradation. These kinetics are considered very slow in cement-based media (approximately 10 % degraded in 100,000 years, the entirety in 1,000,000 years). In addition, the sorption of ISA on cement-based phases limits its content in solution (Giffaut, 2005 ; Glaus & Van Loon, 2004).

In B waste disposal cell conditions, the ISA content in interstitial water is estimated in the region of $2 \cdot 10^{-6}$ mol.L^{-1} (Giffaut, 2005). At these concentrations, the radionuclide distribution constants are not significantly modified (Baston *et al.*, 1994).

Inset 10.9 ***The Solubility and Sorption of Radionuclides in Cement-Based Materials (1/2)***

The solubility of radionuclides is evaluated on the basis of equilibrium calculations (using the Andra thermodynamic database: Thermochimie v.5) compared with data from literature and/or dedicated direct measurements. Sorption is assessed on the basis of measurements from batches of test specimens or on a column, and on literature (Andra, 2005g ; Giffaut, 2005). Schematically, we can differentiate between (Giffaut, 2005):

"Mobile" elements in a cement-based medium, such as Cl, I and Tc

- *Chlorine*, iodine and, in some conditions, technetium are elements that have infinite solubility, but the latter two have sorption properties that are not nil in cement-based phases.

- *Iodine* fixation by cement-based phases is weak (replacement of the sulphates with monosulphoaluminates, affinity for the SCH, etc.): Kd ~ 10^{-3} $m^3.kg^{-1}$ (Giffaut, 2005 ; Nagra, 1999a).

- The behaviour of *technetium* depends on the redox conditions. In fact, two states of oxidation can coexist: Tc^{IV} and Tc^{VII}. Tc^{VII} has an infinite solubility and almost nil retention. At very basic pH imposed by the stages of degradation of the concrete (undisturbed concrete and altered concrete), the reducing conditions of the cement-based materials considered alone (~ -310 mV) are at the limit of the domain of stability between the two states of oxidation of the technetium (-350 mV to pH = 12). Inside the disposal cells, because of the large quantities of steel waste and the formation of hydrogen during their corrosion in reducing conditions, it is probable that the conditions are significantly more anoxic. So, the solubility of the technetium is limited by the precipitation of TcO_2,nH_2O (~ 10^{-7} $mol.L^{-1}$). The sorption of the Tc^{IV} is average for cement-based materials (~ 2 $m^3.kg^{-1}$).

Other elements, with very low solubility and/or (high) sorption in cement-based phases.

- *Caesium* has infinite solubility in cement-based media, but it presents an affinity that is not negligible for CSH phases of the cement-based materials with a Kd of the order of 10^{-2} $m^3.kg^{-1}$.

- *Selenium* is stable in its +IV oxidation level in B waste disposal cell conditions. In spite of its negative charge, the ion SeO_3^{2-} has a certain affinity for CSH surfaces (Kd of the order of 0.1 $m^3.kg^{-1}$). In addition, the portlandite has a high capacity to fix Se^{+IV} probably because of the stability of the solid $CaSeO_3$ (~ 10^{-5} $mol.L^{-1}$) and a tendency to form a solid solution with ettringite.

- *Uranium* is very sensitive to redox conditions. Its behaviour varies considerably between +IV and +VI oxidation states. The alkaline conditions of the B waste disposal cells seem to stabilise the +IV oxidation state. However, determining the solid phase controlling the solubility of the uranium in these conditions is complex, between uraninite (UO_2,xH_2O) and schoepite ($UO_2(OH)_2,H_2O$), passing through the formation of calcic phases such as uranophane ($Ca[(UO_2)(SiO_3OH)]_2,5H_2O$) depending on redox conditions. Calcosilicate phases are probably favoured in the cement-based media of the disposal cells. The solubility of uranium is of the order of 10^{-6} $mol.L^{-1}$. With regard to sorption processes, these are important in cement-based phases (~50 $m^3.kg^{-1}$).

The Solubility and Sorption of Radionuclides in Cement-Based Materials (2/2)

- The solubility of *trivalent lanthanides* (Sm, Eu, Tb, Ho) in cement-based media is governed by the processes of incorporation and coprecipitation with calcic solids (calcium phosphates, calcite, Portlandite, etc.) which gives rise to a very low solubility (~ 10^{-10} mol.L^{-1}). As regards their sorption capacity, these elements have a considerable affinity for cement-based phases, CSH in particular (~ 100 m^3.kg^{--1}). Irreversible sorption processes are also foreseeable, limiting these elements even more.

- *Thorium* has very low mobility in B waste disposal cell conditions. Its solubility is in fact very weak (~ 10^{-11} - ~ 10^{-10} mol.L^{-1}) and its affinity for the mineral phases is very high (~ 20 m^3.kg^{-1}).

- *Neptunium* and *plutonium* are stabilised in a reducing cement-based medium in its +IV oxidation level. Their solubility is governed by phases NpO_2,xH_2O and PuO_2,xH_2O which gives rise to low contents (respectively ~ 5 10^{-9} mol.L^{-1} and ~ 10^{-9} mol.L^{-1}. The sorption of neptunium has not been studied in cement-based phases. By analogy, however, its behaviour can be likened to that of plutonium. They therefore have significant retention on cement-based phases of the order of ~ 20 m^3.kg^{-1}.

- *Americium* is stable with a valence of +III and behaves in a similar way to the lanthanides and europium in particular which is an analogue. Its solubility is, therefore, of the order of ~ 10^{-10} mol.L^{-1}. However, its sorption on cement-based phases appears to be lower than it is for europium (~ 30 m^3.kg^{-1}).

Summary of the Solubility and Retention of Certain Radionuclides of Interest in a Undisturbed to Altered Cement-Based Media

Element	**Solubility (mol.L^{-1})**	**Kd (m^3.kg^{-1})**
Cl^{-I}	infinite	0
I^{-I}	infinite	~ 10^{-3}
Cs^{I}	infinite	~ 10^{-2}
Tc^{IV} / Tc^{VII}	~ 10^{-7} / infinite	~ 2 / 0
C^{IV}	~ 10^{-5} - ~ 10^{-6}	~ 1
Ni^{II}	~ $2 \cdot 10^{-7}$	~ 2
Se^{-IV}	~ 10^{-5}	~ 10^{-1}
Zr^{IV}	~ 10^{-8}	~ 40
Nb^{V}	~ $\cdot 10^{-9}$	~ 100
U^{VI}	~ 10^{-6}	~ 50
Sm^{III}	~ 10^{-10}	~ 100
Eu^{III}	~ 10^{-10}	~ 100
Tb^{III}	~ 10^{-10}	~ 100
Ho^{III}	~ 10^{-10}	~ 100
Th^{IV}	~ 10^{-11} - ~ 10^{-10}	~ 20
Np^{IV}	~ $5 \cdot 10^{-9}$	~ 20
Pu^{IV}	~ 10^{-9}	~ 20
Am^{III}	~ 10^{-10}	~ 30

10.3.3 The Transfer of Radionuclides in the Repository: Transfer Paths and Typical Time Frame

10.3.3.1 Radionuclides in Solution

As a general rule, the main solute transfer path in the disposal cells is the radial path in the direction of the argillites. The solute transfer path through the plug of the C waste disposal cells and the spent fuel disposal cells or the B waste disposal cell seals is a secondary path. Similarly, in the access and connection drifts, the longitudinal transfer path is secondary and transfer essentially takes place by dispersion / diffusion towards the argillites (cf.§ 6). Advection only becomes dominant closer to the shafts. In fact, the branches of the drift network mean increasingly large upstream drainage surface areas the greater the distance from the disposal cells and the closer one is to the shafts. This results in an increase in the water flow rate of the order of 10^{-5} m.year^{-1} to 10^{-4} m.year^{-1} closer to the shafts. These rates are however very slow and correspond to advection transfer times of the order of a few thousand to tens of thousands of years per meter.

- **C Waste Repository Zones and Spent Fuel Repository Zones**

The release of radionuclides by C waste packages and spent fuel packages begins after around 4,000 and 10,000 years, respectively. By this time, the thermal loads in the disposal cells have already significantly decreased: the temperature is almost homogeneous and below 50 °C. The dissolution of the glass in the case of C waste, the corrosion of metal components and the dissolution oxide matrices in the case of spent fuel begins.

The dissolution of the glasses continues for several hundred thousand years and corresponds to a slow release in solution of radionuclides. Essentially, in the case of the latter and actinides in particular, their concentration in the water is governed by their solubility inside the packages or upon contact. Added to this is **(i)** the retention of numerous radionuclides on glass alteration products (alteration layer and secondary layer silicates) and **(ii)** the coprecipitation of radionuclides. The corrosion products in all likelihood present retention properties but they are not quantified to date. A small fraction of the radionuclides released, which is defined by the solubility limits, migrates in solution towards the disposal cells. ^{129}I and ^{36}Cl, which are not governed in solution and whose sorption is therefore nil, migrate immediately beyond the disposal cells into the argillites. These processes continue throughout the dissolution of the glass. The quantity of radionuclides that migrates beyond the disposal cells is therefore governed mainly by the solubility limits of the radionuclides and the diffusion of these in the argillites in the direction of the under- and over-lying surroundings.

An overall similar process affects the spent fuel disposal cells. The difference lies in the presence of the engineered barrier and the particular characteristics of the release of radionuclides from spent fuel assemblies. A fraction of the radionuclide inventory is immediately available for release into solution from the moment water arrives (i.e. the labile fraction). This is particularly the case of mobile radionuclides such as ^{129}I and ^{36}Cl. Their labile fraction then migrates through the engineered barrier to the argillites. The maximum molar flow rate of ^{129}l when leaving the engineered barrier is reached in approximately 200 years. For most other radionuclides, the maximum molar flow rate leaving the engineered barrier is reached after several thousand years (e.g. in the case for ^{59}Ni), several tens of thousands of years (e.g. in the case of ^{99}Tc) or several hundred thousand years (e.g. in the case of uranium) depending on their particular behaviour (Inset 10.6).

In particular, during the several thousand to tens of thousands of years following the discharge of leak tightness of the containers until the return to geothermal temperatures, the temperatures in the engineered barrier and/or the near-field argillites around the disposal cells only result in a slight increase in the retention properties and of the diffusion coefficient (Giffaut & Coelho, 2005), and, therefore, only have a secondary effect on the migration of the radionuclides. Current data indicates a slight increase in retention (less than one order of magnitude) for cationic species sensitive to surface sorption processes (nickel, europium, etc.), whereas, for cations sensitive to ion exchange (caesium, etc.), no temperature effect is visible.

Among the radionuclides that are barely or not at all retained such as ^{129}I, ^{36}CI and ^{14}C, the majority (> 90 %) migrate beyond the disposal cells in the direction of the Callovo-Oxfordian argillites. A small proportion migrates to the drifts (< 10 %, cf. § 10.4), and are not affected by the alkaline disturbance that develops in the clay plug of the disposal cell or the degradation of the concrete support base. The latter give rise to the gradual modification of the solubility and retention of the radionuclides in the external part of the clay plug and in the concrete plug. These chemical processes take place after several hundred thousand years and therefore do not modify the overall pattern of migration. The barely disturbed clay plug area therefore retains its initial retention properties (Giffaut & Coelho, 2005) and the retention properties of the highly remineralised area are very close to those of degraded concrete.

- **The B Waste Repository Zone**

The overall pattern of radionuclide transfer in C waste disposal cells and spent fuel disposal cells applies to B waste disposal cells. The difference lies mainly in the characteristics of the materials (concrete *versus* swelling clay or argillites) and the existence of a non-saturated state of B waste disposal cells. This does not entirely prevent the degradation of waste and the release of radionuclides, but it does delay the migration of radionuclides released in the disposal cells. After a few hundred thousand years, saturation conditions are close to total saturation and this effect disappears. The migration of the radionuclides released takes place preferentially by the radial path towards the argillites. The solubility and sorption of the radionuclides in concrete differs from those in swelling clays and argillites. However, the mobility of elements such as iodine and chlorine is found, although the concrete does present weak but not negligible retention properties in respect of iodine. It is these mobile elements, therefore, that mainly migrate outside the disposal cells. The maximum molar flow rate of the other radionuclides in the disposal cell limits are reached in several thousand to several hundred thousand years.

- **The Shafts**

Only a small proportion of the most mobile radionuclides, such as iodine and chlorine, can migrate through the drift system of the repository to the shafts (cf. § 6.3.3). The proportion leaving the shafts over a time span of a million years is low. For example, in the case of ^{129}I from spent fuel SF1, the fraction of the total inventory leaving via the shafts is of the order of 3.10^{-5} % (Pepin & Vialay, 2005).

10.3.3.2 Gaseous Radionuclides

Of the radionuclides, only ^{14}C can be expressed in gaseous form in the physical and chemical conditions of the repository (Inset 10.10). This would only concern B5-1 type packages. For these packages, the gaseous fraction of the ^{14}C released can migrate during the not totally saturated state phase of the B waste disposal cells and the connection drifts, following the vertical path in the argillites and the horizontal path in the access drifts. However, this would only concern the first few thousand years corresponding to the hydrogen propagation period in the Callovo-Oxfordian formation and in the repository drifts to the shafts. After 10,000 years, hydrogen production diminishes on the scale of the repository which makes the gradual arrival at a state of a total repository saturation possible. In the region of the B waste disposal area, the migration of hydrogen in the Callovo-Oxfordian formation would not exceed 2/3 of the high and low clearance distances (in the direction of the calcareous Oxfordian and Dogger formations) therefore blocking the migration of the gaseous ^{14}C. This can therefore only take place by dissolution and diffusion in the water of the argillites into the surroundings. The hydrogen present in the drifts leading up to the shafts could give rise to the existence of a gas transfer path to the calcareous Oxfordian formation in the shafts thus allowing the migration of ^{14}C directly into the calcareous Oxfordian formation. This transfer path is improbable. Moreover, it would not last longer than 10,000 years. In general, beyond of this period of time, the ^{14}C released by B5.1 packages would gradually migrate preferentially by dissolution and diffusion in the water of the disposal cells and argillites.

Inset 10.10 ***Gaseous Radionuclides in Repository Conditions***

Among the radionuclides of high-level and long-lived level waste and spent fuel, only a few are liable to be found in gaseous form in repository conditions: ^{3}H, ^{14}C, ^{39}Ar and ^{85}Kr. ^{36}Cl and ^{129}I are in a gaseous state (said to be still volatile) in a reactor. Thus, in a reactor ^{129}I can be combined with the caesium to form partially volatile CsI (Nagra, 2002b). In repository conditions in the presence of water, ^{129}I is dissolved in the form of iodide I^-, which is not gaseous. It is very unlikely that it would convert into a volatile form (CH_3I or I_2) since these compounds are very reactive or rather hydrolyse easily again into iodides (Nagra, 2003a). Similarly, in repository conditions, ^{36}Cl would only be found in a non gaseous form (chlorides) (Giffaut, 2005).

^{3}H, ^{39}Ar and ^{85}Kr have very short periods (12.3 years, 269 years and 10.7 years, respectively). They disappear rapidly via radioactive decay and essentially concern the repository operation period. This is the case of ^{3}H in particular which is continually released by B waste packages (Andra, 2005m).

As regards ^{14}C, its gaseous form, mainly methane as it happens, would only be observed in the presence of bacterial activity and only in the case of the organic fraction of ^{14}C (C^{-IV} - C^{-VI}). This would essentially concern the metal compounds of spent fuel (hulls and end caps) and B5 packages. It will be noted that an infimum fraction of carbon, (less than 0.1 % of the total inventory, would be directly present in gaseous form in the clearance of the spent fuel rods when being removed from the reactor vessel. In the case of all other waste, ^{14}C would be in an inorganic form. Its degradation, such as for example the dissolution of iron carbide (Fe_3C), zirconium carbide (ZrC) or spent fuel oxide matrices would give rise to the formation of organic species or non gaseous and soluble carbonates in repository conditions (acetic acid, formic acid, acetaldehyde, formaldehyde, ethanol, methanol, propanol, etc.) (Johnson & Schwyn, 2004).

10.4 Transfer of Radionuclides in Solution in the Callovo-Oxfordian Layer from the Repository and into the Surroundings

10.4.1 Phenomenology of the Callovo-Oxfordian Layer From the Perspective of Radionuclide Release Time for Waste Packages

The hydraulic and chemical evolution of the repository and its surrounding geological medium showed that the Callovo-Oxfordian layer was not significantly affected by the disturbances created by the repository. These are limited to the very near-field of the repository (a few meters maximum). In addition, the duration of this disturbance is limited, for example, to a few thousand to ten thousand years in the case of hydraulic overpressure associated with the thermal load and the production of hydrogen from corrosion in the region of the C waste repository zones and the spent fuel repository zones. Alternatively, this disturbance develops slowly over several hundred thousand years, as in the case of alkaline disturbance in the region of the B waste repository zone. More specifically, the mechanical damage created initially around the repository structure is progressively healed (in a few hundred to a few thousand or tens of thousands of years after the structural work). This healing enables a return to flow properties and solute transfer in the argillites in the repository near-field in the vicinity of those in the initial state prior to the installation of the repository. Finally, on a large scale, the geodynamic evolution does not affect the Callovo-Oxfordian layer directly: after 300,000 to 500,000 years, the vertical hydraulic gradients in the Callovo-Oxfordian layer gradually increase due to variations in hydraulic heads in the Dogger and above all in the calcareous Oxfordian formations.

However, this increase does not change the dominant character of diffusion as the mode of transport of the solutes.

The scale in terms of the time and space mentioned above must be taken into account in relation to the typical times for the release and transfer of radionuclides.

From the chemical perspective:

- the pluridecimetric or plurimetric, at most, thickness of the argillites disturbed by alkaline plume or iron / argillite interaction is negligible over the 50 to 60 meters minimum clearance between the repository and the roof and the wall of the Callovo-Oxfordian layer. In addition, these disturbances do not necessarily lead to a reduction in the retention properties of the radionuclides or the flow and transport of the solutes;
- the thermal load does not modify the retention properties of the argillites in the far-field in particular. It does not give rise to mineralogical transformations likely to irreversibly modify the permeability of the argillites and the diffusion coefficients of the solutes (anions and cations).

From the flow and solute transfer perspective:

- the thermal load and production of hydrogen produced by corrosion gives rise to the transient existence of diverging flows from the repository. However, they only affect a few meters of the repository near-field and will have disappeared after approximately 10,000 years. This means that they only have the potential to affect the transfer of radionuclides for C waste repository zones (the minimum duration of leak tightness of the over-packs is 4,000 years) and the B waste repository zones (radionuclide release is possible from the moment that liquid water comes into contact with the waste, which is in over of several hundred years after the closure of the repository). However, the release of radionuclides by vitrified waste packages extends over a period of several hundred thousand years so that a very small fraction of the radionuclides released is affected by the hydraulic transient. The same is true for B waste. In the case of spent fuel containers, the *minimum* duration leak tightness of 10,000 years results in a release of radionuclides after the period affected by hydraulic disturbance;
- diffusion remains the dominant mode of transport of the solutes, and therefore the radionuclides, on the scale of the Callovo-Oxfordian layer.

10.4.2 Transfer in the Callovo-Oxfordian Layer

After migrating beyond the disposal cells, radionuclides and mobile, long-lived radionuclides (^{129}I, ^{36}Cl, ^{79}Se) in particular can gradually migrate from the repository by diffusion in the Callovo-Oxfordian layer in equal amounts to the calcareous Oxfordian and Dogger formations proportionally to the waste packages.

In the case of the spent fuel zones of the repository, the migration of the mobile radionuclides in the Callovo-Oxfordian layer is mainly influenced by the labile fraction (between 5 % and 35 % of the total inventory) immediately released from the moment that leak tightness of the containers is lost at 10,000 years. The fraction gradually released by the oxide pellets over several tens of thousands to a hundred thousand years only comes into play over the total duration of the release beyond the Callovo-Oxfordian layer. The maximum molar flow rate of ^{129}I at the roof and wall of the Callovo-Oxfordian formation is reached around 250,000 years.

As regards C waste repository zones and B waste repository zones, the overall pattern found is similar to that of spent fuel, but with lower molar flow rates, account taken of the lower initial inventories and labile activity of almost nil (in the case of C waste) or very low (in the case of B waste).

All the other radionuclides, actinides in particular, have low solubility and/or high sorption in argillites. The migration of these in the Callovo-Oxfordian layer is therefore slow. Associated with low release outside the disposal cells, this means that these radionuclides only migrate a few meters into the Callovo-Oxfordian layer on either side of the repository over a time scale of million years.

Consequently, ^{129}I, ^{36}Cl and ^{79}Se (mobile and long-lived radionuclides), are liable to reach the surroundings in one million years' time. This is illustrated in Figure 10.4.2, Figure 10.4.4 and Figure 10.4.6 of the examples of the spent fuel zones SF1 and the C1-C2 zone.

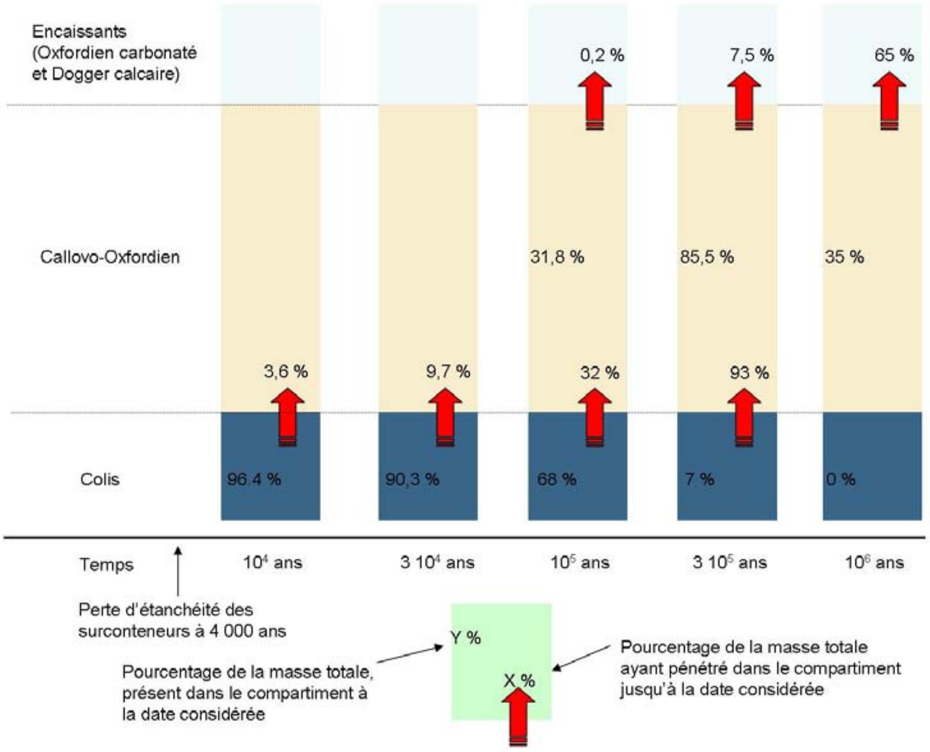

Figure 10.4.1 *Diagram Showing the Distribution of the Mass of Iodine 129 between the Repository Components and the Callovo-Oxfordian Formation at Different Times for Repository Zones C1-C2. The percentages include the mass that has disappeared via radioactive decay (calculated on the basis of Andra, 2005m)*

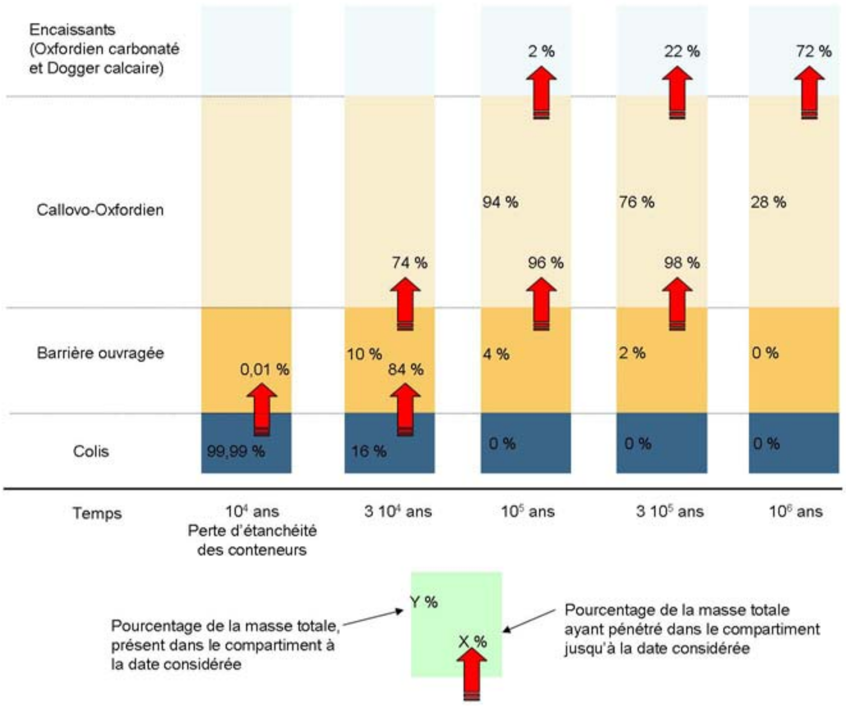

Figure 10.4.2 Diagram Showing the Distribution of the Mass of Iodine 129 between the Repository Components and the Callovo-Oxfordian Layer at Different Times for Repository Zone SF1. The percentages include the mass that has disappeared via radioactive decay (calculated on the basis of Andra, 2005m)

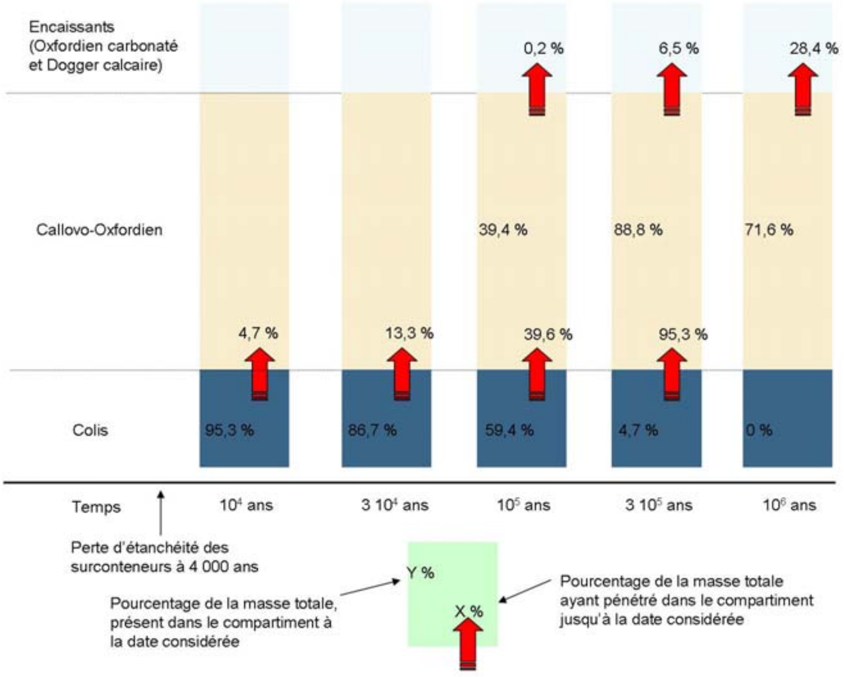

Figure 10.4.3 Diagram Showing the Distribution of the Mass of Chlorine 36 between the Repository Components and the Callovo-Oxfordian Layer at Different Times for Repository Zones C1-C2. The percentages include the mass that has disappeared via radioactive decay (calculated on the basis of Andra, 2005m)

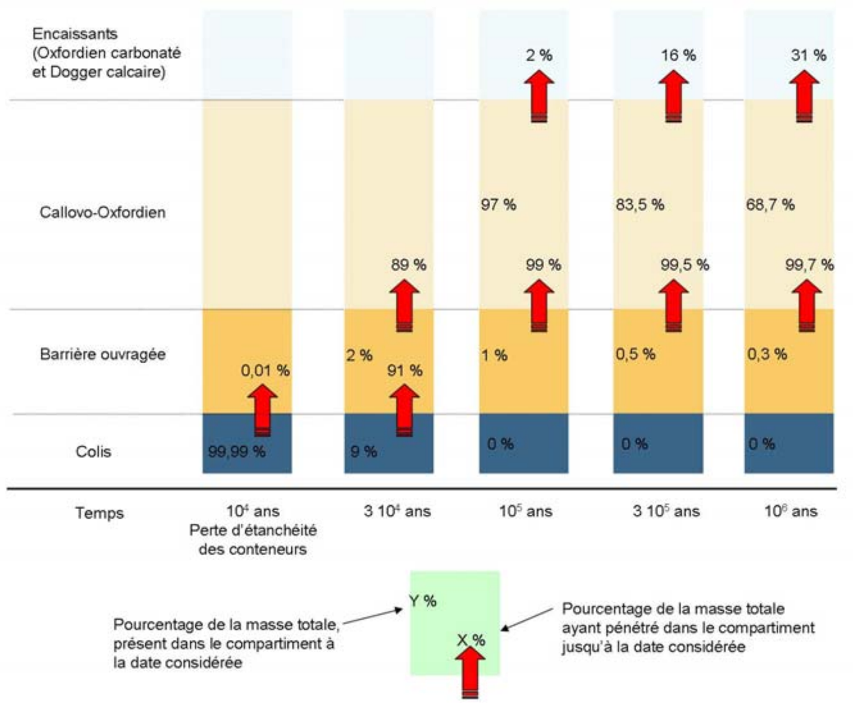

Figure 10.4.4 *Diagram Showing the Distribution of the Mass of Chlorine 36 among the Repository Components and the Callovo-Oxfordian Formation at Different Times for SF1 Spent Fuel Repository Zones. The percentages include the mass that has disappeared via radioactive decay (calculated on the basis of Andra, 2005m)*

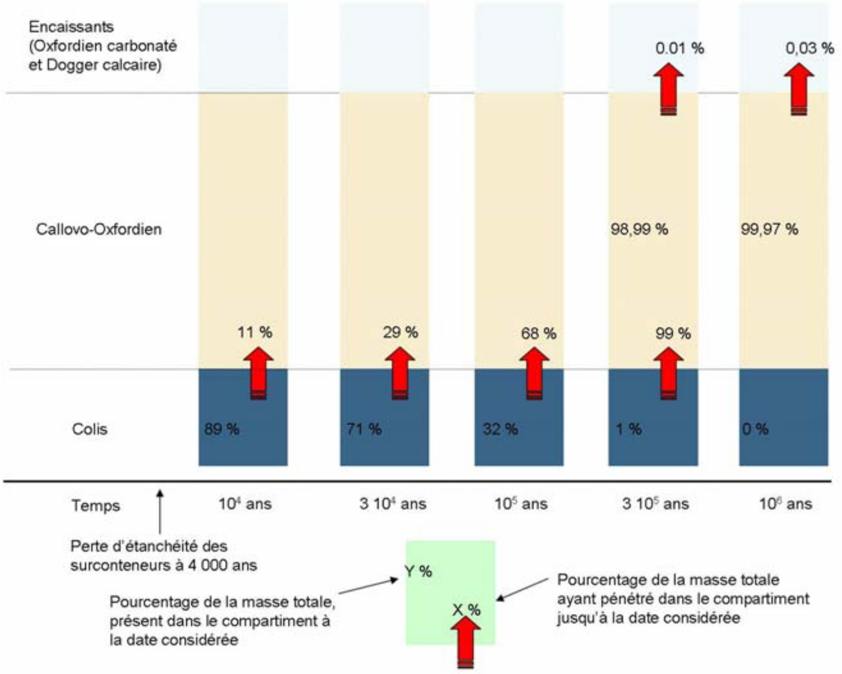

Figure 10.4.5 *Diagram Showing the Distribution of the Mass of Selenium 79 among the Repository Components and the Callovo-Oxfordian Formation at Different Times for the C1-C2 Repository Zone. The percentages include the mass that has disappeared via radioactive decay (calculated on the basis of Andra, 2005m)*

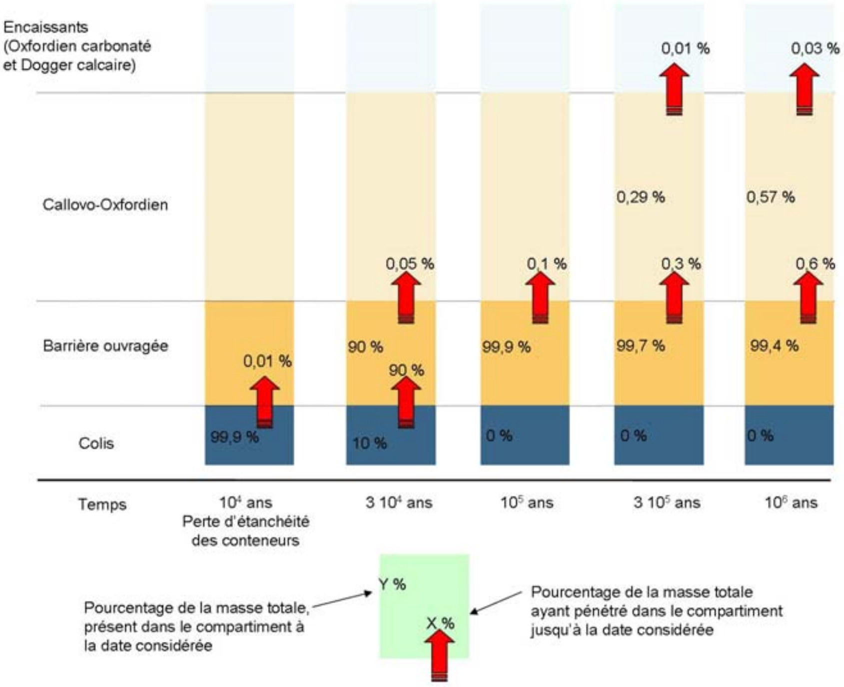

Figure 10.4.6 *Diagram Showing the Distribution of the Mass of Selenium 79 among the Repository Components and the Callovo-Oxfordian Formation at Different Times for SF1 Spent Fuel Repository Zones. The percentages include the mass that has disappeared via radioactive decay (calculated on the basis of Andra, 2005m)*

Inset 10.11 ***The Retention Properties (Solubility and Sorption) of Radionuclides in Callovo-Oxfordian(1/2)***

Numerous experimental studies have been carried out on the retention capacity of Callovo-Oxfordian argillites and the solubility of radionuclides in their interstitial water (Andra, 2005g ; Giffaut & Buschaert, 2005).

Iodine and Chlorine

Chlorine and *Iodine* have infinite solubility. They have no affinity in respect of the clayey phases of the Callovo-Oxfordian argillites.

Other Elements

- *Caesium* is totally soluble, in the form Cs^+. Its retention is governed by the ion exchange processes on clay surfaces. The retention of caesium is contingent upon its concentration in solution; the results of experiments show a variation of several orders of magnitude of the partition coefficient as total Cs varies from trace amounts up to millimolar levels. This sorption is given by a simplified model. Thus, for caesium concentrations lower than 10^{-5} mol.L^{-1}, the retention of caesium is very high and varies between ~ 0.9 m^3.kg^{-1} and ~ 0.1 m^3.kg^{-1} in the case of a caesium concentration varying between 10^{-9} mol.L^{-1} and 10^{-6} mol.L^{-1}respectively. In the case of caesium concentrations lower than 10^{-5} mol.L^{-1}, the retention of caesium is lower, of the order of $2 \cdot 10^{-2}$ m^3.kg^{-1}.

- *Boron* is stable in a soluble form (boric acid H_3BO_3) and has infinite solubility. Its sorption properties on clay are weak but significant (~ $4 \cdot 10^{-3}$ m^3.kg^{-1}).

- The solubility of inorganic *carbon* (~ $5 \cdot 10^{-5}$ mol.L^{-1}) is governed by the formation of calcite. The behaviour of organic carbon is governed by the solubility of the organic compound (acid, alcohol, etc.). Methane is found in gaseous form. Its solubility in the argillite water is therefore close to that of hydrogen. Sorption processes differ according to the form in which they are found, organic or otherwise. In an organic form, the sorption of carbon on the argillites has not been evaluated to date. In organic form (CO_3^{2-}, HCO_3^-), the retention of the carbon takes place mainly by isotopic exchange with the calcareous solids of the media (calcite, dolomite). In view of the long residence times of these solutions in the argillites (at least 100,000 years), this process is not negligible and gives rise to a partition coefficient of the order of 10^{-3} – 10^{-2} m^3.kg^{-1}.

- The solubility of *uranium* is governed by the $UO_{2+x(fuel)}$phase, which is intermediate between amorphous and crystallized species. The solubility of uranium is, therefore, of the order of 10^{-7} mol.L^{-1}. The sorption uranium on the argillites, associated with the great stability of the species $U(OH)_4°$, is of the order of 10 m^3.kg^{-1}.

- Selenium is very significantly influenced by iron content. Therefore, in a milieu that is rich in iron, the species FeSe and FeSe2 can form. In these conditions, the solubility of the selenium is approximately $5 \cdot 10^{-10}$ mol.L^{-1}. In addition, selenium tends to coprecipitate with the pyrite (FeS2) and pyrrhotite ($Fe_{1-x}S$, $0 < x < 0.2$). In this case, the solubility of the selenium diminishes by approximately 4 orders of magnitude. The sorption of selenium in its -II oxidation level on the argillites is not known, it is considered to be nil on account of lack of data.

The Retention Properties (Solubility and Sorption) of Radionuclides in Callovo-Oxfordian Argillites (2/2)

- The behaviour in solution of the *trivalent lanthanides* (samarium, holmium and terbium) is overall similar for all these elements. The solubility is governed by the processes of incorporation and coprecipitation with calcic solids (calcium phosphates, calcite, portlandite, etc.) which give rise to very low solubility (~ 10^{-12} mol.L^{-1}). With regard to the sorption properties of the lanthanides on the Callovo-Oxfordian argillites, no direct measurement has been carried out to date but an analogy can be drawn with Opalinus clay (Nagra, 2003b). Sorption is very high and corresponds to a surface complexing process: the value of the partition coefficient is approximately 50 m^3.kg^{-1}.
- The solubility of *plutonium* is very sensitive to pH and redox conditions, and carbonate content in the argillite conditions of the Callovo-Oxfordian argillites. The redox conditions do not have a great influence on solubility, although their increase stabilises Pu^{IV}, which is less soluble than the form Pu^{III}. With these very reducing redox conditions, the solubility of plutonium is approximately $2 \cdot 10^{-7}$ mol.I^{-1} ; it reduces to approximately $4 \cdot 10^{-9}$ mol.L^{-1} if conditions become less reducing (Eh > -200 mV) or more basic (pH > 7.5). The evaluation of the sorption of plutonium on clay results from the presence of these two redox potentials III and IV. The sorption of Pu^{III} is likened to that of Am^{III} which is analogous. The latter is therefore very high (> 50 m^3.kg^{-1}). The sorption of Pu^{IV} is lower by approximately one order of magnitude (~ 1 m^3.kg^{-1}).
- *Americium* is stable with a valence of +III in argillite conditions. The solubility is close to 10^{-10} mol.L^{-1}, which is consistent with the experiments and the natural analogues. The sorption of americium on Puy illites, which are analogous to the argillites, give rise to a partition coefficient of the order of 50 – 110 m^3.kg^{-1}.

Summary of the Solubility and Retention of Certain Radionuclides of Interest in the Callovo-Oxfordian Argillites

Element	**Solubility (mol.L^{-1})**	**Kd (m^3.kg^{-1})**
Cl^{-I}	INFINITE	0
B^{III}	infinite	~ $4 \cdot 10^{-3}$
I^{-I}	infinite	0
Cs^{I}	infinite	$Kd_{equivalent} = \frac{A}{B + C_{sol}}$ For $[Cs^+] \leq 10^{-5}$ mol.L^{-1}: A=$1.8462 \cdot 10^{-7}$ and B=$4{,}7552 \cdot 10^{-7}$ For $[Cs^+] \geq 10^{-5}$ mol.L^{-1}: A=0.00012 and B=0.00492
Tc^{IV}	~ $4 \cdot 10^{-9}$	~ 10
C^{IV}	~ $5 \cdot 10^{-5}$	10^{-3} – 10^{-2}
Ni^{II}	10^{-5} - 10^{-6}	~ $2 \cdot 10^{-1}$
Se^{-II}	$5 \cdot 10^{-10}$ – 10^{-14}	0*
Zr^{IV}	10^{-11} – $3 \cdot 10^{-6}$	qq 10
Nb^{V}	~ $2 \cdot 10^{-7}$	~ 1.2
U^{IV}	~ 10^{-7}	~ 10
Sm^{III}	~ 10^{-12}	~ 50
Eu^{III}	~ 10^{-12}	~ 50
Tb^{III}	~ 10^{-12}	~ 50
Ho^{III}	~ 10^{-12}	~ 50
Th^{IV}	~ 10^{-9}	~ 60
Np^{IV}	~ $4 \cdot 10^{-9}$	~ 1
Pu^{III} / Pu^{IV}	$2 \cdot 10^{-7}$ - $4 \cdot 10^{-9}$	~ 1 – ~ 50
Am^{III}	~ 10^{-10}	~ 50 - ~ 110

*Value taken as nil due to lack of data

10.5 The Transfer of Radionuclides in the Surroundings

10.5.1 The General Characteristics of Transfer in the Surrounding Formations and the Effects of Geodynamic Evolution

10.5.1.1 General Organisation of Flow and Solute Transfer

The description of the initial geological medium (cf. § 3.6) shows that flows in the surroundings are essentially horizontal and organised into a series of more transmissive porous levels. Solute transport there is advective but slow, so that there is a vertical transport component diffusion between these transmissive levels in the most clayey levels in particular. Transfer in the surroundings therefore generally takes place according to two components, one, horizontal advective, the other, vertical diffusion.

- The flow and transfer of the solutes in the Dogger formation

The hydraulic head gradients in the Dogger formation are small, of the order of 10^{-3} m.m^{-1}, and the permeability is very small (approximately 10^{-8} m.s^{-1} in the more transmissive layers). The quasi horizontal Darcy velocity and direction of flow of the water within the transmissive levels are of the order of some hundred meters per millions of years (a few kilometers per million years for the advective transport velocity of a non-sorbed solute). The directions of flow are generally towards the west-south-west. On the vertical towards the under-lying formations, solute transport is dominated by diffusion.

- The flow and transfer in the calcareous Oxfordian and overlying formations

The Darcy velocity and direction of flow of the water in the porous levels of the calcareous Oxfordian formation are of the order of one kilometre per million years, i.e., advective transport velocities of a non-sorbed solute of the order of a kilometre per hundred thousand years (cf. § 3.3.2.2). At present, the flows downstream of the underground research laboratory are generally directed towards Marne in the west, on the one hand, and follow north-west regional paths on the other.

As a general rule, the behaviour of the solutes in the calcareous Oxfordian formation is similar to that in the Dogger formation. There are, however, two important distinctions: **(i)** part of the solutes can migrate by diffusion across the Kimmeridgian marls to the surface aquifers in the Tithonian (Figure 10.5.1), and **(ii)** flows in the calcareous Oxfordian formation are influenced by climatic and geomorphological evolution from approximately 300,000 years onwards.

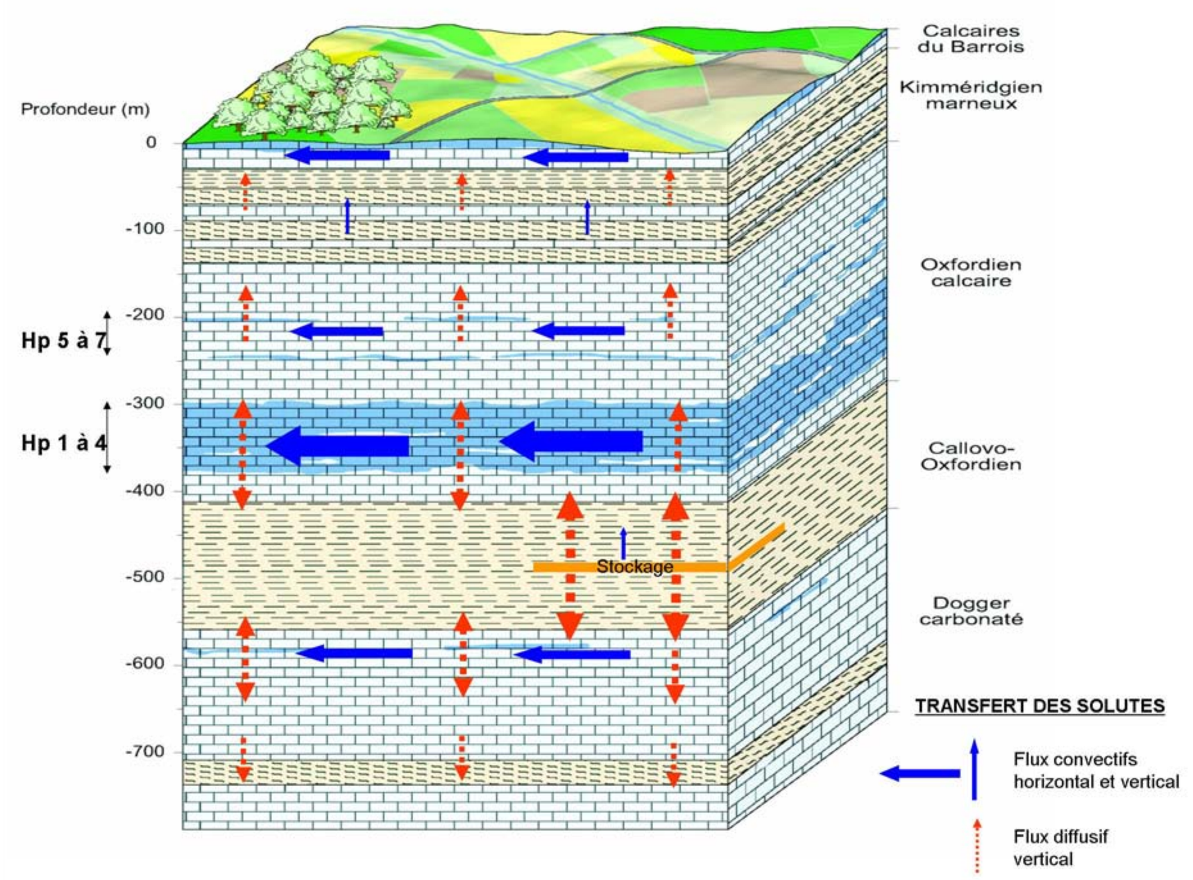

Figure 10.5.1 *Organisation of the (Horizontal and Vertical) Advective and (Essentially Vertical) Diffusive Transport Components in the Callovo-Oxfordian and Surrounding Formations. The size of the arrows are representative of the relative intensity of the transport in the various formations*

10.5.1.2 Retention in the Surrounding Formations

No measurement of retention in surrounding formations over-lying the Callovo-Oxfordian formation in the transposition zone are available. However, it is very likely that the marlaceous levels of the Kimmeridgian formation or the clayey layers of the calcareous Oxfordian wall (basic facies C3a / C3b) present considerable retention properties that could give rise to transfer times of several hundred thousand years in these formations (Buschaert & Giffaut, 2005).

In addition, the samples taken from borehole EST205 show fairly low values (some 10^{-11} to 10^{-12} m².s^{-1} for tritiated water, and 10^{-12} to 10^{-13} m².s^{-1} in the case ^{36}Cl) for the diffusion coefficient in facies C3a / C3b (Trouiller & Benabderrahmane, 2005). Although this data cannot be extrapolated for the whole transposition zone because of the variability of these formations, given the low permeability values of these facies (of the order of 10^{-11} m.s^{-1}), they probably produce a slow transfer by diffusion based on the calcareous Oxfordian formation.

The retention properties of the surroundings of the Callovo-Oxfordian layer are not taken into account in the rest of the analysis.

10.5.1.3 The Influence of Geodynamic Phenomena

- Climate Change

Climate changes directly affect the flows in surface aquifers as periods of extreme glaciation mean the presence of continuous permafrost of a depth of a hundred meters or more.

In the presence of continuous permafrost, the infiltration of water towards deep aquifers is no longer possible. The hydraulic equilibrium is modified because the groundwater is no longer replenished (Figure 10.5.2). The Meuse Haute / Marne site is in the upstream part of the Paris basin. So the groundwater aquifers and those of the calcareous Oxfordian and Dogger formations in particular tend to empty into the regional outlets which are the Manche and the Seuil du Poitou. The hydraulic heads will therefore drop in this sector of the site. During the following thawing period, the arrival of water is again possible and the reverse phenomenon takes place; hydraulic heads increase in the sector of the site. The periodic fluctuation of the water table that results from this have temporal wavelengths of the order of one hundred thousand years and plurimetric amplitudes. (ANTEA, 1999).

Flows from the site in the direction of the local natural outlets correspond to non-sorbed solute advective transfer times of the order of a hundred thousand years (which is the case at present). They would not be significantly influenced by these climatic changes. The natural outlet of Saulx, possible in a million years' time, corresponds to transfer times of several tens of thousands of years. In the case of the establishment of permafrost, flow rates along the paths towards the Saulx could diminish locally by a factor of 2 to 3 during a glacial period. (ANTEA, 1999).

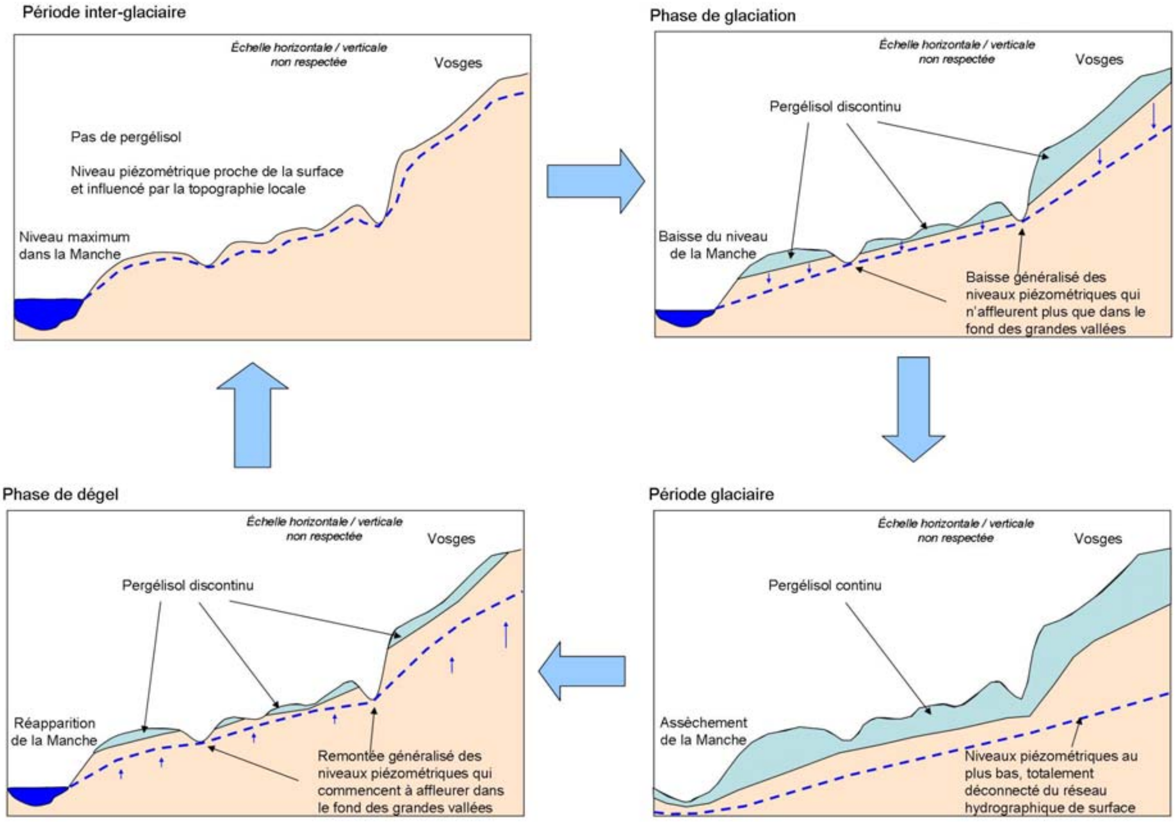

Figure 10.5.2 *Diagram Showing the Fluctuation of the Water Table on the Regional Scale Over the Course of a Glacial Cycle*

Another effect of permafrost is that it prevents the solutes migrating by diffusion from the calcareous Oxfordian to the Tithonian via the Kimmeridgian formations from becoming diluted in the surface water as it is frozen. An increase in their concentration in the liquid water under the permafrost follows. However, continuous permafrost only lasts for a few thousand years maximum. In fact, a glacial cycle of an average duration of one hundred thousand years contains several sub-cycles that vary in intensity. Each includes a period that is cold to a greater or lesser extent and period that is hot to a greater or lesser extent, separated by transition periods. Each of these cold or hot sub-periods lasts for an average period of several thousand years. These durations are short compared with the diffusive transfer time via the Kimmeridgian formation which is several tens of thousands of years at least. The time that could result in an accumulation of the solutes is therefore not significant compared with the total transit time through the Kimmeridgian formations. This effect is therefore negligible.

The maximum depth of permafrost in the Bure sector for 0 °C isotherm conditions is currently estimated at 300 m (cf. § 9.4). The Callovo-Oxfordian layer is not affected by this phenomenon but a significant impact is possible for the groundwater of the calcareous Oxfordian formation. However, at these depths, the pressure conditions are such that ice is concentrated in cracks, fissures and micro fissures. Therefore, all the water present in the calcareous Oxfordian formation will not be frozen. At present, no estimate exists of the impact of permafrost on the "large scale" permeability of the calcareous Oxfordian formation or the potential effect of gas hydrates (cf. § 9.4) but it is improbable that the flows will cease entirely, in particular in lower porous horizons (Hp1 to Hp4). If this were the case, the duration of this phenomenon, which would only occur in the most extreme glaciation, would only last a few thousand years of the whole glacial cycle, the duration of which is approximately a hundred thousand years. This would not have an impact on the flows or on the concentration of the radionuclides for transfer durations of several hundred thousand years.

- The Influence of Surface Erosion

The description of surface geodynamic evolution (cf. § 9.5) over the next million years shows that climatic evolution and alternating freezing and thawing cycles during glaciation in particular significantly modify the topography and, notably, accentuate erosion of river beds. This transformation of surface boundary conditions gradually influences the flows in the calcareous Oxfordian formation. The retrograding of Tithonian cuesta and erosion of valley floors alter the limestone marls of the Kimmeridgian formation, whose permeability increases significantly, in numerous areas of the sector. New outlets associated with advective solute transport in the transmissive strata of the calcareous Oxfordian formation therefore appear downstream from the repository site (Figure 10.5.3). Natural outlets may then arise in the Ornain valley to the north-west of the site after consecutive erosion by several glacial cycles (i.e. after several hundred thousand years) (LSCE / CEA, 2004). They develop to the detriment of the regional paths which disappear in a million years' time. As regards the directions of flow in the direction of the Marl valley, they continue throughout the period. In addition, the erosion of the marlaceous Kimmeridge in the upper course of the Saulx valley to the west of the Meuse/Haute Marne site could also give rise, after a million years, to the emergence of a natural outlet. It would develop to the detriment of paths in the direction of the Marne valley, giving rise, therefore, to non-sorbed solute advective transfer times of the order of several tens of thousands of years from the site to this local outlet.

So, in the region of the site, a solute starting at present at the top of the Callovo-Oxfordian formation could initially take a regional path towards the centre of the Paris basin, then, several hundred thousand years later, take a local path towards the Ornain valley, as the limestone marls of the Kimmeridgian are eroded.

10.5.2 The Transfer of Mobile Radionuclides Leaving the Callovo-Oxfordian Layer

The radionuclides that diffuse through the Callovo-Oxfordian layer from the repository, are distributed roughly equally on either side of the repository towards the over-lying calcareous Oxfordian formation and towards the underlying Dogger formation. The transfer times and concentration flows at the top and wall of the Callovo-Oxfordian layer are identical for each radioactive nuclide considered. On the scale of the transposition zone, the transfer of the radionuclides in the over- and under-lying surroundings can be described independently.

As indicated above, the radionuclides that reach the top and the wall of the Callovo-Oxfordian formation are mainly mobile, long-lived radionuclides ^{129}I and ^{36}Cl, and to a lesser extent ^{79}Se. The general characteristics of the flows and the transfer of the solutes in the surrounding formations indicate that the transfer of these radionuclides will have a significant vertical extent both in the under- and over-lying surroundings, resulting in a spatial dispersion of the radionuclides.

10.5.2.1 Transfer in the Underlying Surroundings

The radionuclides migrate vertically from the repository zones mainly by diffusion towards the underlying Lias. However, the horizontal flow allows the horizontal advective transfer of a fraction of the radionuclides. At a horizontal distance of several kilometers from the repository zones, the concentrations in the solutions become smaller above and below these horizons. The radionuclide plume can, therefore, extend vertically by diffusion in the downwards direction, in the underlying Lias and upwards in the direction of the Callovo-Oxfordian formations (Figure 10.5.1).

Over a million years, the radionuclides have therefore migrated (i) horizontally over several kilometers and (ii) vertically over the entire thickness of the Dogger formation (250 m thickness) and in a large part of the under-lying Lias. A small amount of the radionuclides can migrate again towards the Callovo-Oxfordian layer.

10.5.2.2 Transfer into the Over-Lying Surroundings

The time of the maximum molar flow rates leaving the Callovo-Oxfordian formation are of the order of 250,000 years. At present, there are two directions of flow from the site, one local towards the Marne, and another regional towards the north-west. Geodynamic evolution reveals two new local outlets, (i) one is situated to the north in the Ornain and develops to the detriment of the regional direction after approximately 500,000 years, (ii) the other is situated immediately west of the site in the upper course of the Saulx and develops in a million years' time on part of the flow paths to the Marne.

So, up to approximately 300,000 years, the mobile radionuclides that have reached the calcareous Oxfordian formation either follow the regional direction towards the north-west or the local direction towards the Marne valley. After 300,000 years, the regional direction gradually disappears to the benefit of the local outlet of the Ornain to the north of the site. In a million years' time, the same is true for the local direction towards the Marne to the benefit of the Saulx outlet. From then on there are only two directions: one towards the Ornain and the other towards the Saulx. Consequently, after 300,000 years, the radionuclides that reach the Oxfordian formations will follow paths first in the direction of the Ornain and the Marne, then after a million years, towards the Ornain and the Saulx. The radionuclides that, before 300,000 years have passed, have travelled in the regional direction, by and large remain in the latter (Figure 10.5.3).

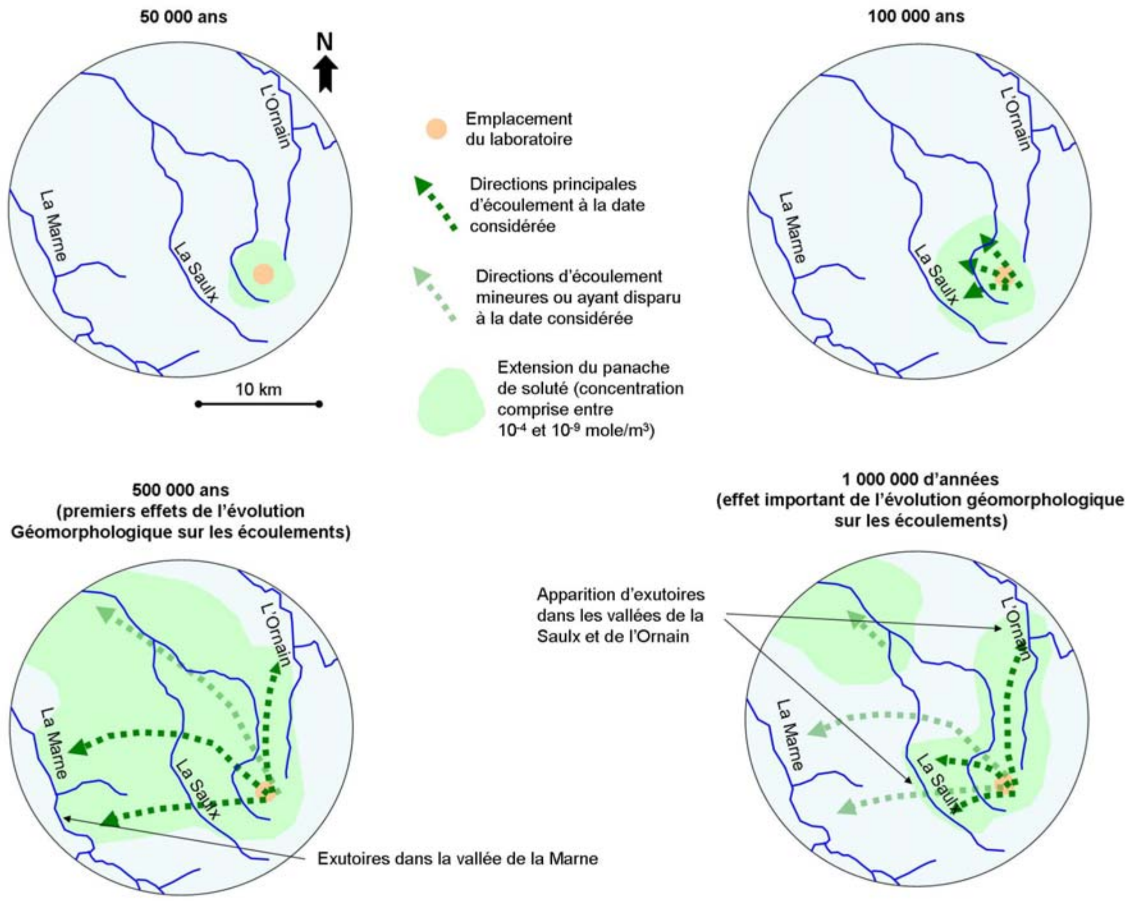

Figure 10.5.3 *Diagram Showing the Development of the Paths and a Plume of Solutes in the Calcareous Oxfordian Formation Downstream from the Meuse/Haute-Marne Site over the Next Million Years*

These different directions correspond to average advective transfer times (corresponding to the maximum molar flow rate) from above the site (i) of the order of a million years for the natural outlet in the Marne valley (current outlet), (ii) several hundred thousand years for the future outlet of the Ornain valley and (iii) several tens of thousands of years for the future outlet of the Saulx valley.

Less than some ten percent of radionuclides that migrate horizontally by advection in the transmissive levels can be conveyed by diffusion to the above-lying layers. An even smaller fraction can be diffused downwards to the Callovo-Oxfordian layer, when concentrations in the latter decrease, some kilometers from the repository zones.

The radionuclides that diffuse towards the Kimmeridgian formations can gradually travel towards the surface. No measurement of the effective diffusion coefficient or measurement of the porosity accessible to diffusion currently exists for the Kimmeridge marls. In this formation, permeability is low (approximately 10^{-12} $m.s^{-1}$, cf. § 3.3.2.3) and the percentage of clay is of the same order of magnitude as that of the Callovo-Oxfordian formation. It is therefore possible to envisage effective diffusion coefficients of the same order of magnitude as those of the Callovo-Oxfordian formation which would increase the durations of migration towards the Tithonian. In any event, the radionuclides that reach the surface water after diffusing vertically through the Kimmeridgian marls would be very much diluted on the surface in the region of the repository.

Whatever path is considered, the radionuclides are naturally diluted by the water that they encounter along their path through the surroundings:

- In the porous levels of the calcareous Oxfordian formations on leaving the Callovo-Oxfordian formation. When the flow rates in the calcareous Oxfordian are taken into account, this dilution is estimated to be of the order of two magnitudes;
- During the horizontal path in the calcareous Oxfordian formation. Dilution may reach a factor of ten at a distance of ten kilometers downstream from the site;
- In the surface water in the alluvium of the Marne or Tithonian limestone. The permeability contrasts between the calcareous Oxfordian buried beneath overlying strata and the alluvium at the outcropping are such that the dilution factor can be estimated at three or four orders of magnitude;
- in the rivers. On the basis of the ratios between the flow of the rivers and the flow drained by the water courses in the alluvial sheets, this dilution is estimated at three to four orders of magnitude.

10.6 The Transfer of Radionuclides to the Biosphere and Humans

The biosphere is the last segment of the transfer of radionuclides to humans. The natural interfaces with the geosphere are the top of free surface groundwater, when the latter is found in Barrois limestone (on the plateaux), outlets from this groundwater in the sides of valleys and outlets from deeper groundwater, the bottom of valleys, in particular, in the case of calcareous Oxfordian formations.

As indicated in the above paragraph, the radionuclides released by the repository and liable to reach the biosphere, with a significant concentration are very small in number and are: iodine, chlorine and selenium in the case of radionuclides and boron in the case of chemical toxins.

Section 10.5 also revealed the spatial scale of the plume of radionuclides to reach this interface after transport in the Callovo-Oxfordian and surrounding formations. In the surroundings, a fraction of these solutes migrates horizontally in the calcareous Oxfordian and, in the sector, reaches the surface towards the Marne valley or the valleys of Ornain and Saulx if the geomorphological modifications over the next million years are taken into account. A smaller proportion migrates vertically through the Kimmeridgian formations, by diffusion, and is dispersed in the surface groundwater of the Barrois limestone which has multiple outlets in the valleys that cut into the plateaux. This spreading of the plume in the surface water means that different surface environments are affected in terms of potential outlets. The possibility of access to underground water resources varies depending on the zone, as do the characteristics of the surface environments (soil, crops, wildlife, human occupations, etc.) in general (cf. § 3.5). In the plateaux zones, which account for the majority of the environment on the scale of the sector, the groundwater of the Barrois limestone is present from 10 to 15 m below the surface of the ground. In valley areas, corresponding to natural outlets of the surface water, the water transporting the solutes reaches the surface directly, then flows into the rivers.

In addition, the flows that reach the surface water or outlets span considerable time scale: of the order of several hundred thousand years (cf. § 10.5). This means that the transfer of radionuclides to the surface does not take place in a single, permanent biosphere for a given geomorphological domain but over a series of alternately temperate then cold biospheres (boreal then tundra), covering several 100,000-year climatic cycles (cf. § 9.4).

Finally, the assessment of radionuclide transfer times in the Callovo-Oxfordian surroundings presented in Sections 10.4 and 10.5 (several hundred thousand years) must be considered in relation to the duration of the possible anthropic disturbance of the 100,000-year glacial/interglacial climatic cycles. Sections 10.4 and 10.5 have demonstrated that this anthropic disturbance could significantly modify the alternating climate of the next 300,000 years, with a dominant temperate biosphere for this period. Up until 600,000 years, the disturbances are attenuated and the natural cycles will begin again thereafter. The majority of the radionuclide flow therefore reaches the biosphere after the most notable effects of this possible disturbance when the climatic cycles return to their natural evolution.

This section first sets out the overall context of the transfer of radionuclides into the biosphere then goes on to consider the effect of various geomorphological situations on the transfer into the biosphere of the radionuclides that reach it. These effects are analysed in the context of a temperate biosphere. Finally, the consequences of climate change on the transfer of these elements are assessed.

10.6.1 The Overall Model of Radionuclide Transfer into the Biosphere: Direct and Indirect Transfer

The transfer of radionuclides into the biosphere involves a large number of actions and retroactions between the various segments of the living media (Albrecht & Gallerand, 2005 ; IAEA, 2003). An example of several components is shown below in the form of a matrix (Figure 10.6.1).

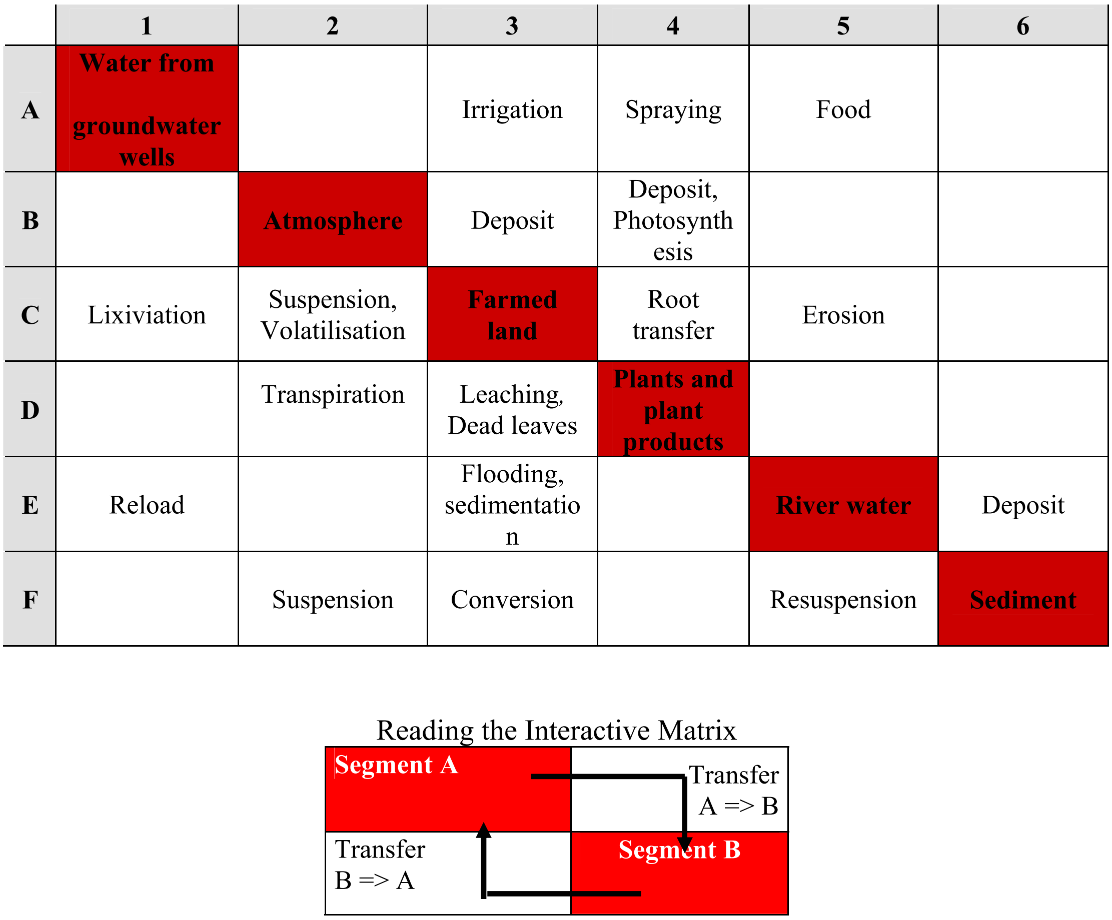

	1	**2**	**3**	**4**	**5**	**6**
A	**Water from groundwater wells**		Irrigation	Spraying	Food	
B		**Atmosphere**	Deposit	Deposit, Photosynthesis		
C	Lixiviation	Suspension, Volatilisation	**Farmed land**	Root transfer	Erosion	
D		Transpiration	Leaching, Dead leaves	**Plants and plant products**		
E	Reload		Flooding, sedimentation		**River water**	Deposit
F		Suspension	Conversion		Resuspension	**Sediment**

Figure 10.6.1 *Model of Transfer in the form of a Matrix in Several Segments of the Biosphere (IAEA, 2003)*

Detailed analysis of each of these phenomena has made it possible to propose a generic pattern showing the main transfer paths in the biosphere. (Albrecht & Gallerand, 2005). This pattern, which this section is structured around is illustrated in Figure 10.6.2.

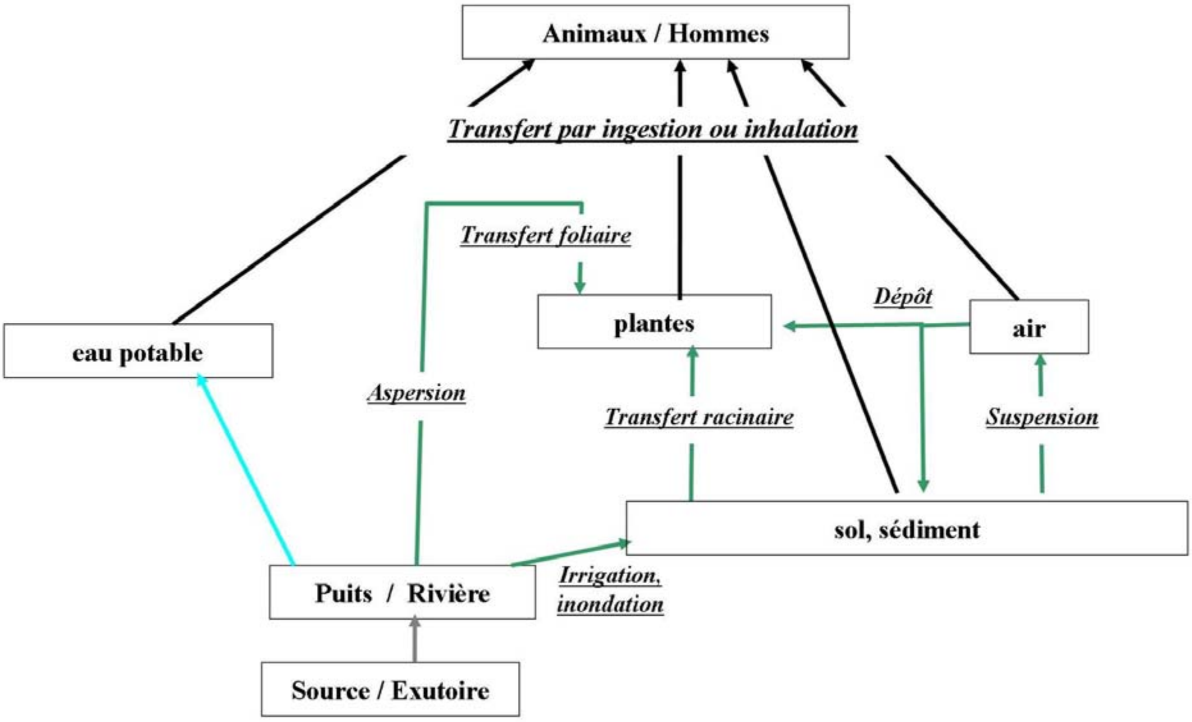

Figure 10.6.2 The Main Transfer Paths in the Biosphere

The radionuclides found directly in the groundwater in the form of traces can immediately be transferred to man:

- this water can be captured by drilling and ingested directly by man (drinking water) and animals;
- in the groundwater outlets, the water transporting the radionuclides reaches the surface in the form of springs or karstic resurgences, depending on the case, then flows into the rivers. This water can also be directly ingested by man, as in the preceding case, possibly after potabilisation. The radionuclide concentrations may, in this case, be diluted because of the flow of the rivers.

More indirectly, the transfer process takes place in the ground (Inset 10.12). This segment, which can lead to accumulations, shows a certain number of actions and retroactions with the atmosphere in particular.

Inset 10.12 ***Model of the Transfer of Radionuclides in Soils***

In the soil, a large number of physical and chemical mechanisms give rise to the mobilisation or immobilisation of trace elements. These phenomena include both dissolution / precipitation reactions and adsorption / desorption reactions in solid phases (Bourrelier & Berthelin, 1998), as in the repository or the geological medium (cf. § 10.3.3 and 10.4)

These reactions are conditioned, in particular, by:

- the acid-base conditions of the soil (pH) that affect speciation,
- the redox potential, an oxidizing medium as is the case for the soils of the Meuse/Haute-Marne sector increasing the mobility of free ions,
- the carbonate, metal oxide or organic matter content as these elements can attach to certain radionuclides, depending on the redox conditions of the milieu and therefore modify their mobility,
- the content and type of minerals present in the soil, of which certain phases (clay in particular) control the adsorption phenomena of certain trace elements.

Finally, the role of micro-organisms that directly or indirectly affect the mineral transformations (dissolution, alteration, etc.) or modify the status of the different elements present (soluble / insoluble, oxidised / reduced, etc.) should be mentioned.

As a general rule, the behaviour of a soil is described by an instantaneous and reversible sorption model as considered in the geological medium (Inset 10.6). For this reason, the same type of parameter is used to express the partition between the solid phase and the liquid phase: the distribution factor (Kd). This macroscopic coefficient makes it possible to integrate numerous physical and chemical phenomena controlling the behaviour of trace elements in the soils.

When they are sorbed to a small degree by the soils and therefore essentially in liquid phase, the radionuclides can be uptaken by plants. Part can also be lixiviated during rainfall, for example, and returned to the sub-soil. The overall model of transfer in soils is therefore a dynamic model that is dependent on the interaction between solid particles and elements in solution but also on the ground-water balance and the use the soils are put to (types of crop and farming methods).

The behaviour of radionuclides in soils is therefore specific to each element.

- As a general rule, iodine is part of the elements least retained in the soils (Deneux-Mustin *et al.*, 2003). Its retention depends little on the percentage of clay in the soil but rather seems linked to the organic matter content with which this element is associated in the anionic state. Micro organisms seem to be directly implicated in the iodine sequestration processes in soils. Direct relationships can therefore be revealed between the quantity of microbial biomass and Kd values.
- Chlorine is considered inert in respect of chemical and biological reactions although an association with organic molecules through chemical or microbial reactions has been demonstrated. (Andra, 2003a). This element is naturally very much present, in its stable form (^{35}Cl and ^{37}Cl), in the environment, very soluble and very mobile. It therefore remains in solution and does not accumulate in the soils (except for precipitation phenomena, which are improbable given the quantities necessary). The transfer of ^{36}Cl from one segment to another can therefore be estimated based on the equality of isotope ratios ^{36}Cl/(^{35}Cl+^{37}Cl) (Albrecht & Gallerand, 2005). The sources of ^{36}Cl in the biosphere originating from the repository are therefore diluted by sources of stable chlorine in the case of each of the segments. In the soils, the main sources of water inflow containing ^{36}Cl originating from the repository (in the form of watering or irrigation for example, see below) are therefore diluted by rainwater.

- Selenium behaves very differently in soils depending on the chemical form present, which depends upon its oxidation level: it is less mobile in the form of selenite ion Se^{IV} than it is in the selenite form Se^{VI} (Andra, 2003a).
- Boron seems able to attach itself to a number of carrier phases: iron or aluminium hydroxides, clay or organic matter. However, on the basis on available analyses, although clay soils sorb this element better than sandy soils(Deneux-Mustin *et al.*, 2003), boron appears to be a relatively mobile element with very low Kd overall. (Andra, 2003a).

From the soil, the main transfer paths to humans are direct (via ingestion or inhalation after placement in suspension in the air) or indirect via plants (Inset 10.12).

The respective participation of leaf and root transfers are very different for the four elements considered (Deneux-Mustin *et al.*, 2003). As a general rule, root transfer is limited by the capacity of the soil to supply radionuclides. In the case of iodine, this transfer is generally low and most of the iodine seems to be retained in the roots. Most of the chlorine (stable or otherwise) in plants comes from the soil, showing that chlorination via the air is not significant. Selenium shows very variable soil-plant transfers depending on the type of soil, the selenium content of the latter or even the type of plant. In general, the behaviour of selenium is directly dependent on the micro-organisms in the soil. Boron, sorbed to a small degree by soils, is an essential element in the development of plants. For this reason it is easily taken up by the roots and largely distributed in the upper parts of the plants in the case of certain leaf-vegetables and certain fruits (rich in polyols) in particular. (Andra, 2003a). The transfer of boron from leaves is little documented.

With regard to soils and plants, another possible transfer path is the deposit of solid particles in suspension in the atmosphere. These deposits can be either on leaves or on soils. The quantities of radionuclides transported in this way are low. They are, moreover, diluted in the total number of particles in suspension.

From plants, radionuclides become mobilisable for animals, then humans, mainly through ingestion (Figure 10.6.2).

Inset 10.13 ***The Model of Radionuclide Transfer to Plants***

There are essentially two main transfer paths to plants: via the roots, from elements in solution in the soil and via leaves through direct interception of watering by the uppermost parts of the plant (Albrecht & Gallerand, 2005).

In soils, the mobilisation of elements in solution, or absorbed to a small extent by solid phases, transportation of these by advection or diffusion to the root or rhizospheric zone, their uptake by the plant and their distribution throughout the latter reveal a certain number of complex phenomena. The latter depend not only on the specific mobility of the elements present in the ground but also on the types of plants envisaged, farming methods and climatic conditions, (Bourrelier & Berthelin, 1998).

Before reaching the root zone, elements in solution, or sorbed to some degree, in the soil are subject to specific conditions governing the vicinity of the latter (the rhizosphere), created, among other things, by root exsudation. The compounds produced by the plant can, depending on the case, mobilise or immobilise trace elements.

The presence of assimilable carbon in this zone contributes to an increase in the number of micro-organisms (bacteria, fungi), that also play a role in transfer to the plant (increase of bioavailability).

Inside the plant, the transfer of radionuclides is conditioned by their internal structure (intercellular spaces, role of the different membranes, etc.) and by the presence of molecules that ensure this transport and are therefore directly dependent on the plant type and the stage of its growth.

Leaf transfer also depends to a very large extent on plant type. The surface area of the leaves determines the interception factor, from which the amount of water effectively in contact with the latter is calculated. Part of this water is retained on the surface of the leaves. The rest is used by the plant. The elements contained in the latter then migrate inside the plant towards the edible parts. This latter transfer from the leaf to the edible part of the plant is described by the translocation factor which depends on the element in question and the stage of growth of the plant.

In the end, the behaviour of radionuclides in plants is very variable depending on the element in question and the type of crop envisaged, some plants demonstrate higher uptake and bioconcentration capacities than others.

10.6.2 The Transfer of Radionuclides in the Current Biosphere for the Plateaux Zones of the Meuse/Haute-Marne Site

On the plateaux, and the Barrois plateau in particular, the unconfined aquifer is reached at a few meters to 10 / 15 meters under the surface (Andra, 2003c). The Barrois limestone formation, fractured to a greater or lesser extent the closer to the surface is overlain by 30 to 50 cm of soil (cf. § 3.5.4). It is only partially saturated (Figure 10.6.3). In this unsaturated area, the movements of the water are, in general, downwards: there is infiltration of rainwater towards the groundwater during heavy rainfall. The replenishing phenomenon is rapid (from a few days to a few weeks), according to the response curves of piezometric levels (cf. § 3.3.2.3) (Andra, 2003c). This rapidity indicates the significant permeability of the non saturated zone.

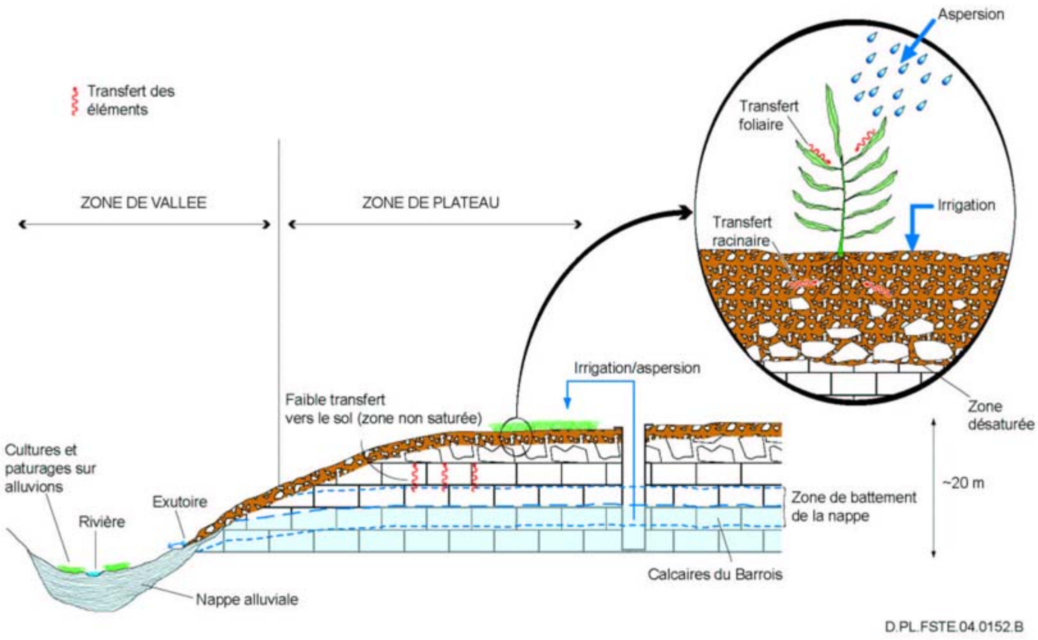

Figure 10.6.3 *Model of Transfer from the Geosphere to the Biosphere on the Meuse/Haute-Marne Site*

Only the first decimeters of soil that are dependent on surface conditions show significant variations in water content (De Marsily, 1981). Below this, throughout the non-saturated zone, it is accepted that there is continuity of the liquid phase, the latter exists essentially at the interface of the solids. Transfer of the radionuclides by diffusion is therefore possible in theory in this liquid phase from the unconfined aquifer of the Barrois limestone to the soil but it is probably small in these conditions with an absence of total saturation. In addition, this non saturated zone is regularly subject to infiltration of water that create leaching and take the solutes downwards. Natural exchanges of solutes between the surface of the groundwater and the soil are therefore very low in plateaux zones.

Greater transfer of radionuclides to the plateaux soil can therefore only occur artificially through the irrigation and spraying of farmland with water taken from a spring or borehole in the groundwater of the Barrois limestone (or calcareous Oxfordian formation if applicable) (Figure 10.6.3).

In this case, the characteristics of the soils of the plateaux, clayey (approximately 40 %) and containing approximately 5 % organic matter (Andra, 2005h, chapitre 22), conditions radionuclide behaviour (Andra, 2003a).

- In the soil, a small proportion of iodine is sorbed (Kd of 10^{-3} $m^3.kg^{-1}$) but most of it remains in the roots. In addition, plants also accumulate this element through transfer by air (spray irrigation water).
- The total chlorine content (stable isotopes and chlorine 36) originating from the groundwater (of the order of 0.02 $g.L^{-1}$) is diluted in the soil by very low-saline (0.005 $g.L^{-1}$) meteoric water the amount of which is greater (by a factor of 4 approximately). The chlorine 36 content is therefore diluted by a factor of approximately 2 in the water in the soil. This chlorine 36 subsequently migrates into the plants mainly via root transfer.
- The most likely form of the selenium in the soils of the Meuse/Haute-Marne site (aerated soils therefore oxidizing medium, neutral to slightly acid pH) is the selenite form. The Kd measurements taken on soil from the site with a selenite solution show values of the order of $5 \cdot 10^{-2}$ $m^3.kg^{-1}$, which are comparable with data for similar soil available elsewhere.
- Boron is retained to a small extent by the soils of the plateaux (Kd in the soil of $1.3 \cdot 10^{-3}$ $m^3.kg^{-1}$. Like chlorine, it is therefore readily available for root transfer, depending on the plant (potatoes,

cereals). Fruit, in particular those rich in polyols (apples, pears, plums, cherries, etc.) tend to show a greater accumulation of boron.

Transfer to humans from plants follows the pattern outlined earlier.

10.6.3 The Transfer of Radionuclides in the Current Biosphere in the Case of the Valley Zones

The natural groundwater outlets flow into the valley areas. They are directly supplied from springs by the water containing radionuclides which is found in river water (Figure 10.6.3). At or near outlets, the concentrations of elements are the same as those of the surface water. From the moment of arrival on the alluvial plain, there is considerable dilution by river water. The rivers in the valleys have very variable flow rates depending on their position in the watershed and the season. The average flow rates measured in the Orge valley give typical flow values of the order of 50 to 100 L.s^{-1} upstream of Biencourt at 300 L.s^{-1} and more downstream (high summer water) (Andra, 2003c). Flow rates measured at springs supplying this stream are some 10 L.s $^{-1}$ upstream to 70 L.s $^{-1}$ downstream, at the same time. The interannual flow rate of the Ornain at the north of the sector (10 m.s^{-1} can also be compared in the karstic context (Andra, 2005h, chapitre 14) with characteristic flow rates of karstic springs (several hundred L.s^{-1}). The dilution of the water from the outlets in the water courses of the valleys therefore appears approximately to be of several orders of magnitude.

In these valleys, the soil is frequently hydromorphic (subject to temporary or permanent over of water), either because the water courses push through marls or because the groundwater associated with the rivers regularly floods these valleys (cf. § 3.5.4). Unlike the plateaux zones, there is therefore more or less permanent direct contact between the solutes and the soil. The latter is deeper on the plateaux. However, the overall characteristics of the soils are fairly similar: the clay content is of the same order of magnitude (30 to 40 %), organic matter is more present in surface horizons (10 %) than on the plateaux (Andra, 2005h, chapitre 22). The behaviour of the radionuclides there is practically identical, as is transfer to the plants. Dilution by river water, however, significantly limits the amounts transported, unless this water is used near outlets (on the slopes) or conditions come close to the situation described on the plateaux in the above paragraph.

10.6.4 The Effect of Geodynamic Evolution on the Transfer of Radionuclides

Over the course of 100,000 year climatic cycles, the evolution of the biospheres significantly modifies the current transfer patterns (c.f § 9.4.2).

The transition from a boreal to a tundra biosphere places considerable restrictions on the plant life on the plateaux. In fact, the initially seasonal then permanent freezing of the first ten meters of the soil prevents the use of water resources in these areas. The bottom of the valley become equally inhospitable: the large flow rates of the rivers following cold seasons makes the beds stony and, during the maximum glacial period, completely destabilises the alluvial deposits. Only some terraces remain, notably during the boreal period, and are periodically flooded. In clay areas, at the top of valleys and therefore less subject to this type of destabilisation, the cooling slows pedogenesis and the organic matter content of the soils increases. Marshes and peat land gradually form in the basins.

On the plateaux, the restriction of farmland, then its absence during the maximum glacial periods no longer allow contamination of the soils. Human activity is then concentrated around the natural outlets. The ground becomes impoverished and stony around the edges of valleys on the terraces not yet dismantled. In this domain, the behaviour of the radionuclides shows the same tendencies as in the valleys during the temperate period. In marlaceous basins, this behaviour is significantly modified to a greater or lesser extent depending on the element in question (Andra, 2003a):

- the enrichment of organic matter in the soils can benefit the sorption of iodine (Kd going from values of the order of $3{\cdot}10^{-2}$ $m^3.kg^{-1}$),
- as the milieu becomes more reducing, it seems to benefit the sorption of selenium: values of some $10^{-1}m^3.kg^{-1}$ are found in cold climates, on some soils that are similar to those of the marlaceous basins of the site,
- the ^{36}Cl content in solution in the soil increases as the negative groundwater balance (reduction of precipitations of a factor in over of 2 (cf. § 9.3) limits dilution,
- boron, which is already very mobile in the soils during temperate periods, remains so. In the event that clay is the key parameter of sorption, it can become even more so because of the reduction in the clay content.

10.7 Summary

10.7.1 The Effects of Thermal, Hydraulic, Chemical, Mechanical and Geomorphicological Evolutions on the Release and Transfer of Radionuclides

The thermal, hydraulic, geochemical and mechanical evolution of the repository and its geological environment define the phenomenological framework of the release of radionuclides from the waste packages, then the possible transfer of these radionuclides from the repository to the biosphere. The description of these evolutions reveals the following major points:

- The thermal loads of the C waste and spent fuel repository zones only affect a short period, approximately ten thousand years, with maximum temperatures reached very early on, between a few years and one hundred years.

The thermal transient is therefore practically finished at the moment of radionuclide release and therefore has no significant influence on their release or transfer.

- The hydraulic evolution of the repository is characterised by a period during which the B waste disposal cells and drifts are in a non-saturated state until total saturation is reached after around 200,000 years' time. During the first several thousand years, conditions that favour advective transport may exist in the very near-field of the repository. They would not affect spent fuel because of the leak tightness of the containers up to 10,000 years. On the scale of transfer over 60 meters on either side of the repository towards the roof and wall of the Callovo-Oxfordian layer, they would have no significant impact on the transfer of radionuclides released by the C waste packages (the overpacks have a specific leak tightness of 4,000 years). Whether that is during this period or after total resaturation and subject to a new hydraulic equilibrium, diffusion is the overall dominant mode of transport in the disposal cells and in the Callovo-Oxfordian layer. This is guaranteed by the mechanical stability of the seals and plugs of the disposal cells, in addition to the significant hydraulic healing of the excavation damaged zone (EDZ) around the structure which does not therefore constitute a preferential transfer path compared with the Callovo-Oxfordian layer.

Radionuclides, therefore, preferentially migrate by diffusion in disposal cells towards the argillites, then in the argillites of the Callovo-Oxfordian formation to the calcareous Oxfordian and the Dogger formations.

- The chemical processes are essentially interface processes. On the scale of a million years, the swelling clay-based repository components, such as the engineered barriers and the C waste disposal cell and spent fuel disposal cell plugs, are only very locally degraded and to a large extent retain their hydraulic properties. The chemical degradation of B waste disposal cells takes place over a time scale of several hundred thousand years during which the disposal packages can be considered a quasi non-failed cement-based environment. The maximum pluridecimetric extensions at less than two meters from the alkaline disturbance around the drifts and B waste disposal cells or iron-argillites around the C waste disposal cells and spent fuel disposal cells are negligible given the pluridecimetric thickness of the Callovo-Oxfordian layer. The thermal load of the repository is insufficient to significantly and irreversibly modify the chemical balance of the Callovo-Oxfordian layer and therefore, indirectly, its permeability and retention properties.

The radionuclides released from disposal cells therefore migrate in a Callovo-Oxfordian formation close to its current state.

- The geomorphological evolutions induce a significant modification of the hydraulic heads and directions of water flows in the above-lying surroundings of the Callovo-Oxfordian formation from 300,000 to 500,000 years onwards to a million years and beyond. In particular, new local outlets for the calcareous Oxfordian are created.

The transfer of radionuclides that migrate through the entire Callovo-Oxfordian layer to reach the surroundings after this time scale is therefore influenced by the modification of the flows under the effect of geodynamic evolutions.

10.7.2 Radionuclides with Specific Behaviour in Terms of Solubility and Retention

Whether in clay media (Callovo-Oxfordian layer, engineered barrier of the spent fuel disposal cells, C waste disposal cell and spent fuel disposal cell plug, B waste disposal cell seal, drift and shaft, drift backfilling) or cement-based media (B waste disposal cells), the radionuclides are distributed schematically into two large families according to their capacity for migration in dissolved form.

- Elements whose solubility is high and retention low or nil, such as iodine or chlorine, for example. These elements are described as being "mobile".
- Other elements, some of which possess high solubility and retention such as caesium, for example, or low solubility and high retention such as actinides and lanthanides.

10.7.3 Slow and Limited Release of Radionuclides Beyond the Repository

10.7.3.1 The Slow Degradation of Metal and Waste Containers

- **The low corrosion kinetics of metal C waste package and spent fuel package containers**

Given slow corrosion rate of steel in repository conditions, specific leak tightness durations of the order of 4,000 years in the case of C waste package overpacks and 10,000 years for spent fuel containers are taken into account. A less conservative approach gives rise to longer leak tightness durations of 15,000 and 30,000 years respectively.

- **The slow aqueous dissolution of the vitrified matrix of vitrified waste and the uranium or uranium-plutonium oxide of spent fuel**

The dissolution of the vitreous matrix and oxide pellets of spent fuel takes place respectively over time scales of the order of 300,000 years after the discharge of leak tightness of the containers and several tens of thousands of years to one hundred thousand years (in the case of radiolytic dissolution) after the discharge of leak tightness of the containers.

- **Varied behaviour depending on the type of B waste, but overall slow degradation**

B waste covers various types of waste (zircaloy hulls and end caps, metal technological waste, salts, organic compounds, etc.) and types of conditioning (bituminisation, compaction, cementation). Consequently, the degradation kinetics of the waste vary but they all take place over a time scale of several thousand to several tens of thousands of years.

10.7.3.2 Disposal Cells: Chemical Environments that Contribute to the Low Mobility of Radionuclides

- **Stable physical and chemical environments for at least several hundred thousand years**

Over the course of a million years, the engineered barrier of the spent fuel disposal cells preserves its overall initial characteristics in equilibrium with the water of the argillites. It is only affected in contact with metal components by interaction with iron. In the case of C waste disposal cells, the argillites are only affected upon contact with the lining.

The degradation of concrete is a slow process in repository conditions. The B waste disposal cells, therefore, preserve overall characteristics that are close to those of undisturbed concrete for a period of over several hundred thousand years. At this time, (i) the degradation of the disposal cells by the water from the argillites is restricted to the periphery of the disposal cells, its chemistry is that of water from altered or degraded concrete, and (ii) the characteristics of the disposal packages at the core of the disposal cells are those of a undisturbed concrete environment.

- **Favourable environments for weak solubility and radionuclide retention**

As a general rule, the disposal cells constitute chemical environments that are favourable to low solubility and the sorption of most radionuclides. With low water flows and the dominant character of diffusion within the repository, these environments combine to produce the low and slow release of radionuclides outside the disposal cells. Therefore, the main radionuclides to migrate outside B waste disposal cells are ^{129}I, ^{36}Cl, ^{135}Cs, ^{99}Tc et ^{79}Se. and ^{129}I, ^{36}Cl and ^{14}C in the case of C waste disposal cells and spent fuel disposal cells. The actinides and lanthanides remain confined in the disposal cells and the near-field of the repository for a million years.

10.7.4 Migration of Very Soluble Long-Lived Radionuclides Not Sorbed in the Callovo-Oxfordian Layer

The Callovo-Oxfordian layer has retention and diffusion characteristics that are favourable to the slow migration of the radionuclides. Associated with the considerable thickness of the layer, these characteristics combine in such a way that only long-lived very soluble and non-sorbed radionuclides released outside the repository reach the above- and under-lying surroundings. The time scale of the maximum molar flow is order of several hundred thousand years. These are ^{129}I, ^{36}Cl, and to a lesser extent ^{79}Se and ^{14}C. Over a million years, the migration of other radionuclides, actinides in particular, remains confined to the Callovo-Oxfordian layer, delimited to some meters around the repository.

10.7.5 Transfer of Radionuclides to the Surroundings Influenced by Geodynamic Evolution

The transfer of iodine and chlorine in the Dogger and calcareous Oxfordian formations takes place mostly by advection - dispersion.

In the Dogger formation, the iodine and chlorine plume progresses horizontally in a west-south-westerly direction. The rate of advection is very low and the extent of the plume is of the order of several kilometers after a million years. In the upper surroundings, maximum molar rates are reached prior to the effect of the evolution of the flows in the surroundings under the effect of geodynamic evolution. Most of the iodine and chlorine therefore first follows directions of flow that are comparable to the current ones.

After 300,000 years, the erosion of the surface gradually modifies the main directions of flow downstream from the underground research laboratory. The Marne valley outlet remains. Regional paths are moving to the benefit of a second local outlet to the north-east of the site in the Ornain valley and, in a million years' time, an outlet in the upper course of the Saulx valley.

Whatever the path, iodine and chlorine are considerably diluted during their transfer to the surface.

10.7.6 The Transfer of Radionuclides to the Biosphere and Humans

The transfer of radionuclides to the biosphere is conditioned by the surface environment. The superficial (Barrois limestone) and deep (calcareous Oxfordian) groundwater outlets situated in the valleys, are the preferential locations from which the radionuclides can be transferred to the soil and plants then on to animals and populations. The concentrations in question are approximately of a lower order of magnitude in the valleys than near the outlets because they are diluted by river water. On the plateaux, this transfer is only possible at present through artificial means in the event of a borehole being drilled down to the groundwater to meet human needs and notably for the purposes of irrigation/spraying of crops.

The characteristics of the soils at present, clay and with an organic matter content of 5 to 10 %, are similar whatever morphological domain is considered (plateau, valleys). These soils allow the sorption of some elements: selenium and iodine, and to a lesser extent boron. Chlorine, not retained, remains in solution. The transfer of radionuclides takes place via the plants to animals and humans.

The evolution of colder biospheres (first boreal then tundra) will limit then prevent farming in the plateau areas, as water supplies will become less accessible on account of the seasonal then permanent deep frost. The transfer of radionuclides to the biosphere is therefore limited to certain areas of the valleys and marlaceous basins.

10.7.7 Important Phenomenological Elements for Reversibility

Reversibility is evaluated in relation to the condition of the repository components. First, the main results of reversibility is summarised then the potential consequences of plurisecular operation is analysed.

10.7.7.1 The Condition of the Repository after the Conventional Standard Secular Period of Repository Operation

After the secular operating period (at the moment of closure), the chemical processes are still limited. This is the case in the C waste repository cells and the used fuel repository cells: they are close to total saturation but corrosion rates are low (a few microns per year maximum) so that the depth of corrosion is a few millimeters. More particularly, the low corrosion rate of the linings during this period enables their mechanical resistance and therefore their leak tightness to be preserved so the packages are in a "dry" environment and are not affected by significant corrosion. The non saturated ("dry") state of B waste disposal cells and drifts contributes to the considerable limitation of degradation processes of the concretes and the corrosion of metal components and also to that of the mechanical processes (argillite creep). There is therefore no release of radionuclides in solution.

10.7.7.2 Influence of a Plurisecular Repository Operation on Reversibility

Maintaining ventilation over a plurisecular period (and therefore a "dry" environment) in the B waste disposal cells would not affect the chemical evolution of the waste packages. There would therefore be no release of radionuclides in solution. If the B waste disposal cells were closed according to the conventional reference operation Chronogram, but the repository remained open for a several centuries, the hydraulic condition of the disposal cells would evolve little during this period. This evolution would be insufficient to bring about a degradation of the waste and a release of radionuclides in solution.

In the case of C waste and spent fuel disposal cells, the prolongation of repository operation over a number of centuries would not contribute to significantly modify the evolution of the different chemical processes taking place over the course of this period. In particular, the rate of corrosion would remain low and would not have an impact on the mechanical strength of the metal components (ground support and lining). The leak tightness of the lining would be preserved as would the absence of corrosion of the disposal packages and therefore the preservation of their physical integrity and the absence of the release of radionuclides.

11

Uncertainties relating to the phenomenological description

11.1 Uncertainty Concerning the Method of Operation and Closure of the Repository 491

11.2 Examination of Uncertainties Concerning the Available Data and Phenomenological Interpretations 492

11.3 Conclusion 498

In describing the historical background of the repository and the phenomena arising from it, the preceding chapters help provide an understanding of the evolution of the various components over time. This work is based on all the knowledge available to date, whether acquired directly from the Callovo-Oxfordian argillites *in situ*, from samples, from modelling, obtained at the Mont Terri laboratory in Switzerland or by transposing results obtained as a part of foreign programmes. It also uses work carried out on the constituent materials of repository structures and waste as well as their changes over time. In view of the complexity of the system and the time scales considered, it is not possible to arrive at a final view of this evolution and its detailed parameters. However, the evolution of the repository as a whole obeys a pattern that is robust to uncertainties, the more so in that it has been designed with caution and with the necessary fine detail for defining possible margins of variation. Hence, the view presented forms a preferred back-up to safety analysis. The latter may then draw up a simplified, more schematic and cautious representation, introducing additional degrees of conservatism, which while obviously removed from reality, ensures that its approach is marked by caution, or even pessimism.

By way of transition with the safety approach, this volume puts forward an initial view of the uncertainties that may affect the narrative history of the repository presented here. These elements have already been described in fragmented form in this account. First of all we therefore need to offer a summary approach rather than putting forward actually new elements.

11.1 Uncertainty Concerning the Method of Operation and Closure of the Repository

The preceding chapters suggested a view of the repository evolution following its closure, i.e. after the access shafts have been sealed. This involved examining how the repository behaved if one wished to utilize its passive safety function, without human intervention. In order to perform such an analysis, the time scales considered need to be defined. Thus, in order to have a starting point, we have adopted a conventional reference timing chart that deals with repository operation over a hundred years, then its closure after that.

The question then arises of knowing to what extent this choice influences the history of the repository as described in this volume. Each chapter relating to a particular category of phenomena has tried to take this parameter into account. Analyses reveal that the scheme described is not very sensitive to the date of closure of the repository since this varies over a period of some hundreds of years, typically from one to several centuries. For such a time interval, the situation of the installations at the beginning of the post-closure phase would vary only slightly, while subsequent evolution would fit overall into the scheme described. It may even be noted that, for certain aspects (thermal, gas), the impact of an extension to the operating period would be rather favourable and would strengthen the overall view. In any case, no consequence capable of undermining the principle of reversibility has been detected. At the same time it should be recalled that this period of several centuries is also derived from assessments associated with engineering and phenomenology. Reversibility may be guaranteed for such a period without any intervention other than conventional monitoring and maintenance actions. Beyond this, it would be necessary to undertake additional works, which would probably range from reinforcing preventive measures to the possible systematic retrieval of packages for reorganizing the structures. However, the broad outlines of the scheme presented would probably remain valid with just a few adaptations. Altogether, the choice of a conventional timing chart for operation has only a slight influence on the general evolution of the repository as described in this volume.

11.2 Examination of Uncertainties Concerning the Available Data and Phenomenological Interpretations

Identifying uncertainties regarding repository evolution is especially associated with safety analysis. The latter is aimed at reviewing and defining options for taking into account the elements identified. This is the specific purpose of the Qualitative Safety Analysis (Andra, 2005c), whose summary is proposed in the volume on safety assessment (Andra, 2005j). Ultimately, this work leads on to defining safety scenarios forming the basis for grasping all the uncertainties and tackling them within a global, consistent framework. The reader will therefore find a framework in these documents for the safety approach, the safety functions and the options adopted for facilitating the control of the uncertainties.

Accordingly, it is not the purpose here to draw up a catalogue of the uncertainties, but merely to recall the determining factors of phenomenological evolution and their sensitivity to present-day knowledge. This exercise forms a backup for safety analysis insofar as it proposes qualitative and quantitative data for assessing the different elements that the latter deals with exhaustively. In this respect, it acts as a complement to the repository evolution narrative of the preceding chapters, with a view to establishing a link with the detailed analysis of uncertainties presented in the volume on safety assessment (Andra, 2005j).

Initially we shall deal with the Callovo-Oxfordian layer, whose characteristics strongly affect repository evolution and, ultimately, the release and transfer of radionuclides. Then we shall deal with the phenomenological evolution of the repository and the Callovo-Oxfordian layer in the near field and finally the surrounding geological formations.

11.2.1 The Characteristics of the Callovo-Oxfordian Layer

The summary of the major determining factors of the phenomenological evolution of the repository and its geological environment has underlined the wide importance of the characteristics of the Callovo-Oxfordian layer on the evolution of the repository and ultimately on the transfer of released radionuclides towards the surrounding formations. In particular, this involves low permeability (and more generally little water circulation), dominant solute transfer by diffusion, high retention properties and low water/rock ratios. All these properties contribute not only to the slow chemical evolution of the repository, but also to the small extent of the disturbances created by the repository in the Callovo-Oxfordian layer. This in itself therefore has characteristics that ensure its stability over a time scale of a million years, and ultimately allow very gradual releases of radionuclides by the waste packages, then their weak migration towards the surrounding formations. This section will discuss the main elements contributing to these properties as a whole by specifying the level of confidence reached in the knowledge and understanding of them.

11.2.2 Bulk Permeability

The characterization of the permeability of the Callovo-Oxfordian layer is based on a large number of works conducted on samples or in boreholes, both on a small scale (several tens of centimeters) and on a large scale (several meters). Geophysics is used to best correlate the data. Backed up by the existence of an overpressure, the whole helps to reinforce the picture of a low bulk permeability of the layer with, in particular, the absence of hydraulically active fractures and an anisotropy in permeability less than one order of magnitude. This can be used to define the permeability values to be taken into consideration with reasonable confidence.

The data has been established at the laboratory scale and corroborated over quite a broad spectrum of studies. The various indices available at present provide a good level of confidence in these assessments. In particular, no great contrasts are expected in the permeability data over the transposition zone. Actually, high bulk permeability levels in the Callovo-Oxfordian layer are very improbable and would not be consistent, for example, with the chloride concentration profiles. A variation of an order of magnitude with respect to the current reference is conceivable. It goes without saying that, as part of a constitution of the research, additional investigations on the transposition zone could be used to refine these conclusions.

The bulk permeability of the Callovo-Oxfordian layer appears to be well-known with a satisfactory level of confidence. Variations around the available values should lie around one order of magnitude.

11.2.3 Diffusion and retention properties

The diffusion and retention capabilities of the Callovo-Oxfordian layer have been characterized in a number of works over the whole thickness of the layer, based on borehole samples. Geological (especially mineralogical) and geophysical studies are used to correlate the results of these works at the scale of the transposition zone. As for permeability, it all leads to the picture of a layer with low diffusion properties and high retention capabilities, which is similar throughout its thickness and on the scale of the transposition zone. There are variations in the diffusion coefficient of the solutes (anions and cations) and K_d, but they remain within a limited range (less than an order of magnitude). Furthermore, the results of the measurements with temperature emphasize the fact that the temperature effects ($T < 80$ °C) are small and within the range of variation of experimental data at ambient temperature (close to the geothermal temperature) for most elements. This range of variation does not appear capable of affecting the broad characteristics of transport in the Callovo-Oxfordian layer. Finally, as for permeability, current data do not cover the transposition zone exhaustively and would benefit from continuing with the programme aimed at refining the conclusions based on experiments on several scales. In any case, the available data and those in the process of being obtained already draw a picture with a reasonable level of confidence.

It will be noted that the porosity accessible to solute advection has not been measured directly. Its common value for anions and cations results from a reasoning based on electroneutrality: by convention it is taken as equal to the kinematic porosity. Although uncertainties regarding the value of advective porosity may have no effect on the representation of solute transfer, its value may be confirmed in order to acquire an additional level of confidence.

The range of variation of diffusion and retention properties has been characterized on a number of samples. Given the current data, it should not in any case exceed one order of magnitude.

11.2.4 The Repository and the Callovo-Oxfordian Layer in the Near Field

This section will address three important aspects for the phenomenological evolution of the repository and of the argillite layer in the near field:

- the role of gases and hydraulic evolution,
- the characteristics and properties of the damaged zone,
- the release models of high-level waste and spent fuel.

11.2.4.1 Gas Production and Hydraulic Transient

The desaturation then resaturation of the repository and the Callovo-Oxfordian layer in the near field form a major process in the phenomenological evolution. It is the presence of water that constitutes the main vector of repository evolution, whether by degradation of the components, initiation of chemical processes or transport of radionuclides. It is therefore important to properly understand their mechanisms and time constants. This section addresses uncertainties regarding the main orders of magnitude and phenomena.

Overall interpretation is made substantially more complicated due to the presence of hydrogen. The corrosion of metal components is initiated during resaturation of the repository. This generates hydrogen, which is then capable of interfering with or slowing down the resaturation process.

Kinetics of Corrosion and Impact of Hydrogen

The description of the hydraulic evolution of the repository under the effect of the corrosion hydrogen from metal components, is the result of assessments obtained by considering a corrosion rate of non-alloy steels of the order of 2 to 3 microns per year, and ignoring the potential effect of the degree of saturation of the metal component environment on the rate of corrosion as well as the water consumption by corrosion.

The assessments currently available (experimentation and modelling) tend to indicate that corrosion rates could be significantly lower, lying between 0.1 and 1 micron per year. While it is reasonable to assume that the degree of saturation in the C waste and spent fuel disposal cells will quickly exceed 97 % in the near field argillites and in the swelling clay (case of spent fuel), it nevertheless appears that very low saturation rates could be maintained over long periods in B waste disposal cells given the hydrological characteristics of the concretes and residual clearances.

Making allowance for lower corrosion rates and the couplings mentioned earlier, means envisaging much lower hydrogen pressures than those adopted in the description presented in this document. They could never exceed the hydrostatic pressure in the Callovo-Oxfordian (5 MPa), and thus not generate any hydraulic overpressure in the near field. Corrosion kinetics less than those adopted by a factor of four would mean reducing the hydrogen production flows by the same factor and spreading out production over longer periods (several tens of thousands of years to several hundreds of thousands of years). Consequently, it is conceivable that there is an absence of significant biphasic flow and a predominance of dissolution-diffusion processes in hydrogen migration. This would result in a gradual removal of hydrogen and a simpler overall scheme for the resaturation process. In particular, it would mean that a higher degree of saturation could be reached earlier than the one hundred to two hundred thousand years adopted as the reference hypothesis in the analysis.

Moreover, under such corrosion conditions the periods of leak tightness of the C waste overpacks and spent fuel containers would be greatly increased with respect to the estimates currently used in connection with dimensioning.

Hydrogen Removal Mechanisms

Under current assessments, there is a large total amount of hydrogen produced in a relatively short time. In this configuration, the hydrogen would therefore tend to migrate via preferential transport paths (damaged zone, drifts, etc.) that appear easier around the disposal cells than in the geological medium itself.

There are uncertainties regarding the transfer properties of the various paths and their respective share in hydrogen circulation. The modelling done to date is still limited in its representations of space and the couplings between corrosion and hydraulics (taking into account simple coupling laws between the degree of saturation and corrosion rates).

At this stage it was assumed that the removal of hydrogen via the damaged zone around the structures or via the drifts then through the Callovo-Oxfordian, would form a preferential path. This option seems reasonable and well reflects the current state of knowledge. Characterization of the mechanisms of transport in the rock would merit further refinement in order to achieve a more detailed physical representation. However, the data adopted at this stage are consistent with the experimental borehole observations, which indicate the possibility of the gas circulating in the rock and rock's hydraulic properties being restored after it passes through. Assessments of the quantities of gas generated and the pressures attained strengthen the plausibility of this mechanism. Moreover, various factors favourable to regulation within the gas circulation period have been ignored. Thus, the three-dimensional geometry of the repository, especially all the volumes and exchange surfaces with the

Callovo-Oxfordian, have only been partially represented. The modelling resources currently available are capable of accounting for gas transfer processes by dissolution-diffusion and by biphasic flow, but are not yet able to represent all the different couplings mentioned above, especially for the actual geometry of the repository and over the long time scales involved. All in all, the representation adopted may be regarded as cautious.

Link with the Safety Approach

Uncertainties exist regarding the resaturation process in the repository. Relatively complex modelling should be carried out to refine the presently available view. However, it may be noted that the scheme outlined in this volume, with staged resaturation over two hundred thousand years, is all-encompassing with respect to conceivable evolutions. Given the pessimistic kinetics adopted for hydrogen production, we have a conservative view of possible resaturation periods. In so doing, we have also dealt with the most complex case and shown that it raised no major difficulties. In particular, the hydrogen did not appear to cause any special damage, nor interfere with radionuclide transport. Thus, reducing uncertainties will tend to produce a simpler, but also less pessimistic view of the resaturation process. Accordingly, taking uncertainties into account by safety calculation may be based on a simplified approach which, in the initial analysis, assumes an immediate resaturation of the repository. The latter places all the components in the presence of water from the first moment, whereas the analysis presented stresses that the arrival of water will occur very gradually and with complete resaturation, which in any event will be delayed. Within such a framework, the limitation of the chemical processes is ignored, which will necessarily produce a reduced quantity of mobilizable water in the structures.

11.2.4.2 Hydraulic Properties of the Damaged Zone Around the Repository Over Time

The mechanical damage of the argillites around the repository structures is an important process insofar as it modifies the near-field hydraulic properties of the repository. In saturated condition and at hydraulic equilibrium, the low bulk permeability of the Callovo-Oxfordian and the design of the swelling clay seals minimize the influence of the damaged zones on the flows and transport of solutes in and around the repository. On the other hand, the hydraulic properties of the EDZ play an important part in transient hydraulic processes, in particular with regard to gas transfer.

The assessment of the extent and hydraulic characteristics of the initial damaged zone around the repository structures is based mainly on sample tests, analogies with deep clay formations (Opalinus clays at Mont Terri and at Benken in Switzerland) and modelling.

The same data lead to the assumption that hydraulic healing of the EDZ over time is very probable. This conclusion is also based on the presence of smectites whose potential for swelling should add to the self-healing capability. This data currently seems the most plausible, but it must be confirmed by additional observations in the Callovo-Oxfordian layer, in particular for assessing the hydraulic properties of the argillites in the near field of the seal hydraulic keys.

In any case, we have a picture of the damaged zone, its properties and the order of magnitude of their variations. This data can be used directly by safety analysis. It will be rendered all the more cautious by ignoring the effects that could lead to healing the damaged zone.

11.2.4.3 Dissolution of the Glass Matrix and Spent Fuel Pellets

The detailed dissolution mechanisms of vitrified waste and spent fuel assembly oxides are still the subject of discussion at the international level. In any event, these involve slow processes spread out over tens to hundreds of thousands of years.

With regard to vitrified waste, we have a range of more or less conservative models covering the different conceivable situations. Prospects are offered for taking into account lower glass dissolution rates. Safety analysis may therefore be based on current data with a high level of confidence by testing the different configurations and their impact.

In the case of spent fuels, the representation adopted is based on a hypothesis of radiolytic dissolution of the matrix. Clearly this option is very conservative and does not coincide with the options adopted at the international level, which appear less conservative. Adopting a conventional dissolution model would in fact lead to clearly longer release periods. However, characterization of spent fuel behaviour again appears to be a complex topic. In addition, a distinction should be made between the various fuels (UOX, MOX). Current uncertainties have meant adopting a cautious approach, but there is most certainly scope for progress in this specific instance.

Thus, the available data offer a solid basis for safety with the identification of safety margins and avenues of progress for representing the source term (whether in terms of a less conservative hypothesis or of heavier constraints).

11.2.5 Surrounding Formations

The surrounding formations do not include components of the repository system. They must nevertheless be represented for assessing the impact of the repository. This assumes a knowledge of the behaviour of the released radionuclides that arrive within them.

11.2.5.1 Initial State and Evolution

The description of the normal evolution of the repository and its geological environment over the next million years emphasizes the expected changes in the flows in the surrounding formations of the Callovo-Oxfordian layer, especially the overlying ones. These changes arise from climatic changes associated with internal geodynamics. Basically they are related to directions of flow. The flow rates should remain of the same order of magnitude. The analysis of these changes is based on characterizing the present flows and on climatic evolution scenarios.

No climatic evolution scenario can be defined as the most probable. There is a range of plausible scenarios. However, whatever the plausible scenario adopted, the evolutionary trends of the flows are similar, especially in terms of the occurrence of local outlets. Similarly, we have a reasonable assessment of orders of magnitude for the period from which the changes become significant. This is a few hundreds of thousands of years.

The representation of the present flows is based mainly on hydraulic measurements in boreholes, geological characterization on the regional scale and over the sector, and on modelling. There is thus great confidence in the general (i.e. regional) directions of flow and in the orders of magnitude of the flow rates, although additional dating information might be useful for quantifying these rates more accurately. However, uncertainties appear in the representation of details:

- we seem to have the picture of unconnected porous horizons in the Dogger, but their organization on the site and sector scale still entails some uncertainties;

- outside the transposition zone, a diffuse fracturing zone is currently represented, appearing in the carbonated Oxfordian from the Saulx, in the direction of the Marne faults. This representation is based on the data from a single borehole, rounded out by interpretation of surface tectonic structures. It is consistent with the variations in salinity observed for the water in the surrounding formations of the Callovo-Oxfordian. It does not alter the general representation of flows both at present and over the next million years. This zone could therefore be better characterized, although this may not cause any change in the overall view. It is up to safety assessments to deal with this point as conservatively as possible. The available characterization can be used to adopt pessimistic representations that broadly overcome this uncertainty.

In conclusion, the available data can be used to build a cautious model representing flows in the surrounding rocks. Additional characterizations would refine this picture.

11.2.5.2 Diffusion and Retention Characteristics of the Base of the carbonated Oxfordian and the Kimmeridgian Marls

At the base of the carbonated Oxfordian is a not very permeable suite approximately 60 meters thick (corresponding to the C3a-C3b facies). Its permeability and its diffusion and retention properties are only presently characterized on a few samples and not at the transposition zone scale. This suite, especially the C3a horizon probably displays characteristics similar to the Callovo-Oxfordian layer. At present, however, we cannot prejudge their homogeneity throughout the transposition zone. Taking into account low diffusion and high retention properties, ruled out in the current representation of normal repository evolution, would alter the picture of the transfer of long-lived, mobile radionuclides like ^{129}I or ^{36}Cl in the form of an increase in times of transfer to the porous levels of the carbonated Oxfordian.

Similarly, the Kimmeridgien displays marl horizons, not characterized particularly at the transposition zone scale, which could present low diffusion and high retention properties leading once again to delaying and further diluting the return of mobile radionuclides to the biosphere. Lacking characterization, these properties have not been taken into account in the description of the phenomenological evolution of the repository.

11.2.6 Representation of Couplings

The description of the evolution of the repository and its geological environment has been broken down according to the main phenomena (thermal, hydraulic, chemical and mechanical – THCM). The narrative highlights a set of temporal and spatial couplings. Their representation is largely based on the results of qualitative analyses. These draw on a set of simulations dealing with the processes in a decoupled fashion, but resorting to simplified or non-continuous couplings as required. This arises from the current capability of the simulation tools. On the other hand, this requires great caution during qualitative analysis in assessing couplings.

A few points deserve further attention:

- the mechanical evolution of the repository structures linked to chemical evolution;
- the possibility of a less conservative representation of gas transfers allowing for the limitations of the process linked to interactions between phenomena;
- the evolution of flows coupled with geodynamic changes and, correlatively, the continuous representation of radionuclide transfer in the overlying surrounding rocks.

This material would lead to achieving a more refined view of evolution, but does not seem likely to undermine the conceptual framework and view of repository history presented in this volume. In fact, it may be assumed that the coupling effects have been identified as arising from an impact of the first order.

11.3 Conclusion

Scrutiny of the uncertainties described in this chapter confirms the overall picture of repository evolution. There is reasonable confidence in the main parameters and the mechanisms liable to affect repository evolution. It goes without saying that additional investigations would refine this view and would probably provide more accurate descriptions, with a still higher level of confidence, but especially resort to less pessimistic hypotheses within the framework of safety approaches. At the current stage, once the uncertainties are taken into account, it is possible to bring to the safety approach a sufficiently clear and thorough view of the repository's behaviour to proceed to cautious and conservative assessments. In particular, the possible ranges of variations of the parameters have been identified, together with the elements likely to cause variations in overall behaviour. In conclusion, the necessary information has been gathered to act as input data for safety analyses, whether within the framework of normal evolution, or in order to take account of altered situations especially reflecting residual uncertainties.

12

Synthesis

12.1 Main characteristics of the approach 501

12.2 General description of repository phenomena and repository life history 502

12.3 Lessons 505

The purpose of the volume on the repository's phenomenological evolution is to describe all processes affecting the repository and its geological environment from the time the repository is built to the post-closure phase, for the million-year reference period selected in view of the lifespan of the radioactive elements in the waste.

The description given is the one considered most likely in the light of current scientific knowledge and expert opinion. It is mainly based on surveys and characterisation work conducted at the Meuse/Haute-Marne site since 1994 (boreholes, geophysical survey, etc.), on data from excavating the underground infrastructures of the research laboratory, on analyses, experiments and modelling based on samples, and on the work of the Mont Terri laboratory in Switzerland. Andra's research results have also been enriched by similar work conducted by Andra's counterpart organisations and, more broadly, knowledge acquired from fields of investigation other than disposal.

12.1 Main characteristics of the approach

The volume first depicts the initial state of the geological medium. It describes the medium and seeks to provide an understanding of the factors that have determined its past evolution and hence its current situation. Starting from this review, it then sets out to identify how the medium is affected by a repository before gradually returning to a stable state.

The approach adopted is to review each major type of phenomenon (thermal, hydraulic, chemical and mechanical) liable to affect the repository and which, together, give a representation of how radionuclides behave in the medium. This breakdown gives a complete and simplified view of all the basic processes. It also provides an understanding of the physical mechanisms involved. The approach does not stop there, however: some phenomena may interact and produce coupled effects. It would be a delicate matter to give an entirely coupled representation of all the phenomena occurring in the repository, particularly in numerical form, which would exceed both computing capacity and the scope of available models.

However, the analysis in this volume does give an understanding of whether, and how, each phenomenon may influence the others, and what couplings should be taken into account. This exercise mainly involves estimating orders of magnitude and partially testing the validity of various hypotheses. All in all, the representation ranks the phenomena, their importance and their interactions on a reasoned basis, in order to identify the main determining factors to be examined. This approach builds up a more readily understandable overall representation which can then be simplified to give a prudent model on which to base the safety analyses.

In this way the volume shows that it is possible to achieve an overall understanding of how the repository would function – an understanding that is sufficiently accurate, but is reduced to the main parameters that would have a real impact on the repository's overall evolution.

This transcription of repository phenomena into a more easily interpreted form is based on meticulous exploitation of the results of research on each component. Each phenomenon has been investigated in detail to calibrate its importance and establish its main effects. Only after this detailed phenomenological approach was it possible to draw up a more general picture showing the main features. The method used was phenomenological analysis of repository situations (PARS).

This innovative approach divides the repository into segments of time and space to give a set of situations that are easier to understand and control, making it possible to transcribe the knowledge acquired into usable material. PARS underpins the work presented in this volume.

The main purpose of this volume is to provide as robust an understanding of the repository's life history as possible. Confidence in the technical structures that make up the repository necessarily depends on the capacity to represent, in a relatively simple and accessible way, the repository's future and the basis for such predictions. However, over and above that representation, it is essential to be able to extract an even more simplified vision that will provide a kind of plan for prudent, well-controlled repository management. Once the main phenomena are understood, the orders of magnitude known and the implications of possible changes understood, this work should be transcribed into a form that (a) can be used for safety analysis and (b) reduces the complexity even further, allowing a simple, unambiguous assessment of the potential repository's performance. The volume on phenomenological assessment of the repository provides this basis, giving a general description of the repository's life history and the main phenomena involved. It informs the safety management approach, highlighting aspects that might be neglected and those that call for prudent representations. In this way is constitutes input data for performance analysis.

An understanding of the repository's life history is also an essential tool for studying reversibility. For the repository to be reversible, one must be able to monitor the phenomena occurring at any moment and take corrective measures if necessary. One must know the characteristic parameters to be able to assess whether they are evolving as predicted. One must know the characteristic lifespan or evolutionary timescale of each component and to understand how each stage in reversible repository management may unfold. This volume shows what factors determine the life of the repository and stresses that, based on these factors, it is possible to envisage reversible repository management lasting a number of centuries without any particular difficulty. Beyond that period reversibility would still be possible, but would require additional activities. This volume also highlights the key points that might prove controversial and call for special attention.

To conclude, describing the broad lines of the repository's life history with a fair level of confidence, this volume lays the groundwork both for reversible management and for a safety assessment based on scientific and technical knowledge acquired in recent years.

12.2 General description of repository phenomena and repository life history

12.2.1 Evolution shaped by the characteristics of the Callovo-Oxfordian stratum and repository design

The normal evolution of the repository and its geological environment at the Meuse/Haute-Marne site is conditioned mainly by the characteristics and properties of the Callovo-Oxfordian formation, especially at the scale of the transposition zone.

The work conducted in boreholes, on samples and during investigations in the underground research laboratory has revealed the outstanding intrinsic properties of the argillite: low permeability, high retention capacity, low chemical reactivity (i.e. high chemical buffer potential) for withstanding such stresses as alkaline disturbance by concrete water or contact with metals, favourable mechanical properties for withstanding excavating engineered structures and a capacity for mechanical and hydraulic self-healing after mechanical rupture or deformation.

The inclined boreholes and interpolation of borehole data combined with geophysical data attest to the uniformity of the argillite throughout the thickness of the Callovo-Oxfordian stratum and within the transposition zone.

- No fault with a slip of more than 5 meters has been detected; this gives to the formation low permeability on a macroscopic scale.
- Although the mineralogical composition of the argillite varies between the top, centre and bottom of the stratum, the chemistry of the interstitial water and the argillite's retention properties appear broadly uniform throughout the thickness of the stratum and throughout the transposition zone.

Together, these features also attest to the stability of the Callovo-Oxfordian at the Meuse/Haute-Marne site, a stability that has lasted for tens of millions of years. In particular, the Meuse/Haute-Marne site is some distance from any active tectonic zone. Around the Meuse/Haute-Marne site and in the transposition zone, flow is particularly slow in the Callovo-Oxfordian stratum and its surrounding formations are poorly aquiferous. These characteristics also determine the potential local and regional hydraulic outlets for any water circulating from the repository zone, so pinpointing the places where the environment might be exposed to radioactivity.

Repository design aims to make the most of all the properties of the Callovo-Oxfordian stratum while keeping to a minimum the thermal, mechanical, hydraulic and chemical stresses generated by the repository. The purpose is to preserve the low reactivity of the Callovo-Oxfordian layer and keep it as close as possible to its current state of equilibrium. The repository is divided into separate disposal zones at some distance from each other, each dedicated to one major type of waste, and divided into disposal modules within each disposal zone. This architecture will prevent or limit phenomenological interactions within the repository and ultimately limit the complexity of the processes taking place there, so that they can be effectively controlled.

12.2.2 A combination of processes that vary in importance over time

The processes taking place in the repository and its geological environment differ not only in their duration and spatial spread but also in their consequences.

Chemical processes take place over timescales ranging from a few thousand to several hundred thousand years**.** Over-packs of C waste packages and containers of spent fuel assemblies will continue to corrode for at least some thousands to tens of thousands of years, and cement water will continue to cause alkaline disturbance to the argillites and swelling clay components for hundreds of thousands of years. However, in spatial terms they will be limited to the repository's near field, i.e. the first meters of argillite. For example, the extent of alkaline disturbance is metric at most, while disturbance caused by iron in the metal components of C waste disposal cells and spent fuel disposal cells is in the decimetre range. Nor will chemical processes spread far within the repository: alkaline disturbance caused by concrete to components based on swelling clay, such as disposal cell plugs and drift and shaft seals, will only affect small volumes. Interactions between waste packages and their near environment within the disposal cells are very weak compared to the metric or plurimetric size of the cells.

The thermal load of the repository affects all the geological formations centred on the repository, the Callovo-Oxfordian stratum particularly. The maximum temperatures reached in these formations are low – 60° at most in the near field of the Callovo-Oxfordian stratum. Furthermore, the thermal load would not last more than about ten thousand years before returning to temperatures close to natural geothermal conditions. Such a moderate heat load is unlikely to have irreversible effects such as mineralogical changes in the argillites, thermal-mechanical stresses or effects on hydraulic and chemical properties (chemistry of interstitial water, retention).

On the mechanical side, the repository generates mechanical disturbance in the near-field argillite, first when the engineered structures are excavated, then during operation (because of the ventilation) and finally in the post-closure phase owing to mechanical changes inside the engineered structures, mainly linked to chemical processes (chemical degradation of concrete). The extent of the mechanical disturbance is plurimetric at most. Its consequences for the permeability of the near-field Callovo-Oxfordian largely fade out within a few thousand years, by self-healing (owing to mechanical compression stresses, swelling of smectite in the argillite and/or precipitation of minerals in fractures and fissures).

The repository also causes considerable ***hydraulic disturbances***. The most significant is that the repository and its near field, at least for some disposal modules, are kept in a relatively desaturated state for a long period. This is largely due to a hydraulic transient linked to hydrogen production caused by corrosion of metal components. The hydrogen slows the repository resaturation process, so that it takes nearly two hundred thousand years for the repository to reach total saturation again. The repository and the surrounding Callovo-Oxfordian stratum then return to a new state of hydraulic equilibrium. In principle, the new hydraulic equilibrium would not be significantly different from the present one. Later still, surface phenomena may affect the formations overlying the argillites, but this will not affect the Callovo-Oxfordian under any circumstances. Broadly speaking, the various hydraulic transients seem to be second-order factors compared to the general pattern governing flows and transport through the medium. Transport remains predominantly diffusive, regardless of when and where convective transport may develop in the repository.

12.2.3 Very limited evolution of the Callovo-Oxfordian layer as a whole over the next million years

The various processes described below only affect the Callovo-Oxfordian layer in the immediate vicinity of the repository installations, through less than one-tenth the total thickness of the layer. Geodynamic changes (mainly climate change above ground affecting the surrounding geological formations, particularly as regards the organisation of flows and the location of outlets) only affect the Callovo-Oxfordian layer by altering hydraulic conditions at its boundaries with the Dogger and carbonated Oxfordian. Overall, the characteristics of the Callovo-Oxfordian layer remain similar to today's.

12.2.4 Evolution of flow in surrounding formations over the next million years

Over the next million years the surrounding formations undergo significant changes due to external geodynamic conditions (climate change), significantly altering the directions of flow. The broad directions and the changes in those directions can be predicted fairly reliably. In particular, with geodynamic changes, new directions of flow appear locally. These changes become significant after a few hundred thousand years and continue to the million-year and beyond.

12.2.5 Slow release of radionuclides from waste packages governed by repository installations and geological medium

The stability of the Callovo-Oxfordian layer and its hydraulic characteristics over time combine to ensure that the repository's disposal cells degrade very slowly and only to a limited extent. This applies to the waste packages themselves and their immediate surroundings, such as the concrete of the B waste disposal cells and the engineered structures of the spent fuel disposal cells. The slow kinetics of the chemical degradation processes results in a very gradual release of radionuclides from the waste packages. Further, the slow corrosion of the metal C waste over-packs does not enable water to reach the glass until several thousands or tens of thousand of years have passed, by which time the thermal load has ceased. The same applies to the spent fuel containers.

Thus broadly speaking, the environment the radionuclides encounter as they are gradually released into the disposal cells is – depending on the waste concerned – a Callovo-Oxfordian stratum close to its present state, swelling clay close to its initial state, or concrete that has suffered little or no deterioration.

Because of the combination of slow diffusive transfer, high retention capacity and low solubility within the disposal cells and the Callovo-Oxfordian stratum, most radionuclides released by the waste packages migrate slowly and do not go far. This particularly applies to actinides, which remain trapped in the repository or migrate only a few meters into the near-field argillite over the next million years. Only "mobile" toxic chemicals and radionuclides (i.e. highly soluble and weakly retained, the main ones being I^{-129} and Cl^{-36}) reach the surrounding formations, and only in very low concentrations after several hundred thousand years.

12.3 Lessons

Several major lessons can be drawn from this volume on the phenomenological evolution of the repository.

In the first place, the understanding acquired of the different phenomena, their characteristic timescales and their mode of representation provides a coherent overall picture of the repository and its evolution over time. This is an important result, since it provides a basis for assessing the repository's performance. The life of the repository is predicted fairly precisely and with a reasonable degree of confidence. True, it cannot be said that we have detailed knowledge of how every factor will evolve, but the general pattern seems to be relatively robust and not very sensitive to uncertainties. Furthermore the uncertainties have been identified, making it possible to assess the importance of different factors in overall performance.

There are still some uncertainties regarding the representation provided. By definition, it would be presumptuous to claim to make absolute predictions on a large spatial scale and for a million-year period. However, we can now outline a general history covering the full spectrum of most likely changes. Within this spectrum the uncertainties seem to be under control insofar as those with a significant impact on the representation, and their associated ranges of variation, have been examined. In this way it is possible to define prudent options with which to encompass possible futures or avoid some uncertainties.

The repository life history presented in this volume is based on concepts and architectures defined after engineering studies. It constitutes ex-post confirmation of the validity of those studies. The concepts have been seen to offer a way of exploiting the favourable properties of the medium to the full and overcoming possible uncertainties. From this standpoint, the overall vision presented appears robust because it is based on realistic, prudent architectural choices that make the most of the geological medium.

The detailed description of the phenomena and associated uncertainties suggest avenues for further research. These are broadly focused on three themes:

- a more detailed, large-scale characterisation of the geological medium to define more precisely the safety margins that have not been taken into account;
- life-size technological constructions, to provide a more detailed understanding of the behaviour of the disposal cells and waste;
- additional studies of the basic mechanisms governing the mechanical behaviour of the host rock and the underground facilities, the release and transport of radionuclides, to produce more accurate models for the representation.

The volume has produced a general picture that constitutes input data directly usable for safety purposes. The suggested ranking order of phenomena lays the groundwork for the safety model in that it provides the necessary information for choosing models, parameters and possible simplifications. The overall understanding we have acquired of the system thus becomes the tool for ensuring that a prudent, conservative vision of the repository's evolution can be developed, ignoring aspects favourable for safety and choosing pessimistic parameters, and so guaranteeing a repository design that is industrially realistic and safe over the long term.

Bibliographic References

Adler M. (2001) Interaction of claystone and hyperalkaline solutions at 30°C: A combined experimental and modelling study; Thèse de l'Université de Bern, Suisse, 119 p.

Advocat T. (1991) Les mécanismes de corrosion en phase aqueuse du verre nucléaire R7T7. Approche expérimentale. Essai de modélisation thermodynamique et cinétique; Thèse de l'Université Louis Pasteur, Strasbourg, France, 213 p.

Advocat T., Crovisier J.L., Fritz B. & Vernaz E. (1990) Thermokinetic model of borosilicate glass dissolution: contextual affinity. *Scientific Basis for Nuclear Waste Management*, XIII, pp. 241-248.

Advocat T., Jollivet P., Crovisier J.L. & del Nero M. (2001) Long-term alteration mechanisms in water for SON68 radioactive borosilicate glass. *Journal of Nuclear Materials*, 298(1-2), pp. 55-62.

Aertsens M. & Van Iseghem P. (1996) Modelling Glass Dissolution with a Monte Carlo Technique. *Mat. Res. Soc. Symp. Proc.*, 412, pp. 271-278.

Albrecht A. & Gallerand M.-O. (2005) Evaluation des facteurs de conversion biospheres pour les radionucléides et des risques associés aux toxiques chimiques. Modélisation de leur comportement dans les biosphères de référence - Site de Meuse / Haute-Marne. Rapport Andra n° C.NT.ASTR.03.110.

Altmann S. & Coelho D. (2005) Le modèle d'écoulement et de transport des solutés dans le Callovo-Oxfordien sain et perturbé - Site de Meuse / Haute-Marne. Rapport Andra n° C.NT.ASTR.03.0022.

Altmann S. & Jacquot E. (2005) La chimie des eaux interstitielles dans la couche du Callovo-Oxfordien à l'état initial - Site de Meuse / Haute-Marne. Rapport Andra n° C.NT.ASTR.03.023.

Andersen B.J. & Borns H.W.J. (1994) The ice age world. An introduction to Quaternary history and research with emphasis on North America and Northerne Europe during the last 2.5 millions years. Scandinavian University Press. Oslo-Copenhagen-Stockolm. Distrib. By Oxford University Press, 208 p.

Andra (2003a) HAVL-Argile. Sélection des valeurs des paramètres de transfert dans la biosphère des radionucléides et toxiques chimiques pour le dossier 2005. Rapport Andra n° SUR.NT.ASTR.03.044.

Andra (2003b) Rapport de synthèse du Kimméridgien - Laboratoire de recherche souterrain de Meuse / Haute-Marne - Lot 4 - Puits d'accès et auxiliaire. Rapport Andra n° D.RP.0ANT.02.021.

Andra (2003c) Synthèse hydrogéologique des calcaires du Barrois. Bilan des connaissances géologiques et hydrogéologiques sur le site de l'Est Laboratoire de recherche souterrain de Meuse / Haute-Marne. Rapport Andra n° D.RP.0HYN.03.004.

Andra (2004a) Forages de reconnaissance de la formation. Synthèse FRF. Laboratoire de recherche souterrain de Meuse / Haute-Marne. Rapport Andra n° D.RP.ADPE.04.1245.

Andra (2004b) Forages Scientifiques Profonds. Synthèse FSP. Laboratoire de recherche souterrain de Meuse / Haute-Marne (3 volumes). Rapport Andra n° D.RP.ADPE.03.0753.

Andra (2004c) Oxfordien calcaire - Rapport de synthèse - Laboratoire de recherche souterrain de Meuse / Haute-Marne. Rapport Andra n° D.RP.ADPE.04.1109.

Andra (2005a) Analyse phénoménologique des situations de stockage (APSS) - Phase d'exploitation d'un stockage en formation argileuse profonde - Site de Meuse / Haute-Marne. Rapport Andra n° C.NT.ASIT.03.077.

Andra (2005b) Analyse phénoménologique des situations de stockage (APSS) - Phase post-fermeture d'un stockage en formation argileuse profonde - Site de Meuse / Haute-Marne. Rapport Andra n° C.NT.ASIT.03.133.

Andra (2005c) Analyse qualitative de sûreté à long terme d'un stockage en formation argileuse profonde - Site de Meuse / Haute-Marne. Rapport Andra n° C.NT.AMES.04.0049.

Andra (2005d) Dossier 2005 - Référentiel de comportement des colis de déchets à haute activité et à vie longue. Rapport Andra n° C.RP.ASCM.04.0017.

Andra (2005e) Dossier 2005 - Référentiel de connaissance et modèle d'inventaire des colis de déchets à haute activité et à vie longue. Rapport Andra n° C.RP.AHVL.04.0006.

Andra (2005f) Dossier 2005 - Référentiel des matériaux d'un stockage de déchets à haute activité et à vie longue. 4 Tomes. Rapport Andra n° C.RP.ACSM.04.0015.

Andra (2005g) Dossier 2005 argile - Référentiel de comportement des radionucléides et des toxiques chimiques d'un stockage dans le Callovo-Oxfordien jusqu'à l'homme - Site de Meuse / Haute-Marne. Rapport Andra n° C.RP.ASTR.04.0032.

Andra (2005h) Dossier 2005 argile - Référentiel du site de Meuse / Haute-Marne. 3 Tomes. Rapport Andra n° C.RP.ADS.04.0022.

Andra (2005i) Dossier 2005 argile - Tome - Architecture et gestion du stockage géologique. Rapport Andra n° C.RP.ADP.04.0001.

Andra (2005j) Dossier 2005 argile - Tome - Evaluation de sûreté du stockage géologique. Rapport Andra n° C.RP.ADSQ.04.0022.

Andra (2005k) Le transitoire redox dans un stockage et dans le Callovo-Oxfordien en champ proche. Site de Meuse / Haute-Marne. Rapport Andra n° C.NT.ASIT.03.127.

Andra (2005l) L'évolution phénoménologique des galeries d'un stockage et le comportement des radionucléides dans les galeries - Site de Meuse / Haute-Marne. Rapport Andra n° C.NT.ASIT.04.0014.

Andra (2005m) Rapport de synthèse des calculs de sûreté du Dossier Argile 2005 - Scénario d'Evolution Normale - Calculs de référence et de sensibilité. Rapport Andra n° C.RP.ACSS.05.0005.

Andra (2005n) Spécification technique de besoin d'un stockage en formation argileuse profonde - Site de Meuse / Haute-Marne. Rapport Andra n° C.SP.AHVL.02.132.

Andra / CNF-INQUA (1999) La France pendant les deux derniers extrêmes climatiques. Variabilité naturelle des environnements (cartes à l'échelle 1/ 1 000 000 et notice). Co-édition Andra/CNF-INQUA, publi. Andra Châtenay-Malabry.

André G. (2003) Caractérisation des déformations méso-cénozoïques et des circulations de fluides dans l'Est du Bassin de Paris. Thèse de doctorat Université Nancy I, 310p.

ANTEA (1999) Site Meuse / Haute-Marne. Mise en oeuvre du modèle hydrodynamique régional pour simuler quelques contextes hydrogéologiques géoprospectifs. Rapport Andra n° D.RP.0ANT.99.056.

Ata A., Shao J.F. & Ozanam O. (2002) Numerical Analysis of Induced Damage due to the Drying in Geological Barrier. Workshop of Hydromechanical and thermohydromechanical behaviour of deep argillaceous rock, Oct 2000, Paris. Balkema-2002 Ed., p. 199-213.

Barnichon J.D. & Su K. (2005a) Le comportement mécanique d'alvéoles de stockage de déchets B dans le temps - Site de Meuse / Haute-Marne. Rapport Andra n° C.RP.ASMG.03.0110.

Barnichon J.D. & Su K. (2005b) Le comportement mécanique des scellements de galeries dans le temps - Site de Meuse / Haute-Marne. Rapport Andra n° C.RP.ASMG.03.111.

Barnichon J.D. & Su K. (2005c) Le comportement mécanique des scellements de puits dans le temps - Site de Meuse / Haute-Marne. Rapport Andra n° C.RP.ASMG.03.112.

Baston G.M.N., Berry J.A., Boult K.A., Brownsword M. & Linklater C.M. (1994) Effects of cellulosic degradation products on uranium sorption in the geosphere. *Journal of alloys and compounds*, 213-214, pp. 475-480.

Bauer C. (2005) La charge thermique d'un stockage - Site de Meuse / Haute-Marne. Rapport Andra n° C.NT.ASIT.03.118.

Bauer C., Piguet J.P. & Wileveau Y. (2003) Disturbance assessment at the wall of a vertical blasted shaft in marls. Proc. of the 10th Int. Congress on Rock Mechanics (ISRM) Vol. 1 - Sandton, Afrique du Sud, 8-12 september 2003, pp 93-98, Ed SANIRE & SAIMM (ISBN 1-919783-52-0).

Berger A. (1992) Le climat de la terre. Un passé pour quel avenir ? Ed. De Boek Université, p. 479.

Bergerat F. (1985) Déformations cassantes et champs de contrainte tertiaires dans la plate-forme européenne.; Thèse Université Pierre & Marie Curie, Paris, 375 p.

Bernat P. (1994) Etude du comportement des enrobés bitumeux sous irradiation gamma. Influence des constituants provenant du procédé ST3 de décontamination des effluents liquides; Thèse de l'Université Paris V, René Descartes, Paris, 240 p.

BIOCLIM (2002) Global climatic features over the next million years and recommendation for specific situations to be considered. Bioclim Delivrable D3.

BIOCLIM (2003a) Development of the rule-based down-scaling methodology for BIOCLIM Workpackage 3. Bioclim Delivrable D8a.

BIOCLIM (2003b) Global climatic characteristics, including vegetation and seasonal cycles over Europe, for snapshots aver the next 200,000 years. Bioclim Delivrable D4-D5.

Boisson J.Y. (1998) Preliminary EDZ investigations in argillaceous rock from old tunnel and new galleries at Tournemire I.P.S.N. site (Aveyron, France). OECD/NEA/RWMC coordination group on site evaluation and design of experiments for radioactive waste disposal SEDE) 9th meeting, 23-25 september 1998, Paris, France.

Bossart P., Meier P.M., Moeri A., Trick T. & Mayor J.C. (2002) Geological and hydraulic characterisation of the excavation disturbed zone in the Opalinus Clay of the Mont Terri Rock laboratory. *Engineering Geology*, 2040, Vol. 66, Issues 1-2, October 2002, pp. 19-38.

Bouchet A., Meunier A. & Sardini P. (2000) Les minéraux argileux : structure cristalline, identification par diffraction de rayons X. *Bull. Centre Rech. Elf Explor. Prod.*, Mém. 23, pp. 136.

Bourbon X. (2005) L'évolution chimique des ouvrages d'un stockage à base de béton : alvéoles de stockage de déchets B, appuis de scellements et de bouchons d'alvéoles, infrastructures des galeries - Site de Meuse / Haute-Marne. Rapport Andra n° C.NT.ASCM.03.021.

Bourcier W.L., Peiffer D.W., Knauss K.G., McKeegan K.D. & Smith D.K. (1990) A kinetic model for borosilicate glass dissolution based on the dissolution affinity of a surface alteration layer. *Scientific Basis for Nuclear Waste Management*, XIII, pp. 209-216.

Bourrelier P.-H. & Berthelin J. (1998) Contamination des sols par les éléments en traces : les risques et leur gestion. Académie des Sciences, Rapport n°42, Lavoisier TEC & DOC, Paris, 440 p.

BRGM & ELF Aquitaine (1976) Potentiel géothermique du Bassin parisien - Rapport de fin de contrat DGRST. Rapport n° 74.7.0990.

Brodersen K. (1999) Hygroscopic materials in bituminized waste : experiments and modelling. Radwaste Bituminization 99, Proceedings of the international workshop on the safety and performance evaluation of bituminization processus for radioactive waste, Prague, Czech Republic, june 29 - july 2, 1999.

Brulhet J. (2005a) L'aléa sismique à long terme et son impact pour un stockage - Site de Meuse / Haute-Marne. Rapport Andra n° C.NT.ASMG.03.0102.

Brulhet J. (2005b) L'évolution géodynamique (tectonique et climatique) et son impact sur l'hydrogéologie et l'environnement de surface - Site de Meuse / Haute-Marne. Rapport Andra n° C.NT.ASMG.03.0106.

Buehler C., Heitz D., Trick T. & Frieg B. (2003) In situ self-healing of the EDZ as a consequence of loading. In Proc. EC CLUSTER conference, Luxembourg, 3-5 nov; 2003, pp. 231-236, to be published in the EUR series.

Buschaert S. (2001) Origine, âge et processus physico-chimiques des circulations dans les fractures. Exemple du socle sous couverture (Vienne) et des formations riches en argiles (Gard et Est). Thèse de doctorat, Université de Nancy I, rapport FORPRO 2001/28Th, 260 p.

Buschaert S., Fourcade S., Cathelineau M., Deloule E., Martineau F., Ayt Ougougdal M. & Trouiller A. (2004) Widespread cementation indiced by inflow of continental water in the eastern part of the Paris basin : O and C isotopic study of carbonate cement. *App. Geochem.*, 19-8, pp. 1201-1215.

Buschaert S. & Giffaut E. (2005) La solubilité et la rétention des radionucléides et des toxiques chimiques dans les encaissants - Site Meuse / Haute-Marne. Rapport Andra n° C.NT.ASTR.03.104.

Camaro S., Simondi-Teisseire B. & Vistoli P.P. (1999) Long-term behaviour of bituminized waste . Radwaste Bituminization 99, Proceedings of the international workshop on the safety and performance evaluation of bituminization processus for radioactive waste, Prague, Czech Republic, june 29 - july 2, 1999.

Carnahan C.L. (1985) Thermodynamically coupled mass transport process in a saturated clay. *Proc. Mat. Res. Soc. Symp*, Vol. 44, pp. 491-498.

Carpentier C. (2004) Géométries et environnements de dépôt de l'Oxfordien de l'est du bassin de Paris. Thèse Université Nancy-1, 470 p., 4 annexes.

Cathelineau M. & Mosser R. (1998) Recherches sur la stabilité thermique des formations argileuses de la Haute-Marne et silteuses du Gard- années 1997-1998 : Rapport final. Rapport Andra n° D.RP.0CRE.98.005.

Caurel J., Vernaz E. & Beaufort D. (1990) Hydrothermal leaching of R7-T7 borosilicates glass (nuclear waste glass). *Scientific Basis for Nuclear Waste Management*, XIII, pp. 309-318.

Cavelier C., Mégnien C., Pomerol C. & Rat P. (1980a) Introduction à la géologie du Bassin de Paris. *Bull. d'inf. géol. du Bassin de Paris*, Vol.16, n°4.

Cavelier *et al.* (1980b) Bassin de Paris, in Géologie de pays européens - France, Belgique, Luxembourg, Dunod.

Chabiron A. & Plas F. (2005) L'évolution phénoménologique normale d'un stockage en formation argileuse profonde - Site de Meuse / Haute-Marne - Les processus majeurs : nature, temps caractéristiques et principaux couplages. Rapport Andra n° C.NT.ASIT.04.0012.

Chamley H. (1989) Clay sedimentology. Spinger-Verlag, 623p.

Chandler N.A. & *et al.* (2002) The five year report on the tuneel sealing experiment : an international project of AECL. Rapport JNC, ANDRA and WIPP, n° AECL-12127.

Charpentier D. (2001) Rôle de l'oxydation chimique et de l'acidification des eaux sur les propriétés minéralogiques et physico-chimiques de la formation argileuse de Tournemire. Thèse de l'Université Henry Poincaré, Nancy I, France, 255 p.

Chermak J.A. (1992a) Low temperature experimental investigation of the effect of high pH KOH solutions on the Opalinus Shale, Switzerland. *Clays Clay Miner*, 41, pp. 365-372.

Chermak J.A. (1992b) Low temperature experimental investigation of the effect of high pH NaOH solutions on the Opalinus Shale, Switzerland. *Clays Clay Miner*, 40, pp. 650-658.

Choquette P.W. & Pray L.C. (1972) Geologic nomenclature and classification of porosity in sedimentary carbonates. *Carbonates rocks II: porosity and classification of reservoir rocks, AAPG Reprint series*, Vol. 5, pp. 154-197.

Clauer N., Buschaert S., Cathelineau M., Disnar J.R., Duplay J., Elie M., Géraud Y., Henry J.P., Javoy M., Landais P., Lavastre V., Liewig N., Marty B., Orberger B., Pagel M., Raynaud S. & Rousset D. (2001) Evolution diagénétique des formations argileuses très imperméables de l'Est et du Gard. Action FORPRO 98 IV. Rapport Forpro 2001/04 Rj. 284 p.

Coelho D. (2005) La thermo-convection dans la couche du Callovo-Oxfordien et les formations géologiques encaissantes sous l'effet de la charge thermique d'un stockage - Site de Meuse / Haute-Marne. Rapport Andra n° C.NT.ASTR.03.105.

Cojan I. (1999) Groupe géoprospective : étude phénoménologiques génériques. Forçage des variations climatiques. Une source de gaz à effet de serre : les hydrates de gaz. Synthèse des connaissances. Rapport Andra n° D.RP.0ARM.98.012.

Colenco Power Engineering (2004) Modélisation de la migration des gaz dans les alvéoles de déchets B. Rapport Andra n° C.RP.OCPE.04.007.

Conrad R., Aragno M. & Seiler W. (1983) Production ans Consumption of Hydrogen in a eutrophic lake. *Appl. Environ. Microbiol.*, 45(2), pp. 502-510.

Coulon M. (1992) La distension oligocène dans le nord-est du bassin de Paris (perturbation des directions d'extension et distribution des stylolites). *Bull. Soc. Géol. Fr., 5*, pp. 531-540.

Crovisier J.L., Advocat T., Petit J.C. & Fritz B. (1989) Alteration of basaltic glass in Iceland as a natural analogue for nuclear waste glasses : geochemical modelling with DISSOL. *Scientific Basis for Nuclear Waste Management*, XII, pp. 57-64.

Crusset D. (2005) La corrosion des composants métalliques d'un stockage : les (sur)conteneurs de colis de déchets vitrifiés et de combustibles usés et les infrastructures métalliques - Site de Meuse / Haute-Marne. Rapport Andra n° C.NT.ASCM.03.0046.

David D. (2003) Analogues archéologique et corrosion. Matériaux. Collection Sciences et Techniques. pp 75.

De Marsily G. (1981) Hydrogéologie quantitative. Masson, Paris, 215 p.

De Windt L., Pellegrini D. & van der Lee J. (2004) Coupled modeling of cement/claystone interactions and radionuclide migration. *J. Contam. Hydrol.*, 68, pp. 165-182.

Dejonghe P. (1999) Development of industry applications of bituminization processes - a historical review. Radwaste bituminization '99, proceedings of the international worshop on the safety and performance evaluation of bituminization processes for radioactive waste. Nuclear research institute rez (Czech Republic) Belgoprocess, Rez near Prague, pp. 11-16.

Del Nero M., Salah S., Miura T., Clément A. & Gauthier-Lafaye F. (1999) Sorption/Desorption Processes of Uranium in Clayey Samples of the Bangombé Natural Reactor Zone, Gabon. *Radiochimica Acta*, 87, pp. 135-149.

Deneux-Mustin S., Roussel-Debet S., Mustin C., Henner P., Munier-Lamy C., Colle C., Berthelin J., Garnier-Laplace J. & Leyval C. (2003) Mobilité et transfert racinaire des éléments en traces : influence des micro-organismes du sol. Editions TEC & DOC, Paris, 282 p.

Dercourt J., Ricou L.E. & Vrielynck B. (1993) Atlas - Thétys - Paleoenvironmental maps. CCGM Diffusion, Paris.

Deschamps P. (2003) Traçage de la mobilité des radionucléides naturels en milieu sédimentaire profond à l'aide des déséquilibres radioactifs (234U/238U) : application aux formations mésozoïques de l'Est du bassin de Paris. Thèse Université du Québec, Montréal / Université Paris-Sud, 191 p. + annexes, Andra, D.RP.0UNQ.03.001.

Deschamps P., Hillaire-Marcel C., Michelot J.L., Doucelance R., Ghaleb B. & Buschaert S. (2004) 234U/238U disequilibrium along stylolitic discontinuities in deep mesozoïc limestone formations of the eastern Paris basin: evidence for discrete uranium mobility over the last 1-2 million years. *Hydrogeoloy and Earth System Science*, 8(1), pp. 35-46.

Dewonck S. (2000) Géochimie isotopique des gaz rares dans les roches sédimentaires et les eaux souterraines de l'Est du Bassin de Paris. Contribution aux transferts massiques intrabassinaux; Thèse INPL, Nancy, France, 247 p.

Donsimoni M. (1981) La bassin houiller lorrain. Mém. 15 pl. ht. BRGM, pp.100.

Elie M., Faure P., Michels R., Landais P. & Griffault L. (2000) Natural and laboratory oxidation of low-organic-carbon-content sediments: comparison of chemical changes in hydrocarbons. *Energy & Fuels*, 14, n°4, pp. 854-861.

Elion P. (2005) Le modèle géologique du Callovo-Oxfordien à l'état initial - Site de Meuse / Haute-Marne. Rapport Andra n° C.NT.ASMG.03.0101.

Espitalié J., Marquis F. & Sage L. (1987) Organic geochemistry of the Paris basin. In Petroleum geology of North West Europe. J. Brooks and K. Glennie, pp.71-86.

European commission (2003) Impact of the excavation disturbed or damaged zone (EDZ) on the performance of radioactive waste geological repositories, Proceedings of a European Commission Cluster conference and workshop, Luxembourg, 3 to 5 November 2003.

Faure P., Landais P. & Griffault L. (1999) Behaviour of organic matter from Callovian shales during low temperature air oxidation. *Fuel*, Vol. 78, pp. 1515-1525.

Fillet S. (1987) Mécanisme de corrosion et comportement des actinides dans le verre nucléaire "R7T7". Thèse de l'Université du Languedoc, Montpellier, France, 338 p.

Forpro (2003) Benchmarck Perméabilités : Caractérisation des milieux de très faible perméabilité. Rapport GdR Forpro 2003/6.

Ganster P. (2004) Modélisation de verres intervenant dans le conditionnement des déchets radioactifs par dynamiques moléculaires classique et ab initio; Thèse de l'université de Montpellier, 177 p.

Gaucher E., Blanc P., Matray J.M. & Michau N. (2004) Modeling diffusion of an alkaline plume in a clay. *Appl. Geochem*, Vol. 19, pp. 1505-1515.

Geotti-Bianchini F. & De Riu L. (1995) Infrared Spectroscopic analysis of water incorporated in the structure of industrial soda-lime-silica glasses. *Glastech. Ber. - Glass Sci. Technol.*, 68, 7, pp. 228-240.

Geotti-Bianchini F., De Riu L., Gagliardi G., Guglielmi M. & Pantano C.G. (1991) New interpretation of the IR reflectance spectra of SiO_2-rich films soda-lime glass. *Glastech. Ber. - Glass Sci. Technol.*, 64, 8, pp. 205-217.

Giffaut E. (2005) La solubilité et la rétention de radionucléides et de toxiques chimiques au sein d'alvéoles de stockage de déchets B - Site de Meuse / Haute-Marne. Rapport Andra n° C.NT.ASTR.03.106.

Giffaut E. & Buschaert S. (2005) La solubilité et la rétention de radionucléides et de toxiques chimiques au sein du Callovo-Oxfordien sain et perturbé - Site de Meuse / Haute-Marne. Rapport Andra n° C.NT.ASTR.03.099.

Giffaut E. & Coelho D. (2005) La solubilité, la rétention et le transport de radionucléides et de toxiques chimiques au sein d'alvéoles de stockage de colis de déchets C et de combustibles usés - Site de Meuse / Haute-Marne. Rapport Andra n° C.NT.ASTR.03.108.

Girard J.P., Flehoc C., Gaucher E., Prinzhofer A. & Chappellaz J. (2002) Isotopic study of CO_2 and CH_4 out-gassed from argillites investigated for radioactive waste repository. *Geochimica and Cosmochimica Acta*, Vol. 66, pp. A274.

Girard J.-P., Fléhoc C., Gaucher E., Prinzhofer A., Huiban Y. & Noirez S. (2003) Projet Isogaz : Caractérisation isotopique des gaz émis par les argilites du Callovo-Oxfordien, Rapport d'avancement de la phase 2. Rap. BRGM/RP-52834-FR. Rapport Andra n° D.RP.PSTR.04.008.

Glaus M.A. & Van Loon L.R. (2004) Cellulose degradation at alkaline conditions: long-term experiments at elevated temperatures. Rapport Nagra n° Technical Report 03-08.

Goguel J. (1987) Hydrogéologie des roches imperméables. *Hydrogéologie*, n°3, pp. 155-160.

Gonçalvès J. (2002) Modélisation 3D de l'évolution géologique du basin de Paris: implications diagénétiques et hydrogéologiques.Thèse Université Paris VI Pierre et Marie Curie, Paris, France, 312 p.

Gonçalvès J., De Marsily G., Violette S. & Wendling J. (2004) Analytical and numerical solutions for alternative overpressuring processes: Application to the Callovo-Oxfordian in the Paris Basin, France. *J. Geophysical Research* (A paraître).

Gorgeon L. (1994) Contribution à la modélisation physico-chimique de la rétention de radioéléments à vie longue par des matériaux argileux; Thèse de l'Université Paris 6.

Grambow B. (1985) A general rate equation for nuclear waste glass corrosion. *Scientific Basis for Nuclear Waste Management*, VIII, pp. 15-27.

Grambow B., Jercinovic M.J., Ewing R.C. & Byers C.D. (1985) Weathered basalt glass: a natural analogue for the effects of reaction progress on nuclear waste glass alteration. *Scientific Basis for Nuclear Waste Management*, IX, pp. 263-272.

Grambow B. & Müller R. (2001) First-order dissolution rate law and the role of surface layers in glass performance assessment. *Journal of Nuclear Materials*, 298, pp. 112-124.

Gras J.M. (2001) Modélisation semi empirique de la corrosion des aciers non alliés en situation de stockage. Actualisation du modèle EDF 1996. Rapport EDR R&D n° HT-40/01/004.

Grauls D. (1999) Overpressures : causal mechanisms, conventional and hydromechanical approches. *Oil & Gas Science and Technology-Rev. IFP*, Vol. 54, N°6, pp. 667-678.

Grellet B., Combes P., Granier T. & Philip H. (1993) Sismotectonique de la France métropolitaine dans son cadre géologique et géophysique, avec atlas de 23 cartes au 1/4 000 000 et une carte au 1/1 000 000. Mém. Soc. Géol. Fr., n°164, 2 vol.

Griffault L., Merceron T., Mossman J.R., Neerdael B., De Cannière P., Beaucaire C., Daumas S., Bianchi A. & Christen R. (1996) Acquisition et régulation de la chimie des eaux en milieu argileux pour le projet de stockage de déchets radioactifs en formation géologique. - Projet Archimède argile, Rapport final (EUR 17454), EC Publ., Luxembourg.

Guillaume D. (2002) Etude expérimentale du système fer - smectite en présence de solutions à 80°C et 300°C. Thèse de l'Université Henry Poincaré, Nancy I, France, 209 p.

Guillaume D., Neaman A., Cathelineau M., Mosser-Ruck R., C. P., Abdelmoula M., Dubessy J., Villiéras F. & Michau N. (2003) Experimental synthesis of chlorite from smectite at 300°C in the presence of metallic iron. *Clay Minerals*, Vol. 38, pp. 281-302.

Guillocheau F., Robin C., Allemand P., Bourquin S., Brault N., Dromart G., Friedenberg R., Garcia J.-P., Gaultier J.-M., Gaumet F., Grosdoy B., Hanot F., Le Strat P., Mettraux M., Nalpas T., Prijac C., Rigollet C., Serrano O. & Grandjean G. (2000) Meso-Cenozoic geodynamic evolution of the Paris Basin : 3D stratigraphic constrains. *Geodin. Acta 13*, pp. 189-246.

Guillocheau F., Robin C., Mettraux M., Dagallier G., Robin F.X. & Le Solleuz A. (2002) Le Jurassique de l'est du Bassin de Paris. *Bull. d'inf. géol. du Bassin de Paris - Volume 39, n°3*, pp. 23-47.

Gwinner B. (2004) Comportement sous eau des déchets radioactifs bitumés : validation expérimentale du modèle de dégradation COLONBO; Thèse de doctorat de l'Institut National Polytechnique de Lorraine, Nancy, 205 p.

Hanzo M. & Espitalié J. (1994) Relationship between organic matter and sedimentation in the Lias of Lorraine. In Hydrocarbon and petroleum geology of France, special publication of E.A.P.G. n°4. *Springer Verlag.*, pp. 121-136.

Hlavacek M. C.P., Doods J.A. & Sardin M. (1995) Interpreting titration data of aqueous lattices by coupling surface ionisation and ion exchange equilibria. *Colloïds and Surfaces. A: Physicochemical and Engineering Aspects*, 95, pp. 101-111.

Hoek E. & Brown E.T. (1980) Empirical strength criterion for rock masses. *J. Geotech. Eng. Div. ASCE*, 106, N° GT9, pp. 1013-1035.

Horie K., Hidaka H. & Gauthier-Lafaye F. (2004) Isotopic evidence for trapped fissiogenic REE and nucleogenic Pu in apatite and Pb evolution at the Oklo natural reactor. *Geochim. Cosmochim. Acta*, 68, pp. 115-125.

Horseman S.-T., Higgo J.J.W., Alexander J. & Harrington J. (1996) Water, Gas and Solute Movement through Argillaceous Media. Report. Rapport NEA n° CC-96/1.

IAEA (2003) "Reference Biospheres" for solid radioactive waste disposal. Rapport International Atomic Energy Agency n° IAEA-BIOMASS-6.

IFP (2004) Site Meuse / Haute-Marne - Evolution du modèle Hydrogéologique Région/Secteur - Ecoulement et transfert en aquifèrer - Rapport Final 2004. 2 tomes. Rapport Andra n° C.RP.0IFP.04.58158.

Jacquot E. & Dimier A. (2005) Multidimensional modelling of clay-cement interactions using the alliances coupling geochemistry-transport tool, Abstracts : 2nd int. meeting - Clays in Natural and Engineered Barriers for Radioactive Waste Confinement, Tours, March 14-18, pp. 21-22.

Jacquot E. & Michau N. (2005) La perturbation alcaline liée à un stockage : les argilites du Callovo-Oxfordien en champ proche et les composants à base d'argile gonflante - Site de Meuse / Haute-Marne. Rapport Andra n° C.NT.ASTR.03.069.

Jégou C., Gin S. & Larché F. (2000) Alteration kinetics of a simplified nuclear glass in an aqueous medium : effects of solution chemistry and of protective gel properties on diminishing the alteration rate. *Journal of Nuclear Materials*, 280, pp. 216-219.

JNC (2000) H12 : project to establish the scientific and technical basis for HLW disposal in Japan. Rapport JNC n° TN1410 2000-003.

Johnson L.H., Niemeyer M., Klubertanz G., Siegel P. & Gribi P. (2002) Calculations of the temperature evolution of a repository for spent fuel, vitrified high-level waste and intermediate level waste in Opalinus clay. Rapport NAGRA Technical n° 01-04.

Johnson L.H. & Schwyn B. (2004) Proceedings of a workshop on the release and transport of C-14 in repository environment. Interner Bericht . Rapport Nagra n° 04-03.

Joussaume S. (1999) Climat d'hier à demain, Ed. CNRS, 144 p.

Koepnick R.B., Denison R.E., Burke W.H., Hetherington E.A. & Dahl D.A. (1990) Construction of the Triassic and Jurassic portion of the Phanerozoic curve of seawater 87Sr/86Sr. *Chemical Geology*, 80, pp. 327-349.

Krakenberger A. (1983) Etude sédimentologique et diagénétique du Bathonien supérieur et du Callovien inférieur carbonatés de la bordure orientale du Bassin de Paris; Thèse Université de Nancy I, Nancy, France, 158 p.

Kruge M.A., Landais P., Bensley D.F., Stankiewicz B.A., Elie M. & Ruau O. (1997) Separation and artificial maturation of macerals from type II kerogen. *Energy & Fuels*, pp. 50-514.

Kull H., Jockwer N., Zhang C.L., Wileveau Y. & Pepa S. (2005) Measurement of thermally-induced pore water pressure increase and gas migration in the Opalinus clay, Clays in

Natural & Engineered Barriers for Radioactive Waste Confinement, Tours 2nd international meeting, March 14-18, 2005 à paraître.

Landais P., Monin J.C., Monthioux M., Poty B. & Zaugg P. (1989) Détermination expérimentale de l'évolution d'indicateurs de maturation de la matière organique. Application aux kérogènes du Toarcien du Bassin de Paris. *C.R.Ac.Sc.*, 308, II, pp. 1161-1166.

Lavastre V. (2002) Evénements sédimentaires, diagénétiques et post-diagénétiques dans la formation argileuse du Callovo-Oxfordien (Bassin de Paris, France) : enregistrement isotopique des minéraux et de l'eau porale. Thèse de doctorat de l'université de Paris VII, Rapport FORPRO 2002/13Th, Paris, France, 195 p.

Le Pichon X. (2004) Origin of post-Eocen extension within the African-Eurasian collision. Réunion des Sciences de la Terre, 20-25 spet. 2004, Strasbourg. Livre des résumés.

Ledieu A. (2004) Altération par l'eau des verres borosilicatés : expériences, modélisation et simulations Monte-Carlo; Thèse de l'Ecole Polytechnique, 190 p.

Leger B., Roussel J.C., Guerpillon Y. & Allagnat D. (1999) Dix ans de mesures géotechniques dans les marnes du tunnel de la Chamoise. Proc. 9ème congrès SIMR, 1999, Paris, pp. 1309-1312.

Leroux J. & Harmand D. (1998) Contrôle morphostructural de l'histoire d'un réseau hydrographique : le site de capture de la Moselle. *Geodin. Acta 13*, Acta 11, 4, pp. 149-162.

Libert M. (2005) Evaluation d'une activité bacterienne dans les colis/alvéoles de stockage - Colis C et CU. Rapport CEA n° DEN/DTN/SMTM/LMTE/04-83.

Libert M.F. (1999) Biodégradation des matériaux utilisés pour l'enrobage de déchets nucléaires : un exemple le bitume. *Bull. Soc. Fr. Microbiol.*, Vol. 14, n°4, pp. 267-271.

Libert M.F. (2004) Evaluation d'une activité bactérienne dans les colis/alvéoles de stockage - colis C et CU. Rapport CEA n° DEN/DTN/SMTM/LMTE/04-83.

Libert M.F., Bilcot J.B., Sellier R. & Bonhomme T.B., B. (1996) Biodégradation d'enrobés bitume STE3 : influence de l'irradiation et d'un pH basique. Rapport CEA n° NT SEP 96/522.

Libert M.F., Sellier R. & Bilcot J.B.B., B. (1998) Influence du pré vieillissement par irradiation gamma et de la nature de l'eau sur la biodégradation d'enrobés bitume de boues STE3. Rapport CEA n° N.T.SEP.98/663.

Lide D.R. (2002) Handbook of Chemistry and Physics, 83rd edition 2002-2003, CRC Press.

Loi n°91-1381 du 30 décembre 1991 relative aux recherches sur la gestion des déchets radioactifs.

Loutre M.F. & Berger A. (2000) Future climatic change : are we entering an exceptionnally long interglacial ? *Climatic change*, 46, pp. 61-90.

LSCE / CEA (2004) Site Meuse / Haute-Marne. Modélisation générique de l'impact de l'évolution géomorphologique sur l'hydrogéologie du site. Rapport Andra n° C.RP.12CEA.04.001.

Lutze W., Malow G., Ewing R.C., Jercinovic M.J. & Keil K. (1985) Alteration of basalt glasses: implications for modelling the long- term stability of nuclear waste glasses. *Nature*, 314, 6008, pp. 252-255.

Mäder U.K. & Mazurek M. (1998) Oxidation phenomena and processes in Opalinus clay: evidence from the excavation disturbed zones in Hauenstein and Mont Terri tunnels, and Siblingen open clay pit. *Material Research Society Symposium Proceedings*, Vol. 506, pp. 731-739.

Maes P. (2002) Circulations de fluids et interactions eau-roches passées et actuelles dans la pile sédimentaire du site de Meuse / Haute-Marne : apport des isotopes du Sr et conséquences. Thèse de doctorat, Université de Montpellier II, Rapport FORPRO 2002/14 Th, 308 p.

Malama B. & Kulatilake P. (2003) Models for normal deformation under compressive loading. *Int. Journal of Rock Mechanics and mining Sciences*, 40 (2003), pp. 893-901.

Malow G. & Ewing R.C. (1981) Nuclear waste glasses and volcanic glasses : a comparison of their stabilities. *Scientific Basis for Nuclear Waste Management*, III, pp. 315-322.

Marty B., Dewonck S. & France-Lanord C. (2003) Geochemical evidence for efficient aquifer isolation over geological timeframes. *Nature*, Vol. 425, pp. 55-58.

Matray J.-M. & Chery L. (1995) Origins and age of deep waters of the Paris Basin. *Hydrologie et géochimie isotopique*. Ed. Orstom, p. 117-133.

Mégnien C. (1980) Synthèse géologique du bassin de Paris - 3 volumes. Mémoires du BRGM n°101, 102 et 103.

Meier P., Trick T., Blümling P. & Volckaert G. (2000) Self-healing of fractures within the EDZ at the Mont Terri rock laboratory : results after one year of experimental work. Proc. If international Workshop on Geomechanics, hydromechanical and thermohydro-mechanical behaviour of deep argillaceous rocks : theory and experiments, October 11-12th 2000, Paris.

Mercier D. & *al.* (2004) Sur le Mio-Pliocène du Bassin de Paris. Journée MINANDRA 2004, livre des résumés.

Michau N. (2005a) ECOCLAY II : Effects of cement on clay barrier performance - Phase II. Final Report. Rapport Andra n° C.RP.ASCM.04.0009.

Michau N. (2005b) L'évolution chimique des ouvrages d'un stockage à base d'argile gonflante : alvéoles de stockage de déchets C et combustibles usés et scellements de galeries et de puits. Site de Meuse / Haute-Marne. Rapport Andra n° C.NT.ASCM.03.043.

Michaux L., Mouche E., Petit J.C. & Fritz B. (1992) Geochemical modelling of the long-term dissolution behaviour of the french nuclear glass R7T7. *Appl. Geochem., Supplementary Issue*, 1, pp. 41-54.

Mosser-Ruck R. & Cathelineau M. (2004) Expérimental transformation of Na,Ca-smectite under basic conditions at 150°C. *App. Clay Sci.*, 26, pp. 259-273.

Munier I., Crovisier J.-L., Grambow B., Fritz B. & Clément A. (2004) Modelling the alteration gel composition of simplified borosilicate glasses by precipitation of an ideal solid solution in equilibrium with leachant. *J. Nuclear Mat.*, 324, 2/3, pp. 97-115.

Nagra (1999a) Diffusion and sorption on hardened cement pastes - experiments and modelling results. Rapport Technique Nagra n° 99-05.

Nagra (1999b) Geochemistry of natural redox fronts - A review. Rapport Technique Nagra n° 99-05.

Nagra (2002a) Cementitious near-field sorption data base for performance assessment of an ILW repository in Opalinius Clay. Rapport Technique Nagra n° 02-20.

Nagra (2002b) Project Opalinus Clay. Safety Report; Demonstration of disposal feasibility for spent fuel, vitrified high-level waste and long-lived intermediate-level waste (Entsorgungsnachweis). Rapport Nagra n° 02-05.

Nagra (2003a) Effects of post disposal gas generation in a repository for spent fuel, high level waste and long live intermediate level sited in Opalinus Clay. Rapport Nagra n° 03-10.

Nagra (2003b) Far-field sorption data bases for performance assessment of a high-level radioactive waste repository in an undisturbed Opalinus clay host rock. Rapport technique Nagra n° TR 02-19.

Nagra (2003c) Redox conditions in the near field of a repository for SF/HLW and ILW in Opalinus clay. Rapport Technique Nagra n° 02-13.

Neuzil C.E. (2000) Osmotic generation of " anomalous " fluid pressures in geological environnement. *Nature*, vol. 403, pp. 182-184.

ONDRAF (2001a) Aperçu technique du rapport Safir 2 - Safety Assessment and Feasibility Interim. Rapport ONDRAF n° 2. NIROND 2001-05 F.

ONDRAF (2001b) Safir 2. Safety Assessment ans Feasibility Interim Report 2. Rapport ONDRAF n° NIROND 2001-06 E.

Ozanam O. & Su K. (2003) Study of EDZ Cutting-off Solutions for Repository Seals Design. In: *Impact of the excavation disturbed or damaged zone (EDZ) on the performance of* *radioactive waste geological repositories* (Ed. by E. commission), pp. 189-194, Luxembourg, 3 to 5 November 2003.

Ozanam O. & Su K. (2004) Projet HAVL-Argile. Site de Meuse / Haute-Marne. Etat des connaissances sur l'EDZ : état initial et mécanismes d'évolution. Rapport Andra n° C.RP.ASMG.03.116.

Panin V.V., Karavaiko G.I. & Pol'kin S.I. (1985) Mechanism and kinetics of bacterial oxidation of sulphide minerals. In : Karavaiko G.I. et Groudev S.N. (Eds) biogeotechnology of metals, Moscou, pp.197-215.

Parkhurst D.L. & Appelo C.A.J. (1999) User's guide to PHREEQC (version 2) - a computer program for specification, reaction-path, ID transport and inverse geochemical calculations. *US Geol. Surv. Water Resour. Inv. Rep. 99-4259, 312 p.*

Pauwels H., Foucher J.-C. & Kloppmann W. (2000) Denitrification and mixing in a schist aquifer: influence on water chemistry and isotopes. *Chem. Geol.*, 168, pp. 307-324.

Pearson F.J., Arcos D., Bath A., Boisson J.Y., Fernandez A.M., Gäbler H.-E., Gaucher E., Gautschi A., Griffault L. & Henàn P.W., H.N. (2003) Mont Terri Project - Geochemistry of water in the Opalinus Clay Formation at the Mont Terri Rock Laboratory. *Rapport de l'OFEG, Série Géologie*, N° 5, p. 143.

Pellenard P., Deconinck, J.F., Marchand D., Thierry J., Fortwengler T. & Vigneron G. (1999) Contrôle géodynamique de la sédimentation argileuse du Callovo-Oxfordien moyen dans l'Est du basin de Paris: influence eustatique et volcanique. *C. R. Acad. Sci. Paris*, 328, pp. 807-813.

Pepin G. & Vialay B. (2005) L'organisation des écoulements dans et autour d'un stockage après resaturation et retour à un état d'équilibre hydraulique. Site de Meuse/Haute-Marne. Rapport Andra n° C.NT.ACSS.03.0111.

Petit J.R., Jouzel J., Raynaud D., Barkov N.I., Barnola J.-M., Basile I., Bender M., Chappellaz J., Davis M., Delayque G., Delmotte M., Kotlyakov V.M., Legrand M., Lipenkov V.Y., Lorius C., Pépin L., Ritz C., Saltzman E. & Stievenard M. (1999) Climate and atmosphéric history of the past 420 000 years from vostock ice core, Antartica. *Nature*, 399, pp. 429-436.

Podlaha O.G., Mutterlose J. & Veizer J. (1998) Preservation of 18O and 13C in belemnite rostra from the Jurassic/early cretaceous successions. *Am. Jr. Sc*, 298, pp. 324-347.

Pokrovski G.S., Schott J., Farges F. & Hazemann J.-L. (2003) Iron(III)-silica interactions in aqueous solution: Insights from X-ray absorption fine structure spectroscopy. *Geochim. Cosmochim. Acta*, Vol. 67, N°19, pp. 3559-3573.

Pomerol C. (1978) Evolution paléogéographique et structurale du bassin de Paris du Précambrien à l'Actuel en relation avec les régions avoisinantes. *Geologie en Mijnbouw*, Vol. 57 (4), pp. 533-543.

Pourbaix M. (1972) Aspects électrochimiques de la corrosion aqueuse, rapport CEBELCOR RT.204 ; 2ème source : Significance of protection potential in pitting, intergranular corrosion ans stress corrosion cracking. *J. of Less-Common Metals*, Vol. 28, pp. 51-65.

Pytte A.M. & Reynolds R.C. (1989) The thermal transformation of smectite to illite. In The thermal history of sedimentary basins. Ed. N.D. Naeser and T.H. McCulloh -Springer-Verlag, pp.133-140.

Ramambasoa N. (2001) Etude du comportement hydro-mécanique des argilites - Application au site de Tournemire; Thèse de l'Ecole Polytechnique, 182 p.

Rebaï S., Philip H. & Taboada A. (1992) Modern tectonic stress field in the méditerranean region: evidences for variation in stress directions at different scales. *Geophys. J. Int.*, 110, pp. 106-140.

Revil A. & Leroy P. (2004) Constitutive equations for ionic transport in porous shales. *Journal of Geophysical Research*, Vol.109, B03208, doi :10.1029/2003BJ002755.

RFS n° III.2.f (10 juin 1991) Règle Fondamentale de Sûreté n° III.2.f relative aux objectifs à retenir dans le phases d'études et de travaux pour le stockage définitif des déchets radioactifs en formation géologique profonde afin d'assurer la sûreté après les périodes d'exploitation du stockage.

Ribet I., Gin S., Godon N., Jollivet P., Minet Y., Grambow B., Abdelouas A., Ferrand K., Lemmens K., Aertsens M., Pirlet V., Jacques D., Crovisier J.L., Aouad G., Art A., Clément A., Fritz B., Morvan G., Munier I., Del Nero M., Ozgümüs A., Curti E., B. L. & B. S. (2003) GLASTAB Long term behaviour of glass: improving the glass source term and substantiating the basic hypotheses. Reporting Period November 1, 2000, to October 31, 2003. Rapport Final Technical European Commission n° 5th Euratom framework programme 1998 - 2002. Contract N° FIKW-CT-2000-00007.

Rimstidt J.D. & Vaughan D.J. (2003) Pyrite oxidation: a state-of-the-art assessment of the reaction mechanism. *Geochim. Cosmochim. Acta*, Vol. 67, 5, pp. 873-880.

Rousset D. & Clauer N. (2003) Discrete clay diagenesis in a very low permeable sequence constrained by an isotopic (K-Ar and Rb-Sr) study. *Min. and Petrol.*, 145, pp. 182-198.

Rutqvist J. & Tsang C.F. (2003) A fully coupled three-dimensional THM analysis of the FEBEX in situ test with the ROCMAS code : prediction of THM behavior in a bentonite barrier. Lawrence Berkeley National laboratory. Paper LBNL-53682.

RWMC (2002) Development of TRU Waste Disposal Packages - Study on concrete packages - Summary report - for meeting Andra/RWMC (Radioactive Waste Management Funding and Research Center) Tokyo, Japan, nov. 2002.

Salah S., Gauthier-Lafaye F. & Del Nero M. (2000) Behaviour of U and REE in the weathering sequence of Bangombé, in Oklo Working Group Proceedings of the second EC-CEA workshop on the Oklo-natural analogue Phase II project held in Helsinki, Finland, from 16-18 june 1998, edited by Marevic, H. von and Louvat, D., Nuclear Science and Technology.

Savage D., Noy D. & Mihara M. (2002) Modelling the interaction of bentonite with hyperalkaline fluids. *Appl. Geochem*, 17, pp. 207-223.

Scholze H. (1991) Glass : Nature, Structure, and properties. Ed. Springer-Verlag. 454 p.

Sercombe J., Adenot F., Tiffreau C., Gwinner B. & Felines I. (2004) Modelling of water uptake and salt leaching in bituminized radioactive waste : comparison between numerical, analytical and experimental results. *Mat. Res. Soc. Symp. Proc.*, Vol. 807, pp. 377-384.

SKB (1996) Revisiting Poços de Caldas. Application of the co-precipitation approach to establish realistic solubility limits for performance assessment. Rapport Technique SKB n° 96-04.

SKB (1999) Experimental determination and chemical modelling of radiolytic processes at the spent fuel/water interface. Rapport SKB Technique n° 99-26.

SKB (2001) Aspö Hard Rock Laboratory. Report on the installation of the Backfill and Plug Test. Rapport International Progress n° IPR-01-07.

SKB (2004) Spent fuel performance under repository conditions: a model for use in SR-Can. Rapport SKB Technique n° 04-19.

Spahiu K., Devoy J., Cui D. & Lundström M. (2004) The reduction of U(VI) by near hydrogen in the presence of UO2(s). *Radiochim. Acta*, 92, pp. 597-601.

Su K. (2003) Development of Hydromechanical Constitutive Models for Callovo-Oxfordian Argilites: the MODEX-REP Project. In: *Impact of the excavation disturbed or damaged zone (EDZ) on the performance of radioactive waste geological repositories* (Ed. by E. commission), pp. 299-303, Luxembourg, 3 to 5 November 2003.

Su K. (2005) Effets d'un stockage sur le comportement mécanique à grande échelle de la couche du Callovo-Oxfordien et des formations géologiques encaissantes - Site de Meuse / Haute-Marne. Rapport Andra n° C.NT.ASMG.04.0046.

Su K. & Barnichon J.D. (2005) Le comportement mécanique d'alvéoles de stockage de déchets C et de combustibles usés dans le temps - Site de Meuse / Haute-Marne. Rapport Andra n° C.RP.ASMG.03.0109.

Talandier J. (2005) La production et le transfert de gaz dans un stockage et dans la couche du Callovo-Oxfordien - Lien avec le transitoire hydraulique - Site de Meuse / Haute-Marne. Rapport Andra n° C.NT.ASCM.03.0042.

Taubald H., Bauer A., Schäfer T., Geckeis H., Satir M. & Kim J.L. (2000) Experimental investigation of the effect of high-pH solutions on Opalinus Shale and theHammerschmiede smectite. *Clay Minerals*, 35, pp. 515-524.

Techer I., Advocat T., Lancelot J. & Liotard J.-M. (2000) Basaltic glass : alteration mechanisms and analogy with nuclear waste glasses. *Journal of Nuclear Materials*, 282, pp. 40-46.

Texier D. & Leclerc-Cessac E. (2005) Les biosphères de référence - Site de Meuse / Haute-Marne. Rapport Andra n° C.RP.ASMG.03.104.

Tournassat C. (2003) Interactions cations - argiles : le cas du Fe(II). Application au contexte de stockage profond des déchets radioactifs; Thèse de l'Université J. Fourier, Grenoble I, France, 199 p.

Trouiller A. & Benabderrahmane H. (2005) Les modèles géologique et hydrogéologique des formations géologiques encaissantes de la couche du Callovo-Oxfordien à l'état initial - Site de Meuse / Haute-Marne. Rapport Andra n° C.NT.ASMG.03.0108.

Tsang C.F., Bernier F. & Davies C. (2005) Geohydromechanical processes in the Excavation Damaged Zone in crystalline rock, rock salt, and indurated and plastic clays - in the context of radioactive waste disposal. *Int. Journal of Rock Mechanics and mining Sciences 2005 42*, pp. pp 109 - 125.

Université de Lyon I (2002) Site de Meuse / Haute-Marne - Modèle sédimentaire de l'Oxfordien calcaire de l'est du bassin de Paris - Intégration des données de terrain à l'interprétation lithostratigraphique du traitement géostatistique de la sismique 3D du site. Rapport Andra n° C.RP.0UCB.02.001.

Valle N. (2001) Traçage isotopique (29Si et 18O) des mécanismes de l'altération du verre de confinement des déchets nucléaires : SON 68. Thèse de l'Université de Lorraine, Nancy, France. 260 p.

Van Iseghem P. & Sneyers A. (1981) The leaching behaviour of bituminized radioactive waste in the geological disposal conditions of the Boom clay formation. *Mat.Res. Soc. Symp Proc*, Vol. 506, pp. 565-572.

Vieillard P., Ramirez S., Bouchet A., Cassagnabère A., Meunier A. & Jacquot E. (2004) Alteration of the Callovo-Oxfordian Clay from Meuse / Haute-Marne underground laboratory (France) by alkaline solutions : II. Modelling of mineral reactions. *Applied Geochemistry*, 19, pp. 1699-1709.

Vigneron G., Delay J., Distinguin M., Lebon P. & Trouiller A. (2004) Apport des investigations multi-échelles pour la construction d'un modèle conceptuel des plateformes carbonatées de l'Oxfordien moyen et supérieur de l'Est du Bassin de Paris. 11èmes journées techniques du Comité Français d'Hydrogéologie de l'AIH - Journées thématiques de l'AGBP. Géologie et hydrogéologie du bassin de Paris. Avancées et perspectives. 16-17 novembre 2004. Actes du Colloque pp.55-62.

Villemin T. (1986) La chronologie des évènements tectoniques dans le Nord-Est de la France et le Sud-Ouest de l'Allemagne du Permien à l'Actuel. *C.R.Ac.Sc., 303, 18*, pp. 1685-1690.

Vincent B. (2001) Sédimentologie et géochimie de la diagenèse des carbonates. Thèse Université de Bourgogne, Dijon, France, 324 p.

Wei H.F., Ledoux E. & De Marsily G. (1990) Regional modelling of groundwater flow and salt and environnemental tracer transport in deep aquifers in the Paris basin. *Journal of Hydrology, 120*, pp. 351-358.

Wendling J. (2005) Le transitoire hydraulique d'un stockage : décharge, désaturation-resaturation, retour à un état d'équilibre hydraulique. Site de Meuse / Haute-Marne. Rapport Andra n° C.NT.ASIT.03.117.

Worden R.H., Coleman M.L. & Matray J.-M. (1999) Basin scale evolution of formation waters : a diagenetic and formation water study of the triassic Chaunoy formation, Paris Basin. *Cosmochim. Actae*, 63(17), pp. 2513-2528.

Worden R.H. & Matray J.M.-M. (1995) Cross formational flow in the Paris basin. *Basin Res.*, 7, pp. 53-66.

Wright A.C. (1994) Neutron scattering from vitreous silica. V. The structure of vitreous silica : what have we learned from 60 years of diffraction studies ? *J. Non-Crist. Solids*, 179, pp. 84-115.

Zachariensen W.H. (1932) The atomic arrangement in glass. *J. Am. Chem. Soc.*, 54, pp. 3841-3851.

Zachariensen W.H. (1933) Die Struktur der Gläser. *Glastech. Ber. -Glass Sci. Technol.*, 11, 4, pp. 120-123.

Zarzycki J. (1982) Les verres et l'état vitreux. Ed. Masson, 391 p.

Zhang C.L. & Rothfuchs T. (2004) Experimental study of the Hydro-mechanical behaviour of the Callovo-Oxfordian argillite. *Applied Clay Science*, 26, pp. 325-336.

Photo Credits:

ANDRA - CEA
GEO-TER - Archividéo - Scétauroute - Intégration

Identifiant : C RP ADS 04 0025 B

The Andra Publication Series

Essential Series

In a few pages, documents in the Essential Series provide simple and illustrated explanations with a view to furthering knowledge on radioactive waste and Andra.

Reference Series

With standard information concerning Andra methods and progress reports on its investigations or activities, the Reference Series presents various technical and other information, especially on the location of radioactive waste.

Periodical Series

On a regular basis, Andra publishes various brochures relating to the environmental monitoring of its disposal and research facilities. The Periodical Series includes those publications as well as the respective news bulletins of each site.

Discovery Series

Videos, CD-ROMs, synthesis images and comic strips… are worth more than a thousand words. The Discovery Series uses vivid illustrations to explain to a broad public the underlying principles of radioactive-waste management.

Science and Technology Series

Taking stock of current knowledge, presenting ongoing research as well as the Agency's methods and approaches constitute the objectives of the Science and Technology Series. Intented for a specialised public, it provides various syntheses and monographs published under the aegis of Andra or in partnership with other scientific organisations.

Report Series

Summaries, reports and seminar proceedings published in the Report Series highlight the advances of Andra's ongoing investigations.

Industrial Practices Series

The Industrial Practices Series includes documents dealing with the acceptance criteria and the management of radioactive waste.

ANDRA
Agence nationale
pour la gestion des déchets radioactifs

Parc de la Croix Blanche - 1/7, rue Jean Monnet - F 92298 Châtenay-Malabry Cedex
Tél. : 01 46 11 80 00
www.andra.fr

© Andra - 269 VA - December 2006 - Graphic design: Mediagérance - ISBN 2-9510108-7-70108-8-5